Stony Brook University

Design, Synthesis and Evaluation of Novel Taxane-Based Anticancer Agents

A Dissertation Presented

by

Yuan Li

to
The Graduate School
in Partial Fulfillment of the
Requirements
for the Degree of

Doctor of Philosophy
in
Chemistry

Stony Brook University

May 2011

Stony Brook University

The Graduate School

Yuan Li

We, the dissertation committee for the above candidate for the
Doctor of Philosophy degree, hereby recommend
acceptance of this dissertation.

Iwao Ojima – Dissertation Advisor
Distinguished Professor, Department of Chemistry

Dale G. Drueckhammer – Chairperson of Defense
Professor, Department of Chemistry

Kathlyn A. Parker– Third Member
Professor, Department of Chemistry

Michael R. Angelastro – Outside Member
Lead Research Investigator, Sanofi-Aventis US Inc.

This dissertation is accepted by the Graduate School

Lawrence Martin
Dean of the Graduate School

Abstract of the Dissertation

Design, Synthesis and Evaluation of Novel Taxane-Based Anticancer Agents

by

Yuan Li

Doctor of Philosophy

in

Chemistry

Stony Brook University

2011

Taxol® (paclitaxel) and Taxotère® (docetaxel) are the most widely used pharmaceuticals in cancer chemotherapy. These drugs have been approved by the FDA for the treatment of advanced ovarian cancer, metastatic breast cancer, Kaposi Sarcoma, non-small cell lung cancer, etc. Both drugs are also under clinical development for additional cancer indications.

Although established great success in the clinic, paclitaxel and docetaxel have exhibited a number of undesirable side effects as well as low efficiency against drug-resistant cancer

phenotypes. Therefore the development of new analogs, which are expected to have higher potency and better pharmacological properties but fewer side effects, is of high value from the cancer chemotherapy perspective.

The dissertation will present the design, synthesis and biological evaluation of the following novel taxane-based anticancer agents:

(1) New generation taxoids: via the highly efficient *β*-Lactam Synthon Method, the design and synthesis of a large number of novel taxoids with systematic modifications has led to the development of highly potent second- and third-generation taxoids. In parallel, taxoids against multi-drug resistance cell lines have also been developed to create the dual functions (the cytotoxicity and the MDR reversal activity) into one molecule.

(2) Macrocyclic taxoids: paclitaxel takes effect by inducing microtubule stabilization, G2/M block and apoptosis. Although this classic mechanism of action has been known for almost 30 years, the binding conformation of paclitaxel to *β*-tubulin is yet to be fully understood. Structurally constrained macrocyclic taxoids were designed, synthesized and evaluated to help identify the bioactive conformation(s).

(3) Novel taxoid conjugates: the undesirable side effects in conventional cancer chemotherapy are generally resulted from the lack of tumor-specificity. Omega-3 fatty acids have been shown to be beneficial for tumor-targeting drug delivery. Novel tumor-targeting conjugates of new generation taxoids were hence designed and synthesized using omega-3 polyunsaturated fatty acids.

Table of Contents

List of Figures viii
List of Schemes x
List of Tables xii
List of Abbreviations xiii
Acknowledgements xvi

CHAPTER 1. CANCER, TAXOIDS, AND β-LACTAM SYNTHON METHOD 1
§1.1 CANCER: STATISTICS, TYPES, CAUSES AND TREATMENTS 1
§1.2 TAXOIDS: DISCOVERY AND STRUCTURE-ACTIVITY RELATIONSHIP STUDIES 3
§1.2.1 Chemotherapy and Anticancer Agents 3
§1.2.2 Paclitaxel: Discovery and Novel Mechanism of Action 4
§1.2.2.1 Discovery of Paclitaxel 4
§1.2.2.2 Paclitaxel: Novel Mechanism of Action 4
§1.2.3 Synthesis of Paclitaxel 7
§1.2.4 Structure-Activity Relationship Studies 9
§1.2.4.1 SAR Studies of the Baccatin Skeleton 10
§1.2.4.2 SAR Studies of the C13 Side Chain 12
§1.3 OJIMA β-LACTAM SYNTHON METHOD 14
§1.3.1 Introduction 14
§1.3.2 Synthesis of Enantiomerically Pure β-Lactam via Asymmetric Ester-Imine Cyclocondensation 14
§1.3.3 Synthesis of Enantiomerically Pure β-Lactam via Staudinger Cycloaddition Reaction Followed by Enzymatic Kinetic Resolution 17
§1.4 EXPERIMENTAL SECTION 20
§1.5 REFERENCES 28

CHAPTER 2. DESIGN, SYNTHESIS AND BIOLOGICAL EVALUATION OF SECOND- AND THIRD- GENERATION TAXOIDS 34
§2.1 DEVELOPMENT OF THE SECOND- AND THIRD-GENERATION TAXOIDS VIA OJIMA β-LACTAM SYNTHON METHOD 34
§2.2 SYNTHESIS AND BIOLOGICAL EVALUATION OF TAXANE-BASED MULTI-DRUG RESISTANCE (MDR) MODULATOR **SB-RA-310124** 37
§2.2.1 Multi-Drug Resistance (MDR) and its Cellular Mechanism 37
§2.2.2 Classical Multidrug Resistance with Efflux Pumps 37
§2.2.3 Design, Synthesis and Biological Evaluation of Taxane-Based MDR Modulators (TRAs) 38
§2.2.3.1 MDR modulators 38
§2.2.3.2 Rational Design of Taxane-Based MDR Modulators (TRAs) 39
§2.2.3.3 Structure-Activity Relations of Taxane-Based MDR Modulators (TRAs) 41
§2.2.4 Taxane-Based Multi-Drug Resistance (MDR) Modulator **SB-RA-310124** 43
§2.2.4.1 Synthesis of **SB-RA-310124** 43
§2.2.4.2 Biological Evaluation 44
§2.3 SECOND-GENERATION TAXOID **SB-T-121303013** 47
§2.3.1 Background 47
§2.3.2 Synthesis of **SB-T-121303013** 47

§2.4 EXPERIMENTAL SECTION 50
§2.5 REFERENCES 54

CHAPTER 3. DESIGN, SYNTHESIS AND BIOLOGICAL EVALUATIONS OF NOVEL MACROCYCLIC TAXOIDS 58
§3.1 INTRODUCTION OF BIOACTIVE CONFORMATION 58
§3.1.1 Nonpolar Conformation 58
§3.1.2 Polar Conformation 60
§3.1.3 T-Taxol 61
§3.1.4 REDOR-Taxol 62
§3.2 DESIGN, SYNTHESIS AND BIOLOGICAL EVALUATION OF THE C4-C2' LINKED MACROCYCLIC TAXOID **SB-TCR-101** 64
§3.2.1 Common Pharmocophore 64
§3.2.2 Design and Synthesis of the C4-C2' Linked Macrocyclic Taxoid **SB-TCR-101** 66
§3.2.3 Biological Evaluations 70
§3.3 DESIGN, SYNTHESIS AND BIOLOGICAL EVALUATION OF THE C14-C3'Bz*N*-LINKED MACROCYCLIC TAXOIDS **SB-T-2055** 71
§3.3.1 Introduction 71
§3.3.2 Design and Synthesis of the C14-C3'Bz*N* Linked Macrocyclic Taxoid **SB-T-2055** 72
§3.3.3 In vitro Biological Evaluations 75
§3.4 EXPERIMENTAL SECTION 77
§3.5 REFERENCES 88

CHAPTER 4. DESIGN, SYNTHESIS, BIOLOGICAL EVALUATION OF NOVEL FLUORINATED TAXOIDS 92
§4.1 INTRODUCTION 92
§4.1.1 Fluorine and Fluorinated Moieties in Medicinal Chemistry 92
§4.1.2 Fluorinated β-Lactam and its Synthetic Applications 93
§4.1.3 Fluorinated Taxoids and its Biological Activities 94
§4.2 GRAM-SCALE SYNTHESIS OF C3'-DIFLUOROVINYL TAXOID **SB-T-12854** 97
§4.2.1 Synthsis of C3'-Difluorovinyl Second-Generation Taxoids 97
§4.2.1.1 Synthesis of (3*R*,4*S*)-1-(*tert*-butoxycarbonyl)-3-triisopropylsiloxy-4-difluorovinylazetidin-2-one 98
§4.2.1.2 Gram-Scale Synthesis of C3'-Difluorovinyl Taxoid **SB-T-12854** 99
§4.2.2 Results and Discussion 100
§4.2.3 Conclusion 102
§4.3 SYNTHESIS AND FLUORESCENCE STUDY OF **C7-FLUORESCEIN-SB-T-12854** 103
§4.3.1 Application of Fluorescein in the Biological Studies 103
§4.3.2 Synthesis of **C7-Fluorescein-SB-T-12854** 103
§4.3.3 Results and Discussion 106
§4.3.4 Conclusion 107
§4.4 EXPERIMENTAL SECTION 109
§4.5 REFERENCES 117

CHAPTER 5. SYNTHESIS AND BIOLOGICAL EVALUATION OF NOVEL FATTY ACID-FLUORINATED TAXOID CONJUGATES 121
§5.1 Introduction.....121
§5.1.1 Development of Tumor-Targeting Conjugate 121
§5.1.2 Docosahexaenoic Acid (DHA) as Cancer-Targeting Moiety 122
§5.1.3 Novel DHA Conjugates with Second- and Third-Generation Taxoids 124
§5.2 RESULTS AND DISCUSSION.....129
§5.2.1 Synthesis of DHA-Fluorinated Second-Generation Taxoid Conjugates 129
§5.2.2 Biological Evaluation of DHA-C3'-Difluorovinyl-Taxoid Conjugate **DHA-SB-T-12854** ... .129
§5.3 CONCLUSION.....131
§5.4 EXPERIMENTAL SECTION.....132
§5.5 REFERENCES 134

References.....136
Appendix.....157

List of Figures

Figure ..... Page

CHAPTER 1

Figure 1-1. Examples of current available anticancer drugs 3
Figure 1-2. Structure of TAXOL® (paclitaxel) 4
Figure 1-3. The cell cycle and the role of taxol as microtubule-stabling agent 5
Figure 1-4. Microtubule formation and mechanism of action of paclitaxel 6
Figure 1-5. 10-Deacetylbaccatin III (10-DAB III) 7
Figure 1-6. Structure of Taxotère® (docetaxel) 9
Figure 1-7. Summary of SAR for paclitaxel 10
Figure 1-8. C-seco taxoid IDN5390 11
Figure 1-9. Chiral auxiliaries 14

CHAPTER 2

Figure 2-1. Second-generation taxoids synthesized from 10-DAB III 35
Figure 2-2. Generic structure of third-generation taxoids 35
Figure 2-3. Structure of second-generation taxoids **SB-T-1103**, **SB-T-1104**, **SB-T-1214** and **SB-T-1216** 36
Figure 2-4. Mechanism of MDR modulator (i.e. MDR reversal agent) 39
Figure 2-5. Structure of the taxane-based MDR modulators 40
Figure 2-6. Taxane-based MDR modulators designed (by Professor Ojima) 40
Figure 2-7. Structure-activity study of TRAs 41
Figure 2-8. Structure of **SB-RA-310124** 43
Figure 2-9. TRAs that modulate all three efflux pumps 45
Figure 2-10. Effect of TRAs on drug efflux in resistant cell lines 45
Figure 2-11. Chemical structure of **SB-T-121303013** 47

CHAPTER 3

Figure 3-1. The chemical structure of paclitaxel and docetaxel 58
Figure 3-2. X-ray structure of docetaxel 59
Figure 3-3. C2-C3'N-linked macrocyclic taxoids 60
Figure 3-4. X-ray structure of paclitaxel 60
Figure 3-5. C2-C3'-linked macrocyclic taxoids 61
Figure 3-6. T-taxol and its interaction with α,β-tubulin 62
Figure 3-7. REDOR-Taxol-1JFF and the atom-atom distance between C14 and the ortho carbon of the C3'Bz*N*-benzoyl group. 63
Figure 3-8. Overlay of the REDOR-Taxol (green) and T-Taxol (yellow) 63
Figure 3-9. Naturally occurring microtubule-stabilizing agents 65
Figure 3-10. Proposed binding conformation of paclitaxel (by Raphal Geney) 66

Figure 3-11. C4-C2' linked and C14-C3'Bz*N* linked macrocyclic taxoids.....66
Figure 3-12. Structure of 14*β*-OH-10-DAB (14-OH-DAB).....71
Figure 3-13. Designed novel C14-C3'Bz*N*-linked macrocyclic taxoids.....71
Figure 3-14. Overlays of REDOR-Taxol (green) with **1a** (cyan), **1b** (red), and **1c** (pink).....72

CHAPTER 4

Figure 4-1. Examples of fluorinated drugs currently on the market.....92
Figure 4-2. Introduction of fluorine atoms prevents oxidation of the phenyl ring.....93
Figure 4-3. Structure of **SB-T-12842-4** and **SB-T-128221-3**.....95
Figure 4-4. Structure of **SB-T-12851**, **SB-T-12852**, **SB-T-12853**, and **SB-T-12854**.....97
Figure 4-5. Structure of fluorescein.....104
Figure 4-6. Flow cytometry / FACS results of **fluorescein-SB-T-12854**.....107

CHAPTER 5

Figure 5-1. Tumor recognition moieties.....122
Figure 5-2. Polyunsaturated fatty acids (PUFAs).....123
Figure 5-3. DHA-paclitaxel conjugate (Taxoprexin).....124
Figure 5-4. Novel DHA conjugates with second- and third-generation taxoids.....125
Figure 5-5. Effect of DHA-Taxoid conjugates on human ovarian tumor xenograft (Pgp-) A121 126
Figure 5-6. Effect of DHA-Taxoid conjugates on human colon tumor xenograft (Pgp+) DLD-1 128

List of Schemes

Scheme ..... Page

CHAPTER 1

Scheme 1-1. The first semisynthesis of paclitaxel by Potier et al 8
Scheme 1-2. Holton semisynthesis of paclitaxel 8
Scheme 1-3. Ojima's *β*-lactam synthon method for semisynthesis of paclitaxel 9
Scheme 1-4. Lithium-chiral ester enolate-imine cyclocondensation method 14
Scheme 1-5. Synthesis of Whitesell chiral auxiliary (1*R*,2*S*)-*trans*-2-phenyl-1-cyclohexanol 15
Scheme 1-6. Synthesis of (1*R*,2*S*)-triisopropylsiloxy-acetic acid 2-phenyl-1-cyclohexyl ester 15
Scheme 1-7. Synthesis of (3*R*,4*S*)-1-(*tert*-butoxycarbonyl)-3-triisopropylsiloxy-4-(2-methyl-propen-2-yl)azetidin-2-one 16
Scheme 1-8. The mechanism of chiral TIPS-ester enolate-imine condensation 16
Scheme 1-9. [2+2] Ketene-imine cycloaddition reaction 17
Scheme 1-10. Synthesis of (3*R*,4*S*)-3-ethoxyethoxy-4-phenylazetidin-2-one 18
Scheme 1-11. Synthesis of (3*R*,4*S*)-1-(*tert*-butoxycarbonyl)-3-triisosiloxy-4-(2-methyl-propen-2-yl)azetidin-2-one 19

CHAPTER 2

Scheme 2-1. Synthesis of 10,13-diacetylbaccatin 43
Scheme 2-2. Synthesis of 4-(4-dimethylaminobenzoyl)cinnamic acid 44
Scheme 2-3. Synthesis of **SB-RA-310124** 44
Scheme 2-4. Synthesis of C2 modified baccatin 48
Scheme 2-5. Synthesis of **SB-T-121303013** 49

CHAPTER 3

Scheme 3-1. Retro-synthetic analysis of macrocyclic taxoid **SB-TCR-101** 67
Scheme 3-2. Preparation of C4 modified baccatin **3-4** 68
Scheme 3-3. Synthesis of modified baccatin **3-7** 68
Scheme 3-4. Synthesis of *β*-lactam **3-12** 69
Scheme 3-5. Synthesis of **SB-TCR-101** 70
Scheme 3-6. Syntheses of modified baccatin **3-19** 73
Scheme 3-7. Syntheses of modified 2-allyloxybenzoyl chloride 73
Scheme 3-8. Attempt of MOP-protected *β*-lactam 74
Scheme 3-9. Syntheses of diene **3-25** 74
Scheme 3-10. Synthesis of (*E*)-**SB-T-2055** and (*Z*)-**SB-T-2055** 75

CHAPTER 4

Scheme 4-1. Representative transformations of *N*-*tert*-Boc-3-PO-4-Rf-*β*-lactams.....94
Scheme 4-2. Primary metabolism site on the second-generation taxoids by the enzyme of P450 family.....96
Scheme 4-3. Retro-synthesis of C3'-difluorovinyl second-generation taxoids.....97
Scheme 4-4. Synthesis of (3*R*,4*S*)-1-(*p*-methoxyphenyl)-3-triisopropylsiloxy-4-(2-methyl-propen-2-yl)azetidin-2-one.....98
Scheme 4-5. Mechanism of 1,1-difluoroolefins formation.....99
Scheme 4-6. (3*R*,4*S*)-1-(*tert*-Butoxycarbonyl)-3-triisopropylsiloxy-4-difluoro-vinyl-azetidin-2-one.....99
Scheme 4-7. Synthesis of C3'-difluorovinyl-taxoids **SB-T-12854**.....100
Scheme 4-8. Modification of Fluorescein.....105
Scheme 4-9. Synthesis of C3'-difluorovinyl-taxoid **SB-T-12854**.....105

CHAPTER 5

Scheme 5-1. Synthesis of **DHA-SB-T-12854**.....129

List of Tables

Table ..... Page

CHAPTER 2

Table 2-1. IC_{50} values of **SB-T-121303013** 47

CHAPTER 3

Table 3-1. Cytotoxicity of **SB-TCR-101** on MCF-7-S and MCR-7-R cell lines 70
Table 3-2. *In vitro* activity of (*E*)-**SB-T-2055** and (*Z*)-**SB-T-2055** 75

CHAPTER 4

Table 4-1. *In vitro* cytotoxicity (IC_{50} nM) of fluoro-taxoids 95
Table 4-2. *In vitro* cytotoxicity (IC_{50} nM) of C3'-difluorovinyl-taxoids 101
Table 4-3. *In vitro* cytotoxicity (IC_{50} nM) of C3'-difluorovinyl-taxoids against pancreatic cancer cell lines 101
Table 4-4. Cytotoxic activity of paclitaxel, **SB-T-12854** and **fluorescein-SB-T-12854** 106

CHAPTER 5

Table 5-1. Antitumor effect of DHA-taxoid conjugates administered i.v. to drug-sensitive human ovarian tumor xenograft (Pgp-) A121 in SCID mice 126
Table 5-2. Antitumor effect of DHA-taxoid conjugates administered i.v. to drug-resistant Pgp+ human colon tumor xenograft DLD-1 in SCID mice 127
Table 5-3. *In vitro* cytotoxicity of **DHA-SB-T-12854** 130

List of Abbreviations

10-DAB III	10-deacetylbaccatin III
Å	angstrom
Ac	acetyl
AcOH	acetic acid
AGM	aminoglutethimide
AML	acute myelogenous leukemia
Anal	analysis
atm	atmosphere
ATP	adenosine triphosphate
bd	broad doublet
Bn	benzyl
bp	boiling point
br	broad
bs	broad singlet
Boc	*tert*-butoxycarbonyl
t-Bu	*tert*-butyl
n-BuLi	*n*-butyllithium
Bz	benzoyl
Calcd	calculated
CAN	Cerium(IV) ammonium nitrate
d	doublet
DCC	N,N'-dicyclohexylcarbodiimide
DCM	dichloromethane
dd	doublet of doublet
DHA	docosahexaenoic acid
DIC	*N,N*-diisopropylcarbodiimide
DIPEA	*N,N*-diisopropylethylamine
DMAP	4-*N,N′*-dimethylaminopyridine
DMF	*N,N′*-dimethylformamide
DMSO	dimethyl sulfoxide
DNA	deoxyribonucleic acid
DOX	doxorubicin
EC_{50}	concentration of drug that produces 50 % effect
EDC.HCl	1-ethyl-3-(3-dimethylaminopropyl)carbodiimide hydrochloride
ee	enantiomeric excess
EE	ethoxyethyl
e.g.	for example
EGFR	epidermal growth factor receptor
EPR	enhanced permeability and retention
eq	equivalent
ESI	electrospray ionization
Et	ethyl
et al.	and others
EtOAc	ethyl acetate

EtOH	ethanol
FDA	Food and Drug Administration
FITC	fluorescein isothiocyanate
FTIR	fourier tranform infrared spectroscopy
g	gram
GC	gas chromatography
GTP	guanosine 5'-triphosphate
h	hour
HA	hyaluronic acid
HATU	2-(1H-7-azabenzotriazol-1-yl)-1,1,3,3-tetramethyl uronium hexafluoro phosphate methanaminium
HMPA	hexamethylphosphoramide
HPLC	high performance liquid chromatography
HRMS	high resolution mass spectrometry
Hz	hertz
IC_{50}	concentration for 50 % inhibition
*i*Pr	isopropyl
IR	infrared spectroscopy
J	coupling constant
Kd	dissociation constant
kDa	kilodalton
kg	kilogram
KHMDS	Potassium 1,1,1,3,3,3-hexamethyldisilazide
L	liter
LC	liquid chromatography
LDA	Lithium diisopropylamide
LiHMDS	Lithium 1,1,1,3,3,3-hexamethyldisilazide
m	multiplet
M	molar or molarity
mAb	monoclonal antibody
MALDI–TOF	matrix-assisted laser desorption ionization time-of-flight
MAPs	microtubule associated proteins
MDR	multi-drug resistance
MDS	methyldisulfanyl
Me	methyl
MeOH	methanol
mg	milligram
MHz	megahertz
min	minute
mL	milliliter
mM	milimolar
mmol	millimole
mol	mole
mp	melting point
MPA	methylpyridinium acetate
MS	mass spectrometry

MTD	maximum tolerated dose
MWNT	multi-walled carbon nanotube
NaHMDS	Sodium 1,1,1,3,3,3-hexamethyldisilazide
NCI	National Cancer Institute
nM	nanomolar
NMR	nuclear magnetic resonance
PBS	phosphate buffered saline
Pgp	P-glycoprotein
Ph	phenyl
PLAP	pig liver acetone powder
PMA	phosphomolybdic acid
PMP	*p*-methoxyphenyl
ppm	parts per million
p-TSA	*p*-toluenesulfonic acid
Py	pyridine
q	quartet
QD	quantum dot
rt	room temperature
s	singlet
SAR	structure-activity relationship
SCID	severe combined immunodeficiency
t	triplet
$t_{1/2}$	half time
TBDMS	*tert*-butyldimethylsilyl
TEA	triethylamine
TEM	Transmission electron microscopy
tert	tertiary
TES	triethylsilyl
Tf	triflouromethanesulfonate
TFA	trifluoroacetic acid
THF	tetrahydrofuran
TIPS	triisopropylsilyl
TLC	thin layer chromatography
TMS	trimethylsilyl
USDA	U.S. Department of Agriculture
U-tube	ultra short carbon nanotube
UV	ultraviolet-visible
wt	weight
β-LSM	β-Lactam Synthon Method
δ	chemical shift
*μ*g	microgram
*μ*L	microliter
*μ*M	micromolar
*μ*m	micrometer
*μ*mol	micromole

Acknowledgments

My deepest gratitude goes to my advisor Professor Iwao Ojima. I have been amazingly fortunate to have an advisor who gives not only invaluable research guidance but also enormous support during my M.S. and Ph.D. study. Professor Ojima set the perfect example of a great scientist with his persistent pursuit of excellence and ingenious insights of research. Besides the scientific direction, Professor Ojima has also given comprehensive guidance for professionalism with a systematic training structure within the group. Professor Ojima's never-ending encouragement have brought out the best in me, making my graduate study at Stony Brook the most memorable years of my life.

I would also like to thank the committee members: Professor Dale Drueckhammer and Professor Kathlyn Parker, the chair and third member of my committee, respectively. Their help as well as insightful comments throughout my advancement in the Ph.D. program have been truly invaluable.

I am grateful to Doctor Michael Angelastro from Sanofi-Aventis, for taking time out of his busy schedule to be the outside member of my committee.

I am also thankful to all the faculty members in the Department of Chemistry at Stony Brook University for their valuable courses and seminars.

A special thank goes to our NMR specialist, Mr. James Marecek, for his kind assistance in NMR spectroscopy and many insightful discussions. I thank Mrs. Katherine Hughes, Student Affairs Coordinator, for her warm-hearted assistance in a variety of matters during my time at Stony Brook.

I want to express my true appreciation to all of the alumni and the current members of Professor Ojima's research group for their support throughout my graduate study at Stony Brook. I would like to thank Dr. Xinyuan Wu, Dr. Zihao Hua, Dr. Larisa Kuznetsova, Dr. Antonella Pepe, Dr. Wen-Hua Chiou, Dr. Bruno Chapsal, Dr. Qing Huang, Dr. Jin Chen, Dr. Greta Varchi, Dr. Bibia Bennacer, Dr. Hojae Choi, Dr. Claude Commandeur, Dr. Stanislav Jaracz, Dr. Seung-Yub Lee, Dr. Kan Ma, Dr. Liang Sun, Dr. Xianrui Zhao, Dr. Shuyi Chen, Dr. Ce Shi, Dr. Manisha Das, Dr. Stephen Chaterpaul, Dr. Joseph Junior Kaloko, Dr. Gary Yu-Han Teng, Kunal Kumar, Ilaria Zanardi, Edison S. Zuniga, Joshua Seitz and Wen Chen for their valuable discussions as well as warm relationships. Special thanks go to Dr. Liang Sun for his valuable

mentoring and discussion on the collaboration on macrocyclic taxoids project, and to Joshua Seitz and Edison Zuniga for their support on conjugate project.

I also want to sincerely thank Ms. Yoko Ojima for her gracious hospitality over the years.

Very special thanks go to Mrs. Patricia Marinaccio, our Project Staff Assistant, who is the "Mom"of the Ojima group. I want to thank her for always being there for help.

I greatly value all my friends from Stony Brook. The warmest friendship made me feel at home while I am thousands of miles away from my home country.

Most importantly, none of this would have been possible without the love, support and patience of my family. My parents and my husband, Shuyi Chen, have been a constant source of love and strength through the years.

Finally, I appreciate the financial support from National Institutes of Health, National Cancer Institute, and the Department of Chemistry at Stony Brook University.

CHAPTER 1. CANCER, TAXOIDS, AND β-LACTAM SYNTHON METHOD

§1.1 Cancer: Statistics, Types, Causes and Treatments

Cancer is one of the major health problems to general public worldwide. It is the leading cause of death in developed countries and the second leading cause of death in developing countries. [1] Based on the GLOBOCAN 2008 estimates, about 12.7 million cancer cases were diagnosed and 7.6 million people died of cancer in 2008. [2]

The global burden of cancer continues to rise as the aging of world population and increasing adoption of cancer-causing behaviors, e.g. smoking and physical inactivity, within developing countries. Deaths from cancer are projected to keep increase worldwide, with an estimated 11 million deaths in 2030. [3]

Currently in the United States, cancer has become the number one cause of death for people under age of 85 years. In 2007, a total of 475,211 people under 85 years died from cancer in the United States, compared with 380,791 deaths from heart disease, which is the leading cause of death for overall population in the United States. [4]

Cancer is a broad term used to cover 100 diseases characterized by uncontrolled growth of abnormal cells which invade or destroy adjacent or distant healthy tissues in the body. These abnormal cells are termed as cancer cells or malignant cells.

As the basic units of living systems, the cells usually grow and divide in a controlled fashion to produce new cells as needed to replace the old or damaged cells. However, this harmonious process sometimes malfunctions when the regulating genetic material is damaged or changed. The balance between new cell growth and old cell death is disrupted, resulting uncontrolled cell growth or loss of apoptosis (self programmed cell death). The excessive cells may form a mass of tissue called tumor or neoplasm. A tumor can be benign or malignant. The benign tumors may grow larger but do not spread to other parts of the body; While malignant cells can spread through the blood and lymph systems to other parts of the body to cause damages, and this process is called metastasis.

The National Cancer Institutes classifies cancers into the following categories:

Carcinoma: cancer that begins in the epithelial tissue of the skin or of the lining of the internal organs;

Sarcoma: cancer that begins in bone, cartilage, fat, muscle, blood vessels, or other connective or non-epithelial tissues;

Leukemia: cancer that begins in blood-forming organ and produces increased numbers of immature or abnormal blood cells;

Lymphoma and myeloma: cancer that begins in the cells of the immune system; and

Central nervous system cancers: cancer that begins in the tissues of the brain and spinal cord.

Cancers are further identified by the name of the tissue or organ of origin, e.g. breast cancer, lung cancer, and colon cancer. The most common cancer types worldwide are lung cancer (1.4 million deaths), stomach cancer (740 000 deaths), liver cancer (700 000 deaths), colorectal cancer (610 000 deaths), and breast cancer (460 000 deaths). [3]

The incidences of cancer death are subjective to many factors, of which 90-95% is environmental factors and 5-10% is genetic factors. Common environmental factors include: smoking (25-30%), diet and obesity (30-35%), infections (15-20%), radiation, stress, physical inactivity, and pollutions.[5] Since cancers are primarily an environmental disease, a significant

portion of them could be prevented through implementation of programs for tobacco control, vaccination and public health campaigns promoting regular screenings, physical activities and healthier dietary.

Many management options for cancer are available including chemotherapy, radiation therapy, surgery, immunotherapy and other methods. The option of treatments is dependent on the type of cancer, the location and grade of the tumor, and the stage of the disease, as well as the general health state of the patients.

Chemotherapy is the treatment of cancer with cytotoxic drugs to destroy cancer cells, stop cancer cells from spreading, and slow the growth of cancer cells. [6]

Radiation therapy (also called irradiation or radiotherapy) is the use of high-energy radiation from X-rays, gamma rays, neutrons, protons, and other sources to kill cancer cells and shrink tumors. Radiation may come from a machine outside the body (external-beam radiation therapy), or it may come from radioactive material placed in the body near cancer cells (internal radiation therapy). [7]

Surgery can be the removal of either only the tumor, or the entire organ. However, complete cure can be difficult when the cancer has metastasized to other part of body.

Immunotherapy is the treatment with monoclonal antibodies, growth factors or vaccines to boost or restore the ability of the immune system to fight cancer.

Today, cancer research is one of the most exciting fields in health programs, medicinal sciences and pharmaceutical development. It comprises of intense scientific effort to understand disease mechanism and discover possible therapies. In the United States only, the investment on cancer research has exceeded $200 billion from public and private sectors and foundations since President Nixon declared “War on Cancer” in 1971. The top cancer research organizations include the American Association for Cancer Research, the American Cancer Society, the American Society of Clinical Oncology, the National Cancer Institute, the European Organisation for Research and Treatment of Cancer, and the National Comprehensive Cancer Network. Just to name a few.

§1.2 Taxoids: Discovery and Structure-Activity Relationship Studies

§1.2.1 Chemotherapy and Anticancer Agents

Chemotherapy is the treatment of cancer with cytotoxic drugs to stop or slow the growth of cancer cells. Tumor with high growth rate, e.g. acute myelogenous leukemia and the aggressive lymphomas, is generally more sensitive to chemotherapy. Depending on the type and stage of cancer, chemotherapy can cure cancers, control cancers or ease cancer symptoms. It could be used as the only treatment method, or along with surgery, radiation therapy, or immunotherapy. Most anticancer drugs are delivered intravenously, while some agents can be administered orally.

The majority of chemotherapeutic drugs can be divided in to alkylating agents (e.g. cisplatin, carboplatin, and oxaliplatin), antimetabolites, anthracyclines, plant alkaloids (e.g. vinca alkaloids and taxanes), topoisomerase inhibitors (e.g. irrinotecan, topotecan, amsacrine, etoposide, and teniposide), and antitumor antibiotics (e.g. dactinomycin). [8] All of these drugs affect cell division (mitosis) or DNA synthesis and function in some way. [6 9] **Figure 1-1** shows some examples of current available anticancer drugs.

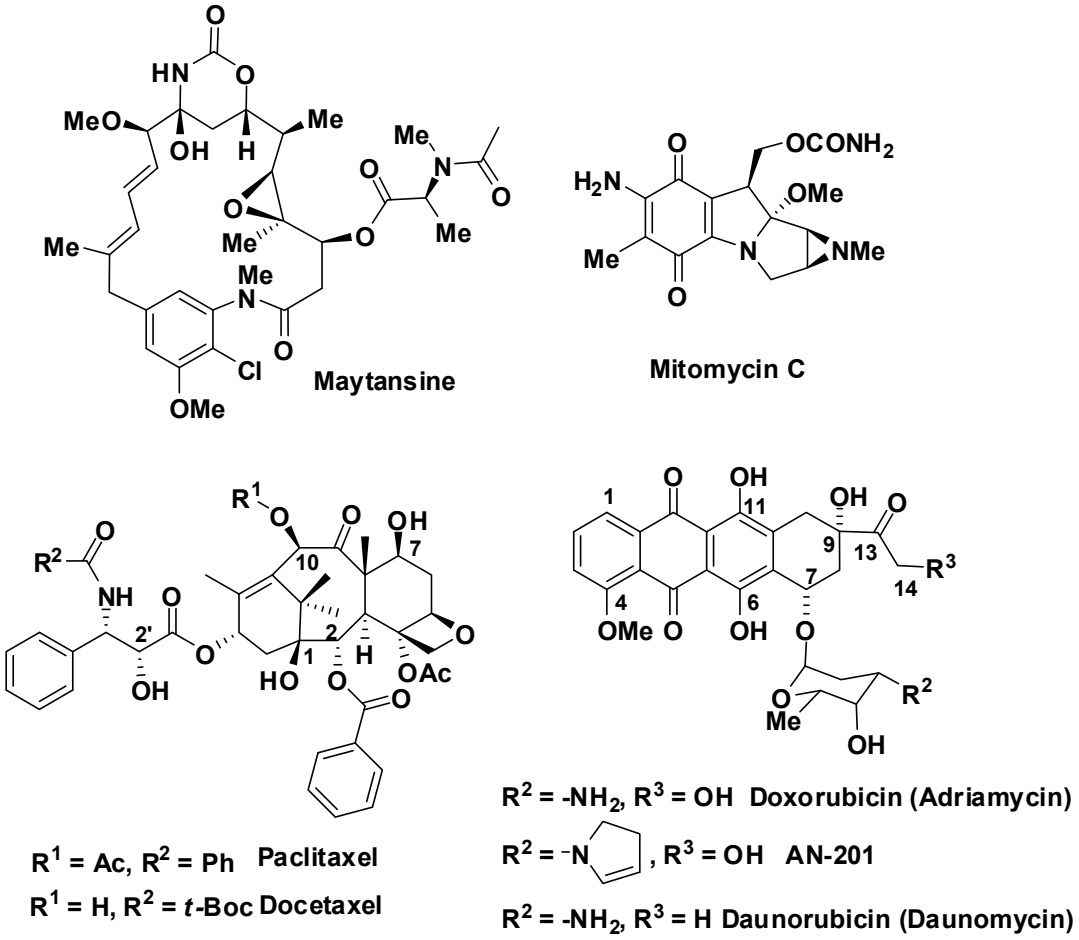

Figure 1-1. Examples of current available anticancer drugs

§1.2.2 Paclitaxel: Discovery and Novel Mechanism of Action

§1.2.2.1 Discovery of Paclitaxel

Development of anticancer drugs has been following discovery of compounds with new structure and mechanism of action, such as the anthracyclines [10] discovered in the sixties, and cisplatin [11] ten years later. In 1955, the National Cancer Institute (NCI) initiated the Cancer Chemotherapy National Service Center (CCNSC) to perform screenings of public-submitted compounds for anticancer activity. [12] This task force has led to a series of work in the sixties in the discovery of a new cytotoxic compound, which was extracted from the bark of the Pacific yew tree, Taxus brevifolia. In 1971, Wani *et al* published the chemical structure of this anticancer agent named taxol, [13] which became the new focus of research interest, and eventually entered clinical development in April 1984. In December 1989, the development of taxol is handed over to the pharmaceutical company Bristol-Myers Squibb (BMS) [12] who successfully brought taxol (trade name TAXOL®, generic name paclitaxel) to the market with New Drug Application (NDA) approval in 1992.

TAXOL® (paclitaxel), a complex diterpenoid, has a tetracyclic 17-carbon skeleton including an acetone D-ring with an *N*-benzoylphenylisoserine side chain attached to the C3-hydroxy group. There are 11 chiral centers and 14 oxygen atoms present in the molecule.

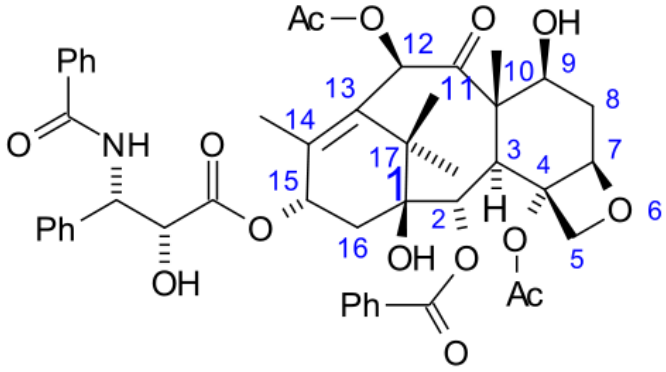

Figure 1-2. Structure of TAXOL® (paclitaxel)

§1.2.2.2 Paclitaxel: Novel Mechanism of Action

In 1979, Horwitz *et al* reported the unique mechanism of action for taxol which is based on a specific interaction between taxol and the microtubules. Distinct from other tubulin-targeted drugs such as colchicine that inhibits microtubule assembly, paclitaxel actually promotes the polymerization by stabilizing and preventing the depolymerization of the microtubules. The inability of the chromosomes to achieve a metaphase spindle configuration leads to a mitotic block, which subsequently triggers apoptosis or return to the G1-phase of the cell cycle. [14 15 16 17] **Figure 1-3** illustrates the cell cycle and the role of taxol as microtubule-stabling agent. [18]

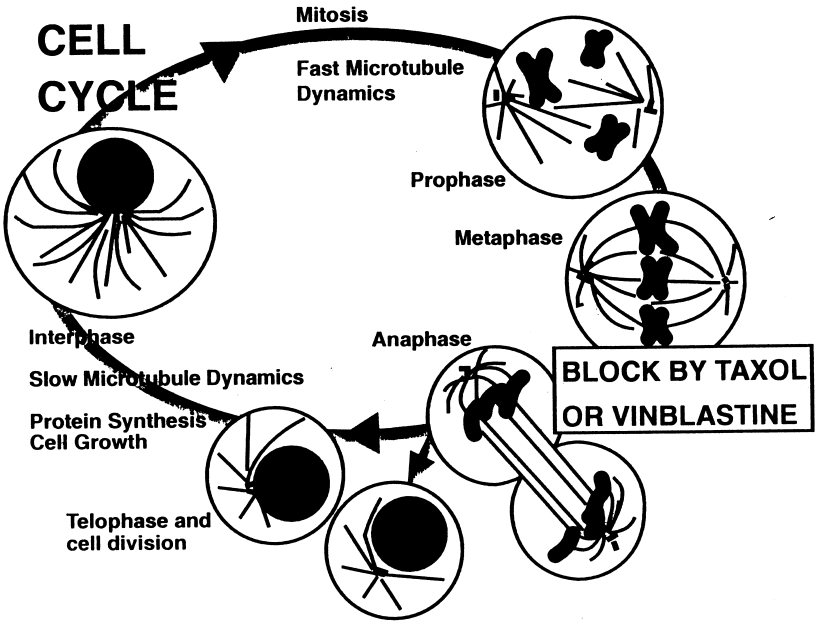

Figure 1-3. The cell cycle and the role of taxol as microtubule-stabling agent [17]

A typical cell cycle of eukaryotes can be divided in two major stages: the mitosis (M) phase during which the cell splits into two distinct "daughter cells" and the interphase during which the cell grows, accumulating nutrients required for mitosis and replicating the DNA.

All of the preparations for cell division are done during the interphase, which proceeds in three steps - Gap 1 (G1), Synthesis (S) and Gap 2 (G2). G1 phase is marked by high rate of biosynthetic activities to generate various enzymes needed for DNA replication. [19] The DNA synthesis then starts as cell cycle enters the S phase. The amount of the DNA has doubled but the numbers of the cell remains the same. G2 phase again involves significant biosynthesis related to the production of microtubules, which are required during the mitosis process.

The mitosis stage can be further broken down into four sequential phases: prophase, metaphase, anaphase and telophase. [20] The names of phases are derived from the ancient Greek, meaning “before stage”, “between stage”, “up stage” and “end stage”, respectively. In prophase, the replicated chromatin condenses into two identical chromosomes, and the duplicated centrosomes move towards the opposite ends of the cell nucleus. The end of prophase is marked by the break down of nuclear envelope, allowing microtubules to reach the kinetochores of the chromosomes. In the following metaphase the chromosomes align in the equatorial plate that is equidistant from the two centrosome poles. After all chromosomes become aligned with every kinetochore properly attached to a bundle of microtubules, the cell then enters anaphase when chromosomes separate. The telophase is roughly opposite to the prophase. As new nuclear envelope forms around each of the two pairs of chromosomes, the nuclear envelopes of two daughter cells are formed. The cell cycle completes with a so-called cytokinesis when cytoplasm is divided into two daughter cells and ensure that chromosome number remains the same from one generation to the next. After the division cycle, cell can either enter the dormant G_0 phase or re-enter the cell cycle.

Horwitz *et al* discovered the function of paclitaxel at the molecular level. It is between metaphase and anaphase that paclitaxel takes effect by stabilizing microtubules and consequently

breaking the dynamic equilibrium required for mitosis.

The normal microtubules are formed by the dimerization of two polypeptide subunits α- and β-tubulin, which are structurally similar proteins with each of approximately 440 amino acid residues and a molecular weight of about 50 kD. In the presence of magnesium ions, guanosine 5'-triphosphate (GTP), and microtubule-associated proteins (MAPs), the α- and β-tubulins aggregate in a 1:1 ratio to form dumbbell-shaped heterodimers which then polymerized into a tubular structure of 13 protofilaments with an average diameter of about 24 nm. Paclitaxel binds to the β-tubulin of the tubulin heterodimer to promote the polymerization and to stabilize the resulting microtubules, either in the presence or the absence of magnesium ions, GTP and MAPs. The microtubule thus formed is quite different from the normal one as only 12 protofilaments are present with an average diameter of about 22 nm, and is irreversibly stabilized against regular microtubule depolymerization conditions (calcium ions or 4 ^{o}C). Paclitaxel was found to enhance the rate, extent, and nucleation phase of tubulin polymerization and to stabilize the microtubules. The apoptosis is eventually induced as a result of this mitotic block by the stabilized microtubules. **Figure 1-4** summarizes the process of microtubule formation and the mechanism of action of paclitaxel. [21]

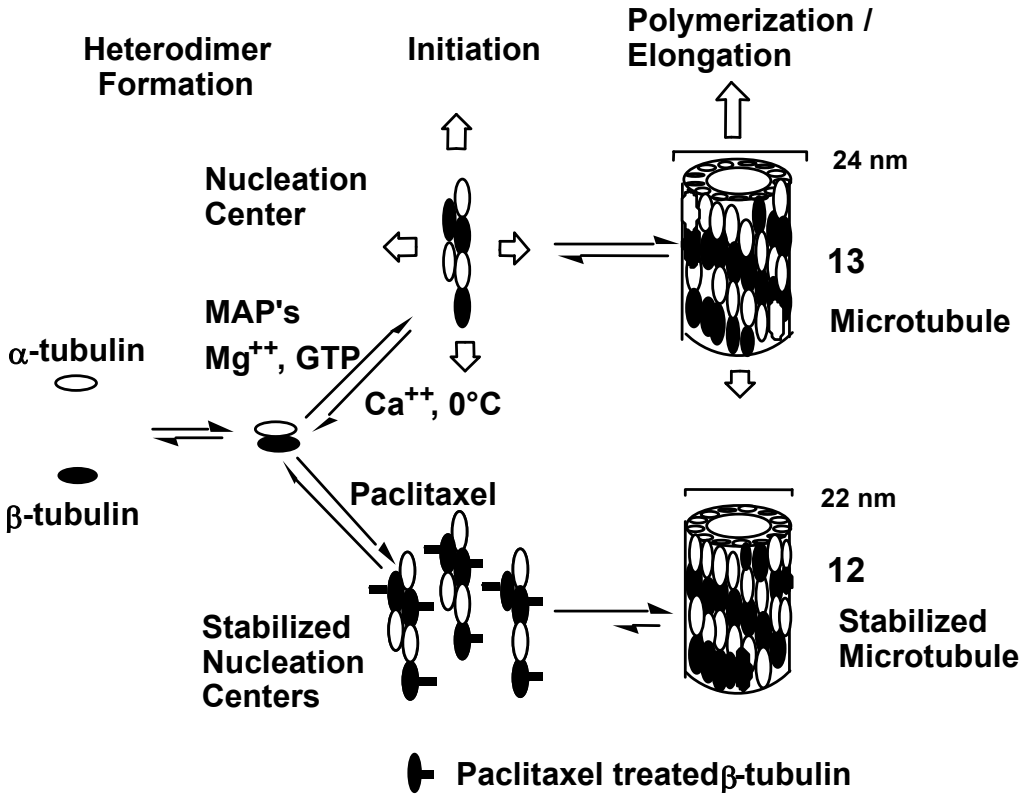

Figure 1-4. Microtubule formation and mechanism of action of paclitaxel

§1.2.3 Synthesis of Paclitaxel

Following the discovery of taxol, the NCI continued work of collection for more Taxus bark to isolate taxol. By 1969, 28 kg of crude extract had been isolated from almost 1,200 kg of bark, although this eventually yielded only 10g of final material. [12] The increased research interest [22] in taxol had lead to substantial needs for purified taxol, for which Taxus bark is the only source at

that time. By 1980, the NCI predicted the need to collect 20,000 lbs of bark. [32] In November 1982, NCI applied for the Investigational New Drug (IND) application and entered clinical trials. The supply of taxol became an increasing challenge as the clinical trials proceeded along. By the time the phase II trial showed efficiency in melanoma patients and a remarkable response rate of 30% in patients with refractory ovarian cancer, [23] Gordon Cragg of the NCI's Natural Product Branch estimated the amount of taxol [24] required to treat all the ovarian cancer and melanoma cases in the US would involve the destruction of 360,000 trees annually. For the first time, serious consideration was given to the problem of supply. [32]

In parallel to the biological study and the subsequent clinical development of taxol, a number of academic groups had attempted total syntheses of taxol since the late 1970s. Total synthesis of taxol has been accomplished by Holton, [25 26] Nicolaou, [27] Danishefsky, [28] Wender, [29] Kuwajima, [30] Mukaiyama [31] and Takahashi [32] research groups. Although being tremendous academic achievement, none of these routes is feasible for large-scale production.

In 1980, 10-deacetylbaccatin III (10-DAB III, **Figure 1-5**), which shared the same tetracyclic framework as that of paclitaxel, was identified as a plausible starting material for the semi-synthesis of paclitaxel. The French group of Pierre Potier had shown the feasibility to isolate relatively large quantities of 10-DAB III from the leaves of European Yew, which is renewable source as opposed to the bark of the Pacific Yew (Taxus brevifolia). Later in 1988, Potier *et al* published the first semisynthesis of paclitaxel. [33]

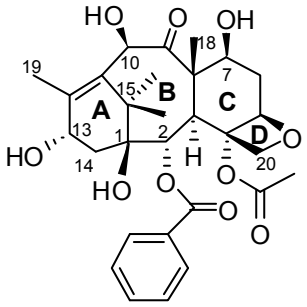

Figure 1-5. 10-Deacetylbaccatin III (10-DAB III)

The different reactivity of the four hydroxyl groups enables the sequential modification of 10-DAB III at C7 and C10 positions. The side chain precursor was synthesized in 8 steps from cis-cinnamyl alcohol with a modest 76-80% e.e. The enantiomeric excess was later improved to 98%. [34 35] Protected side chain precursor was then introduced at C13 position to provide the protected paclitaxel in 80% yield based on 50% conversion. Unfortunately, partial epimerization occurred at the C2' position on the side chain at the high reaction temperature and long reaction time. The final acidic deprotection generated paclitaxel in 89% yield (**Scheme 1-1**).

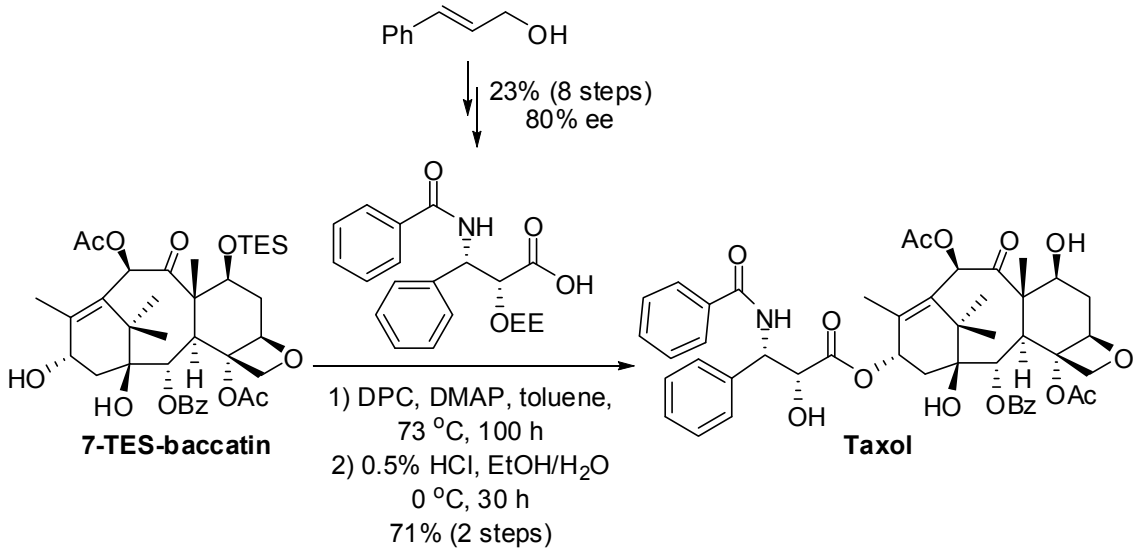

Scheme 1-1. The First semisynthesis of paclitaxel by Potier *et al* [33]

However, this semisynthetic route was not considered as practical for production due to the relatively low overall yield (<52%). Several new methods have since been reported for the coupling of side chain precursors to the modified baccatin, including Holton oxazinone coupling, [36] Ojima-Holton *β*-lactam coupling, [35 37] Commeren oxazolidinecarboxylic acid coupling [38] and Kingston oxazolinecarboxylic acid coupling. [39]

Among all the coupling methods, the Ojima-Holton *β*-lactam coupling has been the most practical method for the semisynthesis of paclitaxel (>80% overall yield). It not only enables the efficient production of the paclitaxel, but also opens the doors for synthesis of paclitaxel analogs and the ensuing structure-activity studies.

Holton's original route started with a direct coupling of (3*R*,4*S*)-*N*-benzoyl-3-*O*-EE-4-phenylazetidin-2-one (5 equiv.; EE = 1-ethoxyethoxyl, obtained from optical resolution of racemic *cis*-3-hydroxy-4-phenylazetidin-2-one) with 7-TES-baccatin III in 92% yield. The generated the 7-TES-2'-*O*-EE-paclitaxel was deprotected in acidic condition providing paclitaxel in 90% yield (**Scheme 1-2**). [40] Although overall yield was high and no epimerization was observed, this protocol had certain limitations including the needs of excess *β*-lactam, slow reaction, and limitation of substrates (i.e. limited to *N*-benzoyl protected *β*-lactam).

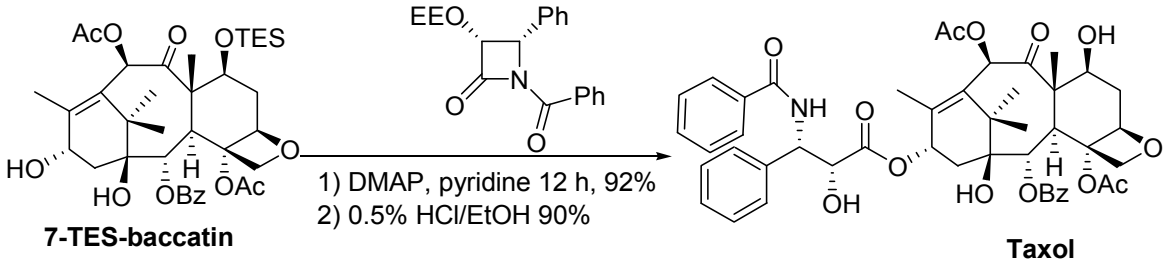

Scheme 1-2. Holton semisynthesis of paclitaxel

A very practical and efficient semisynthesis of paclitaxel was introduced by Ojima *et al* using the so-called *β*-Lactam Synthon Method. [41 42] The optically pure *β*-lactam (3*R*,4*S*)-4-phenylazetidin-2-one was prepared via a greatly efficient lithium chiral ester enolate-imine

cyclocondensation in high yield and with high enantioselectivity (> 96% ee).[43 44 45] Condition for the subsequent coupling of the *β*-lactam to 7-TES-baccatin III was explored with 13-*O*-metalated baccatin derivatives generated from different bases, such as suspension of NaH in THF and DME, *n*-BuLi, LDA, LiHMDS, NaHMDS, and KHMDS in THF, etc. The NaHMDS was found to be the best base for the ring-opening couplings of *N*-acyl-*β*-lactams with baccatins. The ring-opening coupling proceeds smoothly at -30 ~ 0 °C using only a slight excess of *N*-acyl-*β*-lactam to give the coupling product within 30 min in excellent 85-93% yield (**Scheme 1-3**). The subsequent deprotection provided paclitaxel in high overall yield.

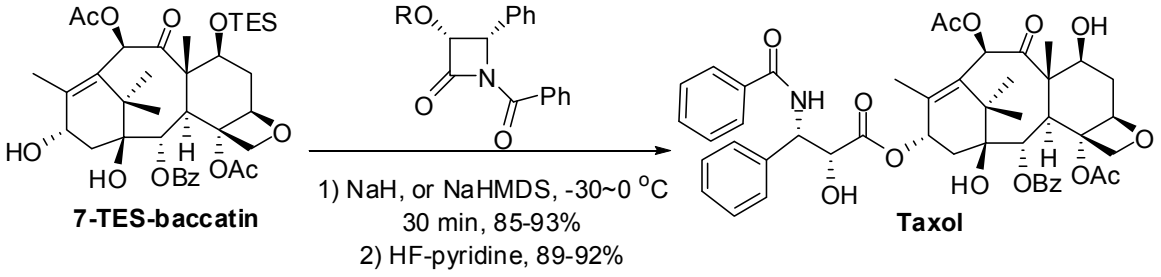

Scheme 1-3. Ojima's *β*-lactam synthon method for semisynthesis of paclitaxel

§1.2.4 Structure-Activity Relationship Studies

With the efficient Ojima-Holton *β*-lactam coupling protocol, the synthesis of paclitaxel analogs became readily feasible. One successful example is the development of Taxotère® (docetaxel, **Figure 1-6**), which was discovered by Potier *et al*. and developed by the French pharmaceutical company Rhône-Poulenc Rorer (now Sanofi-Aventis) in 1984. [46 47 48] It shares the same mechanism of action with paclitaxel, but with twice as high potency as paclitaxel for inhibitory activity of microtubule depolymerization. Currently, paclitaxel and docetaxel are two of the most successful anticancer drugs used in cancer chemotherapy.

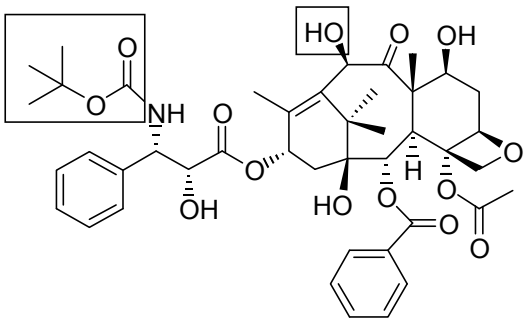

Figure 1-6. Structure of Taxotère® (docetaxel)

Extensive research and development had followed suit, and produced a great number of new generation taxoids (taxol-like compounds). [61] The through structure-activity relationship (SAR) studies was summarized in **Figure 1-7**. [49 50]

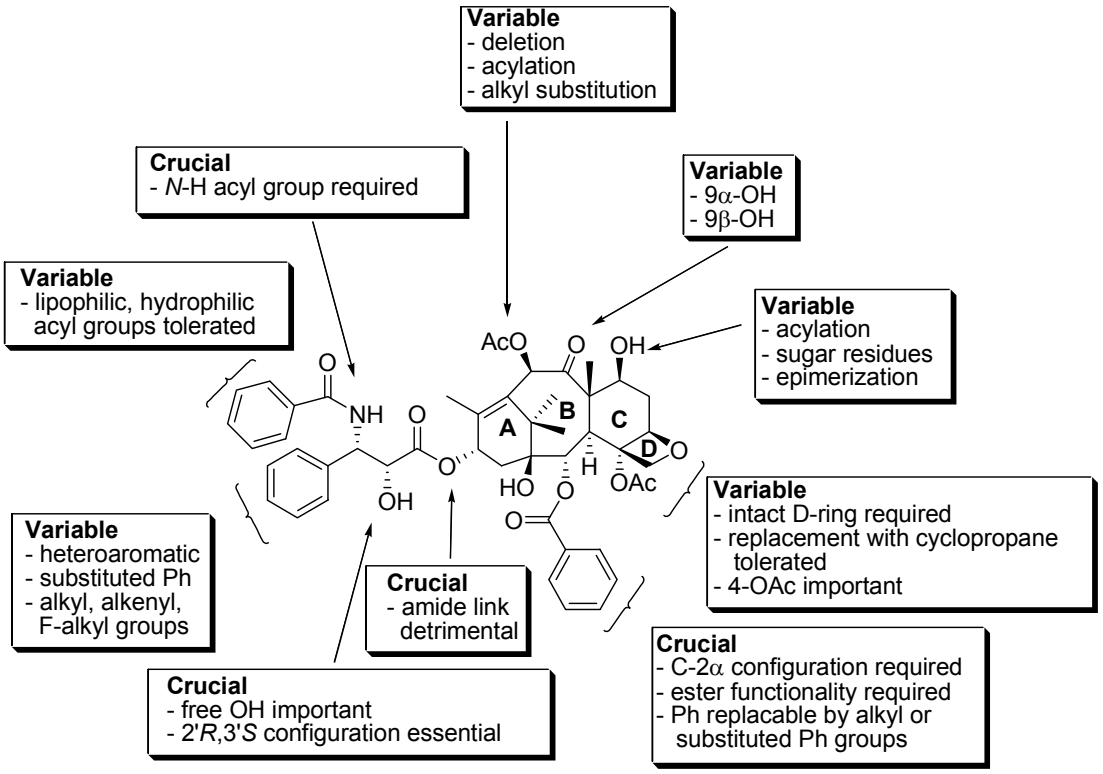

Figure 1-7. Summary of SAR for paclitaxel

§1.2.4.1 SAR Studies of the Baccatin Skeleton

Tetracyclic system

The modification of the baccatin skeleton has included changes of ring sizes and structural integrity as well as modification of various oxygen functionalities. Contraction [51 52] or cleavage of A-rings [53 54] and contraction of C-ring has significantly decreased the compound activities, while those of the contracted B-rings maintain certain level of cytotoxicity.[55] An intact D-ring oxetane is critical to the high level of activity based on the fact that the opening of D-ring,[56 57] the replacement with azetidine ring,[58 59] or the replacement of oxygen with sulfur universally shows the loss of activity. However one recent paper claimed that replacement of oxetane ring with a cyclopropane ring resulted similar activity as paclitaxel. [60]

An interesting type of C-seco taxoids was discovered, of which one compound IDN5390 (**Figure 1-8**) showed potent antiangiogenic and antimetastatic activity with slightly reduced cytotoxicity than paclitaxel.

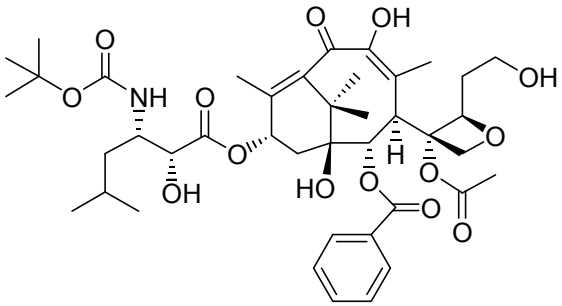

Figure 1-8. C-seco taxoid IDN5390

The C2 position

Hydrolysis of the C2 ester as well as epimerization at C2 position results in drastic decrease of activity. [61] The meta- substitution on the benzoyl group provides derivatives with greater cytotoxicity in the order of -F>-Cl>-OMe>-N_3>-Me>-CH=CH_2, while the para- substitution is detrimental to the activity.

Druing the SAR studies of the C2 position, it is discovered that the meta- position of C2 benzoyl group is involved in the metabolism of paclitaxel. [62] [63] A slower metabolic rate of the meta- substituted analogues may be the reason for the higher activity. Additionally, the para-substitution group disrupts the hydrophobic interactions between the C2 benzoate group and the C3' phenyl group which may account for the active binding conformation, while the meta-substitution group enhances the interaction.[64] Studies in our laboratory have shown that the incorporation of an alkyl or alkenyl group in place of the phenyl group may lead to improved activity. [65]

The C4 position

The loss of C-4 acetoxy group demonstrated a significant decrease in cytotoxicity. [66] [67] Analogs with the acetyl group replaced by a cyclopropanoyl group exhibited slightly increased activity, while analogs bearing a benzoyloxy group at C4 showed greatly reduced activity. [68]

The C7, C9, and C10 position

In contrast to the south part of the taxane skeleton, the north part (specifically C7, C9, and C10) is more tolerable to substitutions. Most of the resulting analogs possess retained or even increased biological activity.

A great deal of structure-activity relationship studies have been performed on the C7 position. [69] [70] [71] The in vitro activity was not significantly impacted with C7 acylation, epimerization or deoxygenation. Therefore, the C7 position has been wildly used for further modification or coupling to delivery moieties (to be illustrated in Chapter 4).

Reduction of the C9 ketone to either an α- or β-hydroxyl group has little effect on the cytotoxicity, [72] [73] while the presence of a C9, C10 diol decreased the analog activity. [74] [75]

Previous studies have concluded that modification of C10 position has little effect on the in vitro cytotoxicity. [76] [77] However, the SAR studies in our group have revealed that the exceptional activity of certain analogs against the drug resistant cell lines is clearly attributed to the C10 modifications. [78] [79] In addition, studies of the advanced second-generation taxoids indicate that the combination of C10 and C2 modifications virtually overcome the P-glycoprotein based MDR in several cancer cell lines (to be elaborated in Chapter 2). [80]

In summary, the structural modifications at the north part of the taxoid skeleton are more feasible than those at the south part in remaining the great in vitro activity of paclitaxel. The role of each part of the taxoid molecule is not completely clear. Further studies are ongoing to develop new generation of taxoids with fewer side effects, superior pharmacological properties, and improved activity against various types of tumors, particularly against drug-resistant phenotypes.

§1.2.4.2 SAR Studies of the C13 Side Chain

The C13 side chain (2*R*,3*S*)-*N*-acyl-3-phenylisoserine moieties has been discovered to be extremely important for the cytotoxicity and antitumor activity of taxoids. The loss of this *β*-amino acid moiety would cause >1,000-hold reduction in the potency. The changes in stereochemistry would also substantially lowers the potency by several to >500 times. [81] [82]

The C2' position

Generally, the protection or elimination of the C2' hydroxyl group would result in significant decrease in the in vitro activity.[83] Recent studies have shown that the presence of hydrogen bonding between the C2' hydroxyl group and either Arg 369 or Gly 370 of the *β*-tubulin backbone. [84] Therefore, any modification of hydroxyl group would interfere with such hydrogen bonding, and decrease the compound activity.

However, if C2' is protected with an ester group which is subject to the hydrolysis by esterases presented in the in vivo system, the C2' ester analogue will demonstrate comparable activity to the parent compound.[85] This strategy actually aligns to the concept of "prodrug" design. [86] [87]

The C3' position

The C3' position has been extensively investigated. [88] [89] [90] Replacement of C3' phenyl group with a range of heteroaromatic rings generates a variety of analogs with comparable or better activity than paclitaxel.[91] A large number of analogs with a *tert*-butoxycarbonyl group in place of the *N*-benzoyl group, such as docetaxel, show increased activity. [81] [92] [93]

Most second-generation taxoids that have been developed in our laboratory include a variety of C3' modifications (e.g. alkyl, alkenyl, fluorinated alkyl, and epoxy groups). The second-generation taxoids generally showed great potency, particularly against multidrug resistant (MDR) cancer cell lines. [80] [94]

The C3'*N* position

The C3'*N* position allows for some structural changes. The compounds with lipophilic and hydrophilic acyl groups exhibit similar activity to paclitaxel. [80] Certain analogs with *N*-cycloalkenoyl substituents also show improved biological activity. [95] The C3'-NH_2 group significantly decreased activity of the analogues compared to their *N*-acyl parent compounds. And the replacement of C3'-*N*-benzoyl with *N*-alkanoyl groups is also detrimental to the activity. [96]

Stereochemistry

The (2'*S*,3'*R*) isomers are significantly less active than the analogs with the (2'*R*,3'*S*)

configuration of the natural product. But epimerization of one of the two stereocenters demonstrated comparable activity to the parent compound. Epimerization of the C13 position or replacement of C13 ester with amide causes complete loss of activity. [80]

§1.3 Ojima *β*-Lactam Synthon Method

§1.3.1 Introduction

The study of *β*-lactam antibiotics has lasted for more than 70 years since the discovery of penicillin. These antibiotics possess very low toxicity. New semisynthetic or total synthetic derivatives with enhanced spectrum have been continuously developed. The structural feature of the *β*-lactam is the the four-membered 2-azetidinone ring. In recent years, *β*-lactam has been found to be a versatile intermediate for the synthesis of non-proteogenic amino acids, peptides, peptide turn mimetics, [97] heterocycles [98] and other types of compounds of biological interests.

In addition, *β*-lactam is also the key-intermediate for synthesis of taxoids using Ojima's *β*-lactam synthon method. [99] The synthesis of *β*-lactam structures has been a subject to research in our laboratory. Two general methods for the enantioselective synthesis of *β*-lactam have been proven to be the most efficient and versatile methods.

§1.3.2 Synthesis of Enantiomerically Pure *β*-Lactam via Asymmetric Ester-Imine Cyclocondensation

In 1992, Ojima group had successfully used lithium-chiral ester enolate-imine cyclocondensation method (**Scheme 1-4**) to synthesize *β*-lactams in good yield and great enantiomeric purity. This method uses a chiral ester as chiral auxiliary, which is eliminated in the cyclocondensation step.

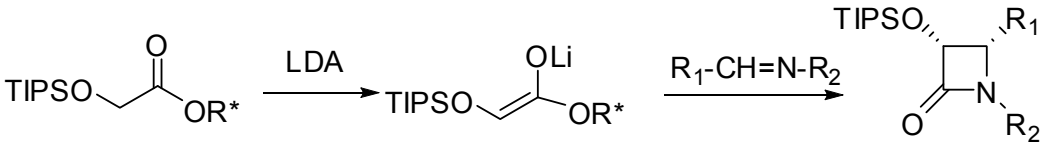

Scheme 1-4. Lithium-chiral ester enolate-imine cyclocondensation method

The chiral auxiliaries that have been successfully employed to prepare highly optically pure *β*-lactams include (1*R*,2*S*)-(-)-trans-2-phenyl-1-cyclohexanol (Whitesell's chiral auxiliary) (**Figure 1-9a**) or (-)-10-dicyclohexylsulfamoylisoborneol (Oppolzer's chiral auxiliary) (**Figure** 1-9**b**).

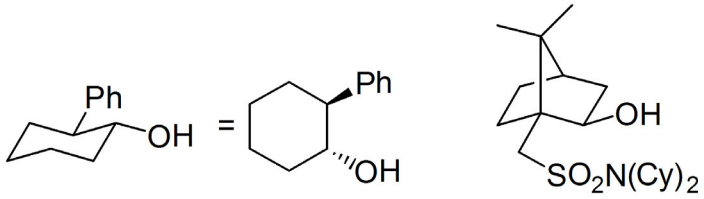

Figure 1-9. Chiral auxiliaries

Whitesell's chiral auxiliary [**(-)-1-2**] was used herein as the source of chirality. CuI-catalyzed ring opening of cyclohexene oxide (**1-1**) with phenylmagnesium bromide provided

racemic *trans*-2-phenylcyclohexanol [**(±)-1-2**]. After acetylation of the alcohol, enzymatic kinetic resolution of the racemic acetate [**(±)-1-3**] using pig liver acetone powder gave chiral auxiliary [**(-)-1-2**] with >99.9% ee in good yield (**Scheme 1-5**).

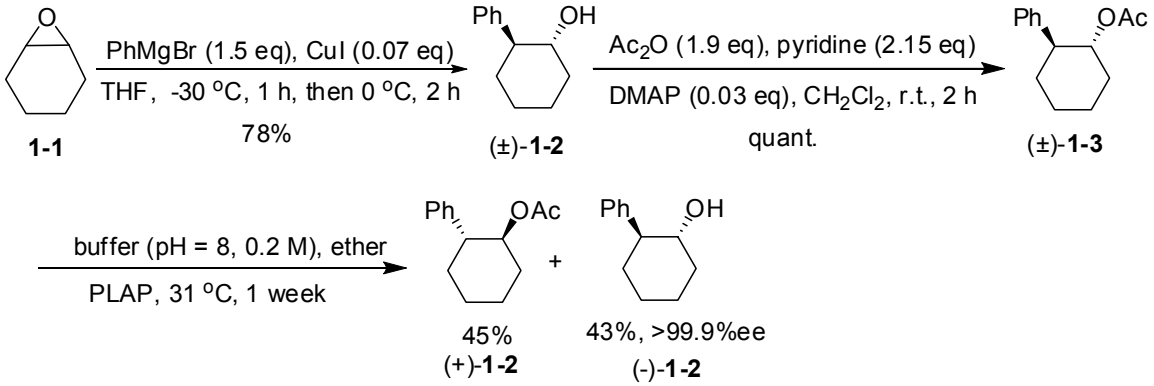

Scheme 1-5. Synthesis of Whitesell chiral auxiliary (1*R*,2*S*)-*trans*-2-phenyl-1-cyclohexanol

The reaction of bromoacetic acid with the sodium alkoxide of benzyl alcohol gave benzyloxyacetic acid (**1-4**), which was then reacted with chiral alcohol [**(-)-1-2**] and yielded ester (**1-5**). Hydrogenolysis followed by TIPS protection of the resulting alcohol gave the chiral TIPS-ester (**1-7**) in good yield (**Scheme 1-6**).

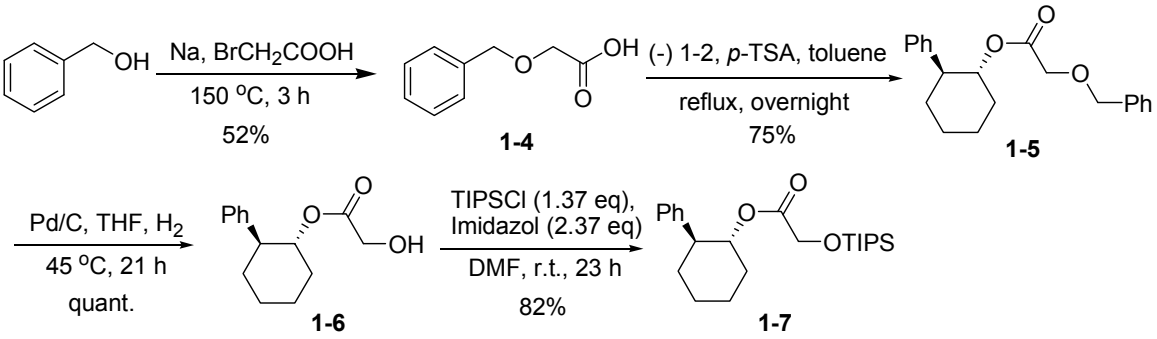

Scheme 1-6. Synthesis of (1*R*,2*S*)-triisopropylsiloxy-acetic acid 2-phenyl-1-cyclohexyl ester

To synthesize the *p*-methoxy phenyl (PMP) *β*-lactam (**1-9**), 3-methylbut-2-enal was first reacted with p-anisidine in methylene chloride to generate *N*-4-methoxyphenyl-iso-butenylaldimine (**1-8**). TIPS ester (**1-7**) in THF was slowly added to freshly prepared LDA. The resulting enolate was then reacted with **1-8** to yield *β*-lactam **1-9**. The 4-methoxyphenyl group was then removed by ceric ammonium nitrate (CAN) oxidation in aqueous acetonitrile. Subsequent standard acylation with di-*tert*-butyl dicarbonate anhydride gave the desired *β*-lactam, (3*R*,4*S*)-1-(*tert*-butoxycarbonyl)-3-triisopropylsilyloxy-4-(2-methyl-propen-2-yl)azetidin-2-one (**1-11**) (**Scheme 1-7**).

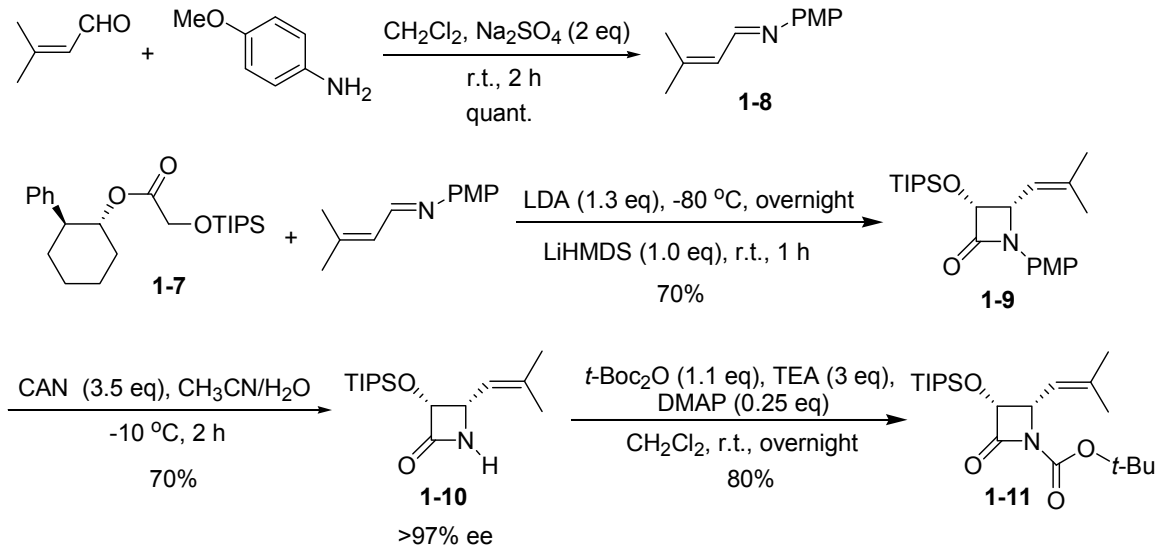

Scheme 1-7. Synthesis of (3*R*,4*S*)-1-(tert-butoxycarbonyl)-3-triisopropylsiloxy-4-(2-methyl-propen-2-yl)azetidin-2-one

The selective formation of *cis*-*β*-lactam with high enatiomeric purity can be explained by the 6-membered ring transition state proposed in **Scheme 1-8**. At low temperature, (*E*)-enolate was predominantly formed and the initial enolate addition to imine would occur from the least hindered face, thus forming the *β*-amino ester intermediate which can be isolated upon quenching the reaction at low temperature. When warmed up to room temperature, this intermediate cyclized to form the chiral *β*-lactam releasing the chiral auxiliary (**Scheme 1-8**).

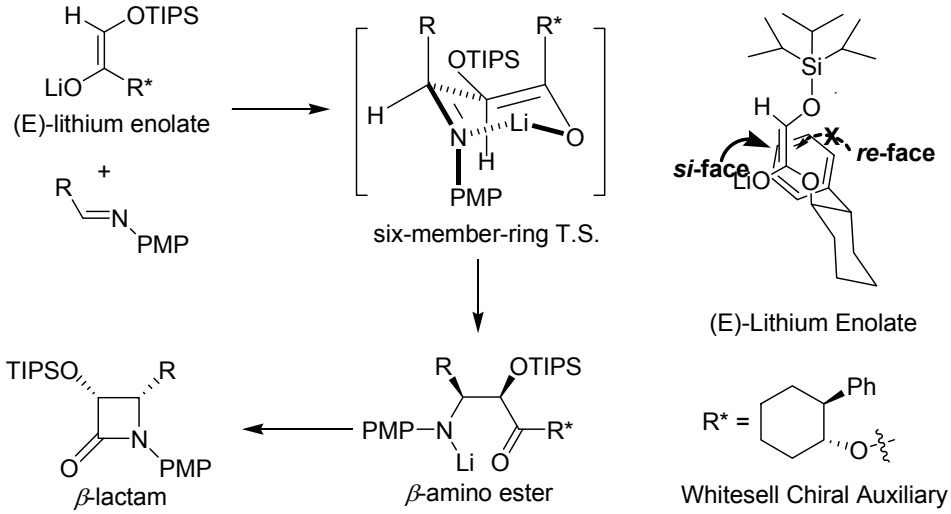

Scheme 1-8. The mechanism of chiral TIPS-ester enolate-imine condensation

§1.3.3 Synthesis of Enantiomerically Pure *β*-Lactam via Staudinger Cycloaddition Reaction Followed by Enzymatic Kinetic Resolution

The second widely used method is Staudinger reaction, also referred to as the [2+2] ketene-imine cycloaddition reactions (**Scheme 1-9**). [100] The mechanism proceeds in a stepwise fashion:

(1) the reaction is initiated by the nucleophilic attack of an imine to a ketene, giving rise to a zwitterionic intermediate; (2) a conrotatory electrocyclic ring closure of the zwitterionic intermediate produces the final *β*-lactam product. This reaction proceeds without a catalyst and its rate is dependent on the nucleophilicity of the imine.

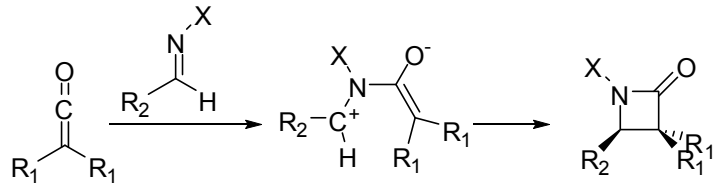

Scheme 1-9. [2+2] Ketene-imine cycloaddition reaction

Acetoxyacetylchloride, in the presence of a tertiary amine, reacted with an imine to give the corresponding racemic *β*-lactam. It had been shown that PS-Amano lipase preferentially hydrolyzes acetate moiety at C3 of the (3*S*,4*R*) enantiomer of **1-13**. A common approach for improving the biocatalytic reaction rate of water-insoluble substrates was the use of co-solvent. Hence 10% CH_3CN was used as co-solvent to improve the rate and the enantioselectivity of the reaction. The 4-methoxyphenyl group can be removed via oxidation with ceric ammonium nitrate, and the acetoxy group can be hydrolyzed to give **(+)-1-15**. The 3-hydroxyl group was protected with 1-ethoxyethyl (EE) group instead of TIPS group, since the relatively small EE group will facilitate the coupling reaction of *β*-lactam to baccatin more easily.

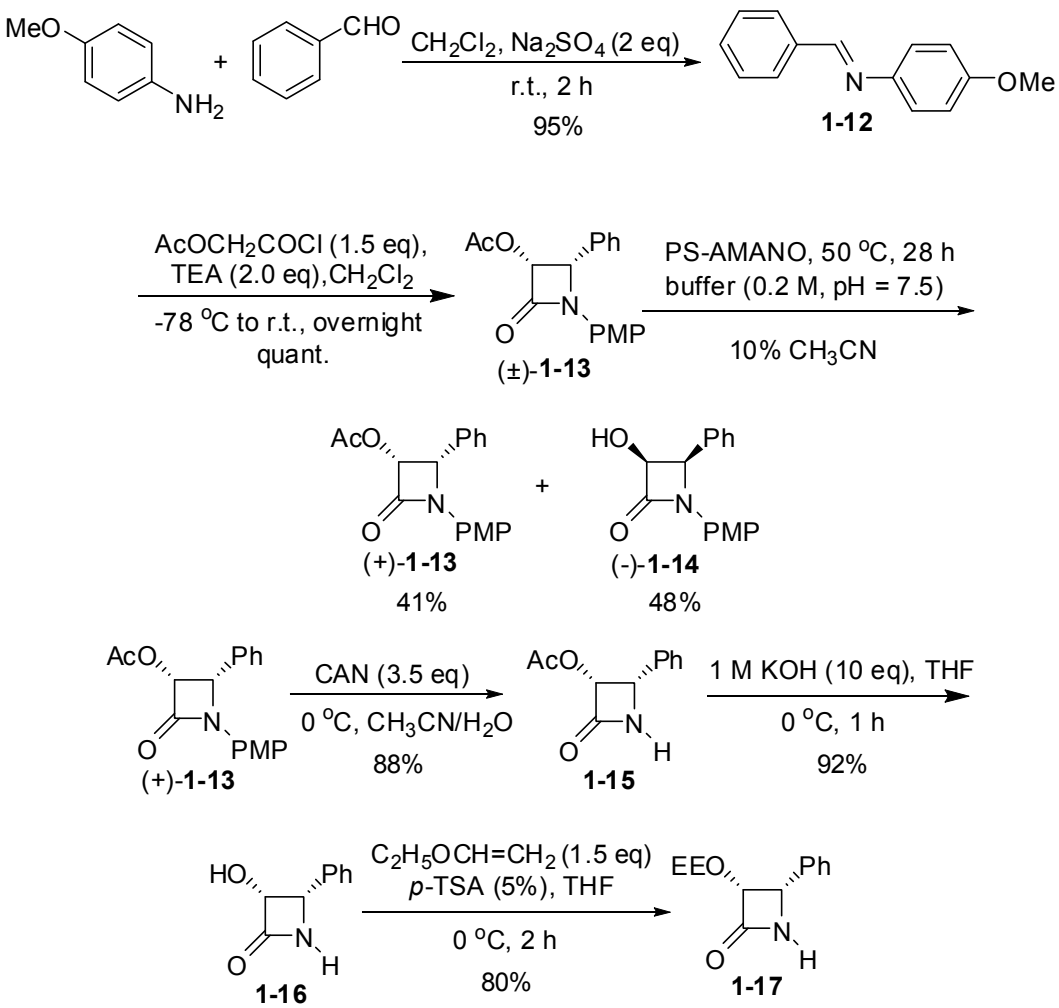

Scheme 1-10. Synthesis of (3*R*,4*S*)-3-ethoxyethoxy-4-phenylazetidin-2-one

The (3*R*,4*S*)-1-(*tert*-butoxycarbonyl)-3-triisopropylsiloxy-4-(2-methyl-propen-2-yl)azetidin-2-one (**1-11**) can be synthesized in similar route (**Scheme 1-11**).

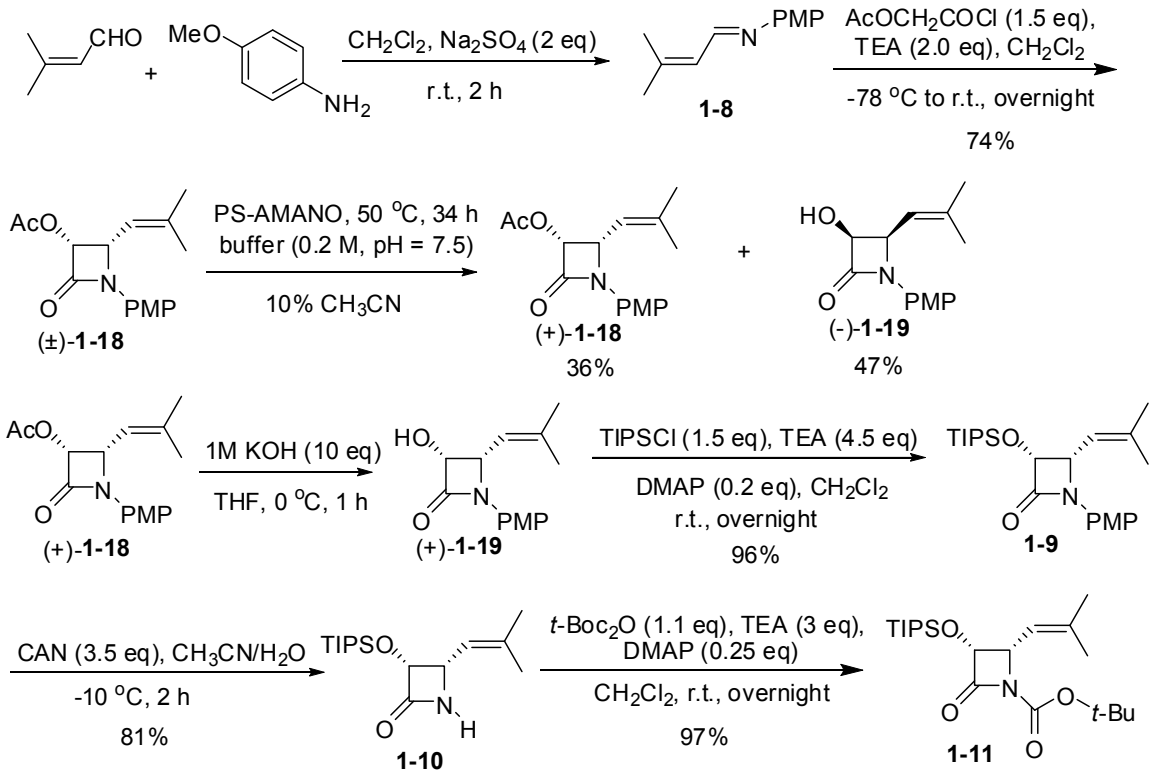

Scheme 1-11. Synthesis of (3*R*,4*S*)-1-(*tert*-butoxycarbonyl)-3-triisosiloxy-4-(2-methyl-propen-2-yl)azetidin-2-one

§1.4 Experimental Section

Materials

The chemicals were purchased from Sigma-Aldrich and/or Fisher Scientific and were used without further purification unless otherwise noted. 10-DAB III and 14β-hydroxy-10-deacetylbaccatin III were gift from Indena, SpA, Italy and used as received. Tetrahydrofuran, dichloromethane, toluene and ethyl ether were obtained from the PureSolv^{TM} Solvent Purification System (Innovative Technology, Inc.) under N_2. The glassware was dried in a 110 ^{o}C oven and allowed to cool to room temperature in a desiccator over "Drierite" (calcium sulfate).

General Methods

^{1}H, ^{13}C and ^{19}F NMR spectra were obtained on Varian 300, 400 or 500 NMR spectrometers. Melting points were measured on a Thomas Hoover Capillary melting point apparatus and are uncorrected. TLC was performed on Merck DC-alufolien with Kieselgel 60F-254 and flash column chromatography was carried out on silica gel 60 (Merck, 230-400 mesh ASTM). Optical rotations were measured on a Perkin-Elmer Model 241 polarimeter. IR spectra were measured on a Shimadzu FTIR-8400s spectrophotometer. Chemical purity was determined on Shimadzu LC-1020A, using a Phenomenex Curosil-B column (5μ, 4.6 × 250 mm), employing CH_3CN/water (40/60, V/V) as the eluent with a flow rate of 1 mL/min. Chiral HPLC analysis for the determination of enantiomeric excess was carried out on a Waters HPLC assembly consist of a Waters M45 solvent delivery system and a Waters 484 detector (at 254 nm) on a PC workstation running Millennium 32 using a DAICEL-CHIRACEL OD chiral column (25 × 0.46 cm), employing n-hexanes/isopropanol (95/5, V/V) as eluent with a flow rate of 1.0 mL/min. High resolution mass spectra were obtained from the Mass Spectrometry Laboratory, University of Illinois at Urbana-Champaign, Urbana, IL.

Racemic *trans*-2-phenylcyclohexanol [(±)-1-2] [38]

A solution of phenylmagnesium bromide in THF (150 mL) was prepared from magnesium (7.317 g, 0.301 mol) and bromobenzene (31.9 mL, 0.300 mol) at room temperature with reflux for overnight. After cooling the Grignard solution to -30 °C, CuI (2.52 g, 13.2 mmol) was added. The resulting solution was stirred for approximately 10 min, and a solution of cyclohexene oxide (20.6 mL, 0.200 mol) in THF (200 mL) was added dropwise over a period of 1 h. The reaction mixture was then allowed to warm up to room temperature and stirred for an additional 2 h. The reaction was quenched with a saturated aqueous NH_4Cl solution and extracted with ethyl ether. The organic layers we washed with a saturated aqueous NH_4Cl solution until no color change in the aqueous layer. The aqueous layer was extracted with ether and then the combined organic layer was dried over anhydrous $MgSO_4$, filtered and concentrated *in vacuo*. Recrystallization from hexanes gave **(±)-1-2** (21.17 g, 60%) as a white solid: ^{1}H NMR (300 MHz, $CDCl_3$) δ 1.25-1.53 (m, 4 H, H on C2, C4, OH), 1.62 (s, 1 H, H on C6), 1.76 (m, 1 H, H on C3), 1.84 (m, 2 H, H on C3), 2.11 (m, 1 H, H of C6), 2.42 (ddd, J = 16.6, 10.8, 5.4 Hz, 1 H, H on C2), 3.64 (ddd, J = 16.6, 10.8, 5.4 Hz, 1 H, H on C1) and 7.17-7.35 (m, 5 H, H on benzene ring) ppm. All data are in agreement with literature values.[38]

Racemic *trans*-2-phenylcyclohexyl acetate [(±)-(1-3)] [26]

To a solution of **(±)-1-2** (17.25 g, 98 mmol), DMAP (0.259 g, 2.94 mmol) and pyridine (10.5 mL) CH_2Cl_2 (14 mL), was added dropwise a solution of acetic anhydride (10.77 mL) in

CH_2Cl_2 (26 mL) over a period of 2 h. The reaction was then poured into a mixture of 6N HCl (30 mL), ice (45 mL) and ether (90 mL). The organic layer was washed with 2N HCl aqueous solution and the combined aqueous layer was extracted with ether. The combined organic layer was washed with a saturated aqueous $NaHCO_3$ solution and dried over anhydrous $MgSO_4$, filtered and concentrated *in vacuo* to afford **(±)-(1-3)** (20.71 g, 97%) as a pale yellow oil: ^{1}H NMR (300 MHz, $CDCl_3$) δ 1.35 (m, 1 H, H on C4), 1.41 (m, 1 H, H on C4), 1.46 (m, 1 H, H on C2), 1.56 (m, 1 H, H on C6), 1.74 (s, 3 H, H on CH_3), 1.78 (m, 1 H, H on C3), 1.84 (m, 1 H, H on C3), 1.93 (m, 1 H, H of C6), 2.65 (ddd, J = 16.6, 11.0, 5.4 Hz, 1 H, H on C2), 4.98 (ddd, J = 16.6, 11.0, 5.4 Hz, 1 H, H on C1) and 7.17-7.35 (m, 5 H, H on benzene ring) ppm. All data are in agreement with literature values. [26]

(+)-*trans*-2-Phenylcyclohexyl acetate [(+)-1-3] and (-)-*trans*-2-phenyl-cyclohexanol [(-)-1-2] [26]

Pig liver acetone powder (PLAP) was obtained following the reported procedure.[101] Freshly purchased pork liver was blended with cold acetone (5 L/kg fresh pork liver) for 10 min. The solution was filtered off and evaporated *in vacuo* to yield the PLAP as pale brown powder.

To a pH 8 phosphate buffer solution (600 mL, 0.5 M) was added a solution of **(±)-(1-3)** (20.70 g, 77.9 mmol) in ether (80 mL) at 31 °C. After stirring for 30 min, 5.40 g of pig liver acetone powder (PLAP) was added. The mixture was stirred for 7 days at 31 °C, until ^{1}H NMR of the crude organic layer showed <50/50 ratio of alcohol **(-)-1-2** and acetate **(+)-1-3**. The reaction mixture was quenched by adding 100 mL of ether and separated. The aqueous layer was extracted with ethyl ether. And the combined organic layer was dried over anhydrous $MgSO_4$, filtered and concentrated *in vacuo*. The crude product was purified via flash column chromatography on silica gel using hexanes/ethyl acetate as the eluent to afford acetate **(+)-1-3** (8.03 g, 39%) as a pale yellow oil and alcohol **(-)-1-2** (5.99 g, 36%, >99% ee) as a white solid. All data are in agreement with literature values. [26]

Benzyloxyacetic acid (1-4) [102]

At room temperature, sodium metal (1.688 g, 73 mmol) was added gradually to benzyl alcohol (27.5 mL, 265 mmol) with mechanical stirring apparatus. After most of the sodium reacted, the reaction mixture was heated up to 150 °C and complete reaction of the sodium was observed. At this point bromoacetic acid (4.436 g, 32 mmol) in THF (10 mL) was added dropwise. The reaction mixture was stirred at 150 °C for 3 h and then cooled down to room temperature. Cold water was added and the two layers were separated. The water layer was acidified with 10% HCl until pH = 2-3 and then extracted with dichloromethane to remove any remaining benzyl alcohol. The organic layer was then dried over anhydrous $MgSO_4$, filtered and concentrated *in vacuo*. The oil residue was distilled under reduced pressure to afford **1-4** (20.44 g, 46%) as colourless oil: b.p. 138-140 °C (0.3 mmHg); ^{1}H NMR (300 MHz, $CDCl_3$) δ 4.17 (s, 2 H, H on benzyl group), 4.67 (s, 2 H, H on C1) and 7.38 (m, 5 H, H on benzene ring) ppm. All data are in agreement with literature values.[102]

(1*R*,2*S*)-(-)-2-Phenylcyclohexyl benzyloxyacetate (1-5) [103]

A solution of **1-2** (2.5486 g, 14.5 mmol), **1-4** (2.3780 g, 14.3 mmol), and a catalytic amount of *p*-toluenesulfonic acid (*p*-TSA) in toluene (35 mL) was refluxed overnight. The toluene was evaporated off *in vacuo* and the reaction mixture was diluted with ethyl ether and washed with saturated aqueous $NaHCO_3$ solution. The organic layer was dried over anhydrous $MgSO_4$,

filtered and concentrated *in vacuo* to afford **1-5** (3.602 g, 77.6%) as a white solid: ^{1}H NMR (300 MHz, $CDCl_3$) δ 1.26-1.63 (m, 4 H, H on C2, C4, C6), 1.76-1.99 (m, 3 H, H on C3,C5,C6), 2.10-2.20 (m, 2 H, H on C6), 2.70 (dt, J = 11.1, 4.1 Hz, 1 H, H on C2), 3.73 (d, J = 16.5 Hz, 1 H, H on acetic acid), 3.84 (d, J = 16.5 Hz, 1 H, H on acetic acid), 4.25 (s, 2 H, H on benzyl group), 5.13 (dt, J = 11.1, 4.2 Hz, 1 H, H on C1) and 7.16-7.39 (m, 10 H, H on benzene ring) ppm. All data are in agreement with literature values. [103]

(1*R*,2*S*)-(-)-2-Phenylcyclohexyl hydroxyacetate (1-6) [29]

A mixture of **1-5** (1.332 g, 4.105 mmol), 10% palladium on carbon (Pd/C, 0.336 g) in THF (12 mL) was stirred overnight at 45 °C under hydrogen. The reaction mixture was filtered through celite and concentrated *in vacuo* to afford **1-6** (0.835 g, 100% based on 85.7% conversion) as a white solid: ^{1}H NMR (300 MHz, $CDCl_3$) δ 1.30-1.66 (m, 4 H, H on C2, C4, C6), 1.78-2.00 (m, 3 H, H on C3, C5, C6), 2.10-2.20 (m, 2 H, H on C6), 2.67 (dt, J = 11.1, 4.2 Hz, 1 H, H on C2), 3.72 (d, J = 17.1 Hz, 1 H, H on acetic acid), 3.93 (d, J = 17.1 Hz, 1 H, H on acetic acid), 5.07 (dt, J = 11.1, 4.2 Hz, 1 H, H on C1) and 7.16-7.32 (m, 5 H, H on benzene ring) ppm. All data are in agreement with literature values. [29]

(-)-(1*R*,2*S*)-2-Phenylcyclohexyl triisopropylsilyloxyacetate (1-7) [29]

To a solution of **1-6** (0.273 g, 4.008 mmol), imidazole (0.6897 g, 2.943 mmol) in DMF (0.7 mL) was added TIPSCl (0.376 mL, 4.032 mmol). The reaction mixture was stirred under nitrogen for 26 h, quenched with water, and extracted with dichloromethane. The organic layer was washed several times with water and brine, dried over anhydrous $MgSO_4$, filtered and concentrated *in vacuo*. The crude product was distilled under reduced pressure to afford **1-7** (0.913 g, 79.4%) as a colorless oil: b.p. 195-205 °C (0.8 mmHg); ^{1}H NMR (300 MHz, $CDCl_3$) δ 0.94-1.25 (m, 21 H, H on TIPS group), 1.35-1.70 (m, 4 H, H on C2, C4, C6), 1.80-2.05 (m, 3 H, H on C3, C5, C6), 2.10-2.20 (m, 1 H, H on C6), 2.70 (dt, J = 11.1, 4.2 Hz, 1 H, H on C2), 3.91 (d, J = 16.5 Hz, 1 H, H on acetic acid), 4.08 (d, J = 16.5 Hz, 1 H, H on acetic acid), 5.07 (dt, J = 11.1, 4.2 Hz, 1 H, H on C1) and 7.16-7.30 (m, 5 H, H on benzene ring) ppm. All data are in agreement with literature values. [29]

1-(4-Methoxyphenyl)-3-methyl-2-butenaldimine (1-8) [29]

To a solution of *p*-anisidine (0.244 g, 1.968 mmol, recrystalized from methanol) and anhydrous Na_2SO_4 (2 eq) in CH_2Cl_2 (10 mL) was added 3-methylbut-2-enal (0.231 mL, 2.45 mmol) dropwise. The reaction mixture was then stirred at room temperature for 2 h. The solution was filtered, and the solvent was removed to yield **1-8** as yellow oil, which was directly used for the next step.

1-(4-Methoxyphenyl)-3-triisopropylsilyloxy-4-(2-methylpropen-2-yl)azetidin-2-one (1-9) [30]

To a solution of diisopropylamine (0.34 mL, 2.418 mmol) in THF (8 mL) was added (2.5 M in *n*-hexane, 0.977 mL, 2.418 mmol) of *n*-butyllithium at -15 °C. After stirring for 60 min, the reaction solution was cooled to -85 °C. A solution of **1-7** (0.5125 g, 1.86 mmol) in THF (5 mL) was slowly added via cannula over a period of 1 h. After stirring for an additional hour, a solution of **1-8** (1.968 mmol in 6.5 mL THF) was carefully added via cannula over a period of 2 h. The reaction was then stirred overnight at -85 °C. Then LiHMDS (1.0 M in THF, 1.312 mmol) was added and the reaction was warmed up after 1 h. The reaction was quenched

with a saturated aqueous NH_4Cl solution. The aqueous layer was extracted with ethyl acetate and the combined organic layer was washed with brine. The organic layer was then dried over $MgSO_4$ and concentrated *in vacuo*. The crude product was then purified by flash column chromatography on silica gel using hexanes/ethyl acetate as eluent to afford **1-9** (0.272 g, 51.5%, >97% ee) as a white solid: ^{1}H NMR (300 MHz, $CDCl_3$) δ 0.97-1.24 (m, 21 H, H on TIPS group), 1.88 (d, J = 2.3 Hz, 3 H, H on CH_3), 1.84 (d, J = 2.3 Hz, 3 H, H on CH_3), 3.77 (s, 3 H, H on CH_3O group), 4.82 (dd, J = 9.9, 5.1 Hz, 1 H, H on vinyl carbon), 5.04 (d, J = 5.1 Hz, 1 H, H on C4), 5.33 (d, J = 9.9 Hz, 1 H, H on C3), 6.84 (d, J = 8.7 Hz, 2 H, H on benzene ring) and 7.32 (d, J = 8.7 Hz, 2 H, H on benzene ring) ppm. All data are in agreement with literature values. [30]

3-Triisopropylsilyloxy-4-(2-methylpropen-2-yl)azetidin-2-one (1-10) [104]

To a solution of **1-9** (0.262 g, 0.649 mmol) in acetonitrile (25 mL) and H_2O (5 mL) was added cerium ammonium nitrate (CAN, 1.244 g, 22 mmol) in H_2O (21 mL) dropwise by dropping funnel at -10 °C. The reaction mixture was allowed to stir for 2 h at -10 °C and then quenched with saturated aqueous Na_2SO_3 solution. The reaction mixture was filtered over celite, and the aqueous layer was extracted with ethyl acetate and the combined organic layer was washed with brine. After drying over anhydrous $MgSO_4$ and concentrating *in vacuo*, the crude product was purified by flash column chromatography on silica gel using hexanes/ethyl acetate as eluent to yield **1-10** (0.125 g, 64.7%) as a white solid: ^{1}H NMR (300 MHz, $CDCl_3$) δ 0.97-1.21 (m, 21 H, H on TIPS group), 1.68 (d, J = 2.4 Hz, 3 H, H on CH_3), 1.19 (d, J = 2.4 Hz, 3 H, H on CH_3), 4.43 (dd, J = 9.6, 4.8 Hz, 1 H, H on vinyl carbon), 4.98 (dd, J = 4.8, 2.4 Hz, 1 H, H on C4) and 5.31 (d, J = 9.6 Hz, 1 H, H on C3) ppm. All data are in agreement with literature values. [104]

1-(*tert*-Butoxycarbonyl)-3-triisopropylsiloxy-4-(2-methylpropen-2-yl)azetidin-2-one (1-11) [104]

To a solution of **1-10** (113 mg, 0.380 mmol), triethylamine (0.197 mL, 1.149 mmol), and a catalytic amount of dimethylaminopyridine (DMAP) in CH_2Cl_2 (2 mL), was added di-tert-butyl dicarbonate (0.091 g, 0.418 mmol) in CH_2Cl_2 (5 mL). The reaction mixture stirred overnight and quenched by saturated NH_4Cl solution. After extraction with ethyl acetate the combined organic layer was washed with brine, dried over anhydrous $MgSO_4$, and concentrated *in vacuo*. The crude product was purified by flash column chromatography on silica gel using hexanes/ethyl acetate as eluent to yield **1-11** (0.141 g, 93.2%) as a cololess oil: ^{1}H NMR (300 MHz, $CDCl_3$) δ 1.02-1.2 (m, 21 H, H on TIPS group), 1.48 (s, 9 H, H on Boc group), 1.77 (d, J = 0.9 Hz, 3 H, H on CH_3), 1.79 (d, J = 0.9 Hz, 3 H, H on CH_3), 4.75 (dd, J = 9.9, 5.7, 1 H, H on vinyl carbon), 4.98 (d, J = 5.7 Hz, 1 H, H on C4) and 5.28 (dd, J = 9.9, 0.9 Hz, 1 H, H on C3) ppm. All data are in agreement with literature values. [104]

1-(4-Methoxyphenyl)benzaldimine (1-12) [104]

To a solution of *p*-anisidine (10.393 g, 83 mmol, recrystallized from methanol) and anhydrous $MgSO_4$ (14.601 g) in CH_2Cl_2 (50 mL) was added benzaldehyde (8.94 mL, 87 mmol) dropwise. The reaction mixture was then stirred at room temperature for 2 h. The solution was filtered and concentrated *in vacuo*. The crude sample was recrystallized (from hexane and little CH_2Cl_2) to yield **1-12** (13.025 g, 78%) as a white solid: ^{1}H NMR (300 MHz, $CDCl_3$) δ 3.84 (s, 3 H), 6.92-6.96 (m, 2 H), 7.23-7.26 (m, 2 H), 7.45-7.48 (m, 3 H), 7.89-7.92 (m, 2 H) and 8.49 (s, 1 H) ppm. All data are in agreement with literature values. [104]

Racemic *cis*-1-(4-methoxyphenyl)-3-acetoxy-4-phenylazetidin-2-one [(±)-1-13] [104]

To a solution of **1-12** (2.473 g, 11.7 mmol) and triethylamine (3.26 mL, 23.4 mmol) in CH_2Cl_2 (45 mL) at -78 °C was added a solution of acetoxyacetyl chloride (1.94 mL, 17.5 mmol) in CH_2Cl_2 (15 mL) dropwise. The reaction mixture was allowed to warm up to room temperature overnight, then diluted with 50 mL CH_2Cl_2. The organic layer was washed with saturated aqueous NH_4Cl solution, dried over anhydrous $MgSO_4$, and concentrated *in vacuo*. The crude product was purified by flash column chromatography on silica gel using hexanes/ethyl acetate as eluent to provide **(±)-1-13** (3.535 g, 97%) as a white solid: ^{1}H NMR (300 MHz, $CDCl_3$) δ 1.68 (s, 3 H, H on acetate group), 3.75 (s, 3 H, H on CH_3O group), 5.34 (d, J = 4.9 Hz, 1 H, H on C4), 5.81(d, 1 H, H on C3), 6.81 (d, J = 9.0 Hz, 2 H, H on PMP group) and 7.35-7,26 (m, 7 H, H on benzene group) ppm. All data are in agreement with literature values. [104]

Enantiomer-selective hydrolysis of *β*-lactam [104]

To a suspension of **(±)-1-13** (3.443 g) in a pH = 7.5 phosphate buffer solution (0.2 M, 300 mL) and acetonitrile (30 mL) was added of PS-Amano lipase (1.53 g), and the mixture was vigorously stirred at 50 °C for 35 h, when ^{1}H NMR of the crude organic layer showed >50/50 ratio of alcohol **(-)-1-14** over acetate **(+)-1-13**. The reaction mixture was cooled down to room temperature and extracted with CH_2Cl_2. The combined organic layer was dried over anhydrous $MgSO_4$, and concentrated *in vacuo* to provide crude products. Then the two products were separated by flash column chromatography on silica gel using hexanes/ethyl acetate as eluent to give **(+)-1-13** (1.32 g, 38%, >99.9% ee) and **(-)-1-14** (1.20 g, 40%). ^{1}H NMR (300 MHz, $CDCl_3$) of **(+)-1-13** δ 1.68 (s, 3 H, H on acetate group), 3.75 (s, 3 H, H on CH_3O group), 5.34 (d, J = 4.9 Hz, 1 H, H on C4), 5.81(d, 1 H, H on C3), 6.81 (d, J = 9.0 Hz, 2 H, H on PMP group) and 7.35-7,26 (m, 7 H, H on benzene group) ppm. All data are in agreement with literature values. [104]

(3*R*,4*S*)-3-Acetoxy-4-phenylazetidin-2-one (1-15) [31]

To a solution of **(+)-1-13** (0.91 g) in acetonitrile (70 mL) and water (10 mL) at -10 °C was slowly added a solution of ceric ammonium nitrate (6.6 g) in of water (60 mL) over 30 min. The mixture was then stirred for 2 h at -10 °C and quenched by saturated Na_2SO_3 solution. After filtered over celite, the aqueous layer was extracted with three portions of ethyl acetate. The combined organic layer was washed with brine, dried over $MgSO_4$, filtered and concentrated *in vacuo*. The crude product was purified by flash column chromatography on silica to yield **1-15** (0.514 g, 85.7%) as a white solid: ^{1}H NMR (300 MHz, $CDCl_3$) δ 1.67 (s, 3 H, H on acetate group), 5.05(d, 1 H, H on C4), 5.87 (dd, J = 4.7, 2.7Hz, 1 H, H on C3), 6.54 (s, exchangeable, 1 H, H on NH) and 7.30-7.38 (m, 5 H, H on benzene ring) ppm. All data are in agreement with literature values. [31]

(3*R*,4*S*)-3-Hydroxy–4-phenylazetidin-2-one (1-16) [105]

To a mixture of THF (6 mL) and aqueous KOH solution (1 M, 25 mL) at 0 °C was added a solution of **1-15** (0.514 g) in THF (32 mL). The solution was stirred at 0 °C for 1 h and quenched with saturated $NaHCO_3$. The mixture was extracted with four portions of ethyl acetate and the combined organic layer was dried over anhydrous $MgSO_4$ and concentrated in vacuo to give **1-16** (0.359 g, quant.) as a white solid: ^{1}H NMR (300 MHz, $CDCl_3$) δ 2.10 (d, 1 H, H on OH), 4.94 (d, J = 4.8 Hz, 1 H, H on C4), 5.04 (d, J = 4.8 Hz, 1H, H on C3), 6.20 (s, exchangeable, 1 H, H

on NH) and 7.25-7.35 (m, 5 H, H on benzene ring) ppm. All data are in agreement with literature values. [105]

(3*R*,4*S*)-3-Ethoxyethoxy-4-phenylazetidin-2-one (1-17) [32]

To a solution of **1-16** (0.359 g) and a catalytic amount of *p*-tolunensulfonic acid in THF (5 mL) at 0 °C was added ethyl vinyl ether (0.64 mL). The mixture was stirred at room temperature for 2 h, quenched with saturated $NaHCO_3$ and extracted with four portions of ethyl acetate. The combined organic layer was washed with brine and dried over anhydrous $MgSO_4$. The product was purified by flash column chromatography on silica gel to yield **1-17** (0.465 g, 70.2%) as a white solid: ^{1}H NMR (300MHz, $CDCl_3$) δ 0.98 (d, J = 5.1 Hz, 1.5 H, $OCH(CH_3)O$), 1.05 (d, J = 5.4 Hz, 1.5 H, $OCH(CH_3)O$), 1.12 (t, J = 7.1 Hz, 3 H, OCH_2CH_3), 3.19-3.25 (m, 0.5 H, OCH_2CH_3), 3.31-3.42 (m, 1 H, OCH_2CH_3), 3.59-3.69 (m, 0.5 H, OCH_2CH_3), 4.47 (q, J = 5.4 Hz, 0.5 H, $OCH(CH_3)O$), 4.68 (q, J = 5.4 Hz, 0.5 H, $OCH(CH_3)O$), 4.82 (dd, J = 11.4, 4.8 Hz, 1H, H on C3), 5.17-5.21 (m, 1 H, H on C4), 6.10 (s, exchangeable, 1 H, H on NH) and 7.35 (m, 5 H, H on benzene ring) ppm. All data are in agreement with literature values. [32]

(±)-1-(4-Methoxyphenyl)-3-acetoxyl-4-(2-methylprop-1-enyl)azetidin-2-one [(±)1-18] [31 32]

To a mixture of anhydrous $MgSO_4$ (2.576 g) and *p*-anisidine (1.396 g, 11.335 mmol) in CH_2Cl_2 (20 mL) was added 3-methylbut-2-enal (1.44 mL, 14.2 mmol). After stirred at room temperature for 2 h, the mixture was filtered and concentrated *in vacuo* to afford 2.52 g crude product (*E*)-4-methoxy-*N*-(3-methylbut-2-enylidene)aniline as a pale red oil: ^{1}H NMR (300 MHz, $CDCl_3$) δ 1.96 (d, J = 0.9 Hz, 3 H, CH_3), 2.01 (d, J = 0.9 Hz, 3 H, CH_3), 3.81 (s, 3 H, OCH_3), 6.21 (td, J = 9.6, 1.2 Hz, 1 H, vinyl-H), 6.89 (td, J = 9.0, 2.1 Hz, 2 H, aryl-H, ortho- to methoxy), 7.11 (td, J = 9.0, 2.1 Hz, 2 H, aryl-H meta- to methoxy) and 8.48 (br d, J = 9.6 Hz, 1 H, N-H) ppm.

The crude product was dissolved in CH_2Cl_2 (40 mL), and triethylamine (5.8 mL) was added at -78 °C. To the mixture was added acetoxyacetyl chloride (5.18 mL) and the reaction mixture was warmed up to room temperature overnight. The reaction was quenched with saturated NH_4Cl solution and the resulting mixture was extracted with three portion of CH_2Cl_2. The combined organic layers was washed with saturated NH_4Cl solution, water and brine, then dried over anhydrous $MgSO_4$, and concentrated *in vacuo*. Flash column chromatography on silica gel gave **(±)-1-18** (2.12 g, 66%) as a white solid: ^{1}H NMR (300 MHz, $CDCl_3$) δ 1.70 (s, 3 H, H on CH_3), 1.72 (s, 3 H, H on CH_3), 2.01 (s, 3 H, H on CH_3 of acetate), 3.67 (s, 3 H, H on CH_3 of PMP), 4.83 (dd, J = 9.9, 4.8 Hz, 1 H, H on CH of isobutenyl), 5.02 (d, J = 9.3 Hz, 1 H, H on C4), 5.67 (d, J = 4.8 Hz, 1 H, H on C3), 6.74 (d, J = 8.9 Hz, 2 H, H on benzene ring) and 7.20 (d, J = 8.9 Hz, 2 H, H on benzene ring) ppm. All data are in agreement with literature values. [31 32]

Enantiomer-selective hydrolysis of *β*-lactam [32]

To a suspension of **(±)-1-18** (0.995 g) in a pH = 7.5 phosphate buffer solution (0.2 M, 120 mL) and acetonitrile (12 mL) was added PS-Amano lipase (413 mg), and the mixture was vigorously stirred at 50 °C for 34 h, until ^{1}H NMR of the crude organic layer showed >50/50 ratio of alcohol and acetate **(+)-1-18**. The reaction was terminated by extraction of the mixture with three portions of ethyl acetate. The crude sample was purified by flash column chromatography on silica gel to give **(+)-1-18** (0.37 g, 37%, >99.9% ee) and **(-)-1-19** (0.43 g, 43.5%).^{1}H NMR (300 MHz, $CDCl_3$) of **(+)-1-18** δ 1.70 (s, 3 H, H on CH_3), 1.72 (s, 3 H, H on

CH_3), 2.01 (s, 3 H, H on CH_3 of acetate), 3.67 (s, 3 H, H on CH_3 of PMP), 4.83 (dd, J = 9.9, 4.8 Hz, 1 H, H on CH of isobutenyl), 5.02 (d, J = 9.3 Hz, 1 H, H on C4), 5.67 (d, J = 4.8 Hz, 1 H, H on C3), 6.74 (d, J = 8.9 Hz, 2 H, H on benzene ring) and 7.20 (d, J = 8.9 Hz, 2 H, H on benzene ring) ppm. ^{1}H NMR (300 MHz, $CDCl_3$) of **(-)-1-19** δ 3.78 (s, 3H), 4.84 (d, J = 4.7 Hz, 1 H, H on C4), 5.04 (d, J = 4.7 Hz, 1 H, H on C3) and 7.25-7.35 (m, 5 H, H on benzene ring) ppm. All data are in agreement with literature values. [32]

(3*R*,4*S*)-1-(4-Methoxyphenyl)-3-hydroxy-4-(2-methylprop-1-enyl)azetidin-2- one (1-19) [32]

To a solution of solution of **(-)-1-19** (360 mg, 1.24 mmol) in THF (22 mL) was added THF (15 mL) and aqueous KOH solution (1 M, 12.5 mL). The reaction mixture was stirred for 1 h and quenched with saturated NH_4Cl solution. The mixture was extracted with four portions of ethyl acetate. The combined organic layer was dried over anhydrous $MgSO_4$, filtered and concentrated to give **1-19** (0.32 g, quant.) as a white solid: ^{1}H NMR (300 MHz, $CDCl_3$) δ 3.78 (s, 3H), 4.84 (d, J = 4.7 Hz, 1 H, H on C4), 5.04 (d, J = 4.7 Hz, 1 H, H on C3) and 7.25-7.35 (m, 5 H, H on benzene ring) ppm. All data are in agreement with literature values. [32]

1-(4-Methoxyphenyl)-3-triisopropylsilyloxy-4-(2-methylpropen-2-yl)azetidin-2-one (1-9) [30]

To a mixture of **1-19** (0.32 g), DMAP (30.6 mg) in CH_2Cl_2 (4 mL) was added TEA (0.70 mL) and TIPSCl (0.36 mL). The reaction solution was stirred overnight at room temperature, and then quenched with a saturated aqueous NH_4Cl solution. The aqueous layer was extracted with CH_2Cl_2 and the combined organic layer was washed with brine. The organic layer was then dried over $MgSO_4$ and concentrated *in vacuo*. The crude product was purified by flash column chromatography on silica gel using hexanes/ethyl acetate as the eluent to afford **1-9** (0.47 g, 93.6%, >99% ee) as a white solid: ^{1}H NMR (300 MHz, $CDCl_3$) δ 0.97-1.24 (m, 21 H, H on TIPS group), 1.88 (d, J = 2.3 Hz, 3 H, H on CH_3), 1.84 (d, J = 2.3 Hz, 3 H, H on CH_3), 3.77 (s, 3 H, CH_3O), 4.82 (dd, J = 9.9, 5.1 Hz, 1 H, H on vinyl carbon), 5.04 (d, J = 5.1 Hz, 1 H, H on C4), 5.33 (d, J = 9.9 Hz, 1 H, H on C3), 6.84 (d, J = 8.7 Hz, 2 H, H on benzene ring) and 7.32 (d, J = 8.7 Hz, 2 H, H on benzene ring) ppm. All data are in agreement with literature values. [30]

3-Triisopropylsilyloxy-4-(2-methylpropen-2-yl)azetidin-2-one (1-10) [30]

To a solution of **1-9** (0.470 g, 1.2 mmol) in acetonitrile (55 mL), water (8 mL) at -10 °C was added cerium ammonium nitrate (2.401 g) in H_2O (40 mL) dropwise. The reaction mixture was allowed to stir for 2 h and then quenched with saturated aqueous Na_2SO_3 solution. The mixture was filtered over celite. Then aqueous layer was extracted three times with ethyl acetate and the combined organic layer was washed with brine. After dried over anhydrous $MgSO_4$ and concentrated in vacuo, the crude product was purified by flash column chromatography on silica gel using hexanes/ethyl acetate as the eluent to yield **1-10** (0.226 g, 65.2%) as a white solid: ^{1}H NMR (300 MHz, $CDCl_3$) δ 0.97-1.21 (m, 21 H, H on TIPS group), 1.68 (d, J = 2.4 Hz, 3 H, H on CH_3), 1.19 (d, J = 2.4 Hz, 3 H, H on CH_3), 4.43 (dd, J = 9.6, 4.8 Hz, 1 H, H on vinyl carbon), 4.98 (dd, J = 4.8, 2.4 Hz, 1 H, H on C4) and 5.31 (d, J = 9.5 Hz, 1 H, H on C3) ppm. All data are in agreement with literature values. [30]

1-(*tert*-Butoxycarbonyl)-3-triisopropylsiloxy-4-(2-methylpropen-2-yl)azetidin-2-one (1-11) [30]

To a solution of **1-10** (226 mg), triethylamine (0.34 mL), dimethylaminopyridine (DMAP, 24.5 mg) in CH_2Cl_2 (4 mL), was added di-tert-butyldicarbonate (0.199 g) in CH_2Cl_2 (4 mL). The reaction mixture was stirred at room temperature overnight and quenched by saturated NH_4Cl solution, and extracted with ethyl acetate three times and the organic layer was washed with brine, dried over anhydrous $MgSO_4$, and concentrated in vacuo. The crude product was purified by flash column chromatography to yield **1-11** (0.280 g, 92.7%) as a cololess oil: ^{1}H NMR (300 MHz, $CDCl_3$) δ 1.02-1.2 (m, 21 H, H on TIPS group), 1.48 (s, 9 H, H on Boc group), 1.77 (d, J = 0.9 Hz, 3 H, H on CH_3), 1.79 (d, J = 0.9 Hz, 3 H, H on CH_3), 4.75 (dd, J = 9.9, 5.7 Hz, 1 H, H on vinyl carbon), 4.98 (d, J = 5.7 Hz, 1 H, H on C4) and 5.28 (dd, J = 9.9, 0.9 Hz, 1 H, H on C3) ppm. All data are in agreement with literature values. [30]

§1.5 References

[1] The Global Burden of Disease: 2004 Update. Geneva: World Health Organization **2008**.

[2] Ferlay, J.; Shin, H. R.; Bray, F.; Forman, D.; Mathers, C. D.; Parkin, D. GLOBOCAN 2008, Cancer Incidence and Mortality Worldwide: IARC CancerBase No. 10. Lyon, France: International Agency for Research on Cancer, **2010**.

[3] World Health Organization, Cancer, Fact sheet N° 297, February **2011**.

[4] National Center for Health Statistics, Division of Vital Statistics, Center for Disease Control **2005-2007**.

[5] Anand, P.; Kunnumakkara, A. B.; Kunnumakara, A. B. Cancer is a preventable disease that requires major lifestyle changes. *Pharm. Res.* **2008**, *25*, 2097-2116.

[6] Cole, W. H. In *Chemotherapy of Cancer*. Lea and Febiger: Philadelphia, **1970**.

[7] Lowry, S. In *Fundamentals of Radiation Therapy and Cancer Chemotherapy*. Engl. Univ. Press: London, **1974**.

[8] Takimoto, C. H.; Calvo, E. Principles of Oncologic Pharmacotherapy. In: *Cancer Management: A Multidisciplinary Approach.* Pazdur, R.; Wagman, L. D.; Camphausen, K. A.; Hoskins, W. J. (Eds.) 11 Ed. **2008**.

[9] Saito, T.; Niitani, H.; Nakao, I. In *Handbook of Advanced Chemotherapies of Cancer*; Life Science Co.: Tokyo, **1989**.

[10] Minotti G, Menna P, Salvatorelli E, Cairo G, Gianni L. Anthracyclines: molecular advances and pharmacologic developments in antitumor activity and cardiotoxicity. *Pharmacol. Rev.* **2004**, 56, 185–229.

[11] Rosenberg, B.; Vancamp, L.; Trosko, J. E.; Mansour, V. H. Platinum Compounds: a New Class of Potent Antitumour Agents. *Nature* **1969,** *222*, 385–386.

[12] Goodman, J.; Walsh, V. In *The Story of Taxol: Nature and Politics in the Pursuit of an Anti-Cancer Drug*. Cambridge University Press, **2001**.

[13] Wani, M. C.; Taylor, H. L.; Wall, M. E.; Coggon, P.; Mc Phail, A.T. *J. Am. Chem. Soc.* **1971**, *93*, 2325-2327.

[14] Bharadwaj, R.; Yu, H. The spindle checkpoint, aneuploidy, and cancer. *Oncogene* **2004**, *23*, 2016–2027.

[15] Schiff, P. B.; Fant, J.; Horwitz, S. *Nature* **1979**, *277*, 665-667.

[16] Schiff, P. B.; Horwitz, S. B. Taxol Stabilizes Microtubules in Mouse Fibroblast Cells. *Proc. Natl. Acad. Sci.* **1980**, *77*, 1561-1565.

[17] Schiff, P. B.; Horwitz, S. B. Taxol Assembles Tubulin in the Absence of Exogenous Guanosine 5'-Triphosphate or Microtubule-Associated Proteins. *Biochemistry*, **1981**, *20*, 3247-3252.

[18] Georg, G. I.; Chen, T. T.; Ojima, I.; Vyas, D. M. In *Taxane Anticancer Agents: Basic Science and Current Status: ACS Symp. Ser. 583*. American Chemical Society, Washington D.C., **1995**.

[19] Smith, J. A.; Martin, L. Do cells cycle? *Proc. Natl. Acad. Sci. U.S.A.* **1973**, *70*, 1263-1267.

[20] De Souza, C. P.; Osmani, S. A. Mitosis, not just open or closed. *Eukaryotic Cell* **2007**, *6*, 1521-1527.

[21] Nicolaou, K. C.; Dai, W.-M.; Guy, R. K. Chemistry and Biology of Taxol. *Angew. Chem. Int. Ed. Engl.* **1994**, *33*, 15-44.

[22] Fuchs, D. A.; Johnson, R. K. Cytologic evidence that taxol, an antineoplastic agent from *Taxus brevifolia*, acts as a mitotic spindle poison. *Cancer Treatment Reports* **1978**, *62*, 1219–1222.

[23] Rowinsky, E. K. *et al*. Phase II study of taxol in advanced epithelial malignancies.

Proceedings of the Association of Clinical Oncology **1988**, *7*, 136.
[24] Morihira, K.; Hara, R.; Kawahara, S.; Nishimori, T.; Nakamura, N.; Kusama, H.; Kuwajima, I. Enantioselective total synthesis of taxol. *J. Am. Chem. Soc.* **1998**, *120*, 12980-12981.
[25] Holton, R. A.; Somoza, C.; Kim, H. B.; Liang, F.; Biediger, R. J.; Boatman, P. D.; Shindo, M.; Smith, C. C.; Kim, S.; Nadizadeh, H.; Suzuki, Y.; Tao, C.; Vu, P.; Tang, S.; Zhang, P.; Murthi, K. K.; Gentile, L. N.; Liu, J. H. First Total Synthesis of Taxol. 1. Functionalization of the B Ring. *J. Am. Chem. Soc.* **1994**, *116*, 1597-1598.
[26] Holton, R. A.; Kim, H. B.; Somoza, C.; Liang, F.; Biediger, R. J.; Boatman, P. D.; Shindo, M.; Smith, C. C.; Kim, S.; Nadizadeh, H.; Suzuki, Y.; Tao, C.; Vu, P.; Tang, S.; Zhang, P.; Murthi, K. K.; Gentile, L. N.; Liu, J. H. First Total Synthesis of Taxol. 2. Completion of the C and D Rings. *J. Am. Chem. Soc.* **1994**, *116*, 1599-1600.
[27] Nicolaou, K. C.; Yang, Z.; Liu, J. J.; Ueno, H.; Nantermet, P. G.; Guy, R. K.; Claiborne, C. F.; Renaud, J.; Couladouros, E. A.; Paulvannan, K.; Sorensen, E. J. Total Synthesis of Taxol. *Nature* **1994**, *367*, 630-634.
[28] Danishefsky, S.; Masters, J.; Young, W.; Link, J.; Snyder, L.; Magee, T.; Jung, D.; Isaacs, R.; Bornmann, W.; Alaimo, C.; Coburn, C.; Di Grandi, M. Total Synthesis of Baccatin III and Taxol. *J. Am. Chem. Soc.* **1996**, *118*, 2843-2859.
[29] Wender, P. A.; Mucciaro, T. P. A New and Practical Approach to the Synthesis of Taxol and Taxol Analogues: The Pinene Path. *J. Am. Chem. Soc.* **1992**, *114*, 5878-5879.
[30] Morihira, K.; Hara, R.; Kawahara, S.; Nishimori, T.; Nakamura, N.; Kusama, H.; Kuwajima, I. Enantioselective total synthesis of taxol. *J. Am. Chem. Soc.* **1998**, *120*, 12980-12981.
[31] Mukaiyama, T.; Shiina, I.; Iwadare, H.; Saitoh, M.; Nishimura, T.; Ohkawa, N.; Sakoh, H.; Nishimura, K.; Tani, Y.; Hasegawa, M.; Yamada, K.; Saitoh, K. Asymmetric total synthesis of Taxol (R). *Chem Eur. J.* **1999**, *5*, 121-161.
[32] Doi, T.; Fuse, S.; Miyamoto, S.; Nakai, K.; Sasuga, D.; Takahashi, T. A Formal Total Synthesis of Taxol Aided by an Automated Synthesizer. *Chemistry an Asian J.* **2006**, *1*, 370-383.
[33] Denis, J.-N.; Greene, A. E.; Gueard, D.; Gueitte-Voegelein, F.; Mangatal, L.; Potier, P. A Highly Efficient, Practical Approach to Natural Taxol. *J. Am. Chem. Soc.* **1988**, *110*, 5917-5919.
[34] Denis, J.-N.; Correa, A.; Greene, A. E. Direct, Highly Efficient Synthesis from (*S*)-(+)-Phenylglycine of the Taxol and Taxotere Side Chains. *J. Org. Chem.* **1991**, *56*, 6939-6942.
[35] Holton, R. A.; Biediger, R. J.; Boatman, D. Semisynthesis of taxol and taxotere. In *Taxol: Science and Applications*; Suffness, M., (Ed.) CRC: Boca Raton, **1995**, 97-121.
[36] Holton, R. A. Method for Preparation of Taxol Using Oxazinone. U.S. Patent, 5015744, **1991**.
[37] Ojima, I.; Sun, C. M.; Zucco, M.; Park, Y. H.; Duclos, O.; Kuduk, S. D. A Highly Efficient Route to Taxotere by the *β*-Lactam Synthon Method. *Tetrahedron Lett.* **1993**, *34*, 4149-4152.
[38] Commeren, A.; Bourzat, J. D.; Didier, E.; Lavelle, F. Practical Semisynthesis and Antimitotic Activity of Docetaxel and Side-Chain Analogues. In *Taxane Anticancer Agents: Basic Science and Current Status*; Georg, G. I., Chan, T. T., Ojima, I., Vyas, D. M., (Eds). American Chemical Society, Washington, D. C., **1995**; 233-246.
[39] Kingston, D. G. I.; Chaudhary, A. G.; Gunatilaka, A. A. L.; Middleton, M. L. Synthesis of Taxol from Baccatin III via an Oxazoline Intermediate. *Tetrahedron Lett.* **1994**, *35*, 4486-4489.
[40] Holton, R. A. Method for Preparation of Taxol. Eur. Pat. Appl., 400971, **1990**.
[41] Ojima, I. *β*-Lactam Synthon Method-Enantiomerically Pure *β*-Lactams as Synthetic Intermediates. In *The Organic Chemistry of β-Lactam Antibiotics*. Georg, G. I., (Ed.) VCH Publishers: New York, **1992**, 197-255.

[42] Ojima, I. Recent Advances in *β*-Lactam Synthon Method. *Acc. Chem. Res.* **1995**, *28*, 383-389.

[43] Ojima, I.; Sun, C. M.; Zucco, M.; Park, Y. H.; Duclos, O.; Kuduk, S. D. A Highly Efficient Route to Taxotere by the β-Lactam Synthon Method. *Tetrahedron Lett.* **1993**, *34*, 4149-4152

[44] Ojima, I.; Park, Y. H.; Sun, C. M.; Brigaud, T.; Zhao, M. New and Efficient Routes to Norstatine and Its Analogs with High Enantiomeric Purity by β-Lactam Synthon Method. *Tetrahedron Lett.* **1992**, *33*, 5737-5740.

[45] Ojima, I.; Zucco, M.; Duclos, O.; Kuduk, S. D.; Sun, C. M.; Park, Y. H. *N*-Acyl-3-hydroxy-*β*-lactams as Key Intermediates for Taxotere and Its Analogs. *Bioorg. Med. Chem. Lett.* **1993**, *3*, 2479-2482.

[46] Gueard, D.; Gueitte-Vogelein, F.; Potier, P. Taxol and Taxotere: Discovery, Chemistry, and Structure-Activity Relationships. *Acc. Chem. Res.* **1993**, *26*, 160-167

[47] Gueitte-Voegelein, F.; Mangatal, L.; Gueard, D.; Potier, P.; Guilhem, J.; Cesario, M.; Pascard, C. Structure of a Synthetic Taxol Precursor: *N-tert*-Butoxycarbonyl-10-deacetyl-*N*-debenzoyltaxol. *Acta Crstallogr.* **1990**, *C46*, 781-784.

[48] Colin, M.; Gueard, D.; Gueitte-Voegelein, F.; Potier, P. Taxotere. Eur. Pat. Appl., 253,738, **1988**.

[49] Ojima, I.; Kuduk, S. D.; Chakravarty, S. Recent Advances in the Medicinal Chemistry of Taxoid Anticancer Agents. *Adv. Med. Chem.* **1998**, 69-124.

[50] Kingston, D. G. I. Recent Advances in the Chemistry and Structure-Activity Relationships of Paclitaxel. In *Taxane Anticancer Agents: Basic Science and Current Status; ACS Symp. Ser. 583*. Georg, G. I., Chen, T. T., Ojima, I., Vyas, D. M., (Eds) American Chemical Society, Washington, D. C., **1995**, 203-216.

[51] Wahl, A.; Gueitte-Voegelein, F.; Gueard, D.; Le Goff, M.-T.; Potier, P. Rearrangement Reactions of Taxanes: Structural Modifications of 10-Deacetylbaccatin III. *Tetrahedron* **1992**, *48*, 6965-6974.

[52] Samaranayake, G.; Magri, N. F.; Jitrangsri, C.; Kingston, D. G. I. Modified Taxols. 5. Reaction of Taxol with Electrophilic Reagents and Preparation of a Rearranged Taxol Derivatives with Tubulin Assembly Activity. *J. Org. Chem.* **1991**, *56*, 5114-5119.

[53] Ojima, I.; Fenoglio, I.; Park, Y. H.; Sun, C.-M.; Appendino, G.; Pera, P.; Bernacki, R. J. Synthesis and Structure-Activity Relationships of Novel Nor-Seco Analogs of Taxol and Taxotere. *J. Org. Chem.* **1994**, *59*, 515-517.

[54] Ojima, I.; Lin, S.; Chakravarty, S.; Fenoglio, I.; Park, Y. H.; Sun, C.-M.; Appendino, G.; Pera, P.; Veith, J. M.; Bernacki, R. J. Synthesis and Structure-Activity Relationships of Novel Nor-seco Taxoids. *J. Org. Chem.* **1998**, *63*, 1637-1645.

[55] Klein, L. L.; Maring, C. J.; Li, L.; Yeung, C. M.; Thomas, S. A.; Grampovnik, D. J.; Plattner, J. J.; Henry, R. F. Synthesis of Ring B-Rearranged Taxane Analogs. *J. Org. Chem.* **1994**, *59*, 2370-2373.

[56] Liang, X.; Kingston, D. G. I.; Lin, C. M.; Hamel, E. Synthesis and Biological Evaluation of Paclitaxel Analogs Modified in Ring C. *Tetrahedron Lett.* **1995**, *36*, 2901-2904.

[57] Liang, X.; Kingston, D. G. I.; Long, B. H.; Fairchild, C. A.; Johnston, K. A. Synthesis, Structure Elucidation, and Biological Evaluation of *C*-Norpaclitaxel. *Tetrahedron Lett.* **1995**, *36*, 7795-7798.

[58] Chen, S.-H.; Fairchild, C.; Long, B. H. Synthesis and Biological Evaluation of Novel C-4 Aziridine-Bearing Paclitaxel. *J. Med. Chem.* **1995**, *38*, 2263-2267.

[59] Marder-Karsenti, R.; Dubois, J.; Bricard, L.; Gueard, D.; Gueitte-Voegelein, F. Synthesis and Biological Evaluation of D-Ring-Modified Taxanes: Azadocetaxel Analogs. *J. Org. Chem.*

1997, *62*, 6631-6637.
[60] Dubois, J.; Thoret, S.; Gueitte, F.; Gueard, D. Synthesis of 5(20)deoxydocetaxel, a new active docetaxel analogue. *Tetrahedron Lett.* **2000**, *41*, 3331-3334.
[61] Chordia, M. D.; Kingston, D. G. I. Synthesis and Biological Evaluation of 2-*epi*-Paclitaxel. *J. Org. Chem.* **1996**, *61*, 799-801.
[62] Monsarrat, B.; Mariel, E.; Cros, S.; Gare, M.; Gueard, D.; Gueitte-Voegelein, F.; Wright, M. Taxol Metabolism. Isolation and Identification of Three Major Metabolites of Taxol in Rat Bile. *Drug Metab. Dispos.* **1990**, *18*, 895-901.
[63] Ojima, I.; Inoue, T.; Slater, J. C.; Lin, S.; Kuduk, S. C.; Chakravarty, S.; Walsh, J. J.; Gilchrist, L.; McDermott, A. E.; Cresteil, T.; Monsarrat, B.; Pera, P.; Bernacki, R. J. Synthesis of Enantiopure F-Containing Taxoids and Their Use as Anticancer Agents as well as Probes for Biomedical Problems. In *Asymmetric Fluoroorganic Chemistry: Synthesis, Application, and Future Directions; ACS Symp. Ser. 746*; Ramachandran, P. V., (Ed.) American Chemical Society, Washington, D. C., **1999**, 158-181.
[64] Chaudhary, A. G.; Gharpure, M. M.; Rimoldi, J. M.; Chordia, M. D.; Gunatilaka, A. A. L.; Kingston, D. G. I.; Grover, S.; Lin, C. M.; Hamel, E. Unexpectedly Facile Hydrolysis of the 2-Benzoate Group of Taxol and Syntheses of Analogs with Increased Activities. *J. Am. Chem. Soc.* **1994**, *116*, 4097-4098.
[65] Ojima, I.; Kuduk, S. D.; Pera, P.; Veith, J. M.; Bernacki, R. J. Synthesis of and Structure-Activity Relationships of Non-Aromatic Taxoids. Effects of Alkyl and Alkenyl Ester Groups on Cytotoxicity. *J. Med. Chem.* **1997**, *40*, 279-285.
[66] Chen, S.-H.; Wei, J.-M.; Long, B. H.; Fairchild, C. A.; Carboni, J.; Mamber, S. W.; Rose, W. C.; Johnston, K.; Casazza, A. M.; Kadow, J. F.; Farina, V.; Vyas, D. M.; Doyle, T. W. Novel C-4 Paclitaxel (Taxol) Analogs: Potent Antitumor Agents. *Bioorg. Med. Chem. Lett.* **1995**, *5*, 2741-2746.
[67] Chen, S.-H.; Kadow, J. F.; Farina, V.; Fairchild, C. R.; Johnston, K. A. First Syntheses of Novel Paclitaxel (Taxol) Analogs Modified at the C-4 Position. *J. Org. Chem.* **1994**, *59*, 6156-6158.
[68] Georg, G. I.; Ali, S. M.; Boge, T. C.; Datta, A.; Falborg, L.; Himes, R. H. Selective C-2 and C-4 Deacylation and Acylation of Taxol: The First Synthesis of a C-4 Substituted Taxol Analogue. *Tetrahedron Lett.* **1994**, *35*, 8931-8934.
[69] Chaudhary, A. G.; Rimoldi, J. M.; Kingston, D. G. I. Modified Taxols. 10. Preparation of 7-Deoxytaxol, a Highly Bioactive Taxol Derivative, and Interconversion of Taxol and 7-*epi*-Taxol. *J. Org. Chem.* **1993**, *58*, 3798-3799.
[70] Chen, S. H.; Wei, J. M.; Vyas, D. M.; Doyle, T. W.; Farina, V. A Facile Synthesis of 7,10-Dideoxy Taxol and 7-*epi*-10-Deoxy Taxol. *Tetrahedron Lett.* **1993**, *34*, 6845-6848.
[71] Chen, S. H.; Kant, J.; Mamber, S. W.; Roth, G. P.; Wei, J.; Marshall, D.; Vyas, D.; Farina, V. Taxol Structure Activity Relationships: Synthesis and Biological Activity of Taxol and Analogs Modified at C-7. *Bioorg. Med. Chem. Lett.* **1994**, *4*, 2223-2228.
[72] Klein, L. L. Synthesis of 9-Dihydrotaxol: A Novel Bioactive Taxane. *Tetrahedron Lett.* **1993**, *34*, 2047-2050.
[73] Pulicani, J.-P.; Bourzat, J.-D.; Bouchard, H.; Commeren, A. Electrochemical Reduction of Taxoids: Selective Preparation of 9-dihydro-, 10-deoxy and 10-deacetoxy-Taxoids. *Tetrahedron Lett.* **1994**, *35*, 4999-5002.
[74] Datta, A.; Vander Velde, D. G.; Georg, G. I.; Himes, R. H. Syntheses of Novel C-9 and C-10 Modified Bioactive Taxanes. *Tetrahedron Lett.* **1995**, *36*, 1985-1988.

[75] Georg, G. I.; Cheruvallath, Z. S.; Vander Velde, D. G.; Himes, R. H. Stereoselective Synthesis of 9-Hydroxytaxanes via Reduction with Samarium Diiodide. *Tetrahedron Lett.* **1995**, *36*, 1783-1786.

[76] Chaudhary, A. G.; Kingston, D. G. I. Synthesis of 10-Deacetoxytaxol and 10-Deoxytaxotere. *Tetrahedron Lett.* **1993**, *34*, 4921-4924.

[77] Kant, J.; O'Keeffe, W. S.; Chen, S.-H.; Farina, V.; Fairchild, C.; Johnston, K.; Kadow, J. F.; Long, B. H.; Vyas, D. A Chemoselective Approach to Functionalize the C-10 Position of 10-Deacetylbaccatin III. Synthesis and Biological Properties of Novel C-10 Taxol Analogues. *Tetrahedron Lett.* **1994**, *35*, 5543-5546.

[78] Ojima, I.; Slater, J. C.; Kuduk, S. D.; Takeuchi, C. S.; Gimi, R. H.; Sun, C.-M.; Park, Y. H.; Pera, P.; Veith, J. M.; Bernacki, R. J. Syntheses and Structure-Activity Relationships of Taxoids Derived from 14*β*-Hydroxy-10-deacetylbaccatin III. *J. Med. Chem.* **1997**, *40*, 267-278.

[79] Ojima, I.; Slater, J. C.; Michaud, E.; Kuduk, S. D.; Bounaud, P.-Y.; Vrignaud, P.; Bissery, M.-C.; Veith, J.; Pera, P.; Bernacki, R. J. Syntheses and Structure-Activity Relationships of the Second Generation Antitumor Taxoids. Exceptional Activity against Drug-Resistant Cancer Cells. *J. Med. Chem.* **1996**, *39*, 3889-3896.

[80] Ojima, I.; Wang, T.; Miller, M. L.; Lin, S.; Borella, C.; Geng, X.; Pera, P.; Bernacki, R. J. Syntheses and Structure-Activity Relationships of New Second-Generation Taxoids. *Bioorg. Med. Chem. Lett.* **1999**, *9*, 3423-3428.

[81] Kingston, D. G. I.; Jagtap, P. G.; Yuan, H.; Samala, L. The chemistry of taxol and related taxoids. *Prog. Chem. Org. Nat. Prod.* **2002**, *84*, 53-225.

[82] Georg, G. I.; Boge, T. C.; Cheruvallath, Z. S.; Clowers, J. S.; Harriman, G. C. B.; Hepperle, M.; Park, H. The Medicinal Chemistry of Taxol. In *Taxol: Science and Applications.* Suffness, M., (Ed.) CRC Press: New York, **1995**, 317-375.

[83] Kant, J.; Huang, S.; Wong, H.; Fairchild, C.; Vyas, D.; Farina, V. Studies Toward Structure-Activity Relationships of Taxol: Synthesis and Cytotoxicity of Taxol Analogues with C-2' Modified Phenylisoserine Side Chains. *Bioorg. Med. Chem. Lett.* **1993**, *3*, 2471-2474.

[84] Geney, R.; Simmerling, C.; Ojima, I. Computational analysis of the paclitaxel binding site in *β*-tubulin. *Abstracts of Papers, 222nd ACS National Meeting*, Chicago, IL, August 26-30, **2001**, MEDI-065.

[85] Nicolaou, K. C.; Dai, W.-M.; Guy, R. K. Chemistry and Biology of Taxol. *Angew. Chem. Int. Ed. Engl.*, **1994**, *33*, 15-44.

[86] Ueda, Y.; Mikkilineni, A. B.; Knipe, J. O.; Rose, W. C.; Casazza, A. M.; Vyas, D. M. Novel Water Soluble Phosphate Prodrugs of Taxol Possessing *in vivo* Antitumor Activity. *Bioorg. Med. Chem. Lett.* **1993**, *3*, 1761-1766.

[87] Ueda, Y.; Wong, H.; Matiskella, J. D.; Mikkilineni, A. B.; Farina, V.; Fairchild, C.; Rose, W. C.; Mamber, S. W.; Long, B. H.; Kerns, E. H.; Casazza, A. M.; Vyas, D. M. Synthesis and Antitumor Evaluation of 2'-Oxycarbonylpaclitaxels (Paclitaxel-2'-carbonates). *Bioorg. Med. Chem. Lett.* **1994**, *4*, 1861-1864.

[88] Boge, T. C.; Georg, G. I. The Medicinal Chemistry of *β*-Amino Acids: Paclitaxel as an Illustrative Example. In *Enantioselective Synthesis of β-Amino Acids*. Juaristi, E. (Ed.) Wiley-VCH: New York, **1997**, 1-43.

[89] Ojima, I.; Lin, S.; Wang, T. The Recent Advances in the Medicinal Chemistry of Taxoids with Novel *β*-Amino Acid Side Chains. *Curr. Med. Chem.* **1999**, *6*, 927-954.

[90] Deng, L.; Jacobsen, E. N. A Practical, Highly Enantioselective Synthesis of the Taxol Side Chain via Asymmetric Catalysis. *J. Org. Chem.* **1992**, *57*, 4320-4323.

[91] Georg, G. I.; Harriman, G. C. B.; Hepperle, M.; Clowers, J. S.; Vander Velde, D. G.; Hines, R. H. Synthesis, Conformational Analysis, and Biological Evaluation of Heteroaromatic Taxanes. *J. Org. Chem.* **1996**, *61*, 2664-2676.

[92] Ojima, I.; Slater, J. C.; Michaud, E.; Kuduk, S. D.; Bounaud, P.-Y.; Vrignaud, P.; Bissery, M.-C.; Veith, J.; Pera, P.; Bernacki, R. J. Syntheses and Structure-Activity Relationships of the Second Generation Antitumor Taxoids. Exceptional Activity against Drug-Resistant Cancer Cells. *J. Med. Chem.* **1996**, *39*, 3889-3896.

[93] Ojima, I.; Slater, J. S.; Kuduk, S. D.; Takeuchi, C. S.; Gimi, R. H.; Sun, C.-M.; Park, Y. H.; Pera, P.; Veith, J. M.; Bernacki, R. J. Syntheses and Structure-Activity Relationships of Taxoids Derived from 14*β*-Hydroxy-10-deacetylbaccatin III. *J. Med. Chem.* **1997**, *40*, 267-278.

[94] Ojima, I.; Duclos, O.; Zucco, M.; Bissery, M.-C.; Combeau, C.; Vrignaud, P.; Riou, J. F.; Lavelle, F. Synthesis and Structure-Activity Relationships of New Antitumor Taxoids. Effects of Cyclohexyl Substitution at the C-3' and/or C-2 of Taxotere (Docetaxel). *J. Med. Chem.* **1994**, *37*, 2602-2608.

[95] Roh, E. J.; Song, C. E.; Kim, D.; Pae, H.; Chung, H.; Lee, K. S.; Chai, K.; Lee, C. O.; Choi, S. U. Synthesis and Biology of 3'-N-Acyl-N-debenzoylpaclitaxel Analogs. *Bioorg. Med. Chem.* **1999**, *7*, 2115-2119.

[96] Georg, G. I.; Harriman, G. C. B.; Hepperle, M.; Clowers, J. S.; Vander Velde, D. G.; Hines, R. H. Synthesis, Conformational Analysis, and Biological Evaluation of Heteroaromatic Taxanes. *J. Org. Chem.* **1996**, *61*, 2664-2676.

[97] Fulop, F.; Bernath, G.; Pihlaja, K. Synthesis, stereochemistry and transformations of cyclopentane-, cyclohexane-, cycloheptane-, and cyclooctane-fused 1,3-oxazines, 1,3-thiazines, and pyrimidines, *Adv. Heterocycl. Chem.* **1998**, *69*, 349-477

[98] Rosenblum, S. B.; Huynh, T.; Afonso, A.; Davis, H. R., Jr.; Yumibe, N.; Clader, J. W.; Burnett, D. A. Discovery of 1-(4-Fluorophenyl)-(3*R*)-[3-(4-fluorophenyl)-(3*S*)-hydroxypropyl]-(4*S*)-(4-hydroxyphenyl)-2-azetidinone (SCH 58235): A Designed, Potent, Orally Active Inhibitor of Cholesterol Absorption, *J. Med. Chem.* **1998**, *41*, 973-980.

[99] Ojima, I.; Habus, I.; Zhao, M.; Zucco, M.; Park, Y. H.; Sun, C. M.; Brigaud, T. New and efficient approaches to the semisynthesis of taxol and its C-13 side chain analogs by means of *β*-lactam synthon method, *Tetrahedron* **1992**, *48*, 6985-7012.

[100] Lynch, J. E.; Riseman, S. M.; Laswell, W. L.; Volante, R. P.; Smith, G. B.; Shinkai, I.; Tschaen, D. M. Mechanism of an acid chloride-imine reaction by low-temperature FT-IR: *β*-lactam formation occurs exclusively through a ketene intermediate, *J. Org. Chem.* **1989**, *54*, 3792-6.

[101] Adachi, K.; Kobayashi, S.; Ohno, M. Creation of novel chiral synthons with enzymes and applications to natural product synthesis. Part 20. Chiral synthons by enantioselective hydrolysis of meso-diesters with pig liver esterase: substrate-stereoselectivity relationships, *Chimia* **1986**, *40*, 311-314.

[102] Yamashita, Y.; Saito, S.; Ishitani, H.; Kobayashi, S. Chiral Hetero Diels-Alder Products by Enantioselective and Diastereoselective Zirconium Catalysis. Scope, Limitation, Mechanism, and Application to the Concise Synthesis of (+)-Prelactone C and (+)-9-Deoxygoniopypyrone, *J. Am. Chem. Soc.* **2003**, *125*, 3793-3798.

[103] Georg, G. I.; Cheruvallath, Z. S.; Himes, R. H.; Mejillano, M. R.; Burke, C. T. Synthesis of biologically active taxol analogs with modified phenylisoserine side chains, *J. Med. Chem.* **1992**, *35*, 4230-4237.

[104] Wu, X. Y. *Ph.D. Dissertation*; SUNY at Stony Brook: Stony brook, **2003**.

[105] Holton, R. A. *Eur. Pat. Appl.* EP 400,971, **1990**.

CHAPTER 2. DESIGN, SYNTHESIS AND BIOLOGICAL EVALUATION OF SECOND- AND THIRD- GENERATION TAXOIDS

§2.1 Development of the Second- and Third-Generation Taxoids via Ojima *β*-Lactam Synthon Method

Paclitaxel (Taxol®, marketed by Bristol-Myers Squibb) and docetaxel (Taxotère®, marketed by Sanofi-Aventis) are currently two of the most widely used drugs for cancer chemotherapy. Paclitaxel has been approved by the U.S. Food and Drug Administration (FDA) for the treatment of advanced ovarian cancer (in 1992), breast cancer (in 1994), Kaposi sarcoma (in 1997) and non-small cell lung cancer (NSCLC, in 1999). Docetaxel has been approved by the FDA for the treatment of breast cancer (in 1996), NSCLC (in 1999), prostate cancer (in 2004), stomach cancer (in 2006) and head and neck cancer (in 2007). Although both paclitaxel and docetaxel possess potent anticancer activity, it has been shown that the treatment with these drugs often produces undesirable side effects as well as drug resistance.[1] Therefore, it is necessary to seek new candidates that have comparable or better anticancer potency with superior pharmacological property but less side effect or drug-resistance.

The discovery of 10-DAB III and the development of efficient semisynthetic Ojima *β*-lactam synthon method not only assured the sufficient supply of paclitaxel and docetaxel, but also made it feasible to synthesize a variety of taxoids for further structure-activity relationship (SAR) studies (details described in Chapter 1).

Over the years our laboratory has performed extensive synthetic work of novel taxoids and has developed numerous highly potent novel taxoids with systematic modifications at the C2, C10 and C3' positions. Our SAR study on taxoids has indicated that the replacement of C3'-phenyl group with an alkenyl or alkyl group and / or the modification of C10 position with certain acyl groups can make the compounds one to two orders of magnitude more potent than the parent drugs (paclitaxel and docetaxel, "first-generation taxoids") against drug-resistant human breast cancer cell lines. These highly potent taxoids were termed as "second-generation taxoids" (**Figure 2-1**). [2] [3]

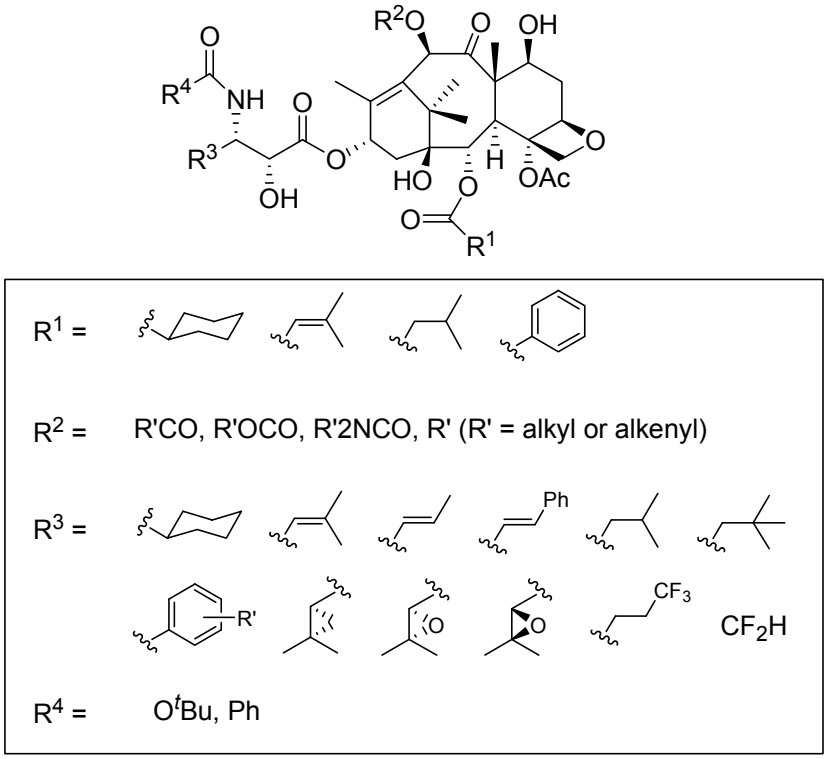

Figure 2-1. Second-generation taxoids synthesized from 10-DAB III

Further modification of the second-generation taxoids included the meta-substitutions on C2-benzoyl group. A number of thus synthesized taxoids has exhibited exceptionally high potency against multidrug-resistant cell lines, even to the extent that virtually no difference in potency against the drug-sensitive versus drug-resistant cell lines was observed. These exceptionally potent taxoids were named as "third-generation taxoids" (**Figure 2-2**). [4 5 6 7]

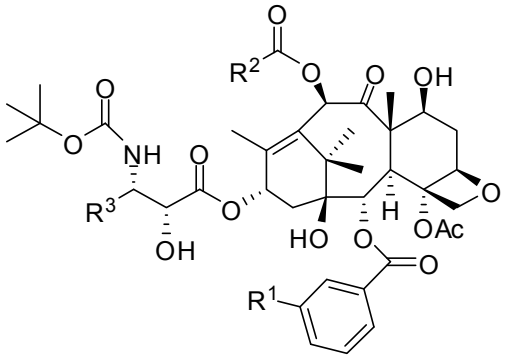

Figure 2-2. Generic structure of third-generation taxoids

Three second-generation taxoids from our group, **SB-T-1103**, **SB-T-1104** and **SB-T-1216**, were selected for further development by Aventis Pharmaceuticals (now Sanofi-Aventis) for their superb pharmacological profile. Another second-generation taxoid **SB-T-1214** was requested by

Abraxis Bioscience Inc. for cytotoxicity assay study.

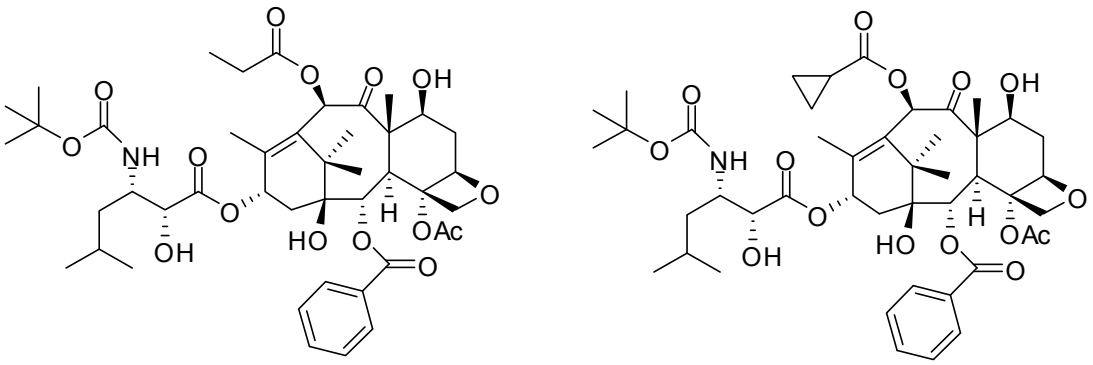

SB-T-1103

SB-T-1104

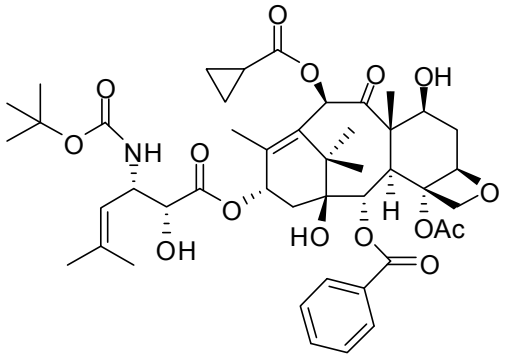

SB-T-1214

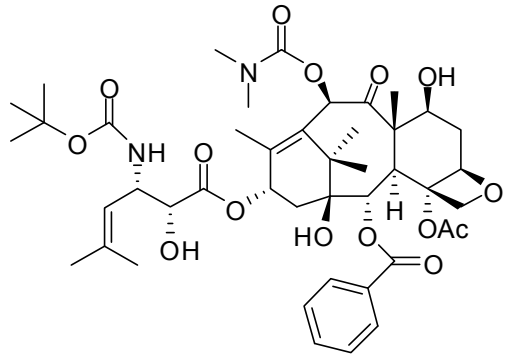

SB-T-1216

Figure 2-3. Structure of second-generation taxoids **SB-T-1103**, **SB-T-1104**, **SB-T-1214** and **SB-T-1216**

§2.2 Synthesis and Biological Evaluation of Taxane-Based Multi-Drug Resistance (MDR) Modulator SB-RA-310124

§2.2.1 Multi-Drug Resistance (MDR) and its Cellular Mechanism

Drug resistance is the reduction in effectiveness of a drug such as an antimicrobial or an anticancer drug after certain period of treatment for a disease or condition. Drug resistance is a consequence of evolution and is a response to pressures imposed on any living organism. Individual organisms vary in their sensitivity to the drug, and some with greater fitness may survive drug treatment and pass the traits of drug resistant onto their subsequent offspring. Unless the drug terminates biological reproduction or cell-division in the entire target population, resistance to the drug will inevitably follow.

When a target organism is resistant to more than one drug, it is called multidrug resistant. Organisms that display multidrug resistance can be pathologic cells, including bacterial and cancer cells. Cancer cells can be resistant to a single drug, a series of drugs with similar mechanism of action, or even cross-resistance to multiple structurally and mechanistically unrelated drugs.

Clinical resistance to drugs is a major barrier in cancer chemotherapy. Although there are many anticancer drugs in use, only a few are effective in the treatment of each specific tumor type because of intrinsic or acquired drug resistance.[8] Generally, there are two types of resistance to cancer chemotherapies. One category arises in the cancer cell itself as a result of genetic and epigenetic alterations that affect drug sensitivity. The other category is the inhibited delivery of anticancer drugs to cancer cells. Decreased drug intake may result from a mechanism referred to as classical MDR. The poor absorption of orally administered drugs, increased drug metabolism, or increased excretion may be responsible for reduced diffusion of drugs from the blood into the cancer cells.[9,10]

Cancer cells become resistant to anticancer drugs by several mechanisms including (a) decreased uptake of drug, (b) reduced intracellular drug concentration by efflux pumps, (e.g. P-glycoprotein, multidrug resistance-associated protein, lung resistance-related protein, and breast cancer resistance protein and reproductive cancer resistance protein), (c) altered cell cycle checkpoints, (d) altered drug targets, (e) increased metabolism of drug and (f) induced emergency response genes to impair apoptotic pathway.[11]

§2.2.2 Classical Multidrug Resistance with Efflux Pumps

Multidrug resistance (MDR) is a phenomenon where cancer cells develop broad resistance to a wide variety of chemotherapeutic drugs. MDR cell lines are characterized by a decreased accumulation and retention of cytotoxic drugs in the cells.[12] The most widely implicated mechanism is often referred to as classical MDR which is associated with accelerated efflux of anticancer agents by an adenosine triphosphate (ATP)-dependent process.[13]

Classical MDR was caused by the over-expression of ATP-binding cassette (ABC) transporters. Typically found in vital organs (i.e. the brain, the kidneys, the liver), ABC transporter is responsible for the key mechanism of metabolic functions in normal cells. However, in cancer cells, they utilized the energy obtained from ATP hydrolysis to pump out a wide range of taxoids and other anticancer agents across a multitude of cellular membranes against concentration gradients.[14]

In 1976, a membrane glycoprotein named P-glycoprotein (Pgp) was isolated and proposed to be the transporter protein that pumps out anticancer agents. [15] [16] [17] Pgp is a broad-spectrum multidrug efflux pump that has twelve transmembrane regions and two ATP-binding sites.[18] The transmembrane regions would bind to hydrophobic drug substrates that are either neutral or positively charged.[19] Once the substrate binds to the transmembrane regions, it will stimulate the ATPase activity of Pgp, and generate a conformational change that releases substrate to the extracellular space. [20] [21] The next ATP site will then be hydrolyzed to reset the transporter completing one catalytic cycle. [22] The continued research of efflux pumps led to the discovery of proteins from the same superfamily, such as multidrug resistance protein (MRP1)[23], lung cancer resistance-related protein (LRP) [24] and breast cancer resistance protein (BCRP). [25]

MRP1 has a similar structure as Pgp. The only difference is an amino terminal extension that contains five-membrane-spanning domains attached to a Pgp-like core. MRP1 transports neutral and anionic hydrophobic natural products, glutathione and other conjugates of these drugs. [26] [27] [28] Eight additional members of the MRP subfamily of transporters have also been discovered, some of which have the five transmembrane amino-terminal extension (MRP1, 2, 3, and 6), while others do not. [29]

§2.2.3 Design, Synthesis and Biological Evaluation of Taxane-Based MDR Modulators (TRAs)

§2.2.3.1 MDR modulators

First-generation taxoids (paclitaxel and docetaxel) had exhibited MDR in clinical applications. The cellular mechanisms of decreased intracellular accumulation of taxoids can be results of (a) overexpression of membrane-bound efflux proteins, such as ABC transporters including P-gp and MRP1; [30] (b) a direct alteration of drug target by mutation; [31] (c) altered expression of tubulin isotypes (for example, overexpression of βIII-tubulin) or MAPs; [32] (d) changes to the microtubules induced by interactions with other cytoskeletal proteins (for example, γ-actin), [33] and/or (e) defects in apoptotic pathways. [33]

MDR modulation of cancer cells is complicated by the fact that there is such a variety of different DNA mutations that contribute to tumor formation, as well as myriad mechanisms by which cells resist drugs. On top of that, since cancer cells are altered human cells, they are difficult to be selectively targeted without causing damages to the normal cells. Although the clinical relevance of multidrug resistance is debated, Pgp and other ABC transporters are viewed

as common targets for therapeutic suppression to increase the susceptibility of multidrug resistant cancers to chemotherapy.[34 35] Chemical and protein inhibitors of ABC transporters have been developed to overcome MDR, and many of the inhibitors have been tested in clinical trials.

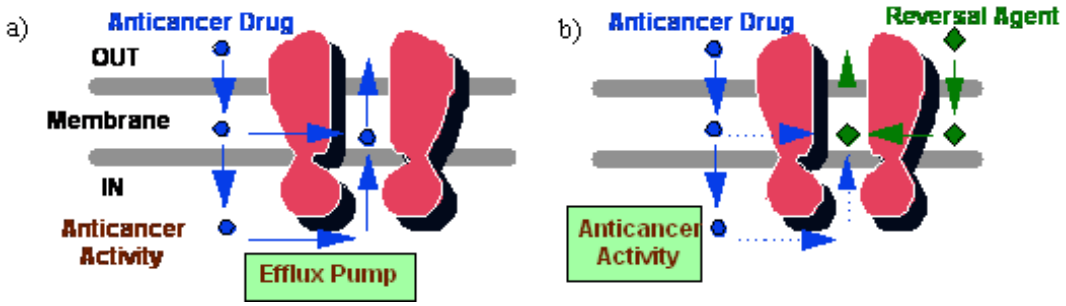

Figure 2-4. Mechanism of MDR modulator (i.e. MDR reversal agent)
a) ABC transporters pump anticancer drugs out of cells against concentration gradients.
b) Reversal agents would be pumped out of cells in lieu of cancer drugs.

§2.2.3.2 Rational Design of Taxane-Based MDR Modulators (TRAs)

A large number of structurally unrelated compounds are known to be Pgp substrates, with limited common features of high hydrophobicity, amphiphilic nature, planar ring structure, and / or a net positive charge.[36]

In the 1990's, several noncytotoxic taxanes from the Japanese yew tree Taxus cuspidate, like taxuspine C,[37 38] taxinine A,[39] taxine II and 2-desacetoxytaxinine J,[39 40] were reported by Kobayashi et al to possess the ability to increase the cellular accumulation of vincristine in MDR tumor cells (**Figure 2-5**). These taxanes, without the phenylisoserine side chain, showed low or no cytotoxicity. This finding had stimulated the investigation into novel taxane-based MDR modulators (TRAs).

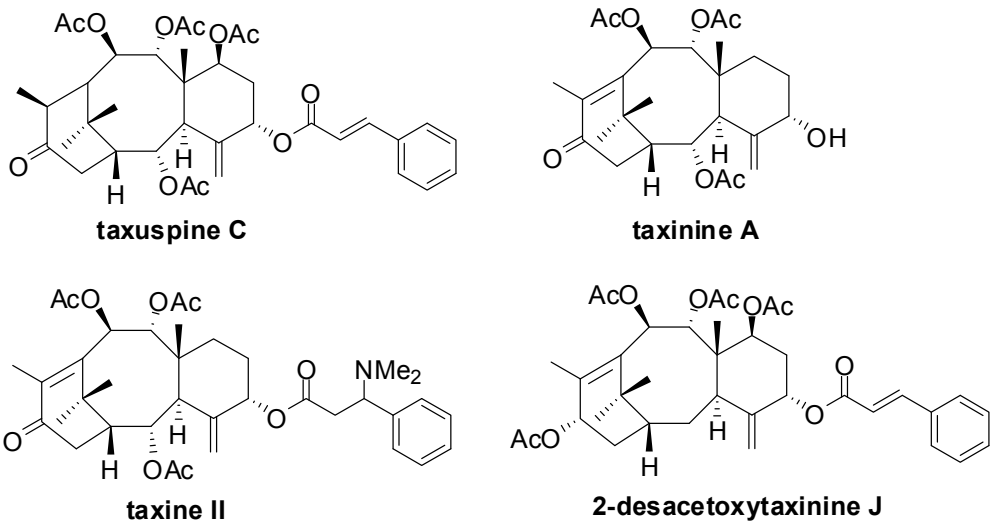

Figure 2-5. Structure of the taxane-based MDR modulators

Previous structure-activity relationship (SAR) studies of structurally different classes of MDR reversal agents pointed out the importance of a hydrophobic, conjugated, planar ring structure. [41 42] Accordingly, benzophenone, naphthalene-containing carboxylic acids and other hydrophobic groups were selected for the modification of 10-DAB III or 14*β*-OH-DAB III. [43 44] Our group has designed and synthesized a series of taxane-based MDR reversal agents by attaching various hydrophobic moieties at the C2, C7, C10, and C13 positions of either 10-DAB III or 14*β*-OH-DAB III (**Figure 2-6**).

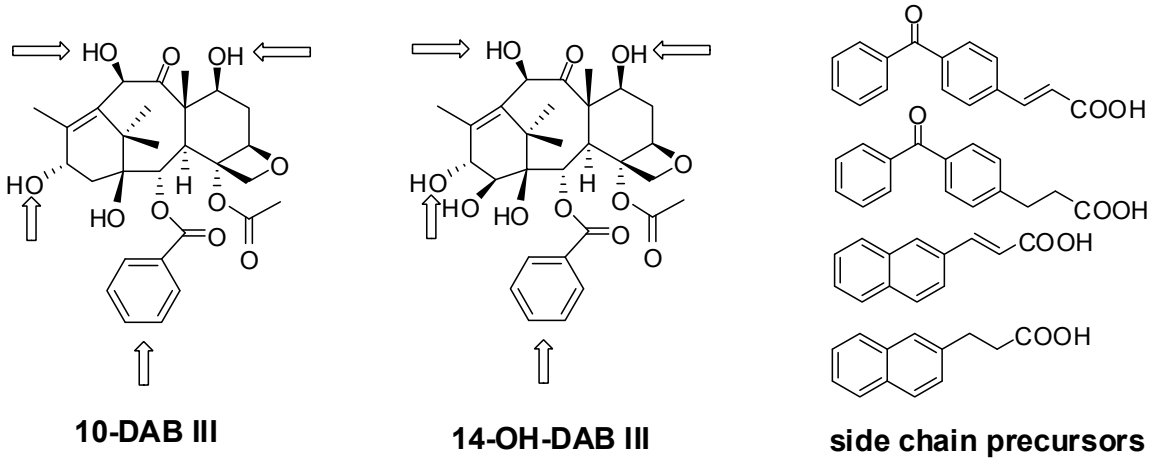

Figure 2-6. Taxane-based MDR modulators designed (by Professor Ojima)

MDR reversal activity of these taxanes was evaluated by testing the cytotoxicity of paclitaxel co-administered with a TRA against drug-resistant human breast cancer cell line MCF7-R or MDA-435/LCC6-MDR. Biological evaluation showed that compounds containing hydrophobic side chain at the C2, C10, or C13 positions had little or no activity, while the ones

substituted at the C7 position proved to be highly effective with >95% reversal activity in most cases. The best activity reached 99.8% recovery of the original antitumor activity of paclitaxel at 1 μM level of a TRA.[46] The compounds bearing a benzoylcinnamoyl or benzoyloxycinnamoyl side chain also showed slightly better activities than those with the napthoyl side chain.[45] The taxane-based MDR reversal agents (TRAs) have dual functions, i.e., both the cytotoxicity and the MDR reversal activity, therefore would bring high potency against Pgp-mediated efflux. [46 47 48]

§2.2.3.3 Structure-Activity Relations of Taxane-Based MDR Modulators (TRAs)

The SAR study of the TRAs focused on two areas: (1) exploring the structural and flexibility requirements of a key hydrophobic pendant group; (2) position of the hydrophobic group. **Figure 2-7** summarizes the results obtained from the SAR studies for the benzoylcinnamoyl side chain attached to a baccatin skeleton.

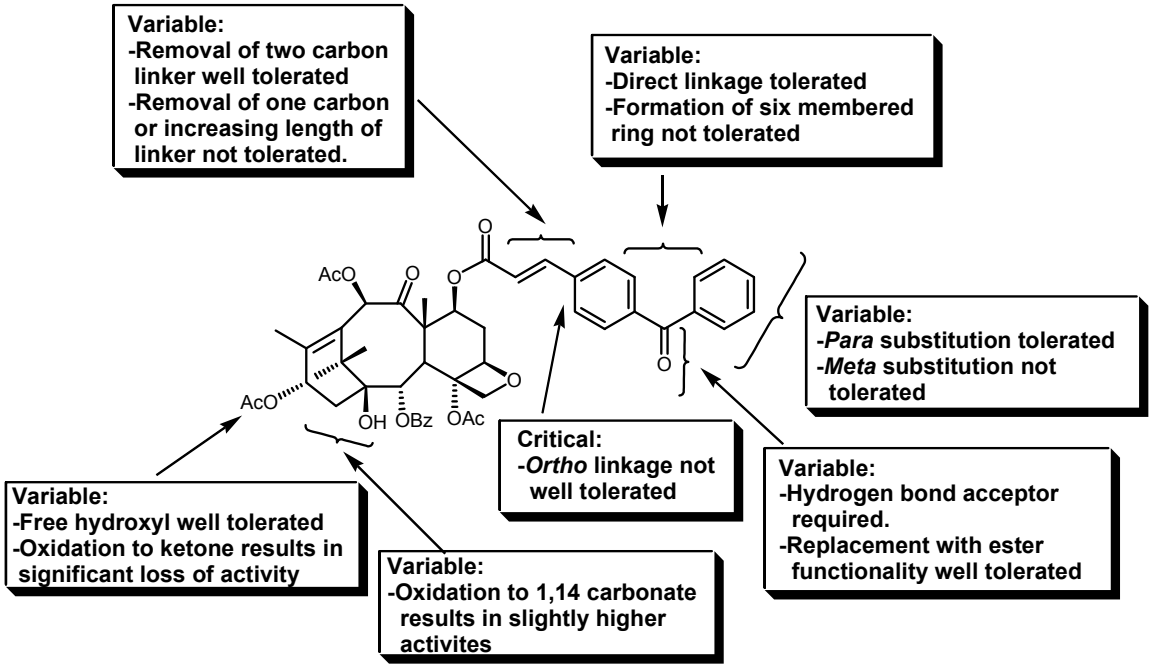

Figure 2-7. Structure-activity study of TRAs

The linker between the benzophenone to the baccatin core is variable. Direct connection is well tolerated, as is the standard two-carbon chain. The one carbon or three and more carbon chain results in loss of activity. [47] For the connections to the benzophenone, the para- substitution exhibits approximated two-order better activity than the ortho-position. [47]

The two aromatic rings of the side chain can be connected to form a 6-5-6 ring system without significant loss of activity, but inserting a second ketone to form an anthraquinone system causes significant loss of activity. [46] The carbonyl can be substituted by an ether linkage

without significant loss of activity. Replacement of the carbonyl by a non hydrogen-bond accepting moiety, like an alkene or reduction to a CH_2, results in severe loss of activity. [49]

Para substitution on the terminal aromatic ring is well tolerated and substitution with a para-*tert*-butyl group increases compound activities. Ortho substitution, on the other hand, is not well tolerated. A 3,5-bis(trifluoromethyl) substitution results in severe loss of activity. [53]

Oxidation of the C13-OH to the ketone is not tolerated resulting significantly reduces activity. [53]

The modulation ability of the TRAs have also been explored in a broad spectrum against MRP-1 and BCRP expressed cell lines, since it was shown that the co-expression of Pgp, MRP-1 and BCRP greatly increases the efflux of chemotherapeutic agents. A subset of the TRAs was further investigated in this context, and **SB-RA-310124** was found to be one of the leading broad-spectrum modulators of ABC transporters. [53]

§2.2.4 Taxane-Based Multi-Drug Resistance (MDR) Modulator SB-RA-310124

Based on previous studies, **SB-RA-310124** (**Figure 2-8**) significantly increases the potency of paclitaxel in MDA-435/LCC6-MDR resistant breast cancer cell lines (89% reduction of IC_{50} value at a concentration of 0.1 mM TRA). [50]
[% Reduction = [1-{IC_{50}(0.1mM reversal agent + paclitaxel) / IC_{50}(paclitaxel)}]x100]

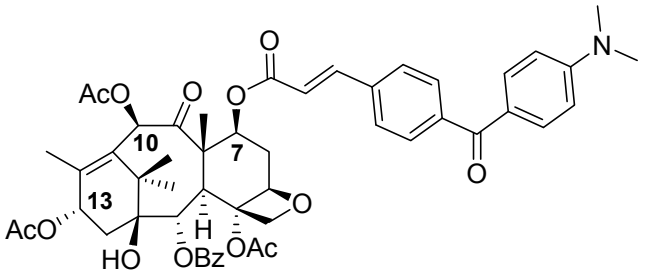

SB-RA-310124

Figure 2-8. Structure of **SB-RA-310124**

§2.2.4.1 Synthesis of SB-RA-310124

The synthesis of modified baccatin was shown in **Scheme 2-1**. Diacetylation at C10 and C13 positions of 7-TES-DAB followed by the deprotection using HF-pyridine gave 13-acetylbaccatin **2-13** in good yield.

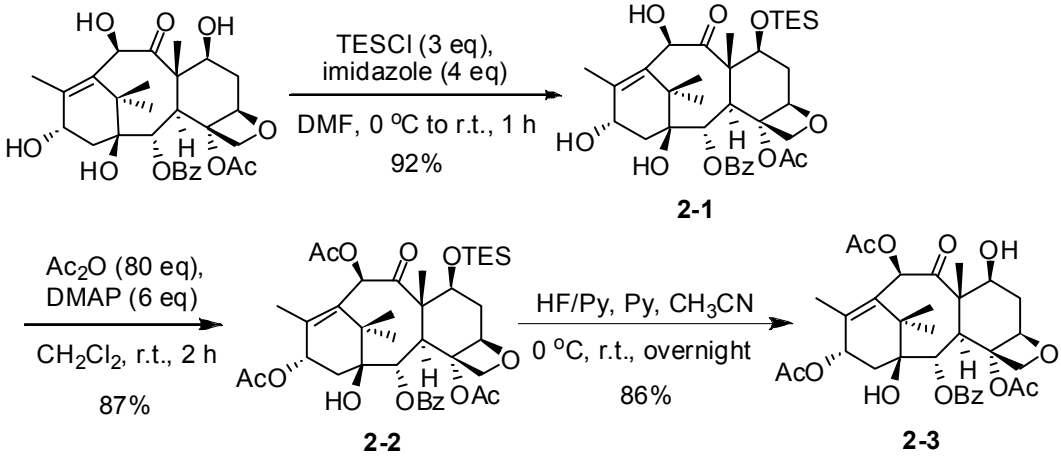

Scheme 2-1. Synthesis of 10, 13-diacetylbaccatin

C7 side chain precursor was synthesized following known procedure (**Scheme 2-2**). [49] The synthesis of 4-(4-dimethylaminobenzoyl)cinnamic acid **2-6** started with the Friedel-Crafts reaction of 4-bromobenzoyl chloride with *N,N*-dimethylaniline in the presence of aluminum

chloride and carbon disulfide. This reaction afforded mostly the p-substituted benzophenone. Relatively high equivalent (3.5 eq) of Lewis acid ($AlCl_3$) helped to increase the yield of the desired p-substituted product against o-substituted product. Heck reaction of **2-4** with methyl acrylate provided the ester **2-5**. Hydrolysis of the ester group afforded the C7 side chain precursor **2-6**.

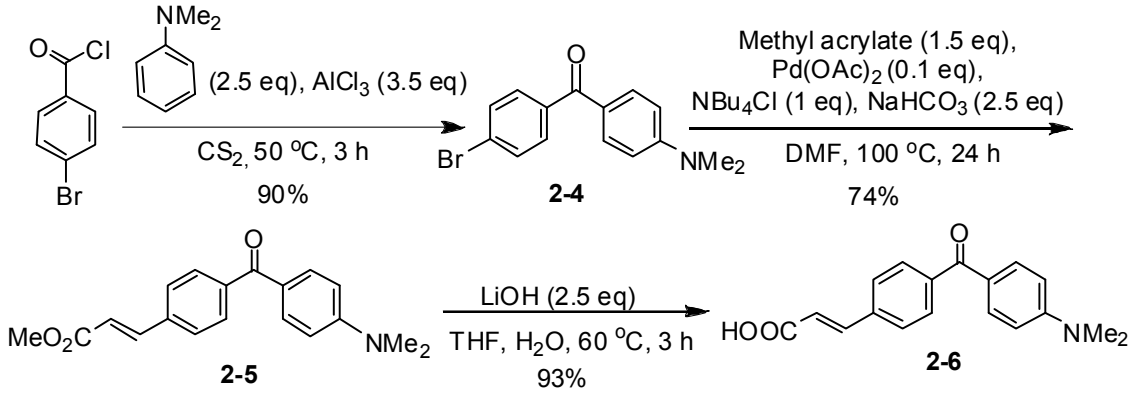

Scheme 2-2. Synthesis of 4-(4-dimethylaminobenzoyl)cinnamic acid

13-Acetylbaccatine **3-3** was coupled with 4-(4-dimethylaminobenzoyl)cinnamic acid (**2-6**) to afford the TRA in high yield as shown in **Scheme 2-3**.

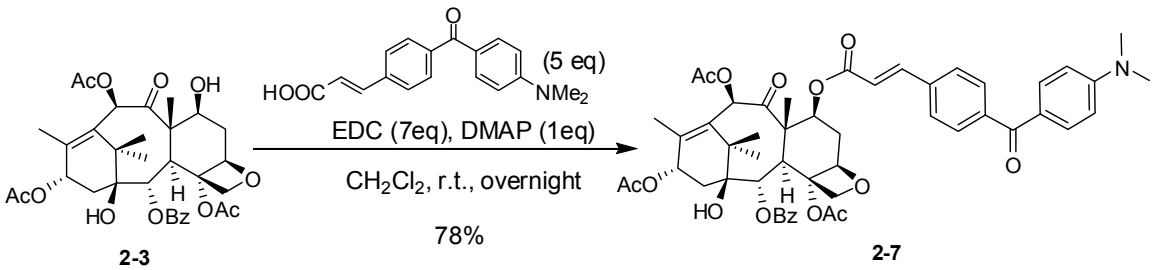

Scheme 2-3. Synthesis of **SB-RA-310124**

§2.2.4.2 Biological Evaluation

Novel TRAs have been designed and synthesized in our laboratory, and sent to Dr. Ralph J. Bernacki's laboratory in Roswell Park Cancer Institute for the assessment against the resistant human breast cancer cell line MCF7-R and/or MDA-435/LCC6-MDR1. These TRAs generally exhibited MDR-reversal activities up to 99.8% when co-administered with paclitaxel, acting as efficient sensitizing agents.

Besides Pgp, selected TRAs were found to modulate efflux pumps mediated by the MRP-1 and BCRP. Six TRAs (**Figure 2-9**) have been identified as triple-modulators to date, which can effectively modulate mitoxantrone efflux from drug-resistant cancer cell lines overexpressing

Pgp, MDR-1 and BCRP. Their broad-spectrum modulatory activities are demonstrated in **Figure 2-10**. [49] Among these, **SB-RA-310124** exhibited the best activity as broad-spectrum modulator, and has been identified as the lead drug candidate.

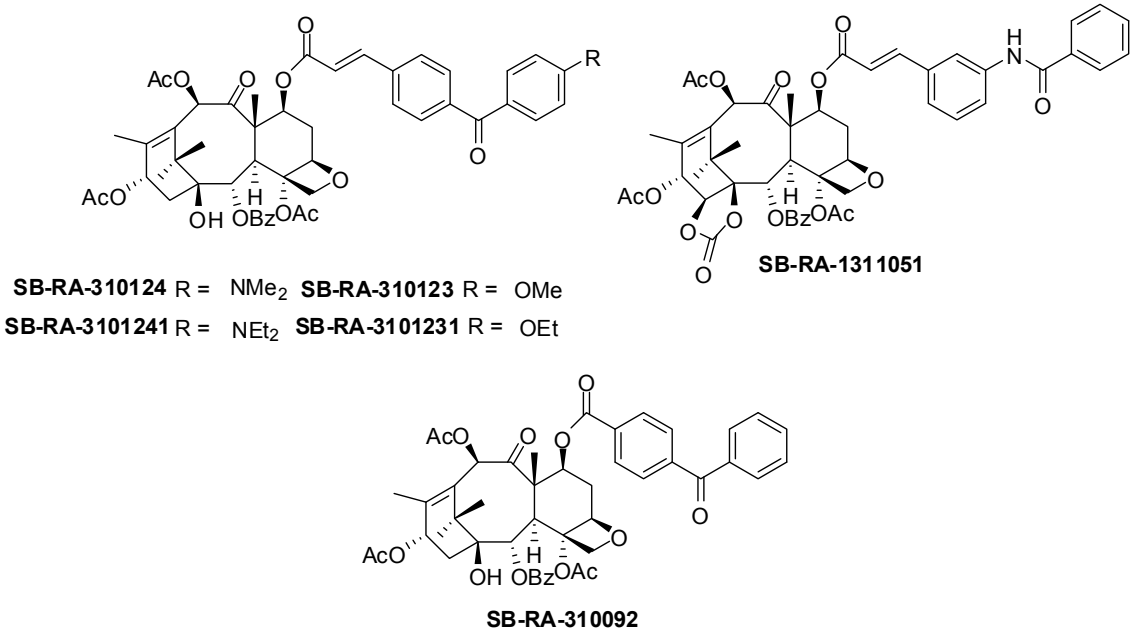

Figure 2-9. TRAs that modulate all three efflux pumps [49]

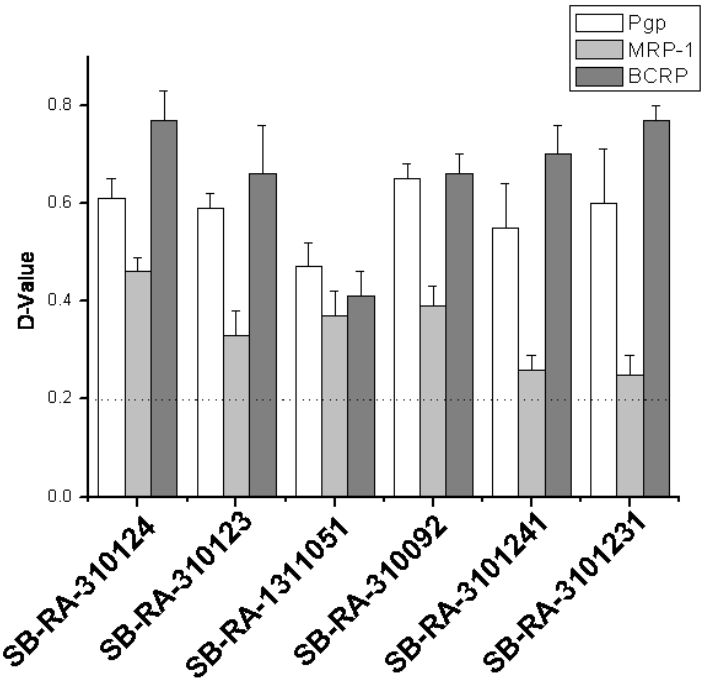

Figure 2-10. Effect of TRAs on drug efflux in resistant cell lines [51]

In the graph, D-values represent the separation of the distribution histograms for uptake in RPMI 1640 + 3 μM mitoxantrone and uptake in RPMI 1640 + 3 μM mitoxantrone + 10 μM TRA in Kolmogorov-Smirnov (KS) statistics. Screening of TRAs for modulation of mitoxantrone efflux mediated by Pgp (8226-Dox6), MRP-1 (HL60-ADR) and BCRP (8226A –MR20) is demonstrated. D-value ≥ 0.20 indicates modulatory activity. The graph shows the mean values from triplicate experiments, with standard errors.

§2.3 Second-Generation Taxoid SB-T-121303013

§2.3.1 Background

One of the second-generation taxoids **SB-T-121303013** (**Figure 2-11**) has showed greater *in vitro* activity compared with paclitaxel against human breast cancer cell lines, as shown in **Table 2-1** (LCC6-WT: human breast carcinoma; LCC6-MDR:MDR1 transduced line. Exposure time: 72 h.) [7 52]

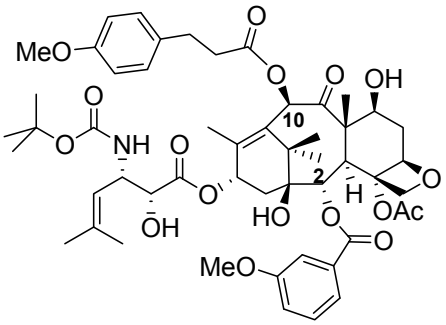

SB-T-121303013

Figure 2-11. Chemical structure of **SB-T-121303013**

Table 2-1. IC_{50} values of SB-T-121303013

	IC_{50} (nM)		
	LCC6-WT	LCC6-MDR	R/S Ratio
paclitaxel	5.9	476	81
SB-T-121303013	3.2	6.7	2.1

This compound was synthesized for anti-Parkinson's disease (anti-PD) studies, which is a collaboration project with Professor Jian Feng's group at State University of New York at Buffalo. It was earlier discovered that parkin, one of the most prevalent genetic factors in Parkinson's disease, binded to *α,β*-tubulin heterodimers and microtubules very strongly and increased the ubiquitination and degradation of *α,β*-tubulins.

§2.3.2 Synthesis of SB-T-121303013

A protocol using tri-TES-baccatin-diol as the key intermediate was employed to synthesize C2-meta-substituted-benzoyl baccatin.[53] As shown in **Scheme 2-4**, the synthesis started with 10-DAB III. The reaction of 10-DAB III with excess TESCl and imidazole in DMF solution afforded 7,10,13-tri-TES-baccatin in high yield. Reductive cleavage at C2 position using Red-Al gave 7,10,13-tri-TES-baccatin-diol in quantitive yield. Then, this diol was mixed with a large

excess of *m*-anisic acid, DIC and DMAP, and the mixture was refluxed in a concentrated dichloromethane solution overnight to give desired C2 modified tri-TES-baccatin in 90% yield. A global removal of the TES groups using HF-pyridine followed by selective protection of the C7-OH using TESCl and imidazole afforded C2-modified 7-TES-baccatin in good yield.

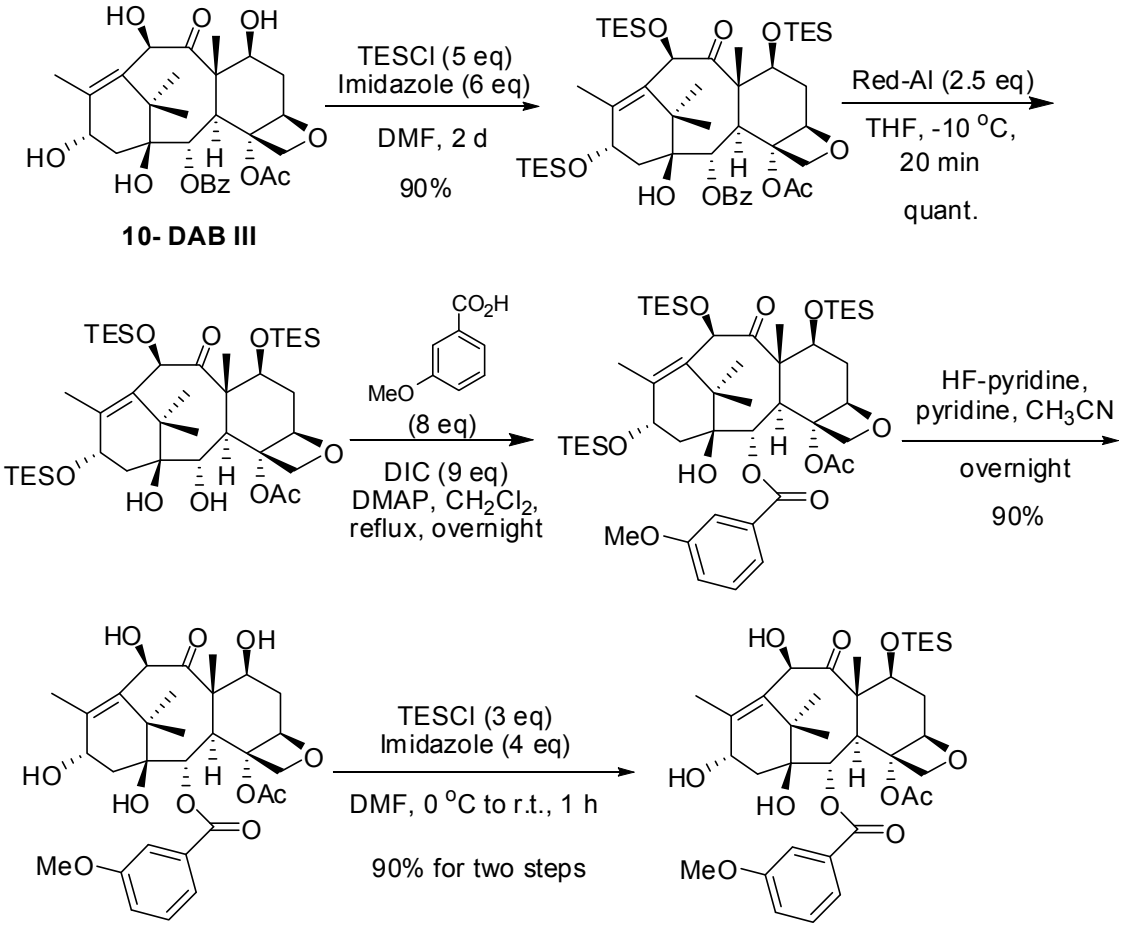

Scheme 2-4. Synthesis of C2 modified baccatin

The synthesis of **SB-T-121303013** was shown in **Scheme 2-5**. 3-(4-Methoxyphenyl)-propionic chloride was obtained from 3-(4-methoxyphenyl) propionic acid by refluxing with thionyl chloride. The C2-*m*-substituted-benzoyl baccatin was then coupled with the freshly distilled chloride to afford protected taxoid in 65% yield. (Byproduct (23%) was also isolated, with coupling at both C10 and C13 positions. The yield can further be optimized with shorter reaction time.) Coupling with *β*-lactam followed by deprotection using HF-pyridine gave **SB-T-121303** (**2-10**) in high yield.

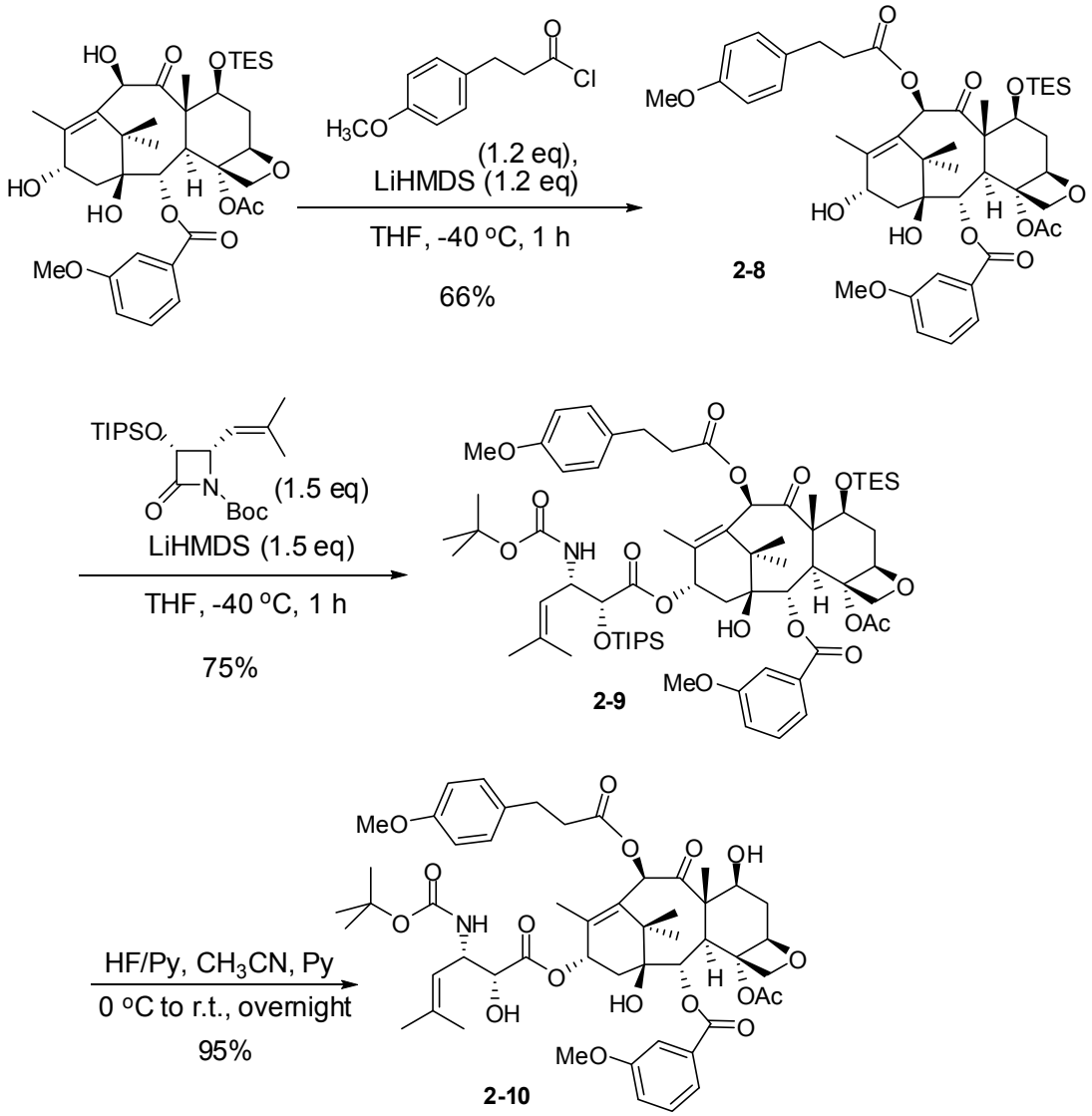

Scheme 2-5. Synthesis of **SB-T-121303013**

The continuing efforts of design and development of novel taxoids will provide us with highly potent new anticancer agents with better activities. The studies of drug-resistant mechanism and tumor-targeting strategies will provide us with valuable information in the design of new generation taxoids for development of anticancer agents.

§2.4 Experimental Section

Materials

The chemicals were purchased from Sigma-Aldrich and/or Fisher Scientific and were used without further purification unless otherwise noted. 10-DAB III and 14β-hydroxy-10-deacetylbaccatin III were gift from Indena, SpA, Italy and used as received. Tetrahydrofuran, dichloromethane, toluene and ethyl ether were obtained from the PureSolv^{TM} Solvent Purification System (Innovative Technology, Inc.) under N_2. The glassware was dried in a 110 ^{o}C oven and allowed to cool to room temperature in a desiccator over "Drierite" (calcium sulfate).

General Methods

^{1}H, ^{13}C and ^{19}F NMR spectra were obtained on Varian 300, 400 or 500 NMR spectrometers. Melting points were measured on a Thomas Hoover Capillary melting point apparatus and are uncorrected. TLC was performed on Merck DC-alufolien with Kieselgel 60F-254 and flash column chromatography was carried out on silica gel 60 (Merck, 230-400 mesh ASTM). Optical rotations were measured on a Perkin-Elmer Model 241 polarimeter. IR spectra were measured on a Shimadzu FTIR-8400s spectrophotometer. Chemical purity was determined on Shimadzu LC-1020A, using a Phenomenex Curosil-B column (5μ, 4.6 × 250 mm), employing CH_3CN/water (40/60, V/V) as the eluent with a flow rate of 1 mL/min. Chiral HPLC analysis for the determination of enantiomeric excess was carried out on a Waters HPLC assembly consist of a Waters M45 solvent delivery system and a Waters 484 detector (at 254 nm) on a PC workstation running Millennium 32 using a DAICEL-CHIRACEL OD chiral column (25 × 0.46 cm), employing n-hexanes/isopropanol (95/5, V/V) as eluent with a flow rate of 1.0 mL/min. High resolution mass spectra were obtained from the Mass Spectrometry Laboratory, University of Illinois at Urbana-Champaign, Urbana, IL.

7-Triethylsilyl-13-acetylbaccatin III (2-2) [45]

To a solution of 68.5 mg **2-1** (0.104 mmol) and 76.9 mg DMAP (0.624 mmol) in dry CH_2Cl_2 (3 mL) was slowly added 0.79 mL acetic anhydride (8.320 mmol). After stirring at room temperature for 2 h, the reaction mixture was quenched with a saturated aqueous $NaHCO_3$ and stirred for another 20 min. The reaction mixture was then extracted with CH_2Cl_2. The combined organic layers were washed with brine and then dried over $MgSO_4$. The solvent was evaporated *in vacuo* and the crude product was purified by flash column chromatography on silica gel to give **2-2** (72.5 mg, 94%) as a white solid: ^{1}H NMR (300 MHz, $CDCl_3$) δ 0.50 (m, 6 H), 0.84 (t, J = 7.8 Hz, 9 H), 1.07 (s, 3 H), 1.12 (s, 3 H), 1.56 (s, 3 H), 1.80 (m, 1 H), 1.95 (s, 3 H), 2.09 (s, 3 H), 2.11 (s, 3 H), 2.12 (m, 2 H), 2.25 (s, 3 H), 2.44 (m, 1 H), 3.74 (d, J = 6.9 Hz, 1 H), 4.06 (d, J = 8.4 Hz, 1 H), 4.21 (d, J = 8.4 Hz, 1 H), 4.39 (m, 1 H), 4.86 (d, J = 8.7 Hz, 1 H), 5.57 (d, J = 7.0 Hz, 2 H), 6.05 (t, J = 8.6 Hz, 1 H), 6.37 (s, 1 H), 7.38 (t, J = 7.5 Hz, 2 H), 7.51 (t, J = 7.3 Hz, 1 H) and 7.98 (d, J = 7.4 Hz, 2 H) ppm. All data are in agreement with literature values. [45]

13-Acetylbaccatin III (2-3) [45]

To a solution of **2-2** (72.5 mg, 0.098 mmol) in a mixture of pyridine and acetonitrile (3 mL, V/V = 1:1) was added dropwise HF-pyridine (0.75 mL) at 0 °C. The mixture was stirred overnight at room temperature, and then quenched with a saturated $NaHCO_3$ solution and diluted with a large amount of EtOAc. The organic layer was washed with saturated $NaHCO_3$ solution, $CuSO_4$ followed by H_2O and brine. And the organic layer was dried over $MgSO_4$ and concentrated *in vacuo*. Purification by flash column chromatography on silica gel gave **2-3** (52.9 mg, 85.7%) as a white solid: ^{1}H NMR (300 MHz, $CDCl_3$) δ 1.08 (s, 3 H), 1.18 (s, 3 H), 1.62 (s, 3 H), 1.86 (m, 4 H), 2.16 (s, 3 H), 2.19 (s, 3 H), 2.22 (m, 2 H), 2.28 (s, 3 H), 2.5 (m, 2 H), 3.78 (d, J = 6.9 Hz, 1 H), 4.12 (d, J = 8.4 Hz, 1 H), 4.25 (d, J = 8.4 Hz, 1 H), 4.38 (m, 1 H), 4.92 (d, J = 7.9 Hz, 2 H), 5.61 (d, J = 7.1 Hz, 1 H), 6.13 (t, J = 8.1 Hz, 1 H), 6.26 (s, 1 H), 7.38 (t, J = 7.5 Hz, 2 H), 7.51 (t, J = 7.3 Hz, 1 H) and 7.98 (d, J = 7.4 Hz, 2 H) ppm. All data are in agreement with literature values. [45]

4-Bromo-4'-*N,N*-dimethylaminobenzophenone (2-4) [45]

To a solution of 4-bromobenzoyl chloride (528 mg, 2.41 mmol) and *N,N*-dimethyl aniline (0.776 mL, 6.12 mmol) in carbon disulfide was added aluminium trichloride (1.125 g, 8.42 mmol) at 0 ^{o}C over a period of 0.5 h. The mixture was then refluxed at 50 ^{o}C for 3 h. The solvent was evaporated and the crude was hydrolyzed with ice and 1 N HCl. The mixture was extracted with diethyl ether and the organic layer was washed with 1 N HCl, followed by water, then dried over $MgSO_4$, filtered and concentrated *in vacuo*. Purification of the residue by flash column chromatography on silica gel afforded **2-4** (589 mg, 80%) as a pale yellow solid: ^{1}H NMR (300 MHz, $CDCl_3$) δ 3.02 (s, 6 H), 6.62 (d, J = 9.0 Hz, 2 H), 7.55 (s, 4 H) and 7.72 (d, J = 9.0 Hz, 2 H) ppm. All data are in agreement with literature values. [45]

4-(4-*N,N*-dimethylaminobenzoyl)cinnamate (2-5) [45]

To a solution of **2-4** (389 mg, 1.279 mmol), tetrabutylammonium chloride (1 eq), $NaHCO_3$ (2.5 eq) and palladium diacetate (0.02 eq) in DMF was added methyl acrylate (1.5 eq). After stirring at 100 ^{o}C for about 24 h, the mixture was cooled down and diluted with EtOAc. The organic layer was washed successively with a saturated solution of $NaHCO_3$ and brine, and the aqueous layer was extracted with EtOAc. The combined organic layers were dried over $MgSO_4$, filtered and concentrated *in vacuo*. Purification of the residue by flash column chromatography on silica gel afforded **2-5** (318 mg, 80%) as a yellow solid: ^{1}H NMR (300 MHz, $CDCl_3$) δ 3.05 (s, 6 H), 3.80 (s, 3 H), 6.50 (d, J = 16.0 Hz, 1 H), 6.65 (d, J = 3.9 Hz, 2 H), 7.58 (d, J = 8.1 Hz, 2 H) and 7.68-7.78 (m, 5 H) ppm. All data are in agreement with literature values. [45]

4-(4-*N,N*-Dimethylaminobenzoyl)cinnamic acid (2-6) [45]

A solution of a methyl ester **2-5** (168.5 mg, 0.545 mmol) and LiOH (2.5 eq) in wet THF was stirred for 3 h. The mixture was partitioned between EtOAc and water. Then the aqueous layer was extracted with EtOAc, and acidified to pH = 1 with 1 N HCl. The white precipitate again

was dissolved in EtOAc. The combined organic layers were dried over $MgSO_4$, filtered and concentrated to give the quantative yield of corresponding acid **2-6** as a yellow solid: ^{1}H NMR (300 MHz, DMSO-d_6) δ 3.04 (s, 6 H), 6.64 (d, J = 16.0 Hz, 1 H), 6.77 (d, J = 8.9 Hz, 2 H), 7.62-7.70 (m, 5 H), 7.83 (d, J = 8.1 Hz, 2 H) and 12.6 (br s, 1 H) ppm. All data are in agreement with literature values. [45]

7-[4-(*N,N*-Dimethylaminobenzoyl)cinnamoyl]-13-acetylbaccatin III (2-7, SB-RA-310124) [45]

The solution of **2-3** (52.9 mg, 0.015-0.02 M), DMAP (2 eq), EDC (7 eq) and 4-(4-*N,N*-dimethylaminobenzoyl)cinnamic acid (**2-6**, 5 eq) in CH_2Cl_2 was stirred at room temperature for about 17 h. Then the reaction mixture was quenched with saturated NH_4Cl solution. The aqueous layer was extracted with CH_2Cl_2. The combined organic layers were washed with three portion of water followed by one portion of brine and then dried over $MgSO_4$. The solvent was evaporated *in vacuo* and the crude product was purified by flash column chromatography on silica gel to give **2-7** (**SB-RA-310124**, 59.9 mg, 79%) as a yellow solid: ^{1}H NMR (300 MHz, $CDCl_3$) δ 1.18 (s, 3 H), 1.20 (s, 3 H), 1.88 (s, 4 H), 2.00 (s, 3 H), 2.08 (s, 3 H), 2.21 (s, 3 H), 2.26 (m, 2 H), 2.35 (s, 3 H), 2.71 (m, 1 H), 3.07 (s, 6 H), 4.01 (d, J = 6.8 Hz, 1 H), 4.18 (d, J = 8.4 Hz, 1 H), 4.34 (d, J = 8.4 Hz, 1 H), 5.00 (d, J = 8.9 Hz, 1 H), 5.70 (m, 2 H), 6.17 (t, J = 8.7 Hz, 1 H), 6.37 (s, 1 H), 6.43 (d, J = 16.0 Hz, 1 H), 6.68 (d, J = 8.9 Hz, 2 H), 7.48 (t, J = 7.4 Hz, 2 H), 7.58-7.79 (m, 8 H) and 8.07 (d, J = 7.5 Hz, 2 H) ppm. All data are in agreement with literature values. [45]

7-Triethylsilyl-2-(3-methoxybenzoyl)-10-(3-*para*-methoxyphenylpropanoyl) baccatin (2-8) [52]

The 7-TES-2-(3-methoxybenzoyl)-10-DAB III was synthesized by Liang Sun. In the solution of 7-TES-2-(3-methoxybenzoyl)-10-DAB III (39 mg, 0.057 mmol) in dry THF (1.4 mL) was added LiHMDS (1.0 M in THF, 0.07 mL, 0.07 mmol) dropwise by syringe at -40 °C. The mixture was stirred at -40 °C for 5 min, and then freshly made 3-(4-methoxyphenyl)propionic chloride (1.2 eq) was added dropwise. After 1 h, the reaction was quenched with saturated aqueous NH_4Cl, extracted with three portion of EtOAc, and the combined organic layers were dried over anhydrous $MgSO_4$ and concentrated *in vacuo*. The crude product was purified by flash column chromatography on silica gel to afford **2-8**(32 mg, 65%) as a white solid: ^{1}H NMR (300 MHz, $CDCl_3$) δ 0.56 (m, 6 H), 0.85 (m, 9 H), 0.92 (s, 3 H), 1.20 (m, 7 H), 1.64 (s, 3 H), 1.87 (m, 1 H), 2.00 (s, 3 H), 2.18 (s, 3 H), 2.26 (s, 3 H), 2.53 (m, 1 H), 2.70 (m, 2 H), 2.95 (t, J = 8.1 Hz, 2 H), 3.77 (s, 3H), 3.86 (m, 4 H), 4.14 (d, J = 8.7 Hz, 1 H), 4.33 (d, J = 8.7 Hz, 1 H), 4.49 (dd, J = 10.2, 6.7 Hz, 1 H), 4.81 (t, J = 7.9 Hz, 1 H), 4.96 (d, J = 8.4 Hz, 1 H), 5.62 (d, J = 6.6 Hz, 1 H), 6.48 (s, 1 H), 6.81 (d, J =8.7 Hz, 2H), 7.14 (d, J = 8.4 Hz, 3 H), 7.37 (t, J = 8.1 Hz, 1 H), 7.60 (s, 1 H) and 7.70 (d, J = 7.5 Hz, 1 H) ppm. All data are in agreement with literature values. [52]

Protected SB-T-121303013 (2-9) [52]

To a solution of baccatin **2-8** (32 mg, 0.037 mmol) and β-lactam **1-11** (22 mg, 0.056 mmol)

in dry THF (1.5 mL) was added LiHMDS (1.0 M in THF, 0.06 mL, 0.06 mmol) dropwise at -40 °C, and the solution was stirred at -40 °C for 1 h. The reaction was then quenched with saturated aqueous NH_4Cl solution, and the aqueous layer was extracted with three portion of EtOAc. The combined organic layers were then dried over anhydrous $MgSO_4$ and concentrated *in vacuo*. The crude product was purified by flash column chromatography on silica gel to afford **2-9** (34.7 mg, 75%) as a white solid: ^{1}H NMR (300 MHz, $CDCl_3$) δ 0.56 (m, 6 H), 0.85 (m, 9 H), 1.14 (s, 3 H), 1.23 (s, 3 H), 1.25 (s, 3 H), 1.68 (s, 3 H), 1.74 (s, 3 H), 1.76 (s, 3 H), 1.86 (s, 3 H), 2.34 (m, 5 H), 2.81 (m, 2 H), 2.95 (t, J = 8.7 Hz, 2 H), 3.38 (m, 1 H), 3.80 (s, 3 H), 3.82 (d, J = 3.6 Hz, 1 H), 3.84 (s, 3 H), 4.19 (d, J = 8.4 Hz, 1 H), 4.35 (d, J = 8.4 Hz, 1 H), 4.42 (m, 1 H), 4.75 (m, 2 H), 4.97 (d, J = 7.5 Hz, 1 H), 5.13 (d, J = 8.1 Hz, 1 H), 5.50 (d, J = 8.4 Hz, 1 H), 6.17 (t, J = 8.7 Hz, 1 H), 6.30 (s, 1 H), 6.81 (d, J = 7.8 Hz, 2 H), 7.14 (d, J = 7.8 Hz, 3 H), 7.37 (t, J = 8.1 Hz, 1 H), 7.63 (s, 1 H) and 7.69 (d, J = 8.1 Hz, 1 H) ppm. All data are in agreement with literature values. [52]

SB-T-121303013 (2-10) [52]

To a solution of **2-9** (34.0 mg, 0.027 mmol) in pyridine/acetonitrile (2.4 mL, V/V = 1:1) was added dropwise HF-pyridine (0.6 ml) at 0 °C, the mixture was then stirred overnight at room temperature. The reaction was quenched with saturated aqueous $NaHCO_3$ solution and stirred for 20 min. The mixture was then diluted with EtOAc, washed with two portions of saturated aqueous $NaHCO_3$ solution, three portions of $CuSO_4$ solution, water and brine, dried over anhydrous $MgSO_4$ and concentrated *in vacuo*. The crude product was purified by flash column chromatography on silica gel to afford **SB-T-121303013** (**2-10**, 25.3 mg, 95%) as a white solid: ^{1}H NMR (300 MHz, $CDCl_3$) δ 1.14 (s, 3 H), 1.23 (s, 3 H), 1.25 (s, 3 H), 1.68 (s, 3 H), 1.74 (s, 3 H), 1.76 (s, 3 H), 1.86 (s, 3 H), 2.34 (m, 5 H), 2.81 (m, 2 H), 2.97 (m, 2 H), 3.38 (m, 1 H), 3.80 (s, 3 H), 3.82 (d, J = 3.6 Hz, 1 H), 3.84 (s, 3 H), 4.19 (m, 2 H), 4.35 (d, J = 8.4 Hz, 1 H), 4.42 (m, 1 H), 4.75 (m, 2 H), 4.97 (d, J = 7.5 Hz, 1 H), 5.13 (d, J = 8.1 Hz, 1H), 5.50 (d, J = 8.4 Hz, 1 H), 6.17 (t, J = 8.7 Hz, 1 H), 6.30 (s, 1 H), 6.81 (d, J = 7.8 Hz, 2H), 7.14 (d, J = 7.8 Hz, 3 H), 7.37 (t, J = 8.1 Hz, 1 H), 7.63 (s, 1 H) and 7.69 (d, J = 8.1 Hz, 1 H) ppm. All data are in agreement with literature values. [52]

§2.5 References

[1] Rowinsky, E. K. The Development and Clinical Utility of the Taxane Class of Antimicrotubule Chemotherapy Agents. *Annu. Re*v. *Med.* **1997**, *48*, 353-374.

[2] Ojima, I.; Slater, J. C.; Michaud, E.; Kuduk, S. D.; Bounaud, P. Y.; Vrignaud, P.; Bissery, M. C.; Veith, J.; Pera, P.; Bernacki, R. J. *J. Med. Chem.* **1996**, 39, 3889-3896.

[3] Ojima, I.; Kuduk, S. D.; Pera, P.; Veith, J. M.; Bernacki, R. J. Synthesis and Structure-Activity Relationships of Non-Aromatic Taxoids. Effects of Alkyl and Alkenyl Ester Groups on Cytotoxicity. *J. Med. Chem.* **1997**, *40*, 279-285.

[4] Ojima, I.; Duclos, O.; Zucco, M.; Bissery, M.-C.; Combeau, C.; Vrignaud, P.; Riou, J. F.; Lavelle, F. Synthesis and Structure-Activity Relationships of New Antitumor Taxoids. Effects of Cyclohexyl Substitution at the C3' and/or C2 of Taxotere (Docetaxel), *J. Med. Chem.* **1994**, *37*, 2602-2608.

[5] Ojima, I.; Park, Y. H.; Sun, C.-M.; Fenoglio, I.; Appendino, G.; Pera, P.; Bernacki, R. J. Structure-Activity Relationships of New Taxoids Derived from 14*β*-Hydroxy-10-deacetylbaccatin III, *J. Med. Chem.* **1994**, *37*, 1408-1410.

[6] Ojima, I.; Slater, J. C.; Michaud, E.; Kuduk, S. D.; Bounaud, P.-Y.; Vrignaud, P.; Bissery, M.-C.; Veith, J. M.; Pera, P.; Bernacki, R. J. Syntheses and Structure-Activity Relationships of the Second-Generation Antitumor Taxoids: Exceptional Activity against Drug-Resistant Cancer Cells, *J. Med. Chem.* **1996**, *39*, 3889-3896.

[7] Ojima, I.; Chen, J.; Sun, L; Borella, C.; Wang, T.; Miller, M.; Lin, S.; Geng, X.; Kuznetsova, L.; Qu, C.; Gallager, D.; Zhao, X.; Zanardi, I.; Xia, S.; Horwitz, S.; Mallen-St. Clair, J.; Guerriero, J.; Bar-Sagi, D.; Veith, J.; Pera, P.; Bernacki, R. Design, Synthesis, and Biological Evaluation of New-Generation Taxoids *J. Med. Chem.* **2008**, *51*, 3203–3221.

[8] Lynch, J. E.; Riseman, S. M.; Laswell, W. L.; Volante, R. P.; Smith, G. B.; Shinkai, I.; Tschaen, D. M. Mechanism of an acid chloride-imine reaction by low-temperature FT-IR: *β*-lactam formation occurs exclusively through a ketene intermediate, *J. Org. Chem.* **1989**, *54*, 3792-3796.

[9] Pluen, A.; Boucher, Y.; Ramanujan, S.; McKee, T. D.; Gohongi, T.; Di Tomaso, E.; Brown, E. B.; Izumi, Y.; Campbell, R. B.; Berk, D. A.; Jain, R. K. Role of tumor-host interactions in interstitial diffusion of macromolecules: cranial vs. subcutaneous tumors. *Proc. Natl. Acad. Sci. USA.* **2001**, *98*, 4628-4633.

[10] Jain, R. K. Delivery of molecular and cellular medicine to solid tumors. *Adv. Drug Deliver. Rev.* **2001**, *46*, 149-168.

[11] Chai *et al. Chinese Medicine* **2010**, 5, 26.

[12] Kessel, D.; Botterill, V.; Wodinsky, I. Uptake and retention of daunomycin by mouse leukemic cells as factors in drug response, *Cancer Res.* **1968**, *28*, 938-41.

[13] Dano, K. Active outward transport of daunomycin in resistant Ehrlich ascites tumor cells, *Biochim. Biophys. Acta* **1973**, *323*, 466-483.

[14] Ferte, J. Analysis of the tangled relationships between P-glycoprotein-mediated multidrug

resistance and the lipid phase of the cell membrane. *Eur. J. Biochem.* **2000**, *267*, 277-294.

[15] Juliano, R. L.; Ling, V. A surface glycoprotein modulating drug permeability in Chinese hamster ovary cell mutants. *Biochim. Biophys. Acta* **1976**, *455*, 152-62.

[16] Safa, A. R. Photoaffinity labeling of P-glycoprotein in multidrug-resistant cells, *Cancer. Invest.* **1992**, *10*, 295-305.

[17] Nielsen, D.; Maare, C.; Skovsgaard, T. Influx of daunorubicin in multidrug resistant Ehrlich ascites tumor cells: correlation to expression of P-glycoprotein and efflux. Influence of verapamil, *Biochem. Pharmacol.* **1995**, *50*, 443-450.

[18] Chen, C. J.; Chin, J. E.; Ueda, K.; Clark, D. P.; Pastan, I.; Gottesman, M. M.; Roninson, I. B. Internal duplication and homology with bacterial transport proteins in the mdr1 (P-glycoprotein) gene from multidrug-resistant human cells. *Cell* **1986**, *47*, 381-389.

[19] Ambudkar, S. V.; Dey, S.; Hrycyna, C. A.; Ramachandra, M.; Pastan, I.; Gottesman, M. M. Biochemical, cellular, and pharmacological aspects of the multidrug transporter. *Annu. Rev. Pharmacol.* **1999**, *39*, 361-398.

[20] Senior, A. E.; Bhagat, S. P-Glycoprotein Shows Strong Catalytic Cooperativity between the Two Nucleotide Sites. *Biochemistry* **1998**, *37*, 831-836.

[21] Ramachandra, M.; Ambudkar, S. V.; Chen, D.; Hrycyna, C. A.; Dey, S.; Gottesman, M. M.; Pastan, I. Human P-Glycoprotein Exhibits Reduced Affinity for Substrates during a Catalytic Transition State. *Biochemistry* **1998**, *37*, 5010-5019.

[22] Sauna, Z. E.; Ambudkar, S. V. Evidence for a requirement for ATP hydrolysis at two distinct steps during a single turnover of the catalytic cycle of human P-glycoprotein. *Proc. Natl. Acad. Sci. USA*. **2000**, *97*, 2515-2520.

[23] Deeley, R. G.; Cole, S. P. C. Function, evolution and structure of multidrug resistance protein (MRP), *Seminars Cancer Biol.* **1997**, *8*, 193-204.

[24] Scheper, R. J.; Broxterman, H. J.; Scheffer, G. L.; Kaaijk, P.; Dalton, W. S.; Van Heijningen, T. H. M.; Van Kalken, C. K.; Slovak, M. L.; De Vries, E. G. E.; et al. Overexpression of a Mr 110,000 vesicular protein in non-P-glycoprotein-mediated multidrug resistance, *Cancer Res.* **1993**, *53*, 1475-1479.

[25] Aszalos, A.; Ross, D. D. Biochemical and clinical aspects of efflux pump related resistance to anti-cancer drugs, *Anticancer Res*. **1998**, *18*, 2937-2944.

[26] Mueller, M.; Meijer, C.; Zaman, G. J. R.; Borst, P.; Scheper, R. J.; Mulder, N. H.; de Vries, E. G. E.; Jansen, P. L. M. Overexpression of the gene encoding the multidrug resistance-associated protein results in increased ATP-dependent glutathione S-conjugate transport. *Proc. Natl. Acad. Sci. USA*. **1994**, *91*, 13033-13037.

[27] Jedlitschky, G.; Leier, I.; Buchholz, U.; Barnouin, K.; Kurz, G.; Keppler, D. Transport of glutathione, glucuronate, and sulfate conjugates by the MRP gene-encoded conjugate export pump. *Cancer Res.* **1996**, *56*, 988-994.

[28] Loe, D. W.; Deeley, R. G.; Cole, S. P. C. Characterization of vincristine transport by the Mr 190,000 multidrug resistance protein (MRP): evidence for cotransport with reduced glutathione. *Cancer Res.* **1998**, *58*, 5130-5136.

[29] Borst, P.; Evers, R.; Kool, M.; Wijnholds, J. A family of drug transporters: The multidrug resistance-associated proteins. *J. Natl. Cancer I.* **2000**, *92*, 1295-1302.

[30] Kyle, A. H., Huxham, L. A., Yeoman, D. M. & Minchinton, A. I. Limited tissue penetration of taxanes: a mechanism for resistance in solid tumors. *Clin. Cancer Res.* **2007**, *13*, 2804-2810.

[31] Bhalla, K. N. Microtubule-targeted anticancer agents and apoptosis. *Oncogene* **2003,** *2*, 9075-9086.

[32] Verrills, N. M. *et al*. Alterations in gamma-actin and tubulin-targeted drug resistance in childhood leukemia. *J. Natl Cancer Inst.* **2006**, 98, 1363-1374.

[33] Attard, G.; Reid, A. H. M.; Yap, T. A.; Raynaud, F.; Dowsett, M.; Settatree, S.; Barrett, M.; Parker, C.; Martins, V.; Folkerd, E.; Clark, J.; Cooper, C. S.; Kaye, S. B.; Dearnaley, D.; Lee, G.; de Bono, J. S. Phase I clinical trial of a selective inhibitor of CYP17, abiraterone acetate, confirms that castration-resistant prostate cancer commonly remains hormone driven. *J. Clin. Oncol.* **2008**, *26*, 4563-4571.

[34] Gottesman, M. M.; Pastan, I. Biochemistry of multidrug resistance mediated by the multidrug transporter *Annu. Rev. Biochem.* **1993**, *62*, 385-427.

[35] Sarkadi, B.; Müller, M. Search for specific inhibitors of multidrug resistance in cancer. *Seminars in Cancer Biology,* **1997**, *8*, 171-182.

[36] Frezard, F.; Pereira-Maia, E.; Quidu, P.; Priebe, W.; Garnier-Suillerot, A. P-glycoprotein preferentially effluxes anthracyclines containing free basic versus charged amine. *Eur. J. Biochem.* **2001**, *268*, 1561-1567.

[37] Kobayashi, J. I.; Ogiwara, A.; Hosoyama, H.; Shigemori, H.; Yoshida, N.; Sasaki, T.; Li, Y.; Iwasaki, S.; Naito, M.; Tsuruo, T. Taxuspines A-C, new taxoids from Japanese yew Taxus cuspidata inhibiting drug transport activity of P-glycoprotein in multidrug-resistant cells. *Tetrahedron* **1994**, *50*, 7401-7416.

[38] Kobayashi, J. I.; Hosoyama, H.; Wang, X.-X.; Shigemori, H.; Sudo, Y.; Tsuruo, T. Modulation of multidrug resistance by taxuspine C and other taxoids from Japanese yew. *Bioorg. Med. Chem. Lett.* **1998**, *8*, 1555-1558.

[39] Hosoyama, H.; Shigemori, H.; Tomida, A.; Tsuruo, T.; Kobayashi, J. I. Modulation of multidrug resistance in tumor cells by taxinine derivative. *Bioorg. Med. Chem. Lett.* **1999**, *9*, 389-394.

[40] Kobayashi, J. I.; Hosoyama, H.; Wang, X.-X.; Shigemori, H.; Koiso, Y.; Iwasaki, S.; Sasaki, T.; Naito, M.; Tsuruo, T. Effects of taxoids from Taxus cuspidata on microtubule depolymerization and vincristine accumulation in MDR cells. *Bioorg. Med. Chem. Lett.* **1997**, *7*, 393-398.

[41] Yamazaki, T.; Hiraoka, S.; Sakamoto, J.; Kitazume, T. Mesyloxy-group migration as the stereoselective preparation method of various functionalized olefins and its reaction mechanism, *Org. Lett.*, **2001**, *3*, 743-746.

[42] Lim, M. H.; Kim, H. O.; Moon, H. R.; Chun, M. W.; Jeong, L. S. Synthesis of Novel D-2'-Deoxy-2'-C-difluoromethylene-4'-thiocytidine as a Potential Antitumor Agent, *Org. Lett.*

2002, *4*, 529-531.

[43] Wu, Q.; Bounaud, P.-Y.; Kuduk, S. D.; Yang, C.-P. H.; Ojima, I.; Horwitz, S. B.; Orr, G. A. Identification of the domains of photoincorporation of the 3'- and 7-benzophenone analogs of Taxol in the carboxyl-terminal half of murine mdr1b P-glycoprotein, *Biochemistry* **1998**, *37*, 11272-11279.

[44] Ojima, I.; Bounaud, P.-Y.; Takeuchi, C.; Pera, P.; Bernacki, R. J. New taxanes as highly efficient reversal agents for multi-drug resistance in cancer cells, *Bioorg. Med. Chem. Lett.* **1998**, *8*, 189-194.

[45] Fumero, C. L., *Ph.D. Dissertation*; SUNY at Stony Brook: Stony Brook, **2000**.

[46] Ojima, I.; Borella, C.; Wu, X.; Bounaud, P.; Oderda, C.; Sturm, M.; Miller, M.; Chakravarty, S.; Chen, J.; Huang, Q.; Pera, P.; Brooks, T.; Baer, M.; Bernacki, R. Design, Synthesis and Structure-Activity Relationships of Novel Taxane-Based Multidrug Resistance Reversal Agents, *J. Med. Chem.* **2005,** *48,* 2218-2228.

[47] Ojima, I.; Bounaud, P.-Y.; Bernacki, R. J. New weapons in the fight against cancer. *Chemtech*, **1998**, *28*, 31-36.

[48] Geney, R.; Ungureanu, I. M.; Li, D.; Ojima, I. Overcoming multidrug resistance in taxane chemotherapy. *Clin. Chem. Lab. Med.* **2002**, *40*, 918-925.

[49] Chen, J., *Ph.D. Dissertation*; SUNY at Stony Brook: Stony Brook, **2006**.

[50] Wu, X., *Ph.D. Dissertation*; SUNY at Stony Brook: Stony Brook, **2003**.

[51] Brooks, T.; Minderman, H.; O'Loughlin, K. L.; Pera, P.; Ojima, I.; Baer, M. R.; Bernacki, R. J. Taxane-based reversal agents modulate drug resistance mediated by P-glycoprotein, multidrug resistance protein, and breast cancer resistance protein. *Mol. Cancer Ther.* **2003**, *2*, 1195-1205.

[52] Borella, C. P., *Ph.D. Dissertation*; SUNY at Stony Brook: Stony Brook, **2001**.

[53] Ojima, I.; Wang, T.; Miller, M. L.; Lin, S.; Borella, C. P.; Geng, X.; Pera, P.; Bernacki, R. J. Synthesis and structure-activity relationships of new second-generation taxoids, *Bioorg. Med. Chem. Lett.* **1999**, *9*, 3423-3428.

CHAPTER 3. DESIGN, SYNTHESIS AND BIOLOGICAL EVALUATIONS OF NOVEL MACROCYCLIC TAXOIDS

§3.1 Introduction of Bioactive Conformation

The diterpenoid natural product paclitaxel [1] and its semisynthetic analogue docetaxel [2] are two important antitumor drugs currently used in the treatment of refractory ovarian cancer, small-cell lung cancer, metastatic breast disease, etc. (**Figure 3-1**) [3 4] Paclitaxel binds to the *β*-tubulin component of the *α,β*-tubulin heterodimer, promotes the polymerization of tubulin, stabilizes microtubules, therefore disrupts the equilibrium of the microtubular dynamics, and eventually causes apoptosis. [5 6]

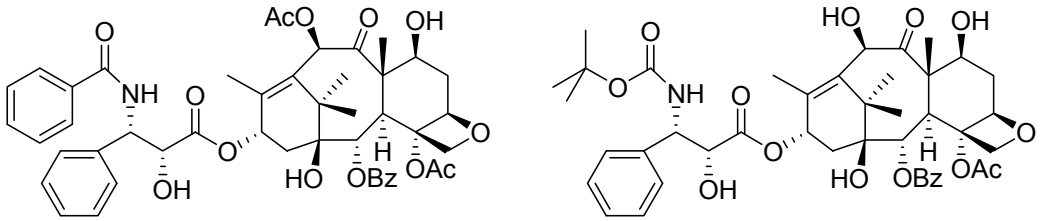

Figure 3-1. The chemical structure of paclitaxel and docetaxel

Although the unique mechanism of action of paclitaxel has been discovered almost thirty years ago, [7 8] their exact binding conformation with microtubule is yet to be fully understood. The investigation of possible bioactive conformation of paclitaxel has attracted much interest among organic and medicinal chemists, as well as molecular pharmacologists and structural biologists. [9 10] The bioactive conformation of paclitaxel is intriguing not only because of the genuine curiosity for the structural study, but more importantly of the possibility to develop the novel anticancer candidates with simplified structure designed based on the bioactive confirmation of paclitaxel.

Extensive studies have been carried out relating to this topic. [11] X-ray crystallography, [12 13] solution NMR spectroscopy, [14 15] photolabeling affinity study, [16 17] fluorescence spectroscopy, [18 19] solid-state NMR studies, [13] mutagenesis, [20] computational modeling [21] and electron crystallography [22] have afforded much information about the bioactive conformation.

Four different conformations have been proposed to be the bioactive conformation of paclitaxel: nonpolar conformation, [9-23] polar conformation, [10 24] T-Taxol, [10 16] and REDOR-Taxol. [10] Although the first two proved less likely to be the bioactive conformation of paclitaxel in the microtubule-bound complex, they have played an important role in the conformational studies and are worth reviewing in this chapter.

§3.1.1 Nonpolar Conformation

The initial conformational analysis was performed by NMR and X-ray crystallography of paclitaxel in solution and in solid state, which led to the proposals of the “nonpolar” conformation and the “polar” conformation marked by the hydrophobic collapse between either

C3' *N*-benzoyl or C3' phenyl with the C2 benzoyl groups. [25 26 27]

The nonpolar confirmation was also reported for docetaxel by Guilhem *et al* in 1990 based on the X-ray structure (**Figure 3-2**). [7] This confirmation was characterized with a hydrophobic collapse between C2 benzoyl phenyl ring, C4 acetyl group and ^{t}Boc group of the C13 side chain. The folded C13 side chain also included intramolecular hydrogen bonds between the C2'-hydroxyl group with the C1'-carbonyl oxygen and the amide nitrogen.

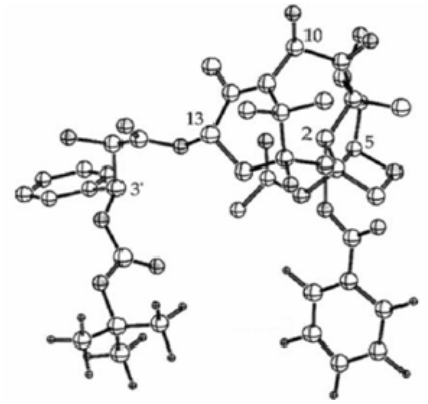

Figure 3-2. X-ray structure of docetaxel [7]

A similar conformation was found later in the solution NMR of paclitaxel and analogue in aprotic solvent (e.g. $CDCl_3$, CD_2Cl_2). [9 18 28 29] These observations as well as the previously found docetaxel X-ray structure have brought forward the proposal of non-polar conformation.

A powerful tool for obtaining information regarding the binding confirmation at the receptor site is by introducing conformational restrains. It is generally assumed that the analogs with similar confirmation would demonstrate similar biological activity to the same receptor. Based on this hypothesis, extensive synthetic efforts have been made to restrict the flexible C13 side chain and to correlate them with biological activity of paclitaxel or docetaxel. Several series of C2-C3'*N*-linked macrocyclic taxoids were reported to mimic the "nonpolar" conformation (**Figure 3-3**). However, none of the compounds showed comparable activity to paclitaxel.[30 31 32 33 34]

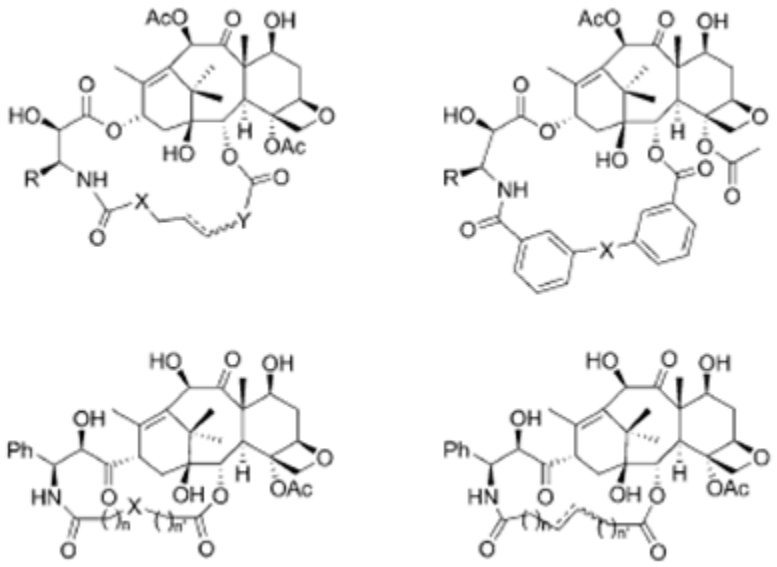

Figure 3-3. C2-C3'*N*-linked macrocyclic taxoids

§3.1.2 Polar Conformation

Besides aprotic solvent, protic solvent was also used for NMR studies. Due to the poor solubility of paclitaxel in water, D_2O/DMSO-d_6 mixture was used as an aqueous surrogate. In this solvent system, the paclitaxel adopted a very different conformation. [19] This new conformer was characterized by a hydrophobic collapse of C2-benzoyl phenyl ring, C4 acetyl group and C3' phenyl group. The intramolecular hydrogen bonds were lost with the concomitant appearance of new hydrophobic interactions. [10] X-ray structure of paclitaxel was reported later by Mastropaolo and Camerman *et al*.(**Figure 3-4**) [8] Two molecules were found in the asymmetric unit, one of which was very similar to the conformer mentioned above found in the polar NMR. This conformer was then names as "polar" conformation.

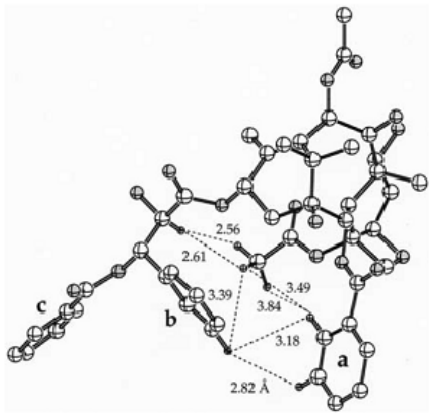

Figure 3-4. X-ray structure of paclitaxel [8]

The first attempt to orient the C13 side chain to mimic the polar conformation includes

synthesis of the C4-C3'-linked macrocyclic taxoids (**Figure 3-5**) by Heck reaction, esterification [35] and olefin metathesis. [30 36] But none of the reported taxoids were as active as paclitaxel: most of them showed IC_{50} value of submicromolar to more than two-digit micromolar, [37 38] or even completely loss of activity.

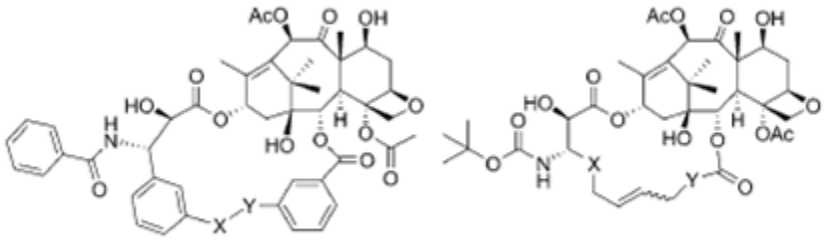

Figure 3-5. C2-C3'-linked macrocyclic taxoids

The experimental results indicated that neither the "nonpolar" conformation nor the "polar" conformation were the correct binding structure of paclitaxel. The disagreement of the activity data and the proposed conformation derived from structure studies could be explained from two aspects. Firstly, the NMR parameters, i.e. NOE's and J's, only reflected an AVERAGE value of the multiple individual conformations in rapid exchange. For a very flexible molecule like paclitaxel, the single derived conformation could not represent all the possible conformations that exist in the real solution. Secondly, the ligand conformation could change drastically when binding to the protein, due to the various interactions between protein residues and the ligand. The prevalence of either of the two conformers was likely dependent on the nature of the solvent rather than representative of the bioactive conformation.

Nevertheless, the early endeavors in the synthetic strategy has proved the olefin metathesis to be a powerful method to synthesize conformationally restrained macrocyclic paclitaxel analogues, and could be applied to further investigations. [39]

§3.1.3 T-Taxol

In 2000, Snyder et al. proposed another conformer, which was derived from Monte Carlo conformational search and NMR-based analysis of ROESY and NOESY data of paclitaxel in $CDCl_3$.[40] Three conformations were identified, two of which corresponded to nonpolar and polar conformation, respectively. The third one, with an open C13-side chain, was considered to be a novel bioactive conformation, named as "T-Taxol" (**Figure 3-6**).

The first cryo-electron microscopy (cryo-EM) structure of paclitaxel-bound Zn^{2+}-stabilized α,β-tubulin heterodimer was reported in 1998 at 3.7 Å resolution (1TUB structure). [41] The 1TUB structure was later refined to 3.5 Å resolution (1JFF structure) in 2001. [42] However, the resolution of these cryo-EM structures was still not high enough to solve the binding conformation of paclitaxel. Thus, a computational study of the electron-density map was performed, which generated the same conformer as "T-Taxol". [21]

In order to validate the "T-Taxol" structure, rigidified paclitaxel congeners were designed, synthesized, and assayed for their tubulin polymerization ability and cytotoxicity. [43 44 45] Among those "T-Taxol" mimics, C4-C3'-linked macrocyclic taxoids showed higher activities than

paclitaxel in the cytotoxicity and tubulin polymerization assays. [44]

The open C13-side chain of "T-taxol" allows inter- and intramolecular hydrophobic interactions among C3' benzamido, C2 benzoyl moieties and His-229. His-229 had already been proved to be an essential residue for the interaction between paclitaxel and *α,β*-tubulin by mutagenesis study. [16]

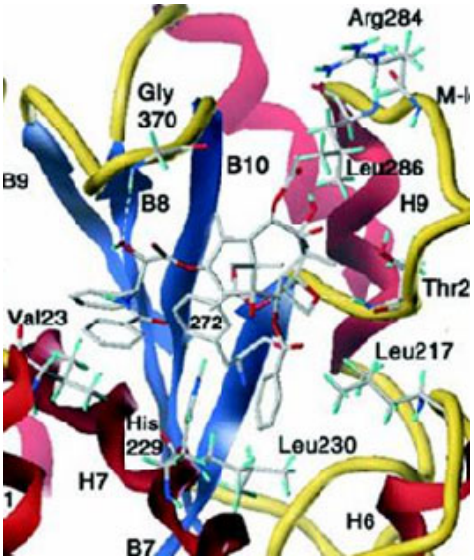

Figure 3-6. T-taxol and its interaction with *α,β*-tubulin [16]

§3.1.4 REDOR-Taxol

Our group has also been working on the conformational studies of paclitaxel. Monte Carlo dynamic studies incorporating REDOR-NMR results [13] yielded 16 different conformers. Docking of the conformers in to EC coordinate [31] of *α,β*-tubulin deduced a new conformer, named as REDOR-Taxol (**Figure 3-7**). [69]

In the meantime, two ^{13}C-^{19}F intramolecular distances of the microtubule-bound 2-(4-fluorobenzoyl)paclitaxel were experimentally obtained by means of the REDOR NMR study in 2000. [46] On the basis of the REDOR distances, MD analysis of paclitaxel conformers, photoaffinity labeling, [47] and molecular modeling studies using the 1TUB coordinate, [22] we proposed the "REDOR-Taxol" as a valid microtubule-bound paclitaxel structure in 2005. We have further refined the "REDOR-Taxol" using the 1JFF coordinate and found that the "REDOR-Taxol" is not only fully consistent with the new REDOR-experiments [48] but also accommodates highly active macrocyclic paclitaxel analogues designed on the basis of the "T-Taxol" structure. [49]

According to the "REDOR-Taxol", we have designed novel macrocyclic taxoids by linking the C14 and C3'*N* groups to examine whether these conformationally restricted taxoids exhibit the same level of biological activity as that of paclitaxel. [49]

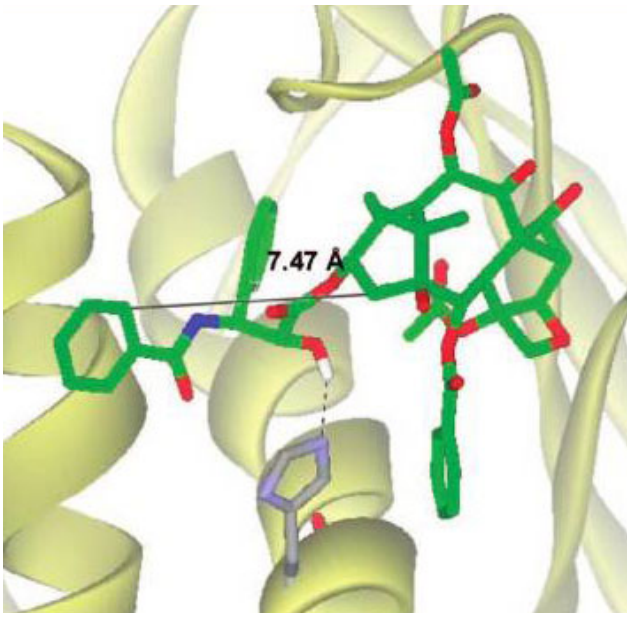

Figure 3-7. REDOR-Taxol 1JFF and the atom-atom distance between C14 and the *ortho*-carbon of the C3'*N*-benzoyl group [69]

The critical difference between the "T-Taxol" and "REDOR-Taxol" is the orientation of the C2'-OH group. In the "REDOR-Taxol", the C2'-OH group interacts with His227 as the hydrogen bond donor; While in the "T-Taxol", the hydrogen bond resides between the C2'-OH and the backbone carbonyl oxygen of Arg369 (**Figure 3-8**).[50]

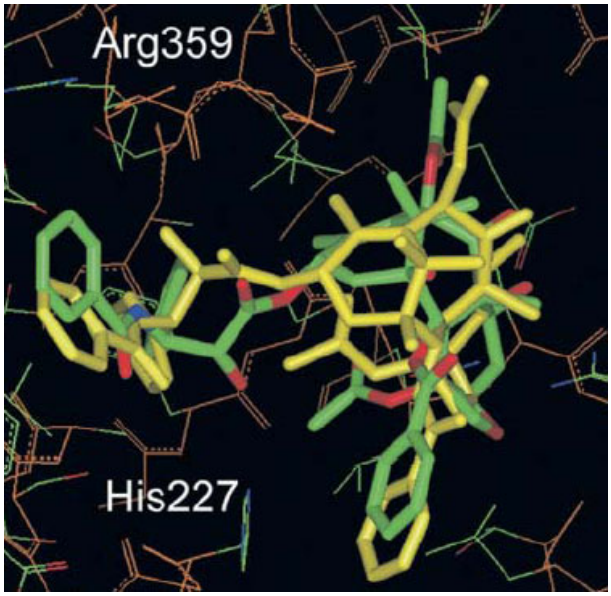

Figure 3-8. Overlay of the REDOR-Taxol (green) and T-Taxol (yellow) [50]

Both T-Taxol and REDOR-Taxol were supported by experimental results, and were good models for the bound paclitaxel. Macrocyclic taxoids based on these two models showed good to excellent cytotoxicity.[44 49]

§3.2 Design, Synthesis and Biological Evaluation of the C4-C2' Linked Macrocyclic Taxoid SB-TCR-101

§3.2.1 Common Pharmocophore

The novel mechanism of action of paclitaxel, which was originally thought to be unique, was later found to be shared by several other natural products of anticancer properties. Epothilones A and B (from the mycobacterium, Sorangium cellulosum), [51] [52]eleutherobin (from a soft coral of the Eleutherobia sp.), [53] discodermolide (from the marine sponge Discodermia dissoluta), [54] showed activities comparable to those of paclitaxel in cytotoxicity assays and inhibition of microtubules disassembly in purified tubulin assembly assays (**Figure 3-9**). These compounds also competitively inhibit [^{3}H]-paclitaxel binding to microtubules, which strongly suggests the existence of a common, or closely overlapping, binding site. [55] [56] More recently, two other novel compounds, laulimalide [57] and FR181277, [58] were reported to share the same mechanism of action as paclitaxel.

The fact that the structurally distinct compounds shared the same mechanism of action and / or binding site has intrigued the research effort to seek a common pharmacophore of all the microtubule-stabilizing agents (MSA), which would shed light on the rational design of the next generation microtubule-stabilizing anticancer agents.

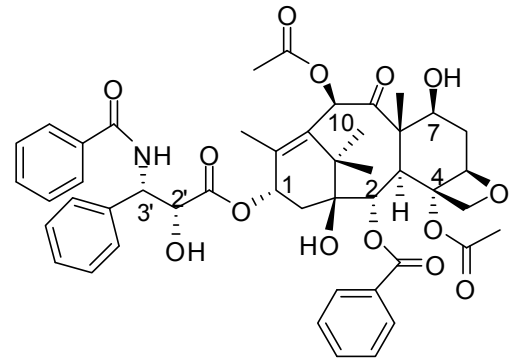

Taxol® (paclitaxel)

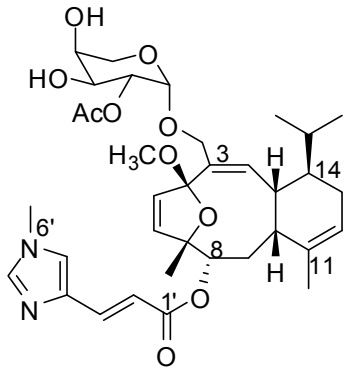

Eleutherobin

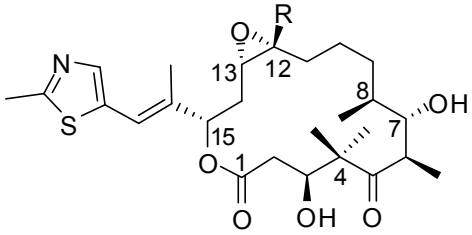

R=H Epothilone A
R=CH_3 Epothilone B

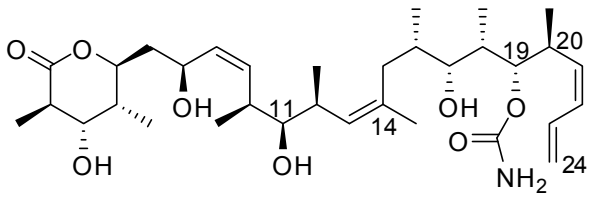

Discodermolide

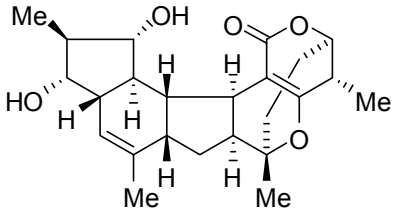

FR182877

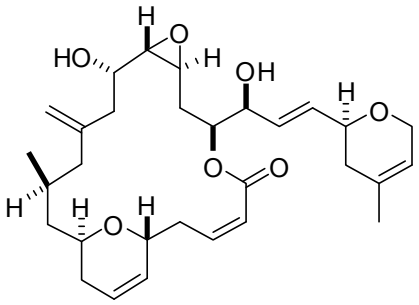

Laulimalide

Figure 3-9. Naturally occurring microtubule-stabilizing agents

In our efforts to elucidate the bioactive conformation of paclitaxel, our laboratory has proposed a binding conformation of paclitaxel based on docking studies of paclitaxel with *α,β*-tubulin dimer (**Figure 3-10**, by Raphael Geney in our laborotary). [59] This preliminary proposal has contributed to the discovery of the "REDOR-Taxol" and is worth discussion.

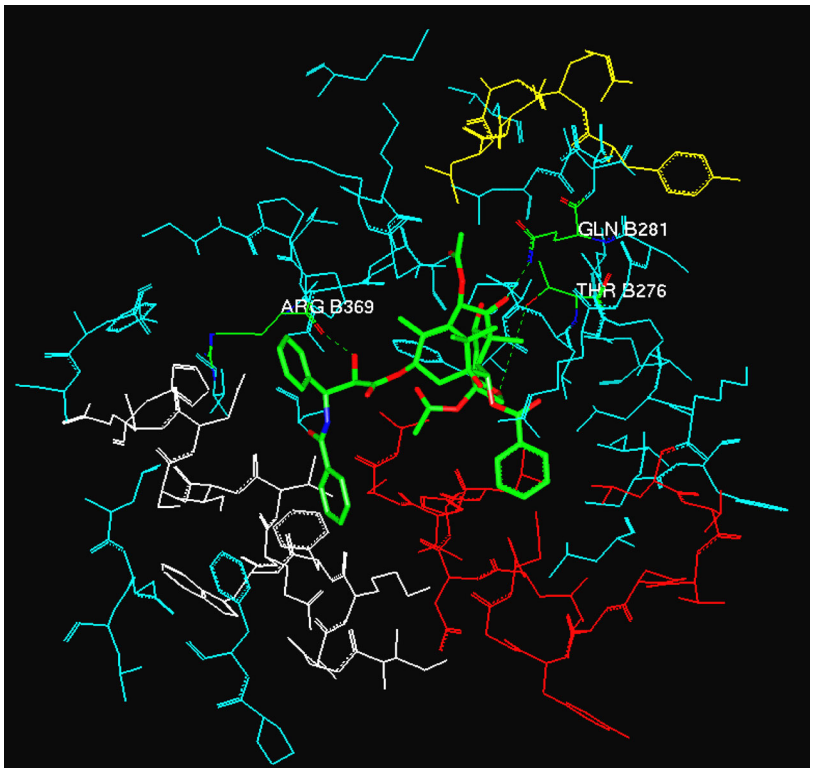

Figure 3-10. Proposed binding conformation of paclitaxel (by Raphael Geney)

Upon examining the conformation described above, we believe that the C4 acetyl group and the C2' carbon atom should be close in space; and the C14 position and the meta position of the C3' benzoyl group should also be close in distance. Accordingly, the C4-C2' linked and the C14-C3'Bz*N* taxoids were designed to mimic this conformation (**Figure 3-11**).

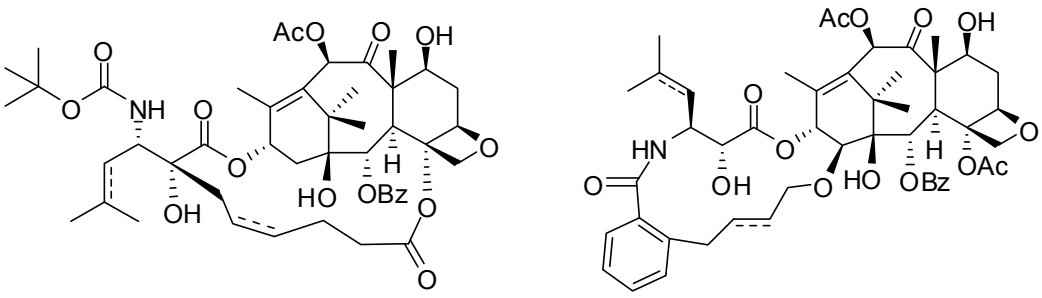

Figure 3-11. C4-C2' linked and C14-C3'Bz*N* linked macrocyclic taxoids

§3.2.2 Design and Synthesis of the C4-C2' Linked Macrocyclic Taxoid SB-TCR-101

The synthesis of **SB-TCR-101** required *a,β*-lactam with a quaternary carbon center which poses certain difficulties in the synthesis. The retro-synthetic analysis of **3-16** is shown in **Scheme 3-1**. Using the RCM protocol, macrocyclic taxoid can be obtained from diene **3-14**, which was prepared though ring-opening coupling of *β*-lactam **3-12** with modified baccatin **3-7**. [60]

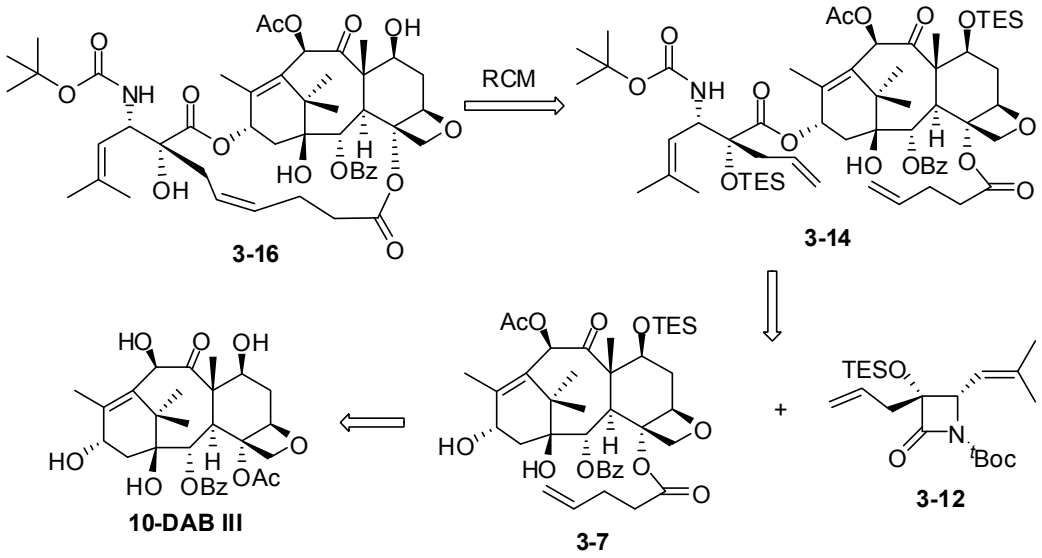

Scheme 3-1. Retro-synthetic analysis of macrocyclic taxoid **SB-TCR-101**

The C4 modification was carried out using a reported protocol with little modification. [61] To prevent concomitant C2 reduction, the coordination of Red-Al with the C1 hydroxy group was blocked. As shown in **Scheme 3-2**, 7, 10, 13-*tri*-TES-10-DAB was treated with chlorodimethylsilane in the presence of imidazole in DMF to protect the hydroxyl group at the C1 position. This protection successfully resulted in the specific coordination of Red-Al with the oxetane ring oxygen, and facilitated the selective reduction of the C4 acetate. [62] The obtained free hydroxy group was then reacted with LiHMDS and 4-pentenoyl chloride to afford C4-modified baccatin **3-4** in good yield.

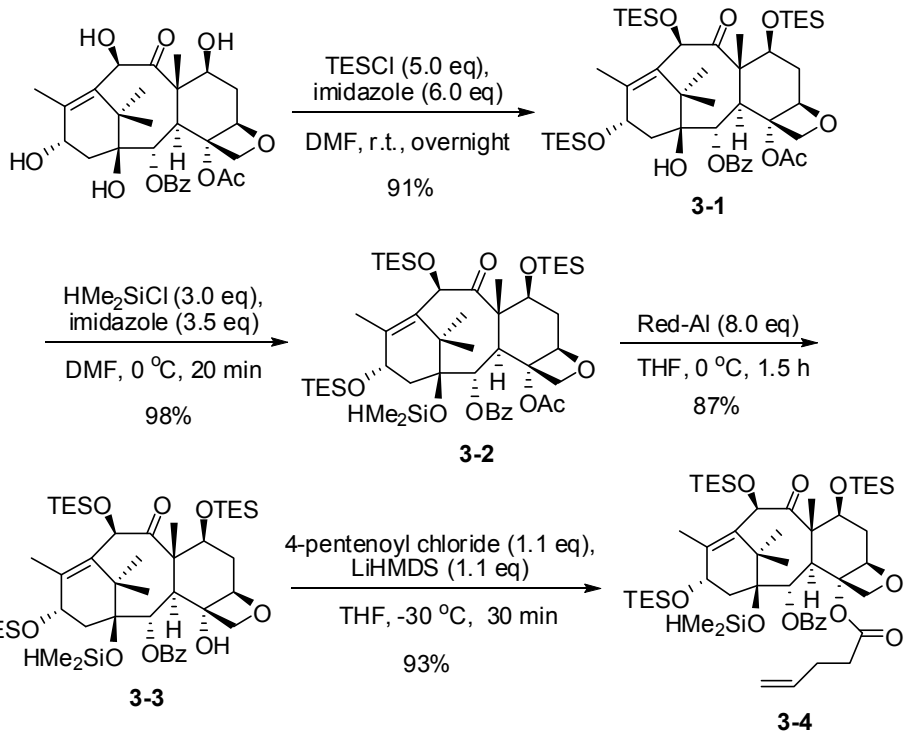

Scheme 3-2. Preparation of C4 modified baccatin **3-4**

The silyl groups of **3-4** were removed using HF-pyridine, followed by a selective 7-TES protection to afford baccatin **3-5** in 83% yield for two steps. Finally, C10 acylation of **3-5** using LiHMDS and acetyl chloride at -40 °C afforded desired baccatin **3-7**, as shown in **Scheme 3-3**.

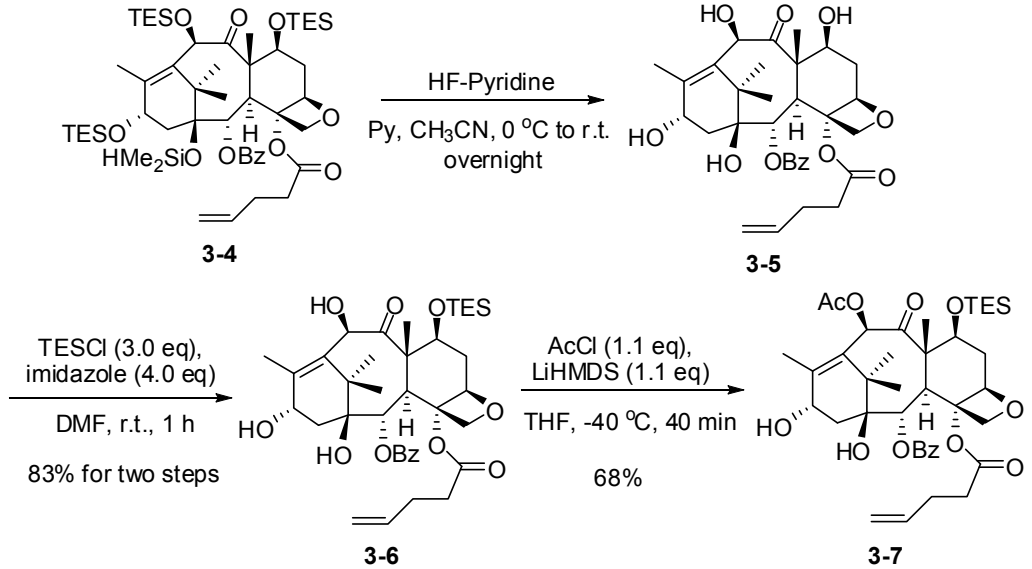

Scheme 3-3. Synthesis of modified baccatin **3-7**

The synthesis of C3 allyl-substituted *β*-lactam **3-12** was shown in **Scheme 3-4** following the Ojima-Holton coupling protocol. [63] The enatiopure *β*-lactam was synthesized by [2+2]

cycloaddition reaction followed by enzymatic resolution. Hydrolysis reaction gave free hydroxy group ready for the subsequent TES protection. Then, treatment of **3-9** with LDA followed by allyl bromide at low temperature gave the allylated *β*-lactam **3-10** in 58% yield. Standard oxidative removal of *p*-methoxyphenyl (PMP) group using cerium(IV) ammonium nitrate (CAN) followed by ^{t}Boc protection afforded desired *β*-lactam **3-12**.

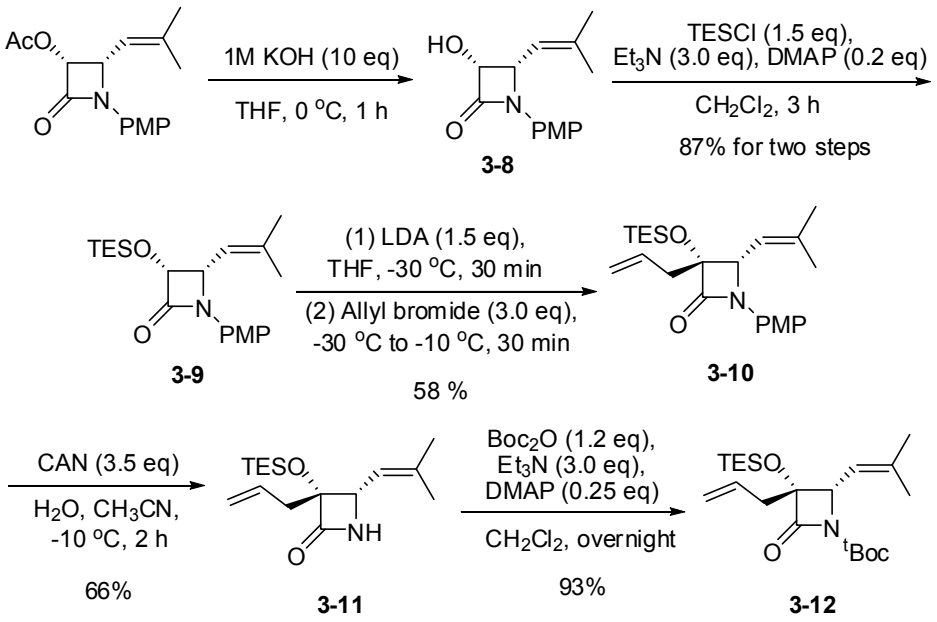

Scheme 3-4. Synthesis of *β*-lactam **3-12**

The allyl group at the C3 position of *β*-lactam **3-12** introduced extra steric hindrance in the coupling reaction. Accordingly, sodium bis(trimethylsilyl)amide (NaHMDS) was utilized instead of lithium bis(trimethylsilyl)amide (LiHMDS) as the base and 5 equivalents of *β*-lactam **3-12** was used. Desired diene **3-14** was obtained in 54% yield along with side product **3-13** in 25% yield, due to the steric hindrance of the C2 carbonyl group of *β*-lactam. Diene **3-14** was then subjected to RCM reaction to afford macrocyclic taxoid **3-15**. After HF-pyridine desilylation, the purification with flash column chromatography afforded **SB-TCR-101** (**3-16**) in 35% yield for two steps (**Scheme 3-5**).

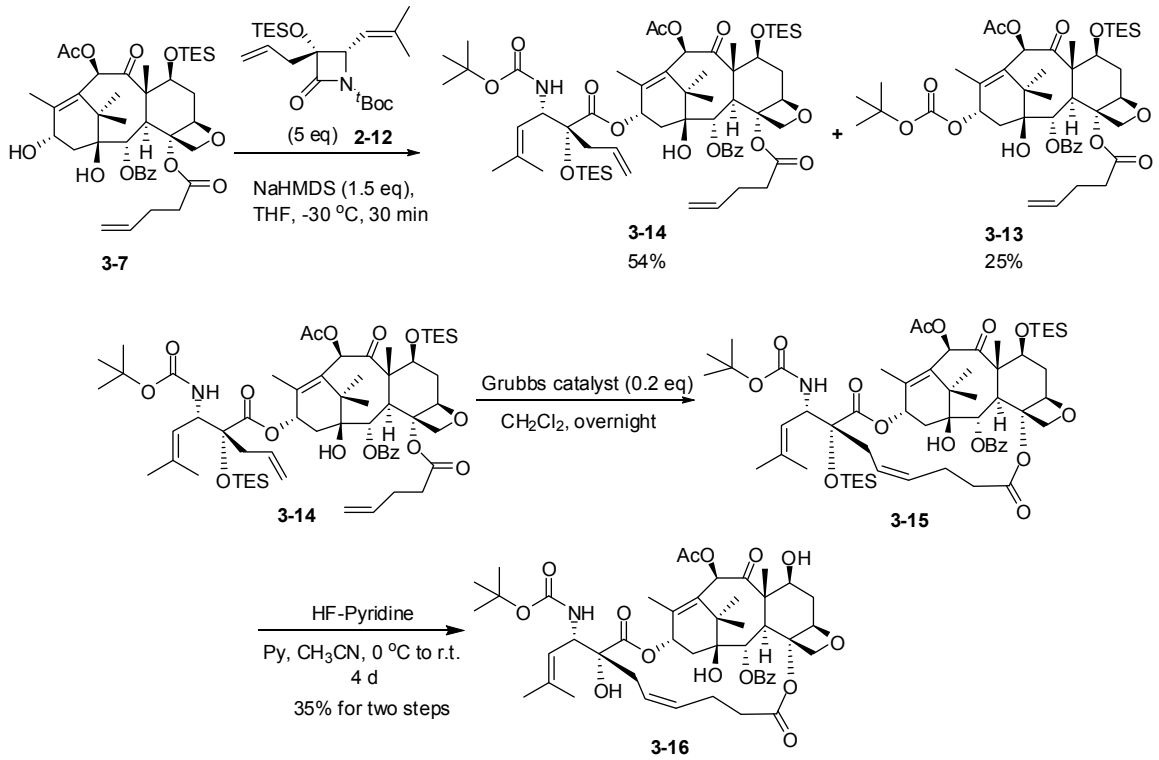

Scheme 3-5. Synthesis of **SB-TCR-101** (**3-16**)

§3.2.3 Biological Evaluations

SB-TCR-101 was synthesized and sent for *in vitro* evaluation to Dr. Ralph J. Bernacki's group (Department of Pharmacology and Therapeutics, Roswell Park Cancer Institute) with results shown in **Table 3-1**.

Table 3-1. Cytotoxicity of **SB-TCR-101** on MCF-7-S and MCR-7-R cell lines
Assay: SRB-96 well plate, solvent: DMSO, incubation: 72h

IC_{50} (nM)	MCF7-S	MCF7-R	R/S ratio
paclitaxel	0.7 ±.08	386 ±43	551
SB-TCR-101	8000 ±1000	22000 ±1800	2.8

.

Unfortunately, the compound did not possess comparable activity to paclitaxel. Modification to the original computational model was considered as necessary, and further studies led to a more validated bioactive conformer as described in the earlier section, known as "REDOR-Taxol".

§3.3 Design, Synthesis and Biological Evaluation of the C14-C3'Bz*N*-Linked Macrocyclic Taxoids SB-T-2055

In 1992, a novel taxane diterpenoid, 14*β*-hydroxy-10-deacetylbaccatin III (14*β*-OH-10-DAB, **Figure 3-12**), was isolated from the needles of *Taxus wallichiana Zucc.* as well as other plant parts. [64] This baccatin possesses an extra hydroxyl group at the C14*β* position, offering another modification site for the SAR studies as well as making it more water soluble than the usual 10-DAB III. Thus, the new anticancer taxoids derived from 14*β*-OH-10-DAB could be expected to have improved water solubility, bioavailability, and less hydrophobicity-related drug resistance.[65]

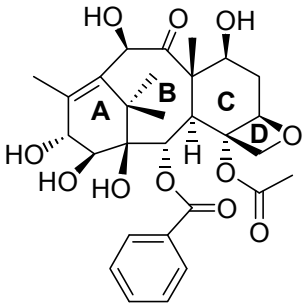

Figure 3-12. Structure of 14*β*-OH-10-DAB (14-OH-DAB)

§3.3.1 Introduction

Computational analysis of the "REDOR-Taxol" revealed that this structure could be rigidified by connecting the C14 position of the baccatin moiety and the ortho position of C3'*N*-benzoyl group, which are c.a. 7.5Å apart, with a short linker (4-6 atoms). Also, the same analysis indicated that the use of such linkers would not interfere with the amino acid residues in the paclitaxel binding site. Since the naturally occurring 14*β*-OH-10-deacetylbaccatin (14-OH-DAB) is readily available to us and we have performed substantial SAR studies on the taxoids derived from this material, we chose 14-OH-DAB as a key starting material for the synthesis of novel macrocyclic taxoids (**Figure 3-13**).

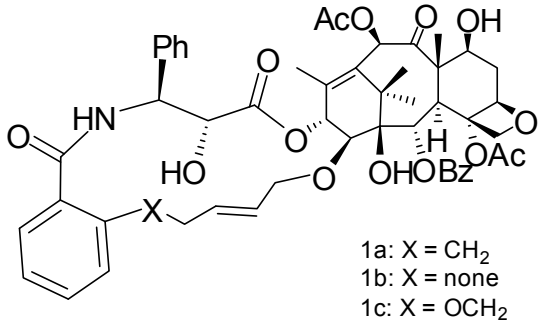

Figure 3-13. Designed novel C14-C3'Bz*N*-linked macrocyclic taxoids

As the overlays in **Figure 3-14** illustrate, the designed macrocyclic taxoids **1a** and **1c** appear

to mimic the REDOR-Taxol structure very well, while the C3'*N*-benzoyl group of **1b** deviates from the rest.

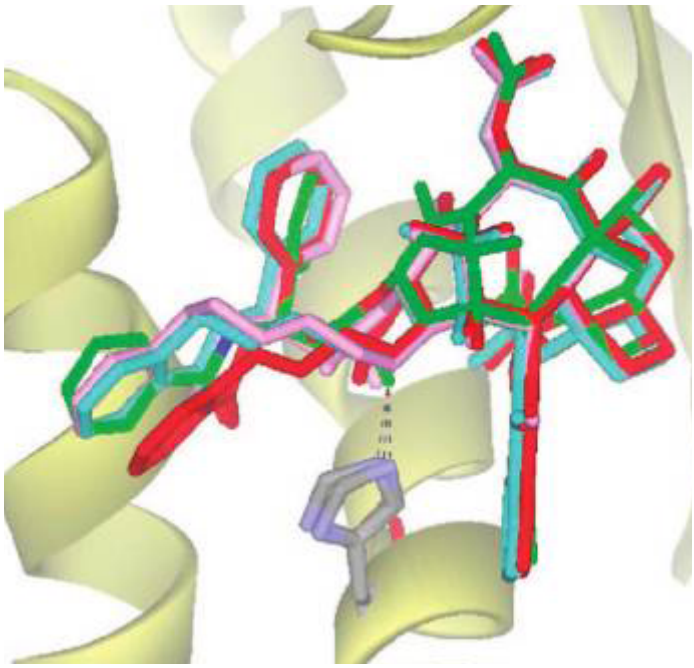

Figure 3-14. Overlays of REDOR-Taxol (green) with **1a** (cyan), **1b** (red), and **1c** (pink) [49]

§3.3.2 Design and Synthesis of the C14-C3'Bz*N* Linked Macrocyclic Taxoid SB-T-2055

The C14-C3'Bz*N* linked macrocyclic taxoid **SB-T-2055** was synthesized following the general protocol. [22] Ring Closing Metathesis (RCM) was introduced as the key step to generate the macrocycle. The diene substrate was obtained by using Ojima-Holton coupling protocol. The modified baccatin was synthesized using standard methods (**Scheme 3-6**). [22] C10 acetylation and C7 TES protection were utilized to give **3-18** in good yield. The following C14 coupling reaction successfully installed the terminal double bond which was essential for the RCM step.

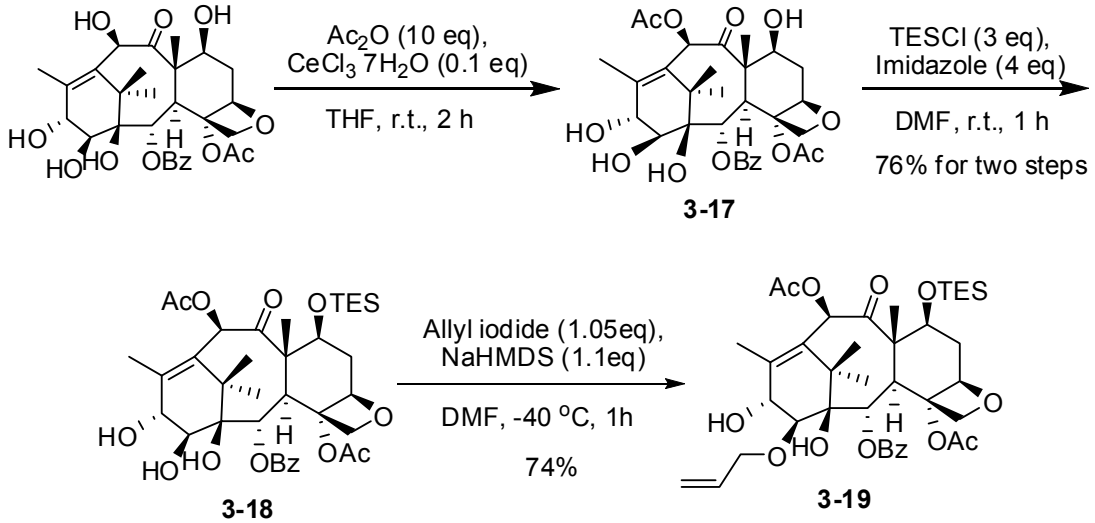

Scheme 3-6. Syntheses of modified Baccatin **3-19**

Following a reported method, [66] 2-allyloxybenzoyl chloride was synthesized (**Scheme 3-7**). Reflux of salicylic acid with potassium carbonate gave dianion, which reacted with allyl bromide to give desired ester. Hydrolysis of the ester yield 2-allyloxybenzoic acid (**3-20**), which was transformed into acid chloride by reflux with thionyl chloride.

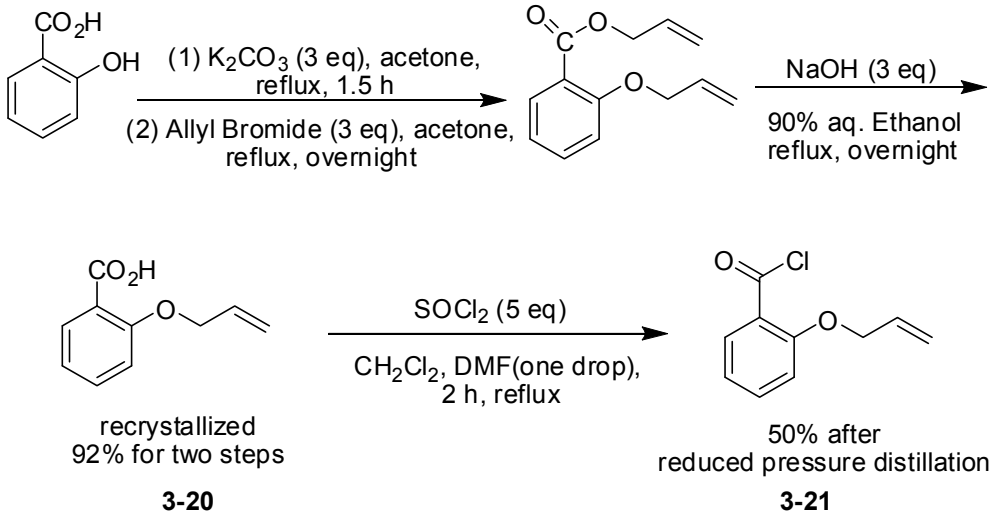

Scheme 3-7. Syntheses of modified 2-allyloxybenzoyl chloride

Theoretically, the *β*-lactam should tolerate different protected groups in C3 position. 2-Methoxypropyl group was firstly tried herein. The etherification of C3 hydroxyl group and subsequent acylation of NH gave the desired MOP-protected *β*-lactam **3-23** in high yield. However, the coupling of *β*-lactam **3-23** with modified baccatin **3-19** did not succeed (**Scheme 3-8**).

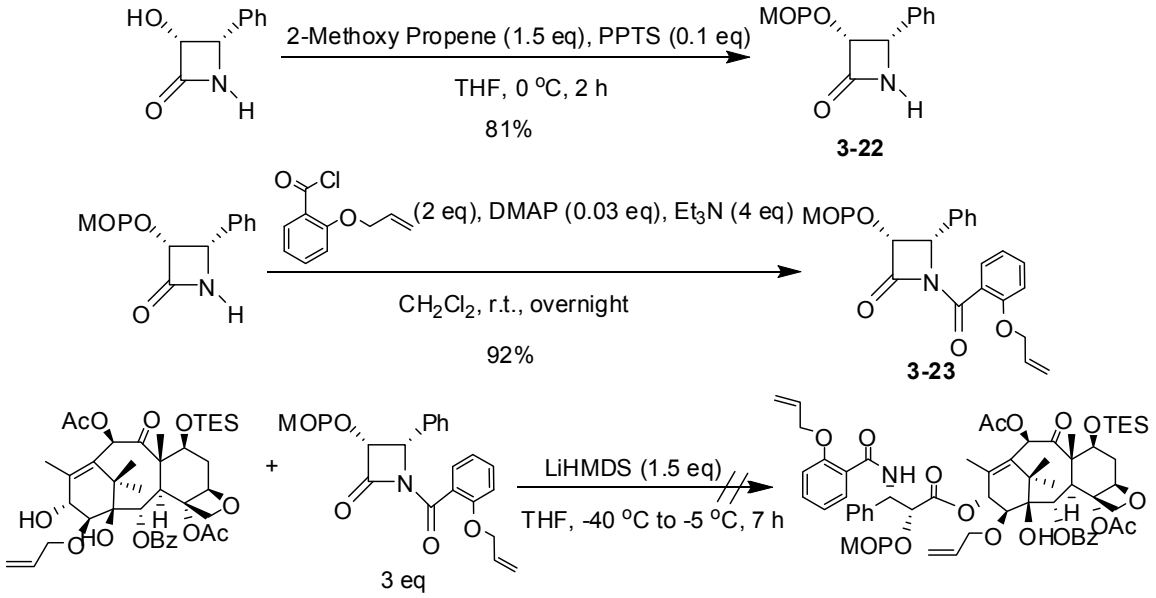

Scheme 3-8. Attempt of MOP-protected *β*-lactam

Common TES-protected *β*-lactam was utilized. The acylation gave desired *β*-lactam **3-24** in high yield. The coupling of *β*-lactam **3-24** with modified baccatin **3-19** succeeded to give desired diene **3-25** in 70% yield (**Scheme 3-9**).

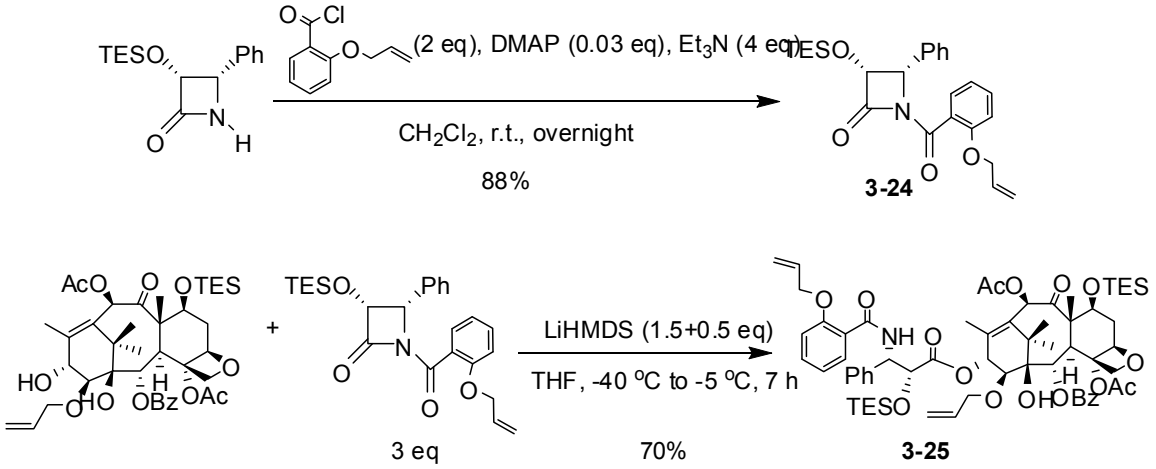

Scheme 3-9. Syntheses of diene **3-25**

RCM of diene **3-25** yielded two stereoisomers in 1:1 ratio, both of which were exposed to HF-pyridine condition to afford (*E*)- and (*Z*)- **SB-T-2055** (**Scheme 3-10**, **3-27a** and **3-27b**).

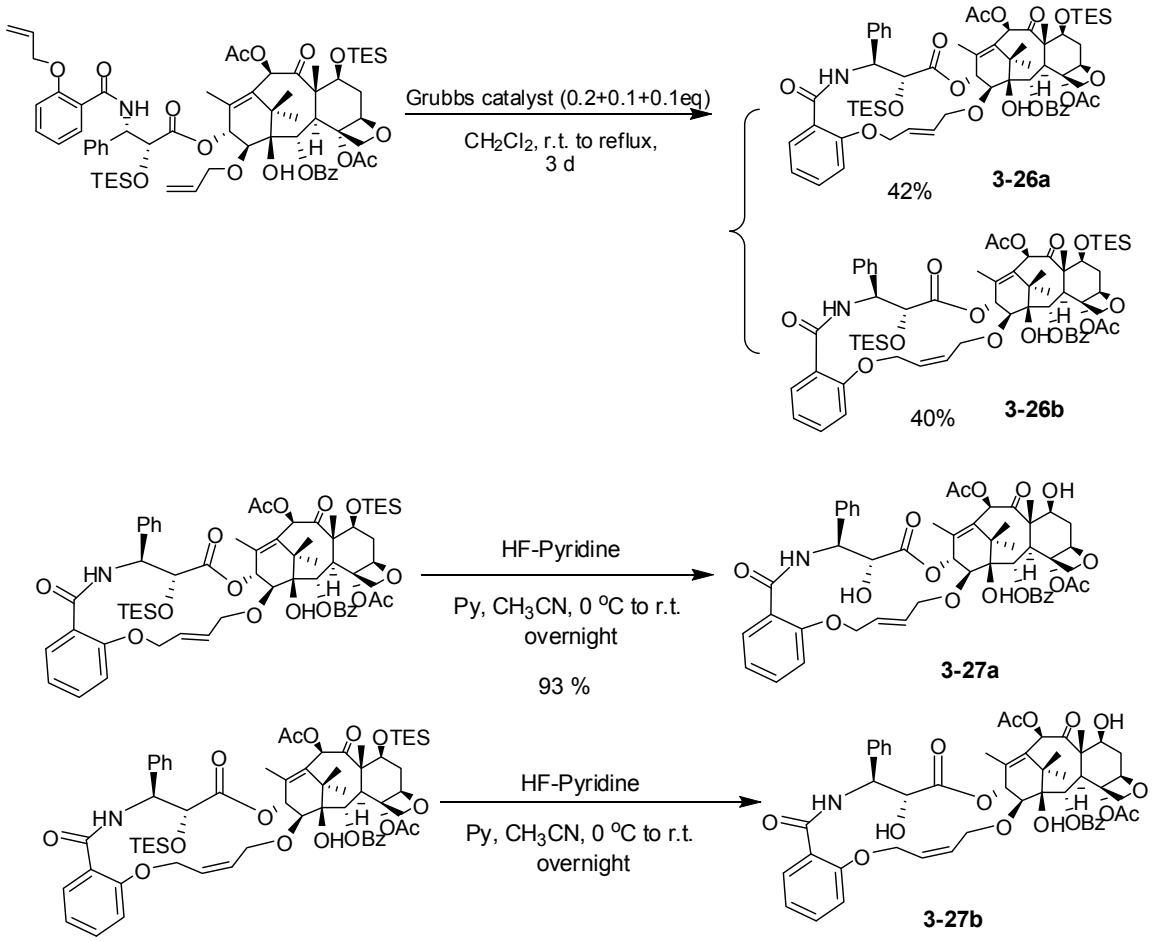

Scheme 3-10. Synthesis of (*E*)-**SB-T-2055** and (*Z*)-**SB-T-2055**

§3.3.3 *In vitro* Biological Evaluations

The synthesized (*E*)- and (*Z*)-**SB-T-2055** were sent to Dr. Bernacki's laboratory at Roswell Park Cancer Institute for cytotoxicity assays. The results were shown in **Table 3-2**. Both of the two macrocyclic taxoids were less active than paclitaxel, showing submicromolar level IC_{50}.

Table 3-2. *In vitro* activity of (*E*)-**SB-T-2055** and (*Z*)-**SB-T-2055**
MCF7-S: human breast cancer cell line; MCF7-R: MDR cell line

IC_{50} nM (±S.E.)	MCF7-S	MCF7-R	R/S Ratio
paclitaxel	1.4 ±.17	747 ±75	534
(*E*)-**SB-T-2055**	880 ± 120	8100 ±1000	9.2
(*Z*)-**SB-T-2055**	130 ± 20	3500 ± 210	27

Although the (*E*)-**SB-T-2055** and (*Z*)-**SB-T-2055** well overlay to the energy minimized structures of the REDOR-Taxol model, the Monte Carlo simulation (in 1JFF using the Macromodel program, MMFF94 force field33) show that their overall confirmations

substantially deviates from that of REDOR-Taxol due to the structural flexibility. The MD simulation analysis indicates that the conformational instability of the paclitaxel mimics needs to be addressed to improve their potency, besides structural over-simplification.

§3.4 Experimental Section

Materials

The chemicals were purchased from Sigma-Aldrich and/or Fisher Scientific and were used without further purification unless otherwise noted. 10-DAB III and 14β-hydroxy-10-deacetylbaccatin III were gift from Indena, SpA, Italy and used as received. Tetrahydrofuran, dichloromethane, toluene and ethyl ether were obtained from the PureSolv^{TM} Solvent Purification System (Innovative Technology, Inc.) under N_2. The glassware was dried in a 110 ^{o}C oven and allowed to cool to room temperature in a desiccator over "Drierite" (calcium sulfate).

General Methods

^{1}H, ^{13}C and ^{19}F NMR spectra were obtained on Varian 300, 400 or 500 NMR spectrometers. Melting points were measured on a Thomas Hoover Capillary melting point apparatus and are uncorrected. TLC was performed on Merck DC-alufolien with Kieselgel 60F-254 and flash column chromatography was carried out on silica gel 60 (Merck, 230-400 mesh ASTM). Optical rotations were measured on a Perkin-Elmer Model 241 polarimeter. IR spectra were measured on a Shimadzu FTIR-8400s spectrophotometer. Chemical purity was determined on Shimadzu LC-1020A, using a Phenomenex Curosil-B column (5μ, 4.6 × 250 mm), employing CH_3CN/water (40/60, V/V) as the eluent with a flow rate of 1 mL/min. Chiral HPLC analysis for the determination of enantiomeric excess was carried out on a Waters HPLC assembly consist of a Waters M45 solvent delivery system and a Waters 484 detector (at 254 nm) on a PC workstation running Millennium 32 using a DAICEL-CHIRACEL OD chiral column (25 × 0.46 cm), employing *n*-hexanes/isopropanol (95/5, V/V) as eluent with a flow rate of 1.0 mL/min. High resolution mass spectra were obtained from the Mass Spectrometry Laboratory, University of Illinois at Urbana-Champaign, Urbana, IL.

7,10,13-Tris(triethylsilyl)-10-deacetylbaccatin III (3-1) [67]

Under a nitrogen atmosphere, chlorotriethylsilane (0.43 mL, 2.5 mmol) was added dropwise to a solution of 10-DAB (275 mg, 0.5 mmol) and imidazole (208 mg, 3.0 mmol) in dry DMF (1 mL) at room temperature. The reaction mixture was stirred for overnight at room temperature, quenched with saturated aqueous NH_4Cl solution (10 mL) and diluted with EtOAc (150 mL). The mixture was then washed with water (20 mL × 3) and brine (20 mL), dried over anhydrous $MgSO_4$ and concentrated *in vacuo*. Flash column chromatography on silica gel (Hexanes/EtOAc = 15/1) gave **3-1** (408 mg, 91%) as a white solid: mp 187-189 °C; ^{1}H NMR (300 MHz, $CDCl_3$) δ 0.65 (m, 18 H), 0.99 (m, 27 H), 1.11 (s, 3 H), 1.18 (s, 3 H),1.64 (s, 3 H), 1.87 (m, 1 H), 1.97 (s, 3 H), 2.08 (dd, J = 15.2, 8.8 Hz, 1 H), 2.21 (dd, J = 15.1, 8.2 Hz, 1 H), 2.27 (s, 3 H), 2.51 (m, 1 H), 3.84 (d, J = 7.0 Hz, 1 H), 4.13 (d, J = 8.3 Hz, 1 H), 4.27 (d, J = 8.3 Hz, 1 H), 4.40 (dd, J = 10.5, 6.6 Hz, 1 H), 4.92 (m, 2 H), 5.18 (s, 1 H), 5.61 (d, J = 7.1 Hz, 1 H), 7.44 (t, J = 7.3 Hz, 2 H), 7.57 (t, J = 7.3 Hz, 1 H) and 8.07 (d, J = 7.4 Hz, 1 H) ppm; ^{13}C NMR (75 MHz, $CDCl_3$) δ 4.7, 5.2, 5.9, 6.9, 10.4, 14.8, 20.5, 22.4, 26.3, 37.3, 19.8, 42.4, 46.8, 58.2, 68.3, 72.6, 75.4, 75.7, 76.6, 79.5, 80.7, 83.9, 128.5, 129.6, 130.0, 133.4, 135.7, 139.3, 167.1, 169.7 and 205.6 ppm; $[\alpha]_D^{20}$ -38.8 (c 0.28, $CHCl_3$). All data are in agreement with literature values. [67]

Dimethylsilyl-7,10,13-tris(triethylsilyl)-10-deacetylbaccatin III (3-2)

Under a nitrogen atmosphere, chlorodimethylsilane (0.086 mL, 0.66 mmol) was added to a

solution of **3-1** (197 mg, 0.22 mmol) and imidazole (53 mg, 0.77 mmol) in dry DMF (3.5 mL) at 0 °C. The mixture was stirred at 0 °C for 20 min and the reaction was quenched with saturated aqueous NH_4Cl solution (10 mL) and diluted with EtOAc (100 mL). The organic layer was washed with H_2O (10 mL × 3) and brine (10 mL), dried over anhydrous $MgSO_4$ and concentrated *in vacuo*. Flash column chromatography on silica gel (Hexanes/EtOAc = 15/1) gave **3-2** (206 mg, 98%) as a white solid: mp 85-87 °C; ^{1}H NMR (300 MHz, $CDCl_3$) δ -0.31 (d, J = 2.6 Hz, 3 H), 0.04 (d, J = 2.5 Hz, 1 H), 0.51-0.72 (m, 18 H), 0.88-1.63 (m, 27 H), 1.13 (s, 3 H), 1.22 (s, 3 H), 1.63 (s, 3 H), 1.68 (s, 3 H), 1.95 (m, 1 H), 2.01 (s, 3 H), 2.70 (m, 2 H), 2.32 (s, 3 H), 2.50 (m, 1 H), 3.88 (d, J = 6.9 Hz, 1 H), 4.26 (br s, 2 H), 4.34 (dd, J = 3.6, 2.9 Hz, 1 H), 4.56 (m, 1 H), 5.00 (m, 2 H), 5.20 (s, 1 H), 5.74 (d, J = 6.6 Hz, 1 H), 7.44 (m, 2 H), 7.55 (m, 1 H) and 8.08 (m, 2 H) ppm; ^{13}C NMR (75 MHz, $CDCl_3$) δ -0.3, 0.1, 4.1, 4.6, 5.0, 5.2, 5.5, 5.8, 6.2, 6.6, 6.7, 10.1, 13.9, 14.2, 20.6, 21.1, 22.1, 27.0, 37.2, 39.1, 43.8, 46.4, 58.0, 60.0, 68.2, 72.5, 75.5, 75.6, 76.3, 80.8, 81.8, 83.8, 128.1, 129.8, 130.3, 132.9, 135.7, 138.4, 165.1, 167.3, 168.1, 169.6 and 205.2 ppm; HRMS (FAB) m/z calcd. for $C_{49}H_{84}O_{10}Si_4H^+$: 945.5220, found: 945.5220 (Δ = -0.2 ppm). All data are in agreement with literature values. [67]

Dimethylsilyl-4-deacetyl-7,10,13-tris(triethylsilyl)-10-deacetylbaccatin (3-3)

Under a nitrogen atmosphere, Red-Al (3.5 M in toluene, 0.51 mL, 1.76 mmol) was added to a solution of **3-2** (210 mg, 0.22 mmol) in dry THF (4 mL) at 0 °C and the mixture was stirred for 2 h. The reaction was quenched with saturated aqueous NH_4Cl solution (5 mL) and extracted with EtOAc (50 mL × 3). The organic layer was washed with H_2O (5 mL × 3) and brine (5 mL), dried over anhydrous $MgSO_4$ and concentrated *in vacuo*. Flash column chromatography on silica gel (Hexanes/EtOAc = 10/1) gave **3-3** (174 mg, 87%) as a white solid: mp 86-88 °C; ^{1}H NMR (300 MHz, $CDCl_3$) δ -0.32 (d, J = 2.7 Hz, 3 H), 0.00 (d, J = 3.0 Hz, 1 H), 0.51-0.70 (m, 18 H), 0.86-1.09 (m, 27 H), 1.09 (s, 3 H), 1.17 (s, 3 H), 1.54 (s, 3 H), 1.94 (s, 3 H), 1.99-2.04 (m, 1 H), 2.39-2.58 (m, 2 H), 2.80 (dd, J = 15.3, 2.1 Hz, 1 H), 3.59 (d, J = 5.4 Hz, 1 H), 3.81 (br s, 1 H), 4.01 (dd, J = 11.7, 5.7 Hz, 1 H), 4.20 (d, J = 7.5, 1 H), 4.29 (d, J = 7.5, 1 H), 4.56 (dd, J = 5.4, 2.7 Hz, 1 H), 4.64 (m, 1 H), 4.67 (d, J = 3.6 Hz, 1 H), 5.21 (s, 1 H), 5.59 (d, J = 5.1 Hz, 1 H), 7.42 (m, 2 H), 7.54 (m, 1 H) and 8.13 (m, 2 H) ppm; ^{13}C NMR (75 MHz, $CDCl_3$) δ 0.2, 0.6, 4.6, 5.1, 5.9, 6.7, 6.8, 6.9, 9.9, 17.0, 18.3, 29.9, 37.6, 38.3, 42.9, 51.5, 59.2, 69.9, 73.0, 73.5, 74.7, 76.4, 79.5, 80.2, 88.3, 128.2, 130.2, 132.9, 135.6, 140.3, 165.0 and 205.5 ppm; HRMS (FAB) m/z calcd for $C_{47}H_{82}O_9Si_4H^+$: 903.5114, found: 903.5110 (Δ = 0.5 ppm).

Dimethylsilyl-4-deacetyl-4-(4-pentenoyl)-7,10,13-tris(triethylsilyl)-10-deacetyl-baccatin III (3-4)

Under a nitrogen atmosphere, LiHMDS (1.0 M in THF, 0.15 mL, 0.15 mmol) was added to a solution of **3-3** (123 mg, 0.14 mmol) in dry THF (2 mL) at -30 °C. 4-pentenoyl chloride (0.016 mL, 0.15 mmol) was added after 5 min and the reaction mixture was stirred at -30 °C for 30 min. The reaction mixture was quenched with saturated aqueous NH_4Cl solution (5 mL) and extracted with EtOAc (50 mL × 3). The organic layer was washed with H_2O (5 mL × 3) and brine (5 mL), dried over anhydrous $MgSO_4$ and concentrated *in vacuo*. Flash column chromatography on silica gel (Hexanes/EtOAc = 20/1) gave **3-4** (124 mg, 93%) as a white solid: mp 132-134 °C; ^{1}H NMR (300 MHz, $CDCl_3$) δ -0.30 (d, J = 2.7 Hz, 3 H), 0.05 (d, J = 3.0 Hz, 1 H), 0.53-0.73 (m, 18 H), 0.85-1.02 (m, 27 H), 1.10 (s, 3 H), 1.18 (s, 3 H), 1.65 (s, 3 H), 1.82-1.91 (m, 1 H), 1.96 (s, 3 H), 2.20-2.37 (m, 2 H), 2.45-2.56 (m, 3 H), 2.60-2.80 (m, 2 H), 3.82 (d, J = 6.9 Hz, 1 H), 4.22 (m, 2 H), 4.38 (dd, J = 10.5, 6.6 Hz, 1 H), 4.52 (m, 1 H), 4.87 (d, J = 7.8, 1 H), 4.95 (d, J = 9.9, 1 H),

5.08-5.19 (m, 2 H), 5.70 (d, J = 6.9 Hz, 1 H), 5.84-5.98 (m, 1 H), 7.45 (m, 2 H), 7.57 (m, 1 H) and 8.10 (m, 2 H) ppm; ^{13}C NMR (75 MHz, $CDCl_3$) δ 0.0, 0.3, 4.8, 4.9, 5.2, 6.0, 6.8, 6.9, 10.4, 14.3, 21.5, 27.3, 29.0, 34.5, 37.3, 39.3, 44.0, 46.6, 58.2, 68.3, 72.6, 75.6, 75.9, 76.5, 76.6, 81.1, 82.0, 84.2, 116.0, 128.3, 130.1, 130.5, 133.1, 135.9, 136.2, 138.5, 165.3, 171.6 and 205.5 ppm; HRMS (FAB) m/z calcd for $C_{52}H_{88}O_{10}Si_4H^+$: 985.5533, found: 985.5530 (Δ = 0.3 ppm).

7-Triethylsilyl-4-deacetyl-4-(4-pentenoyl)-10-deacetylbaccatin (3-6)

Under a nitrogen atmosphere, HF-pyridine (70:30, 2.5 mL) was added dropwise to a solution of **3-4** (124 mg, 0.12 mmol) in pyridine/acetonitrile (10 mL, V/V = 1:1) at 0 °C, and the mixture was stirred for overnight. The reaction was quenched with a saturated aqueous $NaHCO_3$ solution (5 mL). The mixture was then diluted with EtOAc (100 mL), washed with saturated $NaHCO_3$ aqueous solution (10 mL × 3), saturated $CuSO_4$ aqueous solution (10 mL × 3), H_2O (10 mL × 3) and brine (10 mL). The combined organic layer was dried over anhydrous $MgSO_4$ and concentrated *in vacuo* to afford crude **3-5** as a white solid.

Under a nitrogen atmosphere, chlorotriethylsilane (0.06 mL, 0.38 mmol) was added dropwise to a solution of **3-5** thus obtained (80 mg, crude) and imidazole (34 mg, 0.50 mmol) in dry DMF (2 mL) at room temperature. The reaction mixture was stirred for 1 h at room temperature and diluted with EtOAc (100 mL). The mixture was then washed with H_2O (15 mL × 3), brine (10 mL), dried over $MgSO_4$ and concentrated *in vacuo*. Flash column chromatography on silica gel (Hexanes/EtOAc = 3/1) gave **3-6** (73 mg, 83%) as a white solid: mp 120-122 °C; ^{1}H NMR (300 MHz, $CDCl_3$) δ 0.50-0.59 (m, 6 H), 0.87-0.95 (m, 9 H), 1.06 (br s, 6 H), 1.30 (m, 1 H), 1.72 (s, 3 H), 1.85 (m, 1 H), 2.05 (s, 3 H), 2.30 (m, 2 H), 2.48 (m, 3 H), 2.66 (m, 2 H), 3.93 (d, J = 6.6 Hz, 1 H), 4.15 (d, J = 8.1 Hz, 1 H), 4.29 (d, J = 8.1 Hz, 1 H), 4.40 (dd, J = 10.5, 6.3 Hz, 1 H), 4.83 (t, J = 7.5 Hz, 1 H), 4.90 (d, J = 9.0 Hz, 1 H), 5.08 (m, 2 H), 5.16 (s, 1 H), 5.58 (d, J = 7.2 Hz, 1 H), 5.84-5.95 (m, 1 H), 7.46 (m, 2 H), 7.60 (m, 1 H) and 8.10 (m, 2 H) ppm; ^{13}C NMR (75 MHz, $CDCl_3$) δ 5.1, 6.7, 9.9, 15.0, 19.5, 26.7, 28.7, 34.5, 37.2, 38.7, 42.6, 47.0, 57.9, 67.7, 72.8, 74.6, 74.8, 78.7, 80.6, 84.3, 115.7, 128.5, 129.4, 130.0, 133.5, 134.9, 136.6, 142.0, 166.9, 172.3 and 210.3 ppm; HRMS (FAB) m/z calcd for $C_{38}H_{54}O_{10}SiH^+$: 699.3564, found: 699.3562 (Δ = 0.4 ppm).

7-Triethylsilyl-4-deacetyl-4-(4-pentenoyl)baccatin (3-7)

Under a nitrogen atmosphere, LiHMDS (1.0 M in THF, 0.11 mL, 0.11 mmol) and AcCl (8 μL, 0.11 mmol) were successively added to a solution of **3-6** (73 mg, 0.10 mmol) in dry THF (5 mL) at -40 °C. The reaction mixture was stirred for 40 min, then quenched with a saturated NH_4Cl aqueous solution (5 mL) and extracted with EtOAc (50 mL × 3). The organic layer was washed with H_2O (5 mL × 3) and brine (5 mL), dried over anhydrous $MgSO_4$ and concentrated *in vacuo*. Flash column chromatography on silica gel (Hexanes/EtOAc = 5/1) gave **3-7** (73 mg, 83%) as a white solid: mp 114-116 °C; ^{1}H NMR (300 MHz, $CDCl_3$) δ 0.58 (m, 6 H), 0.92 (m, 9 H), 1.03 (s, 3 H), 1.19 (s, 3 H), 1.62 (s, 3 H), 1.87 (dt, J = 12.4, 2.0 Hz, 1 H), 2.03 (d, J = 5.2 Hz, 1 H), 2.17 (s, 3 H), 2.26 (m, 2 H), 2.51 (m, 3 H), 2.68 (t, J = 8.0 Hz, 2 H), 3.87 (d, J = 7.2 Hz, 1 H), 4.14 (d, J = 8.0 Hz, 1 H), 4.30 (d, J = 8.0, 1 H), 4.49 (d, J = 6.8 Hz, 1 H), 4.82 (m, 1 H), 4.91 (d, J = 7.6 Hz, 1 H), 5.07 (dd, J = 9.2, 1.2 Hz, 1 H), 5.14 (d, J = 14.0 Hz, 1 H), 5.63 (d, J = 7.2 Hz, 1 H), 5.91 (m, 1 H), 6.45 (s, 2 H), 7.47 (t, J = 7.6 Hz, 2 H), 7.60 (t, J = 7.6 Hz, 1 H) and 8.11 (d, J = 7.2 Hz, 2 H) ppm; ^{13}C NMR (75 MHz, $CDCl_3$) δ 5.5, 7.0, 10.2, 15.1, 20.3, 21.2, 27.0, 29.0, 34.9, 37.5, 38.5, 43.0, 47.6, 58.9, 68.2, 72.6, 75.0, 76.0, 76.8, 79.0, 81.1, 84.5, 116.1, 128.8, 129.6, 130.3, 132.9, 133.9, 136.9, 144.1, 167.3, 169.6, 172.7 and 202.4 ppm; HRMS

(FAB/DCM/NaCl) m/z calcd for $C_{40}H_{56}O_{11}Si_3H^+$: 741.3670, found: 741.3668 (Δ = 0.2 ppm).

(3*R*,4*S*)-1-(4-Methoxyphenyl)-3-triethylsilyloxy-4-(2-methylpropen-1-yl)azetidin-2-one (3-9) [68]

To a solution of THF (8 mL) and aqueous KOH solution (1 M, 12 mL) was added a solution of **(+)-1-18** (336 mg, 1.16 mmol) in dry THF (12 mL). The solution was stirred for 1 h at 0 °C and quenched with saturated NH_4Cl solution (5 mL). The mixture was extracted with EtOAc (50 mL × 4). The combined organic layers were washed with brine (15 mL), dried over anhydrous $MgSO_4$ and concentrated *in vacuo* to give **3-8** (297 mg, crude) as a white solid.

Under a nitrogen atmosphere, triethylamine (0.5 mL, 3.6 mmol) and TESCl (0.30 mL, 1.8 mmol) were added to a solution of **3-8** (297 mg, crude) thus obtained and DMAP (30 mg, 0.24 mmol) in dry CH_2Cl_2 (10 mL). The reaction mixture was stirred at room temperature for 2 h, quenched with saturated NH_4Cl aqueous solution (10 mL), and extracted with EtOAc (30 mL × 3). The organic layer was washed with brine (10 mL), dried with anhydrous $MgSO_4$ and concentrated *in vacuo*. Flash column chromatography on silica gel (Hexanes/EtOAc = 10/1) gave **3-9** (364 mg, 87% for two steps) as a white solid: ^{1}H NMR (300 MHz, $CDCl_3$) δ 0.64-0.73 (m, 6 H), 0.99-1.02 (m, 9 H), 1.84 (d, J = 1.5 Hz, 3 H), 1.89 (d, J = 1.5 Hz, 3 H), 3.81 (s, 1 H), 4.82 (dd, J = 9.6, 4.8 Hz, 1 H), 5.01 (d, J = 4.8 Hz, 1 H), 5.33 (d, J = 9.6 Hz, 1 H), 6.88 (m, 2 H) and 7.35 (m, 2 H) ppm.

(3*R*,4*S*)-1-(4-Methoxyphenyl)-3-triethylsilyloxy-3-allyl-4-(2-methylpropen-1-yl)azetidin-2-one (3-10)

Under a nitrogen atmosphere, *n*-butyllithium (2.5 M in *n*-hexane, 0.56 mL, 1.4 mmol) was added to a solution of diisopropylamine (0.20 mL, 1.4 mmol) in dry THF (5 mL) at -20 °C and the mixture was stirred for 20 min at the same temperature. The solution was then cooled down to -30 °C and a solution of *β*-lactam **3-9** (339 mg, 0.94 mmol) in THF (3 mL) was added slowly via cannula. The reaction mixture was stirred at -30 °C for 30 min and allyl bromide (0.246 mL, 2.8 mmol) was added, and then the rection mixture was warmed up to -10 °C. The reaction was quenched with saturated NH_4Cl aqueous solution (10 mL) and extracted with EtOAc (30 mL × 3). The combined organic layer was washed with brine (10 mL), dried over anhydrous $MgSO_4$ and concentrated *in vacuo*. Flash column chromatography on silica gel (Hexanes/EtOAc = 50/1) gave **3-10** (218 mg, 58%) as a colorless oil: ^{1}H NMR (300 MHz, $CDCl_3$) δ 0.60-0.80 (m, 6 H), 0.85-1.05 (m, 9 H), 1.79 (s, 3 H), 2.59 (m, 2 H), 3.77 (s, 3 H), 4.56 (d, J = 9.3 Hz, 1 H), 5.15 (m, 2 H), 5.83 (m, 1 H), 6.84 (d, J = 8.9 Hz, 2 H) and 7.32 (d, J = 8.9 Hz, 2 H) ppm; ^{13}C NMR (62.9 MHz, $CDCl_3$) δ 5.9, 6.9, 18.5, 25.1, 41.2, 55.5, 60.9, 86.8, 114.3, 118.5, 118.8, 120.4, 131.3, 132.5, 138.8, 156.1 and 166.8 ppm; $[\alpha]_D^{20}$ +13.9 (c 0.36, $CHCl_3$).

(3*R*,4*S*)-3-triethylsilyloxy-3-allyl-4-(2-methylpropen-1-yl)azetidin-2-one (3-11)

To a solution of **3-10** (218 mg, 0.54 mmol) in acetonitrile (12 mL) at -10 °C was added cerium ammonium nitrate (CAN) (1.06 g, 1.89 mmol) in H_2O (10 mL) dropwise via addition funnel. The reaction mixture was stirred for 2 h at the same temperature and the reaction was quenched with saturated Na_2SO_3 aqueous solution. The mixture was filtered over celite, and extracted with EtOAc (50 mL × 3) and the combined organic layers were washed with brine (15 mL), dried over anhydrous $MgSO_4$ and concentrated *in vacuo*. Flash column chromatography on silica gel (Hexanes/EtOAc = 5/1) gave **3-11** (105 mg, 66%) as a white solid: ^{1}H NMR (250 MHz, $CDCl_3$) δ 0.64-0.73 (m, 6 H), 0.95 (m, 9 H), 1.64 (s, 3 H), 1.75 (s, 3 H), 2.50 (m, 2 H), 4.20 (d, J

= 8.8 Hz, 1 H), 5.13 (m, 2 H), 5.80 (m, 1 H) and 5.97 (br s, 1 H) ppm; ^{13}C NMR (62.9 MHz, $CDCl_3$) δ 5.8, 6.9, 18.4, 26.1, 41.1, 56.8, 88.7, 118.7, 121.7, 132.5, 137.8 and 170.8 ppm; HRMS (CI) m/z calcd for $C_{16}H_{29}O_2NSiH^+$: 296.2032, found: 296.2046 (Δ = 4.7 ppm); $[\alpha]_D^{20}$ +12.5 (c 0.08, $CHCl_3$).

(3*R*,4*S*)-1-*tert*-Butoxycarbonyl-3-triethylsilyloxy-3-allyl-4-(2-methylpropen-1-yl)azetidin-2-one (3-12)

Under a nitrogen atmosphere, di-*tert*-butyl dicarbonate (89 mg, 0.39 mmol) in dry CH_2Cl_2 (1 mL) was added to a solution of **3-11** (105 mg, 0.357 mmol), DMAP (11 mg, 0.089 mmol) and triethylamine (0.15 mL, 1.07 mmol) in dry CH_2Cl_2 (3 mL) at room temperature. The reaction mixture was stirred overnight and quenched with saturated NH_4Cl aqueous solution (4 mL). The reaction mixture was extracted with EtOAc (50 mL × 3). The organic layer was washed with brine (10 mL), dried over $MgSO_4$ and concentrated *in vacuo*. Flash column chromatography on silica gel (Hexanes/EtOAc = 50/1) gave **3-12** (131 mg, 93%) as a clear oil: ^{1}H NMR (250 MHz, $CDCl_3$) δ 0.63-0.72 (m, 6 H), 0.91-0.96 (m, 9 H), 1.48 (s, 9 H), 1.70 (s, 3 H), 1.78 (s, 3 H), 2.47 (dd, J = 14.1, 7.2 Hz, 1 H), 2.50 (dd, J = 14.1, 7.2 Hz, 1 H), 4.48 (d, J = 9.3 Hz, 1 H), 5.12-5.23 (m, 2 H) and 5.72-5.85 (m, 1 H) ppm; ^{13}C NMR (62.9 MHz, $CDCl_3$) δ 5.7, 6.7, 18.3, 26.0, 27.9, 40.9, 60.4, 83.0, 86.7, 119.1, 119.5, 131.6, 139.1, 148.4 and 169.7 ppm; HRMS (CI) m/z calcd for $C_{21}H_{37}O_4NSiNH_4^+$: 413.2815, found: 413.2836 (Δ = 5.0 ppm); $[\alpha]_D^{20}$ +18.1 (c 2.6, $CHCl_3$).

10-Acetyl-4-deacetyl-4-(pent-4-enoyl)-7-triethylsilyl-2'-allyl-2'-triethylsilyl-3'-dephenyl-3'-(2-methylpropenyl)docetaxel (3-14)

Under a nitrogen atmosphere, NaHMDS (1.0 M in THF, 0.11 mL, 0.11 mmol) was added to a solution of **3-7** (50 mg, 0.067 mmol) and *β*-lactam **3-12** (131 mg, 0.33 mmol) in dry THF (6 mL) at -30 °C. The reaction mixture was stirred for 30 min and quenched with saturated NH_4Cl aqueous solution (10 mL). The mixture was extracted with EtOAc (40 mL × 3). The combined organic layer was washed with brine (15 mL), dried over anhydrous $MgSO_4$ and concentrated *in vacuo*. Flash column chromatography on silica gel (Hexanes/EtOAc = 12/1) gave **3-14** (43 mg, 54%) as a white solid: mp 105-108 °C; ^{1}H NMR (300 MHz, $CDCl_3$) δ 0.53-0.61 (m, 6 H), 0.66-0.75 (m, 6 H), 0.85-0.99 (m, 18 H), 1.26 (m, 15 H), 1.64-1.70 (m, 6 H), 1.75 (s, 3 H), 1.76 (s, 3 H), 1.82-1.90 (m, 1 H), 1.96 (s, 3 H), 2.18 (s, 3 H), 2.20-2.32 (m, 2 H), 2.50-2.60 (m, 5 H), 3.77 (d, J = 7.2 Hz, 1 H), 4.20 (d, J = 7.8 Hz, 1 H), 4.29 (d, J = 7.8 Hz, 1 H), 4.40-4.46 (m, 1 H), 4.55-4.68 (m, 2 H), 4.86 (d, J = 9.6 Hz, 1 H), 5.07-5.24 (m, 5 H), 5.69 (d, J = 7.2 Hz, 1 H), 5.75-5.94 (m, 2 H), 6.16 (t, J = 9.6 Hz, 1 H), 6.45 (s, 1 H), 7.45-7.50 (m, 2 H), 7.58-7.63 (m, 1 H) and 8.15-8.17 (m, 2 H) ppm; ^{13}C NMR (75.0 MHz, $CDCl_3$) δ 5.3, 5.8, 6.9, 7.1, 7.4, 10.2, 14.6, 18.9, 20.9, 22.1, 26.0, 26.9, 28.2, 29.8, 35.1, 35.7, 37.2, 41.5, 43.4, 46.4, 54.9, 58.3, 72.2, 72.5, 74.9, 75.1, 76.6, 79.2, 81.1, 83.5, 84.4, 116.6, 119.3, 121.3, 128.5, 129.4, 130.4, 132.3, 133.5, 135.5, 136.6, 141.1, 154.5, 166.9, 169.2, 170.5, 171.9, 174.4 and 201.9 ppm; HRMS (FAB/DCM/NaCl) m/z calcd for $C_{61}H_{93}NO_{15}Si_2H^+$: 1137.6240, found: 1137.6238 (Δ = 0.2 ppm).

Macrocyclic Taxoid SB-TCR-101 (3-16)

Under a nitrogen atmosphere, bis(tricyclohexylphosphine)benzylideneruthenium(IV) dichloride ("Grubbs's catalyst" 4.6 mg, 5.6 μmol) in 0.6 mL dry CH_2Cl_2 was added to a solution of **3-14** (32 mg, 0.028 mmol) in CH_2Cl_2 (20 mL). The mixture was stirred overnight and the solvent was removed under reduced pressure. The crude product was passed through a short silica gel column to remove remained catalyst and byproduct to afford **3-15** (20.4 mg, crude) as a

yellow solid.

Under a nitrogen atmosphere, HF-pyridine (70:30, 0.2 mL) was added dropwise to a solution of **3-15** thus obtained in CH_3CN (0.4 mL) and pyridine (0.4 mL) at 0 °C and stirred overnight. The reaction mixture was diluted with EtOAc (100 mL) and washed with saturated aqueous $NaHCO_3$ solution (10 mL × 3), $CuSO_4$ solution (8 mL × 3), water (10 mL × 3) and brine (10 mL). The organic layer was dried over anhydrous $MgSO_4$ and concentrated *in vacuo*. Flash column chromatography on silica gel (Hexanes/EtOAc = 12/1) gave **SB-TCR-101** (**3-16,** 5.7 mg, 35% for two steps) as a white solid: mp 148-150 °C; ^{1}H NMR (300 MHz, $CDCl_3$) δ 0.85-0.99 (m, 6 H), 1.14 (s, 3 H), 1.25 (s, 3 H), 1.26 (s, 3 H), 1.28 (s, 3 H), 1.34 (s, 9 H), 1.67 (s, 3 H), 1.78 (s, 3 H), 1.80 (s, 3 H), 1.85 (s, 3 H), 2.04 (s, 3 H), 2.24 (s, 3 H), 2.52 (m, 2 H), 2.42-2.45 (m, 2 H), 2.83-2.88 (m, 1 H), 3.59 (m, 1 H), 4.16 (d, J = 8.7 Hz, 1 H), 4.33 (d, J = 8.7 Hz, 1 H), 4.40-4.51 (m, 2 H), 4.65 (d, J = 9.0 Hz, 1 H), 5.05 (d, J = 7.5 Hz, 1 H), 5.25 (d, J = 9.9 Hz, 1 H), 5.51 (m, 1 H), 5.69 (d, J = 6.9 Hz, 1 H), 5.88 (m, 1 H), 5.99 (m, 1 H), 6.27 (s, 1 H), 7.45-7.51 (m, 2 H), 7.60-7.64 (m, 1 H) and 8.10-8.12 (m, 2 H) ppm; ^{13}C NMR (62.9 MHz, $CDCl_3$) δ 6.6, 9.7, 15.4, 18.7, 20.9, 21.3, 23.0, 25.8, 26.7, 28.3, 29.7, 32.5, 33.1, 35.2, 35.7, 43.3, 46.0, 55.2, 58.1, 72.1, 75.3, 75.6, 79.2, 79.7, 79.8, 80.6, 84.3, 117.5, 119.2, 126.0, 128.5, 129.3, 130.2, 131.6, 135.5, 138.8, 143.9, 166.8, 171.4, 172.1, 176.6 and 203.9 ppm; HRMS (FAB/DCM/NaCl) m/z calcd for $C_{47}H_{61}NO_{15}H^+$: 880.4119, found: 880.4119 (Δ = 0.0 ppm); $[\alpha]_D^{20}$ -36.0 (c 0.02, $CHCl_3$).

14*β*-Hydroxybaccatin III (3-17) [69]

Under a nitrogen atmosphere, acetic anhydride (0.34 mL, 3.6 mmol) was dropwise added to a solution of 14*β*-hydroxy-10-deacetylbaccatin III (204 mg, 0.36 mmol) and $CeCl_37H_2O$ (13.5 mg, 0.036 mol) in dry THF (12 mL) at room temperature. The reaction mixture was stirred for 2 h at the same temperature and then quenched with a saturated aqueous $NaHCO_3$ solution (10 mL). The mixture was extracted with EtOAc (30 mL × 3), washed with brine (15 mL), dried over anhydrous $MgSO_4$, and concentrated *in vacuo*. The crude product **3-17** (249 mg, a white solid) was directly used for the next step without further purification. ^{1}H NMR (300 MHz, $CDCl_3$) δ 1.13 (s, 3 H, CH_3 at C16 or 17), 1.26 (s, 3 H, CH_3 at C16 or 17), 1.68 (s, 3 H, CH_3 at C19), 1.87 (m, 1 H, H6a), 2.04 (s, 3 H, CH_3 at C18), 2.24 (s, 3 H, OAc at C4 or C10), 2.30 (s, 3 H OAc at C4 or C10), 2.44 (br s, 1 H, OH), 2.49-2.67 (m, 2 H, H6b and OH), 2.96 (br s, 1 H, OH), 3.23 (s, 1 H, OH), 3.81 (d, J = 7.5 Hz, 1 H, H3), 4.01 (d, J =6.6 Hz, 1 H, H14), 4.16 (d, J = 8.1 Hz, 1 H, H20a), 4.24 (d, J = 8.1 Hz, 1 H, H20b), 4.44 (dd, J = 6.5, 10.3 Hz, 1 H, H7), 4.77 (d, J = 6.6, 1 H, H13), 4.98 (d, J = 7.8 Hz, 1 H, H5), 5.80 (d, J = 7.5 Hz, 1 H, H2), 6.31 (s, 1 H, H10), 7.48 (t, J = 7.5 Hz, 2 H, C2Bz-o), 7.62 (t, J = 7.5 Hz, 1 H, C2Bz-p) and 8.02 (d, J = 7.2 Hz, 2 H, C2Bz-m) ppm. All data are in agreement with literature values. [69]

7-Triethylsilyl-14*β*-Hydroxybaccatin III (3-18) [69]

Under a nitrogen atmosphere, chlorotriethylsilane (0.18 mL, 1.07 mmol) was dropwise added to a solution of **3-17** (249 mg, crude) and imidazole (97 mg, 1.42 mmol) in anhydrous DMF (5 mL) at room temperature. The reaction mixture was stirred for 2 h at the same temperature, and quenched with saturated aqueous NH_4Cl solution (5 mL). The mixture was extracted with EtOAc (30 mL × 3) and then washed with H_2O (10 mL x 2) and brine (10 mL). The organic layer was dried over anhydrous $MgSO_4$, and concentrated *in vacuo*. Flash column chromatography on silica gel (Hexanes/EtOAc = 2/1 followed by 1/1) gave **3-18** (197 mg, 76% for 2 steps) as a white solid: mp 156–159 °C; ^{1}H NMR (300 MHz, $CDCl_3$) δ 0.48–0.61 (m, 6 H, $SiCH_2CH_3$), 0.82-0.92 (m, 9 H, $SiCH_2CH_3$), 1.00 (s, 3 H, CH_3 at C16 or 17), 1.20 (s, 3 H, CH_3 at

C16 or 17), 1.66 (s, 3 H, CH_3 at C19), 1.79-1.88 (m, 1 H, H6a), 2.12 (s, 3 H, CH_3 at C18), 2.14 (s, 3 H, OAc), 2.26 (s, 3 H, OAc), 2.43-2.53 (m, 1 H, H6b), 3.78 (d, J = 7.2 Hz, 1 H, H3), 3.84 (br s, 1 H, OH), 4.00 (d, J = 6.3 Hz, 1 H, H14), 4.16 (d, J = 8.7 Hz, 1 H, H20a), 4.23 (d, J = 8. 1 Hz, 1 H, H20b), 4.45 (dd, J = 6.6, 10.2 Hz, 1 H, H7), 4.64 (d, J = 5.7, 1 H, H13), 4.92 (d, J = 8.4 Hz, 1 H, H5), 5.76 (d, J = 7.2 Hz, 1 H, H2), 6.42 (s, 1 H, H10), 7.38 (t, J = 7.5 Hz, 2 H, C2Bz-m), 7.52 (t, J = 7.5 Hz, 1 H, C2Bz-p) and 8.00 (d, J = 7.5 Hz, 2 H, C2Bz-o) ppm; ^{13}C NMR (75 MHz, $CDCl_3$) δ 5.2, 6.7, 10.0, 14.6, 20.8, 21.8, 22.3, 26.2, 37.1, 42.8, 46.5, 58.6, 72.2, 74.1, 74.3, 75.5, 76.3, 76.7, 80.7, 84.1, 128.6, 129.3, 133.5, 141.3, 165.4, 169.3, 170.3, and 202.3 ppm; HRMS (FAB/DCM/NaCl) m/z calcd $C_{37}H_{52}O_{12}SiH^+$, 717.3306; found, 717.3276 (Δ = -4.2 ppm). All data are in agreement with literature values. [69]

14-Allyl-7-Triethylsilyl-14*β*-Hydroxybaccatin III (3-19)

Under a nitrogen atmosphere, NaHMDS (1.0 M in THF, 0.1 mL, 0.1 mmol) was added to a solution of **3-18** (74 mg, 0.10 mmol) in anhydrous DMF (3 mL) at −40 °C. The reaction mixture was stirred for 5 min at the same temperature, and then allyl iodide (0.010 mL, 0.1mmol) was added. The reaction was quenched after 1 h with a saturated NH_4Cl aqueous solution (20 mL) and extracted with EtOAc (30 mL × 3). The organic layer was washed with H_2O (10 mL × 2) and brine (10 mL), dried over anhydrous $MgSO_4$ and concentrated *in vacuo*. Flash column chromatography on silica gel (Hexanes/EtOAc = 4/1) afforded **3-19** (58 mg, 74%) as a white solid: mp 133–135 °C; ^{1}H NMR (300 MHz, $CDCl_3$) δ 0.53-0.62 (m, 6 H, $SiCH_2CH_3$), 0.88-0.95 (m, 9 H, $SiCH_2CH_3$), 0.97 (s, 3 H, CH_3 at C16 or 17), 1.24 (s, 3 H, CH_3 at C16 or 17), 1.71 (s, 3 H, H19), 1.84-1.94 (m, 1 H, H6a), 2.10-2.22 (m, 4 H, CH_3 at C18 and OAc), 2.32 (s, 3 H, OAc), 2.44 (d, J = 5.4 Hz, 3 H, OH), 2.46-2.60 (m, 1 H, H6b), 3.71-3.74 (m, 2 H, H3 and OH), 3.82 (d, J = 7.2 Hz, 1 H, H14), 4.10 (dd, J = 5.7, 12.0 Hz, 1 H, CH_2:$CHCH_2OC14$), 4.24 (d, J = 8.1 Hz, 1 H, H20a), 4.31 (dd, J = 5.7, 12.0 Hz, 1 H, CH_2:$CHCH_2OC14$), 4.46 (dd, J = 6.6, 10.2 Hz, 1 H, H7), 4.74 (m, 1 H, H13), 4.93-5.05 (m, 3 H, H5 and CH_2:$CHCH_2OC14$), 5.68–5.74 (m, 1 H, CH_2:$CHCH_2OC14$), 5.88 (d, J = 7.2 Hz, 1 H, H2), 6.42 (s, 1 H, H10), 7.46 (t, J = 7.5 Hz, 2 H, C2Bz-m), 7.58 (t, J = 7.5 Hz, 1 H, C2Bz-p) and 8.11 (d, J = 7.5 Hz, 2 H, C2Bz-o) ppm; ^{13}C NMR (75 MHz, $CDCl_3$) δ 5.1, 5.4, 6.6, 6.7, 9.7, 10.0, 14.7, 20.8, 21.4, 22.4, 26.2, 37.1, 42.7, 46.4, 58.7, 72.1, 73.0, 74.5, 75.6, 75.7, 76.2, 76.4, 80.9, 81.5, 82.0, 84.0, 117.4, 128.4, 129.7, 129.8, 133.3, 133.6, 133.7, 141.2, 165.6, 169.3, 170.1 and 201.9 ppm; HRMS (FAB/DCM/NaCl) m/z calcd for $C_{40}H_{56}O_{12}SiH^+$, 757.3619; found, 757.3643 (Δ = 3.2 ppm).

2-Allyloxybenzoic acid (3-20) [66]

A mixture of salicylic acid (6.7 g, 0.05 mol) and potassium carbonate (20 g, 0.15 mol) in dry acetone (80 mL) was refluxed while stirring under nitrogen atmosphere for 1 h. After the reaction mixture was cooled to room temperature, a solution of allyl bromide (12.6 mL, 0.15 mol) in dry acetone (50 mL) was added dropwise and the reaction mixture was refluxed for 36 h. The reaction mixture was then cooled to room temperature, filtered over celite to remove the potassium carbonate and concentrated to give the crude ester. The obtained ester and sodium hydroxide (5.7 g, 0.15 mol) in 90% aqueous ethanol (70 mL) were refluxed overnight. Evaporation of the solvent yielded crude product which was then recrystallized from ethyl ether/hexanes to give **3-20** (8.6 g, 92%) as a pale white crystal: mp 63-65 °C; ^{1}H NMR (300 MHz, $CDCl_3$) δ 4.76 (d, J = 5.4 Hz, 2 H, OCH_2CH:CH_2), 5.41 (d, J = 10.5 Hz, 1 H, cis-OCH_2CH:CH_2), 5.48 (d, J = 17.1 Hz, 1 H, trans-OCH_2CH:CH_2), 6.01-6.14 (m, 1 H, OCH_2CH:CH_2), 7.03 (d, J = 8.4 Hz, 1 H, o- of allyloxy group), 7.10 (t, J = 7.5 Hz, 1 H, p- of

allyloxy group), 7.52 (dt, J = 1.8, 7.8 Hz, 1 H, p- of carboxylic group), 8.15 (dd, J = 1.5, 7.8 Hz, 1H, o- of carboxylic group) and 10.9 (br s, 1 H, CO_2H) ppm; MS (API-ES) m/z calcd for $C_{10}H_{10}O_3H^+$: 178.063, found: 179.1 (Δ = 5.8 ppm). All data are in agreement with literature values. [66]

2-Allyloxybenzoyl chloride (3-21)

A mixture of **3-20** (2 g, 11.2 mmol) and thionyl chloride (4 mL, 56 mmol) in dry CH_2Cl_2 (15 mL) was refluxed under a nitrogen atmosphere for 2 h. The reaction mixture was then cooled to room temperature and concentrated *in vacuo*. Distillation at 108-110 °C at 0.5 Torr gave **3-21** (1.1 g, 50%) as a colorless oil: ^{1}H NMR (300 MHz, $CDCl_3$) δ 4.66 (m, 2 H, $OCH_2CH{:}CH_2$), 5.41 (qd, J = 1.5, 10.5 Hz, 1 H, cis-$OCH_2CH{:}CH_2$), 5.48 (qd, J = 1.5, 17.1 Hz, 1 H, trans-$OCH_2CH{:}CH_2$), 5.98-6.11 (m, 1 H, $OCH_2CH{:}CH_2$), 7.03 (d, J = 8.4 Hz, 1 H, o- of allyloxy group), 7.10 (dt, J = 0.6, 8.1 Hz, 1 H, p- of allyloxy group), 7.52 (m, 1 H, p- of carboxylic group) and 8.09 (dd, J = 1.5, 7.8 Hz, 1 H, o- of carboxylic group) ppm.

(3*R*,4*S*)-3-(1-Methoxy-1-methylethoxy)-4-phenylazetidin-2-one (3-22) [70]

Under a nitrogen atmosphere, 2-methoxypropene (0.08 mL, 0.8 mmol) was added to a solution of **1-16** (90 mg, 0.5 mmol) and PPTS (14 mg, 0.05 mmol) in dry THF (6 mL) at 0 °C. The reaction mixture was stirred for 2 h at the same temperature and then quenched with a saturated $NaHCO_3$ solution (10 mL). The mixture was extracted with ethyl acetate (30 mL × 3). The combined organic layer was washed with brine (10 mL), dried over anhydrous $MgSO_4$, and concentrated *in vacuo*. Flash column chromatography on silica gel (Hexanes/EtOAc = 4/1) gave **3-22** (104 mg, 81%) as a white solid: ^{1}H NMR (300 MHz, distilled $CDCl_3$) δ 0.92 (s, 3 H, CH_3 of MOP), 1.20 (s, 3 H, CH_3 of MOP), 3.13 (s, 3 H, OCH_3 of MOP), 4.79 (d, J = 4.5 Hz, 1 H, H3), 5.18 (dd, J = 2.1, 4.8 Hz, 1 H, H4), 6.24 (br s, 1 H, NH) and 7.32-7.37 (m, 5 H, Ar-H) ppm. All data are in agreement with literature values. [70]

(3*R*,4*S*)-1-(2-Allyloxybenzoyl)-3-(1-methoxy-1-methylethoxy)-4-phenyl-azetidin-2-one (3-23) [70]

Under a nitrogen atmosphere, **3-21** (157 mg, 0.8 mmol) in CH_2Cl_2 (2 mL) was added dropwise to a solution of β-lactam **3-22** (94 mg, 0.4 mmol), triethylamine (0.22 mL, 1.6 mmol), and DMAP (1.5 mg, 0.012 mmol) in CH_2Cl_2 (3 mL) at room temperature. The mixture was stirred overnight at room temperature, and quenched with pure water (20 mL). The mixture was then extracted with ethyl acetate (30 mL × 3). The combined organic layer was washed with brine (10 mL), dried over anhydrous $MgSO_4$ and concentrated *in vacuo*. Flash column chromatography on silica gel (Hexanes/EtOAc = 12/1) gave **3-23** (145 mg, 92%) as a white solid: mp 109-111 °C; ^{1}H NMR (300 MHz, CD_3OD) δ 0.96 (s, 3 H, CH_3 of MOP), 1.15 (s, 3 H, CH_3 of MOP), 3.09 (s, 3 H, OCH_3 of MOP), 4.62 (d, J = 5.4 Hz, 2 H, $OCH_2CH{:}CH_2$), 5.28 (d, J = 8.0 Hz, 1 H, H3), 5.32 (qd, J = 1.5, 10.5 Hz, 1 H, cis-$OCH_2CH{:}CH_2$), 5.38 (d, J = 6.3 Hz, 1 H, H4), 5.45 (qd, J = 1.8, 17.4 Hz, 1 H, trans-$OCH_2CH{:}CH_2$), 7.08 (d, J = 8.7 Hz, 1 H, p- of allyloxy group on C1-benzamido group), 6.97-7.02 (d, J = 7.5 Hz, 1 H, o- of allyloxy group on C1-benzamido group) and 7.31-7.49 (m, 7 H, o- and p- of carbonyl group on C1-benzamido group and C3-Ar-H) ppm. [70]

(3*R*,4*S*)-1-(2-Allyloxybenzoyl)-4-phenyl-3-triethylsilanyloxyazetidin-2-one (3-24)

Under a nitrogen atmosphere, **3-21** (120 mg, 0.6 mmol) in CH_2Cl_2 (1 mL) was added

dropwise to a solution of **3-23** (85 mg, 0.3 mmol), triethylamine (0.17 mL, 1.2 mmol), and DMAP (1.2 mg, 0.009 mmol) in CH_2Cl_2 (2 mL) at room temperature. The mixture was stirred overnight at room temperature, and quenched with a saturated NH_4Cl aqueous solution (20 mL). The mixture was then extracted with ethyl acetate (30 mL × 3). The combined organic layer was washed with brine (10 mL), dried over anhydrous $MgSO_4$ and concentrated *in vacuo*. Flash column chromatography on silica gel (Hexanes/EtOAc = 25/1) gave **3-24** (118 mg, 88%) as a colorless oil: ^{1}H NMR (300 MHz, $CDCl_3$) δ 0.40-0.50 (m, 6 H, $SiCH_2CH_3$), 0.75-0.81 (m, 9 H, $SiCH_2CH_3$), 4.62 (dd, J = 1.2, 5.7 Hz, 2 H, $OCH_2CH{:}CH_2$), 5.10 (d, J = 6.0 Hz, 1 H, H3), 5.22 (dd, J = 0.9, 10.5 Hz, 1 H, $OCH_2CH{:}CH_2$, the cis-), 5.36 (d, J = 6.0 Hz, 1 H, H4), 5.45 (dd, J =1.8, 17.4 Hz, 1 H, $OCH_2CH{:}CH_2$, the trans-), 6.04-6.20 (m, 1 H, $OCH_2CH{:}CH_2$), 6.96-7.03 (m, 2 H, o- and p- of allyloxy group on C1-benzamido group) and 7.32-7.45 (m, 7 H, o- and p- of carbonyl group on C1-benzamido group and C3-Ar-H) ppm; ^{13}C NMR (75 Hz, $CDCl_3$) δ 4.34, 6.15, 61.5, 69.7, 70.1, 112.2, 118.3, 120.5, 124.2, 127.8, 127.9, 128.0, 129.4, 132.8, 132.9, 133.6, 156.9, 164.6 and 165.0 ppm; HRMS (FAB/DCM/NaCl) m/z calcd for $C_{25}H_{31}NO_4SiH^+$: 438.2100, found: 438.2088 (Δ = -2.7 ppm).

14*β*-Alloxy-3'*N*-debenzoyl-3'*N*-(2-allyloxybenzoyl)-7,2'-triethylsilylpaclitaxel (3-25)

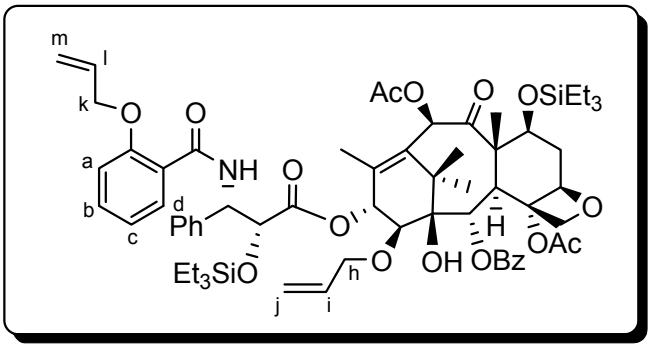

To a solution of **3-19** (55 mg, 0.07 mmol) and *β*-lactam **3-24** (96 mg, 0.22 mmol) in dry THF (7 mL) was added LiHMDS (1.0 M in THF, 0.11 mL, 0.11 mmol) at -40 °C under a nitrogen atmosphere. The reaction mixture was stirred for 7 h and then quenched with a saturated NH_4Cl aqueous solution (10 mL) and extracted with EtOAc (30 mL × 3). The organic layer was washed with brine (10 mL), dried over anhydrous $MgSO_4$ and concentrated *in vacuo*. Flash column chromatography on silica gel (Hexanes/EtOAc = 25/1 followed by 7/1) afforded **3-25** (60 mg, 70%) as a white solid: mp 205-207 °C; ^{1}H NMR (400 MHz, $CDCl_3$) δ 0.28-0.48 (m, 6 H, $SiCH_2CH_3$), 0.52-0.66 (m, 6 H, $SiCH_2CH_3$), 0.76-0.86 (m, 9 H, $SiCH_2CH_3$), 0.88-0.98 (m, 9 H, $SiCH_2CH_3$), 1.11 (s, 3 H, CH_3 at C16 or 17), 1.25 (s, 3 H, CH_3 at C16 or 17), 1.73 (s, 3 H, CH_3 at C19), 1.88-1.98 (m, 1 H, H6a), 2.01 (s, 3 H, CH_3 at C8), 2.17 (s, 3 H, OAc), 2.50-2.60 (m, 1 H, H6b), 2.66 (s, 3 H, OAc), 3.74 (s, 1 H, OH), 3.76-3.88 (m, 3 H, H3, H14 and Hh), 4.20 (dd, J = 4.4, 10.8 Hz, 1 H, Hh), 4.28 (d, J = 8.4 Hz, 1 H, H20a), 4.42-4.55 (m, 4 H, H20b, H7 and Hj), 4.70 (d, J = 1.6 Hz, 1 H, H2'), 4.74-4.83 (dd, J = 5.2, 13.2 Hz, 1 H, Hk), 4.83-4.89 (dd, J = 12.8, 5.6 Hz, 1 H, Hk), 5.0 (d, J = 8.4 Hz, 1 H, H5), 5.20-5.30 (m, 1 H, Hi), 5.34 (d, J = 10.4 Hz, 1 H, cis-Hm), 5.44 (d, J = 16.4 Hz, 1 H, trans-Hm), 5.64 (d, J = 6.4 Hz, 1 H, H3'), 5.96 (d, J = 7.2 Hz, 1 H, H2), 6.16-6.30 (m, 2 H, H13 and Hl), 6.45 (s, 1 H, H10), 6.92-7.0 (m, 2 H, Ha and Hc), 7.26-7.42 (m, 6 H, C3'Ph and Hb), 7.48 (t, J = 7.2 Hz, 2 H, C2Bz-m), 7.59 (t, J = 7.6 Hz, 1 H, C2Bz-p), 8.02 (dd, J = 1.6, 8 Hz, 1 H, Hd), 8.10 (d, J= 7.2 Hz, 2 H, C2Bz-o) and 9.09 (d, J = 7.6

Hz, 1 H, NH) ppm; ^{13}C NMR (100 MHz, $CDCl_3$) δ 4.28, 4.31, 5.26, 5.29, 6,46, 6.52, 6.72, 6.78, 9.90, 14.3, 20.9, 22.4, 23.4, 26.0, 29.7, 37.3, 43.4, 45.9, 56.6, 58.8, 70.3, 72.2, 72.7, 74.7, 74.9, 75.1, 76.6, 78.2, 78.5, 81.6, 84.2, 113.0, 117.2, 118.6, 121.1, 126.6, 127.6, 128.5, 128.6, 129.6, 129.9, 132.5, 132.8, 132.9, 133.4, 135.4, 136.4, 139.0, 157.1, 164.6, 165.6, 169.4, 170.0, 171.2 and 201.0 ppm; HRMS (FAB/DCM/NaCl) m/z calcd for $C_{65}H_{87}NO_{16}Si_2H^+$: 1194.5641, found: 1194.5692 (Δ = 4.3 ppm).

Macrocyclic Taxoid SB-T-2055 (3-27a, 3-27b)

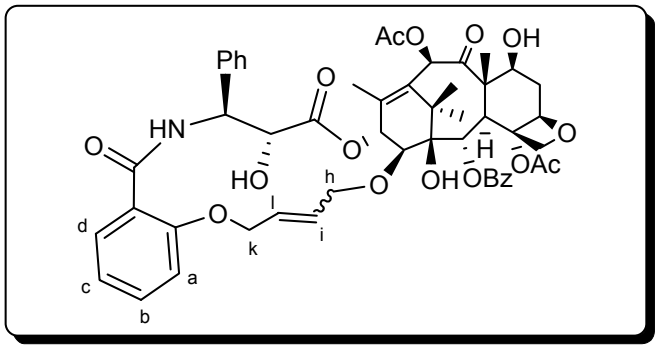

To a solution of **3-25** (60 mg, 0.05 mmol) in dry CH_2Cl_2 (20 mL) was added bis(tricyclohexylphosphine)benzylideneruthenium(IV) dichloride ("Grubbs's catalyst" 8 mg, 0.015 mmol) in dry CH_2Cl_2 (1.5 mL) under a nitrogen atmosphere. The reaction was stirred for 2 days of room temperature and 1 day of 40 °C reflux to convert all of the starting materials. Solvent was removed *in vacuo*. Two products were separated with a short column (Hexanes/EtOAc = 5/1) to afford **3-26a** (25 mg, 42%) and **3-26b** (24 mg, 40%) as crude yellow solid.

^{1}H NMR (300 MHz, $CDCl_3$) of **3-26a** δ 0.46-0.66 (m, 12 H, $SiCH_2CH_3$), 0.84-0.89 (t, J = 7.8 Hz, 9 H, $SiCH_2CH_3$), 0.93-0.98 (t, J = 7.5 Hz, 9 H, $SiCH_2CH_3$), 1.20 (s, 3 H, CH_3 at C16 or C17), 1.31 (s, 3 H, CH_3 at C16 or C17), 1.74 (s, 3 H, CH_3 at C19), 1.88-1.98 (m, 1 H, H6a), 2.12 (s, 3 H, H18), 2.19 (s, 3 H, OAc), 2.54 (s, 3 H, OAc), 2.50-2.62 (m, 1 H, H6b), 3.27 (s, 1 H, OH), 3.72 (d, J = 15.0 Hz, 1 H, Hh), 3.81 (d, J = 7.5 Hz, 1 H, H3 or H14), 3.85 (d, J = 7.5 Hz, 1 H, H3 or H14), 3.95 (dd, J = 4.8, 15.3 Hz, 1 H, Hh), 4.19 (d, J = 8.4 Hz, 1 H, Hk), 4.24 (d, J = 8.4 Hz, 1 H, H20a), 4.39 (d, J = 8.1 Hz, 1 H, H20b), 4.50 (dd, J = 6.6, 10.5 Hz, 2 H, H7), 4.66 (d, J = 1.8 Hz, 1 H, H2'), 4.80 (dd, J = 4.8, 11.1 Hz, 1 H, Hk), 4.97 (d, J = 8.1 Hz, 1 H, H5), 5.32 (d, J = 14.1 Hz, 1 H, Hi), 5.84 (dd, J = 1.8, 8.1 Hz, 1 H, H3'), 5.91-6.06 (m, 1 H, Hl), 6.00 (d, J = 7.2 Hz, 1 H, H2), 6.46 (s, 1 H, H10), 6.48 (d, J = 7.8 Hz, 1 H, H13), 7.03 (d, J = 7.5 Hz, 1 H, Ha), 7.15 (dt, J = 1.2, 7.5 Hz, 1 H, Hc), 7.26-7.6 (m, 9 H, C3'Ph, C2Bz-p, C2Bz-m and Hb), 7.92 (dd, J = 1.8, 8.1 Hz, 1 H, Hd) and 8.05-8.14 (m, 2 H, C2Bz-o and NH) ppm.

^{1}H NMR (300 MHz, $CDCl_3$) of **3-26b** δ 0.53-0.64 (m, 12 H, $SiCH_2CH_3$), 0.84-0.94 (m, 18 H, $SiCH_2CH_3$), 1.14 (s, 3 H, CH_3 at C16 or C17), 1.27 (s, 3 H, CH_3 at C16 or C17), 1.71 (s, 3 H, CH_3 at C19), 1.82-1.96 (m, 1 H, H6a), 2.00 (s, 3 H, H18), 2.17 (s, 3 H, OAc), 2.29 (s, 3 H, OAc), 2.48-2.58 (m, 1 H, H6b), 3.69 (s, 1 H, OH), 3.78-3.83 (m, 2 H, H3 and H14), 3.87 (d, J = 11.4 Hz, 1H, Hh), 4.19-4.29 (m, 3 H, H20a, Hh and Hk), 4.43-4.49 (m, 2 H, H20b and H2'), 4.59 (dd, J =12.3, 7.2 Hz, 1 H, Hk), 4.70 (dd, J = 11.4, 9.0 Hz, 1 H, H7), 4.86 (m, 1 H, H5), 5.49-5.67 (m, 3 H, Hl, Hi and H3'), 5.90 (d, J = 7.5 Hz, 1 H, H2), 6.26 (dd, J = 5.7 Hz, 1 H, H13), 6.44 (s, 1 H, H10), 6.93 (d, J = 8.1 Hz, 1 H, Ha), 7.16 (t, J = 7.5 Hz, 1 H, Hc), 7.29-7.38 (m, 7 H, C3'Ph and

C2Bz-m), 7.49-7.58 (m, 2 H, C2Bz-p and Hb), 8.00 (d, J = 7.2 Hz, 2 H, C2Bz-o) and 8.09-8.18 (m, 2 H, Hd and NH) ppm.

Under a nitrogen atmosphere, HF-pyridine (70:30, 0.25 mL) was added to a solution of **3-26a** (25 mg) in CH_3CN (0.5 mL) and pyridine (0.5 mL) at 0 °C and the reaction mixture was stirred overnight. The reaction mixture was diluted with EtOAc (60 mL) and washed with a saturated aqueous $NaHCO_3$ solution (10 mL × 2), a $CuSO_4$ solution (8 mL × 3), water (10 mL × 3), and brine (5 mL). The organic layer was dried over anhydrous $MgSO_4$, and solvent was removed *in vacuo*. Flash column chromatography on silica gel (Hexanes/EtOAc = 1/2) afforded (*E*)-**SB-T-2055**, (**3-27a**, 18.8 mg, 93%) as a white solid: mp 194-196 °C; ^{1}H NMR (400 MHz, $CDCl_3$) δ 1.08 (s, 3 H, CH_3 at C16 or C17), 1.12 (s, 3 H, CH_3 at C16 or C17), 1.60 (s, 3 H, CH_3 at C19), 1.64 (s, 3 H, CH_3 at C18), 1.78-1.86 (m, 1 H, H6a), 2.13 (s, 3 H, OAc), 2.34 (s, 1 H, OH), 2.36 (s, 3 H, OAc), 2.44-2.56 (m, 1 H, H6b), 3.27 (s, 1 H, OH), 3.69-3.77 (m, 3 H, OH, H3 and H14), 4.08-4.19 (m, 3 H, H20a and Hh), 4.30-4.33 (m, 3 H, H20b, H7 and H2'), 4.60-4.68 (m, 2 H, Hk), 4.92 (d, J = 8.4 Hz, 1 H, H5), 5.57 (d, J = 15.6 Hz, 1 H, Hi), 5.82 (dd, J = 9.2, 3.2 Hz, 1 H, H3'), 5.86 (d, J = 7.2 Hz, 1 H, H2), 5.94 (m, 1 H, Hl), 6.16 (s, 1 H, H10), 6.25 (d, J = 6.0 Hz, 1 H, H13), 6.89 (d, J = 8.4 Hz, 1 H, Ha), 7.04 (t, J = 7.6 Hz, 1 H, Hc), 7.17-7.24 (m, 3 H, Hb and C3'Ph-o), 7.40 (t, J = 7.6 Hz, 3 H, C2Bz-m and C3'Ph-p), 7.47 (d, J = 7.2 Hz, 2 H, C3'Ph-m), 7.53 (t, J = 7.2 Hz, 1 H, C2Bz-p), 7.92 (dd, J = 1.2, 7.6 Hz, 1 H, Hd), 8.02 (d, J = 7.6 Hz, 2 H, C2Bz-o) and 8.52 (d, J = 9.2 Hz, 1 H, NH) ppm; ^{13}C NMR (100 MHz, $CDCl_3$) δ 4.29, 4.31, 4.70, 5.27, 5.30, 6.48, 6.52, 6.73, 6.78, 9.90, 14.3, 20.8, 22.4, 23.4, 26.0, 37.3, 43.4, 46.0, 56.6, 58.8, 70.3, 72.2, 72.7, 74.7, 74.9, 75.1, 76.7, 78.3, 78.5, 81.6, 84.2, 85.8, 113.0, 117.2, 118.6, 121.1, 126.6, 127.6, 128.5, 128.7, 129.6, 129.9, 132.5, 132.8, 132.9, 133.4, 135.4, 136.5, 139.0, 157.1, 164.6, 165.6, 169.4, 170.0, 171.2, 201.0 and 211.8 ppm; HRMS m/z calcd for $C_{51}H_{55}NO_{16}H^+$, 938.3599; found, 938.3590 (Δ = -0.9 ppm); $[\alpha]_D^{20}$ -107 (c 12.7, $CHCl_3$).

The (*Z*)-**SB-T-2055** was synthesized in the similar fashion. However, a taxoid derivative impurity (with same mass) was observed, whose close Rf value made the flash column chromatography failed. Preparative TLC was used to finally get the pure (*Z*)-**SB-T-2055** (**3-27a**, 5.8 mg, 40%): mp 166-168 °C; ^{1}H NMR (500 MHz, $CDCl_3$) δ 1.22 (s, 3 H, CH_3 at C16 or C17), 1.24 (s, 3 H, CH_3 at C16 or C17), 1.69 (s, 3 H, CH_3 at C19), 1.84 (s, 3 H, CH_3 at C18), 1.87 (m, 1 H, H6a), 2.04 (s, 3 H, OAc), 2.24 (s, 3 H, OAc), 2.40 (d, J = 4.0 Hz, 1 H, OH), 2.50-2.51 (m, 1 H, H6b), 2.97 (d, J = 8.5 Hz, 1 H, OH), 3.44 (s, 1 H, OH), 3.74 (d, J = 7.5 Hz, H3), 3.85 (d, J = 8.0 Hz, 1 H, H14), 4.14 (d, J = 11.0 Hz, 1 H, Hh), 4.19 (d, J = 8.0 Hz, 1 H, H20a), 4.20 (d, J = 8.5 Hz, 1 H, H20b), 4.34-4.44 (m, 3 H, Hk and Hh), 4.60 (dd, J = 8.5, 12.5 Hz, 1 H, H7), 4.91 (d, J = 9.0 Hz, 1 H, H5), 5.03 (dd, J = 3.5, 8.5 Hz, 1 H, H2'), 5.49 (dd, J = 4.0, 5.5 Hz, 1 H, H3'), 5.70-5.77 (m, 1 H, Hl or Hi), 5.82 (t, J = 9 Hz, 1 H, Hl or Hi), 5.92 (d, J = 7.5 Hz, 1 H, H2), 6.20 (d, J = 6.5 Hz, 1 H, H13), 6.28 (s, 1 H, H10), 7.00 (d, J = 8 Hz, 1 H, Ha), 7.24-7.26 (m, 1 H, Hc), 7.34-7.44 (m, 7 H, C3'Ph and C2Bz-m), 7.60-7.66 (m, 2 H, C2Bz-p and Hb), 8.03 (d, J = 7.5 Hz, 2 H, C2Bz-o), 8.35 (dd, J = 1, 7.5 Hz, 1 H, Hd) and 8.49 (d, J = 6 Hz, 1 H, NH) ppm; HRMS m/z calcd for $C_{51}H_{55}NO_{16}H^+$, 938.3599; found, 938.3589 (Δ = -1.0 ppm); $[\alpha]_D^{20}$ -73 (c 3.7, $CHCl_3$).

§3.5 References

[1] McGuire, W. P.; Hoskins, W. J.; Brady, M. F.; Kucera, P. R.; Partridge, E. E.; Look, K. Y.; Clarke-Pearson, D. L.; Davidson, M. Cyclophosphamide and cisplatin compared with paclitaxel and cisplatin in patients with stage III and stage IV ovarian cancer, *New Engl. J. Med.* **1996**, *334*, 1-6.

[2] Holmes, F. A.; Kudelka, A. P.; Kavanagh, J. J.; Huber, M. H.; Ajani, J. A.; Valero, V. In *Taxane Anticancer Agents. Basic Science and Current Status*, Georg, G. I.; Chen, T. T.; Ojima, I.; Vyas, D. M. (Eds.) American Chemical Society: Washington, **1995,** 31-57.

[3] Gelmon, K. The Taxoids-Paclitaxel and Docetaxel, *The Lancet* **1994**, *344*, 1267-1272.

[4] Rowinsky, E. K.; Donehover, R. C. Drug-Therapy - Paclitaxel (Taxol), *New Engl. J. Med.* **1995**, *332*, 1004-1014.

[5] Schiff, P. B.; Fant, J.; Horwitz, S. B. *Nature* **1979**, *277*, 665–667.

[6] Jordan, M. A.; Wilson, L. *Nat. Rev. Cancer* **2004**, *4*, 253–265.

[7] Vallee, R. B., In *Taxol: Science and Applications*, Suffness, M. (Ed.) CRC Press: Boca Raton, **1995**, 259-274.

[8] Jordon, M. A.; Wilson, L., In *Taxane Anticancer Agents. Basic Science and Current Status*, Georg, G. I.; Chen, T. T.; Ojima, I.; Vyas, D. M. (Eds.) American Chemical Society: Washington, **1995**, 138-153.

[9] Kingston, D. G.; Bane, S.; Snyder, J. P. *Cell Cycle* **2005**, *4*, 279–289.

[10] Snyder, J. P.; Nevins, N.; Cicero, D. O.; Jansen, J. The Conformations of Taxol in Chloroform, *J. Am. Chem. Soc.* **2000**, *122*, 724-725.

[11] Sun, L.; Simmerlin, C.; Ojima, I. Recent Advances in the Study of the Bioactive Conformation of Taxol, *ChemMedChem* **2009**, *4*, 719 – 731.

[12] Gueritte-Voegelein, F.; Guenard, D.; Mangatal, L.; Potier, P.; Guilhem, J.; Cesario, M.; Pascard, C. Structure of a Synthetic Taxol Precursor: *N*-*tert*-Butoxycarbonyl-10-deacetyl-*N*-debenzoyltaxol, *Acta Cryst.* **1990**, *C46*, 781-784.

[13] Mastropaolo, D.; Camerman, A.; Luo, Y.; Brayer, G. D.; Camerman, N. Crystal and molecular structrue of paclitaxel (taxol), *Proc. Natl. Acad. Sci. USA*, **1995**, *92*, 6920-6924.

[14] Hilton, B. D.; Chmurny, G. N.; Muschik, G. M. Taxol: Quantitative Internuclear Proton-Proton Distances in $CDCl_3$ Solution from nOe Data: 2D NMR ROESY Buildup Rates at 500 MHz, *J. Nat. Prod.* **1992**, *55*, 1157-1161.

[15] Vander Velde, D. G.; Georg, G. I.; Grunewald, G. L.; Gunn, C. C.; Mitscher, L. A. "Hydrophobic Collapse" of Taxol and Taxotere Solution Conformations in Mixtures of Water and Organic Solvent, *J. Am. Chem. Soc.* **1993**, *115*, 11650-11651.

[16] Rao, S.; Orr, G. A.; Chaudhary, A. G.; Kingston, D. G. I.; Horwitz, S. B. Characterization of the Taxol Binding Site on the Microtubule, *J. Biol. Chem.* **1995**, *270*, 20235-20238.

[17] Rao, S.; Krauss, N. E.; Heerding, J. M.; Swindell, C. S.; Ringel, I.; Orr, G. A.; Horwitz, S. B. 3'-(*p*-Azidobenzamido)taxol Photolabels the *N*-terminal 31 Amino Acids of *β*-Tubulin, *J. Biol. Chem.* **1994**, *269*, 3132-3134.

[18] Li, Y.; Cegelski, L.; Poliks, M.; Gryczynsli, Z.; Piszczek, G.; Jagtap, P. G.; Studelska, D.; Kingston, D. G.; Schaefer, J.; Bane, S. Conformation of Microtubule-Bound Paclitaxel Determined by Fluorescence Spectroscopy and REDOR NMR, *Biochemistry* **2000**, *39*, 281-291.

[19] Sengupta, S.; Boge, T. C.; Liu, Y.; Hepperle, M.; Georg, G. I.; Himes, R. H. Probing the

Enviroment of Tubulin-Bound Paclitaxel Using Florescent Paclitaxel Analogues, *Biochemistry* **1997**, *36*, 5179-5184.
[20] Gupta, M. L., Jr.; Bode, C. J.; Georg, G. I.; Himes, R. H. Understanding tubulin-Taxol interactions: Mutations that impart Taxol binding to yeast tubulin., *Proc. Natl. Acad. Sci. USA* **2003**, *100*, 6394-6397.
[21] Snyder, J. P.; Nettles, J. H.; Cornett, B.; Dowing, K. H.; Nogales, E. The binding conformation of Taxol in *β*-tubulin: A model based on electron crystallographic density, *Proc. Natl. Acad. Sci. USA* **2001**, *98*, 5312-5316.
[22] Nogales, E.; Wolf, S. G.; Downing, K. H. Structure of the alpha, *β*-Tubulin Dimer by Electron Crystallography, *Nature* **1998**, *391*, 199-203.
[23] Falzon, C. J.; Benesi, A. J.; Lecomte, J. T. J. Characterization of Taxol in Methylene Chloride by NMR Spectroscopy, *Tetrahedron Lett.* **1992**, *33*, 1169-1172.
[24] Williams, H. J.; Scott, A. I.; Dieden, R. A.; Swindell, C. S.; Chirlian, L. E.; Francl, M. M.; Heerding, J.; Krauss, N. E. NMR and Molecular Modeling Study of the Conformations of Taxol and Its Side Chain Methylester in Aqueous and Non-aqueous Solution, *Tetrahedron* **1993**, *49*, 6545-6560.
[25] Dubois, J.; Guenard, D.; Gueritte-Voegelein, F.; Guedira, N.; Potier, P.; Gillet, B.; Beloeil, J. C. *Tetrahedron* **1993**, *49*, 6533–6544.
[26] Vander Velde, D. G.; Georg, G. I.; Grunewald, G. L.; Gunn, C. W.; Mitscher, L. A. *J. Am. Chem. Soc.* **1993**, *115*, 11650–11651.
[27] Lin, S.; Ojima, I. *Expert Opin. Ther. Pat.* **2000**, *10*, 869–889.
[28] Chmurny, G. N.; Hilton, B. D.; Brobst, S.; Look, S. A.; Witherup, K. M.; Beutler, J. A. ^{1}H- and ^{13}C-NMR Assignments for Taxol, 7-*epi*-Taxol, and Cephalomannine, *J. Nat. Prod.* **1992**, *55*, 414-423.
[29] Balasubramanian, S. V.; Alderfer, J. L.; Straubinger, R. M. Solvent-Dependent and Concentration-Dependent Molecular-Interactions of Taxol (Paclitaxel), *J. Pharm. Sci.*, **1994**, *83*, 1470-1476.
[30] Ojima, I.; Lin, S.; Inoue, T.; Miller, M. L.; Borella, C. P.; Geng, X.; Walsh, J. J. *J. Am. Chem. Soc.* **2000**, *122*, 5343–5353.
[31] Ojima, I.; Geng, X.; Lin, S.; Pera, P.; Bernacki, R. J. *Bioorg. Med. Chem. Lett.* **2002**, *12*, 349–352.
[32] Geng, X.; Miller, M. L.; Lin, S.; Ojima, I. *Org. Lett.* **2003**, *5*, 3733–3736.
[33] Querolle, O. D.; Thoret, J.; Dupont, S.; Gueritte, C.; Guenard, F.; *Eur. J. Org. Chem.* **2003**, 542–550.
[34] Querolle, O. D.; Dupont, S.; Thoret, S.; Roussi, F.; Montiel-Smith, S.; Gueritte, S.; Guenard, D. *J. Med. Chem.* **2003**, *46*, 3623–3630.
[35] Boge, T. C.; Wu, Z.-J.; Himes, R. H.; Vander Velde, D. G.; Georg, G. I. *Bioorg. Med. Chem. Lett.* **1999**, *9*, 3047–3052.
[36] Ojima, I.; Chakravarty, S.; Inoue, T.; Lin, L.; He, L.; Horwitz, S. B.; Kuduk, S. D.; Danishefsky, S. J. *Proc. Natl. Acad. Sci. USA* **1999**, *96*, 4256–4261.
[37] Boge, T.; Wu, Z.; Himes, R.; Vander Velde, D.; Georg, G. Conformationally Restricted Paclitaxel Analogues: Macrocyclic Mimics of the "Hydrophobic Collapse" Conformation, *Bioorg. Med. Chem. Lett.* **1999**, *9*, 3047-3052.
[38] Querolle, O.; Dubois, J.; Thoret, S.; Roussi, F.; Montiel-Smith, S.; Gueritte, F.; Guenard, D. Synthesis of Novel Macrocyclic Docetaxel Analogues. Influence of Their Macrocyclic Ring Size on Tubulin Activity, *J. Med. Chem.* **2003**, *46*, 3623-3630.

[39] Kingston, D. G.; Bane, S.; Snyder, J. P. *Cell Cycle* **2005**, *4*, 279–289.
[40] Snyder, J. P.; Nevins, N.; Cicero, D. O.; Jansen, J. The Conformations of Taxol in Chloroform, *J. Am. Chem. Soc.* **2000**, *122*, 724-725.
[41] Nogales, E.; Wolf, S. G.; Downing, K. H. *Nature* **1998**, *391*, 199–203.
[42] Lowe, J.; Li, H.; Downing, K. H.; Nogales, E. *J. Mol. Bol.* **2001**, *313*, 1045–1057.
[43] Kingston, D. G. I.; Bane, S.; Snyder, J. P. *Cell Cycle* **2005**, *4*, 279–289
[44] Ganesh, T.; Guza, R. C.; Bane, S.; Ravindra, R.; Shanker, N.; Lakdawala, A. S.; Snyder, J. P.; Kingston, D. G. I. *Proc. Natl. Acad. Sci. U.S.A.* **2004**, *101*, 10006-10011.
[45] Larroque, A.-L.; Dubois, J.; Thoret, S.; Aubert, G.; Chiaroni, A.; Gueritte, F.; Guenard, D. *Bioorg. Med. Chem.* **2007**, *15*, 563–574.
[46] Li, Y.; Poliks, B.; Cegelski, L.; Poliks, M.; Cryczynski, A.; Piszcek, G.; Jagtap, P. G.; Studelska, D. R.; Kingston, D. G. I.; Schaefer, J.; Bane, S. *Biochemistry* **2000**, *39*, 281–291.
[47] Rao, S.; He, L.; Chakravarty, S.; Ojima, I.; Orr, G. A.; Horwitz, S. B. *J. Biol. Chem.* **1999**, *274*, 37990–37994.
[48] Paik, Y.; Yang, C.; Metaferia, B.; Tang, S.; Bane, S.; Ravindra, R.; Shanker, N.; Alcaraz, A. A.; Johnson, S. A.; Schaefer, J.; O'Connor, R. D.; Cegelski, L.; Snyder, J. P.; Kingston, D. G. I. *J. Am. Chem. Soc.* **2007**, *129*, 361–370.
[49] Sun, L.; Geng, X.; Geney, R.; Li, Y.; Simmerling, C.; Li, Z.; Lauher, J. W.; Xia, S.; Horwitz, S. B.; Veith, J. M.; Pera, P.; Bernacki, R. J.; Ojima, I. *J. Org. Chem.* **2008**, *73*, 9584–9593.
[50] Geney, R.; Sun, L.; Pera, P.; Bernacki, R. J.; Xia, S.; Horwitz, S. B.; Simmerline, C. L.; Ojima, I. Use of the Tubulin Bound Paclitaxel Conformation for Structure-Based Rational Drug Design. *Chemistry & Biology*, **2005**, *12*, 339-348.
[51] Bollag, D. M.; McQueney, P. A.; Zhu, J.; Hensens, O.; Koupal, L.; Liesch, J.; Goetz, M.; Lazarides, E.; Woods, C. M. *Cancer Res.* **1995**, *55*, 2325-2333.
[52] Kowalski, R. J.; Giannakakou, P.; Hamel, E. *J. Biol. Chem.* **1997**, *272*, 2534-2541.
[53] Lindel, T.; Jensen, P. R.; Fenical, W.; Long, B. H.; Casazza, A. M.; Carboni, J.; Fairchild, C. R. *J. Am. Chem. Soc.* **1997**, *119*, 8744-8745.
[54] ter Haar, E.; Kowalski, R. J.; Hamel, E.; Lin, C. M.; Longley, R. E.; Gunasekera, S. P.; Rosenkranz, H. S.; Day, B. W. *Biochemistry* **1996**, *35*, 243-250.
[55] Kowalski, R. J.; ter Haar, E.; Longley, R. E.; Gunasekera, S. P.; Lin, C. M.; Day, B. W.; Hamel, E. *Mol Biol. Cell* **1995**, *6*, 368a.
[56] Hung, D. T.; Chen, J.; Schreiber, S. L. *Chem. Biol.* **1996**, *3*, 287-293.
[57] Mooberry, S. L.; Tien, G.; Hernandez, A. H.; Plubrukarn, A.; Davidson, B. S. *Cancer Res.* **1999**, *59*, 653-660.
[58] Sato, B.; Muramatsu, H.; Miyauchi, M.; Hori, Y.; Takase, S.; Hino, M.; Hashimoto, S.; Terano, H. *J. Antibiot.* **2000**, *53*, 123-130.
[59] Geney, R.; Simmerling, C.; Ojima, I. *Abstr. Pap. - Am. Chem. Soc.* **2001**, 222nd, MEDI-065.
[60] Ojima, I.; Geng, X.; Lin, S.; Pera, P.; Bernacki, R. J. Design, Synthesis and Biological Activity of Novel C2-C3'*N*-Linked Macrocyclic Taxoids, *Bioorg. Med. Chem. Lett.* **2002**, *12*, 349-352.
[61] Ojima, I.; Wang, T.; Delaloge, F. Extremely Stereoselective Alkylation of 3-siloxy-*β*-lactams and its applications to the asymmetric syntheses of novel 2-alkylisoserines, their dipeptides, and taxoids, *Tetrahedron Lett.* **1998**, *39*, 3663-3666.
[62] Chen, S. H.; Kadow, J. F.; Farina, V.; Fairchild, C. R.; Johnston, K. A. First Syntheses of Novel Paclitaxel (Taxol) Analogs Modified at the C4-Position, *J. Org. Chem.*, **1994**, *59*, 6156-6158.
[63] Ojima, I.; Habus, I.; Zhao, M.; Zucco, M.; Park, Y. H.; Sun, C. M.; Brigaud, T. New and Efficient Approaches to the Semisynthesis of Taxol and Its C-13 Side Chain Analogs by

Means of *β*-Lactam Synthon Method, *Tetrahedron*, **1992**, *48*, 6985-7012.

[64] Appendino, G.; Gariboldi, P.; Gabetta, B.; Pace, R.; Bombardelli, E.; Viterbo, D. 14□-Hydroxy-10-deacetylbaccatin III, a New Taxane from Himalayan Yew (*Taxus Wallichiana Zucc.*). *J. Chem. Soc., Perkins Trans 1* **1992**, 2925-2929.

[65] Horowitz, S. B. Taxol: Mechanism of Action and Resistance. *Stony Brook Symposium on Taxol and Taxotere*, Stony Brook, NY, May 14-15, **1993**; Abstracts 1923-1924.

[66] Ye, T.; Garcia, C. F.; McKervey, M. A. Chemoselectivity and Stereoselectivity of Cyclization of alpha-Diazocarbonyls Leading to Oxygen and Sulfur Heterocycles Catalyzed by Chiral Rhodium and Copper-Catalysts, *J. Chem. Soc. - Perkin Trans. I* **1995**, *11*, 1373-1379.

[67] Ojima, I.; Wang, T.; Miller, M. L.; Lin, S.; Borella, C. P.; Geng, X.; Pera, P.; Bernacki, R. J. Synthesis and structure-activity relationships of new second-generation taxoids, *Bioorg. Med. Chem. Lett.* **1999**, *9*, 3423-3428.

[68] Geng, X. D. *Ph.D. Dissertation;* SUNY at Stony Brook: Stony Brook, **2002**.

[69] Geney, R.; Sun, L.; Pera, P.; Bernacki, R. J.; Xia, S.; Horwitz, S. B.; Simmerling, C. L.; Ojima, I. Use of the Tubulin Bound Paclitaxel Conformation for Structure-Based Rational Drug Design, *Chem. Biol.*, **2005**, *12*, 339-348.

[70] Kant, J.; Schwartz, W. S.; Fairchild, C.; Gao, Q.; Huang, S.; Long, B. H.; Kadow, J. F.; Langley, D. R.; Farina, V.; Vyas, D. Diastereoselective addition of Grignard reagents to azetidine-2,3-dione: Synthesis of novel Taxol® analogues, *Tetrahedron Lett.* **1996**, *37*, 6496-6498.

CHAPTER 4. DESIGN, SYNTHESIS, BIOLOGICAL EVALUATION OF NOVEL FLUORINATED TAXOIDS

§4.1 Introduction

§4.1.1 Fluorine and Fluorinated Moieties in Medicinal Chemistry

The successful application of fluorine in medicinal chemistry[1] has been demonstrated by a large number of fluorinated pharmaceuticals currently on the market (**Figure 4-1**). [2 3]

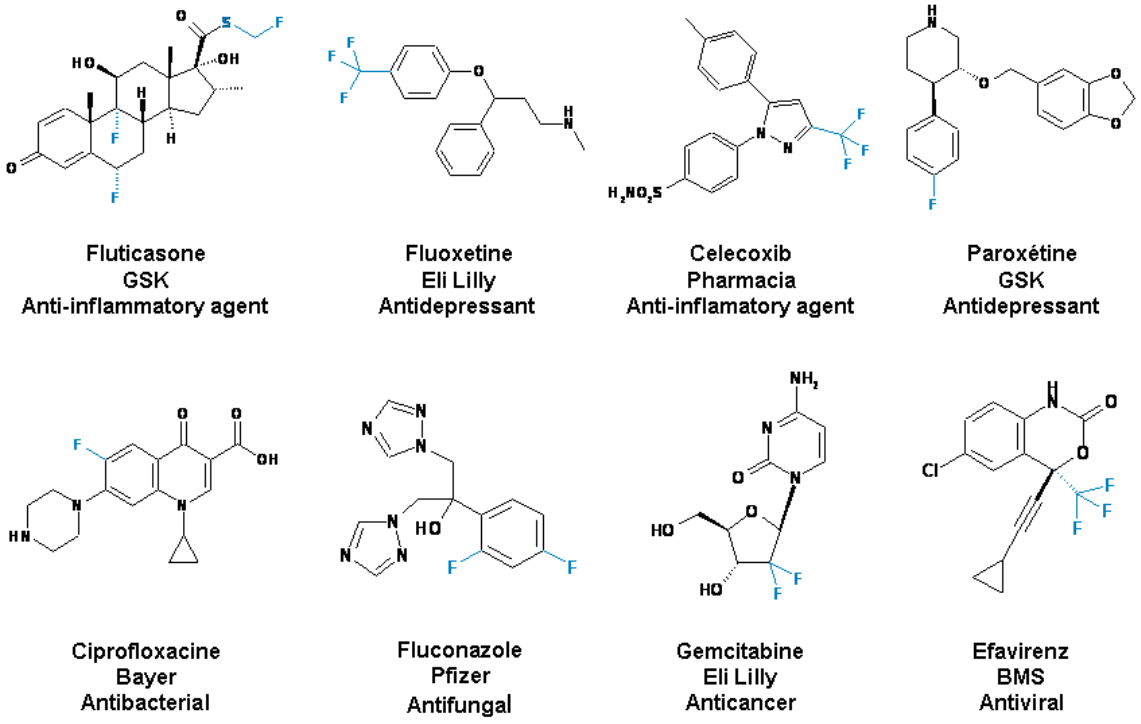

Figure 4-1. Examples of fluorinated drugs currently on the market

Fluorine is a unique atom. It has a van der waals radius of 1.47 Å (Bondi value), [4] which is closest to that of hydrogen atom (1.20 Å) among all the elements. Actually, fluorine is the only element which can replace hydrogen without notable steric consequence.

As the most electronegative element, fluorine binds very tightly to its valence electrons, which results in low atomic polarizability. The extreme electronegativity of the fluorine atom can also confer strong inductive electron withdrawing effects therefore change the reactivity of the surrounding substitution groups.

Low metabolic stability is a recurring challenge in many drug discovery projects. Lipophilic compound has the tendency to be oxidized by liver enzymes (e.g. CYP450) and cause an unappealing pharmacokinetics profile. The energy of C-F bond ranges is around 116 kcal/mol, approximately 18 kcal/mol higher than that of the C-H bond. [5] It proves to be an effective

strategy to block the enzymatic cleavage by introducing a fluorine atom or fluorinated moieties ($-CF_3$, $-CF_2H$, $-CFH_2$) at the active site. [6] The example of Ezetimib is shown in **Figure 4-2**. [7] [8]

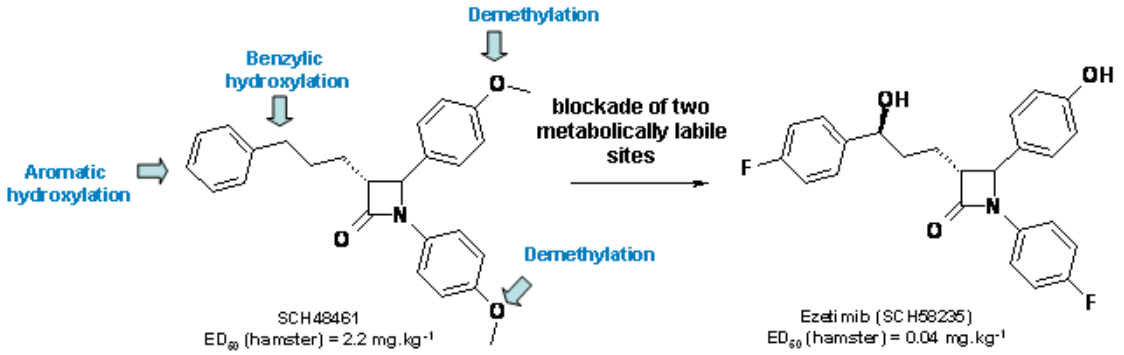

Figure 4-2. Introduction of fluorine atoms prevents oxidation of the phenyl ring

Incorporation of fluorine can also alter the lipophilicity of a molecule. Fluorination usually increases the compound lipophilicity therefore increase the hydrophobic binding and the membrane permeability. [9] Aromatic fluorination and perfluorination almost always increases lipophilicity. Fluorination adjacent to atoms with π-bonds generally increases lipophilicity, with exceptions for some fluorinated *α*-carbonyl compounds. In contrast to aromatic substitution, terminal fluorination of saturated alkyl groups typically decreases lipophilicity. It is a direct consequence of the relatively polar character of monofluoro- and trifluoromethylalkanes with their strong C-F and C-CF_3 bond dipoles. When heterosubstituents are present, the situation is more complex and less predictable.

Moreover, fluorine substitution could increase the binding affinity of the ligand with the targeting protein. This result can be ascribed to F-protein interaction or fluorine modulation of the polarity of other groups on the ligand. [10] In addition, Fluorine also can serve as a unique and valuable tool for *in vitro* and *in vivo* ^{19}F NMR studies of protein structures and drug-protein interactions by taking advantage of the fact that fluorine is virtually absent in the living tissue.

Selective introduction of fluorine atoms or fluorinated moieties into a biologically active molecule have been a very effective tool for modification of its physicochemical properties and its physiological behavior. [10] [11] [12] It appears that fluorine has become a widely used heteroatom in rational design of drug discovery. [13] [14]

§4.1.2 Fluorinated *β*-Lactam and its Synthetic Applications

β-Lactams have intrinsic importance as a pharmacophore of various therapeutic agents. They are found in numerous pharmacologically active molecules possessing antibacterial, [15] antifungal, [16] antitumor, [17] and plasma cholesterol lowering activities. [18] [19] Because of the aforementioned advantages of introducing fluorine into medicinally active molecules, fluorinated

β-lactams have been synthesized to investigate the effects of strategic incorporation of fluorine or fluorinated moieties. As described in the previous chapters, the applications of the β-Lactam Synthon Method (β-LSM) have been well developed and established. [20] [21] [22] As part of the continuing efforts in our laboratory, the β-LSM has been expanded to the syntheses of fluorinated α-hydroxy-β-amino acids, dipeptides, and fluorinated taxoids. **Scheme 4-1** illustrates representative transformations of *N*-*t*-Boc-3-PO-4-R_f-β-lactams (P = hydroxyl protecting group).

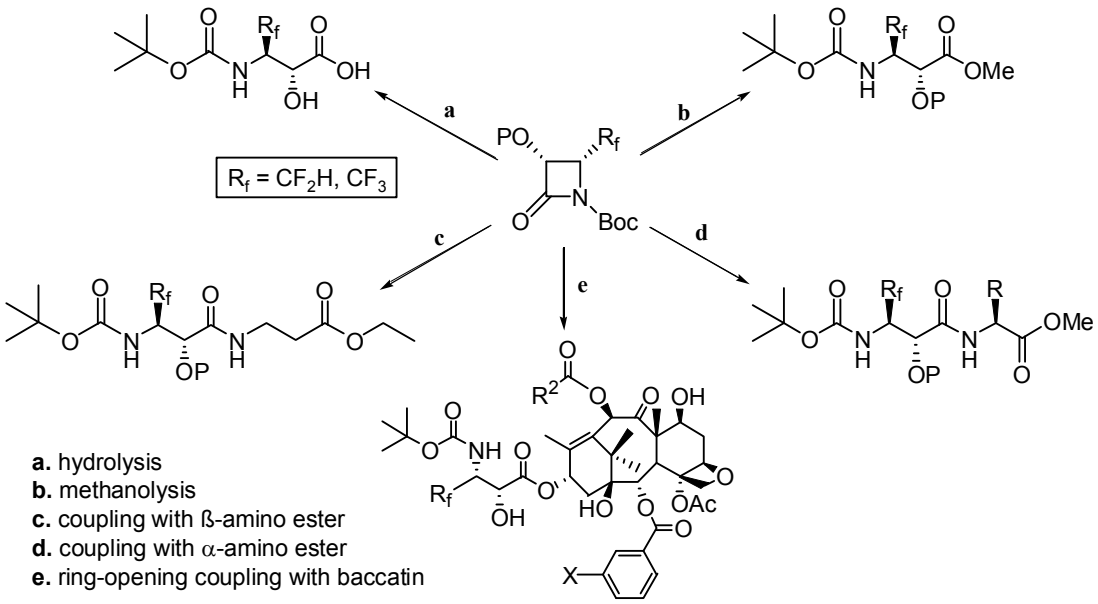

Scheme 4-1. Representative transformations of *N*-*t*-Boc-3-PO-4-R_f-β-lactams

§4.1.3 Fluorinated Taxoids and its Biological Activities

Although paclitaxel and docetaxel have very promising anticancer activity, they both displayed a number of undesirable side effects as well as inherent weakness against drug-resistant cancer cells expressing multi-drug resistance (MDR) phenotypes. These inherent issues can be overcome by the development of new analogs with maximizing the utility of the taxane-based analogues. [23] Selective introduction of a fluorine atom or fluorinated moieties into a biologically active molecule becomes very effective tool for modification of its physicochemical properties and pharmacokinetic behavior.

Systematic structure–activity relationship (SAR) studies of novel fluorinated taxoids have been carried out in our laboratory with the highly efficient Ojima-Holton coupling protocol based on the β-Lactam Synthon Method. [24] [25] A series of novel C2- and C10- modified C3'-difluoromethyl- and trifluoromethyl- taxoids have been synthesized and exhibited substantially better *in vitro* potency than paclitaxel and docetaxel against several human cancer cell lines, i.e., ovarian (A121), colon (HT-29), non-small cell lung (A549), breast (MCF-7, LCC6-WT) and drug resistant breast (MCF7-R, LCC6-MDR) cancer cell lines. [26] [27]

Illustrated in **Figure 4-3** are two representatives of the second-generation fluorinated taxoids, **SB-T-12842-4** and **SB-T-128221-3**, which possess more than two orders of magnitude higher cytotoxicity than paclitaxel against the drug-resistant cell lines, MCF7-R and LCC6-MDR, and even more impressively, several magnitude higher potency than paclitaxel against the drug-sensitive cell lines, MCF7-S and LCC6-WT (**Table 4-1**). [28]

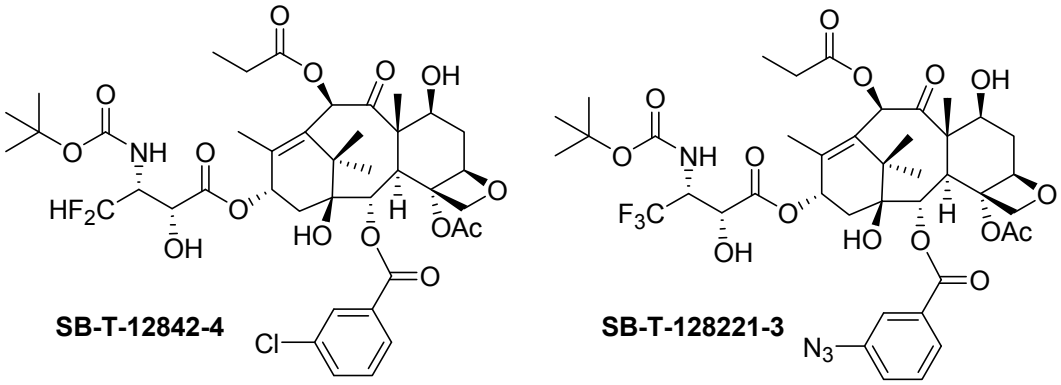

Figure 4-3. Structure of **SB-T-12842-4** and **SB-T-128221-3**

Table 4-1. *In vitro* cytotoxicity (IC_{50} nM)[a] of fluorinated taxoids [30]

Taxoid	MCF7-S (breast)	MCF7-R (breast)	R/S[b]	LCC6-WT (breast)	LCC6-MDR (breast)	R/S[b]	H460 (ovarian)	HT-29 (colon)
Paclitaxel	1.8	484	269	3.4	216	64	5.5	3.6
SB-T-12842-4	0.6	6.4	11	0.6	3.1	5.2	0.3	0.5
SB-T-128221-3	0.4	2.6	6.5	1.2	1.6	1.3	0.2	0.4

[a] The concentration of compound which inhibits 50% (IC_{50}) of the growth of the human tumor cell line after 72 h drug exposure.

[b] R/S = drug-resistant factor = IC_{50} (drug-resistant cell line)/IC_{50} (drug-sensitive cell line).

On the other hand, recent metabolism studies on second-generation taxoids have shown that the metabolism of the second-generation taxoids (e.g. **SB-T-1214**, **SB-T-1216**, and **SB-T-1103**) is noticeably different from those of docetaxel. [29] In contrast to the dominant metabolic site of *tert*-butyl group of the C3'*N*-*t*-Boc moiety in docetaxel, these taxoids are metabolized by CYP3A4 primarily at the two allylic methyl groups of the C3'-isobutenyl group and the methine moiety of the 3'-isobutyl group (**Scheme 4-2**). [30 31] Prompted by the above findings, the C3'-difluorovinyl-taxoids have been designed and synthesized to block the allylic oxidation by CYP3A4 and increase the metabolic stability and *in vivo* activity.

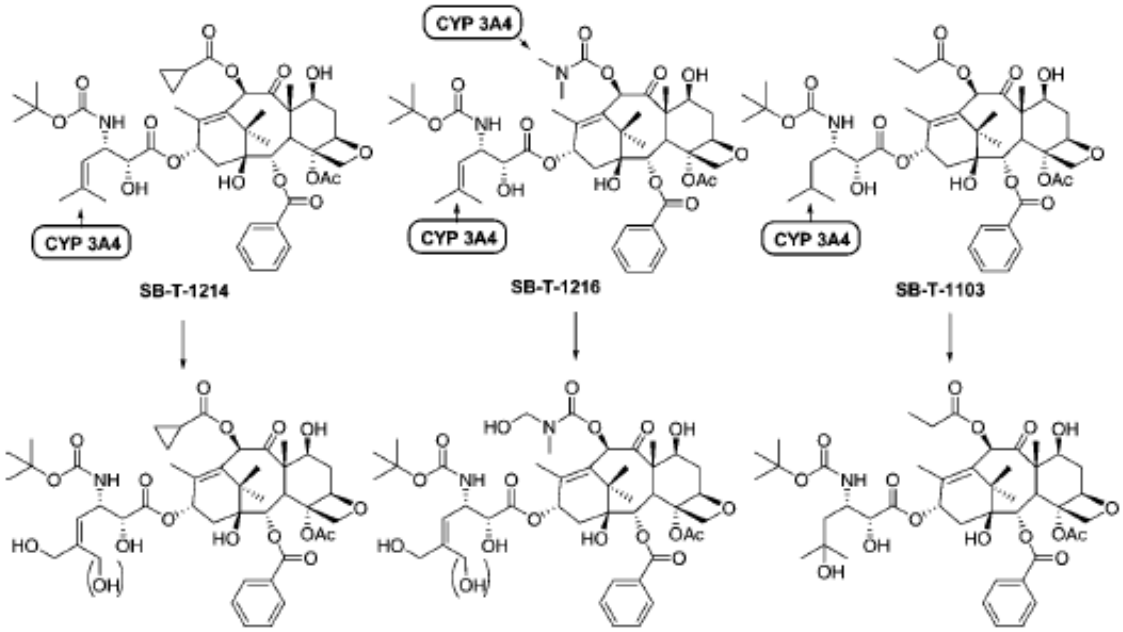

Scheme 4-2. Primary metabolism site on the second-generation taxoids by the enzyme of P450 family [27]

§4.2 Gram-Scale Synthesis of C3'-Difluorovinyl Taxoid SB-T-12854

§4.2.1 Synthsis of C3'-Difluorovinyl Second-Generation Taxoids

Within the framework of structure-activity relationship studies of fluorinated taxoids, the synthesis of difluorovinyl second-generation taxoids was proposed using the highly efficient Ojima-Holton coupling protocol, as illustrated in **Scheme 4-3**.

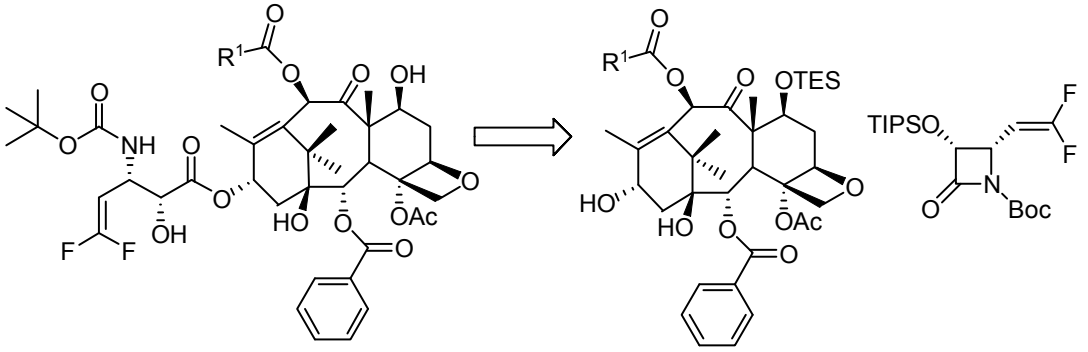

Scheme 4-3. Retro-synthesis of C3'-difluorovinyl second-generation taxoids

The robustness of the Ojima-Holton coupling protocol is also demonstrated, as this is the first time in our laboratory to prepare second-generation taxoids in gram scales (**Figure 4-4**).

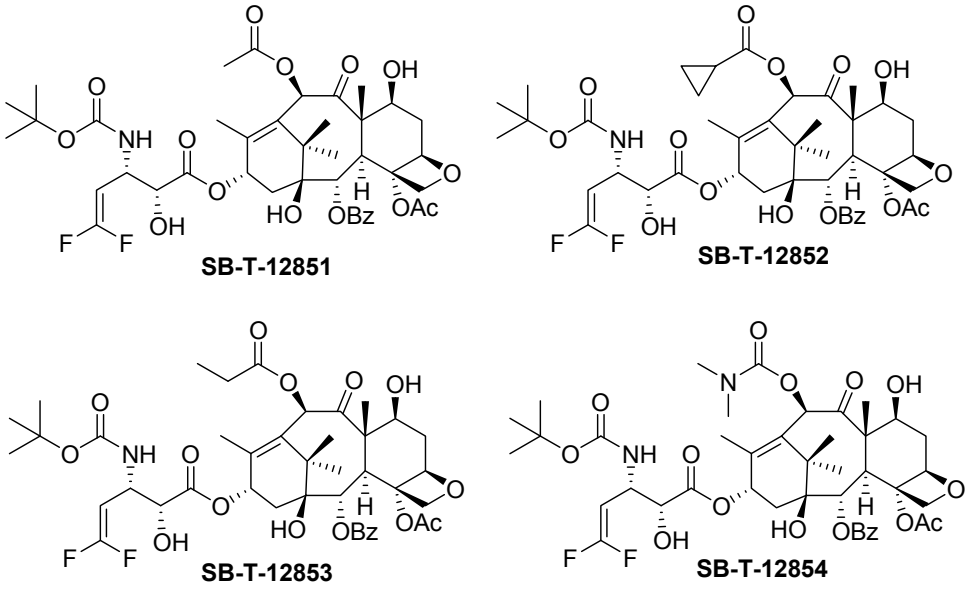

Figure 4-4. Structures of **SB-T-12851**, **SB-T-12852**, **SB-T-12853,** and **SB-T-12854**

§4.2.1.1 Synthesis of (3*R*,4*S*)-1-(*tert*-butoxycarbonyl)-3-triisopropylsiloxy-4-difluoro-vinyl-azetidin-2-one

(3*R*,4*S*)-1-(*p*-Methoxy-phenyl)-3-triisopropylsiloxy-4-(2-methyl-propen-2-yl)azetidin-2-one was prepared through [2+2] ketene-imine cycloaddition followed by the enzymatic resolution using the procedure described in Chapter 1. The protecting group of the 3-acetoxy moiety of (3*R*,4*S*)-3-AcO-*β*-lactam **4-4** was replaced with triisopropylsilyl (TIPS) via subsequent hydrolysis and silylation (**Scheme 4-4**).

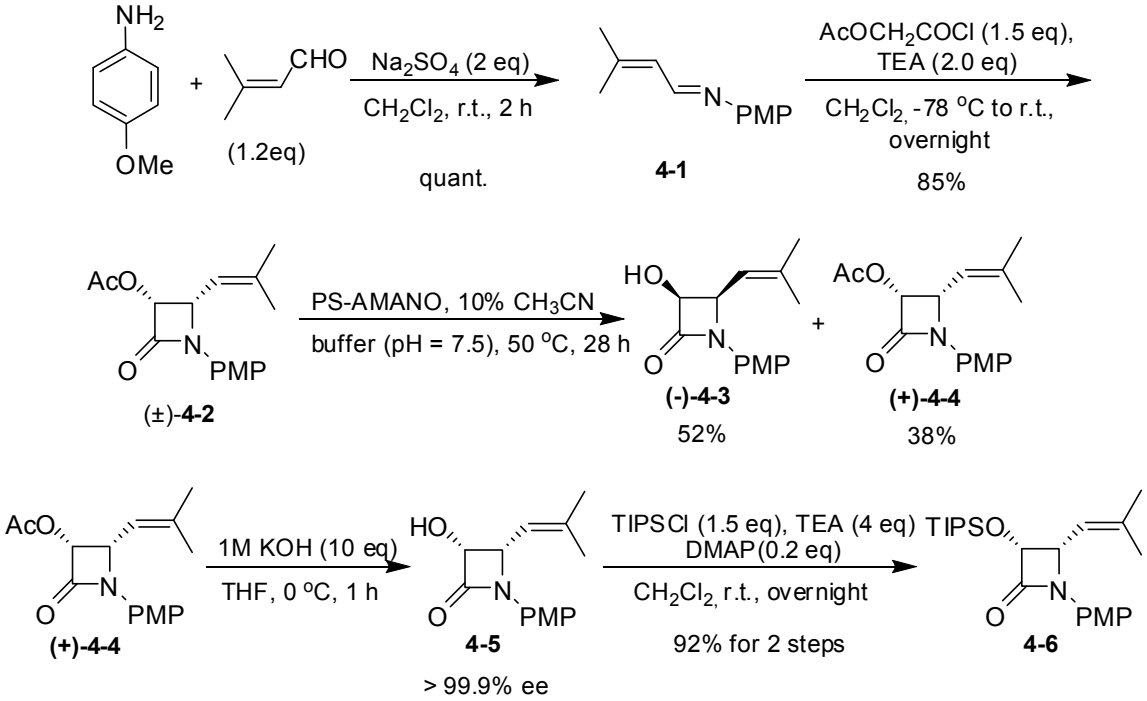

Scheme 4-4. Synthesis of (3*R*,4*S*)-1-(*p*-methoxyphenyl)-3-triisopropylsiloxy-4-(2-methyl-propen-2-yl)azetidin-2-one

Compound **4-6** was then subjected to ozonolysis to give (3*R*,4*S*)-1-(4-methoxy-phenyl)-3-triisopropylsiloxy-4-formylazetidin-2-one **4-7** (**Scheme 4-5**). Enantiopure **4-7** was transformed to (3*R*,4*S*)-1-(*p*-methoxyphenyl)-3-triisopropylsiloxy-4-difluorovinyl- 2-one **4-8** following Wittig reaction using CBr_2F_2, hexamethylphosphoroustriamide (HMPT), and Zn in THF. [32] [33] [34]

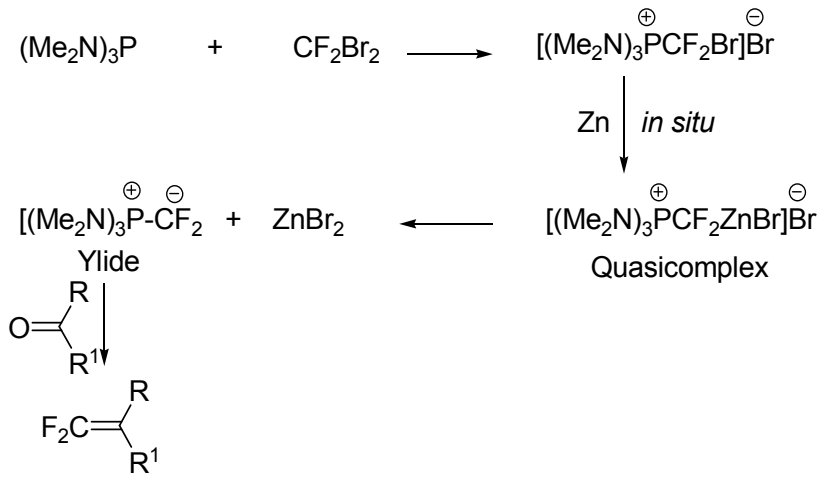

Scheme 4-5. Mechanism of 1,1-difluoroolefins formation [34]

Finally the PMP group was removed using cerium ammonium nitrate (CAN) to give enantiopure (3*R*,4*S*)-3-TIPSO-4-difluovinylazetidin-2-one **4-9** followed by carbalkoxylation with *di-tert*-butyl dicarbonate (Boc_2O) to give desired (3*R*,4*S*)-*N*-boc-3-TIPSO-4-difluorovinylazetidin-2-one **4-10** in excellent yield (**Scheme 4-6**).

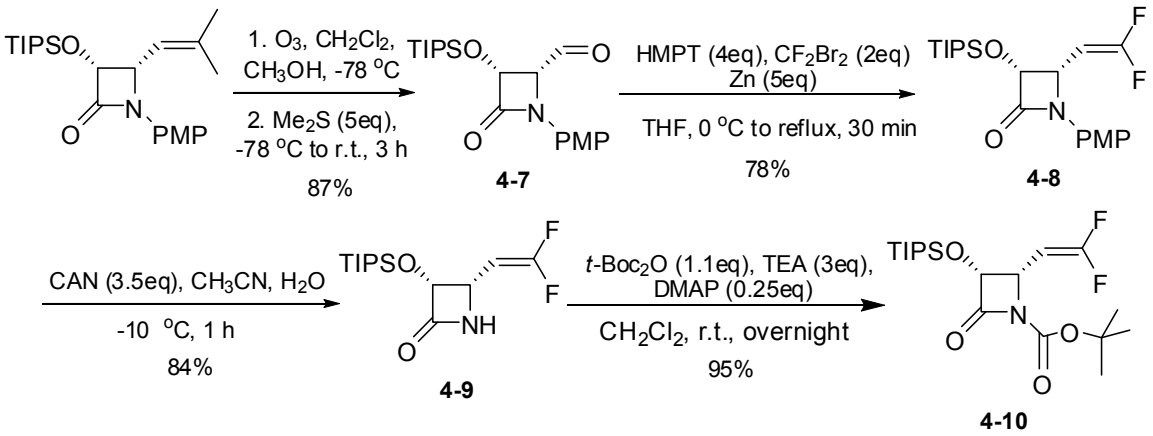

Scheme 4-6. (3*R*,4*S*)-1-(*tert*-Butoxycarbonyl)-3-triisopropylsiloxy-4-difluoro-vinyl-azetidin-2-one

§4.2.1.2 Gram-Scale Synthesis of C3'-Difluorovinyl Taxoid SB-T-12854

The synthesis of modified baccatin started from 10-DAB III (**Scheme 4-7**). C7-TES protection followed by C10-modification yielded the designed modified baccatin in excellent yield.[35] Ring-opening coupling of *β*-lactam **4-10** with modified baccatin **4-12** was carried out at -40 °C in THF at the presence of LiHMDS. [36] [37] The subsequent removal of the silyl protecting groups by HF-pyridine gave the corresponding C3'-difluorovinyl- taxoids **4-14** in good overall

yields.

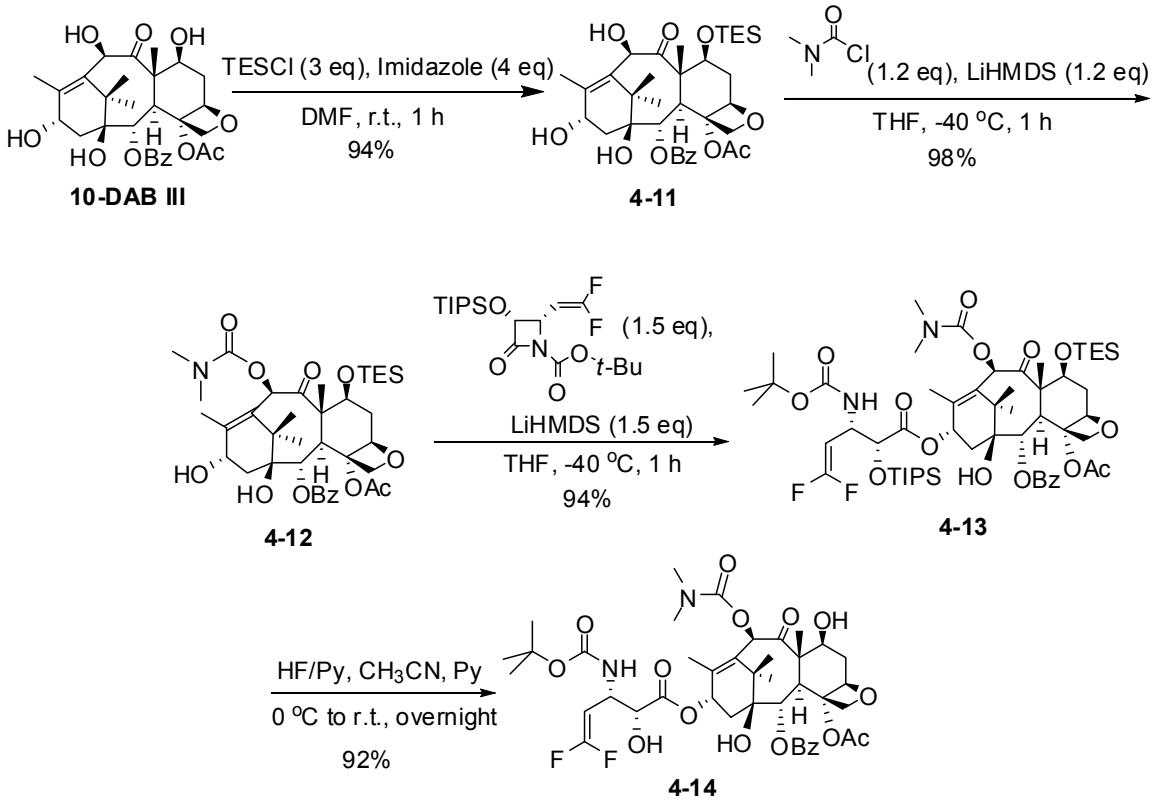

Scheme 4-7. Synthesis of C-3' difluorovinyl-taxoids **SB-T-12854**

§4.2.2 Results and Discussion

Novel difluorovinyl taxoids **SB-T-12851**, **SB-T-12852**, **SB-T-12853**, and **SB-T-12854** was previously synthesized by Dr. Larisa Kuzentsova for biological evaluation by our collaborator in the Department of Pharmacology and Therapeutic in Roswell Park Center Institute. [38] *In vitro* cytotoxicity was tested against both drug sensitive and drug resistant human breast cancer cell lines, MCF7-S and MCF7-R, respectively. The IC_{50} values were determined through 72 h exposure of the taxoids to the cancer cells (**Table 4-2**). The difluorovinyl taxoids consistently showed one order of magnitude higher than paclitaxel potency on sensitive breast cancer cell line MCF7-S, and two to three orders of magnitude higher on resistant cell line MCF7-R.

Table 4-2. In vitro cytotoxicity (IC_{50} nM) of C-3'-difluorovinyl-taxoids

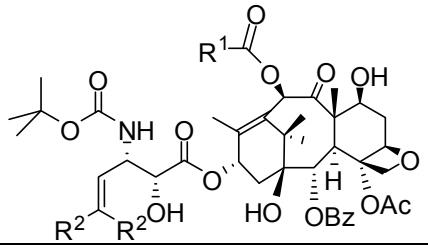

Taxoid	R^1	R^2	MCF7-S (breast)	MCF7-R (breast)	R/S
Paclitaxel	Me	Ph	1.7	300	176
SB-T-1213	Et	CH_3	0.18	2.2	12
SB-T-12851	Ac	F	0.14	0.95	6.7
SB-T-12852	c-Pr-CO	F	0.17	6.03	35.5
SB-T-12853	Et-CO	F	0.17	1.2	7.06
SB-T-12854	Me_2N-CO	F	0.19	4.27	22.5

With the large quantity (3 gram each) of difluorovinyl taxoids **SB-T-12851**, **SB-T-12852**, **SB-T-12853** and **SB-T-12854** (synthesized by J. Chen, L. Sun, S. Chen and Y. Li), a series studies have been supported with sufficient compound supply.

SB-T-12851 and **SB-T-12854** were tested against two drug-resistant pancreatic cancer cell lines, CFPac and Panc1, in Professor Weixing Zong's research group in the department of molecular genetics and microbiology at Stony Brook University. The preliminary results were summarized in **Table 4-3**. **SB-T-12851** and **SB-T-12854** have shown IC_{50} values of 0.0056-2.2 nM, four times or more magnitude higher potent than paclitaxel. It is noteworthy that the efficacy of the compounds does not appear to be affected by the expression of multidrug resistance proteins.

Table 4-3. *In vitro* cytotoxicity (IC_{50} nM) of C3'-difluorovinyl-taxoids against pancreatic cancer cell lines

Taxoids	CFPac	Panc1
Paclitaxel	15.8	4.7
SB-T-12851	0.0056	1.3
SB-T-12854	2.2	0.83

Recently, Gut and Ojima *et al* has reported the in vitro cytotoxicity study results of the fluorinated taxoids **SB-T-12851**, **SB-T-12852**, **SB-T-12853** and **SB-T-12854** in comparison with the first- and second-generation taxoids in two human cancer cell lines, paclitaxel sensitive MDA-MB-435 cells and highly paclitaxel-resistant NCI/ADR-RES cells. [39] One objective of the study is to explore the details of the well-known mechanism of actions of paclitaxel, and to

elucidate the causal relationship of the mitotic arrest induced by paclitaxel and/or its analogs to the cell apoptosis. Although it is generally believed that taxoids induce apoptosis via the release of proapoptotic proteins such as cytochrome c from the mitochondria into the cytosol, [40] [41] it seems that paclitaxel-induced cell death pathways varies in cancer cell lines of different origin. [42] [43] The studies evaluate the release of cytochrome c, the cell growth and survival rate, caspases activites of the aforementioned fluorinated and non-fluorinated taxoids with paclitaxel as standard references in the two cell lines.

The results demonstrated that fluorinated taxoids appear to share the same mechanism of cell death induction to exert their in vitro anticancer effects as compared with non-fluorinated taxoid **SB-T-1216** and the paclitaxel. Also, the cell death inducing concentration of fluorinated taxoids is comparable to the second-generation non-fluorinated taxoids **SB-T-1216**, both of which are around five times more potent than paclitaxel. What is more impressive is that these fluorinated taxoids are significantly more effective than paclitaxel against MDA-MB-435 resistant cell lines, similar to what has been observed in other breast and pancreatic cancer cell lines as described earlier. Therefore, the non-fluorinated or fluorinated novel taxoids are excellent candidates for further development and may lead to great treatment options for patients who are refractory to the conventional paclitaxel treatment.

The fluorinated taxoids have been further investigated in vivo in a subcutaneous rat lymphoma model. **SB-T-12854** was reported to significantly suppress the spontaneous rat lymphoma. [44]

Fluorinated taxoid **SB-T-12854** was also provided to American BioScience, Inc (now Abraxis BioScience, Inc.) under the collaboration for formulation studies of novel taxoids. American BioScience, Inc has invented a novel albumin-bound formulation for paclitaxel that has gained FDA approval in January 2005 under the trade name Abraxane®. Abraxane® is an injectable suspension using albumin as delivery system, instead of conventional Cremophor EL/ethanol formulation in Taxol®. The human serum albumin was employed as the stabilizer, as it creates protein-stabilized nanoparticle colloidal suspension and can increase the concentration of paclitaxel to 2-10 mg/mL in normal saline. This eliminates the need for pre-medication with steroids or antihistamines for hypersensitivity reactions caused by these solvents. Abraxane ® is 59-fold less toxic than paclitaxel alone, and 29-fold less toxic than the excipients of Paclitaxel. [45]

§4.2.3 Conclusion

C3' difluorovinyl second-generation taxoid **SB-T-12854** was successfully synthesized in gram scale, and was evaluated for their antitumor activity against various drug-sensitive and drug-resistant human cancer cell lines. It was found that **SB-T-12854** consistently exhibited higher potency than paclitaxel, i.e. one magnitude higher potency in sensitive cancer cell lines, as well as two magnitudes higher in resistant cancer cell lines. These results showed that C3' difluorovinyl taxoid **SB-T-12854** is a very promising development candidates for treatment of cancer patients, particularly those who are refractory to treatment with paclitaxel.

§4.3 Synthesis and Fluorescence Study of C7-Fluorescein-SB-T-12854

§4.3.1 Application of Fluorescein in the Biological Studies

The unique mechanism of action of paclitaxel discovered around thirty years ago [46] [47] had spurred the rapid progression in research and development of paclitaxel, which led to its current status as a widely used clinical agent for cancer treatment. Its microtubule-stabilizing property has shed light on the normal process of microtubule dynamics and highlighted the importance of this process in cellular events. [48] The "dynamic instability" of microtubules [49] is critical to many cellular processes, particularly the assembly and function of a mitotic spindle during cell division. [50] Paclitaxel reversibly binds to the *β*-tubulin and stabilizes the microtubule and prevents the normal microtubule dynamics. Meanwhile, it also sets off a number of morphological changes in the cells, [51] [52] e.g. the formation of an atypical microtubule bundles. [53]

In order to make observations, an anti-tubulin/microtubule immunofluorescence or fluorescent-labeled ligand is commonly used before treated cells were subject to fluorescence microscopy or flow cytometry to collect qualitative or quantitative results.

The technology of flow cytometry (also called FACS - fluorescence-activated cell sorting) is one of the greatest invention in the field of cell biology, and now has broad applications in a number of fields, including molecular biology, pathology, immunology, medicine, genetics, etc. Modern flow cytometers allow simultaneous multiparametric analysis of the physical and/or chemical characteristics of up to thousands of particles per second.

A flow cytometer is similar to a microscope, except that, instead of producing an image of the cell, flow cytometry offers high-throughput and automated quantification of cells based on specific set properties.

Fluorescent paclitaxel is a commonly used molecular probe in the studies of cellular microtubules, as well as the microtubule-stabilizing mechanisms of paclitaxel. [54] [55] [56] It is reasonable to envision that a bioactive fluorescence-labeled paclitaxel or its analogs, together with FACS technology, would allow the study of previously unprobed areas, such as the localization of paclitaxel, the exploration of a secondary receptor site, and the elucidation of mechanism of actions of paclitaxel analogues.

§4.3.2 Synthesis of C7-Fluorescein-SB-T-12854

As mentioned in §4.2, the C3'-difluorovinyl-taxoid **SB-T-12854** demonstrated a one to two orders of magnitude higher potency than paclitaxel in different sensitive cancer cell lines and two to three orders of magnitude higher potency than paclitaxel in different resistant cancer cell lines. The mechanistic study of C3'-difluorovinyl-taxoid has yet to be extensively performed.

The synthesis of fluorescence-labeled C3'-difluorovinyl-taxoids are of interest, as they would allow us to elucidate cellular uptake of the tumor-targeting molecule, and pioneered further cellular / molecular biology studies.

Based on the established SAR of the paclitaxel (in Chapter 1), modifications to the C13-sidechain and to the substituents on the 'Southern' region are less tolerated while modifications on the 'Northern' region have much less impact to the drug's activity. On top of that, the C7-hydroxy generally exhibits a better reactivity than C10-hydroxy group and thus is selected as the position to link the fluorescent moiety.

In cellular biology, fluorescein and its isothiocyanate derivative FITC are often used to label and track cells in fluorescence microscopy or flow cytometry. Additional biologically active molecules (such as antibodies) may also be attached to fluorescein, allowing biologists to target the fluorophore to specific proteins or structures within cells. The fluorescein is selected due to its high synthetic yields and good water solubility (**Figure 4-5**).

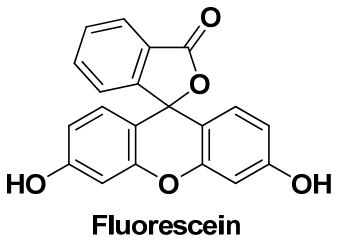

Figure 4-5. Structure of fluorescein

Tethered fluorescein was provided by courtesy of J. Seize in our laboratory with the following synthetic route. Fluorescein was converted to methyl ester, followed by Mitsunobu coupling with 4-hydroxy-butyric acid *tert*-butyl ester to give the precursor of tethered fluorescein. Deprotection of *tert*-butyl group afforded 2-[6-(3-carboxy-propoxy)-3-oxo-3H-xanthen-9-yl]benzoic acid methyl ester (**Scheme 4-8**).

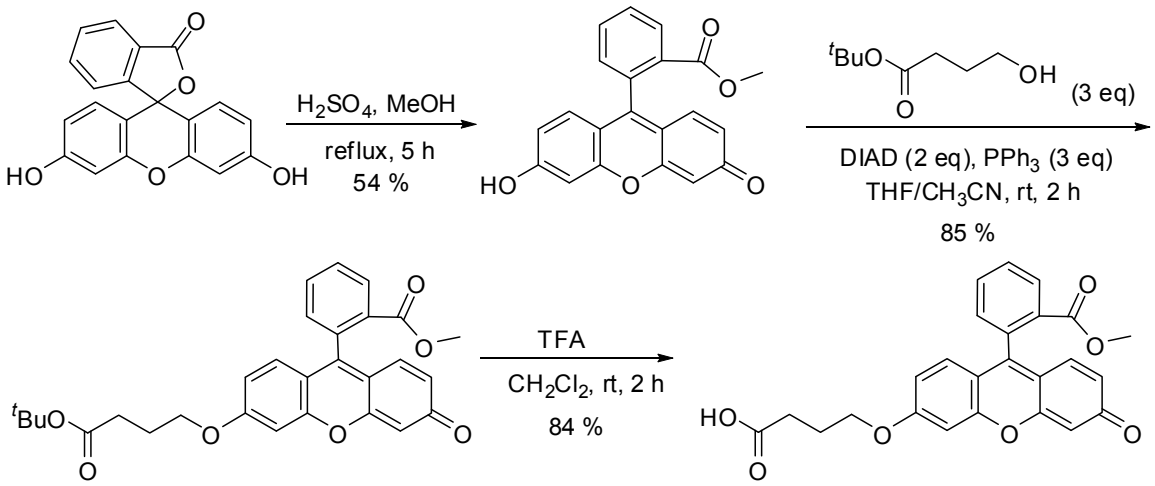

Scheme 4-8. Modification of Fluorescein

C2' hydroxy group of **SB-T-12854** was protected by TBDMS group, followed by C7 coupling with the tethered fluorescein. Deprotection with HF/pyridine generated desired **fluorescein-SB-T-12854** conjugate (**Scheme 4-9**).

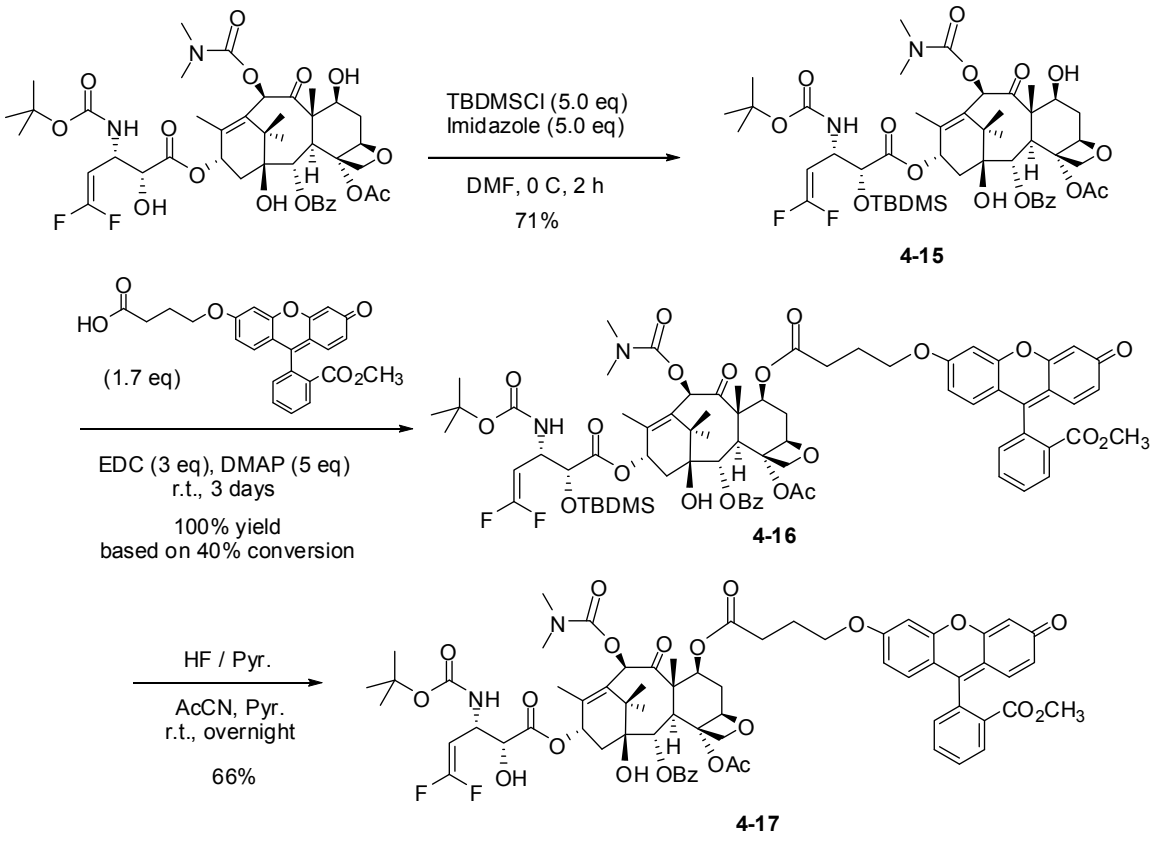

Scheme 4-9. Synthesis of C3'-Difluorovinyl-taxoid **SB-T-12854**

§4.3.3 Results and Discussion

The synthesized **fluorescein-SB-T-12854** is subject to cytotoxic study and flow cytometry. The assays were conducted by E. Zuniga in our laboratory. **Table 4-4** showed that **SB-T-1284** exhibits much better potency than paclitaxel in colon carcinoma cell line DLD-1, Human colon adenocarcinoma grade II cell line HT-29 and the murine ovarian cancer cell line ID8.

The additional substitution with C7-fluorescein, although showing lower potency of **SB-T-12854**, still exhibits comparable cytotoxicity to that of paclitaxel in the DLD-1 colon carcinoma cell line.

Table 4-4. Cytotoxic activity of paclitaxel, **SB-T-12854** and **fluorescein-SB-T-12854**
Cells were incubated for 48h at 37°C with 5% CO_2 after treatment with taxoids.

Cancer Cell Line	Compound	IC_{50} (nM)	Average IC_{50} (nM)
DLD-1	Paclitaxel	128, 144, 139	137 ± 8.19
	SB-T-12854	0.44, 0.22, 0.09	0.25 ± 0.18
	Fluorescein-SB-T-12854	156, 241, 251	216 ± 52.2
HT-29	Paclitaxel	35.8, 42.6, 13.2	30.5 ± 15.4
	SB-T-12854	0.57, 0.51, 0.54	0.54 ± 0.03
	Fluorescein-SB-T-12854	572, 557, 536	555 ± 18.1
ID8	Paclitaxel	14.2, 6.94, 6.74	9.29 ± 4.25
	SB-T-12854	0.44, 0.23, 0.16	0.28 ± 0.15
	Fluorescein-SB-T-12854	146, 218, 283	216 ± 68.5

The **fluorescein-SB-T-12854** was also evaluated by flow cytometry in different cancer cell lines (**Figure 4-6**). The fuorescein labeled compound across the board showed good uptake by cancel cells.

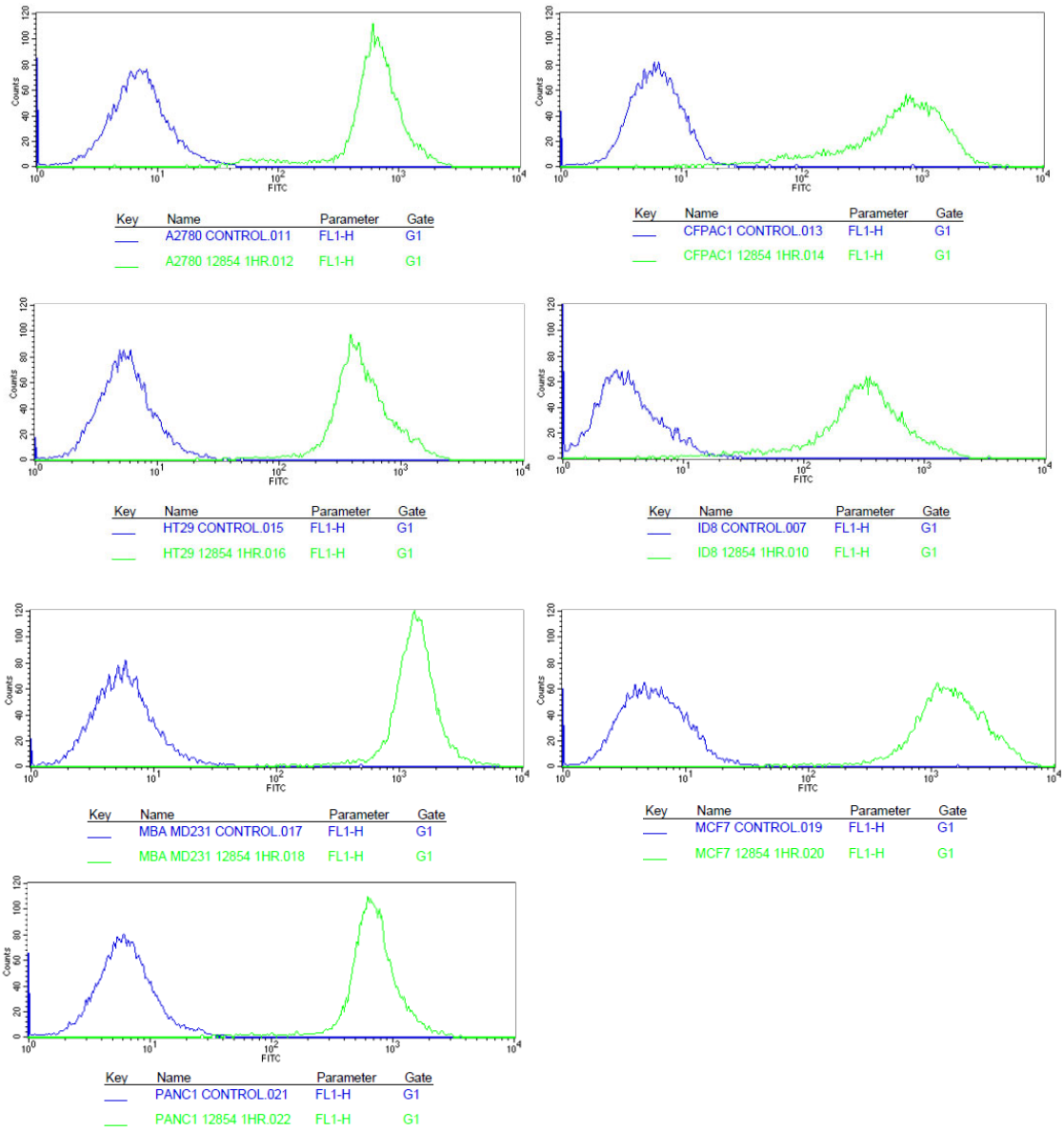

Figure 4-6. Flow cytometry / FACS results of **fluorescein-SB-T-12854** in human ovarian cancer cell line A2780, human colon adenocarcinoma grade II cell line HT-29, human breast cancer cell MBA-MD-231, human pancreatic carcinoma, epithelial-like cell line Pacn-1, human pancreatic adenocarcinoma cell lines CFPAC-1, the murine ovarian cancer cell line ID8 and human breast cancer cell line MCF-7. Cells incubated with 10μM for 1 h at 37 °C with 5% CO_2.

§4.3.4 Conclusion

The work presented above shows that the C7 position of C3'-difluorovinyl-taxoid **SB-T-12854** can be substituted with a fluorescein label via a four-carbon long linker. The defined synthetic route can be further applied to other C3'-difluorovinyl-taxoids with good overall yield.

The method should easily adapt to the production of any labeled taxoid of interest.

According to the biological studies, substitutions at the C7 position of C3'-difluorovinyl-taxoid retain reasonable biological activity. Although the activity is lower than that of fluorescein-free taxoid, it is still comparable to that of paclitaxel.

This conjugate and its analogue would enable the study of microtubule-based cytoskeleton of living cells without using invasive techniques such as the microinjection of fluorescently labeled proteins or the more severe fixation procedures required for immunofluorescence. Also, the attachment of a fluorescent probe to a tumor-targeting drug conjugate make it possible to clarify the interaction between the tumor-targeting taxoid and its receptors, the internalization into cancer cells and the real-time distribution of the conjugate.

§4.4 Experimental Section

Materials

The chemicals were purchased from Sigma-Aldrich and/or Fisher Scientific and were used without further purification unless otherwise noted. 10-DAB III and 14β-hydroxy-10-deacetylbaccatin III were gift from Indena, SpA, Italy and used as received. Tetrahydrofuran, dichloromethane, toluene and ethyl ether were obtained from the PureSolv^{TM} Solvent Purification System (Innovative Technology, Inc.) under N_2. The glassware was dried in a 110 ^{o}C oven and allowed to cool to room temperature in a desiccator over "Drierite" (calcium sulfate).

General Methods

^{1}H, ^{13}C and ^{19}F NMR spectra were obtained on Varian 300, 400 or 500 NMR spectrometers. Melting points were measured on a Thomas Hoover Capillary melting point apparatus and are uncorrected. TLC was performed on Merck DC-alufolien with Kieselgel 60F-254 and flash column chromatography was carried out on silica gel 60 (Merck, 230-400 mesh ASTM). Optical rotations were measured on a Perkin-Elmer Model 241 polarimeter. IR spectra were measured on a Shimadzu FTIR-8400s spectrophotometer. Chemical purity was determined on Shimadzu LC-1020A, using a Phenomenex Curosil-B column (5μ, 4.6 × 250 mm), employing CH_3CN/water (40/60, V/V) as the eluent with a flow rate of 1 mL/min. Chiral HPLC analysis for the determination of enantiomeric excess was carried out on a Waters HPLC assembly consist of a Waters M45 solvent delivery system and a Waters 484 detector (at 254 nm) on a PC workstation running Millennium 32 using a DAICEL-CHIRACEL OD chiral column (25 × 0.46 cm), employing n-hexanes/isopropanol (95/5, V/V) as eluent with a flow rate of 1.0 mL/min. High resolution mass spectra were obtained from the Mass Spectrometry Laboratory, University of Illinois at Urbana-Champaign, Urbana, IL.

1-(4-Methoxyphenyl)-3-(methyl-but-2-enyl)imine (4-1) [57]

To a mixture of *p*-anisidine (7.11 g, 57 mmol) and anhydrous Na_2SO_4 (24.20 g, 0.17 mol) in CH_2Cl_2 (114 mL, c = 0.5 M) was added 3-methylbut-2-enal (6.9 ml, 72 mmol) dropwise, and the mixture was stirred at room temperature for 2 h. The mixture was filtered and concentrated in vacuo to afford 10.2 g crude product **4-1** as a pale red oil: ^{1}H NMR (300 MHz, $CDCl_3$) δ 1.96 (d, J = 0.9 Hz, 3 H, CH_3), 2.01 (d, J = 0.9 Hz, 3 H, CH_3), 3.81 (s, 3 H, OCH_3), 6.21 (td, J = 9.6, 1.2 Hz, 1 H, vinyl-H), 6.89 (td, J = 9.0, 2.1 Hz, 2 H, aryl-H, ortho- to methoxy), 7.11 (td, J = 9.0, 2.1 Hz, 2 H, aryl-H meta- to methoxy) and 8.48 (br d, J = 9.6 Hz, 1 H, N-H) ppm. All data are in agreement with literature values. [57]

(±)-1-(4-Methoxyphenyl)-3-acetoxyl-4-(2-methylprop-1-enyl)azetidin-2-one [(±)-4-2] [57]

The crude product was dissolved in CH_2Cl_2 (200 mL) and triethylamine (16 mL, 0.10 mol), then the reaction mixture was cooled down to -78 °C. To the mixture was added acetoxyacetyl

chloride (9.3 mL, 86 mmol) and stirred overnight to reach room temperature. The reaction was quenched with saturated NH_4Cl solution (20 mL) and the resulting mixture was separated. The aqueous layer was extracted with CH_2Cl_2 (50 ml × 3). The combined organic layers was washed with water (30 mL × 2) and brine (30 mL), then dried over anhydrous $MgSO_4$, filtered and concentrated in vacuo. Flash column chromatography on silica gel using hexanes/ethyl acetate (5/1) gave **(±)-4-2** (12.5 g, 75% for two steps) as a white solid: ^{1}H NMR (300 MHz, $CDCl_3$) δ 1.79 (d, J = 1.5 Hz, 3 H, CH_3), 1.82 (d, J = 1.5 Hz, 3 H, CH_3), 2.11 (s, 3 H, acyl-CH_3), 3.78 (s, 3 H, OCH_3), 4.96 (dd, J = 4.8, 9.3 Hz, 1 H, C3-H), 5.13 (td, J = 1.2, 9.3 Hz, 1 H, vinyl-H), 6.89 (td, J = 2.1, 9.0 Hz, 2 H, aryl-H), 5.80 (d, J = 4.8 Hz, 1 H, H on C3), 6.86 (td, J = 3.0, 9.6 Hz, 2 H, aryl-H ortho- to methoxy group) and 7.31 (td, J = 2.1, 9.0 Hz, 2H, aryl-H meta- to methoxy group) ppm. All data are in agreement with literature values. [57]

Enantiomer-selective hydrolysis of *β*-lactam [57]

To a suspension of **(±)-4-2** (12.5 g, 43 mmol) in acetonitrile (140 mL) and a pH = 7.5 phosphate buffer solution (1.40 L, c = 0.2 M) was added PS-Amano lipase (4.6 g), and the mixture was vigorously stirred at 50 °C, until ^{1}H NMR of the crude sample shows >50/50 ratio of alcohol **(-)-3-6** over acetate **(+)-3-5**. The reaction mixture was then filtered and extracted with CH_2Cl_2 (800 mL × 3). The combined organic layers was washed with brine (100 mL), then dried over anhydrous $MgSO_4$, filtered and concentrated in vacuo. Flash column chromatography on silica gel using hexanes/ethyl acetate (5/1) gave **(+)-4-4** (4.73 g, 38%), and hexanes/ethyl acetate (3/1) gave **(-)-4-3** (5.55 g, 52%), both as white solid: **(+)-4-4** ^{1}H NMR (300 MHz, $CDCl_3$) δ 1.79 (d, J = 1.5 Hz, 3 H, CH_3), 1.82 (d, J = 1.5 Hz, 3 H, CH_3), 2.11 (s, 3 H, acyl-CH_3), 3.78 (s, 3 H, OCH_3), 4.96 (dd, J = 4.8, 9.3 Hz, 1 H, C3-H), 5.13 (td, J = 1.2, 9.3 Hz, 1 H, vinyl-H), 6.89 (td, J = 2.1, 9.0 Hz, 2 H, aryl-H), 5.80 (d, J = 4.8 Hz, 1 H, H on C3), 6.86 (td, J = 3.0, 9.6 Hz, 2 H, aryl-H ortho- to methoxy group) and 7.31 (td, J = 2.1, 9.0 Hz, 2H, aryl-H meta- to methoxy group) ppm; **(-)-4-3** ^{1}H NMR (300 MHz, $CDCl_3$) δ 1.86 (s, 6 H, CH_3), 2.91 (br s, 1 H, OH), 3.78 (s, 3 H, OCH_3), 4.88 (dd, J = 5.1, 8.7 Hz, 1 H, C3-H), 5.20 (dd, J = 5.1, 7.5 Hz, 1 H, C2-H), 5.27 (d, J = 8.4 Hz, 1 H, vinyl-H), 7.83 (d, J = 9.0 Hz, 2 H, aryl-H o- to methoxy group) and 7.31 (d, J = 9.0 Hz, 2 H, aryl-H m- to methoxy group) ppm.All data are in agreement with literature values. [57]

(3*R*,4*S*)-1-(4-Methoxyphenyl)-3-hydroxy-4-(2-methylprop-1-enyl)azetidin-2-one (4-5) [57]

To a solution of **(+)-4-4** (4 g, 14 mmol) in THF (140 mL) was added a KOH aqueous solution (140 mL, c = 1 M) dropwise. The solution was stirred for 1 h and quenched with saturated NH_4Cl solution (100 mL). The mixture was extracted with CH_2Cl_2 (200 mL × 4). The combined organic layer was dried over anhydrous $MgSO_4$, filtered and concentrated to give **4-5** (3.48 g, quant., 100% ee) as a white solid: ^{1}H NMR (300 MHz, $CDCl_3$) δ 1.86 (s, 6 H, CH_3), 2.91 (br s, 1 H, OH), 3.78 (s, 3 H, OCH_3), 4.88 (dd, J = 5.1, 8.7 Hz, 1 H, C3-H), 5.20 (dd, J = 5.1, 7.5 Hz, 1 H, C2-H), 5.27 (d, J = 8.4 Hz, 1 H, vinyl-H), 7.83 (d, J = 9.0 Hz, 2 H, aryl-H o- to methoxy group) and 7.31 (d, J = 9.0 Hz, 2 H, aryl-H m- to methoxy group) ppm. Chiral HPLC analysis for the determination of enantiomeric excess was carried out on a Waters HPLC

assembly consist of a Waters M45 solvent delivery system and a Waters 484 detector (at 254 nm) using a DAICEL-CHIRACEL OD chiral column (25 × 0.46 cm), employing n-hexane/2-propanol (92/8, V/V) as the eluent with a flow rate of 0.5 mL/min. The retention time of the desired enatiomer was 25.85 min, while retention time of the other enatiomer (from a racemic reference) was 21.29 min. All data are in agreement with literature values. [57]

1-(4-Methoxyphenyl)-3-triisopropylsilyloxy-4-(2-methylpropen-2-yl)azetidin-2-one (4-6) [57]

To a solution of **4-5** (3.48 g crude) and DMAP (0.34 g, 2.8 mmol) in CH_2Cl_2 (50 mL) was added TEA (7.7 mL, 55 mmol) and TIPSCl (4.44 mL, 20 mmol). The reaction solution was stirred overnight at room temperature, and quenched with a saturated aqueous NH_4Cl solution (10 mL). The aqueous layer was extracted with CH_2Cl_2 (20 mL × 3) and the combined organic layer was washed with brine (10 mL), then dried over $MgSO_4$, filtered and concentrated in vacuo. The crude product was purified by flash column chromatography on silica gel using hexanes/ethyl acetate (15/1) to afford **4-6** (4.87 g, 87% for two steps) as a white solid: ^{1}H NMR (300 MHz, $CDCl_3$) δ 1.00 - 1.25 (m, 21 H, from TIPS group), 1.79 (d, J = 0.9 Hz, 3 H, CH_3), 1.84 (d, J = 1.5 Hz, 3 H, CH_3), 3.77 (s, 3 H, OCH_3), 4.80 (dd, J = 4.8, 9.9 Hz, 1 H, C3-H), 5.05 (d, J = 5.1 Hz, 1 H, C2-H), 5.33 (d, J = 9.9 Hz, 1 H, vinyl-H), 6.84 (td, J = 2.1, 9.3 Hz, 2 H, aryl-H ortho- to methoxy group) and 7.32 (td, J = 2.1, 9.0 Hz, 2 H, meta- to methoxy group) ppm. All data are in agreement with literature values. [57]

(3*R*,4*S*)-1-4-Methoxyphenyl-3-triisopropylsiloxy-4-formylazetidin-2-one (4-7) [38]

To a solution of **4-6** (1.96 g, 4.85 mmol) in CH_2Cl_2 was bubbled in O_3 at -78 °C until the solution turns into blue, when N_2 was bubbled instead to exclude the excess mount of O_3 until the solution turned to colorless. Then dimethyl sulfide (5 eq) was added dropwise and the reaction mixture was allowed to ward up during 3 h. The crude product was obtained after solvent removal in vacuo, and further purified by flash column chromatography on neutral alumina (Hexanes/EtOAc = 8/1 then 3/1) to yield **4-7** (1.56 g, 87%) as a white solid: ^{1}H NMR (300 MHz, $CDCl_3$) δ 1.00-1.25 (m, 21 H, from TIPS group), 3.76 (s, 3 H, OCH_3), 4.44 (dd, J = 4.5, 5.4 Hz, 1 H, C3-H), 5.27 (d, J = 5.4 Hz, 1 H, C2-H), 6.84 (d, J = 9.3 Hz, 2 H, aryl-H o- to methoxy group), 7.24 (d, J = 9.0 Hz, 2 H, m- to methoxy group) and 9.74 (d, J = 4.2 Hz, 1 H, CHO) ppm. All data are in agreement with literature values. [38]

(3*R*,4*S*)-1-(4-Methoxyphenyl)-3-triisopropylsiloxy-4-(2,2-difluorovinyl)azetidin-2-one (4-8)

To a solution of dibromodifluoromethane (0.67 mL, 4.34 mmol) in THF (20 mL) at 0 °C was added hexamethylphosphorous triamide (1.62 mL, 8.68 mmol). The formed white suspension was quickly transferred to a solution of **4-7** (820 mg, 2.17 mmol) and Zn (0.71 g, 10.85 mmol) in THF (20 mL). The reaction mixture was then refluxed for 30 min. After cooled down to room temperature, the reaction mixture was filtered over celite to remove excess Zn powder. After solvent was evaporated in vacuo, the residue was purified by a short silica gel

column to yield **4-8** (600 mg, 67%) as a colorless oil: ^{1}H NMR (300 MHz, $CDCl_3$) δ 1.08-1.15 (m, 21 H), 3.79 (s, 3 H), 4.54 (ddd, J = 1.5, 6.3, 16.5 Hz, 1 H), 4.83 (m, 1 H), 5.14 (d, J = 5.1 Hz, 1 H), 6.87 (d, J = 9.0 Hz, 2H) and 7.32 (d, J = 9.0 Hz, 2H) ppm; ^{13}C NMR (75.5 MHz, $CDCl_3$) δ 12.1, 17.9, 54.1 (d, J = 8.5 Hz), 55.8, 75.8 (dd, J = 5.0, 22.1 Hz), 76.9, 77.4, 114.8, 118.6, 130.9, 156.7 and 164.9 ppm; ^{19}F NMR (282 MHz, $CDCl_3$) δ -80.80 (d, J = 32.7 Hz, 1 F) and -86.34 (dd, J = 2.8, 28.2, 1 F) ppm; HRMS (FAB$^+$) m/z calcd. for $C_{21}H_{31}F_2NO_3SiH^+$, 412.2114; found, 412.2127.

(3*R*,4*S*)-3-Triisopropylsiloxy-4-(2,2-difluorovinyl)azetidin-2-one (4-9)

To a solution of **4-8** (2.28 g, 5.53 mmol) in acetonitrile (150 mL) and H_2O (30 mL), was added dropwise a solution of ceric ammonium nitrate (10.8 g, 19.4 mmol) in water (40 mL). The reaction mixture was stirred for 2 h and quenched with saturated Na_2SO_3 solution. The aqueous layer was extracted with EtOAc, and the combined organic layer was washed with H_2O, dried over $MgSO_4$ and concentrated in vacuo. The product mixture was purified by flash column chromatography on silica gel to yield **4-9** (1.42 g, 84%) as a colorless oil: ^{1}H NMR (400 MHz, $CDCl_3$) δ 1.03-1.18 (m, 21 H), 4.44-4.54 (m, 2 H), 5.04 (dd, J = 1.6, 2.4 Hz, 1 H) and 6.59 (br s, 1 H) ppm; ^{13}C NMR (100 MHz, $CDCl_3$) δ 12.1, 17.8 (d, J = 4.6 Hz), 50.4 (d, J = 7.6 Hz), 77.1 (dd, J = 15.9, 23.5 Hz), 79.3, 157.6 (t, J = 289.9 Hz) and 169.4 ppm; ^{19}F NMR (282 MHz, $CDCl_3$) δ -82.33 (d, J = 34.7 Hz, 1 F), -87.50 (dd, J = 9.3, 25.7 Hz, 1 F).

1-(*tert*-Butoxycarbonyl)-3-triisopropylsiloxy-4-(2,2-difluorovinyl)azetidin-2-one (4-10)

To a solution of **4-9** (1.32 g, 4.33 mmol), triethylamine (2.1 mL, 13.0 mmol), and DMAP (134 mg, 1.08 mmol) in CH_2Cl_2 (15 mL), was added Boc_2O (1.06 g, 4.76 mmol) at room temperature. The reaction mixture was stirred overnight and quenched with aqueous NH_4Cl. The reaction mixture was diluted with EtOAc and the organic layer was washed with brine, dried over $MgSO_4$, and concentrated in vacuo. Crude product was purified by flash column chromatography to yield **4-10** (1.68 g, 95%) as a colorless oil: ^{1}H NMR (300 MHz, $CDCl_3$) δ 1.04-1.17 (m, 21 H), 1.49 (s, 9 H), 4.49 (ddd, J = 1.6, 13.8, 23.7 Hz, 1 H), 4.75 (dddd, J = 0.9, 2.4, 5.1, 9.0 Hz, 1 H), 5.04 (d, J = 5.7 Hz, 1 H) and 6.59 (br s, 1 H) ppm; ^{13}C NMR (100 MHz, $CDCl_3$) δ 12.0, 17.8 (d, J = 5.3 Hz), 28.2, 53.6 (d, J = 8.4 Hz), 74.5 (dd, J = 10.6, 26.5 Hz), 77.2, 83.9, 147.9, 158.5 (t, J = 292.2 Hz) and 165.3 ppm; ^{19}F NMR (282 MHz, $CDCl_3$) δ -81.20 (d, J = 31.0 Hz, 1 F), -85.83 (dd, J = 5.6, 29.3 Hz, 1 F) ppm; HRMS (FAB$^+$) m/z calcd. for $C_{19}H_{33}F_2NO_4SiNa^+$, 428.2039; found, 428.2050; $[\alpha]_D^{20}$ +24.17 (c 14.4, $CHCl_3$).

7-Triethylsilyl-10-deacetylbaccatin III (4-11) [58]

Under a nitrogen atmosphere, chlorotriethylsilane (1.7 mL, 10.8 mmol) was added dropwise to a solution of 10-DAB III (2.00 g, 3.67 mmol) and imidazole (0.98 g, 14.7 mmol) in dry DMF (60 mL) 0 °C. The reaction mixture was then stirred for 1 h at room temperature and diluted with EtOAc (250 mL). The mixture was then washed with H_2O (15 mL × 5), brine (25 mL), dried over $MgSO_4$ and concentrated in vacuo. Flash column chromatography on silica gel (Hexanes/EtOAc = 3/1) gave **4-11** (2.32 g, 94%) as a white solid: ^{1}H NMR (300 MHz, $CDCl_3$) δ

0.56 (m, 6 H), 0.94 (m, 9 H), 1.08 (s, 6 H), 1.59 (d, J = 2.5 Hz, 1 H), 1.73 (s, 3 H), 1.90 (dt, 1 H, H6a), 2.05 (d, J = 4.8 Hz, 1 H), 2.08 (s, 3 H), 2.24 (s, 1 H), 2.28 (s, 3 H, OAc), 2.48 (ddd, 1 H, H6b), 3.95 (d, J = 7.1 Hz, 1 H, H3), 4.16 (d, J = 8.3 Hz, 1 H, H20a), 4.25 (s, 1 H), 4.31 (d, J = 8.3 Hz, 1 H, H20b), 4.40 (dd, J = 6.4, 10.5 Hz, 1 H, H7), 4.85 (t, 1 H, H13), 4.95 (d, J = 8.0 Hz, 1 H, H5), 5.17 (s, 1 H, H10), 5.60 (d, J = 7.0 Hz, 1 H, H2), 7.47 (t, J = 7.5 Hz, 2 H), 7.60 (t, J = 7.5 Hz, 1 H) and 8.10 (d, J = 7.3 Hz, 2 H) ppm; ^{13}C NMR (75.0 MHz, $CDCl_3$) δ 5.1, 6.7, 9.9, 15.1, 19.5, 22.6, 26.8, 37.2, 38.6, 42.7, 47.0, 57.9, 67.9, 72.9, 74.6, 74.8, 76.5, 78.8, 80.7, 84.2, 87.6, 128.6, 129.4, 130.0, 133.6, 135.1, 141.8, 167.0, 170.7 and 210.3 ppm. All data are in agreement with literature values. [58]

7-Triethylsilyl-10-deacetyl-10-*N*,*N*-dimethylcarbamoylbaccatin III (4-12) [35]

In the solution of **4-11**(1.62 g, 4.11 mmol) in dry THF (80 mL) was added LiHMDS (1.0 M in THF, 4.93 ml, 4.93 mmol) dropwise by syringe at -40 °C. The mixture was stirred at -40 °C for 5 min, and then freshly made 3-(4-methoxyphenyl)propionic chloride (1.2 eq) was added dropwise. After 1 h, the reaction was quenched with saturated aqueous NH_4Cl, extracted with three portion of EtOAc, and the combined organic layers were dried over anhydrous $MgSO_4$ and concentrated in vacuo. The crude product was purified by flash column chromatography on silica gel to afford **4-12** (1.73 g, 97%) as a white solid: ^{1}H NMR (300 MHz, $CDCl_3$) δ 0.56 (m, 6 H), 0.85 (m, 9 H), 0.92 (s, 3 H), 1.20 (m, 7 H), 1.64 (s, 3 H), 1.87 (m, 1 H), 2.00 (s, 3 H), 2.18 (s, 3 H), 2.26 (s, 3 H), 2.53 (m, 1H), 2.70 (m, 2 H), 2.95 (t, J = 8.1 Hz, 2 H), 3.77 (s, 3 H), 3.86 (m, 4 H), 4.14 (d, J = 8.7 Hz, 1 H), 4.33 (d, J = 8.7 Hz, 1 H), 4.49 (dd, J = 10.2, 6.7 Hz, 1 H), 4.81 (t, J = 7.9 Hz, 1 H), 4.96 (d, J = 8.4 Hz, 1 H), 5.62 (d, J = 6.6 Hz, 1 H), 6.48 (s, 1 H), 6.81 (d, J=8.7 Hz, 2 H), 7.14 (d, J = 8.4 Hz, 3 H), 7.37 (t, J = 8.1 Hz, 1 H), 7.60 (s, 1 H) and 7.70 (d, J = 7.5 Hz, 1 H) ppm. All data are in agreement with literature values. [35]

3'-Dephenyl-3'-(2,2-difluorovinyl)-10-dimethylcarbamoyl-7-triethylsilyl-2'-triisopropylsilyldocetaxel (4-13)

To a solution of modified baccatin **4-12** (2.52 g, 4.11 mmol) and difluorovinyl-β-lactam 3-11 (2.43 g, 6.16 mmol) in 100 mL THF at -40 °C, was added LiHMDS (1M in THF, 6.16 mL, 6.16 mmol). The reaction was stirred for 2 h at -40 °C and quenched with 10 mL of NH_4Cl, the aqueous layer was extracted with ethyl acetate, and the combined organic layers were dried with brine and $MgSO_4$. The crude was purified by flash column chromatography on silica gel to yield **4-13** (3.69 g, 94%) as a white solid: ^{1}H NMR (300 MHz, $CDCl_3$) δ 0.57-0.62 (m, 6 H, $SiCH_2CH_3$), 0.88-0.94 (m, 9 H, $SiCH_2CH_3$), 1.08-1.13 (m, 21 H, H on TIPS), 1.20 (s, 3 H, H on C16 or C17), 1.22 (s, 3 H, H on C16 or C17), 1.30 (s, 9 H, H on Boc), 1.65 (br s, exchangeable, 1 H, OH), 1.68 (s, 3 H, H on C19), 2.05 (s, 3 H, H on C18), 2.16-2.30 (m, 1 H, H14), 2.36 (s, 3 H, H on OAc), 2.93 (s, 3 H, H on $N(CH_3)_2$), 3.06 (s, 3 H, H on $N(CH_3)_2$), 3.84 (d, J = 6.6 Hz, 1 H, H3), 4.18 (d, J = 8.4 Hz, 1H, H20), 4.31 (d, J = 8.4 Hz, 1H, H20), 4.42-4.54 (m, 3 H, H7, H2' and H3'), 4.86-4.97 (m, 3 H, H5, vinyl H, and NH), 5.69 (d, J =6.9 Hz, 1 H, H2), 6.18 (d, J =8.1 Hz, 1 H, H13), 6.39 (s, 1 H, H10), 7.48 (t, J = 7.2 Hz, 2 H, m-H on benzoyl group), 7.59 (t, J = 7.2 Hz, 1 H, p-H on benzoyl group) and 8.11 (d, J = 7.5 Hz, 2 H, o-H on benzoyl group) ppm.

3'-Dephenyl-3'-(2,2-difluorovinyl)-10-dimethylcarbamoyldocetaxel (SB-T-12854, 4-14)

To a solution of **4-13** (2.33 g, 3.80 mmol) in of a 1:1 mixture of pyridine and CH_3CN (46 mL, V/V = 1:1), was added 23 mL of HF-pyridine at 0 °C. The reaction was stirred and allowed to warm up to room temperature overnight. The reaction was then quenched with aqueous $NaHCO_3$ solution and stirred for 10 min. After diluted with ethyl acetate, the organic layers were washed with $NaHCO_3$, $CuSO_4$, brine, and dried over $MgSO_4$ and concentrate in vacuo. The residue was purified by flash column chromatography on silica gel using hexanes/ethyl acetate (1/1) as eluent to afford **4-14** (1.51 g, 96%) as a white solid: ^{1}H NMR (500 MHz, $CDCl_3$) δ 1.15 (s, 3 H, H-16), 1.25 (s, 3 H, H-17), 1.30 (s, 9 H, Boc), 1.66 (s, 3 H, H-19), 1.75 (br s, 1 H, OH), 1.87 (m, 1 H, H-6b), 1.90 (s, 3 H, H-18), 2.31 (m, 2 H, H-14), 2.39 (br s, 3 H, 4-OAc), 2.54 (ddd, J = 7.0, 10.0, 15.5 Hz, 1 H, H-6a), 2.96 (s, 3 H, N-Me), 3.04 (s, 3 H, N-Me), 3.56 (br s, 1 H, OH), 3.81 (d, J = 7.0 Hz, 1 H, H-3), 4.16 (d, J = 8.5 Hz, 1 H, H-20b), 4.27 (s, 1 H, H-2'), 4.32 (d, J = 8.5 Hz, 1 H, H-20a), 4.45 (dd, J = 6.5, 10.5 Hz, 1 H, H-7), 4.57 (ddd, J = 1.0, 9.0, 24.0 Hz, 1 H, H-3' vinyl), 4.85 (t, J = 8.0 Hz, 1 H, H-3'), 4.97 (m, 2 H, H-5, NH-3'), 5.65 (d, J = 7.0 Hz, 1 H, H-2), 6.23 (t, J = 9.5 Hz, 1 H, H-13), 6.25 (s, 1 H, H-10), 7.23 (dd, J = 1.5, 8.5 Hz, 1 H), 7.47 (t, J = 8.0 Hz, 1 H), 7.80 (s, 1 H) and 7.89 (d, J = 8.0 Hz, 1 H) ppm; ^{13}C NMR (75.5 MHz, $CDCl_3$) δ 9.3, 14.9, 22.3, 26.9, 28.1, 35.4 (d, J = 6.6 Hz), 36.0, 36.6, 43.2, 58.5, 72.4, 72.6, 73.1, 75.6, 76.1, 76.3, 79.2, 80.1, 84.7, 120.7, 120.2, 124.3, 126.7, 130.2, 130.9, 133.4, 140.9, 142.6, 154.9, 156.1, 166.1, 170.3 and 205.5 ppm; ^{19}F NMR (282 MHz, $CDCl_3$) δ –84.06 (dd, J = 25.7, 34.7 Hz, 1 F), –86.17 (d, J = 36.7 Hz, 1 F); HRMS (FAB$^+$) m/z calcd. for $C_{42}H_{53}F_2N_5O_{15}H^+$, 906.3579; found 906.3588 (Δ = 0.99 ppm); $[\alpha]_D^{20}$ -75.39 (c 4.51, $CHCl_3$). Certain steps were repeated to obtain target amount of 3 g for **SB-T-12854**.

2'-(*tert*-Butyldimethylsilyl-3'-dephenyl-3'-difluorovinyl-10-(*N*,*N*-dimethyl) carbamatecarbonyldocetaxel (4-15)

To a solution of **4-14** (135 mg, 0.16 mmol) and imidazole (53 mg, 0.78 mmol) in *N,N*-dimethylformamide (DMF, 0.64 mL) was added t-butyldimethylsilyl chloride (118 mg, 0.78 mmol) dropwise via syringe at at 0 ˚C, and then the reaction mixture was stirred for 4 h at RT and diluted with EtOAc. The mixture was then washed with H_2O (200 mL x 3), brine (150 mL), dried over $MgSO_4$ and concentrated. The crude product was purified on a silica gel column using hexane/EtOAc (80:20) as eluent to give **4-15** as a white solid (111 mg, 71% yield): ^{1}H NMR (400 MHz, $CDCl_3$) δ 8.12 (d, J = 7.6 Hz, 2H), 7.61 (t, J = 7.2 Hz, 1H), 7.50 (t, J = 7.5 Hz, 2H), 6.35 – 6.11 (m, 2H), 5.66 (d, J = 7.1 Hz, 1H), 5.08 – 4.76 (m, 3H), 4.56 – 4.36 (m, 2H), 4.31 (d, J = 8.0 Hz, 2H), 4.19 (d, J = 8.3 Hz, 1H), 3.81 (d, J = 7.3 Hz, 1H), 3.20 (s, 1H), 3.03 (s, 3H), 2.95 (s, 3H), 2.53 (s, 1H), 2.46 – 2.29 (m, 4H), 2.17 (t, J = 23.7 Hz, 1H), 1.88 (d, J = 21.0 Hz, 4H), 1.67 (s, 4H), 1.28 (d, J = 16.8 Hz, 12H), 1.15 (s, 3H), 0.95 (s, 9H), 0.15 (s, 3H) and 0.10 (s, 3H) ppm; ^{13}C NMR (101 MHz, $CDCl_3$) δ 205.62, 170.73, 170.03, 167.10, 156.10, 154.68, 142.93, 133.59, 133.19, 130.18, 129.18, 128.67, 84.65, 81.10, 80.14, 79.35, 76.10, 75.28, 74.38, 72.42, 71.50, 58.45, 45.51, 43.25, 36.60, 35.98, 35.55, 35.34, 28.13, 26.87, 25.64, 22.55, 22.40, 18.35, 14.92, 9.38, -4.84 and -5.46 ppm; ^{19}F NMR (376 MHz, $CDCl_3$) δ -88.80 (dd, J = 37.9, 25.3 Hz)

and -90.48 (d, J = 38.0 Hz) ppm.

7-Fluorescein-2'-TBDMS- SB-T-12854 (4-16)

A solution of **4-15** (110 mg, 0.10 mmol), EDC (57 mg, 0.14 mmol), DMAP (61 mg, 0.50 mmol) and 4-(9-(2-(methoxycarbonyl)phenyl)-3-oxo- 3H-xanthen-6-yloxy)butanoic acid (60 mg, 0.14 mmol) in DMF (1.5 mL) was stirred at room temperature for 3 days. The mixture was then diluted with 50 mL EtOAc, washed with H_2O (10 mL x 3), brine (10 mL), dried over $MgSO_4$ and concentrated. The crude product was purified on a silica gel column using hexane/EtOAc (85:15) as eluant to give **4-16** as a orange solid (63 mg, 100 % yield based on 40% conversion): ^{1}H NMR (400 MHz, $CDCl_3$) δ 8.23 (d, J = 7.0 Hz, 1H), 8.10 (d, J = 7.5 Hz, 2H), 7.76 – 7.54 (m, 3H), 7.49 (t, J = 7.7 Hz, 2H), 7.29 (d, J = 7.5 Hz, 1H), 6.96 (dd, J = 5.1, 2.3 Hz, 1H), 6.84 (t, J = 9.5 Hz, 2H), 6.71 (dd, J = 9.0, 2.3 Hz, 1H), 6.52 (d, J = 9.8 Hz, 1H), 6.44 (s, 1H), 6.29 – 6.14 (m, 2H), 5.68 (d, J = 6.9 Hz, 1H), 5.62 (dd, J = 10.4, 7.2 Hz, 1H), 5.04 – 4.78 (m, 3H), 4.42 (dd, J = 25.2, 9.5 Hz, 1H), 4.32 (d, J = 8.5 Hz, 2H), 4.23 – 3.91 (m, 5H), 3.62 (d, J = 1.3 Hz, 3H), 2.99 (s, 3H), 2.91 (d, J = 19.1 Hz, 3H), 2.58 – 2.45 (m, 2H), 2.39 (d, J = 9.5 Hz, 3H), 2.16 (tdd, J = 20.4, 12.9, 7.1 Hz, 3H), 1.97 (s, 3H), 1.80 (s, 4H), 1.32 (s, 9H), 1.21 (d, J = 16.2 Hz, 8H), 0.95 – 0.90 (m, 9H), 0.13 (s, 3H) and 0.08 (d, J = 11.3 Hz, 3H) ppm; ^{13}C NMR (101 MHz, $CDCl_3$) δ 203.69, 185.55, 171.79, 170.70, 169.81, 166.93, 165.53, 163.52, 158.91, 156.20, 154.83, 154.27, 150.10, 140.90, 134.61, 133.61, 133.01, 132.55, 131.05, 130.51, 130.35, 130.09, 129.80, 129.53, 129.09, 128.68, 117.44, 114.63, 113.81, 105.68, 100.75, 83.96, 80.80, 80.08, 78.71, 76.29, 75.83, 74.60, 74.24, 71.52, 71.32, 68.05, 60.29, 55.89, 53.34, 52.30, 48.53, 46.89, 43.25, 36.52, 36.01, 35.34, 33.34, 31.51, 30.47, 29.62, 28.10, 26.22, 25.61, 23.72, 22.57, 22.30, 21.57, 18.29, 14.50, 14.03, 10.73, -4.85 and -5.49 ppm; ^{19}F NMR (376 MHz, $CDCl_3$) δ -84.88 (dd, J = 37.7, 25.1 Hz) and -86.60 (d, J = 38.0 Hz) ppm.

7-Fluorescein- SB-T-12854 (4-17)

To a solution of **4-16** (63 mg, 0.045 mmol) in 2.5 mL pyridine and 2.5 mL CH_3CN at 0°C was added 0.63 mL HF/Py. The mixture was stirred overnight, and was diluted with 40 mL EtOAc, washed with water, Cu_2SO_4 saturated solution, water and brine. The organic layer was dried over anhydrous $MgSO_4$ and concentrated in vacuo. The crude product was purified on a silica gel column (40% EtOAc in dichloromethane) to afford **4-17** as an orange solid (38 mg, 66 % yield): ^{1}H NMR (400 MHz, $CDCl_3$) δ 8.24 (d, J = 7.0 Hz, 1H), 8.12 (d, J = 7.4 Hz, 2H), 7.79 – 7.58 (m, 3H), 7.51 (t, J = 7.5 Hz, 2H), 7.32 (s, 2H), 6.95 – 6.81 (m, 2H), 6.73 (dd, J = 8.9, 2.3 Hz, 1H), 6.57 (d, J = 9.3 Hz, 1H), 6.43 (s, 1H), 6.29 (d, J = 3.5 Hz, 1H), 6.21 (d, J = 8.6 Hz, 1H), 5.75 (s, 1H), 5.70 (d, J = 6.9 Hz, 1H), 5.19 (s, 1H), 4.99 (d, J = 8.8 Hz, 1H), 4.91 (s, 1H), 4.65 (dd, J = 25.0, 9.8 Hz, 1H), 4.37 (d, J = 22.3 Hz, 2H), 4.27 (d, J = 8.7 Hz, 1H), 4.19 (d, J = 8.4 Hz, 2H), 4.02 (d, J = 5.3 Hz, 1H), 3.62 (d, J = 7.1 Hz, 3H), 3.35 (s, 1H), 3.00 (s, 3H), 2.88 (d, J = 5.0 Hz, 3H), 2.58 (s, 2H), 2.43 (s, 3H), 2.34 (d, J = 7.1 Hz, 2H), 2.11 (d, J = 6.7 Hz, 5H), 1.83 (s, 4H), 1.34 (s, 9H) and 1.22 (d, J = 6.3 Hz, 8H) ppm; ^{13}C NMR (101 MHz, $CDCl_3$) δ 204.01, 185.74, 172.51, 170.34, 167.17, 165.78, 164.10, 159.53, 154.99, 141.04, 134.80, 133.32, 132.71, 131.41, 131.20, 130.51, 130.29, 129.82, 129.27, 128.86, 117.44, 115.03, 114.78, 105.77, 101.18,

101.00, 84.37, 81.16, 80.32, 78.83, 76.33, 74.62, 72.30, 71.94, 71.78, 68.19, 56.22, 52.61, 47.51, 43.50, 35.64, 33.69, 29.91, 28.45, 28.34, 23.45, 15.02, 14.33 and 11.10 ppm; ^{19}F NMR (376 MHz, $CDCl_3$) δ -84.83 (dt, J = 35.7, 24.4 Hz) and -86.77 (dd, J = 36.4, 27.8 Hz) ppm. HRMS sample was submitted, waiting for the result.

§4.5 References

[1] Ojima, I. Use of Fluorine in the Medicinal Chemistry and Chemical Biology of Bioactive Compounds-A Case Study on Fluorinated Taxane Anticancer Agents. *ChemBioChem* **2004**, *5*, 628-635.

[2]Begue, J. P.; Bonnet-Delpon, D. Recent advances (1995-2005) in fluorinated pharmaceuticals based on natural products. *J. Fluor. Chem*. **2006**, *127*, 992–1012.

[3] Isanbor, C.; O'Hagan, D. Fluorine in medicinal chemistry: A review of anti-cancer agents. *J. Fluor. Chem.* **2006**, *127*, 303–319.

[4] Bondi, A. van der Waals volumes and radii. *J. Phys. Chem.*, **1964**, *68*, 441-451.

[5] Jeschke, P. The Unique Role of Fluorine in the Design of Active Ingredients for Modern Crop Protection *ChemBioChem* **2004**, *5*, 570-589.

[6] Penning, J. D.; Talley, J. J.; Bertenshaw, S. R. Carter, J. S.; Collins, P. W.; Docter, S.; Graneto, M. J.; Lee, L. F.; Malecha, J. W.; Miyashiro, J. M.; Rogers, R. S.; Rogier, D. J.; Yu, S. S.; Anderson, G. D.; Burton, E. G.; Cogburn, J. N.; Gregory, S. A.; Koboldt, C. M.; Perkins, W. E.; Seibert, K.; Veenhuizen, A. W.; Zhang, Y. Y.; Isakson, P. C. Synthesis and biological evaluation of the 1,5-diarylpyrazole class of cyclooxygenase-2 inhibitors:Identification of SC-56835 (celecoxib). *J. Med. Chem.* **1997**, *40*, 1347-1365.

[7] Clader, J. W. The Discovery of Ezetimibe: A View from Outside the Receptor. *J. Med. Chem.* **2004**, *47*, 1-9.

[8] Dugar, S.; Yumibe, N.; Clader, J.; W.; Vizziano, M.; Huie, K.; van Heek, M.; Compton, D. S.; Davis, H. R., Jr. Metabolism and structure activity data based drug design: discovery of (−) SCH 53079 an analog of the potent cholesterol absorption inhibitor (−) SCH 48461. *Bioorg. Med. Chem.Lett.* **1996**, *6*, 1271-1274.

[9] Smart, B. E. Fluorine substituent effects (on bioactivity). *J. Fluorine Chem*. **2001**, *109* 3-11.

[10] Böhm, H.-J.; Banner, D.; Bendels, S.; Kansy, M.; Kuhn, B.; Mueller, K.; Obst-Sander, U.; Stahl, M. Fluorine in medicinal chemistry. *ChemBioChem*, **2004**, *5*, 637-643.

[11] Ojima, I.; Kuduk, S. D.; Slater, J. C.; Gimi, R. H.; Sun, C. M. Syntheses of new fluorine-containing taxoids by means of *β*-lactam synthon method. *Tetrahedron* **1996**, *52*, 209-224.

[12] Ojima, I.; McCarthy, J. R.; Welch, J. T. (Eds.) Biomedical Frontiers of Fluorine Chemistry. *ACS symposium series*, American Chemical Society, Volume 639, 1st Ed., **1996,** pp 356.

[13] Cottet, F.; Marull, M.; Lefebvre, O.; Schlosser,M. Recommendable Routes to Trifluoromethyl-Substituted Pyridine- and Quinolinecarboxylic Acids. *Eur. J. Org. Chem.* **2003,** *8*, 1559–1568.

[14] Kirk, K. L. Fluorine in medicinal chemistry: Recent therapeutic applications of fluorinated small molecules. *J. Fluor. Chem*. **2006**, *127,* 1013–1029.

[15] Page, M. I. The mechanisms of reactions of *β*-lactam antibiotics. *Acc. Chem. Res.*, **1984**, *17*, 144-151.

[16] Khalafallah, A. K.; Hassan, M. E.; Soleman, H. A. Synthesis and biological studies on some spiro Schiff base derivatives. *J. Ind. Chem. Soc.*, **1992**, *69*, 318-320.

[17]Lukic, I. Preparation of novel derivatives of 3-bromo and 3,3-dibromo-4-oxo-1-azetidines for their use in antibacterial or antitumor therapy. **1997**, *Eur. Pat. Appl. 791580*.

[18] Borthwick, A. D.; Weingarten, G.; Haley, T. M.; Tomaszewski, M.; Wang, W.; Hu, Z.; Bedard,

J.; Jin, H.; Yuen, L.; Mansour, T. S. Design and synthesis of monocyclic β-lactams as mechanism-based inhibitors of human cytomegalovirus protease. *Bioorg. Med. Chem. Lett.* **1998**, *8*, 365-370.

[19] Ogilvie, W.; Bailey, M.; Poupart, M.-A.; Abraham, A.; Bhavsar, A.; Bonneau, P.; Bordeleau, J.; Bousquet, Y.; Chabot, C.; Duceppe, J.-S.; Fazal, G.; Goulet, S.; Grand-Maitre, C.; Guse, I.; Halmos, T.; Lavallee, P.; Leach, M.; Malenfant, E.; O'Meara, J.; Plante, R.; Plouffe, C.; Poirier, M.; Soucy, F.; Yoakim, C.; Deziel, R. Peptidomimetic Inhibitors of the Human Cytomegalovirus Protease. *J. Med. Chem.* **1997**, *40*, 4113-4135.

[20] Ojima, I. Recent Advances in the *β*-Lactam Synthon Method. *Acc. Chem. Res.* **1995**, *28*, 383-389.

[21] Ojima, I.; Delaloge, F. Asymmetric synthesis of building-blocks for peptides and peptidomimetics by means of the β-lactam synthon method. *Chem. Soc. Rev.* **1997**, *26*, 377-386.

[22] Ojima, I.; Delaloge, F. Syntheses of norstatine, its analogs, and dipeptide isosteres by means of *β*-lactam synthon method. *Methods Mol. Med.* **1999**, *23*, 137-160.

[23] Pepe, A.; Kuznetsova, L.; Sun, L.; Ojima, I. Fluoro-taxoid anticancer agents. In: *Fluorine in medical chemistry and chemical biology*. Ojima, I. (Ed.) 1st Ed., Wiley-Blackwell, Chichester, pp 117–139, **2009**.

[24] Ojima, I.; Kuduk, S. D.; Slater, J. C.; Gimi, R. H.; Sun, C. M.; Chakravarty, S.; Ourevitch, M.; Abouabdellah, A.; Bonnet-Delpon, D.; Begue, J.-P.; Veith, M.; Pera, P.; Bernacki, R. J. In: *Biomedical Frontiers of Fluorine Chemistry.* Ojima, I.; McCarthy, J. R.; Welch J. T. (Eds.) ACS Symposium Series 639, American Chemical Society, Washington, DC, pp. 228–243, **1996**.

[25] Ojima, I.; Inoue, T.; Slater, J. C.; Lin, S.; Kuduk, S. C.; Chakravarty, S.; Walsh, J. J.; Gilchrist, L.; McDermott, A. E.; Cresteil, T.; Monsarrat, B.; Pera, P.; Bernacki, R. J. In: *Asymmetric Fluoroorganic Chemistry: Synthesis, Application, and Future Directions.* Ramachandran P. V. (Ed.) ACS Symposium Series 746, American Chemical Society, Washington, DC, pp. 158–181, **1999**.

[26] Ojima, I.; Kuduk, S. C.; Chakravarty, S.; Ourevitch, M.; Begue, J.-P. *J. Am. Chem. Soc*. **1997**, *119*, 5519–5527.

[27] Ojima, I.; Lin, S.; Slater, J. C.; Wang, T.; Pera, P.; Bernacki, R. J.; Ferlini, C.; Scambia, G. *Bioorg. Med. Chem.* **2000**, *8*, 1619–1628.

[28] Kuznetsova, L.; Ungureanu, I. M.; Pepe, A.; Zanardi, I.; Wu, X.; Ojima, I. Trifluoromethyl- and difluoromethyl-*β*-lactams as useful building blocks for the synthesis of fluorinated amino acids, dipeptides, and fluoro-taxoids. *J. Fluorine Chem.* **2004**, *125*, 487-500.

[29] Gut, I.; Ojima, I.; Vaclavikova, R.; Simek, P.; Horsky, S.; Soucek, P.; Kondrova, E.; Kuznetsova, L. V.; Chen, J. *Xenobiotica* **2006**, *36*, 772–792.

[30] Vuilhorgne, M.; Gaillard, C.; Sanderlink, G. J.; Royer, I.; Monsarrat, B.; Dubois, J.; Wright, M. In: *Taxane Anticancer Agents: Basic Science and Current Status.* Georg, G. I., Chen, T. T., Ojima, I., Vyas, D. M. (Eds.) ACS Symp. Ser. 583; American Chemical Society: Washington, D.C., pp 98-110, **1995**.

[31] Ojima, I.; Das, M. Recent Advances in the Chemistry and Biology of New Generation Taxoids, *J. Nat. Prod.* **2009**, *72,* 554–565.

[32] Yamazaki, T.; Hiraoka, S.; Sakamoto, J.; Kitazume, T. Mesyloxy-group migration as the stereoselective preparation method of various functionalized olefins and its reaction mechanism, *Org. Lett.* **2001**, *3*, 743-746.

[33] Lim, M. H.; Kim, H. O.; Moon, H. R.; Chun, M. W.; Jeong, L. S. Synthesis of Novel D-2'-Deoxy-2'-C-difluoromethylene-4'-thiocytidine as a Potential Antitumor Agent, *Org. Lett.* **2002**, *4*, 529-531.

[34] Bhadury, P. S.; Palit, M.; Sharma, M.; Raza, S. K.; Jaiswal, D. K. Fluorinated phosphonium ylides: versatile *in situ* Wittig intermediates in the synthesis of hydrofluorocarbons, *J. Fluorine Chem.* **2002**, *116*, 75-80.

[35] Ojima, I.; Slater, J.; Michaud, E.; Kuduk, S.; Bounaud, P.; Vrignaud, P.; Bissery, M.; Veith, J.; Pera, P.; Bernacki, R. Syntheses and Structure-Activity Relationships of the Second-Generation Antitumor Taxoids: Exceptional Activity against Drug-Resistant Cancer Cells. *J. Med. Chem.* **1996**, *39*, 3889–3896.

[36] Ojima, I.; Slater, J. C.; Pera, P.; Veith, J. M.; Abouabdellah, A.; Bégué, J.-P.; Bernacki, R. J. *Bioorg. Med. Chem. Lett.* 1997, *7*, 133-138.

[37] Ojima, I.; Lin, S. N.; Slater, J. C.; Wang, T.; Pera, P.; Bernacki, R. J.; Ferlini, C.; Scambia, G. *Bioorg. Med. Chem.* **2000**, *8*, 1619-1628.

[38] Kuznetsova, L., *Ph.D. Dissertation*; SUNY at Stony Brook: Stony Brook, **2005**.

[39] Vobořilová, J.; Němcová-Fürstov, V.; Neubauerová, J.; Ojiman I.; Zanardi, I.; Gut, I.; Kovář, J. Cell death induced by novel fluorinated taxanes in drug-sensitive and drug-resistant cancer cells. *Investigational New Drugs* **2009**, *29*, 411-423.

[40] Bhalla, K. N. Microtubule-targeted anticancer agents and apoptosis. *Oncogene* **2003,** *22*, 9075–9085.

[41] Liao, P. C.; Tan, S. K.; Lieu, C. H.; Jung, H. K. Involvement of endoplasmic reticulum in paclitaxel-induced apoptosis. *J. Cell Biochem.* **2008**, *104*, 1509–1523.

[42] Mhaidat, N. M.; Wang, Y.; Kiejda, K. A.; Zhang, X. D.; Hersey, P. Docetaxel-induced apoptosis in melanoma cells is dependent on activation of caspase-2. *Mol Cancer Ther* **2007**, *6*, 752–761.

[43] Shi, J.; Orth, J. D.; Mitchison, T. Cell type variation in responses to antimitotic drugs that target microtubules and kinesin-5. *Cancer Res* **2008**, *68*, 3269–3276.

[44] Otová1, B.; Ojima, I.; Václavíková, R; Ehrlichová, J.; Souček, P.; Vobořilová, J.; Němcová, V.; Zanardi, I.; Horský, S.; Kovář, J.; Gut, I. Effects of novel taxanes on subcutaneous lymphoma in Sprague-Dawley/Cub rats: role of disposition, transport, in vitro efficiency and expression of relevant genes, submitted for publication.

[45] Damascelli, B.; Cantu, G.; Mattavelli, F.; Tamplenizza, P.; Bidoli, P.; Leo, E.; Dosio, F.; Cerrotta, A. M.; Di Tolla, G.; Frigerio, L. F.; Garbagnati, F.; Lanocita, R.; Marchiano, A.; Patelli, G.; Spreafico, C.; Ticha, V.; Vespro, V.; Zunino, F. Intraarterial chemotherapy with polyoxyethylated castor oil free paclitaxel, incorporated in albumin nanoparticles (ABI-007): Phase II study of patients with squamous cell carcinoma of the head and neck and anal canal: preliminary evidence of clinical activity, *Cancer*, **2001**, *92*, 2592-602.

[46] Schiff, P. B.; Fant, J.; Horwitz, S. B. Promotion of microtubule assembly *in vitro* by taxol. *Nature* **1979**, 277, 665-667.

[47] Manfredi, J. J.; Horwitz, S. B. Taxol: an antimitotic agent with a new mechanism of action. *Pbarrmcol. Tber.* **1984**, *25*, 83-l 25.

[48] Wuthers, J. C., Mitchison, T. J., Reider, C. L.; Salmon, E. D. The kinetochore microtubule minus-end disassembly associated with poleward flux produces a force that can do work. *Mol. Biol. Cell* **1996,** *7*, 1547-l 558.

[49] Cassimeris, L. Regulation of microtubule dynamic instability. *Cell Motil. Cytoskeleton.* **1993**, *26*, 275-281.

[50] Inoue, S.; Salmon, E. D.; Force generation by microtubule assembly/disassembly in mitosis and related movements. *Mol. Biol. Cell* **1995**, *6*, 1619-1640.

[51] Keller, H. U.; Zimmermann, A. Shape changes and chemokinesis of Walker 256 carcinosarcoma cells in response to colchicine, vinblastine, nocodazole and taxol. Invasion. *Metastasis* **1986,** *6*, 33-43.

[52] Masurovsky, E. B., Peterson, E. R., Crain, S. M.; Horwitz, S. B. Morphological alterations in dorsal root ganglion neurons and supporting cells of organotypic mouse spinal cord ganglion cultures exposed to taxol. *Neuroscience* **1983**, *10*, 491-509.

[53] Green, K. J.; Goldman, R. D. The effects of taxol on cytoskeletal components in cultured fibroblasts and epithelial cells. *Cell Motif. Cytoskeleton* **1983**, *3*, 283-305.

[54] Evangelio, J. A.; Abal, M.; Barasoain, I.; Souto, A. A.; Lillo, M. P.; Acuna, A. U.; Amat-Guerri, F.; Andreu, J. M. Fluorescent taxoids as probes of the microtubule cytoskeleton. *Cell Motil. Cytoskeleton*, **1998**, *39*, 73-90.

[55] Guy, R. K.; Scott, Z. A.; Sloboda, R. D.; Nicolaou, K. C. Fluorescent taxoids. *Chem. Biol.* **1996**, *3*, 1021-1031.

[56] Rao, C. S.; Chu, J.-J.; Liu, R.-S.; Lai, Y.-K. Synthesis and evaluation of [^{14}C]-labeled and fluorescent-tagged paclitaxel derivatives as new biological probes. *Bioorg. Med. Chem.* **1998**, *6*, 2193-2204.

[57] Wu, X., *Ph.D. Dissertation*; SUNY at Stony Brook: Stony Brook, **2003**.

[58] Ojima, I.; Habus, I.; Zhao, M.; Zucco, M.; Park, Y. H.; Sun, C. M.; Brigaud, T. New and Efficient Approaches to the Semisynthesis of Taxol and Its C-13 Side Chain Analogs by Means of β-Lactam Synthon Method, *Tetrahedron*, **1992**, *48*, 6985-7012.

CHAPTER 5. SYNTHESIS AND BIOLOGICAL EVALUATION OF NOVEL FATTY ACID-FLUORINATED TAXOID CONJUGATES

§5.1 Introduction

§5.1.1 Development of Tumor-Targeting Conjugate

One of the biggest challenges in conventional chemotherapy is the lack of tumor-specificity of the treatment drug. Unlike bacteria or viruses, cancer cells originate from the healthy host cells and therefore resemble the normal cells in many characteristics and properties. As a consequence, it is difficult for the therapeutic agents to differentiate the cancer cells from the normal cells. The conventional cancer chemotherapy is based on the assumption that the anticancer agents are more likely to exert cytotoxic effect to cancer cells than normal cells simply because cancer cells exhibit faster cell proliferation. [1]

The lack of tumor-specificity of commonly used anticancer drugs, e.g. paclitaxel, cisplatin, and doxorubin, causes mild to severe side effects by impairing normal cells and tissues. [2] Common side effects include nausea and vomiting, loss of appetite, thinned or brittle hair, pain in the joints, changes in the color of the nails, and tingling in the hands or toes. More serious side effects such as unusual bruising or bleeding, pain and swelling at the injection site, fever, chills, difficulty swallowing, shortness of breath, severe exhaustion, skin rash, facial flushing and chest pain can also occur.

In order to mitigate the side effects of chemotherapeutic agents, considerable amount of efforts has been put into identifying unique properties of cancer cells, which can be exploited for the drug to selectively treat cancer cells but not normal cells.

Extensive research has been recently focused on targeting technologies which can be either active or passive. Passive targeting is typically accomplished through the enhanced permeability and retention (EPR) effect using macromolecules for delivery. This can be used to produce higher accumulation of the drug in tumor tissue as opposed to normal tissues. [3] [4] Cell Therapeutics has developed a formulated polyglutamate polymer (PG) bonded paclitaxel. Tumor cells are significantly more porous to polyglutamate polymers than normal cells, due to the leaky endothelial membranes of tumor cells. PG-paclitaxel has been introduced into clinical use, and has proven to exert very mild side effects with effective treatment for paclitaxel non-responders. [5]

Active targeting is accomplished through direction of the drug to specific body tissues. Examples of this include routes of administration directly to the tumor site, and antibodies / ligands binding to receptors over-expressed on particular cancer cells.

One of the most promising approaches of active targeting is the development of so-called "tumor-targeting conjugate", which is generally comprised of a cytotoxic drug and a tumor-specific moiety. Ideally, the conjugate should have a minimal systemic toxicity therefore minimize its damage to the healthy tissues, but would effectively release the parent cytotoxic drugs into cancer tissues via certain specific mechanism possessed by cancer cells such as endocytosis and transcytosis. The reported tumor-targeting conjugate systems (**Figure 5-1**) can be classified based on the type of tumor-specific molecules, e.g. monoclonal antibodies (mAb), folic acids, hyaluronic acids, polyunsaturated fatty acids and oligopeptides. [6] [7]

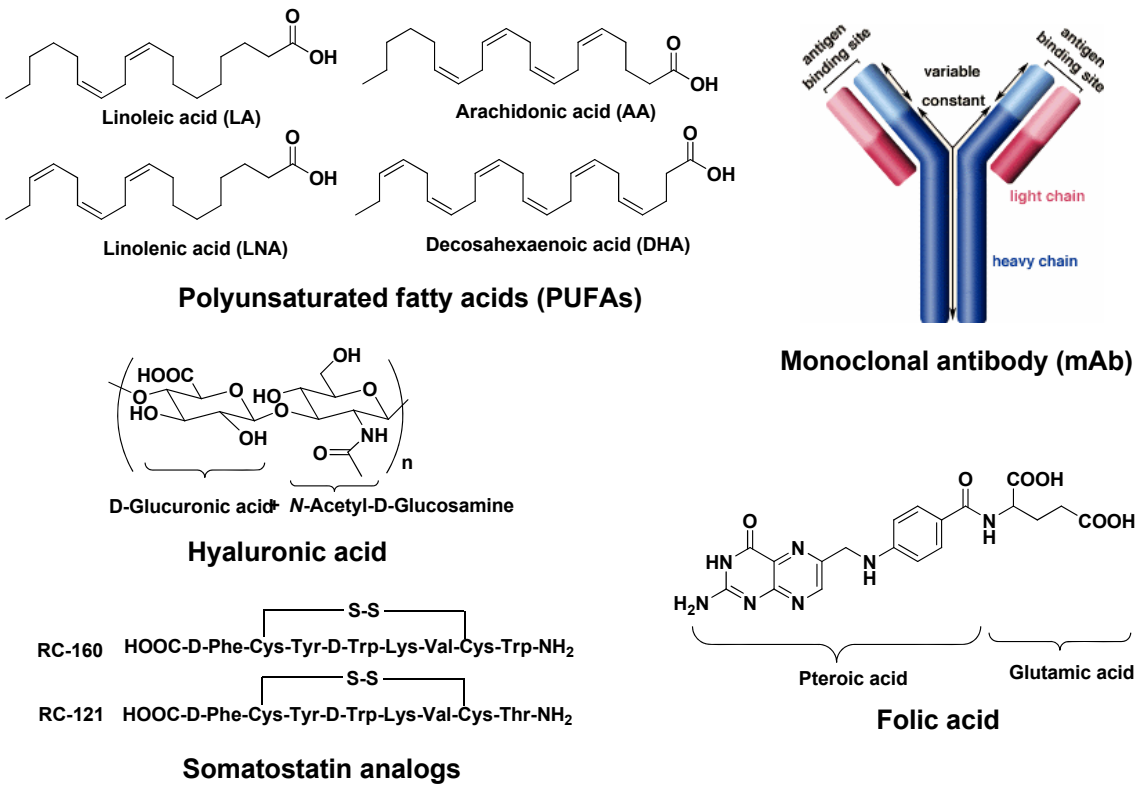

Figure 5-1. Tumor recognition moieties [6]

ImmunoGen has introduced the tumor-activated pro-drug (TAP) technology, which was designed for accurate tumor-targeting by the action of a monoclonal antibody specifically binding to certain cancer cells.

AngioChem has developed a conjugate with paclitaxel bonded to peptide Angiopep-2, which targets lipoprotein receptor-related protein (LRP-1) over-expressed in some cancer cells. [8] It is currently in phase I studies for advanced cancer and brain metastases, as well as recurrent malignant glioma.

Protarga has developed the docosahexaenoic acid (DHA) linked paclitaxel which exerts low-to-none systematic cytotoxicity until the ester bond to DHA is cleaved within the cell. The advantage of the conjugate is its ability to carry much higher concentrations of paclitaxel to the cells, which is also maintained for longer periods in the cancer cells, thus increasing their action.

It is conceivable that the next generation of cancer chemotherapy relies on developing effective tumor-targeting drug delivery system with accurate selectivity to cancer cells.

§5.1.2 Docosahexaenoic Acid (DHA) as Cancer-Targeting Moiety

Polyunsaturated fatty acids (PUFAs, **Figure 5-2**) are fatty acids that contain more than one double bond in their backbone. The PUFAs are present in vegetable oils, cold water fish, and meat. PUFAs and their metabolites have a variety of physiological roles, including energy provision, membrane structure, cell signaling and regulation of gene expression. Omega-3 fatty acids (or ω-3 fatty acids) are a series of PUFAs that have in common a carbon-carbon double

bond in the third bond from the methyl end of the fatty acid. Nutritionally important ω-3 fatty acids include α-linolenic acid (ALA), eicosapentaenoic acid (EPA), and docosahexaenoic acid (DHA). The human body cannot synthesize ω-3 fatty acids *de novo*, [9] but it has a limited ability to form the long chain ω-3 fatty acids EPA (20 carbon atoms) and DHA (22 carbon atoms) from the short chain 18-carbon $\omega-3$ fatty acid ALA. [10 11]

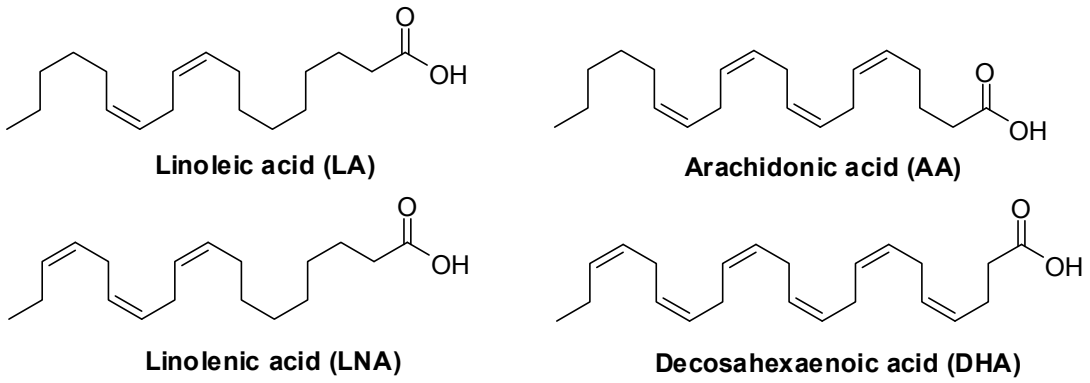

Figure 5-2. Polyunsaturated fatty acids (PUFAs)

PUFAs are ideal candidates as tumor-targeting moiety. They have been previously reported to exhibit anticancer activity against CFPAC, PANC-1, and Mia-Pa-Ca-2 pancreatic and HL-60 leukemia cell lines, and their anticancer activities have been evaluated in preclinical and clinical studies. [12 13] Additional perfusion studies of tissue isolated hepatomas demonstrated that some PUFAs can be taken up more rapidly by cancer cells than by normal cells, presumably as biochemical precursors and energy sources. [14 15] It has also been reported that PUFAs are readily incorporated into the lipid bilayer of cancer cells, causing disruption of membrane structure and fluidity. [16 17] These findings have clearly demonstrated the relationship between PUFAs intake and cancer cells, and encourage the application of PUFAs as tumor-targeting moieties to the design of cancer-targeting conjugates.

DHA is classified as a nutritional additive by the US Food and Drug Administration (FDA), and therefore is considered to be safe to humans. [18 19] Bradely *et al* in Protarga, Inc. PA, hypothesized that the conjugation of DHA to anticancer drugs would produce a new chemical entity that have more accurate tumor-targeting property and thus reduce toxicity to normal tissues. [20] The hypothesis has been supported by their successful clinical development of DHA-paclitaxel conjugate (Taxoprexin, **Figure 5-3**). The drug shows low-to-none systematic cytotoxicity until locally activated by cancer cells. Effective tumor-targeting property of the conjugate was demonstrated by nonclinical pharmacokinetic studies in M109 tumor-bearing mice. The concentration of DHA-paclitaxel in tumors is 8-fold higher than paclitaxel at equimolar doses and 57-fold higher at equitoxic doses. Additionally, since DHA-paclitaxel is slowly converted to cytotoxic parent drug, it remains in tumor cells for a relative long time at high concentration. It is believed that DHA-paclitaxel may treat the slowly circulating or residual cancer cells eventually. In October 2002, Taxoprexin proceeded in two phase III trials in metastatic melanoma and pancreatic cancer with FDA endorsement.

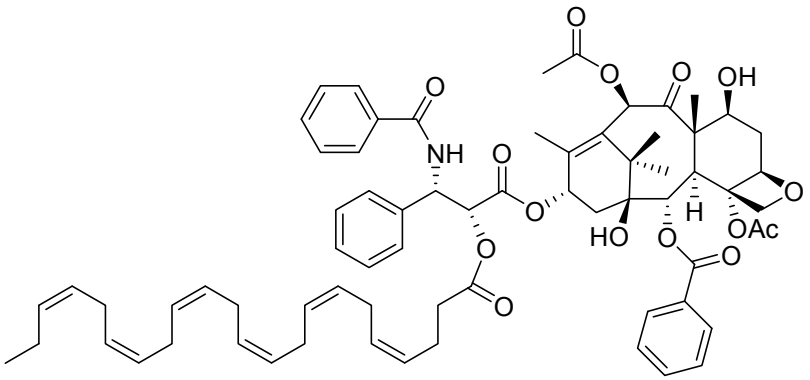

Figure 5-3. DHA-paclitaxel conjugate (Taxoprexin)

§5.1.3 Novel DHA Conjugates with Second- and Third-Generation Taxoids

Paclitaxel, although is undoubtedly one of the most efficient cancer chemotherapeutic agents, is known for its limitation in the treatment of certain cancers marked with over-expression of ATP-dependent drug-efflux pumps.[21] In the contrast, several second-generation taxoids previously developed in our laboratory, e.g **IDN5109** (**SB-T-101131**), **SB-T-1213**, **SB-T-1216** and more others, have shown excellent *in vitro* activity against drug resistant cancer cells. **IDN5109** also exhibited impressive *in vivo* activity against human colon carcinoma SW-620 xenografts in mice. [22 23] Although DHA-paclitaxel conjugate was claimed as a weak substrate of efflux pump as opposed to the paclitaxel, the released paclitaxel will eventually be captured by the Pgp efflux pump resulting decreased effectiveness. Therefore, it is crucial to develop novel DHA conjugates with the second- and third-generation taxoids of superior potency against resistant cancer phenotypes.

DHA-, LNA- and LA-taxoid conjugates (**Figure 5-4**) have been synthesized in our laboratory and subject to *in vivo* biological evaluation in a drug-sensitive human ovarian tumor xenograft (Pgp-) A121 model and a drug-resistant human colon tumor xenograft (Pgp+) DLD-1 model in SCID mice. [24]

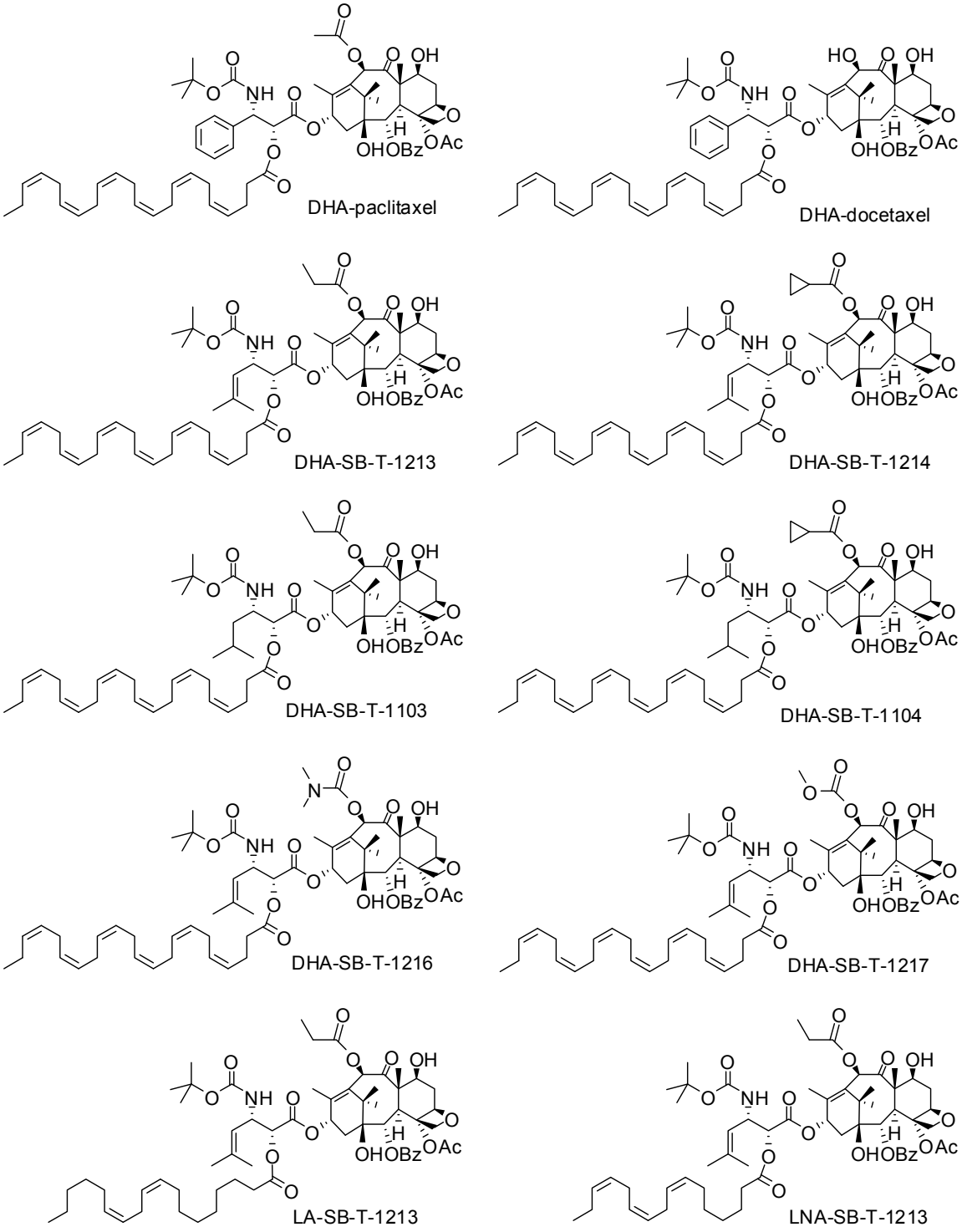

Figure 5-4. Novel DHA conjugates with second- and third-generation taxoids [24]

As shown in **Table 5-1**, **Figure 5-5**, in the drug-sensitive tumor xenograft A121 model, DHA-paclitaxel (80 mg/kg, i.v., q3d; 240 mg/kg/day) demonstrated delayed tumor growth about one time longer than paclitaxel. Two of the novel DHA conjugates, **DHA-SB-T-1213** and **DHA-**

SB-T-1216, had exhibited similar delayed tumor growth with much lower dose (30 mg/kg, i.v., q3d; 90 mg/kg/day).

Table 5-1. Antitumor effect of DHA-taxoid conjugates administered i.v. to drug-sensitive human ovarian tumor xenograft (Pgp-) A121 in SCID mice [24]

Treatment[a] (i.v.)	Total Dose (mg/kg)	Growth Delay (days)	Toxicity[b]	Cured mice[c]/ group
Control	0	---	0	0 / 10
Vehicle-Cremophor:EtOH	0	3	0	0 / 5
Vehicle-Tween : EtOH	0	3	0	0 / 5
Paclitaxel	60	83	0	0 / 5
DHA-paclitaxel	240	>186	0	2 / 5
DHA-SB-T-1216	90	>186	4	1 / 5
DHA-SB-T-1213	90	>186	1	4 / 5
DHA-SB-T-1104	240	115	0	0 / 5

[a] Treatment given i.v. to SCID mice on days 5, 8 and 11 tumor implant, paclitaxel and DHA-paclitaxel formulated in Cremophor:EtOH; DHA-taxoid conjugates formulated in Tween:EtOH. [b]Number of animals that either died or lost greater than 20% body weight. [c]Number of SCID mice with no measurable tumor after 197 days.

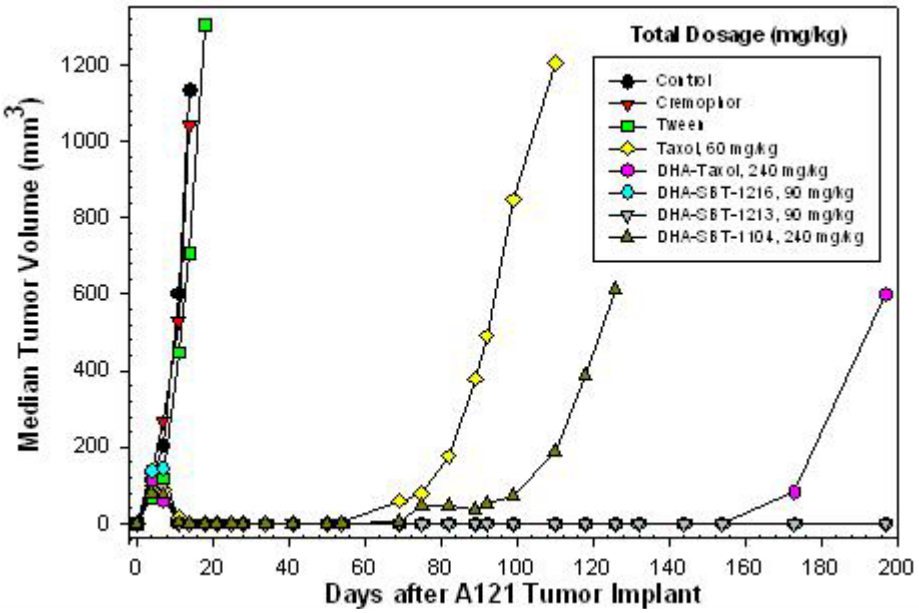

Figure 5-5. Effect of DHA-Taxoid conjugates on human ovarian tumor xenograft A121 (Pgp-) model [24]

In the drug-resistant tumor xenograft DLD-1 model (**Table 5-2**, **Figure 5-6**), **DHA-SB-T-1214** achieved complete regression of the DLD-1 tumor in 5 of 5 mice at 240 mg/kg/day (80 mg/kg/day, i.v., q3d, administered on days 5, 8 and 11), and tumor growth delay is more than 187 days, as opposed to zero efficiency of paclitaxel or DHA-paclitaxel. This promising result promotes the interest in the further preclinical studies for this compound.

Table 5-2. Antitumor effect of DHA-taxoid conjugates administered i.v. to drug-resistant (Pgp+) human colon tumor xenograft DLD-1 in SCID mice [24]

Treatment[a] (i.v.)	Total Dose (mg/kg)	Growth Delay (days)	Toxicity[b]	Cured mice[c]/ group
Control	0	---	0	0 / 7
Vehicle-Cremphor:EtOH	0	--	0	0 / 3
Vehicle-Tween:EtOH	0	--	0	0 / 3
Paclitaxel	60	8	0	0 / 3
DHA-Paclitaxel	240	4	0	0 / 5
DHA-SB-T-1213	75	54	0	0 / 5
DHA-SB-T-1103	75	4	0	0 / 5
DHA-SB-T-1214	240	>187	0	5 / 5
DHA-SB-T-1104	240	4	0	0 / 5
DHA-Docetaxel	75	17	0	0 / 4
DHA-Docetaxel	150	34	0	0 / 4

[a]Treatment given i.v. to SCID mice on days 5, 8 and 11 tumor implant, paclitaxel and DHA-paclitaxel formulated in Cremophor:EtOH; DHA-taxoid conjugates formulated in Tween:EtOH. [b]Number of animals that either died or lost greater than 20% body weight. [c]Number of SCID mice with tumors less than 600 mm^3 after 201 days.

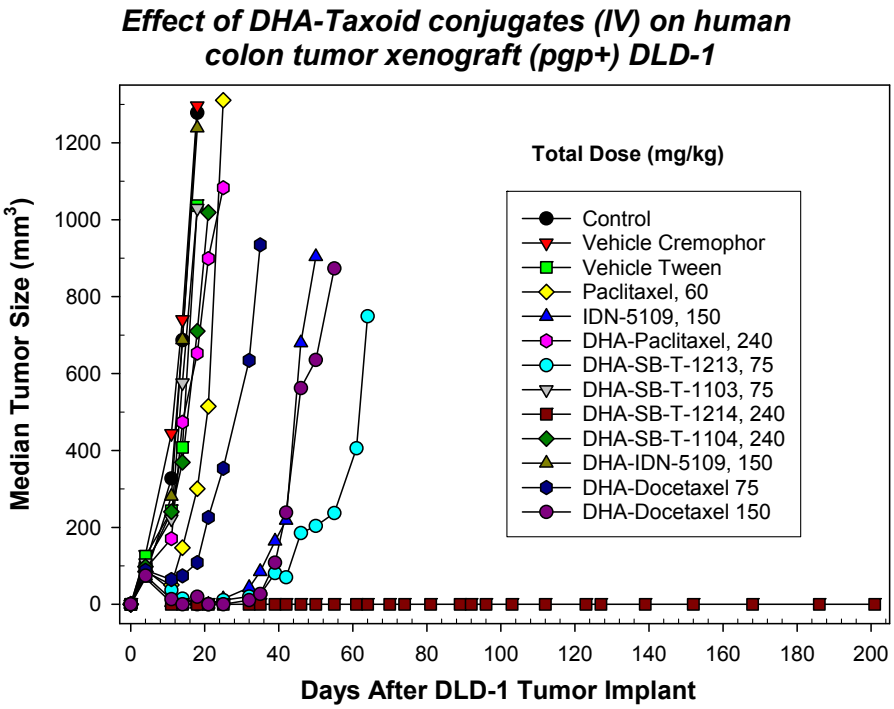

Figure 5-6. Effect of DHA-Taxoid conjugates on human colon tumor xenograft (Pgp+) DLD-1 model [24]

Additional comparison studies of **DHA-SB-T-1214** and **SB-T-1214** at 360 mg/kg/day (120 mg/kg, i.v., q3d) showed that the treatment of **DHA-SB-T-1214** resulted complete tumor regression without any systemic toxicity, while **SB-T-1214** led to elevated systemic toxicity, i.e. 2/5 mice died. This result clearly indicates the effective tumor-targeting property of DHA-second-generation taxoid conjugates.

§5.2 Results and Discussion

As part of the ongoing effort in the development of tumor-targeting taxoid conjugates, a series of DHA- or LNA- conjugates of the second- and third-generation taxoids have been developed in our laboratory.

The previous studies have demonstrated that the difluorovinyl taxoids consistently showed approximate one order of magnitude higher than paclitaxel potency on sensitive cancer cell lines, and two to three orders of magnitude higher potency on resistant cell lines. Therefore, it is meaningful to synthesize the DHA-fluorinated taxoid conjugate. Since **SB-T-12854** is one of the leading fluorinated taxoids, this section will present the synthesis of **DHA-SB-T-12854** conjugate.

§5.2.1 Synthesis of DHA-Fluorinated Second-Generation Taxoid Conjugates

The synthesis of the DHA-taxoids is quite straightforward (**Scheme 5-1**). Based on the SAR studies, C2'-OH is less hindered and thus more reactive than the C7-OH group. [25] [26] Direct coupling of DHA in the presence of *N,N'*-diisopropylcarbodiimide (DIC) and 4-(dimethylamino)pyridine (DMAP) afforded the DHA-taxoid conjugates in good yield.

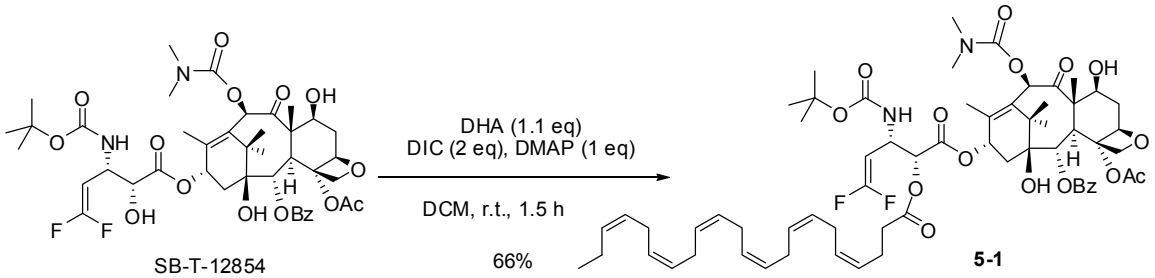

Scheme 5-1. Synthesis of **DHA-SB-T-12854**

§5.2.2 Biological Evaluation of DHA-C3'-Difluorovinyl-Taxoid Conjugate DHA-SB-T-12854

Cytotoxicity of **DHA-SB-T-12854** was evaluated in different types of cancer cell lines, including human ovarian cancer cell line A2780, human pancreatic adenocarcinoma cell line CFPAC-1, human breast cancer cell line MDA-MB-231, human breast cancer cell line MCF-1 and pancreatic cancer cell line Panc-1. Cytotoxicity assays were performed by courtesy of E. Zuniga in our group (**Table 5-3**).

Table 5-3. *In vitro* cytotoxicity of DHA-SB-T-12854
Cells were incubated for 48 h at 37 °C with 5% CO_2 after treatment with taxoid.

Cancer Cell Line	Compound	IC_{50} (nM)	Average IC_{50} (nM)
A2780	Paclitaxel	4.12, 4.07, 4.35	4.18 ± 0.15
	SB-T-12854	5.33, 1.70, 2.36	3.13 ± 0.93
	DHA-SB-T-12854	362, 153, 124	213 ± 130
CFPac-1	Paclitaxel	28.6, 15.6, 66.0	36.7 ± 26.2
	SB-T-12854	0.19, 0.38, 0.49	0.35 ± 0.15
	DHA-SB-T-12854	47.9, 44.9, 84.4	59.1 ± 22.0
MBA MD 231	Paclitaxel	20.9, 11.6, 11.0	14.5 ± 5.55
	SB-T-12854	0.77, 0.62, 0.16	0.52 ± 0.32
	DHA-SB-T-12854	211, 461, 147	276 ± 166
MCF-7	Paclitaxel	1.76, 4.84, 8.87	5.16 ± 3.57
	SB-T-12854	0.37, 0.88, 0.29	0.51 ± 0.32
	DHA-SB-T-12854	111, 122, 99.4	111 ± 11.3
Panc-1	Paclitaxel	4.23, 4.27, 4.50	4.33 ± 0.15
	SB-T-12854	5.70, 5.37, 6.99	6.02 ± 0.86
	DHA-SB-T-12854	128, 157, 122	136 ± 18.7

Overall, the **DHA-SB-T-12854** showed two to three orders of magnitude lower cytotoxicity than that of the free **SB-T-12854**. Compared to the cases of DHA-paclitaxel and DHA-docetaxel, where the differences between the conjugates and the free drug are generally less than 10 times, the **DHA-SB-T-12854** is expected to demonstrate even lower systematic cytotoxicity while eventually releasing **SB-T-12854** with potency higher that of paclitaxel. The greater difference in the potencies could potentially provide a larger therapeutic window of the conjugate.

§5.3 Conclusion

DHA-C3'-difluorovinyl-taxoid conjugate **DHA-SB-T-12854** was successfully synthesized by coupling DHA with **SB-T-12854** at the C2'-OH position. The conjugate was evaluated against various cancer cell lines, and showed two to three orders of magnitude lower cytotoxicity than the free taxoid *in vitro*. This set of data would strongly support further investigation of the DHA-fluorinated taxoid conjugates and potential nonclinical studies and clinical development.

§5.4 Experimental Section

General Methods

Materials

The chemicals were purchased from Sigma-Aldrich and/or Fisher Scientific and were used without further purification unless otherwise noted. 10-DAB III and 14β-hydroxy-10-deacetylbaccatin III were gift from Indena, SpA, Italy and used as received. Tetrahydrofuran, dichloromethane, toluene and ethyl ether were obtained from the PureSolv^{TM} Solvent Purification System (Innovative Technology, Inc.) under N_2. The glassware was dried in a 110 ^{o}C oven and allowed to cool to room temperature in a desiccator over "Drierite" (calcium sulfate).

General Methods

^{1}H, ^{13}C and ^{19}F NMR spectra were obtained on Varian 300, 400 or 500 NMR spectrometers. Melting points were measured on a Thomas Hoover Capillary melting point apparatus and are uncorrected. TLC was performed on Merck DC-alufolien with Kieselgel 60F-254 and flash column chromatography was carried out on silica gel 60 (Merck, 230-400 mesh ASTM). Optical rotations were measured on a Perkin-Elmer Model 241 polarimeter. IR spectra were measured on a Shimadzu FTIR-8400s spectrophotometer. Chemical purity was determined on Shimadzu LC-1020A, using a Phenomenex Curosil-B column (5μ, 4.6 × 250 mm), employing CH_3CN/water (40/60, V/V) as the eluent with a flow rate of 1 mL/min. Chiral HPLC analysis for the determination of enantiomeric excess was carried out on a Waters HPLC assembly consist of a Waters M45 solvent delivery system and a Waters 484 detector (at 254 nm) on a PC workstation running Millennium 32 using a DAICEL-CHIRACEL OD chiral column (25 × 0.46 cm), employing n-hexanes/isopropanol (95/5, V/V) as eluent with a flow rate of 1.0 mL/min. High resolution mass spectra were obtained from the Mass Spectrometry Laboratory, University of Illinois at Urbana-Champaign, Urbana, IL.

10-(*N*,*N*-dimethyl)carbamatecarbonyl-2'-docosahexaenoyl-3'-dephenyl-3'-difluorovinyldocetaxel (DHA-SB-T-12854)

To a solution of **SB-T-12854** (20 mg, 0.023 mmol) and 4-dimethylaminopyridine (2.8 mg, 0.023 mmol) in dichloromethane (0.3 mL) under nitrogen were added a solution of DHA (8.8 μL, 0.025 mmol) in dichloromethane (1.2 mL) followed with addition of 1,3-dicyclohexylcarbodiimide (7.1 μL, 0.046 mmol). The reaction mixture was stirred at ambient temperature for 1.5 h. The reaction mixture was diluted in EtOAc (20mL), washed with saturated ammonium chloride solution (5 mL), water (5 mL) and brine (5 mL). The organic layer was dried over $MgSO_4$, filtered and concentrated in vacuo. Flash column chromatography on silica gel (Hexanes/EtOAc = 3/1) afforded 31 mg **DHA-SB-T-12854** (quant. yield) as colorless oil. Reaction was repeated on 100 mg starting material SB-T-12854 to afford 78 mg DHA-SB-T-12854 (57 % yield). ^{1}H NMR (400 MHz, $CDCl_3$) δ 8.10 (d, J = 7.8 Hz, 2H), 7.59 (t, J = 6.9 Hz, 1H), 7.49 (t, J = 7.6 Hz, 2H), 6.25 (d, J = 12.6 Hz, 2H), 5.65 (d, J = 7.0 Hz, 1H), 5.37 (d, J = 5.3 Hz, 12H), 5.16 - 4.83 (m, 4H), 4.46 (s, 2H), 4.30 (d, J = 8.4 Hz, 1H), 4.17 (d, J = 8.3 Hz, 1H), 3.80 (d, J = 6.9 Hz, 1H), 3.24 (d, J = 3.4 Hz, 1H), 3.02 (s, 3H), 2.94 (s, 3H), 2.84 (s, 10H), 2.60 – 2.48 (m, 3H), 2.47 – 2.41 (m, 2H), 2.38 (s, 4H), 2.21 (dd, J = 15.2, 9.0 Hz, 1H), 2.13 – 2.00 (m, 2H), 1.94 (s, 3H), 1.91 – 1.81 (m, 1H), 1.77 (d, J = 14.5 Hz, 1H), 1.66 (s, 3H), 1.30 (s, 9H), 1.24

(s, 3H), 1.13 (d, J = 3.5 Hz, 3H) and 0.96 (s, 3H) ppm; ^{13}C NMR (101 MHz, $CDCl_3$) δ 205.94, 172.03, 169.94, 167.47, 167.31, 157.06, 156.76, 156.29, 154.74, 143.42, 133.85, 133.24, 132.31, 132.12, 130.46, 130.28, 130.08, 129.88, 129.40, 128.96, 128.78, 128.59, 128.48, 128.38, 128.12, 127.92, 127.63, 127.43, 127.09, 84.97, 84.75, 81.22, 80.72, 79.56, 76.58, 76.35, 76.31, 75.56, 75.41, 72.72, 72.56, 72.00, 58.64, 45.76, 45.73, 43.41, 35.68, 35.51, 33.76, 28.43, 28.34, 28.24, 27.14, 27.06, 25.93, 25.82, 25.72, 23.69, 23.62, 22.65, 22.51, 22.35, 20.74, 15.07, 14.93, 14.46, 14.42, 9.63 and 9.50 ppm; ^{19}F NMR (376 MHz, $CDCl_3$) δ -83.61 (dd, J = 34.5, 24.4 Hz) and -85.38 (d, J = 34.8 Hz) ppm; HRMS m/z calcd for $C_{64}H_{84}F_2N_2O_{16}H^+$, 1175.5867; found, 1175.5856 (Δ = -0.9 ppm).

§5.5 References

[1] Chari, R. V. J. Targeted delivery of chemotherapeutics: tumor-activated prodrug therapy. *Adv. Drug Deliv. Rev.* **1998**, *31*, 89-104.

[2] Ojima, I.; Geng, X.; Wu, X.; Qu, C.; Borella, C. P.; Xie, H.; Wilhelm, S. D.; Leece, B. A.; Bartle, L. M.; Goldmacher, V. S.; Chari, R. V. J. Tumor-Specific Novel Taxoid-Monoclonal Antibody Conjugates. *J. Med. Chem.* **2002**, *45*, 5620-5623.

[3] Matsumura, Y.; Maeda, H. A new concept for macromolecular therapeutics in cancer chemotherapy: mechanism of tumoritropic accumulation of proteins and the antitumor agent smancs. *Cancer Res.* **1986**, *46*, 6387–6392.

[4]Maeda, H.; Matsumura, Y. Tumoritropic and lymphotropic principles of macromolecular drugs. *Crit. Rev. Ther. Drug Carr. Syst.* **1989**, *6*, 193–210.

[5] Whelan, J. Targeted Taxane Therapy for Cancer. *Drug Discovery Today* **2002**, *7*, 90–92.

[6] Chen, J.; Jaracz, S.; Zhao, X.; Chen, S.; Ojima, I. Antibody-cytotoxic agent conjugates for cancer therapy. *Expert Opin. Drug Delivery* **2005**, *2*, 873-890.

[7] Jaracz, S.; Chen, J.; Kuznetsova, L. V.; Ojima, I. Recent advances in tumor-targeting anticancer drug conjugates. *Bioorg. Med. Chem.* **2005**, *13*, 5043-5054.

[8] Régina, A.; Demeule, M.; Ché, C.; Lavallée, I.; Poirier, J.; Gabathuler, R.; Béliveau, R.; Castaigne, J. P. Antitumour activity of ANG1005, a conjugate between paclitaxel and the new brain delivery vector Angiopep-2. *Br J Pharmacol* **2008**, *155*, 185–197.

[9] Goodhart, R. S.; Shils. M. E. In: *Modern Nutrition in Health and Disease.* 6th Ed., Lea and Febiger. Philadelphia, PA **1980**, 134-138.

[10] Widmer, C., Jr.; Holman, R. T. Polyethenoid fatty acid metabolism. II. Deposition of polyunsaturated fatty acids in fat-deficient rats upon single fatty acid supplementation. *Arch. Biochem.* **1950**, *25*, 1-12.

[11] Tapiero, H.; Nguyen Ba, G.; Couvreur, P.; Tew, K. D. Polyunsaturated fatty acids (PUFA) and eicosanoids in human health and pathologies. *Biomed. Pharmacother.* **2002**, *56*, 215-222.

[12] Wigmore, S. J.; Ross, J. A.; Falconer, J. S.; Plester, C. E.; Tisdale, M. J.; Carter, D. C.; Fearon, K. C. H. The effect of polyunsaturated fatty acids on the progress of cachexia in patients with pancreatic cancer. *Nutrition* **1996**, *12*, S27-S30.

[13] Hawkins, R. A.; Sangster, K.; Arends, M. J. Apoptotic death of pancreatic cancer cells induced by polyunsaturated fatty acids varies with double bond number and involves an oxidative mechanism. *J. Pathol.* **1998**, *185*, 61-70.

[14] Sauer, L. A.; Dauchy, R. T. Tumor-host metabolic interrelationships. *Biochem.l Soc. T.* **1990**, *18*, 80-82.

[15] Sauer, L. A.; Dauchy, R. T. The effect of omega-6 and omega-3 fatty acids on 3H-thymidine incorporation in hepatoma 7288CTC perfused in situ. *Brit. J. Cancer* **1992**, *66*, 297-303.

[16] Takahashi, M.; Przetakiewicz, M.; Ong, A.; Borek, C.; Lowenstein, J. M. Effect Of Omega-3 And Omega-6 Fatty-Acids On Transformation Of Cultured-Cells By Irradiation And Transfection. *Cancer Res.* **1992**, *52*, 154-162.

[17] Grammatikos, S. I.; Subbaiah, P. V.; Victor, T. A.; Miller, W. M. N-3 And N-6 Fatty-Acid Processing And Growth Effects In Neoplastic And Non-Cancerous Human Mammary Epithelial-Cell Lines. *Brit. J. Cancer* **1994**, *70*, 219-227.

[18] Moser, U. N-3 and N-6 PUFAS in healthy and diseased skin. *J. Appl. Cosmetology* **2002**, *20*, 137-142.

[19] Heird, W. C.; Lapillonne, A. The role of essential fatty acids in development. *Annu. Rev. Nutr.* **2005**, *25*, 549-571.

[20] Bradley, M. O.; Webb, N. L.; Anthony, F. H.; Devanesan, P.; Witman, P. A.; Hemamalini, S.; Chander, M. C.; Baker, S. D.; He, L. F.; Horwitz, S. B.; Swindell, C. S. Tumor targeting by covalent conjugation of a natural fatty acid to paclitaxel. *Clin. Cancer Res.* **2001**, *7*, 3229-3238.

[21] Vredenburg, M. R.; Ojima, I.; Veith, J.; Pera, P.; Kee, K.; Cabral, F.; Sharma, A.; Kanter, P.; Greco, W. R.; Bernacki, R. J. Effects of orally active taxanes on P-glycoprotein modulation and colon and breast carcinoma drug resistance. *J. Natl. Cancer. Inst.* **2001**, *93*, 1234-1245.

[22] Lin, S.; Geng, X.; Qu, C.; Tynebor, R.; Gallagher, D. J.; Pollina, E.; Rutter, J.; Ojima, I. Synthesis of highly potent second-generation taxoids through effective kinetic resolution coupling of racemic *β*-lactams with baccatins. *Chirality* **2000**, *12*, 431-441.

[23] Ojima, I.; Wang, T.; Miller, M. L.; Lin, S.; Borella, C. P.; Geng, X.; Pera, P.; Bernacki, R. J. Synthesis and structure-activity relationships of new second-generation taxoids. *Bioorg. Med. Chem. Lett.* **1999**, *9*, 3423-3428.

[24] Kuznetsova, L.; Chen, J.; Sun, L.; Wu, X.; Pepe, A.; Veith, J. M.; Pera, P.; Bernacki, R. J.; Ojima, I. Syntheses and evaluation of novel fatty acid-second-generation taxoid conjugates as promising anticancer agents. *Bioorg. Med. Chem. Lett.* **2006**, *16*, 974-977.

[25] Chordia, M. D.; Gharpure, M. M.; Kingston, D. G. I. Facile AB ring cleavage reactions of taxoids. *Tetrahedron* **1995**, *51*, 12963-12970.

[26] Georg, G. I.; Harriman, G. C. B.; Datta, A.; Ali, S.; Cheruvallath, Z.; Dutta, D.; Vander Velde, D. G.; Himes, R. H. The Chemistry of the Taxane Diterpene: Stereoselective Reductions of Taxanes. *J. Org. Chem.* **1998**, *63*, 8926-8934.

References

References for Chapter 1

[1] The Global Burden of Disease: 2004 Update. Geneva: World Health Organization **2008**.

[2] Ferlay, J.; Shin, H. R.; Bray, F.; Forman, D.; Mathers, C. D.; Parkin, D. GLOBOCAN 2008, Cancer Incidence and Mortality Worldwide: IARC CancerBase No. 10. Lyon, France: International Agency for Research on Cancer, **2010**.

[3] World Health Organization, Cancer, Fact sheet N° 297, February **2011**.

[4] National Center for Health Statistics, Division of Vital Statistics, Center for Disease Control 2005-2007.

[5] Anand, P.; Kunnumakkara, A. B.; Kunnumakara, A. B. Cancer is a preventable disease that requires major lifestyle changes. *Pharm. Res.* **2008**, *25*, 2097-2116.

[6] Cole, W. H. In *Chemotherapy of Cancer*. Lea and Febiger: Philadelphia, **1970**.

[7] Lowry, S. In *Fundamentals of Radiation Therapy and Cancer Chemotherapy*. Engl. Univ. Press: London, **1974**.

[8] Takimoto, C. H.; Calvo, E. Principles of Oncologic Pharmacotherapy. In: *Cancer Management: A Multidisciplinary Approach.* Pazdur, R.; Wagman, L. D.; Camphausen, K. A.; Hoskins, W. J. (Eds.) 11 Ed. **2008**.

[9] Saito, T.; Niitani, H.; Nakao, I. In *Handbook of Advanced Chemotherapies of Cancer*; Life Science Co.: Tokyo, **1989**.

[10] Minotti G, Menna P, Salvatorelli E, Cairo G, Gianni L. Anthracyclines: molecular advances and pharmacologic developments in antitumor activity and cardiotoxicity. *Pharmacol. Rev.* **2004**, 56, 185–229.

[11] Rosenberg, B.; Vancamp, L.; Trosko, J. E.; Mansour, V. H. Platinum Compounds: a New Class of Potent Antitumour Agents. *Nature* **1969,** *222*, 385–386.

[12] Goodman, J.; Walsh, V. In *The Story of Taxol: Nature and Politics in the Pursuit of an Anti-Cancer Drug*. Cambridge University Press, **2001**.

[13] Wani, M. C.; Taylor, H. L.; Wall, M. E.; Coggon, P.; Mc Phail, A.T. *J. Am. Chem. Soc.* **1971**, *93*, 2325-2327.

[14] Bharadwaj, R.; Yu, H. The spindle checkpoint, aneuploidy, and cancer. *Oncogene* **2004**, *23*, 2016–2027.

[15] Schiff, P. B.; Fant, J.; Horwitz, S. *Nature* **1979**, *277*, 665-667.

[16] Schiff, P. B.; Horwitz, S. B. Taxol Stabilizes Microtubules in Mouse Fibroblast Cells. *Proc. Natl. Acad. Sci.* **1980**, *77*, 1561-1565.

[17] Schiff, P. B.; Horwitz, S. B. Taxol Assembles Tubulin in the Absence of Exogenous Guanosine 5'-Triphosphate or Microtubule-Associated Proteins. *Biochemistry*, **1981**, *20*, 3247-3252.

[18] Georg, G. I.; Chen, T. T.; Ojima, I.; Vyas, D. M. In *Taxane Anticancer Agents: Basic Science and Current Status: ACS Symp. Ser. 583*. American Chemical Society, Washington D.C., **1995**.

[19] Smith, J. A.; Martin, L. Do cells cycle? *Proc. Natl. Acad. Sci. U.S.A.* **1973**, *70*, 1263-1267.

[20] De Souza, C. P.; Osmani, S. A. Mitosis, not just open or closed. *Eukaryotic Cell* **2007**, *6*, 1521-1527.

[21] Nicolaou, K. C.; Dai, W.-M.; Guy, R. K. Chemistry and Biology of Taxol. *Angew. Chem. Int. Ed. Engl.* **1994**, *33*, 15-44.

[22] Fuchs, D. A.; Johnson, R. K. Cytologic evidence that taxol, an antineoplastic agent from *Taxus brevifolia*, acts as a mitotic spindle poison. *Cancer Treatment Reports* **1978**, *62*, 1219–1222.

[23] Rowinsky, E. K. *et al*. Phase II study of taxol in advanced epithelial malignancies. *Proceedings of the Association of Clinical Oncology* **1988**, *7*, 136.

[24] Morihira, K.; Hara, R.; Kawahara, S.; Nishimori, T.; Nakamura, N.; Kusama, H.; Kuwajima, I. Enantioselective total synthesis of taxol. *J. Am. Chem. Soc.* **1998**, *120*, 12980-12981.

[25] Holton, R. A.; Somoza, C.; Kim, H. B.; Liang, F.; Biediger, R. J.; Boatman, P. D.; Shindo, M.; Smith, C. C.; Kim, S.; Nadizadeh, H.; Suzuki, Y.; Tao, C.; Vu, P.; Tang, S.; Zhang, P.; Murthi, K. K.; Gentile, L. N.; Liu, J. H. First Total Synthesis of Taxol. 1. Functionalization of the B Ring. *J. Am. Chem. Soc.* **1994**, *116*, 1597-1598.

[26] Holton, R. A.; Kim, H. B.; Somoza, C.; Liang, F.; Biediger, R. J.; Boatman, P. D.; Shindo, M.; Smith, C. C.; Kim, S.; Nadizadeh, H.; Suzuki, Y.; Tao, C.; Vu, P.; Tang, S.; Zhang, P.; Murthi, K. K.; Gentile, L. N.; Liu, J. H. First Total Synthesis of Taxol. 2. Completion of the C and D Rings. *J. Am. Chem. Soc.* **1994**, *116*, 1599-1600.

[27] Nicolaou, K. C.; Yang, Z.; Liu, J. J.; Ueno, H.; Nantermet, P. G.; Guy, R. K.; Claiborne, C. F.; Renaud, J.; Couladouros, E. A.; Paulvannan, K.; Sorensen, E. J. Total Synthesis of Taxol. *Nature* **1994**, *367*, 630-634.

[28] Danishefsky, S.; Masters, J.; Young, W.; Link, J.; Snyder, L.; Magee, T.; Jung, D.; Isaacs, R.; Bornmann, W.; Alaimo, C.; Coburn, C.; Di Grandi, M. Total Synthesis of Baccatin III and Taxol. *J. Am. Chem. Soc.* **1996**, *118*, 2843-2859.

[29] Wender, P. A.; Mucciaro, T. P. A New and Practical Approach to the Synthesis of Taxol and Taxol Analogues: The Pinene Path. *J. Am. Chem. Soc.* **1992**, *114*, 5878-5879.

[30] Morihira, K.; Hara, R.; Kawahara, S.; Nishimori, T.; Nakamura, N.; Kusama, H.; Kuwajima, I. Enantioselective total synthesis of taxol. *J. Am. Chem. Soc.* **1998**, *120*, 12980-12981.

[31] Mukaiyama, T.; Shiina, I.; Iwadare, H.; Saitoh, M.; Nishimura, T.; Ohkawa, N.; Sakoh, H.; Nishimura, K.; Tani, Y.; Hasegawa, M.; Yamada, K.; Saitoh, K. Asymmetric total synthesis of Taxol (R). *Chem Eur. J.* **1999**, *5*, 121-161.

[32] Doi, T.; Fuse, S.; Miyamoto, S.; Nakai, K.; Sasuga, D.; Takahashi, T. A Formal Total Synthesis of Taxol Aided by an Automated Synthesizer. *Chemistry an Asian J.* **2006**, *1*, 370-383.

[33] Denis, J.-N.; Greene, A. E.; Gueard, D.; Gueitte-Voegelein, F.; Mangatal, L.; Potier, P. A Highly Efficient, Practical Approach to Natural Taxol. *J. Am. Chem. Soc.* **1988**, *110*, 5917-5919.

[34] Denis, J.-N.; Correa, A.; Greene, A. E. Direct, Highly Efficient Synthesis from (*S*)-(+)-Phenylglycine of the Taxol and Taxotere Side Chains. *J. Org. Chem.* **1991**, *56*, 6939-6942.

[35] Holton, R. A.; Biediger, R. J.; Boatman, D. Semisynthesis of taxol and taxotere. In *Taxol: Science and Applications*; Suffness, M., (Ed.) CRC: Boca Raton, **1995**, 97-121.

[36] Holton, R. A. Method for Preparation of Taxol Using Oxazinone. U.S. Patent, 5015744, **1991**.

[37] Ojima, I.; Sun, C. M.; Zucco, M.; Park, Y. H.; Duclos, O.; Kuduk, S. D. A Highly Efficient Route to Taxotere by the *β*-Lactam Synthon Method. *Tetrahedron Lett.* **1993**, *34*, 4149-4152.

[38] Commeren, A.; Bourzat, J. D.; Didier, E.; Lavelle, F. Practical Semisynthesis and Antimitotic Activity of Docetaxel and Side-Chain Analogues. In *Taxane Anticancer Agents: Basic Science and Current Status*; Georg, G. I., Chan, T. T., Ojima, I., Vyas, D. M., (Eds). American Chemical Society, Washington, D. C., **1995**; 233-246.

[39] Kingston, D. G. I.; Chaudhary, A. G.; Gunatilaka, A. A. L.; Middleton, M. L. Synthesis of Taxol from Baccatin III via an Oxazoline Intermediate. *Tetrahedron Lett.* **1994**, *35*, 4486-4489.

[40] Holton, R. A. Method for Preparation of Taxol. Eur. Pat. Appl., 400971, **1990**.

[41] Ojima, I. *β*-Lactam Synthon Method-Enantiomerically Pure *β*-Lactams as Synthetic Intermediates. In *The Organic Chemistry of β-Lactam Antibiotics*. Georg, G. I., (Ed.) VCH

Publishers: New York, **1992**, 197-255.

[42] Ojima, I. Recent Advances in *β*-Lactam Synthon Method. *Acc. Chem. Res.* **1995**, *28*, 383-389.

[43] Ojima, I.; Sun, C. M.; Zucco, M.; Park, Y. H.; Duclos, O.; Kuduk, S. D. A Highly Efficient Route to Taxotere by the β-Lactam Synthon Method. *Tetrahedron Lett.* **1993**, *34*, 4149-4152

[44] Ojima, I.; Park, Y. H.; Sun, C. M.; Brigaud, T.; Zhao, M. New and Efficient Routes to Norstatine and Its Analogs with High Enantiomeric Purity by β-Lactam Synthon Method. *Tetrahedron Lett.* **1992**, *33*, 5737-5740.

[45] Ojima, I.; Zucco, M.; Duclos, O.; Kuduk, S. D.; Sun, C. M.; Park, Y. H. *N*-Acyl-3-hydroxy-*β*-lactams as Key Intermediates for Taxotere and Its Analogs. *Bioorg. Med. Chem. Lett.* **1993**, *3*, 2479-2482.

[46] Gueard, D.; Gueitte-Vogelein, F.; Potier, P. Taxol and Taxotere: Discovery, Chemistry, and Structure-Activity Relationships. *Acc. Chem. Res.* **1993**, *26*, 160-167

[47] Gueitte-Voegelein, F.; Mangatal, L.; Gueard, D.; Potier, P.; Guilhem, J.; Cesario, M.; Pascard, C. Structure of a Synthetic Taxol Precursor: *N-tert*-Butoxycarbonyl-10-deacetyl-*N*-debenzoyltaxol. *Acta Crstallogr.* **1990**, *C46*, 781-784.

[48] Colin, M.; Gueard, D.; Gueitte-Voegelein, F.; Potier, P. Taxotere. Eur. Pat. Appl., 253,738, **1988**.

[49] Ojima, I.; Kuduk, S. D.; Chakravarty, S. Recent Advances in the Medicinal Chemistry of Taxoid Anticancer Agents. *Adv. Med. Chem.* **1998**, 69-124.

[50] Kingston, D. G. I. Recent Advances in the Chemistry and Structure-Activity Relationships of Paclitaxel. In *Taxane Anticancer Agents: Basic Science and Current Status; ACS Symp. Ser. 583*. Georg, G. I., Chen, T. T., Ojima, I., Vyas, D. M., (Eds) American Chemical Society, Washington, D. C., **1995**, 203-216.

[51] Wahl, A.; Gueitte-Voegelein, F.; Gueard, D.; Le Goff, M.-T.; Potier, P. Rearrangement Reactions of Taxanes: Structural Modifications of 10-Deacetylbaccatin III. *Tetrahedron* **1992**, *48*, 6965-6974.

[52] Samaranayake, G.; Magri, N. F.; Jitrangsri, C.; Kingston, D. G. I. Modified Taxols. 5. Reaction of Taxol with Electrophilic Reagents and Preparation of a Rearranged Taxol Derivatives with Tubulin Assembly Activity. *J. Org. Chem.* **1991**, *56*, 5114-5119.

[53] Ojima, I.; Fenoglio, I.; Park, Y. H.; Sun, C.-M.; Appendino, G.; Pera, P.; Bernacki, R. J. Synthesis and Structure-Activity Relationships of Novel Nor-Seco Analogs of Taxol and Taxotere. *J. Org. Chem.* **1994**, *59*, 515-517.

[54] Ojima, I.; Lin, S.; Chakravarty, S.; Fenoglio, I.; Park, Y. H.; Sun, C.-M.; Appendino, G.; Pera, P.; Veith, J. M.; Bernacki, R. J. Synthesis and Structure-Activity Relationships of Novel Nor-seco Taxoids. *J. Org. Chem.* **1998**, *63*, 1637-1645.

[55] Klein, L. L.; Maring, C. J.; Li, L.; Yeung, C. M.; Thomas, S. A.; Grampovnik, D. J.; Plattner, J. J.; Henry, R. F. Synthesis of Ring B-Rearranged Taxane Analogs. *J. Org. Chem.* **1994**, *59*, 2370-2373.

[56] Liang, X.; Kingston, D. G. I.; Lin, C. M.; Hamel, E. Synthesis and Biological Evaluation of Paclitaxel Analogs Modified in Ring C. *Tetrahedron Lett.* **1995**, *36*, 2901-2904.

[57] Liang, X.; Kingston, D. G. I.; Long, B. H.; Fairchild, C. A.; Johnston, K. A. Synthesis, Structure Elucidation, and Biological Evaluation of *C*-Norpaclitaxel. *Tetrahedron Lett.* **1995**, *36*, 7795-7798.

[58] Chen, S.-H.; Fairchild, C.; Long, B. H. Synthesis and Biological Evaluation of Novel C-4 Aziridine-Bearing Paclitaxel. *J. Med. Chem.* **1995**, *38*, 2263-2267.

[59] Marder-Karsenti, R.; Dubois, J.; Bricard, L.; Gueard, D.; Gueitte-Voegelein, F. Synthesis and

Biological Evaluation of D-Ring-Modified Taxanes: Azadocetaxel Analogs. *J. Org. Chem.* **1997**, *62*, 6631-6637.

[60] Dubois, J.; Thoret, S.; Gueitte, F.; Gueard, D. Synthesis of 5(20)deoxydocetaxel, a new active docetaxel analogue. *Tetrahedron Lett.* **2000**, *41*, 3331-3334.

[61] Chordia, M. D.; Kingston, D. G. I. Synthesis and Biological Evaluation of 2-*epi*-Paclitaxel. *J. Org. Chem.* **1996**, *61*, 799-801.

[62] Monsarrat, B.; Mariel, E.; Cros, S.; Gare, M.; Gueard, D.; Gueitte-Voegelein, F.; Wright, M. Taxol Metabolism. Isolation and Identification of Three Major Metabolites of Taxol in Rat Bile. *Drug Metab. Dispos.* **1990**, *18*, 895-901.

[63] Ojima, I.; Inoue, T.; Slater, J. C.; Lin, S.; Kuduk, S. C.; Chakravarty, S.; Walsh, J. J.; Gilchrist, L.; McDermott, A. E.; Cresteil, T.; Monsarrat, B.; Pera, P.; Bernacki, R. J. Synthesis of Enantiopure F-Containing Taxoids and Their Use as Anticancer Agents as well as Probes for Biomedical Problems. In *Asymmetric Fluoroorganic Chemistry: Synthesis, Application, and Future Directions; ACS Symp. Ser. 746*; Ramachandran, P. V., (Ed.) American Chemical Society, Washington, D. C., **1999**, 158-181.

[64] Chaudhary, A. G.; Gharpure, M. M.; Rimoldi, J. M.; Chordia, M. D.; Gunatilaka, A. A. L.; Kingston, D. G. I.; Grover, S.; Lin, C. M.; Hamel, E. Unexpectedly Facile Hydrolysis of the 2-Benzoate Group of Taxol and Syntheses of Analogs with Increased Activities. *J. Am. Chem. Soc.* **1994**, *116*, 4097-4098.

[65] Ojima, I.; Kuduk, S. D.; Pera, P.; Veith, J. M.; Bernacki, R. J. Synthesis of and Structure-Activity Relationships of Non-Aromatic Taxoids. Effects of Alkyl and Alkenyl Ester Groups on Cytotoxicity. *J. Med. Chem.* **1997**, *40*, 279-285.

[66] Chen, S.-H.; Wei, J.-M.; Long, B. H.; Fairchild, C. A.; Carboni, J.; Mamber, S. W.; Rose, W. C.; Johnston, K.; Casazza, A. M.; Kadow, J. F.; Farina, V.; Vyas, D. M.; Doyle, T. W. Novel C-4 Paclitaxel (Taxol) Analogs: Potent Antitumor Agents. *Bioorg. Med. Chem. Lett.* **1995**, *5*, 2741-2746.

[67] Chen, S.-H.; Kadow, J. F.; Farina, V.; Fairchild, C. R.; Johnston, K. A. First Syntheses of Novel Paclitaxel (Taxol) Analogs Modified at the C-4 Position. *J. Org. Chem.* **1994**, *59*, 6156-6158.

[68] Georg, G. I.; Ali, S. M.; Boge, T. C.; Datta, A.; Falborg, L.; Himes, R. H. Selective C-2 and C-4 Deacylation and Acylation of Taxol: The First Synthesis of a C-4 Substituted Taxol Analogue. *Tetrahedron Lett.* **1994**, *35*, 8931-8934.

[69] Chaudhary, A. G.; Rimoldi, J. M.; Kingston, D. G. I. Modified Taxols. 10. Preparation of 7-Deoxytaxol, a Highly Bioactive Taxol Derivative, and Interconversion of Taxol and 7-*epi*-Taxol. *J. Org. Chem.* **1993**, *58*, 3798-3799.

[70] Chen, S. H.; Wei, J. M.; Vyas, D. M.; Doyle, T. W.; Farina, V. A Facile Synthesis of 7,10-Dideoxy Taxol and 7-*epi*-10-Deoxy Taxol. *Tetrahedron Lett.* **1993**, *34*, 6845-6848.

[71] Chen, S. H.; Kant, J.; Mamber, S. W.; Roth, G. P.; Wei, J.; Marshall, D.; Vyas, D.; Farina, V. Taxol Structure Activity Relationships: Synthesis and Biological Activity of Taxol and Analogs Modified at C-7. *Bioorg. Med. Chem. Lett.* **1994**, *4*, 2223-2228.

[72] Klein, L. L. Synthesis of 9-Dihydrotaxol: A Novel Bioactive Taxane. *Tetrahedron Lett.* **1993**, *34*, 2047-2050.

[73] Pulicani, J.-P.; Bourzat, J.-D.; Bouchard, H.; Commeren, A. Electrochemical Reduction of Taxoids: Selective Preparation of 9-dihydro-, 10-deoxy and 10-deacetoxy-Taxoids. *Tetrahedron Lett.* **1994**, *35*, 4999-5002.

[74] Datta, A.; Vander Velde, D. G.; Georg, G. I.; Himes, R. H. Syntheses of Novel C-9 and C-10

Modified Bioactive Taxanes. *Tetrahedron Lett.* **1995**, *36*, 1985-1988.

[75] Georg, G. I.; Cheruvallath, Z. S.; Vander Velde, D. G.; Himes, R. H. Stereoselective Synthesis of 9-Hydroxytaxanes via Reduction with Samarium Diiodide. *Tetrahedron Lett.* **1995**, *36*, 1783-1786.

[76] Chaudhary, A. G.; Kingston, D. G. I. Synthesis of 10-Deacetoxytaxol and 10-Deoxytaxotere. *Tetrahedron Lett.* **1993**, *34*, 4921-4924.

[77] Kant, J.; O'Keeffe, W. S.; Chen, S.-H.; Farina, V.; Fairchild, C.; Johnston, K.; Kadow, J. F.; Long, B. H.; Vyas, D. A Chemoselective Approach to Functionalize the C-10 Position of 10-Deacetylbaccatin III. Synthesis and Biological Properties of Novel C-10 Taxol Analogues. *Tetrahedron Lett.* **1994**, *35*, 5543-5546.

[78] Ojima, I.; Slater, J. C.; Kuduk, S. D.; Takeuchi, C. S.; Gimi, R. H.; Sun, C.-M.; Park, Y. H.; Pera, P.; Veith, J. M.; Bernacki, R. J. Syntheses and Structure-Activity Relationships of Taxoids Derived from 14*β*-Hydroxy-10-deacetylbaccatin III. *J. Med. Chem.* **1997**, *40*, 267-278.

[79] Ojima, I.; Slater, J. C.; Michaud, E.; Kuduk, S. D.; Bounaud, P.-Y.; Vrignaud, P.; Bissery, M.-C.; Veith, J.; Pera, P.; Bernacki, R. J. Syntheses and Structure-Activity Relationships of the Second Generation Antitumor Taxoids. Exceptional Activity against Drug-Resistant Cancer Cells. *J. Med. Chem.* **1996**, *39*, 3889-3896.

[80] Ojima, I.; Wang, T.; Miller, M. L.; Lin, S.; Borella, C.; Geng, X.; Pera, P.; Bernacki, R. J. Syntheses and Structure-Activity Relationships of New Second-Generation Taxoids. *Bioorg. Med. Chem. Lett.* **1999**, *9*, 3423-3428.

[81] Kingston, D. G. I.; Jagtap, P. G.; Yuan, H.; Samala, L. The chemistry of taxol and related taxoids. *Prog. Chem. Org. Nat. Prod.* **2002**, *84*, 53-225.

[82] Georg, G. I.; Boge, T. C.; Cheruvallath, Z. S.; Clowers, J. S.; Harriman, G. C. B.; Hepperle, M.; Park, H. The Medicinal Chemistry of Taxol. In *Taxol: Science and Applications*. Suffness, M., (Ed.) CRC Press: New York, **1995**, 317-375.

[83] Kant, J.; Huang, S.; Wong, H.; Fairchild, C.; Vyas, D.; Farina, V. Studies Toward Structure-Activity Relationships of Taxol: Synthesis and Cytotoxicity of Taxol Analogues with C-2' Modified Phenylisoserine Side Chains. *Bioorg. Med. Chem. Lett.* **1993**, *3*, 2471-2474.

[84] Geney, R.; Simmerling, C.; Ojima, I. Computational analysis of the paclitaxel binding site in *β*-tubulin. *Abstracts of Papers, 222nd ACS National Meeting*, Chicago, IL, August 26-30, **2001**, MEDI-065.

[85] Nicolaou, K. C.; Dai, W.-M.; Guy, R. K. Chemistry and Biology of Taxol. *Angew. Chem. Int. Ed. Engl.*, **1994**, *33*, 15-44.

[86] Ueda, Y.; Mikkilineni, A. B.; Knipe, J. O.; Rose, W. C.; Casazza, A. M.; Vyas, D. M. Novel Water Soluble Phosphate Prodrugs of Taxol Possessing *in vivo* Antitumor Activity. *Bioorg. Med. Chem. Lett.* **1993**, *3*, 1761-1766.

[87] Ueda, Y.; Wong, H.; Matiskella, J. D.; Mikkilineni, A. B.; Farina, V.; Fairchild, C.; Rose, W. C.; Mamber, S. W.; Long, B. H.; Kerns, E. H.; Casazza, A. M.; Vyas, D. M. Synthesis and Antitumor Evaluation of 2'-Oxycarbonylpaclitaxels (Paclitaxel-2'-carbonates). *Bioorg. Med. Chem. Lett.* **1994**, *4*, 1861-1864.

[88] Boge, T. C.; Georg, G. I. The Medicinal Chemistry of *β*-Amino Acids: Paclitaxel as an Illustrative Example. In *Enantioselective Synthesis of β-Amino Acids*. Juaristi, E. (Ed.) Wiley-VCH: New York, **1997**, 1-43.

[89] Ojima, I.; Lin, S.; Wang, T. The Recent Advances in the Medicinal Chemistry of Taxoids with Novel *β*-Amino Acid Side Chains. *Curr. Med. Chem.* **1999**, *6*, 927-954.

[90] Deng, L.; Jacobsen, E. N. A Practical, Highly Enantioselective Synthesis of the Taxol Side

Chain via Asymmetric Catalysis. *J. Org. Chem.* **1992**, *57*, 4320-4323.

[91] Georg, G. I.; Harriman, G. C. B.; Hepperle, M.; Clowers, J. S.; Vander Velde, D. G.; Hines, R. H. Synthesis, Conformational Analysis, and Biological Evaluation of Heteroaromatic Taxanes. *J. Org. Chem.* **1996**, *61*, 2664-2676.

[92] Ojima, I.; Slater, J. C.; Michaud, E.; Kuduk, S. D.; Bounaud, P.-Y.; Vrignaud, P.; Bissery, M.-C.; Veith, J.; Pera, P.; Bernacki, R. J. Syntheses and Structure-Activity Relationships of the Second Generation Antitumor Taxoids. Exceptional Activity against Drug-Resistant Cancer Cells. *J. Med. Chem.* **1996**, *39*, 3889-3896.

[93] Ojima, I.; Slater, J. S.; Kuduk, S. D.; Takeuchi, C. S.; Gimi, R. H.; Sun, C.-M.; Park, Y. H.; Pera, P.; Veith, J. M.; Bernacki, R. J. Syntheses and Structure-Activity Relationships of Taxoids Derived from 14*β*-Hydroxy-10-deacetylbaccatin III. *J. Med. Chem.* **1997**, *40*, 267-278.

[94] Ojima, I.; Duclos, O.; Zucco, M.; Bissery, M.-C.; Combeau, C.; Vrignaud, P.; Riou, J. F.; Lavelle, F. Synthesis and Structure-Activity Relationships of New Antitumor Taxoids. Effects of Cyclohexyl Substitution at the C-3' and/or C-2 of Taxotere (Docetaxel). *J. Med. Chem.* **1994**, *37*, 2602-2608.

[95] Roh, E. J.; Song, C. E.; Kim, D.; Pae, H.; Chung, H.; Lee, K. S.; Chai, K.; Lee, C. O.; Choi, S. U. Synthesis and Biology of 3'-N-Acyl-N-debenzoylpaclitaxel Analogs. *Bioorg. Med. Chem.* **1999**, *7*, 2115-2119.

[96] Georg, G. I.; Harriman, G. C. B.; Hepperle, M.; Clowers, J. S.; Vander Velde, D. G.; Hines, R. H. Synthesis, Conformational Analysis, and Biological Evaluation of Heteroaromatic Taxanes. *J. Org. Chem.* **1996**, *61*, 2664-2676.

[97] Fulop, F.; Bernath, G.; Pihlaja, K. Synthesis, stereochemistry and transformations of cyclopentane-, cyclohexane-, cycloheptane-, and cyclooctane-fused 1,3-oxazines, 1,3-thiazines, and pyrimidines, *Adv. Heterocycl. Chem.* **1998**, *69*, 349-477

[98] Rosenblum, S. B.; Huynh, T.; Afonso, A.; Davis, H. R., Jr.; Yumibe, N.; Clader, J. W.; Burnett, D. A. Discovery of 1-(4-Fluorophenyl)-(3*R*)-[3-(4-fluorophenyl)-(3*S*)-hydroxypropyl]-(4*S*)-(4-hydroxyphenyl)-2-azetidinone (SCH 58235): A Designed, Potent, Orally Active Inhibitor of Cholesterol Absorption, *J. Med. Chem.* **1998**, *41*, 973-980.

[99] Ojima, I.; Habus, I.; Zhao, M.; Zucco, M.; Park, Y. H.; Sun, C. M.; Brigaud, T. New and efficient approaches to the semisynthesis of taxol and its C-13 side chain analogs by means of *β*-lactam synthon method, *Tetrahedron* **1992**, *48*, 6985-7012.

[100] Lynch, J. E.; Riseman, S. M.; Laswell, W. L.; Volante, R. P.; Smith, G. B.; Shinkai, I.; Tschaen, D. M. Mechanism of an acid chloride-imine reaction by low-temperature FT-IR: *β*-lactam formation occurs exclusively through a ketene intermediate, *J. Org. Chem.* **1989**, *54*, 3792-6.

[101] Adachi, K.; Kobayashi, S.; Ohno, M. Creation of novel chiral synthons with enzymes and applications to natural product synthesis. Part 20. Chiral synthons by enantioselective hydrolysis of meso-diesters with pig liver esterase: substrate-stereoselectivity relationships, *Chimia* **1986**, *40*, 311-314.

[102] Yamashita, Y.; Saito, S.; Ishitani, H.; Kobayashi, S. Chiral Hetero Diels-Alder Products by Enantioselective and Diastereoselective Zirconium Catalysis. Scope, Limitation, Mechanism, and Application to the Concise Synthesis of (+)-Prelactone C and (+)-9-Deoxygoniopypyrone, *J. Am. Chem. Soc.* **2003**, *125*, 3793-3798.

[103] Georg, G. I.; Cheruvallath, Z. S.; Himes, R. H.; Mejillano, M. R.; Burke, C. T. Synthesis of biologically active taxol analogs with modified phenylisoserine side chains, *J. Med. Chem.* **1992**, *35*, 4230-4237.

[104] Wu, X. Y. *Ph.D. Dissertation*; SUNY at Stony Brook: Stony brook, **2003**.

[105] Holton, R. A. *Eur. Pat. Appl.* EP 400,971, **1990**.

References for Chapter 2

[1] Rowinsky, E. K. The Development and Clinical Utility of the Taxane Class of Antimicrotubule Chemotherapy Agents. *Annu. Rev. Med.* **1997**, *48*, 353-374.

[2] Ojima, I.; Slater, J. C.; Michaud, E.; Kuduk, S. D.; Bounaud, P. Y.; Vrignaud, P.; Bissery, M. C.; Veith, J.; Pera, P.; Bernacki, R. J. *J. Med. Chem.* **1996**, 39, 3889-3896.

[3] Ojima, I.; Kuduk, S. D.; Pera, P.; Veith, J. M.; Bernacki, R. J. Synthesis and Structure-Activity Relationships of Non-Aromatic Taxoids. Effects of Alkyl and Alkenyl Ester Groups on Cytotoxicity. *J. Med. Chem.* **1997**, *40*, 279-285.

[4] Ojima, I.; Duclos, O.; Zucco, M.; Bissery, M.-C.; Combeau, C.; Vrignaud, P.; Riou, J. F.; Lavelle, F. Synthesis and Structure-Activity Relationships of New Antitumor Taxoids. Effects of Cyclohexyl Substitution at the C3' and/or C2 of Taxotere (Docetaxel), *J. Med. Chem.* **1994**, *37*, 2602-2608.

[5] Ojima, I.; Park, Y. H.; Sun, C.-M.; Fenoglio, I.; Appendino, G.; Pera, P.; Bernacki, R. J. Structure-Activity Relationships of New Taxoids Derived from 14*β*-Hydroxy-10-deacetylbaccatin III, *J. Med. Chem.* **1994**, *37*, 1408-1410.

[6] Ojima, I.; Slater, J. C.; Michaud, E.; Kuduk, S. D.; Bounaud, P.-Y.; Vrignaud, P.; Bissery, M.-C.; Veith, J. M.; Pera, P.; Bernacki, R. J. Syntheses and Structure-Activity Relationships of the Second-Generation Antitumor Taxoids: Exceptional Activity against Drug-Resistant Cancer Cells, *J. Med. Chem.* **1996**, *39*, 3889-3896.

[7] Ojima, I.; Chen, J.; Sun, L; Borella, C.; Wang, T.; Miller, M.; Lin, S.; Geng, X.; Kuznetsova, L.; Qu, C.; Gallager, D.; Zhao, X.; Zanardi, I.; Xia, S.; Horwitz, S.; Mallen-St. Clair, J.; Guerriero, J.; Bar-Sagi, D.; Veith, J.; Pera, P.; Bernacki, R. Design, Synthesis, and Biological Evaluation of New-Generation Taxoids *J. Med. Chem.* **2008**, *51*, 3203–3221.

[8] Lynch, J. E.; Riseman, S. M.; Laswell, W. L.; Volante, R. P.; Smith, G. B.; Shinkai, I.; Tschaen, D. M. Mechanism of an acid chloride-imine reaction by low-temperature FT-IR: *β*-lactam formation occurs exclusively through a ketene intermediate, *J. Org. Chem.* **1989**, *54*, 3792-3796.

[9] Pluen, A.; Boucher, Y.; Ramanujan, S.; McKee, T. D.; Gohongi, T.; Di Tomaso, E.; Brown, E. B.; Izumi, Y.; Campbell, R. B.; Berk, D. A.; Jain, R. K. Role of tumor-host interactions in interstitial diffusion of macromolecules: cranial vs. subcutaneous tumors. *Proc. Natl. Acad. Sci. USA.* **2001**, *98*, 4628-4633.

[10] Jain, R. K. Delivery of molecular and cellular medicine to solid tumors. *Adv. Drug Deliver. Rev.* **2001**, *46*, 149-168.

[11] Chai *et al. Chinese Medicine* **2010**, 5, 26.

[12] Kessel, D.; Botterill, V.; Wodinsky, I. Uptake and retention of daunomycin by mouse leukemic cells as factors in drug response, *Cancer Res.* **1968**, *28*, 938-41.

[13] Dano, K. Active outward transport of daunomycin in resistant Ehrlich ascites tumor cells, *Biochim. Biophys. Acta* **1973**, *323*, 466-483.

[14] Ferte, J. Analysis of the tangled relationships between P-glycoprotein-mediated multidrug

resistance and the lipid phase of the cell membrane. *Eur. J. Biochem.* **2000**, *267*, 277-294.

[15] Juliano, R. L.; Ling, V. A surface glycoprotein modulating drug permeability in Chinese hamster ovary cell mutants. *Biochim. Biophys. Acta* **1976**, *455*, 152-62.

[16] Safa, A. R. Photoaffinity labeling of P-glycoprotein in multidrug-resistant cells, *Cancer. Invest.* **1992**, *10*, 295-305.

[17] Nielsen, D.; Maare, C.; Skovsgaard, T. Influx of daunorubicin in multidrug resistant Ehrlich ascites tumor cells: correlation to expression of P-glycoprotein and efflux. Influence of verapamil, *Biochem. Pharmacol.* **1995**, *50*, 443-450.

[18] Chen, C. J.; Chin, J. E.; Ueda, K.; Clark, D. P.; Pastan, I.; Gottesman, M. M.; Roninson, I. B. Internal duplication and homology with bacterial transport proteins in the mdr1 (P-glycoprotein) gene from multidrug-resistant human cells. *Cell* **1986**, *47*, 381-389.

[19] Ambudkar, S. V.; Dey, S.; Hrycyna, C. A.; Ramachandra, M.; Pastan, I.; Gottesman, M. M. Biochemical, cellular, and pharmacological aspects of the multidrug transporter. *Annu. Rev. Pharmacol.* **1999**, *39*, 361-398.

[20] Senior, A. E.; Bhagat, S. P-Glycoprotein Shows Strong Catalytic Cooperativity between the Two Nucleotide Sites. *Biochemistry* **1998**, *37*, 831-836.

[21] Ramachandra, M.; Ambudkar, S. V.; Chen, D.; Hrycyna, C. A.; Dey, S.; Gottesman, M. M.; Pastan, I. Human P-Glycoprotein Exhibits Reduced Affinity for Substrates during a Catalytic Transition State. *Biochemistry* **1998**, *37*, 5010-5019.

[22] Sauna, Z. E.; Ambudkar, S. V. Evidence for a requirement for ATP hydrolysis at two distinct steps during a single turnover of the catalytic cycle of human P-glycoprotein. *Proc. Natl. Acad. Sci. USA*. **2000**, *97*, 2515-2520.

[23] Deeley, R. G.; Cole, S. P. C. Function, evolution and structure of multidrug resistance protein (MRP), *Seminars Cancer Biol.* **1997**, *8*, 193-204.

[24] Scheper, R. J.; Broxterman, H. J.; Scheffer, G. L.; Kaaijk, P.; Dalton, W. S.; Van Heijningen, T. H. M.; Van Kalken, C. K.; Slovak, M. L.; De Vries, E. G. E.; et al. Overexpression of a Mr 110,000 vesicular protein in non-P-glycoprotein-mediated multidrug resistance, *Cancer Res.* **1993**, *53*, 1475-1479.

[25] Aszalos, A.; Ross, D. D. Biochemical and clinical aspects of efflux pump related resistance to anti-cancer drugs, *Anticancer Res*. **1998**, *18*, 2937-2944.

[26] Mueller, M.; Meijer, C.; Zaman, G. J. R.; Borst, P.; Scheper, R. J.; Mulder, N. H.; de Vries, E. G. E.; Jansen, P. L. M. Overexpression of the gene encoding the multidrug resistance-associated protein results in increased ATP-dependent glutathione S-conjugate transport. *Proc. Natl. Acad. Sci. USA*. **1994**, *91*, 13033-13037.

[27] Jedlitschky, G.; Leier, I.; Buchholz, U.; Barnouin, K.; Kurz, G.; Keppler, D. Transport of glutathione, glucuronate, and sulfate conjugates by the MRP gene-encoded conjugate export pump. *Cancer Res.* **1996**, *56*, 988-994.

[28] Loe, D. W.; Deeley, R. G.; Cole, S. P. C. Characterization of vincristine transport by the Mr 190,000 multidrug resistance protein (MRP): evidence for cotransport with reduced glutathione. *Cancer Res.* **1998**, *58*, 5130-5136.

[29] Borst, P.; Evers, R.; Kool, M.; Wijnholds, J. A family of drug transporters: The multidrug resistance-associated proteins. *J. Natl. Cancer I.* **2000**, *92*, 1295-1302.

[30] Kyle, A. H., Huxham, L. A., Yeoman, D. M. & Minchinton, A. I. Limited tissue penetration of taxanes: a mechanism for resistance in solid tumors. *Clin. Cancer Res.* **2007**, *13*, 2804-2810.

[31] Bhalla, K. N. Microtubule-targeted anticancer agents and apoptosis. *Oncogene* **2003,** *2*, 9075-9086.

[32] Verrills, N. M. *et al*. Alterations in gamma-actin and tubulin-targeted drug resistance in childhood leukemia. *J. Natl Cancer Inst.* **2006**, 98, 1363-1374.

[33] Attard, G.; Reid, A. H. M.; Yap, T. A.; Raynaud, F.; Dowsett, M.; Settatree, S.; Barrett, M.; Parker, C.; Martins, V.; Folkerd, E.; Clark, J.; Cooper, C. S.; Kaye, S. B.; Dearnaley, D.; Lee, G.; de Bono, J. S. Phase I clinical trial of a selective inhibitor of CYP17, abiraterone acetate, confirms that castration-resistant prostate cancer commonly remains hormone driven. *J. Clin. Oncol.* **2008**, *26*, 4563-4571.

[34] Gottesman, M. M.; Pastan, I. Biochemistry of multidrug resistance mediated by the multidrug transporter *Annu. Rev. Biochem.* **1993**, *62*, 385-427.

[35] Sarkadi, B.; Müller, M. Search for specific inhibitors of multidrug resistance in cancer. *Seminars in Cancer Biology,* **1997**, *8*, 171-182.

[36] Frezard, F.; Pereira-Maia, E.; Quidu, P.; Priebe, W.; Garnier-Suillerot, A. P-glycoprotein preferentially effluxes anthracyclines containing free basic versus charged amine. *Eur. J. Biochem.* **2001**, *268*, 1561-1567.

[37] Kobayashi, J. I.; Ogiwara, A.; Hosoyama, H.; Shigemori, H.; Yoshida, N.; Sasaki, T.; Li, Y.; Iwasaki, S.; Naito, M.; Tsuruo, T. Taxuspines A-C, new taxoids from Japanese yew Taxus cuspidata inhibiting drug transport activity of P-glycoprotein in multidrug-resistant cells. *Tetrahedron* **1994**, *50*, 7401-7416.

[38] Kobayashi, J. I.; Hosoyama, H.; Wang, X.-X.; Shigemori, H.; Sudo, Y.; Tsuruo, T. Modulation of multidrug resistance by taxuspine C and other taxoids from Japanese yew. *Bioorg. Med. Chem. Lett.* **1998**, *8*, 1555-1558.

[39] Hosoyama, H.; Shigemori, H.; Tomida, A.; Tsuruo, T.; Kobayashi, J. I. Modulation of multidrug resistance in tumor cells by taxinine derivative. *Bioorg. Med. Chem. Lett.* **1999**, *9*, 389-394.

[40] Kobayashi, J. I.; Hosoyama, H.; Wang, X.-X.; Shigemori, H.; Koiso, Y.; Iwasaki, S.; Sasaki, T.; Naito, M.; Tsuruo, T. Effects of taxoids from Taxus cuspidata on microtubule depolymerization and vincristine accumulation in MDR cells. *Bioorg. Med. Chem. Lett.* **1997**, *7*, 393-398.

[41] Yamazaki, T.; Hiraoka, S.; Sakamoto, J.; Kitazume, T. Mesyloxy-group migration as the stereoselective preparation method of various functionalized olefins and its reaction mechanism, *Org. Lett.*, **2001**, *3*, 743-746.

[42] Lim, M. H.; Kim, H. O.; Moon, H. R.; Chun, M. W.; Jeong, L. S. Synthesis of Novel D-2'-Deoxy-2'-C-difluoromethylene-4'-thiocytidine as a Potential Antitumor Agent, *Org. Lett.*

2002, *4*, 529-531.

[43] Wu, Q.; Bounaud, P.-Y.; Kuduk, S. D.; Yang, C.-P. H.; Ojima, I.; Horwitz, S. B.; Orr, G. A. Identification of the domains of photoincorporation of the 3'- and 7-benzophenone analogs of Taxol in the carboxyl-terminal half of murine mdr1b P-glycoprotein, *Biochemistry* **1998**, *37*, 11272-11279.

[44] Ojima, I.; Bounaud, P.-Y.; Takeuchi, C.; Pera, P.; Bernacki, R. J. New taxanes as highly efficient reversal agents for multi-drug resistance in cancer cells, *Bioorg. Med. Chem. Lett.* **1998**, *8*, 189-194.

[45] Fumero, C. L., *Ph.D. Dissertation*; SUNY at Stony Brook: Stony Brook, **2000**.

[46] Ojima, I.; Borella, C.; Wu, X.; Bounaud, P.; Oderda, C.; Sturm, M.; Miller, M.; Chakravarty, S.; Chen, J.; Huang, Q.; Pera, P.; Brooks, T.; Baer, M.; Bernacki, R. Design, Synthesis and Structure-Activity Relationships of Novel Taxane-Based Multidrug Resistance Reversal Agents, *J. Med. Chem.* **2005,** *48,* 2218-2228.

[47] Ojima, I.; Bounaud, P.-Y.; Bernacki, R. J. New weapons in the fight against cancer. *Chemtech*, **1998**, *28*, 31-36.

[48] Geney, R.; Ungureanu, I. M.; Li, D.; Ojima, I. Overcoming multidrug resistance in taxane chemotherapy. *Clin. Chem. Lab. Med.* **2002**, *40*, 918-925.

[49] Chen, J., *Ph.D. Dissertation*; SUNY at Stony Brook: Stony Brook, **2006**.

[50] Wu, X., *Ph.D. Dissertation*; SUNY at Stony Brook: Stony Brook, **2003**.

[51] Brooks, T.; Minderman, H.; O'Loughlin, K. L.; Pera, P.; Ojima, I.; Baer, M. R.; Bernacki, R. J. Taxane-based reversal agents modulate drug resistance mediated by P-glycoprotein, multidrug resistance protein, and breast cancer resistance protein. *Mol. Cancer Ther.* **2003**, *2*, 1195-1205.

[52] Borella, C. P., *Ph.D. Dissertation*; SUNY at Stony Brook: Stony Brook, **2001**.

[53] Ojima, I.; Wang, T.; Miller, M. L.; Lin, S.; Borella, C. P.; Geng, X.; Pera, P.; Bernacki, R. J. Synthesis and structure-activity relationships of new second-generation taxoids, *Bioorg. Med. Chem. Lett.* **1999**, *9*, 3423-3428.

References for Chapter 3

[1] McGuire, W. P.; Hoskins, W. J.; Brady, M. F.; Kucera, P. R.; Partridge, E. E.; Look, K. Y.; Clarke-Pearson, D. L.; Davidson, M. Cyclophosphamide and cisplatin compared with paclitaxel and cisplatin in patients with stage III and stage IV ovarian cancer, *New Engl. J. Med.* **1996**, *334*, 1-6.

[2] Holmes, F. A.; Kudelka, A. P.; Kavanagh, J. J.; Huber, M. H.; Ajani, J. A.; Valero, V. In *Taxane Anticancer Agents. Basic Science and Current Status*, Georg, G. I.; Chen, T. T.; Ojima, I.; Vyas, D. M. (Eds.) American Chemical Society: Washington, **1995,** 31-57.

[3] Gelmon, K. The Taxoids-Paclitaxel and Docetaxel, *The Lancet* **1994**, *344*, 1267-1272.

[4] Rowinsky, E. K.; Donehover, R. C. Drug-Therapy - Paclitaxel (Taxol), *New Engl. J. Med.* **1995**, *332*, 1004-1014.

[5] Schiff, P. B.; Fant, J.; Horwitz, S. B. *Nature* **1979**, *277*, 665–667.

[6] Jordan, M. A.; Wilson, L. *Nat. Rev. Cancer* **2004**, *4*, 253–265.

[7] Vallee, R. B., In *Taxol: Science and Applications*, Suffness, M. (Ed.) CRC Press: Boca Raton, **1995**, 259-274.

[8] Jordon, M. A.; Wilson, L., In *Taxane Anticancer Agents. Basic Science and Current Status*, Georg, G. I.; Chen, T. T.; Ojima, I.; Vyas, D. M. (Eds.) American Chemical Society: Washington, **1995**, 138-153.

[9] Kingston, D. G.; Bane, S.; Snyder, J. P. *Cell Cycle* **2005**, *4*, 279–289.

[10] Snyder, J. P.; Nevins, N.; Cicero, D. O.; Jansen, J. The Conformations of Taxol in Chloroform, *J. Am. Chem. Soc.* **2000**, *122*, 724-725.

[11] Sun, L.; Simmerlin, C.; Ojima, I. Recent Advances in the Study of the Bioactive Conformation of Taxol, *ChemMedChem* **2009**, *4*, 719 – 731.

[12] Gueritte-Voegelein, F.; Guenard, D.; Mangatal, L.; Potier, P.; Guilhem, J.; Cesario, M.; Pascard, C. Structure of a Synthetic Taxol Precursor: *N*-*tert*-Butoxycarbonyl-10-deacetyl-*N*-debenzoyltaxol, *Acta Cryst.* **1990**, *C46*, 781-784.

[13] Mastropaolo, D.; Camerman, A.; Luo, Y.; Brayer, G. D.; Camerman, N. Crystal and molecular structrue of paclitaxel (taxol), *Proc. Natl. Acad. Sci. USA*, **1995**, *92*, 6920-6924.

[14] Hilton, B. D.; Chmurny, G. N.; Muschik, G. M. Taxol: Quantitative Internuclear Proton-Proton Distances in $CDCl_3$ Solution from nOe Data: 2D NMR ROESY Buildup Rates at 500 MHz, *J. Nat. Prod.* **1992**, *55*, 1157-1161.

[15] Vander Velde, D. G.; Georg, G. I.; Grunewald, G. L.; Gunn, C. C.; Mitscher, L. A. "Hydrophobic Collapse" of Taxol and Taxotere Solution Conformations in Mixtures of Water and Organic Solvent, *J. Am. Chem. Soc.* **1993**, *115*, 11650-11651.

[16] Rao, S.; Orr, G. A.; Chaudhary, A. G.; Kingston, D. G. I.; Horwitz, S. B. Characterization of the Taxol Binding Site on the Microtubule, *J. Biol. Chem.* **1995**, *270*, 20235-20238.

[17] Rao, S.; Krauss, N. E.; Heerding, J. M.; Swindell, C. S.; Ringel, I.; Orr, G. A.; Horwitz, S. B. 3'-(*p*-Azidobenzamido)taxol Photolabels the *N*-terminal 31 Amino Acids of *β*-Tubulin, *J. Biol. Chem.* **1994**, *269*, 3132-3134.

[18] Li, Y.; Cegelski, L.; Poliks, M.; Gryczynsli, Z.; Piszczek, G.; Jagtap, P. G.; Studelska, D.; Kingston, D. G.; Schaefer, J.; Bane, S. Conformation of Microtubule-Bound Paclitaxel Determined by Fluorescence Spectroscopy and REDOR NMR, *Biochemistry* **2000**, *39*, 281-291.

[19] Sengupta, S.; Boge, T. C.; Liu, Y.; Hepperle, M.; Georg, G. I.; Himes, R. H. Probing the

Enviroment of Tubulin-Bound Paclitaxel Using Florescent Paclitaxel Analogues, *Biochemistry* **1997**, *36*, 5179-5184.
[20] Gupta, M. L., Jr.; Bode, C. J.; Georg, G. I.; Himes, R. H. Understanding tubulin-Taxol interactions: Mutations that impart Taxol binding to yeast tubulin., *Proc. Natl. Acad. Sci. USA* **2003**, *100*, 6394-6397.
[21] Snyder, J. P.; Nettles, J. H.; Cornett, B.; Dowing, K. H.; Nogales, E. The binding conformation of Taxol in *β*-tubulin: A model based on electron crystallographic density, *Proc. Natl. Acad. Sci. USA* **2001**, *98*, 5312-5316.
[22] Nogales, E.; Wolf, S. G.; Downing, K. H. Structure of the alpha, *β*-Tubulin Dimer by Electron Crystallography, *Nature* **1998**, *391*, 199-203.
[23] Falzon, C. J.; Benesi, A. J.; Lecomte, J. T. J. Characterization of Taxol in Methylene Chloride by NMR Spectroscopy, *Tetrahedron Lett.* **1992**, *33*, 1169-1172.
[24] Williams, H. J.; Scott, A. I.; Dieden, R. A.; Swindell, C. S.; Chirlian, L. E.; Francl, M. M.; Heerding, J.; Krauss, N. E. NMR and Molecular Modeling Study of the Conformations of Taxol and Its Side Chain Methylester in Aqueous and Non-aqueous Solution, *Tetrahedron* **1993**, *49*, 6545-6560.
[25] Dubois, J.; Guenard, D.; Gueritte-Voegelein, F.; Guedira, N.; Potier, P.; Gillet, B.; Beloeil, J. C. *Tetrahedron* **1993**, *49*, 6533–6544.
[26] Vander Velde, D. G.; Georg, G. I.; Grunewald, G. L.; Gunn, C. W.; Mitscher, L. A. *J. Am. Chem. Soc.* **1993**, *115*, 11650–11651.
[27] Lin, S.; Ojima, I. *Expert Opin. Ther. Pat.* **2000**, *10*, 869–889.
[28] Chmurny, G. N.; Hilton, B. D.; Brobst, S.; Look, S. A.; Witherup, K. M.; Beutler, J. A. ^{1}H- and ^{13}C-NMR Assignments for Taxol, 7-*epi*-Taxol, and Cephalomannine, *J. Nat. Prod.* **1992**, *55*, 414-423.
[29] Balasubramanian, S. V.; Alderfer, J. L.; Straubinger, R. M. Solvent-Dependent and Concentration-Dependent Molecular-Interactions of Taxol (Paclitaxel), *J. Pharm. Sci.*, **1994**, *83*, 1470-1476.
[30] Ojima, I.; Lin, S.; Inoue, T.; Miller, M. L.; Borella, C. P.; Geng, X.; Walsh, J. J. *J. Am. Chem. Soc.* **2000**, *122*, 5343–5353.
[31] Ojima, I.; Geng, X.; Lin, S.; Pera, P.; Bernacki, R. J. *Bioorg. Med. Chem. Lett.* **2002**, *12*, 349–352.
[32] Geng, X.; Miller, M. L.; Lin, S.; Ojima, I. *Org. Lett.* **2003**, *5*, 3733–3736.
[33] Querolle, O. D.; Thoret, J.; Dupont, S.; Gueritte, C.; Guenard, F.; *Eur. J. Org. Chem.* **2003**, 542–550.
[34] Querolle, O. D.; Dupont, S.; Thoret, S.; Roussi, F.; Montiel-Smith, S.; Gueritte, S.; Guenard, D. *J. Med. Chem.* **2003**, *46*, 3623–3630.
[35] Boge, T. C.; Wu, Z.-J.; Himes, R. H.; Vander Velde, D. G.; Georg, G. I. *Bioorg. Med. Chem. Lett.* **1999**, *9*, 3047–3052.
[36] Ojima, I.; Chakravarty, S.; Inoue, T.; Lin, L.; He, L.; Horwitz, S. B.; Kuduk, S. D.; Danishefsky, S. J. *Proc. Natl. Acad. Sci. USA* **1999**, *96*, 4256–4261.
[37] Boge, T.; Wu, Z.; Himes, R.; Vander Velde, D.; Georg, G. Conformationally Restricted Paclitaxel Analogues: Macrocyclic Mimics of the "Hydrophobic Collapse" Conformation, *Bioorg. Med. Chem. Lett.* **1999**, *9*, 3047-3052.
[38] Querolle, O.; Dubois, J.; Thoret, S.; Roussi, F.; Montiel-Smith, S.; Gueritte, F.; Guenard, D. Synthesis of Novel Macrocyclic Docetaxel Analogues. Influence of Their Macrocyclic Ring Size on Tubulin Activity, *J. Med. Chem.* **2003**, *46*, 3623-3630.

[39] Kingston, D. G.; Bane, S.; Snyder, J. P. *Cell Cycle* **2005**, *4*, 279–289.
[40] Snyder, J. P.; Nevins, N.; Cicero, D. O.; Jansen, J. The Conformations of Taxol in Chloroform, *J. Am. Chem. Soc.* **2000**, *122*, 724-725.
[41] Nogales, E.; Wolf, S. G.; Downing, K. H. *Nature* **1998**, *391*, 199–203.
[42] Lowe, J.; Li, H.; Downing, K. H.; Nogales, E. *J. Mol. Bol.* **2001**, *313*, 1045–1057.
[43] Kingston, D. G. I.; Bane, S.; Snyder, J. P. *Cell Cycle* **2005**, *4*, 279–289
[44] Ganesh, T.; Guza, R. C.; Bane, S.; Ravindra, R.; Shanker, N.; Lakdawala, A. S.; Snyder, J. P.; Kingston, D. G. I. *Proc. Natl. Acad. Sci. U.S.A.* **2004**, *101*, 10006-10011.
[45] Larroque, A.-L.; Dubois, J.; Thoret, S.; Aubert, G.; Chiaroni, A.; Gueritte, F.; Guenard, D. *Bioorg. Med. Chem.* **2007**, *15*, 563–574.
[46] Li, Y.; Poliks, B.; Cegelski, L.; Poliks, M.; Cryczynski, A.; Piszcek, G.; Jagtap, P. G.; Studelska, D. R.; Kingston, D. G. I.; Schaefer, J.; Bane, S. *Biochemistry* **2000**, *39*, 281–291.
[47] Rao, S.; He, L.; Chakravarty, S.; Ojima, I.; Orr, G. A.; Horwitz, S. B. *J. Biol. Chem.* **1999**, *274*, 37990–37994.
[48] Paik, Y.; Yang, C.; Metaferia, B.; Tang, S.; Bane, S.; Ravindra, R.; Shanker, N.; Alcaraz, A. A.; Johnson, S. A.; Schaefer, J.; O'Connor, R. D.; Cegelski, L.; Snyder, J. P.; Kingston, D. G. I. *J. Am. Chem. Soc.* **2007**, *129*, 361–370.
[49] Sun, L.; Geng, X.; Geney, R.; Li, Y.; Simmerling, C.; Li, Z.; Lauher, J. W.; Xia, S.; Horwitz, S. B.; Veith, J. M.; Pera, P.; Bernacki, R. J.; Ojima, I. *J. Org. Chem.* **2008**, *73*, 9584–9593.
[50] Geney, R.; Sun, L.; Pera, P.; Bernacki, R. J.; Xia, S.; Horwitz, S. B.; Simmerline, C. L.; Ojima, I. Use of the Tubulin Bound Paclitaxel Conformation for Structure-Based Rational Drug Design. *Chemistry & Biology*, **2005**, *12*, 339-348.
[51] Bollag, D. M.; McQueney, P. A.; Zhu, J.; Hensens, O.; Koupal, L.; Liesch, J.; Goetz, M.; Lazarides, E.; Woods, C. M. *Cancer Res.* **1995**, *55*, 2325-2333.
[52] Kowalski, R. J.; Giannakakou, P.; Hamel, E. *J. Biol. Chem.* **1997**, *272*, 2534-2541.
[53] Lindel, T.; Jensen, P. R.; Fenical, W.; Long, B. H.; Casazza, A. M.; Carboni, J.; Fairchild, C. R. *J. Am. Chem. Soc.* **1997**, *119*, 8744-8745.
[54] ter Haar, E.; Kowalski, R. J.; Hamel, E.; Lin, C. M.; Longley, R. E.; Gunasekera, S. P.; Rosenkranz, H. S.; Day, B. W. *Biochemistry* **1996**, *35*, 243-250.
[55] Kowalski, R. J.; ter Haar, E.; Longley, R. E.; Gunasekera, S. P.; Lin, C. M.; Day, B. W.; Hamel, E. *Mol Biol. Cell* **1995**, *6*, 368a.
[56] Hung, D. T.; Chen, J.; Schreiber, S. L. *Chem. Biol.* **1996**, *3*, 287-293.
[57] Mooberry, S. L.; Tien, G.; Hernandez, A. H.; Plubrukarn, A.; Davidson, B. S. *Cancer Res.* **1999**, *59*, 653-660.
[58] Sato, B.; Muramatsu, H.; Miyauchi, M.; Hori, Y.; Takase, S.; Hino, M.; Hashimoto, S.; Terano, H. *J. Antibiot.* **2000**, *53*, 123-130.
[59] Geney, R.; Simmerling, C.; Ojima, I. *Abstr. Pap. - Am. Chem. Soc.* **2001**, 222nd, MEDI-065.
[60] Ojima, I.; Geng, X.; Lin, S.; Pera, P.; Bernacki, R. J. Design, Synthesis and Biological Activity of Novel C2-C3'*N*-Linked Macrocyclic Taxoids, *Bioorg. Med. Chem. Lett.* **2002**, *12*, 349-352.
[61] Ojima, I.; Wang, T.; Delaloge, F. Extremely Stereoselective Alkylation of 3-siloxy-*β*-lactams and its applications to the asymmetric syntheses of novel 2-alkylisoserines, their dipeptides, and taxoids, *Tetrahedron Lett.* **1998**, *39*, 3663-3666.
[62] Chen, S. H.; Kadow, J. F.; Farina, V.; Fairchild, C. R.; Johnston, K. A. First Syntheses of Novel Paclitaxel (Taxol) Analogs Modified at the C4-Position, *J. Org. Chem.*, **1994**, *59*, 6156-6158.
[63] Ojima, I.; Habus, I.; Zhao, M.; Zucco, M.; Park, Y. H.; Sun, C. M.; Brigaud, T. New and Efficient Approaches to the Semisynthesis of Taxol and Its C-13 Side Chain Analogs by

Means of *β*-Lactam Synthon Method, *Tetrahedron*, **1992**, *48*, 6985-7012.

[64] Appendino, G.; Gariboldi, P.; Gabetta, B.; Pace, R.; Bombardelli, E.; Viterbo, D. 14□-Hydroxy-10-deacetylbaccatin III, a New Taxane from Himalayan Yew (*Taxus Wallichiana Zucc.*). *J. Chem. Soc., Perkins Trans 1* **1992**, 2925-2929.

[65] Horowitz, S. B. Taxol: Mechanism of Action and Resistance. *Stony Brook Symposium on Taxol and Taxotere*, Stony Brook, NY, May 14-15, **1993**; Abstracts 1923-1924.

[66] Ye, T.; Garcia, C. F.; McKervey, M. A. Chemoselectivity and Stereoselectivity of Cyclization of alpha-Diazocarbonyls Leading to Oxygen and Sulfur Heterocycles Catalyzed by Chiral Rhodium and Copper-Catalysts, *J. Chem. Soc. - Perkin Trans. I* **1995**, *11*, 1373-1379.

[67] Ojima, I.; Wang, T.; Miller, M. L.; Lin, S.; Borella, C. P.; Geng, X.; Pera, P.; Bernacki, R. J. Synthesis and structure-activity relationships of new second-generation taxoids, *Bioorg. Med. Chem. Lett.* **1999**, *9*, 3423-3428.

[68] Geng, X. D. *Ph.D. Dissertation;* SUNY at Stony Brook: Stony Brook, **2002**.

[69] Geney, R.; Sun, L.; Pera, P.; Bernacki, R. J.; Xia, S.; Horwitz, S. B.; Simmerling, C. L.; Ojima, I. Use of the Tubulin Bound Paclitaxel Conformation for Structure-Based Rational Drug Design, *Chem. Biol.*, **2005**, *12*, 339-348.

[70] Kant, J.; Schwartz, W. S.; Fairchild, C.; Gao, Q.; Huang, S.; Long, B. H.; Kadow, J. F.; Langley, D. R.; Farina, V.; Vyas, D. Diastereoselective addition of Grignard reagents to azetidine-2,3-dione: Synthesis of novel Taxol® analogues, *Tetrahedron Lett.* **1996**, *37*, 6496-6498.

References for Chapter 4

[1] Ojima, I. Use of Fluorine in the Medicinal Chemistry and Chemical Biology of Bioactive Compounds-A Case Study on Fluorinated Taxane Anticancer Agents. *ChemBioChem* **2004**, *5*, 628-635.

[2]Begue, J. P.; Bonnet-Delpon, D. Recent advances (1995-2005) in fluorinated pharmaceuticals based on natural products. *J. Fluor. Chem*. **2006**, *127*, 992–1012.

[3] Isanbor, C.; O'Hagan, D. Fluorine in medicinal chemistry: A review of anti-cancer agents. *J. Fluor. Chem.* **2006**, *127*, 303–319.

[4] Bondi, A. van der Waals volumes and radii. *J. Phys. Chem.*, **1964**, *68*, 441-451.

[5] Jeschke, P. The Unique Role of Fluorine in the Design of Active Ingredients for Modern Crop Protection *ChemBioChem* **2004**, *5*, 570-589.

[6] Penning, J. D.; Talley, J. J.; Bertenshaw, S. R. Carter, J. S.; Collins, P. W.; Docter, S.; Graneto, M. J.; Lee, L. F.; Malecha, J. W.; Miyashiro, J. M.; Rogers, R. S.; Rogier, D. J.; Yu, S. S.; Anderson, G. D.; Burton, E. G.; Cogburn, J. N.; Gregory, S. A.; Koboldt, C. M.; Perkins, W. E.; Seibert, K.; Veenhuizen, A. W.; Zhang, Y. Y.; Isakson, P. C. Synthesis and biological evaluation of the 1,5-diarylpyrazole class of cyclooxygenase-2 inhibitors:Identification of SC-56835 (celecoxib). *J. Med. Chem.* **1997**, *40*, 1347-1365.

[7] Clader, J. W. The Discovery of Ezetimibe: A View from Outside the Receptor. *J. Med. Chem.* **2004**, *47*, 1-9.

[8] Dugar, S.; Yumibe, N.; Clader, J.; W.; Vizziano, M.; Huie, K.; van Heek, M.; Compton, D. S.; Davis, H. R., Jr. Metabolism and structure activity data based drug design: discovery of (−) SCH 53079 an analog of the potent cholesterol absorption inhibitor (−) SCH 48461. *Bioorg. Med. Chem.Lett.* **1996**, *6*, 1271-1274.

[9] Smart, B. E. Fluorine substituent effects (on bioactivity). *J. Fluorine Chem*. **2001**, *109* 3-11.

[10] Böhm, H.-J.; Banner, D.; Bendels, S.; Kansy, M.; Kuhn, B.; Mueller, K.; Obst-Sander, U.; Stahl, M. Fluorine in medicinal chemistry. *ChemBioChem*, **2004**, *5*, 637-643.

[11] Ojima, I.; Kuduk, S. D.; Slater, J. C.; Gimi, R. H.; Sun, C. M. Syntheses of new fluorine-containing taxoids by means of *β*-lactam synthon method. *Tetrahedron* **1996**, *52*, 209-224.

[12] Ojima, I.; McCarthy, J. R.; Welch, J. T. (Eds.) Biomedical Frontiers of Fluorine Chemistry. *ACS symposium series*, American Chemical Society, Volume 639, 1st Ed., **1996,** pp 356.

[13] Cottet, F.; Marull, M.; Lefebvre, O.; Schlosser,M. Recommendable Routes to Trifluoromethyl-Substituted Pyridine- and Quinolinecarboxylic Acids. *Eur. J. Org. Chem.* **2003,** *8*, 1559–1568.

[14] Kirk, K. L. Fluorine in medicinal chemistry: Recent therapeutic applications of fluorinated small molecules. *J. Fluor. Chem*. **2006**, *127,* 1013–1029.

[15] Page, M. I. The mechanisms of reactions of *β*-lactam antibiotics. *Acc. Chem. Res.*, **1984**, *17*, 144-151.

[16] Khalafallah, A. K.; Hassan, M. E.; Soleman, H. A. Synthesis and biological studies on some spiro Schiff base derivatives. *J. Ind. Chem. Soc.*, **1992**, *69*, 318-320.

[17]Lukic, I. Preparation of novel derivatives of 3-bromo and 3,3-dibromo-4-oxo-1-azetidines for their use in antibacterial or antitumor therapy. **1997**, *Eur. Pat. Appl. 791580*.

[18] Borthwick, A. D.; Weingarten, G.; Haley, T. M.; Tomaszewski, M.; Wang, W.; Hu, Z.; Bedard,

J.; Jin, H.; Yuen, L.; Mansour, T. S. Design and synthesis of monocyclic β-lactams as mechanism-based inhibitors of human cytomegalovirus protease. *Bioorg. Med. Chem. Lett.* **1998**, *8*, 365-370.

[19] Ogilvie, W.; Bailey, M.; Poupart, M.-A.; Abraham, A.; Bhavsar, A.; Bonneau, P.; Bordeleau, J.; Bousquet, Y.; Chabot, C.; Duceppe, J.-S.; Fazal, G.; Goulet, S.; Grand-Maitre, C.; Guse, I.; Halmos, T.; Lavallee, P.; Leach, M.; Malenfant, E.; O'Meara, J.; Plante, R.; Plouffe, C.; Poirier, M.; Soucy, F.; Yoakim, C.; Deziel, R. Peptidomimetic Inhibitors of the Human Cytomegalovirus Protease. *J. Med. Chem.* **1997**, *40*, 4113-4135.

[20] Ojima, I. Recent Advances in the *β*-Lactam Synthon Method. *Acc. Chem. Res.* **1995**, *28*, 383-389.

[21] Ojima, I.; Delaloge, F. Asymmetric synthesis of building-blocks for peptides and peptidomimetics by means of the β-lactam synthon method. *Chem. Soc. Rev.* **1997**, *26*, 377-386.

[22] Ojima, I.; Delaloge, F. Syntheses of norstatine, its analogs, and dipeptide isosteres by means of *β*-lactam synthon method. *Methods Mol. Med.* **1999**, *23*, 137-160.

[23] Pepe, A.; Kuznetsova, L.; Sun, L.; Ojima, I. Fluoro-taxoid anticancer agents. In: *Fluorine in medical chemistry and chemical biology*. Ojima, I. (Ed.) 1st Ed., Wiley-Blackwell, Chichester, pp 117–139, **2009**.

[24] Ojima, I.; Kuduk, S. D.; Slater, J. C.; Gimi, R. H.; Sun, C. M.; Chakravarty, S.; Ourevitch, M.; Abouabdellah, A.; Bonnet-Delpon, D.; Begue, J.-P.; Veith, M.; Pera, P.; Bernacki, R. J. In: *Biomedical Frontiers of Fluorine Chemistry.* Ojima, I.; McCarthy, J. R.; Welch J. T. (Eds.) ACS Symposium Series 639, American Chemical Society, Washington, DC, pp. 228–243, **1996**.

[25] Ojima, I.; Inoue, T.; Slater, J. C.; Lin, S.; Kuduk, S. C.; Chakravarty, S.; Walsh, J. J.; Gilchrist, L.; McDermott, A. E.; Cresteil, T.; Monsarrat, B.; Pera, P.; Bernacki, R. J. In: *Asymmetric Fluoroorganic Chemistry: Synthesis, Application, and Future Directions.* Ramachandran P. V. (Ed.) ACS Symposium Series 746, American Chemical Society, Washington, DC, pp. 158–181, **1999**.

[26] Ojima, I.; Kuduk, S. C.; Chakravarty, S.; Ourevitch, M.; Begue, J.-P. *J. Am. Chem. Soc*. **1997**, *119*, 5519–5527.

[27] Ojima, I.; Lin, S.; Slater, J. C.; Wang, T.; Pera, P.; Bernacki, R. J.; Ferlini, C.; Scambia, G. *Bioorg. Med. Chem.* **2000**, *8*, 1619–1628.

[28] Kuznetsova, L.; Ungureanu, I. M.; Pepe, A.; Zanardi, I.; Wu, X.; Ojima, I. Trifluoromethyl- and difluoromethyl-*β*-lactams as useful building blocks for the synthesis of fluorinated amino acids, dipeptides, and fluoro-taxoids. *J. Fluorine Chem.* **2004**, *125*, 487-500.

[29] Gut, I.; Ojima, I.; Vaclavikova, R.; Simek, P.; Horsky, S.; Soucek, P.; Kondrova, E.; Kuznetsova, L. V.; Chen, J. *Xenobiotica* **2006**, *36*, 772–792.

[30] Vuilhorgne, M.; Gaillard, C.; Sanderlink, G. J.; Royer, I.; Monsarrat, B.; Dubois, J.; Wright, M. In: *Taxane Anticancer Agents: Basic Science and Current Status.* Georg, G. I., Chen, T. T., Ojima, I., Vyas, D. M. (Eds.) ACS Symp. Ser. 583; American Chemical Society: Washington, D.C., pp 98-110, **1995**.

[31] Ojima, I.; Das, M. Recent Advances in the Chemistry and Biology of New Generation Taxoids, *J. Nat. Prod.* **2009**, *72,* 554–565.

[32] Yamazaki, T.; Hiraoka, S.; Sakamoto, J.; Kitazume, T. Mesyloxy-group migration as the stereoselective preparation method of various functionalized olefins and its reaction mechanism, *Org. Lett.* **2001**, *3*, 743-746.

[33] Lim, M. H.; Kim, H. O.; Moon, H. R.; Chun, M. W.; Jeong, L. S. Synthesis of Novel D-2'-Deoxy-2'-C-difluoromethylene-4'-thiocytidine as a Potential Antitumor Agent, *Org. Lett.* **2002**, *4*, 529-531.

[34] Bhadury, P. S.; Palit, M.; Sharma, M.; Raza, S. K.; Jaiswal, D. K. Fluorinated phosphonium ylides: versatile *in situ* Wittig intermediates in the synthesis of hydrofluorocarbons, *J. Fluorine Chem.* **2002**, *116*, 75-80.

[35] Ojima, I.; Slater, J.; Michaud, E.; Kuduk, S.; Bounaud, P.; Vrignaud, P.; Bissery, M.; Veith, J.; Pera, P.; Bernacki, R. Syntheses and Structure-Activity Relationships of the Second-Generation Antitumor Taxoids: Exceptional Activity against Drug-Resistant Cancer Cells. *J. Med. Chem.* **1996**, *39*, 3889–3896.

[36] Ojima, I.; Slater, J. C.; Pera, P.; Veith, J. M.; Abouabdellah, A.; Bégué, J.-P.; Bernacki, R. J. *Bioorg. Med. Chem. Lett.* 1997, *7*, 133-138.

[37] Ojima, I.; Lin, S. N.; Slater, J. C.; Wang, T.; Pera, P.; Bernacki, R. J.; Ferlini, C.; Scambia, G. *Bioorg. Med. Chem.* **2000**, *8*, 1619-1628.

[38] Kuznetsova, L., *Ph.D. Dissertation*; SUNY at Stony Brook: Stony Brook, **2005**.

[39] Vobořilová, J.; Němcová-Fürstov, V.; Neubauerová, J.; Ojiman I.; Zanardi, I.; Gut, I.; Kovář, J. Cell death induced by novel fluorinated taxanes in drug-sensitive and drug-resistant cancer cells. *Investigational New Drugs* **2009**, *29*, 411-423.

[40] Bhalla, K. N. Microtubule-targeted anticancer agents and apoptosis. *Oncogene* **2003,** *22*, 9075–9085.

[41] Liao, P. C.; Tan, S. K.; Lieu, C. H.; Jung, H. K. Involvement of endoplasmic reticulum in paclitaxel-induced apoptosis. *J. Cell Biochem.* **2008**, *104*, 1509–1523.

[42] Mhaidat, N. M.; Wang, Y.; Kiejda, K. A.; Zhang, X. D.; Hersey, P. Docetaxel-induced apoptosis in melanoma cells is dependent on activation of caspase-2. *Mol Cancer Ther* **2007**, *6*, 752–761.

[43] Shi, J.; Orth, J. D.; Mitchison, T. Cell type variation in responses to antimitotic drugs that target microtubules and kinesin-5. *Cancer Res* **2008**, *68*, 3269–3276.

[44] Otová1, B.; Ojima, I.; Václavíková, R; Ehrlichová, J.; Souček, P.; Vobořilová, J.; Němcová, V.; Zanardi, I.; Horský, S.; Kovář, J.; Gut, I. Effects of novel taxanes on subcutaneous lymphoma in Sprague-Dawley/Cub rats: role of disposition, transport, in vitro efficiency and expression of relevant genes, submitted for publication.

[45] Damascelli, B.; Cantu, G.; Mattavelli, F.; Tamplenizza, P.; Bidoli, P.; Leo, E.; Dosio, F.; Cerrotta, A. M.; Di Tolla, G.; Frigerio, L. F.; Garbagnati, F.; Lanocita, R.; Marchiano, A.; Patelli, G.; Spreafico, C.; Ticha, V.; Vespro, V.; Zunino, F. Intraarterial chemotherapy with polyoxyethylated castor oil free paclitaxel, incorporated in albumin nanoparticles (ABI-007): Phase II study of patients with squamous cell carcinoma of the head and neck and anal canal: preliminary evidence of clinical activity, *Cancer*, **2001**, *92*, 2592-602.

[46] Schiff, P. B.; Fant, J.; Horwitz, S. B. Promotion of microtubule assembly *in vitro* by taxol. *Nature* **1979**, 277, 665-667.

[47] Manfredi, J. J.; Horwitz, S. B. Taxol: an antimitotic agent with a new mechanism of action. *Pbarrmcol. Tber.* **1984**, *25*, 83-l 25.

[48] Wuthers, J. C., Mitchison, T. J., Reider, C. L.; Salmon, E. D. The kinetochore microtubule minus-end disassembly associated with poleward flux produces a force that can do work. *Mol. Biol. Cell* **1996,** *7*, 1547-l 558.

[49] Cassimeris, L. Regulation of microtubule dynamic instability. *Cell Motil. Cytoskeleton.* **1993**, *26*, 275-281.

[50] Inoue, S.; Salmon, E. D.; Force generation by microtubule assembly/disassembly in mitosis and related movements. *Mol. Biol. Cell* **1995**, *6*, 1619-1640.

[51] Keller, H. U.; Zimmermann, A. Shape changes and chemokinesis of Walker 256 carcinosarcoma cells in response to colchicine, vinblastine, nocodazole and taxol. Invasion. *Metastasis* **1986,** *6*, 33-43.

[52] Masurovsky, E. B., Peterson, E. R., Crain, S. M.; Horwitz, S. B. Morphological alterations in dorsal root ganglion neurons and supporting cells of organotypic mouse spinal cord ganglion cultures exposed to taxol. *Neuroscience* **1983**, *10*, 491-509.

[53] Green, K. J.; Goldman, R. D. The effects of taxol on cytoskeletal components in cultured fibroblasts and epithelial cells. *Cell Motif. Cytoskeleton* **1983**, *3*, 283-305.

[54] Evangelio, J. A.; Abal, M.; Barasoain, I.; Souto, A. A.; Lillo, M. P.; Acuna, A. U.; Amat-Guerri, F.; Andreu, J. M. Fluorescent taxoids as probes of the microtubule cytoskeleton. *Cell Motil. Cytoskeleton*, **1998**, *39*, 73-90.

[55] Guy, R. K.; Scott, Z. A.; Sloboda, R. D.; Nicolaou, K. C. Fluorescent taxoids. *Chem. Biol.* **1996**, *3*, 1021-1031.

[56] Rao, C. S.; Chu, J.-J.; Liu, R.-S.; Lai, Y.-K. Synthesis and evaluation of [^{14}C]-labeled and fluorescent-tagged paclitaxel derivatives as new biological probes. *Bioorg. Med. Chem.* **1998**, *6*, 2193-2204.

[57] Wu, X., *Ph.D. Dissertation*; SUNY at Stony Brook: Stony Brook, **2003**.

[58] Ojima, I.; Habus, I.; Zhao, M.; Zucco, M.; Park, Y. H.; Sun, C. M.; Brigaud, T. New and Efficient Approaches to the Semisynthesis of Taxol and Its C-13 Side Chain Analogs by Means of β-Lactam Synthon Method, *Tetrahedron*, **1992**, *48*, 6985-7012.

References for Chapter 5

[1] Chari, R. V. J. Targeted delivery of chemotherapeutics: tumor-activated prodrug therapy. *Adv. Drug Deliv. Rev.* **1998**, *31*, 89-104.

[2] Ojima, I.; Geng, X.; Wu, X.; Qu, C.; Borella, C. P.; Xie, H.; Wilhelm, S. D.; Leece, B. A.; Bartle, L. M.; Goldmacher, V. S.; Chari, R. V. J. Tumor-Specific Novel Taxoid-Monoclonal Antibody Conjugates. *J. Med. Chem.* **2002**, *45*, 5620-5623.

[3] Matsumura, Y.; Maeda, H. A new concept for macromolecular therapeutics in cancer chemotherapy: mechanism of tumoritropic accumulation of proteins and the antitumor agent smancs. *Cancer Res.* **1986**, *46*, 6387–6392.

[4]Maeda, H.; Matsumura, Y. Tumoritropic and lymphotropic principles of macromolecular drugs. *Crit. Rev. Ther. Drug Carr. Syst.* **1989**, *6*, 193–210.

[5] Whelan, J. Targeted Taxane Therapy for Cancer. *Drug Discovery Today* **2002**, *7*, 90–92.

[6] Chen, J.; Jaracz, S.; Zhao, X.; Chen, S.; Ojima, I. Antibody-cytotoxic agent conjugates for cancer therapy. *Expert Opin. Drug Delivery* **2005**, *2*, 873-890.

[7] Jaracz, S.; Chen, J.; Kuznetsova, L. V.; Ojima, I. Recent advances in tumor-targeting anticancer drug conjugates. *Bioorg. Med. Chem.* **2005**, *13*, 5043-5054.

[8] Régina, A.; Demeule, M.; Ché, C.; Lavallée, I.; Poirier, J.; Gabathuler, R.; Béliveau, R.; Castaigne, J. P. Antitumour activity of ANG1005, a conjugate between paclitaxel and the new brain delivery vector Angiopep-2. *Br J Pharmacol* **2008**, *155*, 185–197.

[9] Goodhart, R. S.; Shils. M. E. In: *Modern Nutrition in Health and Disease.* 6th Ed., Lea and Febiger. Philadelphia, PA **1980**, 134-138.

[10] Widmer, C., Jr.; Holman, R. T. Polyethenoid fatty acid metabolism. II. Deposition of polyunsaturated fatty acids in fat-deficient rats upon single fatty acid supplementation. *Arch. Biochem.* **1950**, *25*, 1-12.

[11] Tapiero, H.; Nguyen Ba, G.; Couvreur, P.; Tew, K. D. Polyunsaturated fatty acids (PUFA) and eicosanoids in human health and pathologies. *Biomed. Pharmacother.* **2002**, *56*, 215-222.

[12] Wigmore, S. J.; Ross, J. A.; Falconer, J. S.; Plester, C. E.; Tisdale, M. J.; Carter, D. C.; Fearon, K. C. H. The effect of polyunsaturated fatty acids on the progress of cachexia in patients with pancreatic cancer. *Nutrition* **1996**, *12*, S27-S30.

[13] Hawkins, R. A.; Sangster, K.; Arends, M. J. Apoptotic death of pancreatic cancer cells induced by polyunsaturated fatty acids varies with double bond number and involves an oxidative mechanism. *J. Pathol.* **1998**, *185*, 61-70.

[14] Sauer, L. A.; Dauchy, R. T. Tumor-host metabolic interrelationships. *Biochem.l Soc. T.* **1990**, *18*, 80-82.

[15] Sauer, L. A.; Dauchy, R. T. The effect of omega-6 and omega-3 fatty acids on 3H-thymidine incorporation in hepatoma 7288CTC perfused in situ. *Brit. J. Cancer* **1992**, *66*, 297-303.

[16] Takahashi, M.; Przetakiewicz, M.; Ong, A.; Borek, C.; Lowenstein, J. M. Effect Of Omega-3 And Omega-6 Fatty-Acids On Transformation Of Cultured-Cells By Irradiation And Transfection. *Cancer Res.* **1992**, *52*, 154-162.

[17] Grammatikos, S. I.; Subbaiah, P. V.; Victor, T. A.; Miller, W. M. N-3 And N-6 Fatty-Acid Processing And Growth Effects In Neoplastic And Non-Cancerous Human Mammary Epithelial-Cell Lines. *Brit. J. Cancer* **1994**, *70*, 219-227.

[18] Moser, U. N-3 and N-6 PUFAS in healthy and diseased skin. *J. Appl. Cosmetology* **2002**, *20*, 137-142.

[19] Heird, W. C.; Lapillonne, A. The role of essential fatty acids in development. *Annu. Rev. Nutr.* **2005**, *25*, 549-571.

[20] Bradley, M. O.; Webb, N. L.; Anthony, F. H.; Devanesan, P.; Witman, P. A.; Hemamalini, S.; Chander, M. C.; Baker, S. D.; He, L. F.; Horwitz, S. B.; Swindell, C. S. Tumor targeting by covalent conjugation of a natural fatty acid to paclitaxel. *Clin. Cancer Res.* **2001**, *7*, 3229-3238.

[21] Vredenburg, M. R.; Ojima, I.; Veith, J.; Pera, P.; Kee, K.; Cabral, F.; Sharma, A.; Kanter, P.; Greco, W. R.; Bernacki, R. J. Effects of orally active taxanes on P-glycoprotein modulation and colon and breast carcinoma drug resistance. *J. Natl. Cancer. Inst.* **2001**, *93*, 1234-1245.

[22] Lin, S.; Geng, X.; Qu, C.; Tynebor, R.; Gallagher, D. J.; Pollina, E.; Rutter, J.; Ojima, I. Synthesis of highly potent second-generation taxoids through effective kinetic resolution coupling of racemic *β*-lactams with baccatins. *Chirality* **2000**, *12*, 431-441.

[23] Ojima, I.; Wang, T.; Miller, M. L.; Lin, S.; Borella, C. P.; Geng, X.; Pera, P.; Bernacki, R. J. Synthesis and structure-activity relationships of new second-generation taxoids. *Bioorg. Med. Chem. Lett.* **1999**, *9*, 3423-3428.

[24] Kuznetsova, L.; Chen, J.; Sun, L.; Wu, X.; Pepe, A.; Veith, J. M.; Pera, P.; Bernacki, R. J.; Ojima, I. Syntheses and evaluation of novel fatty acid-second-generation taxoid conjugates as promising anticancer agents. *Bioorg. Med. Chem. Lett.* **2006**, *16*, 974-977.

[25] Chordia, M. D.; Gharpure, M. M.; Kingston, D. G. I. Facile AB ring cleavage reactions of taxoids. *Tetrahedron* **1995**, *51*, 12963-12970.

[26] Georg, G. I.; Harriman, G. C. B.; Datta, A.; Ali, S.; Cheruvallath, Z.; Dutta, D.; Vander Velde, D. G.; Himes, R. H. The Chemistry of the Taxane Diterpene: Stereoselective Reductions of Taxanes. *J. Org. Chem.* **1998**, *63*, 8926-8934.

Appendix

^{1}H NMR Spectrum of **(+)-1-2**

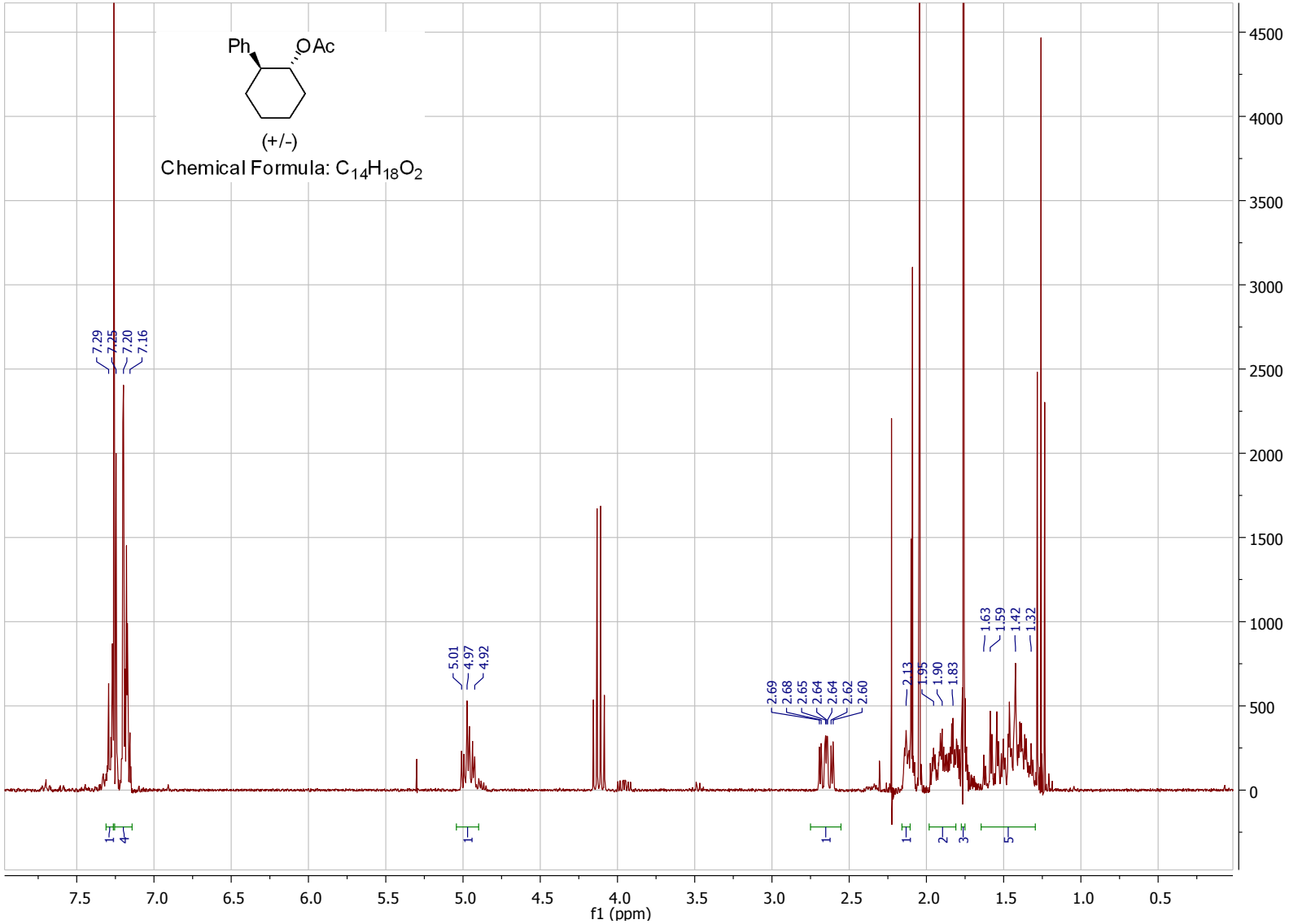

^{1}H NMR Spectrum of **1-5**

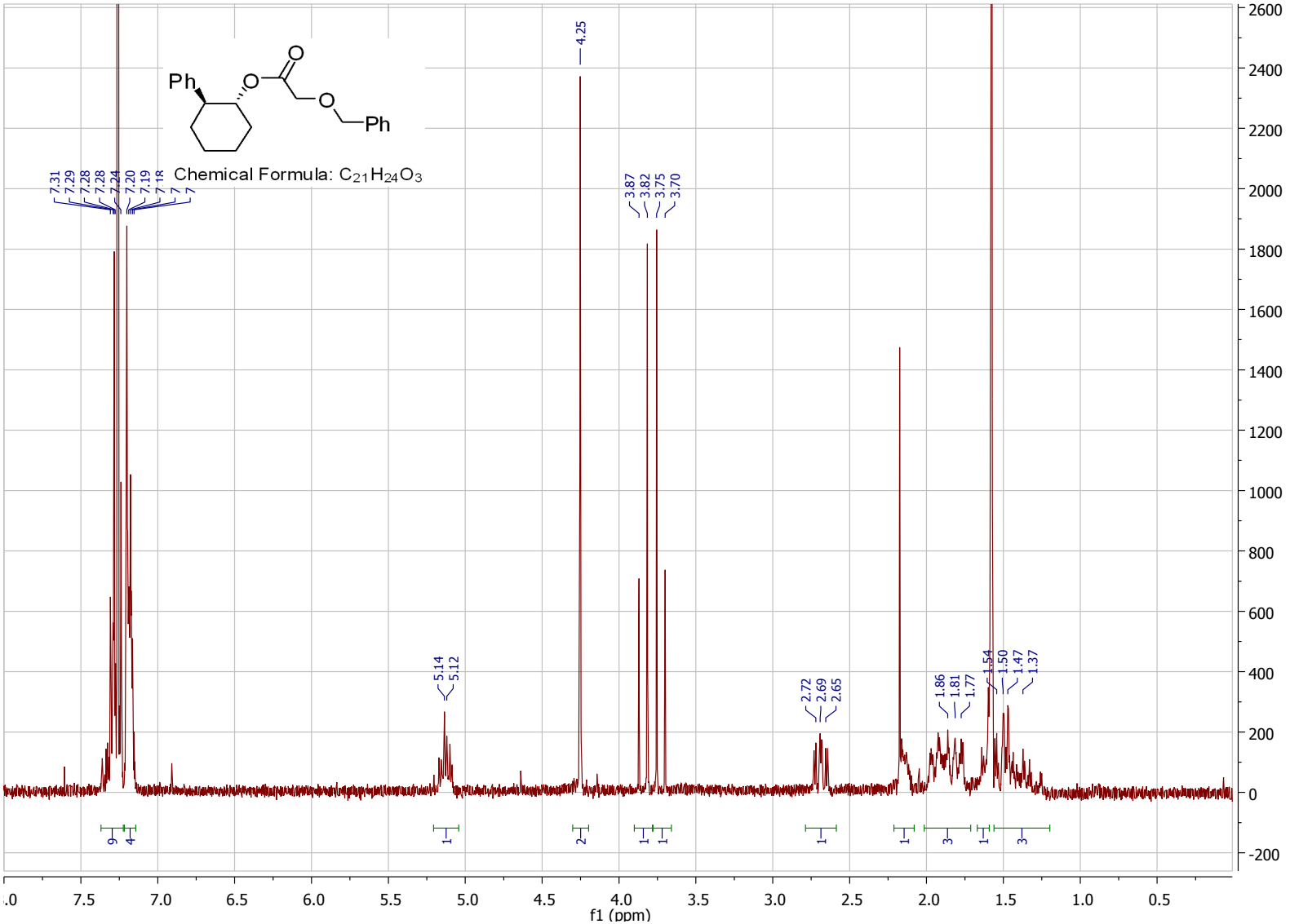

^{1}H NMR Spectrum of **1-6**

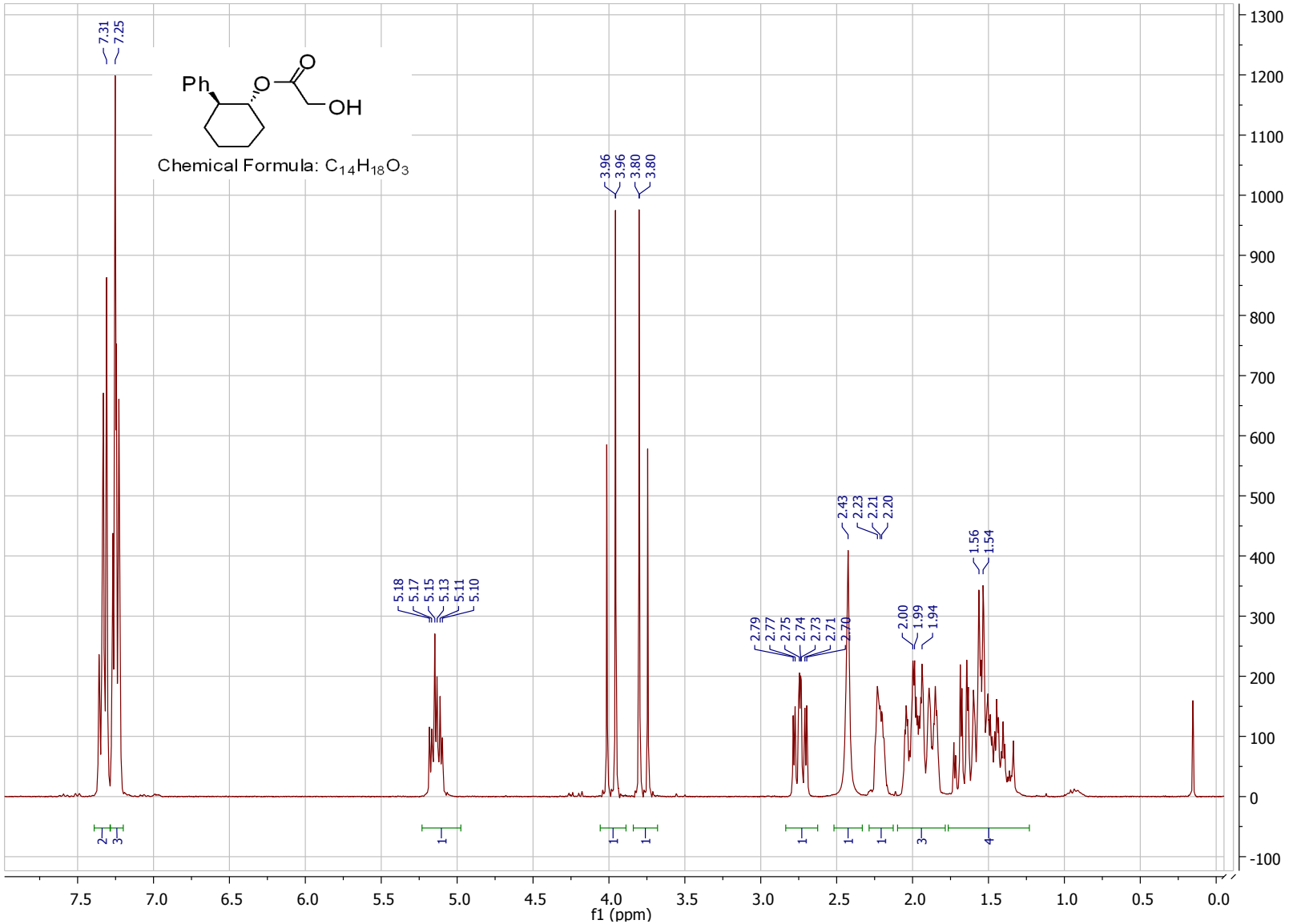

^{1}H NMR Spectrum of **1-8**

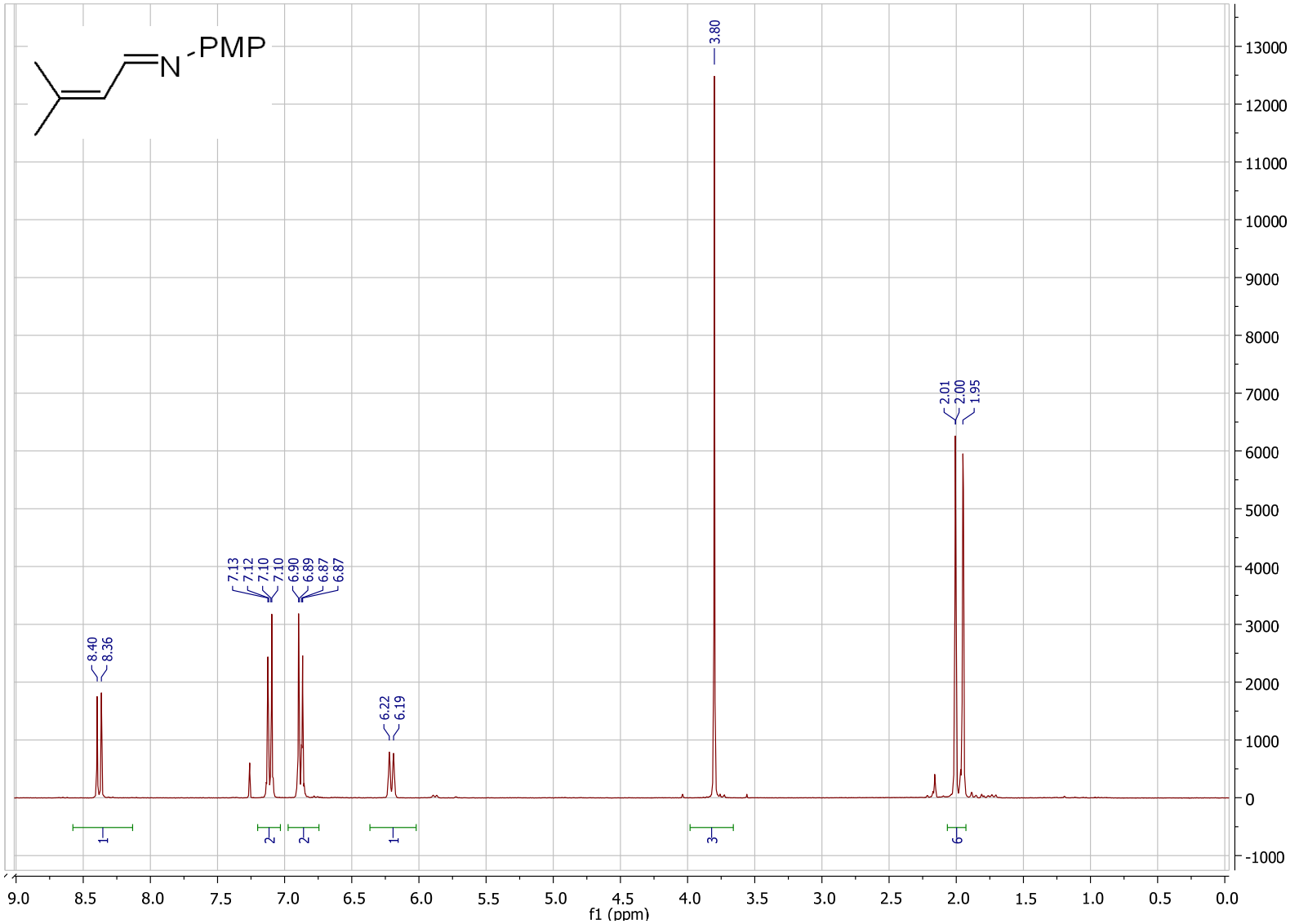

^{1}H NMR Spectrum of **1-9**

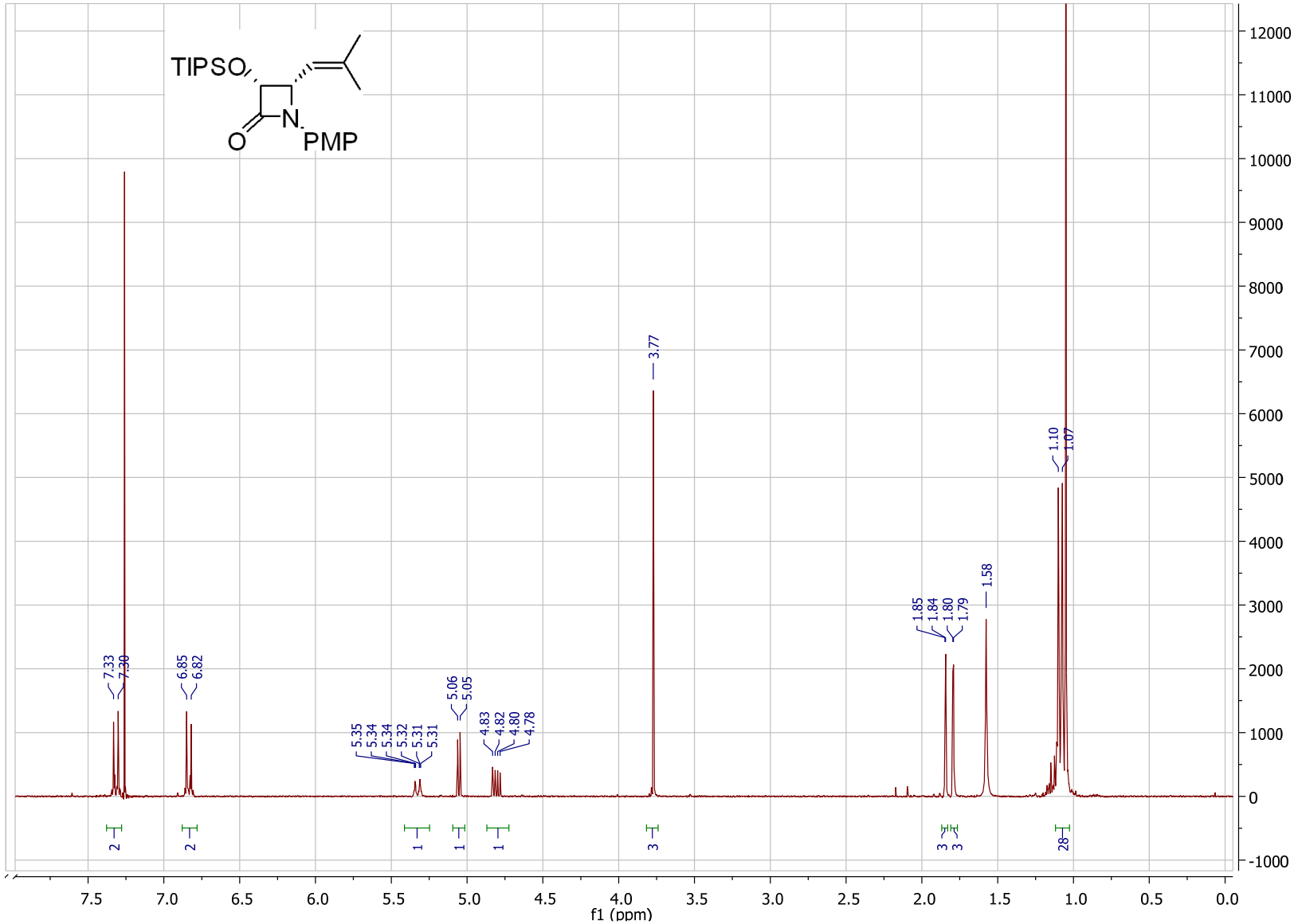

^{1}H NMR Spectrum of **1-10**

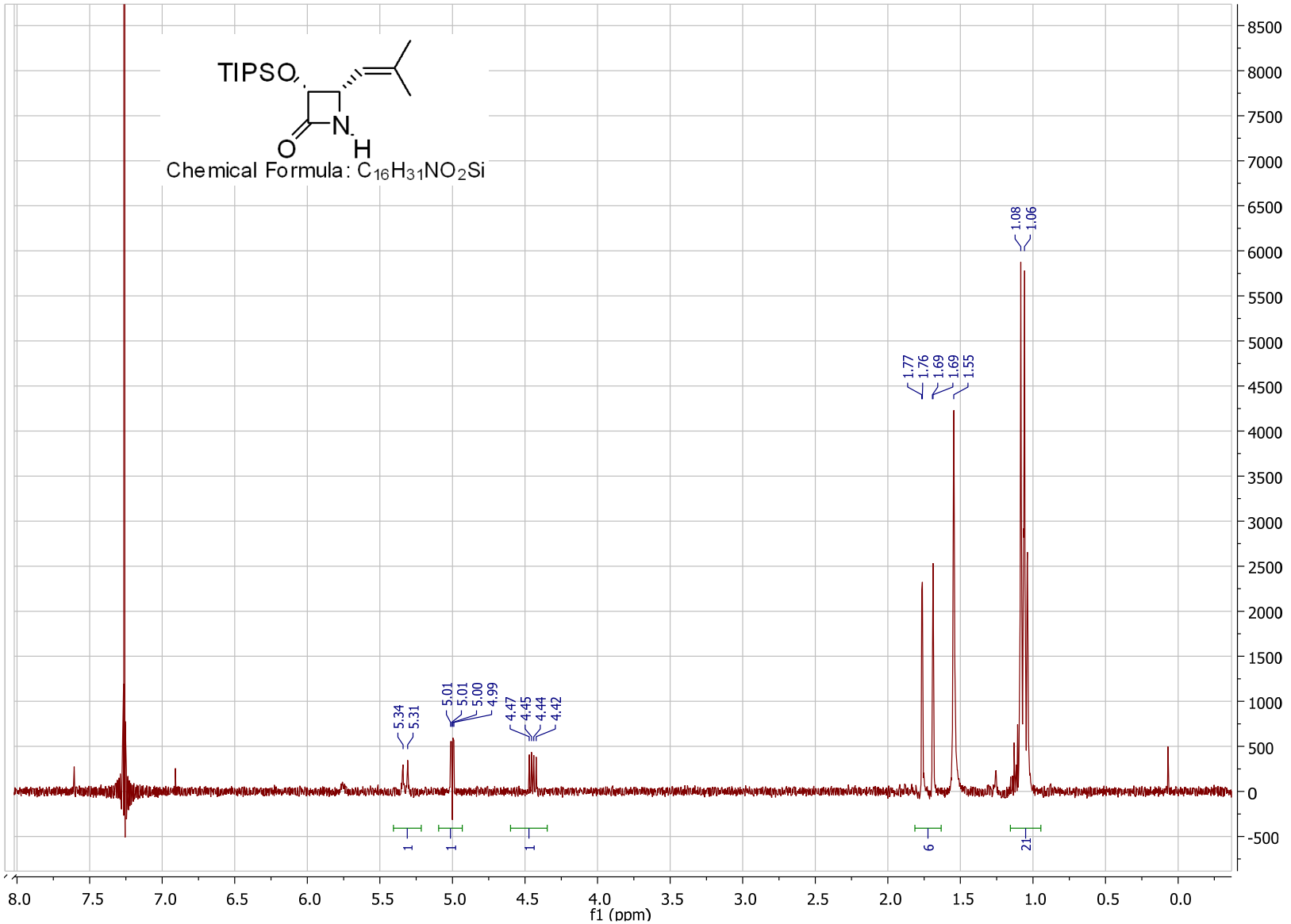

^{1}H NMR Spectrum of **1-11**

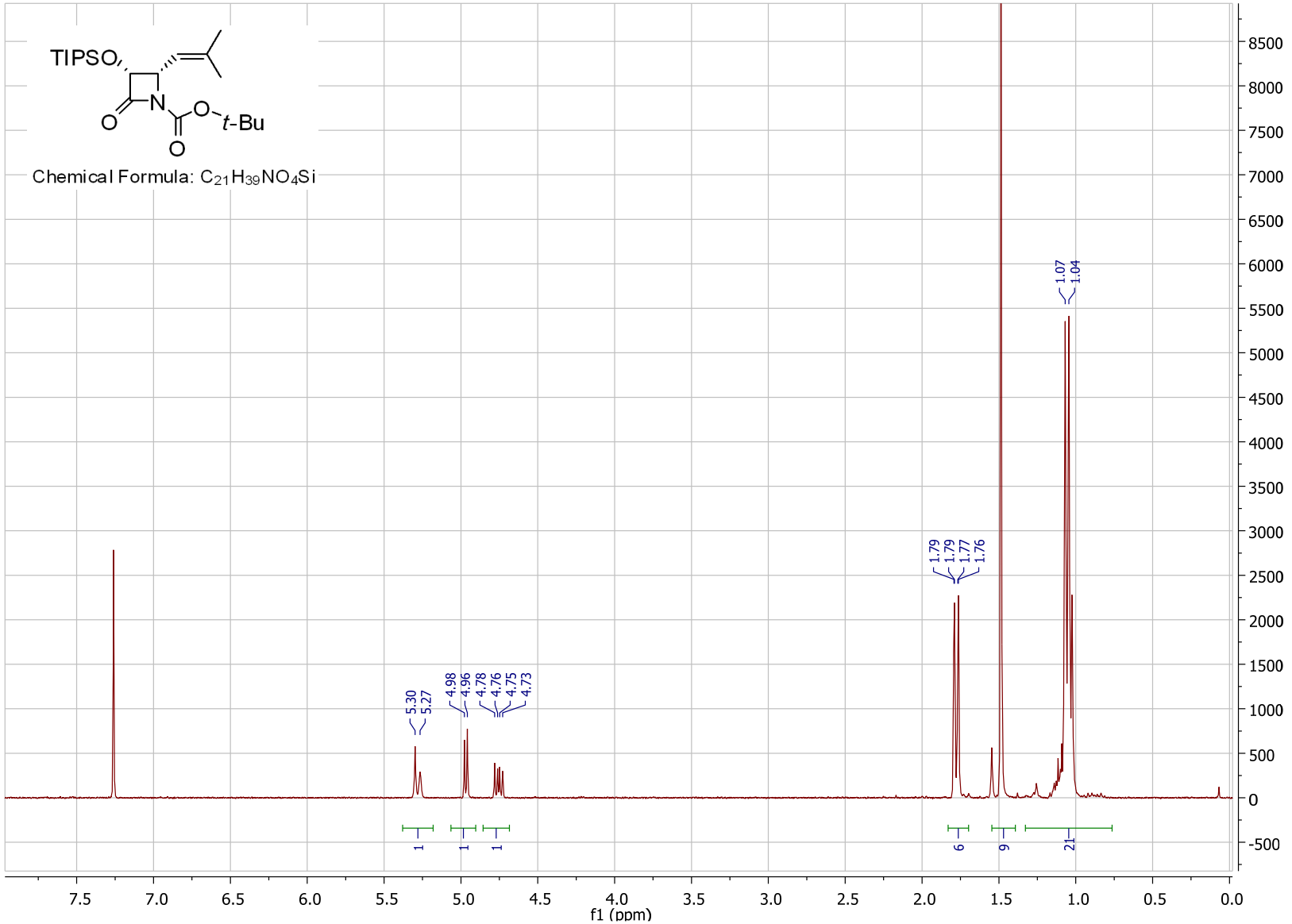

^{1}H NMR Spectrum of **1-12**

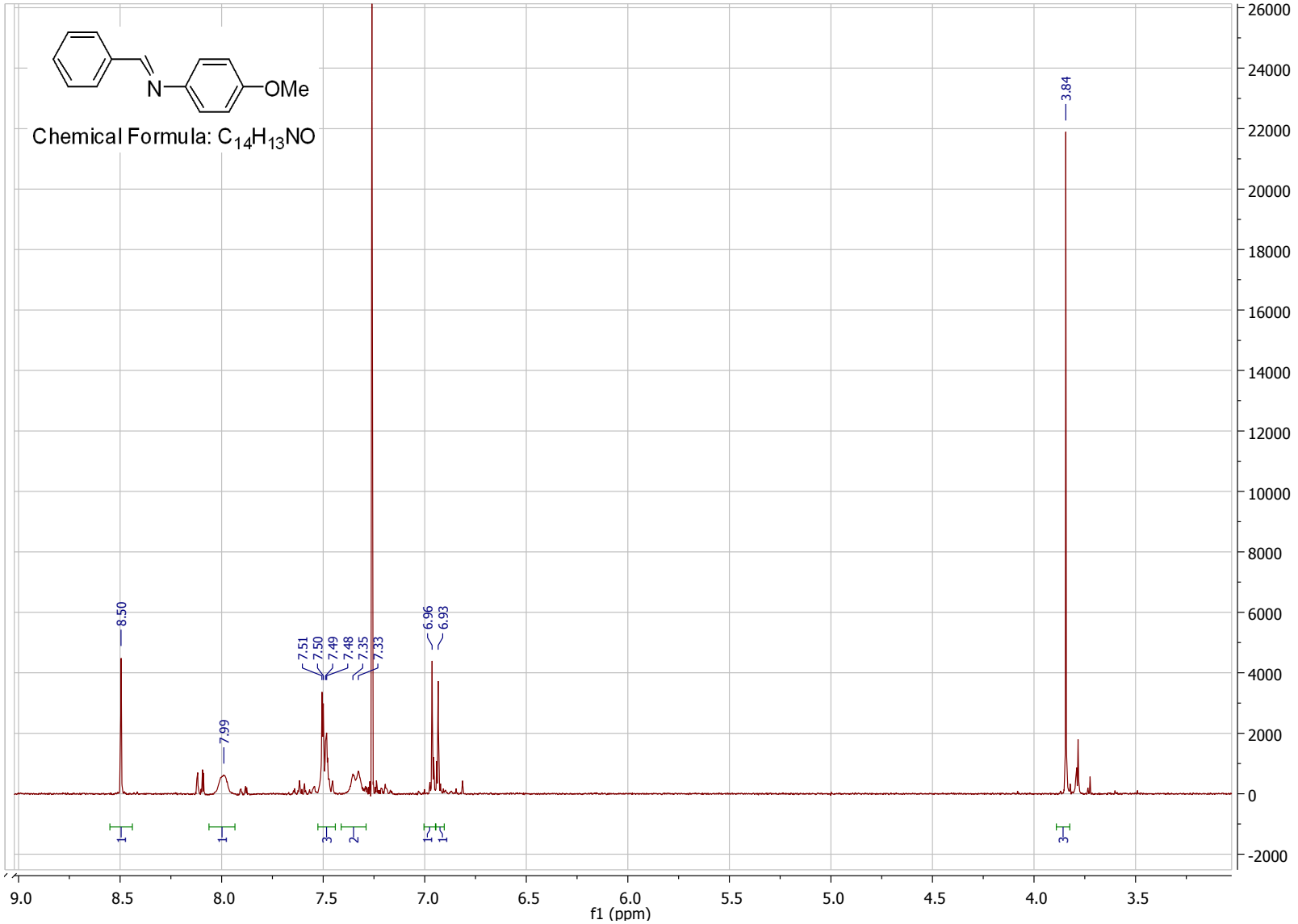

^{1}H NMR Spectrum of **(±)-1-13**

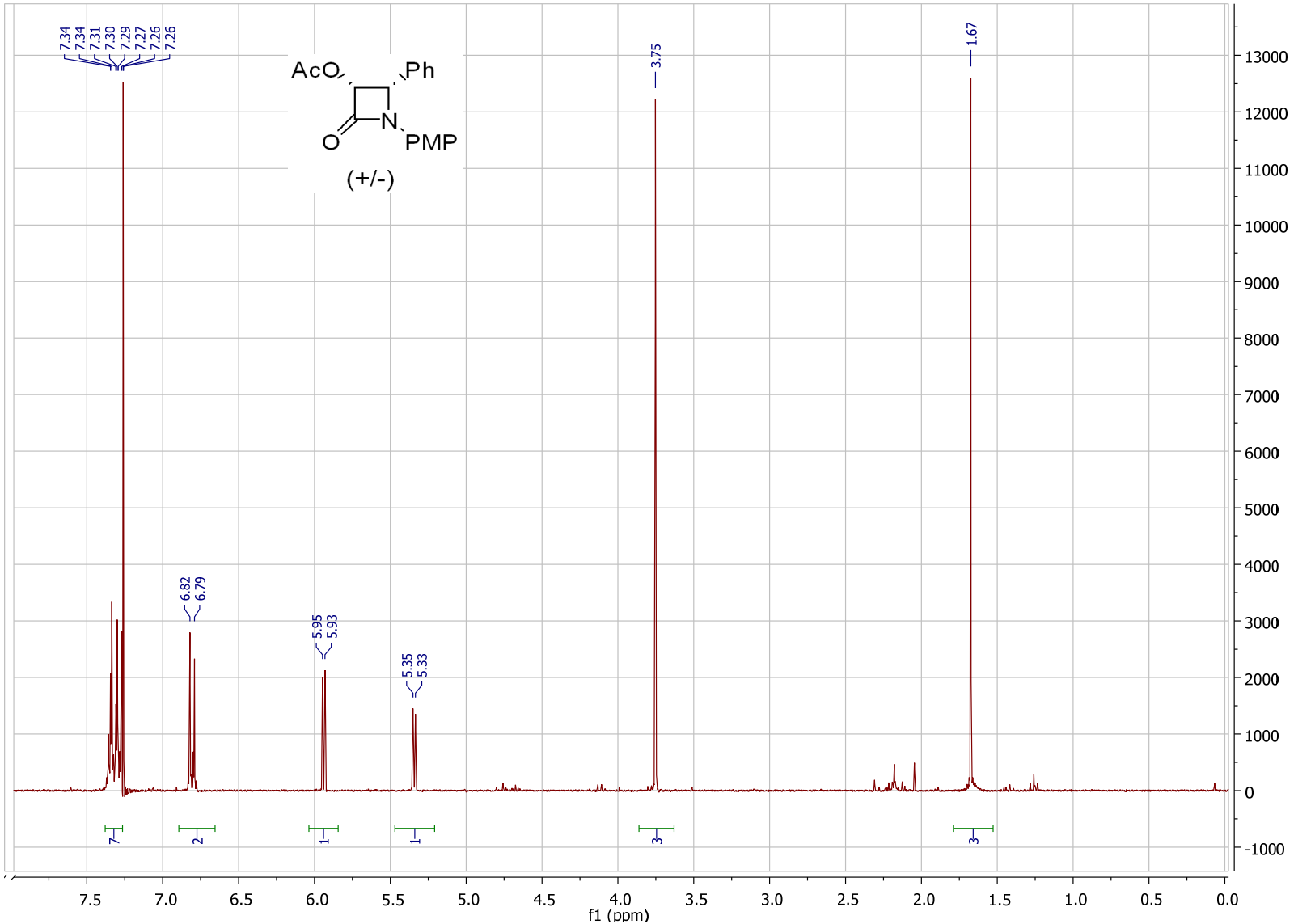

^{1}H NMR Spectrum of **(+)-1-13**

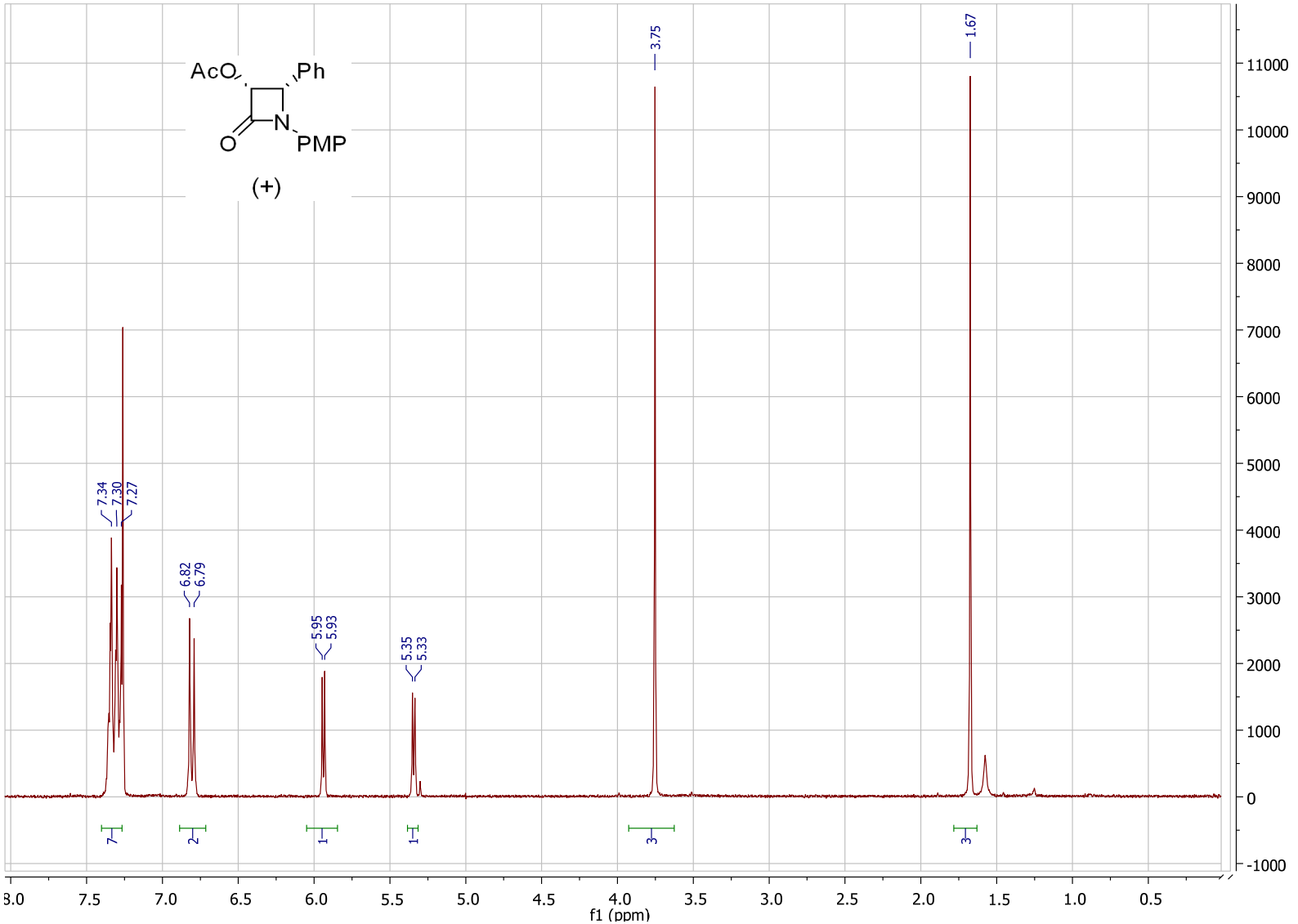

^{1}H NMR Spectrum of **(-)-1-14**

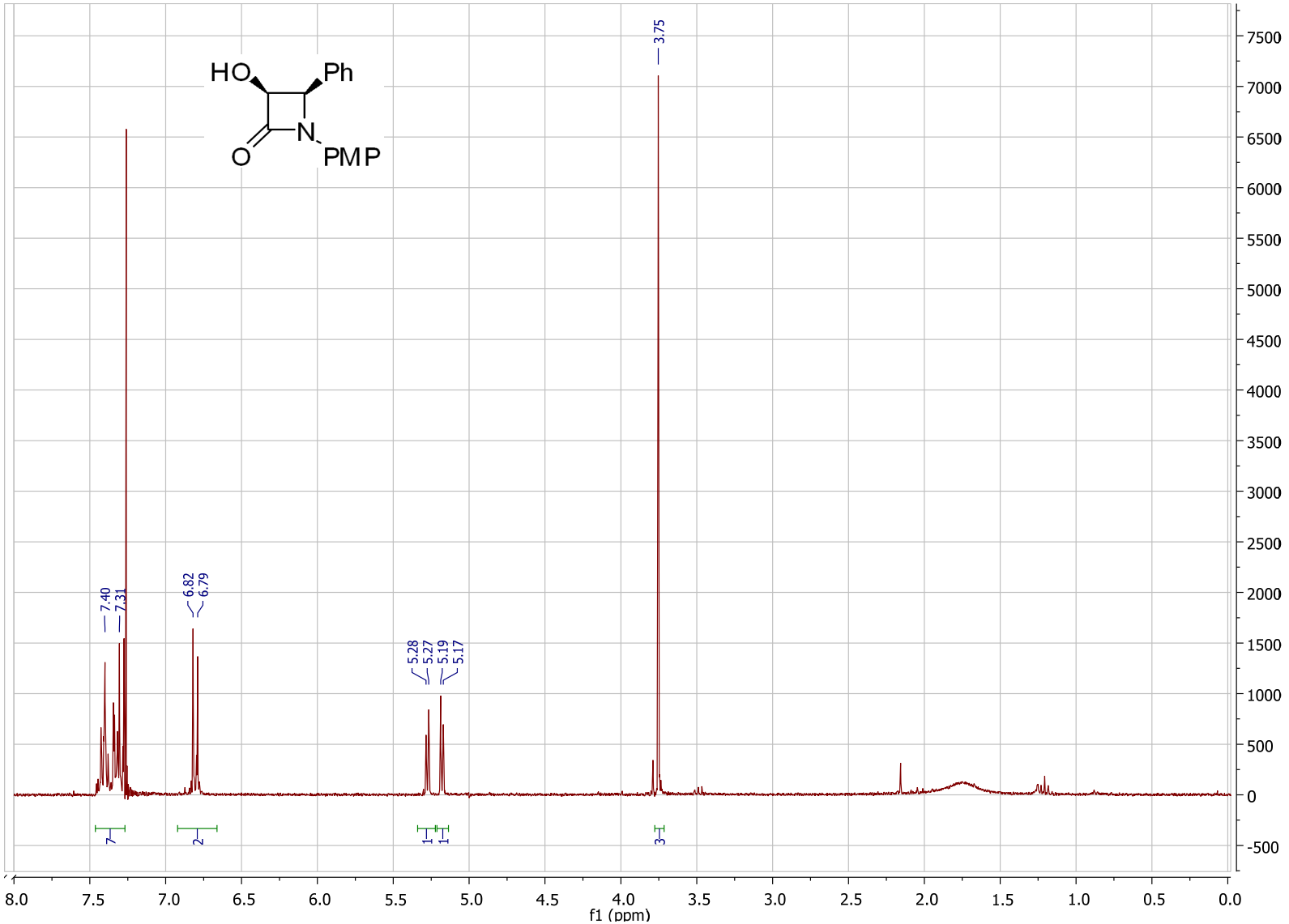

^{1}H NMR Spectrum of **1-15**

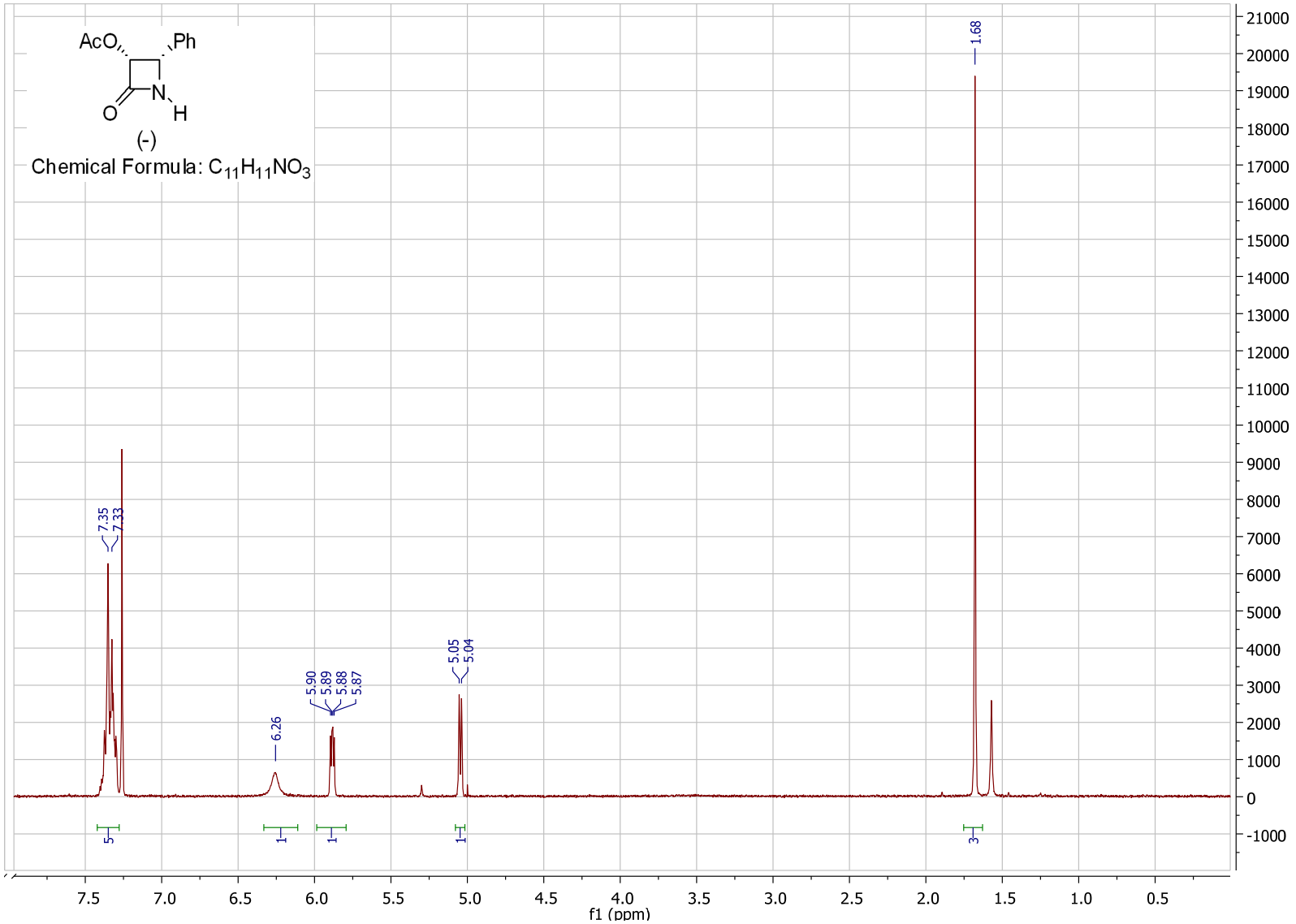

^{1}H NMR Spectrum of **1-17**

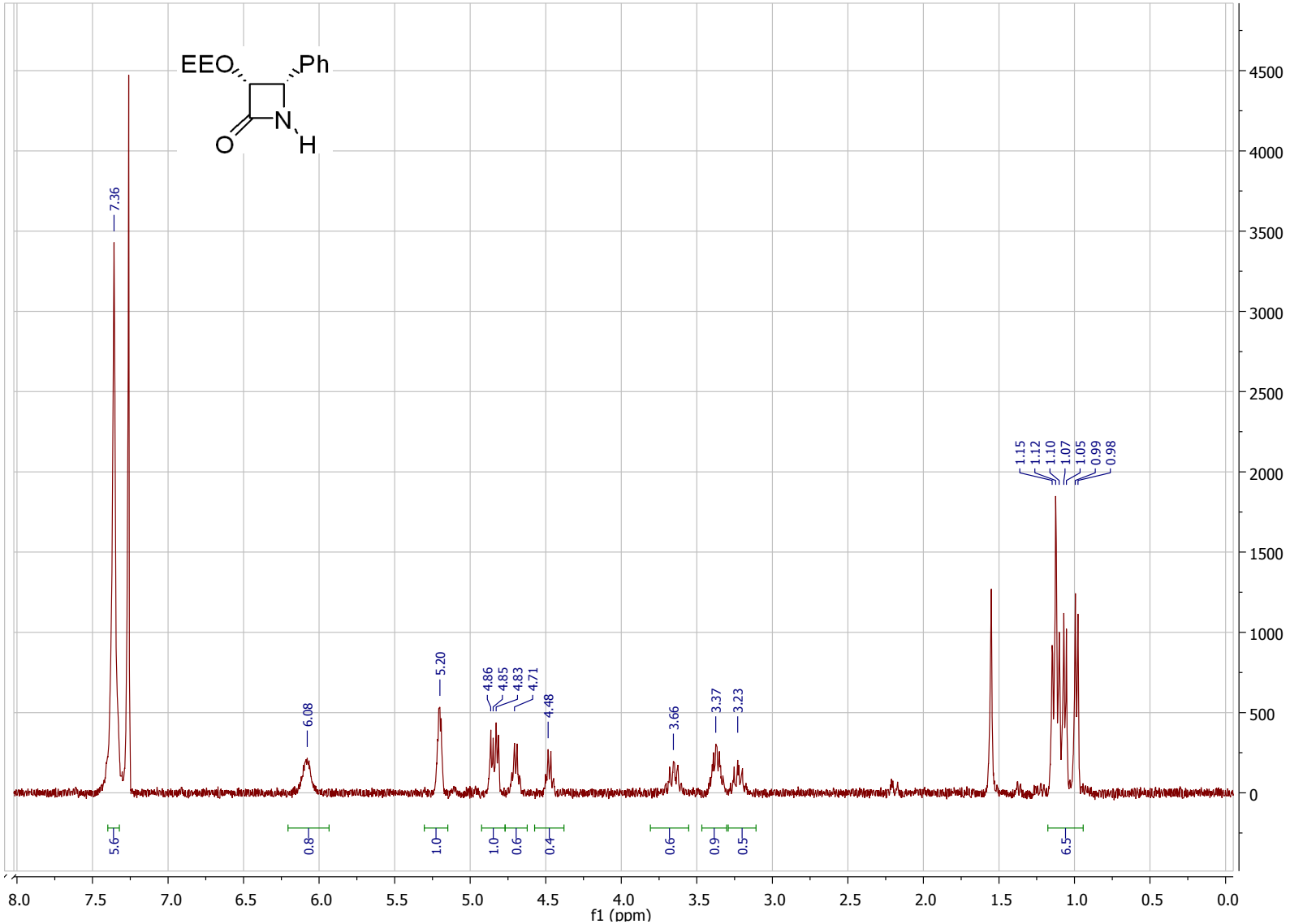

^{1}H NMR Spectrum of **(+)-1-18**

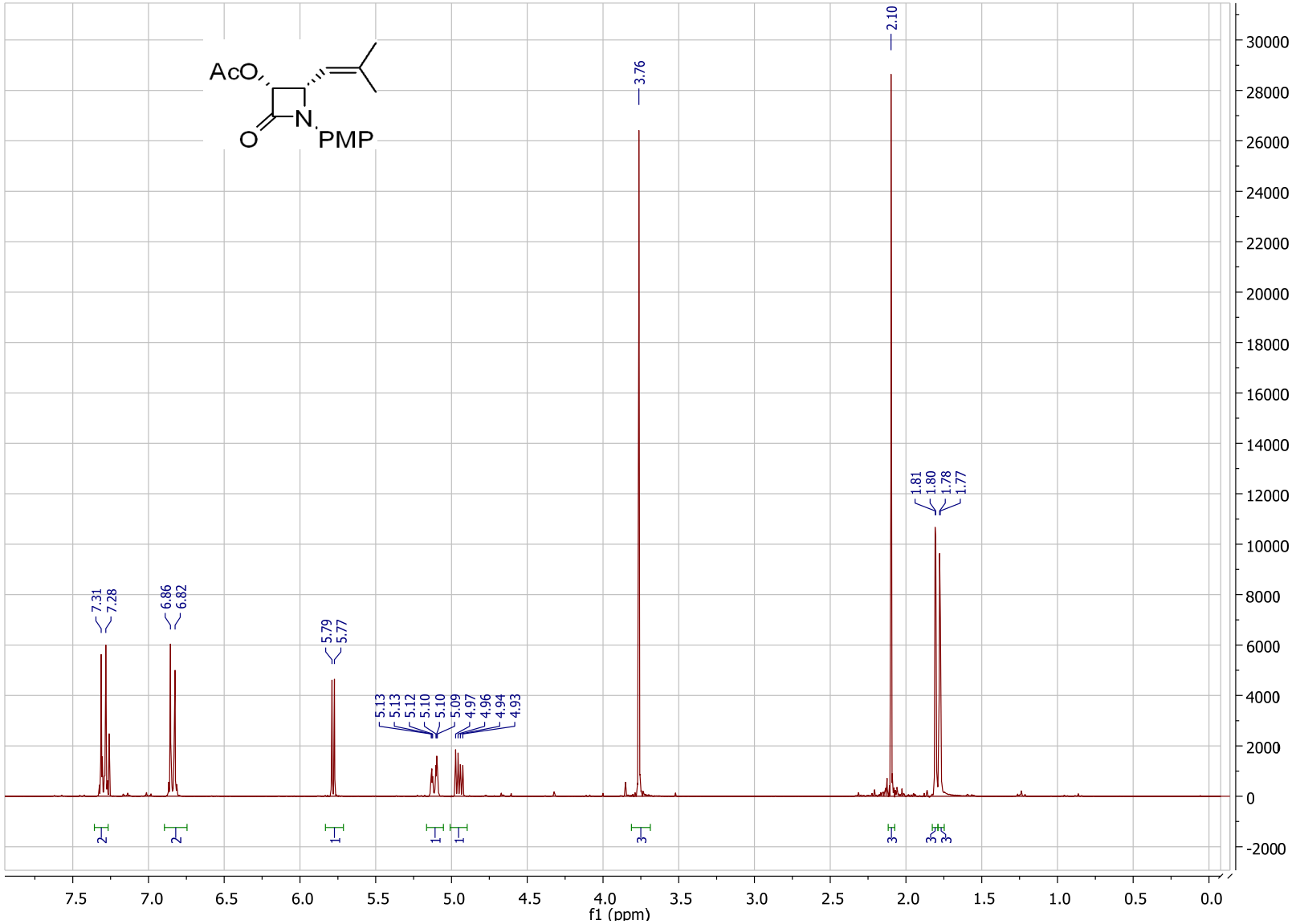

^{1}H NMR Spectrum of **(+)-1-19**

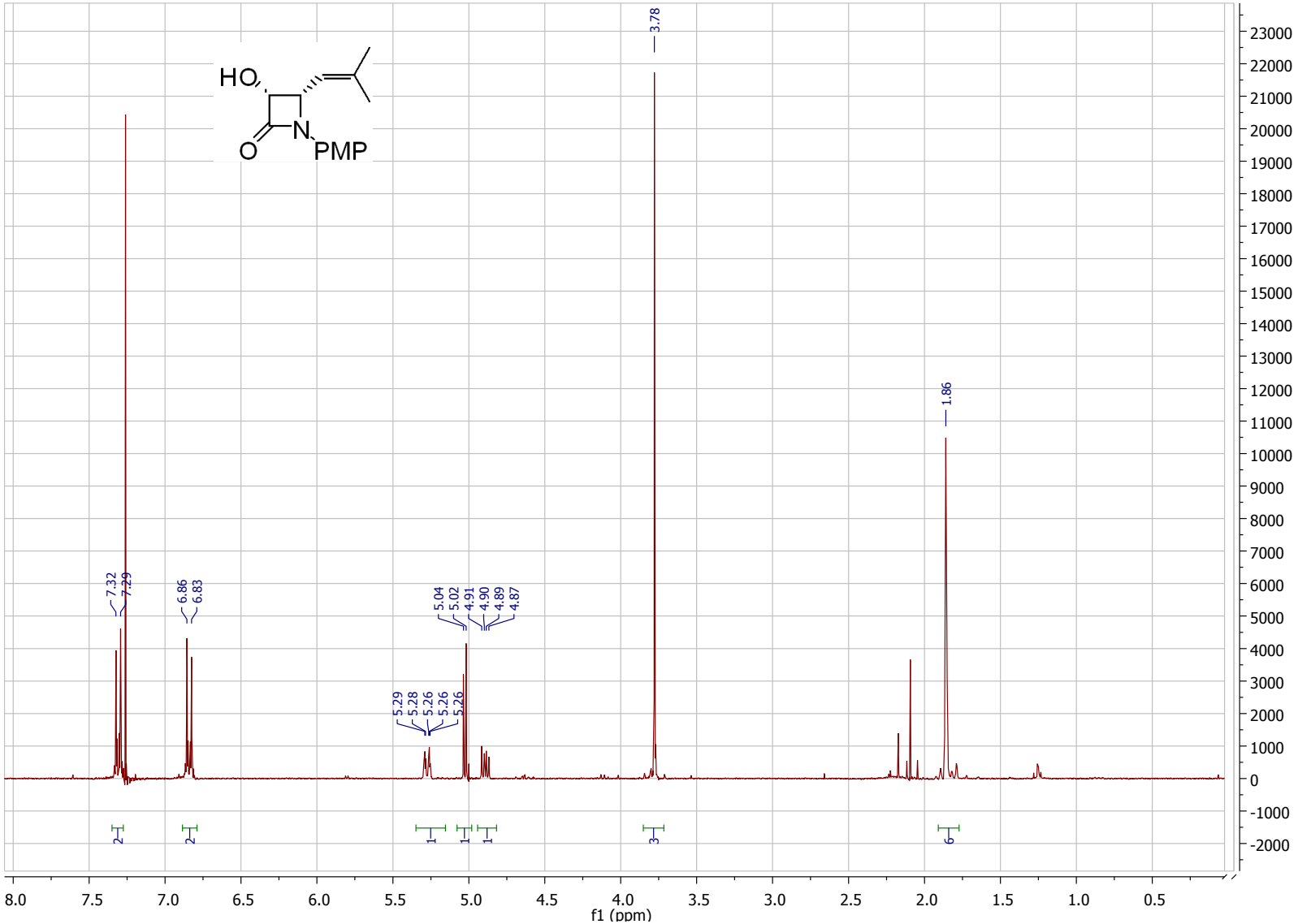

^{1}H NMR Spectrum of **2-1**

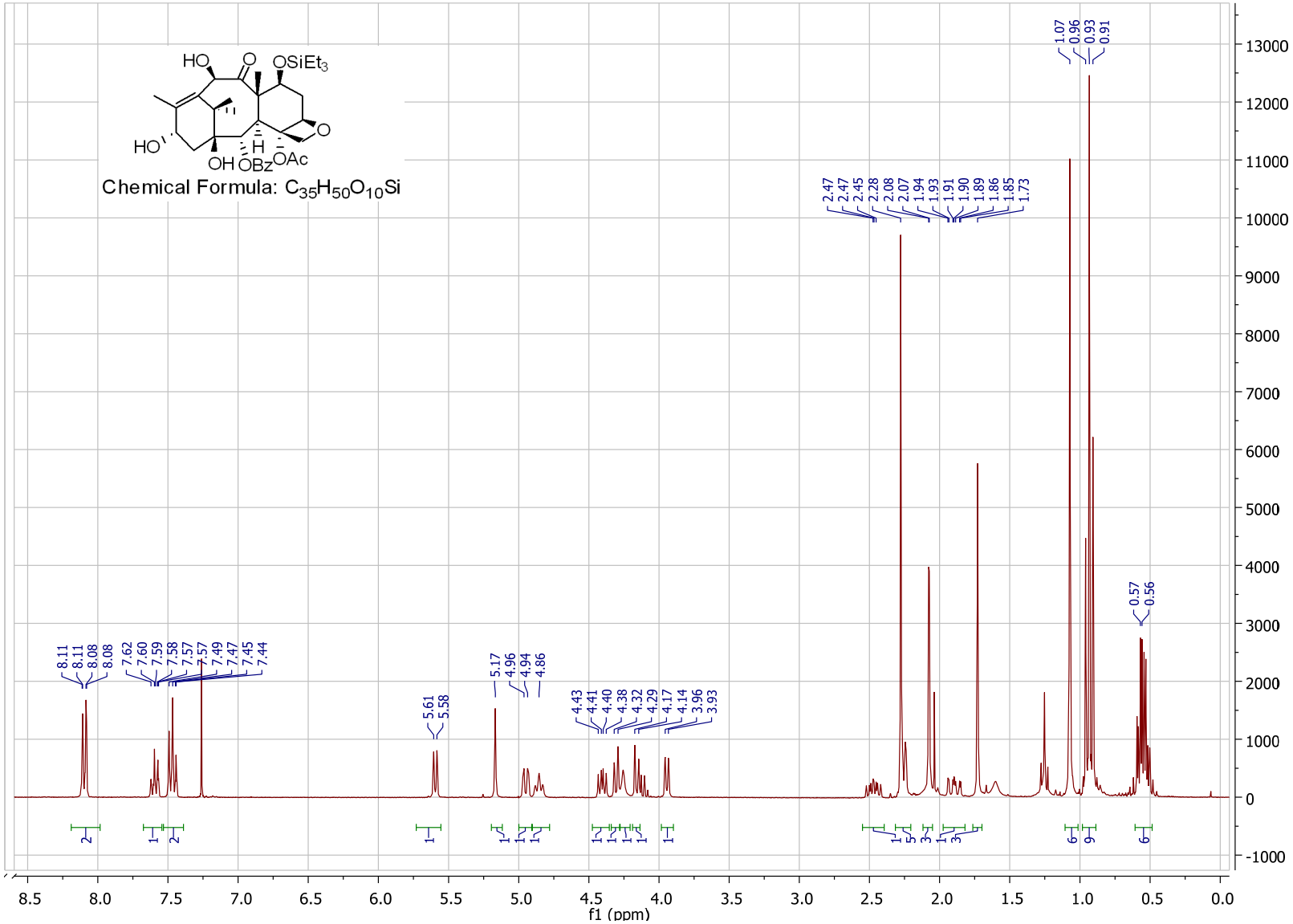

^{1}H NMR Spectrum of **2-2**

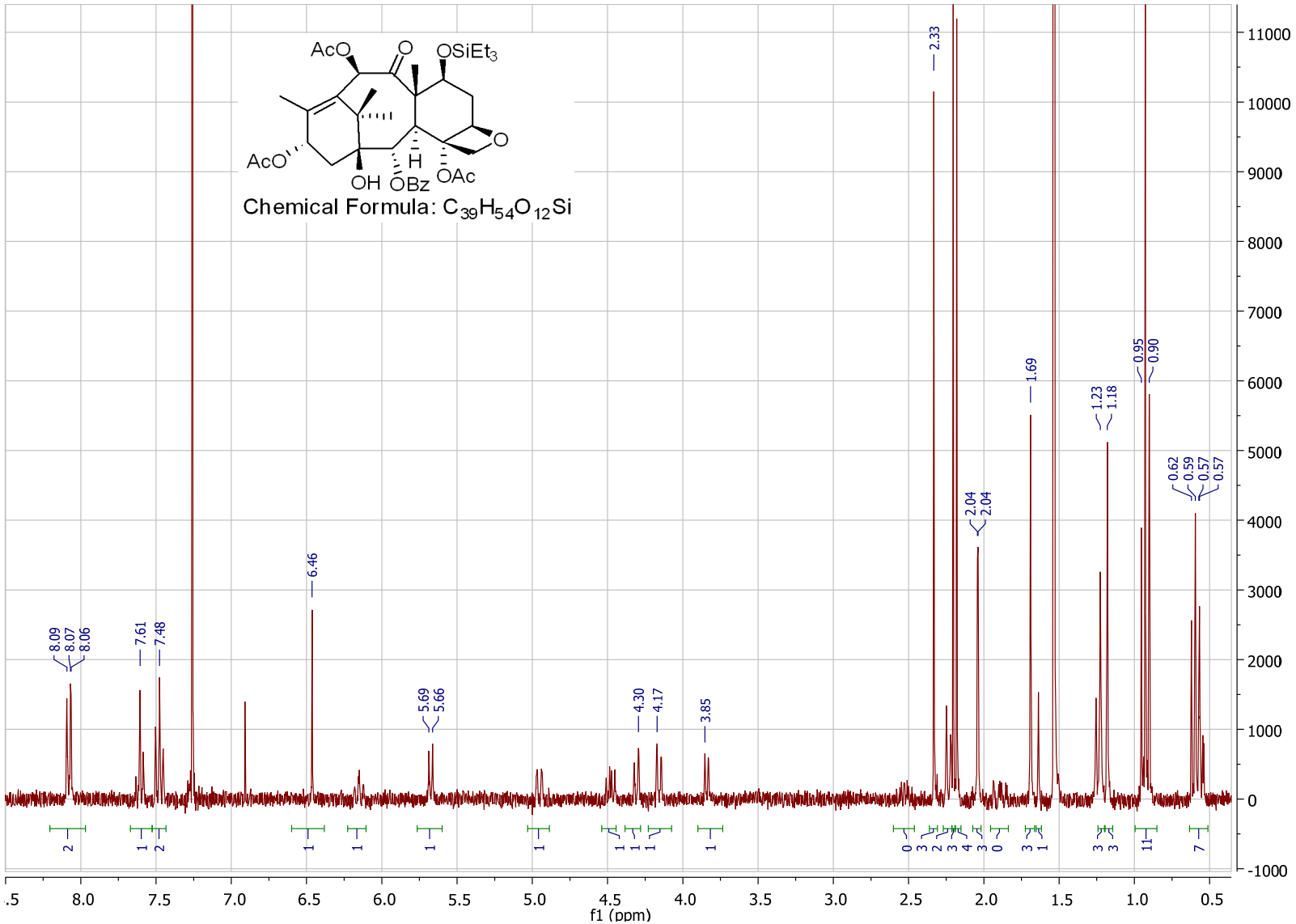

^{1}H NMR Spectrum of **2-3**

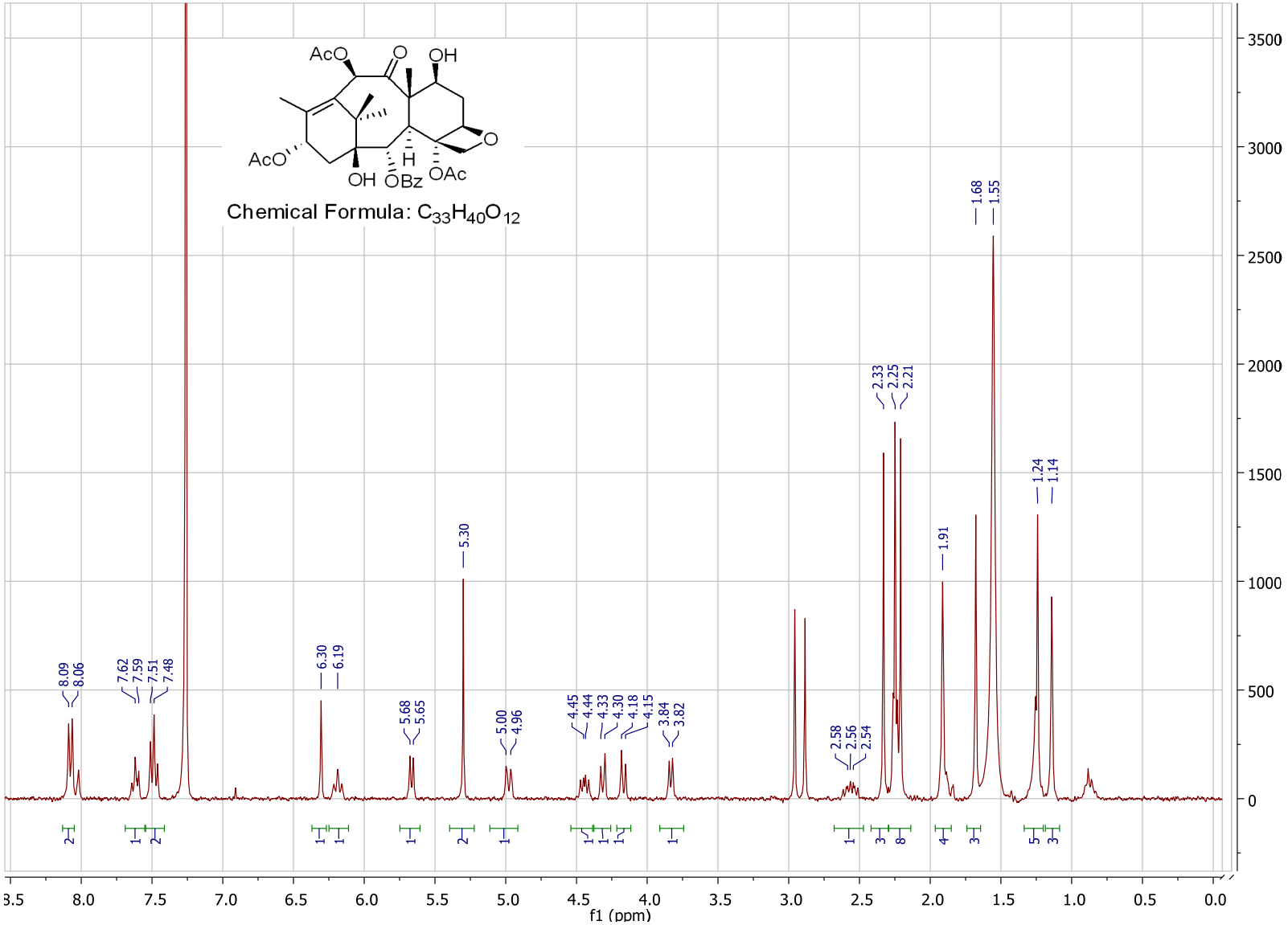

^{1}H NMR Spectrum of **2-4**

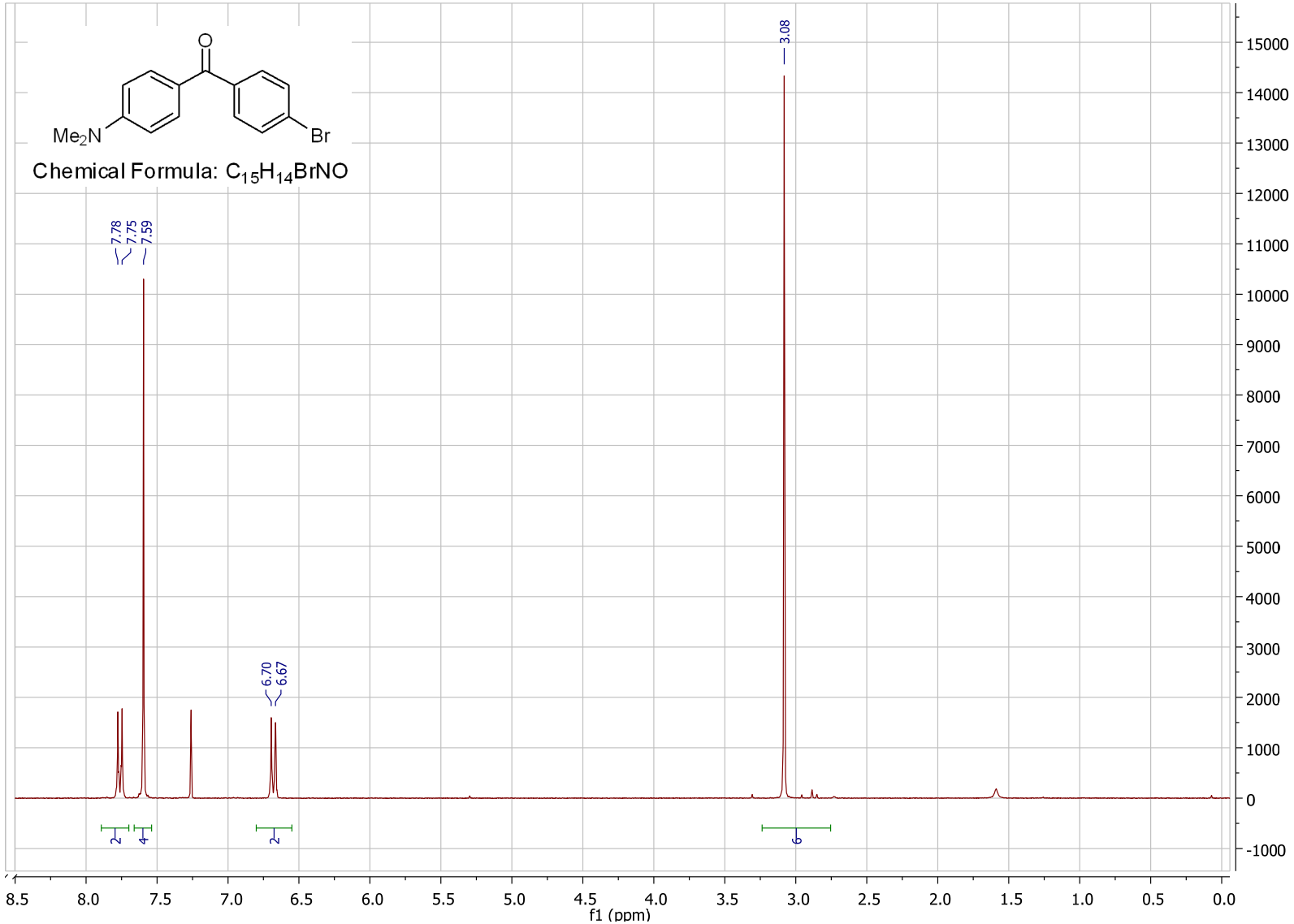

^{13}C NMR Spectrum of **2-4**

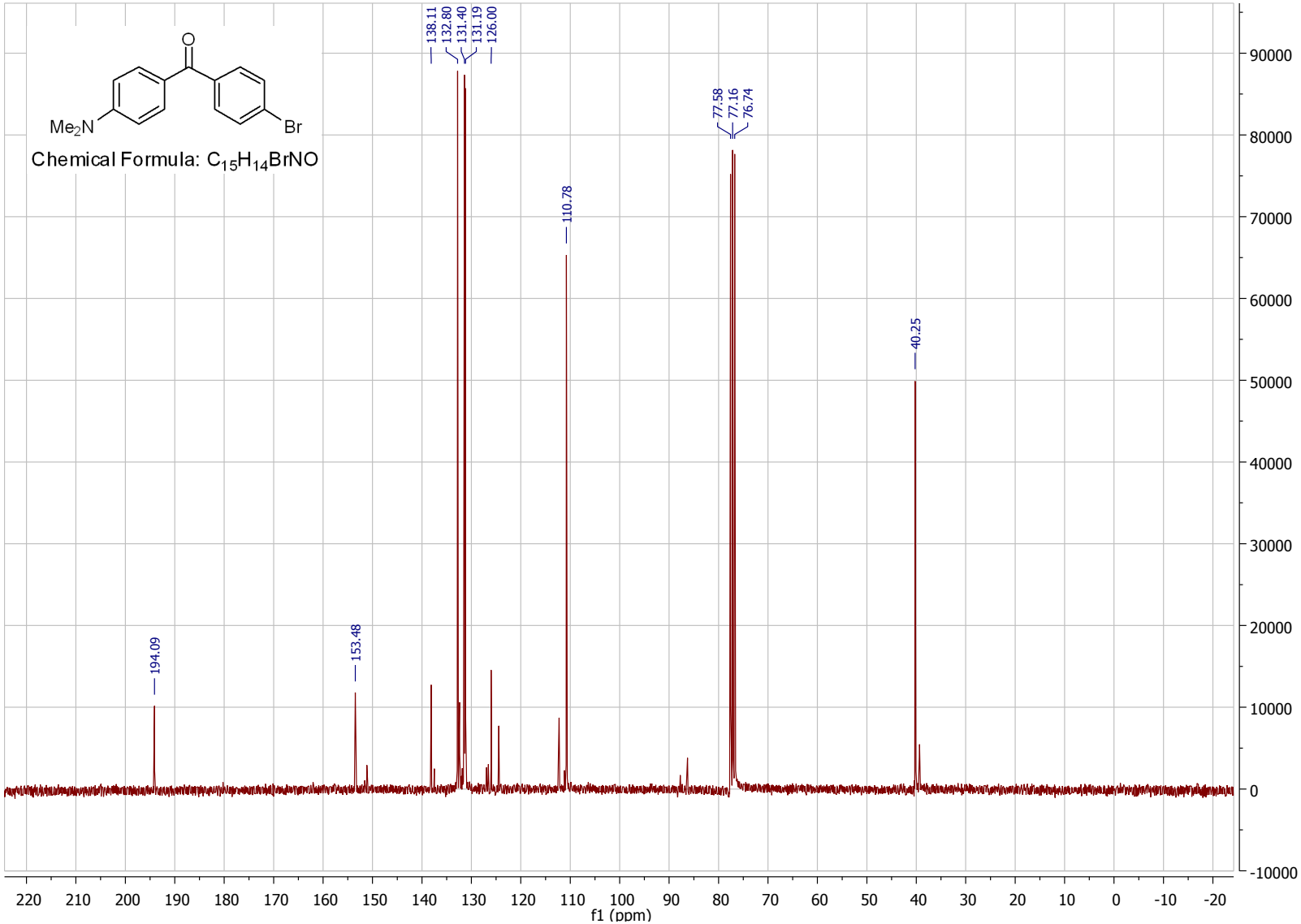

^{1}H NMR Spectrum of **2-5**

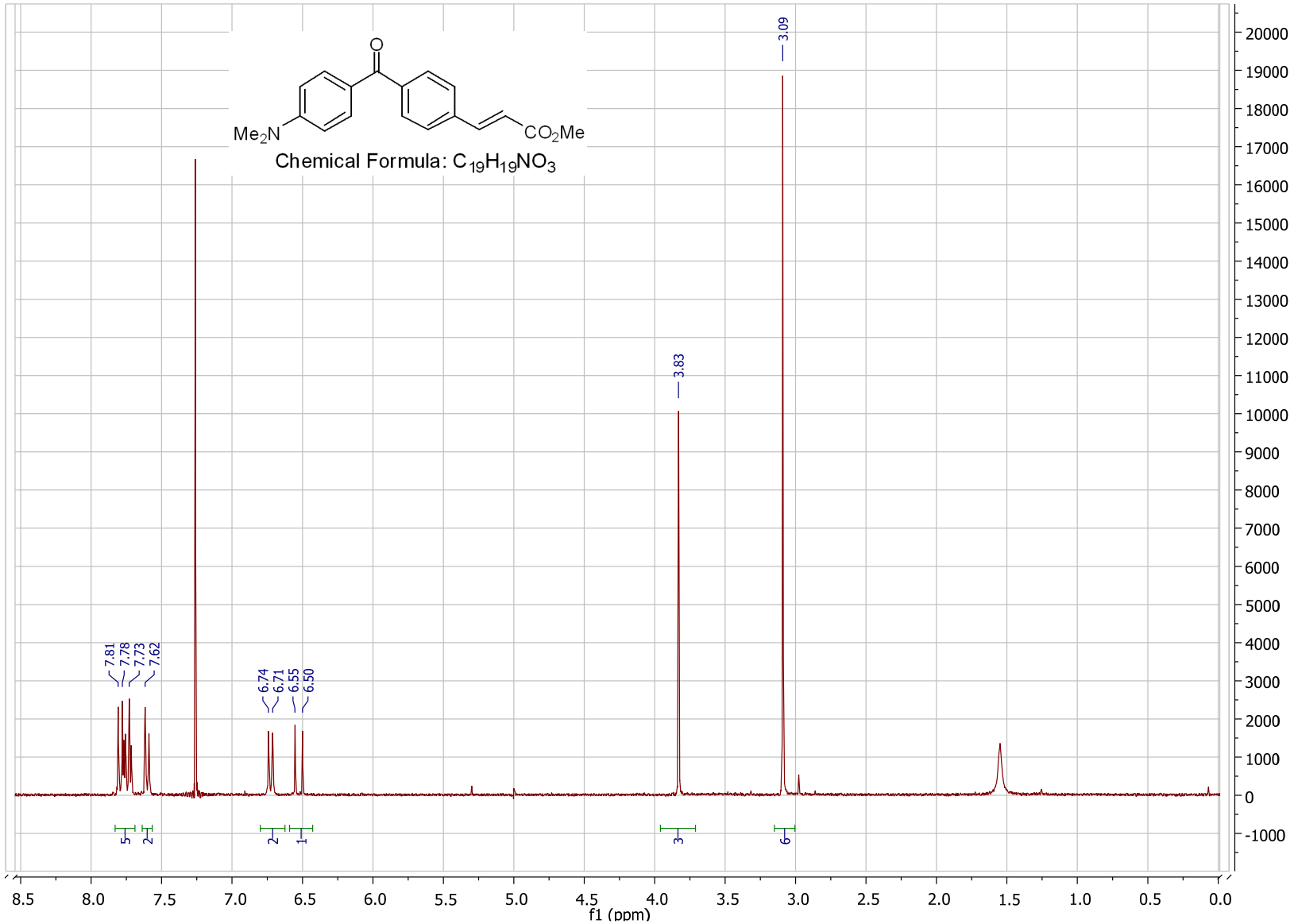

^{1}H NMR Spectrum of **2-6**

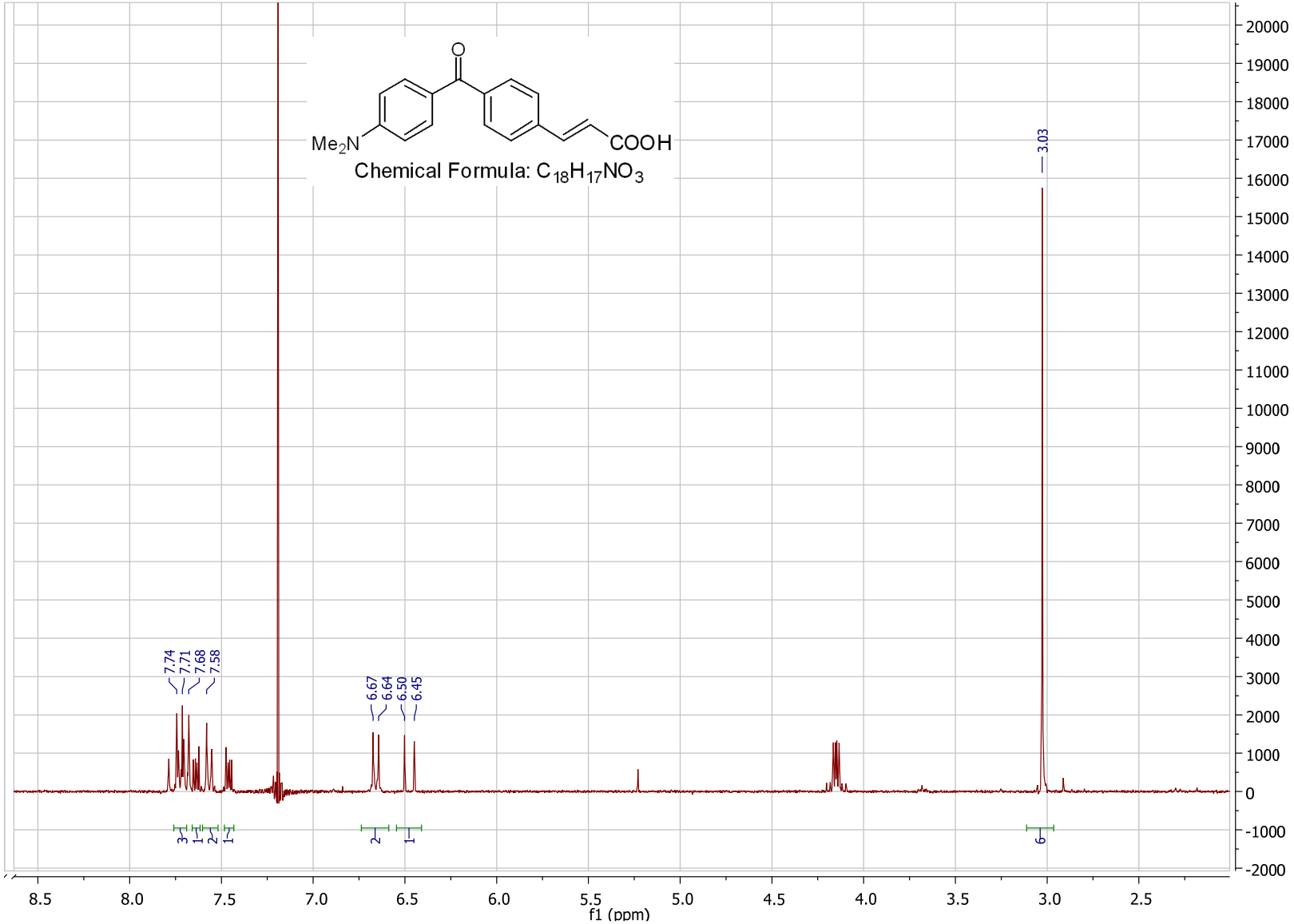

^{1}H NMR Spectrum of **2-7**

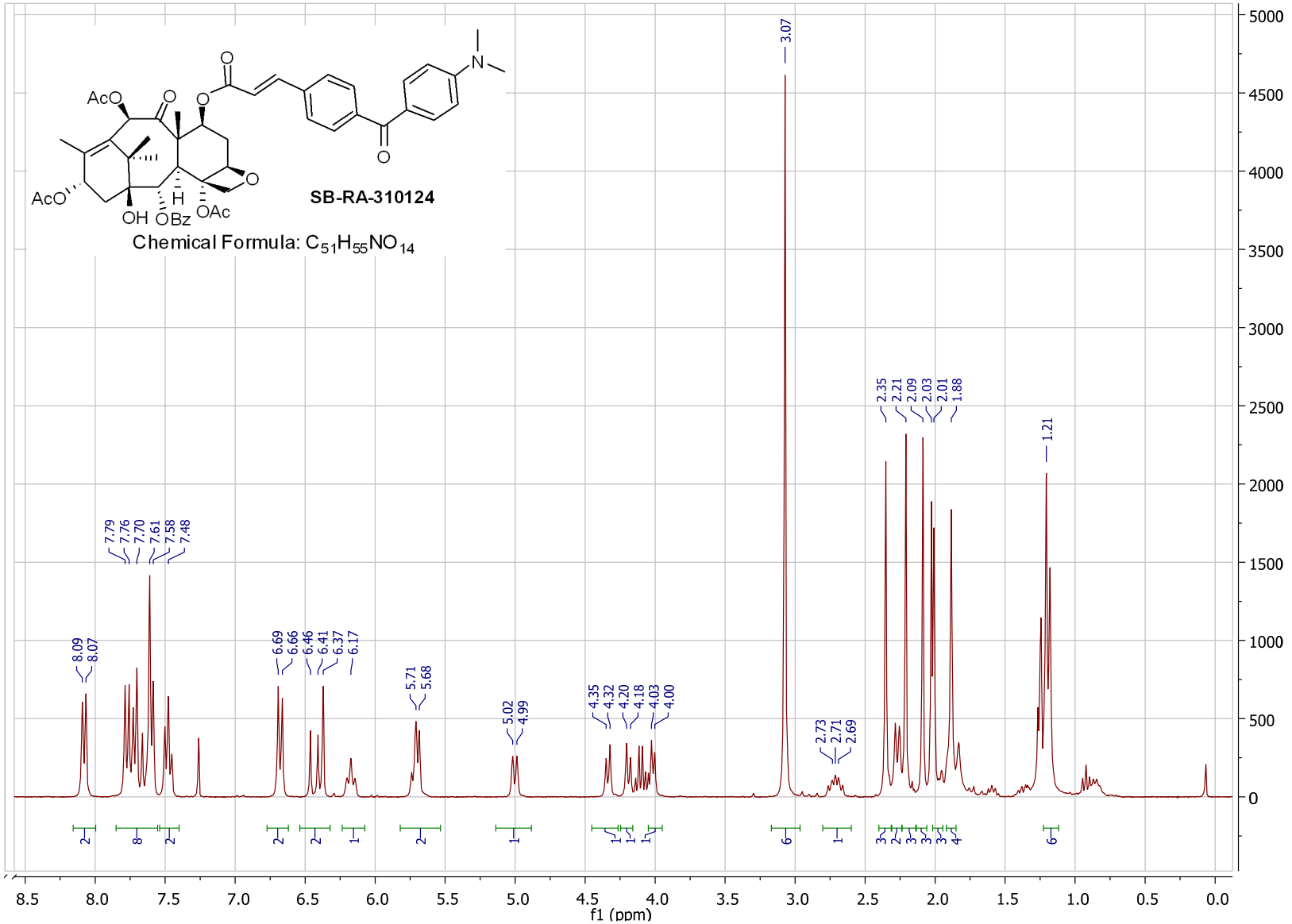

^{13}C NMR Spectrum of **2-7**

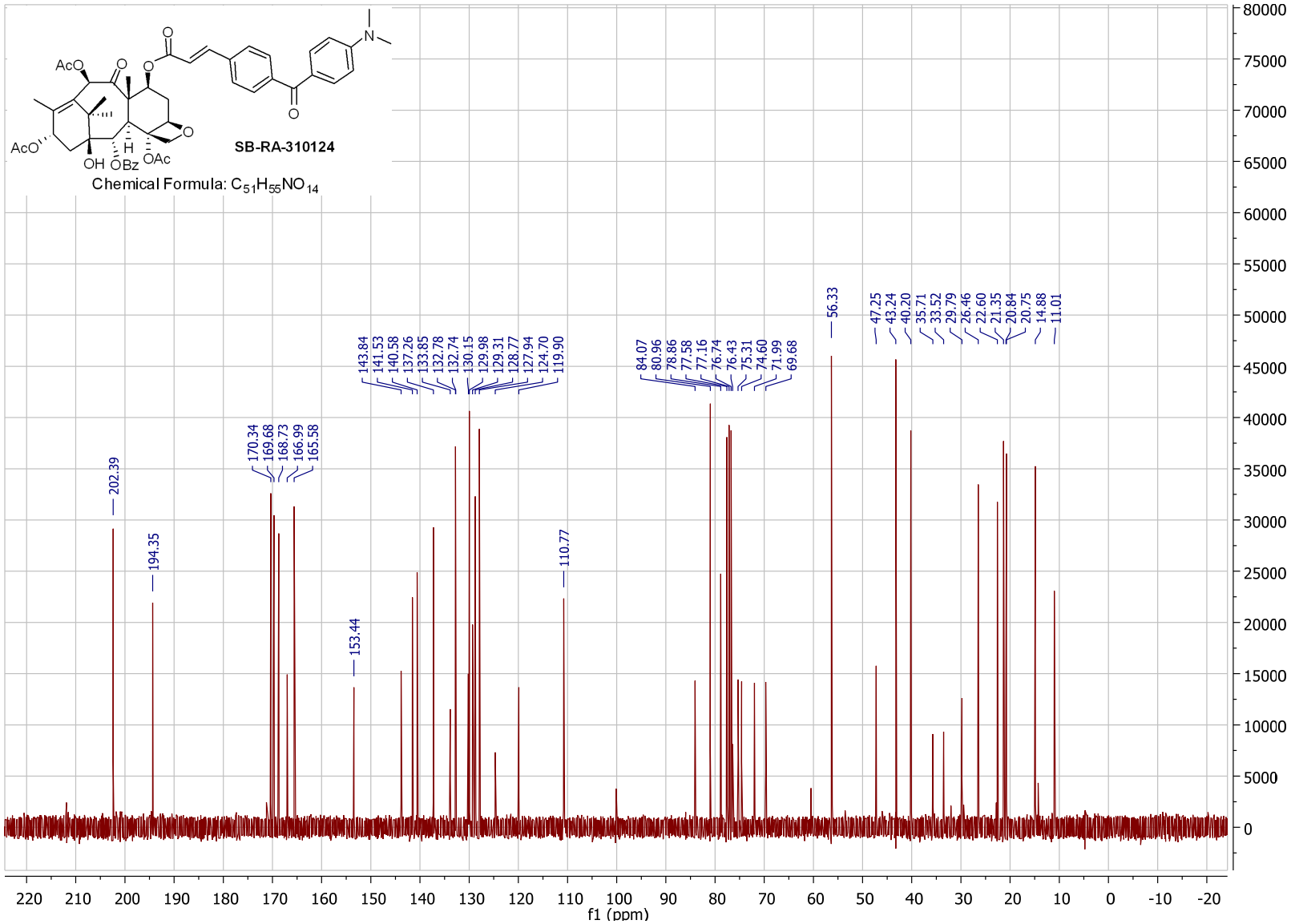

^{1}H NMR Spectrum of **2-8**

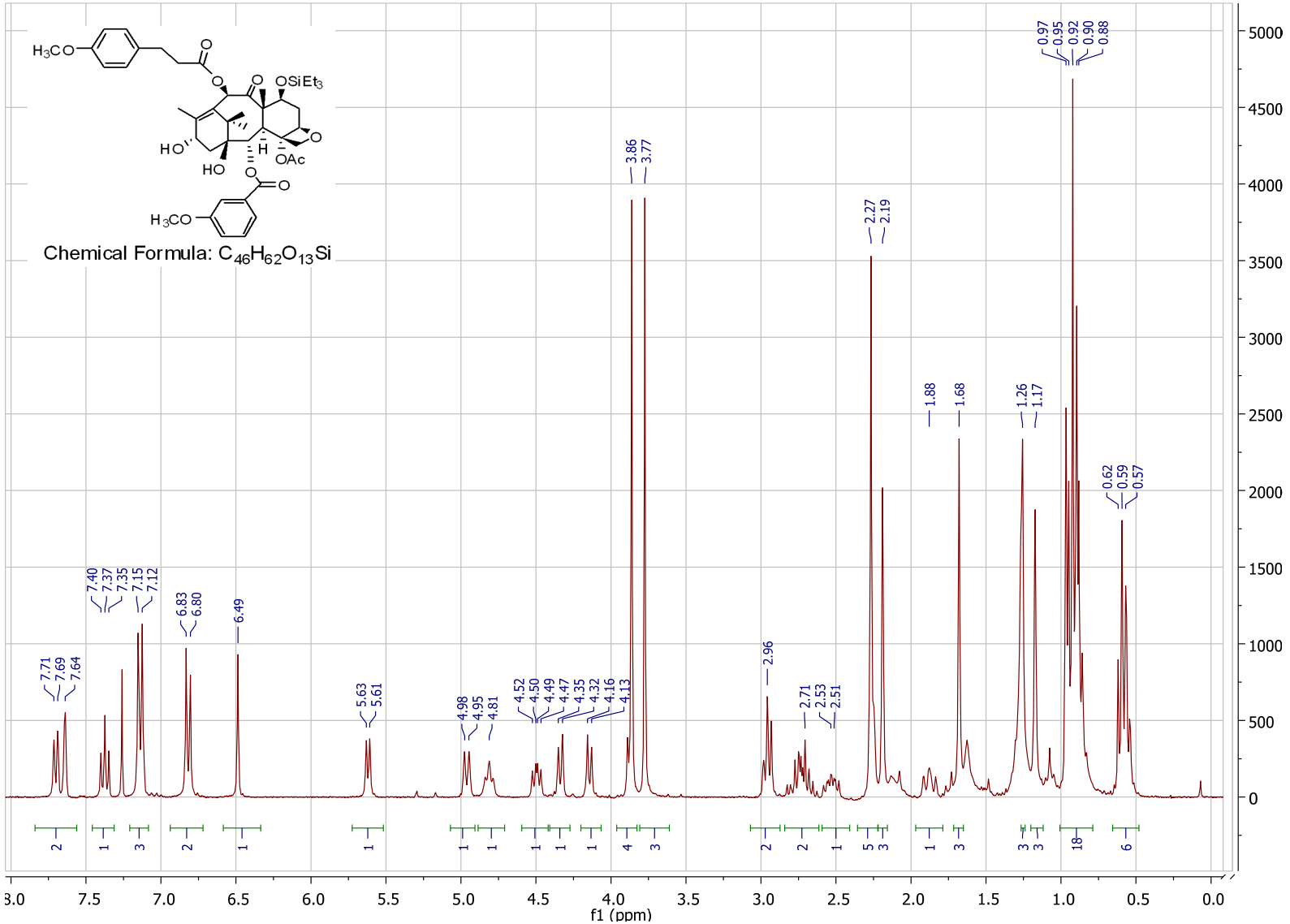

^{1}H NMR Spectrum of **2-9**

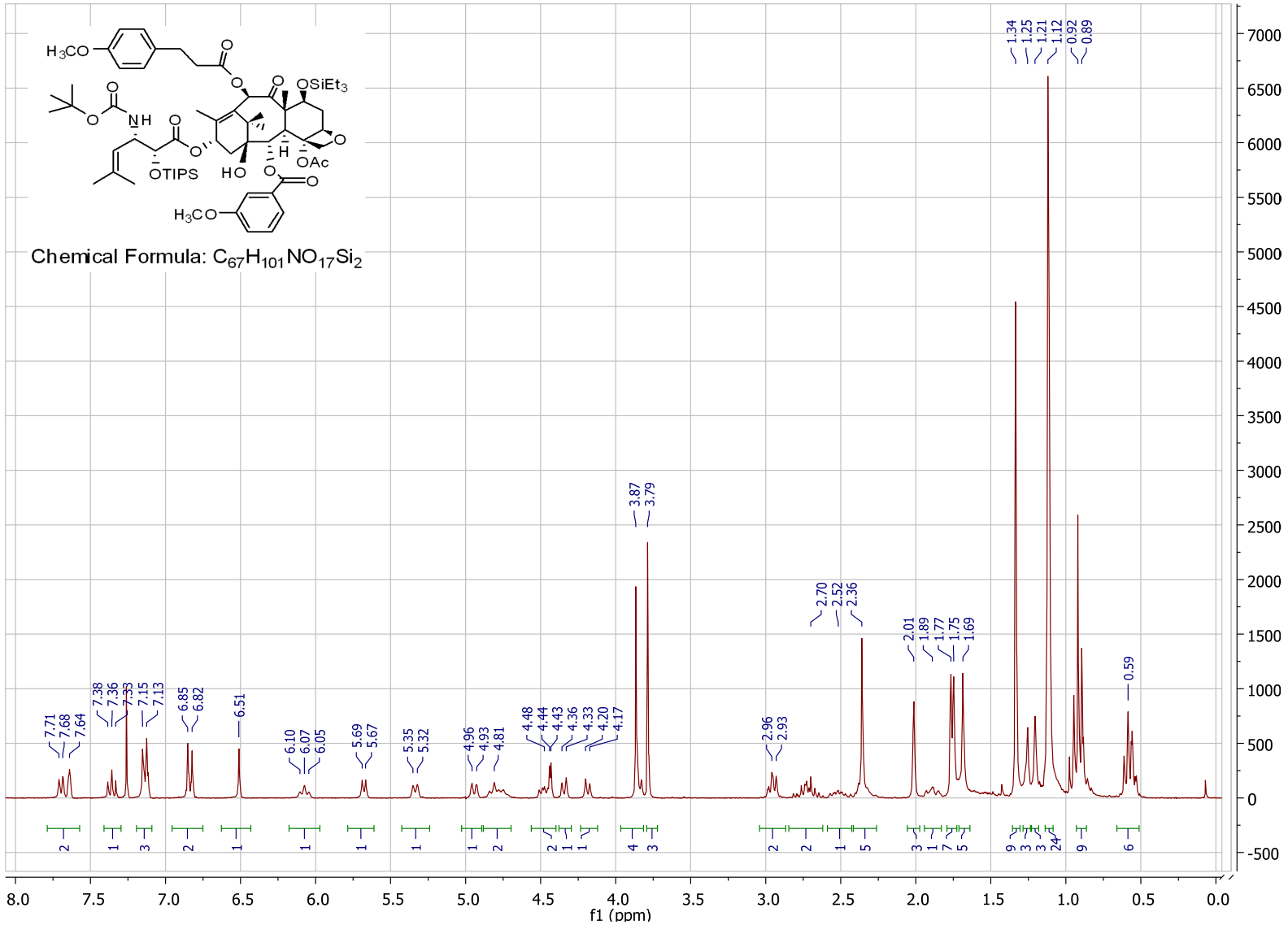

^{1}H NMR Spectrum of **2-10**

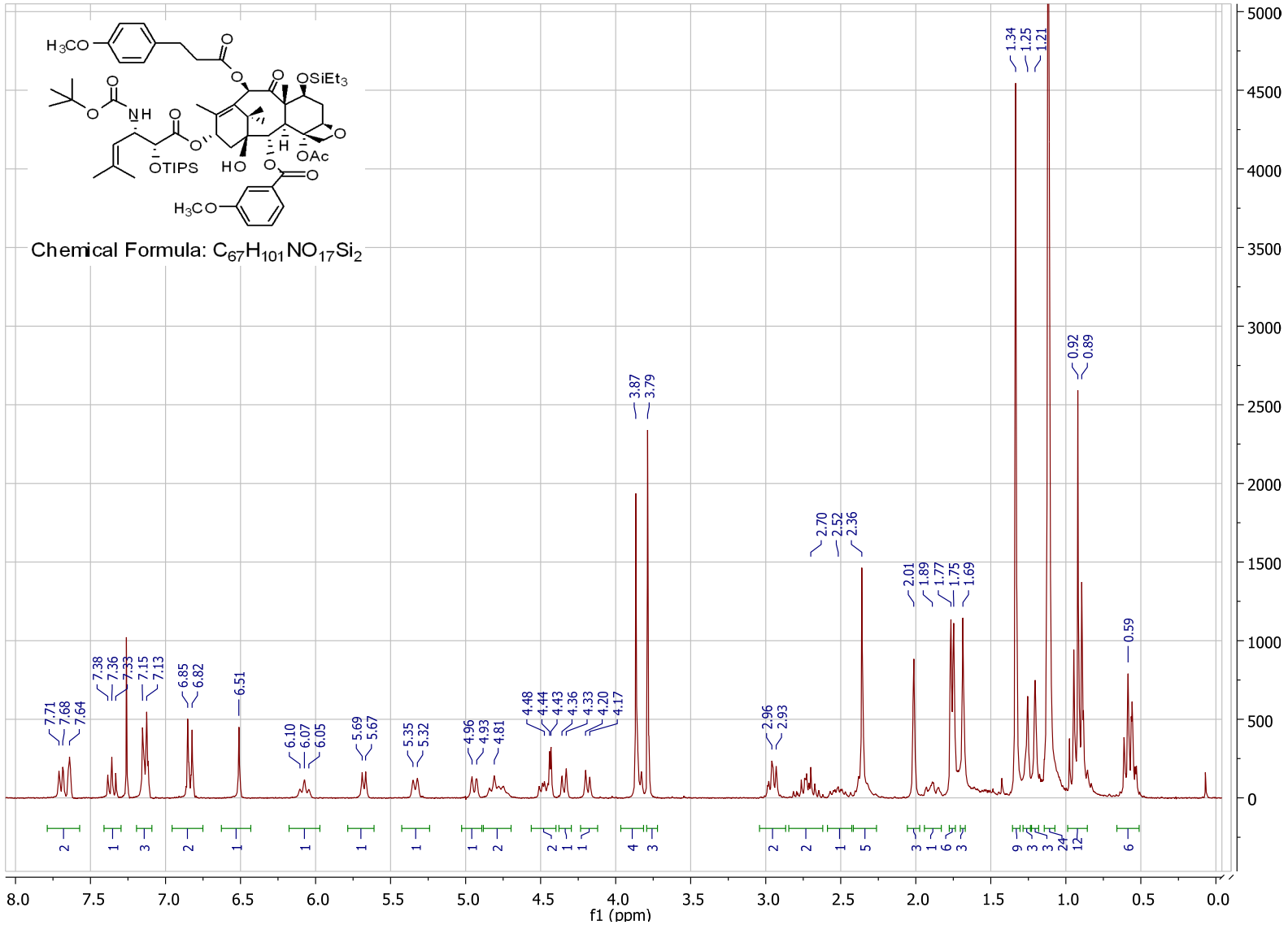

^{13}C NMR Spectrum of **2-10**

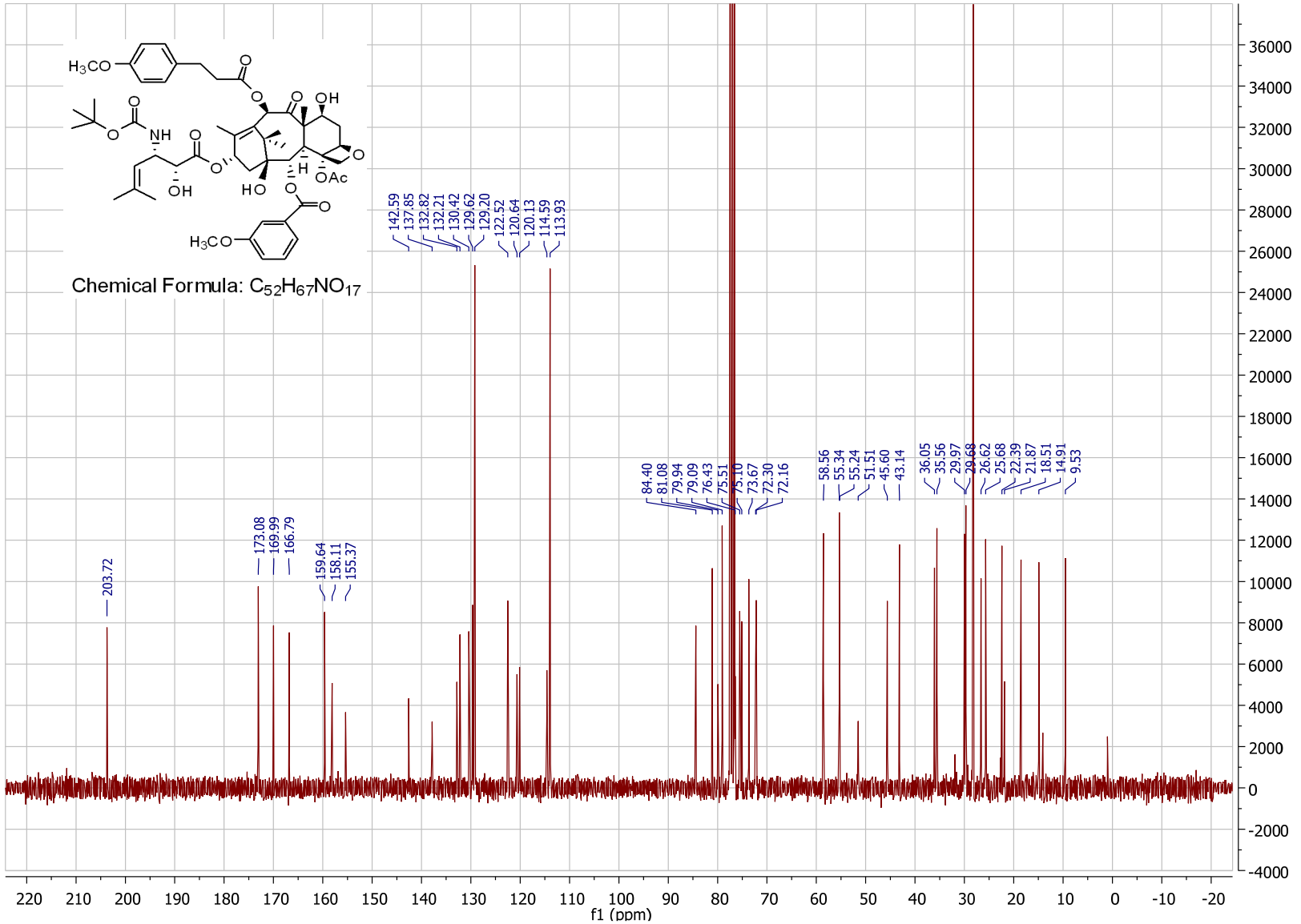

^{1}H NMR Spectrum of **3-1**

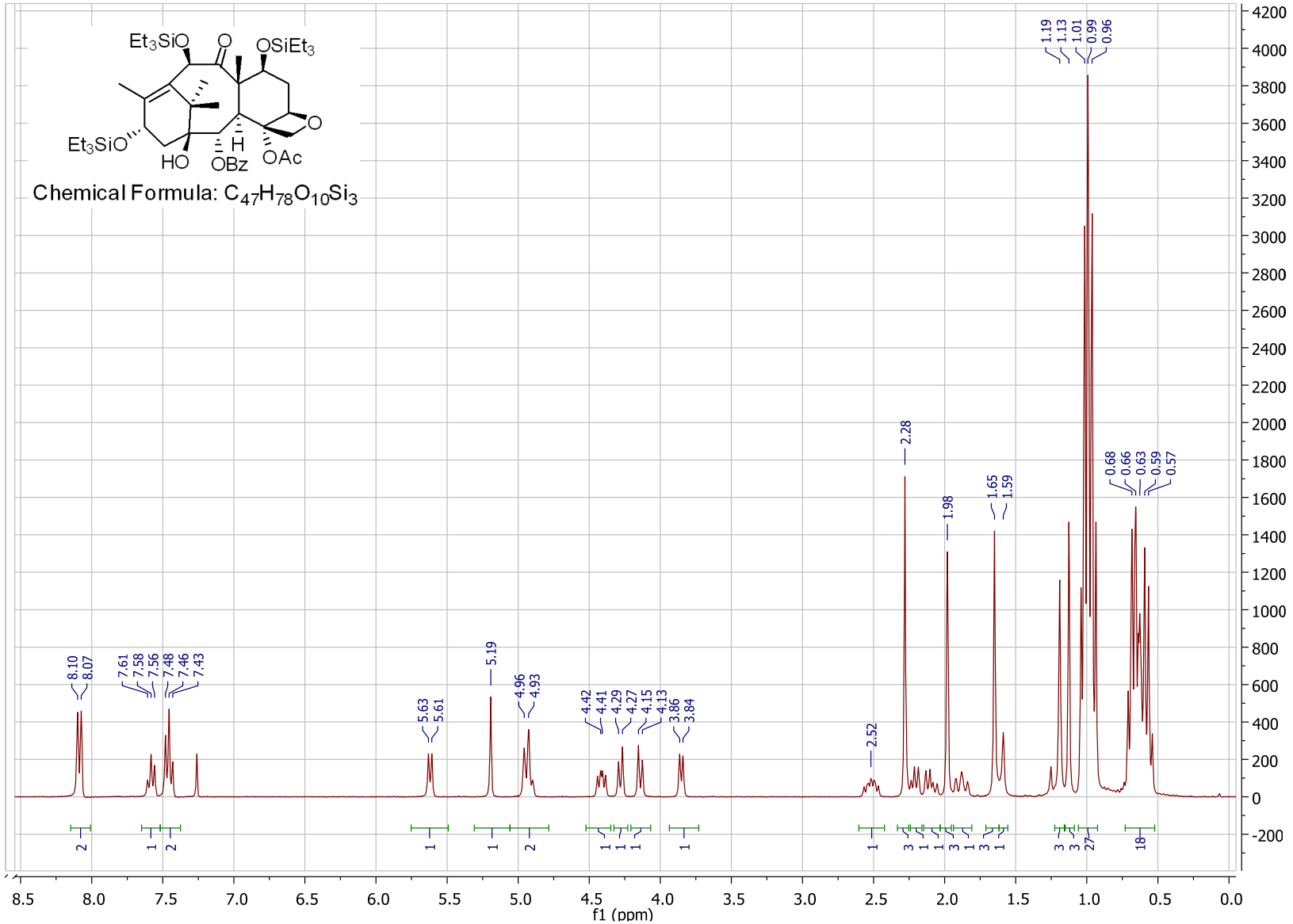

^{1}H NMR Spectrum of **3-2**

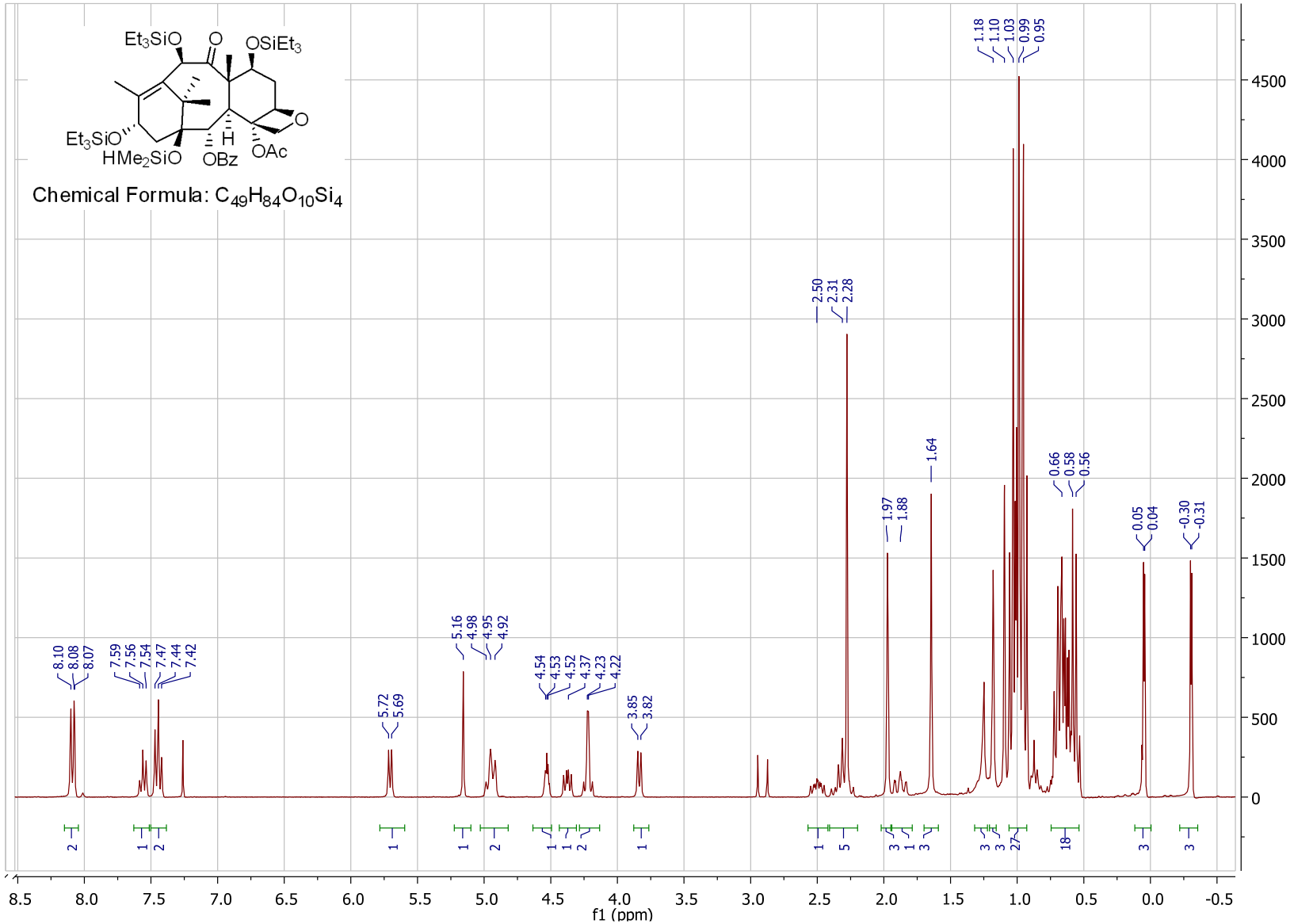

^{1}H NMR Spectrum of **3-3**

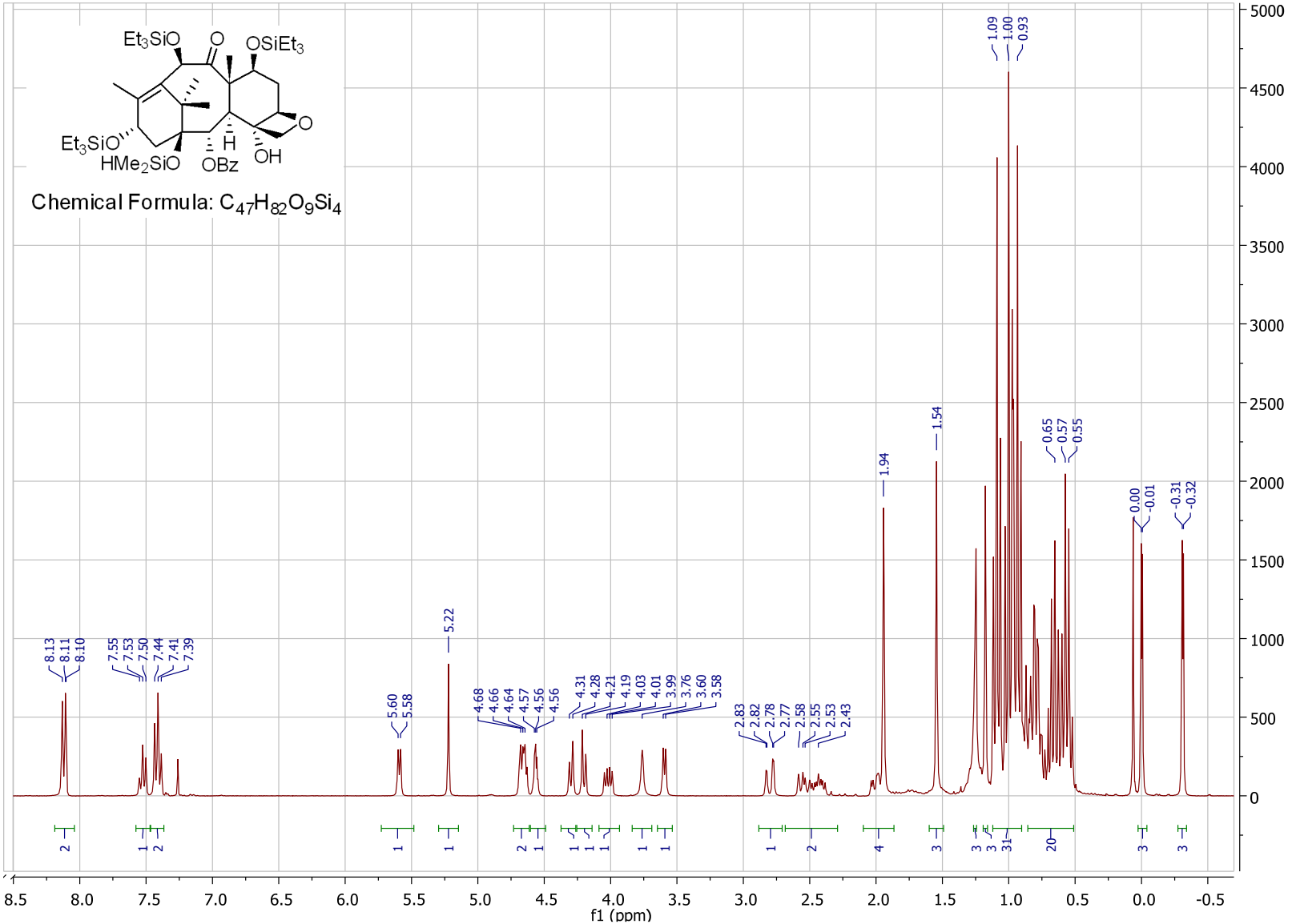

^{1}H NMR Spectrum of **3-4**

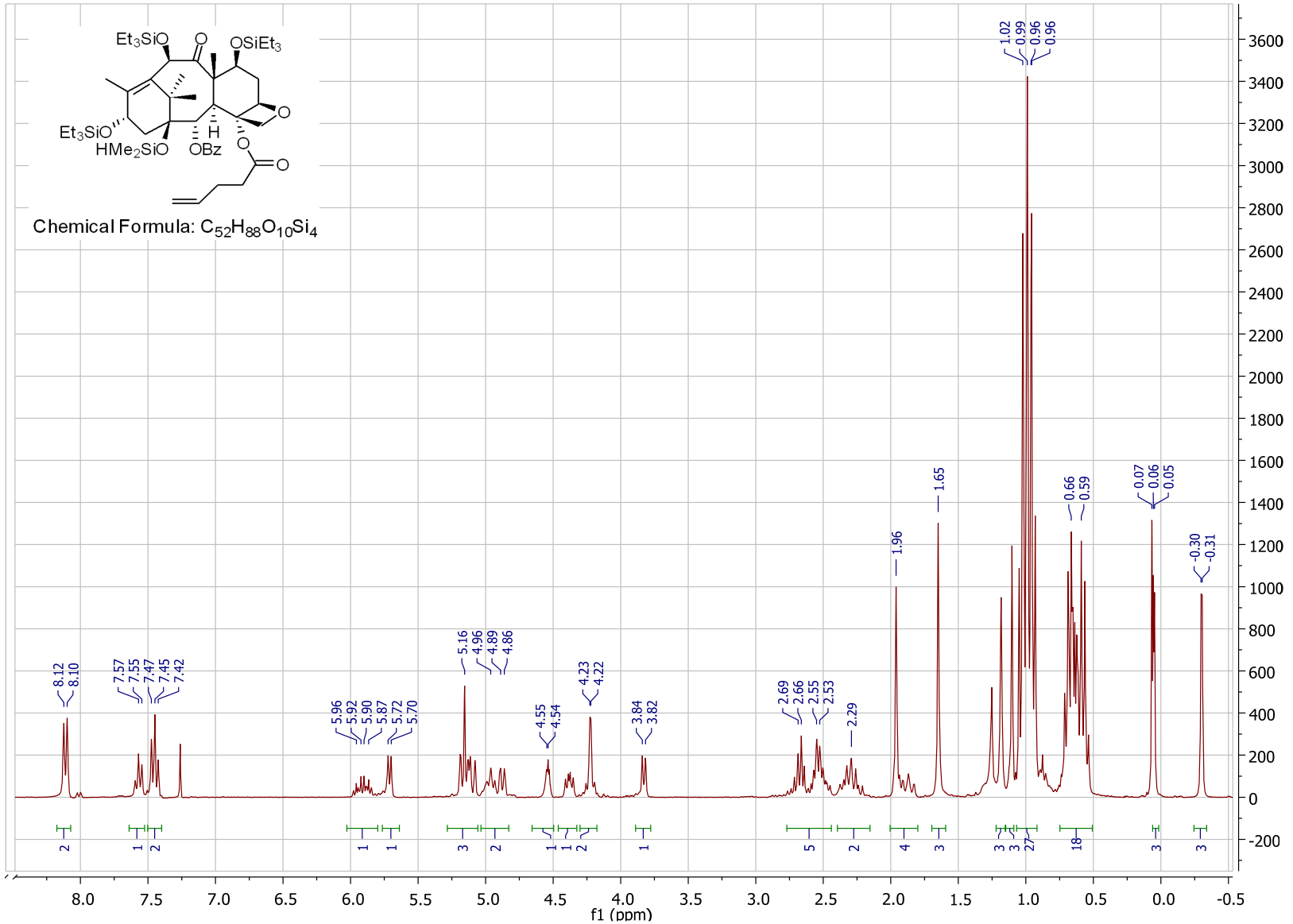

^{1}H NMR Spectrum of **3-6**

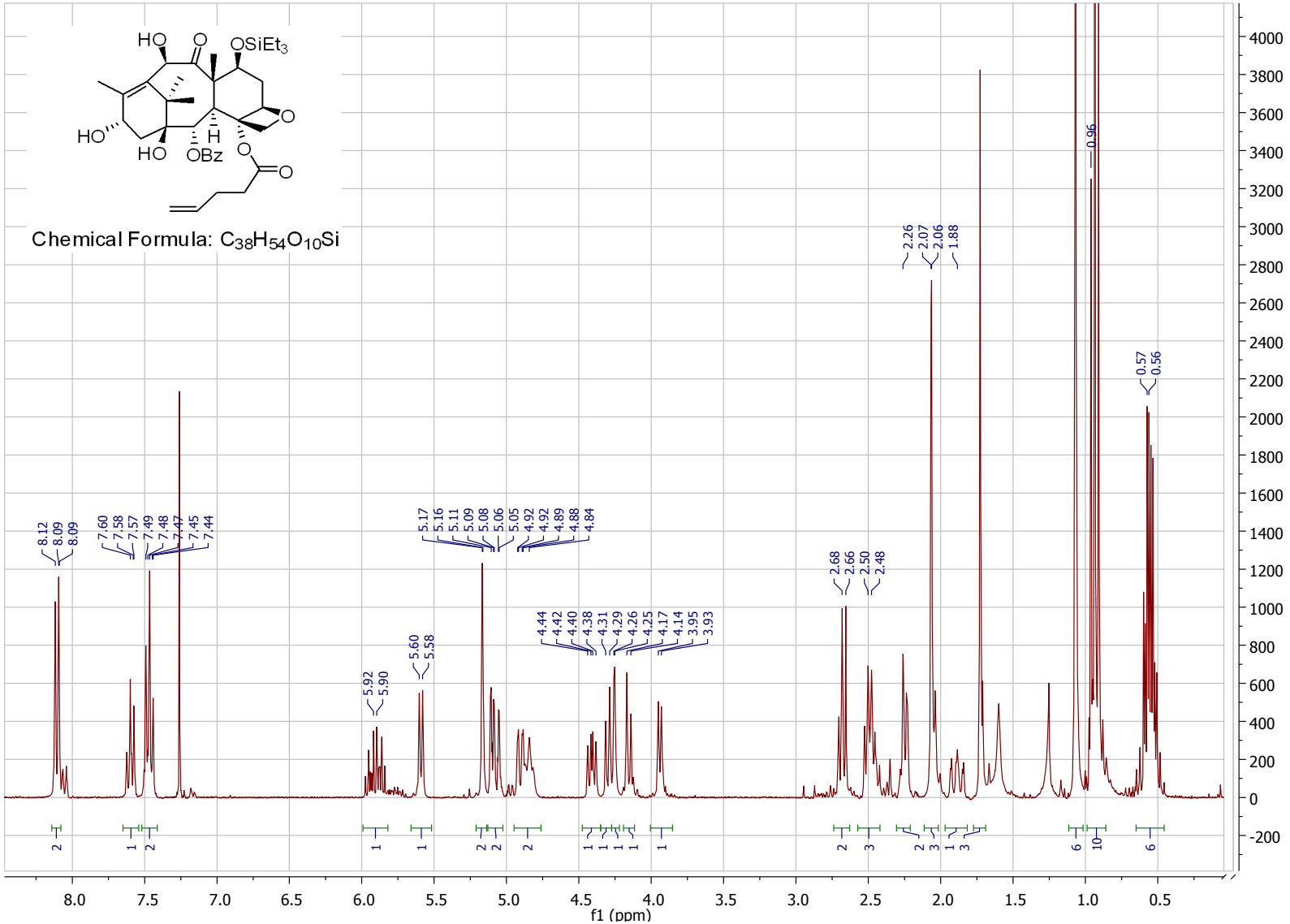

^{1}H NMR Spectrum of **3-7**

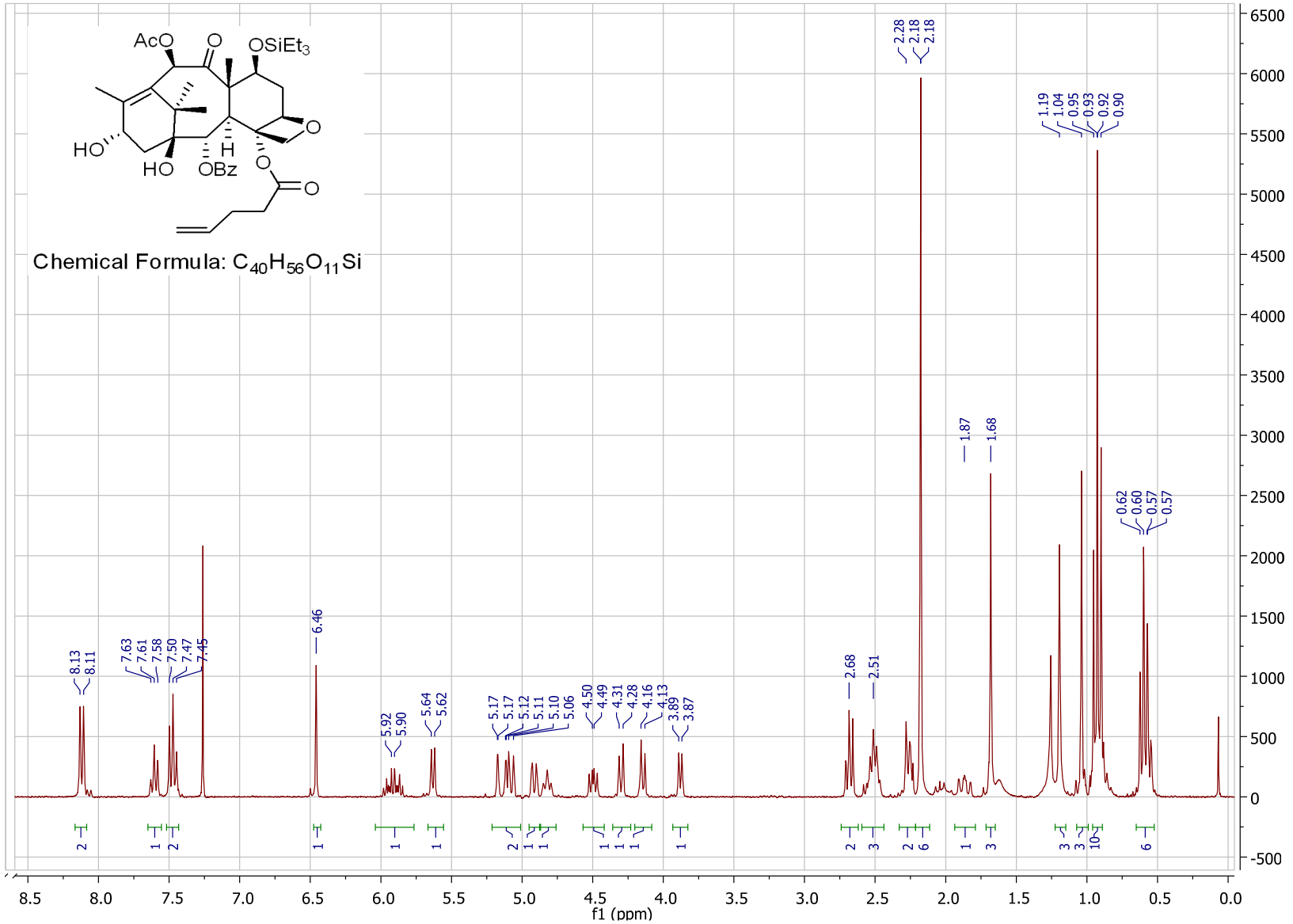

^{1}H NMR Spectrum of **3-9**

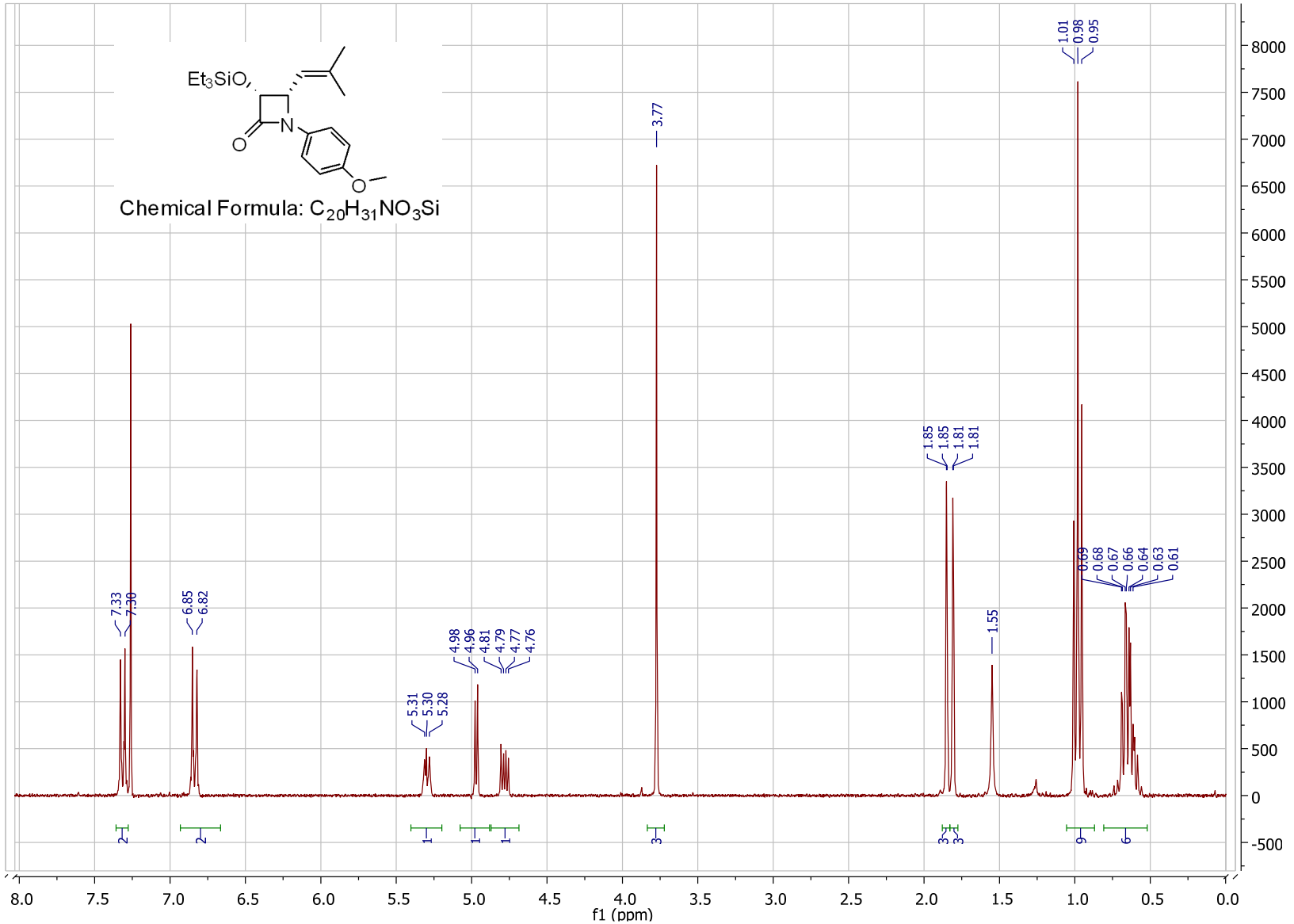

^{1}H NMR Spectrum of **3-10**

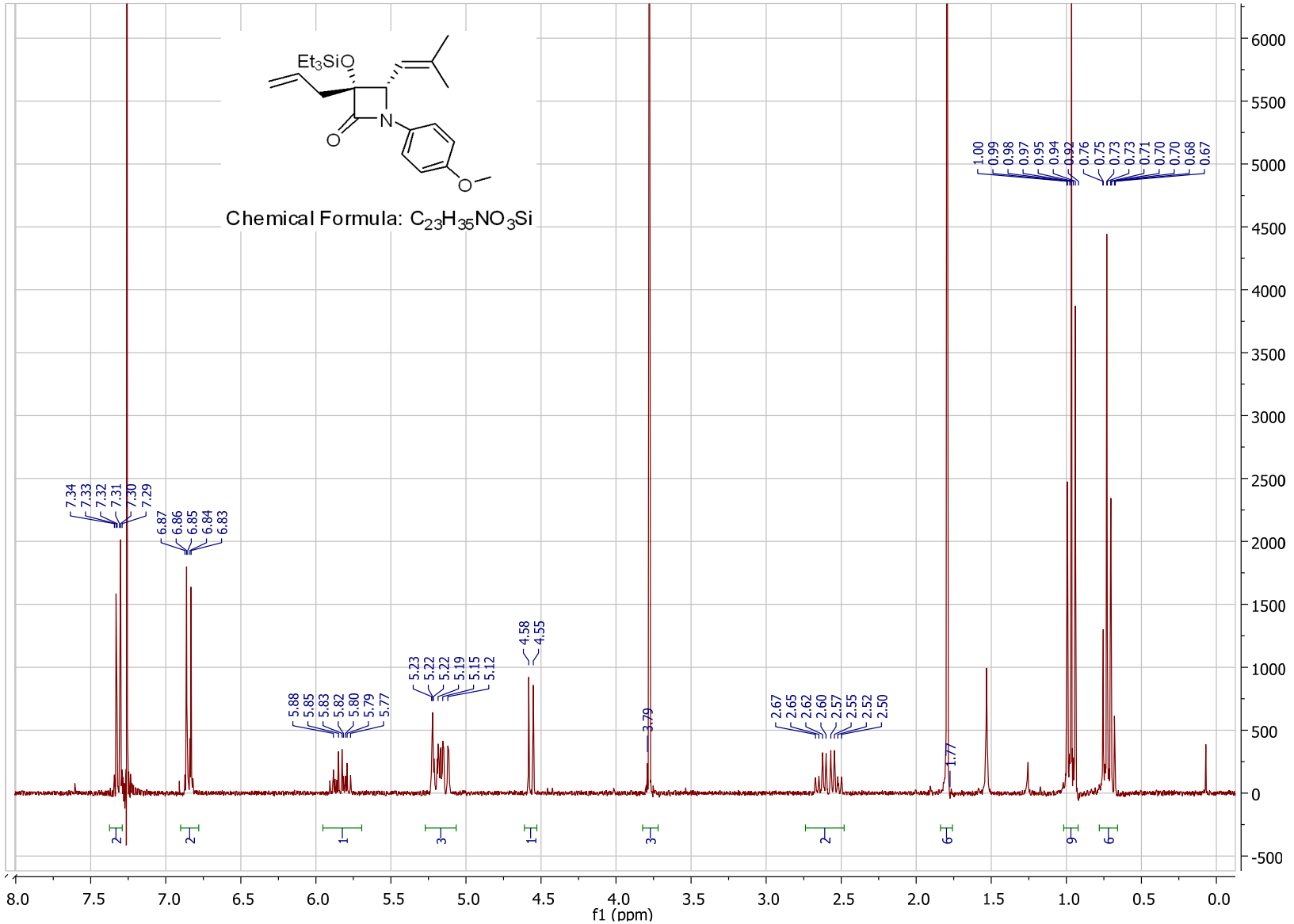

^{1}H NMR Spectrum of **3-11**

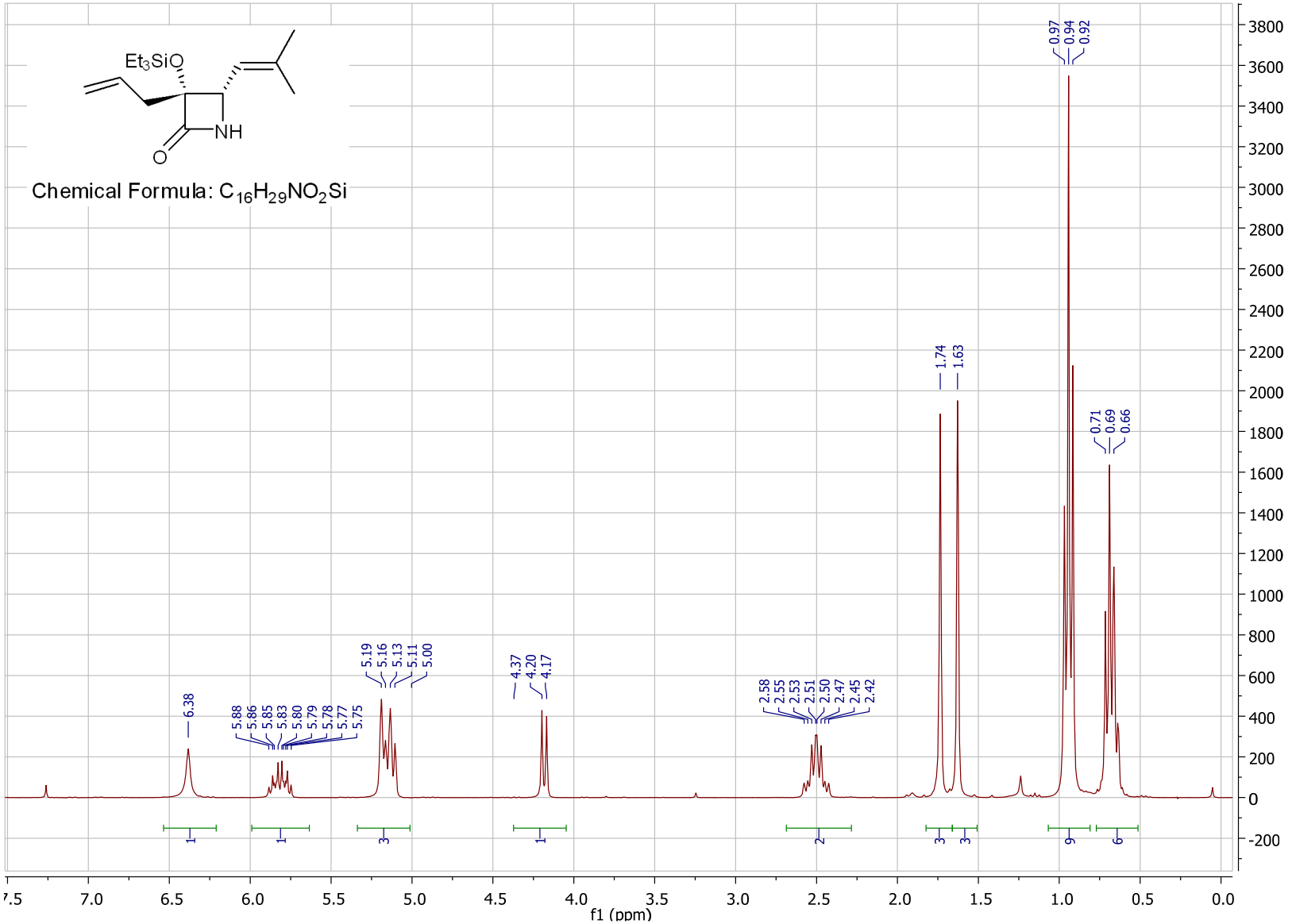

^{1}H NMR Spectrum of **3-12**

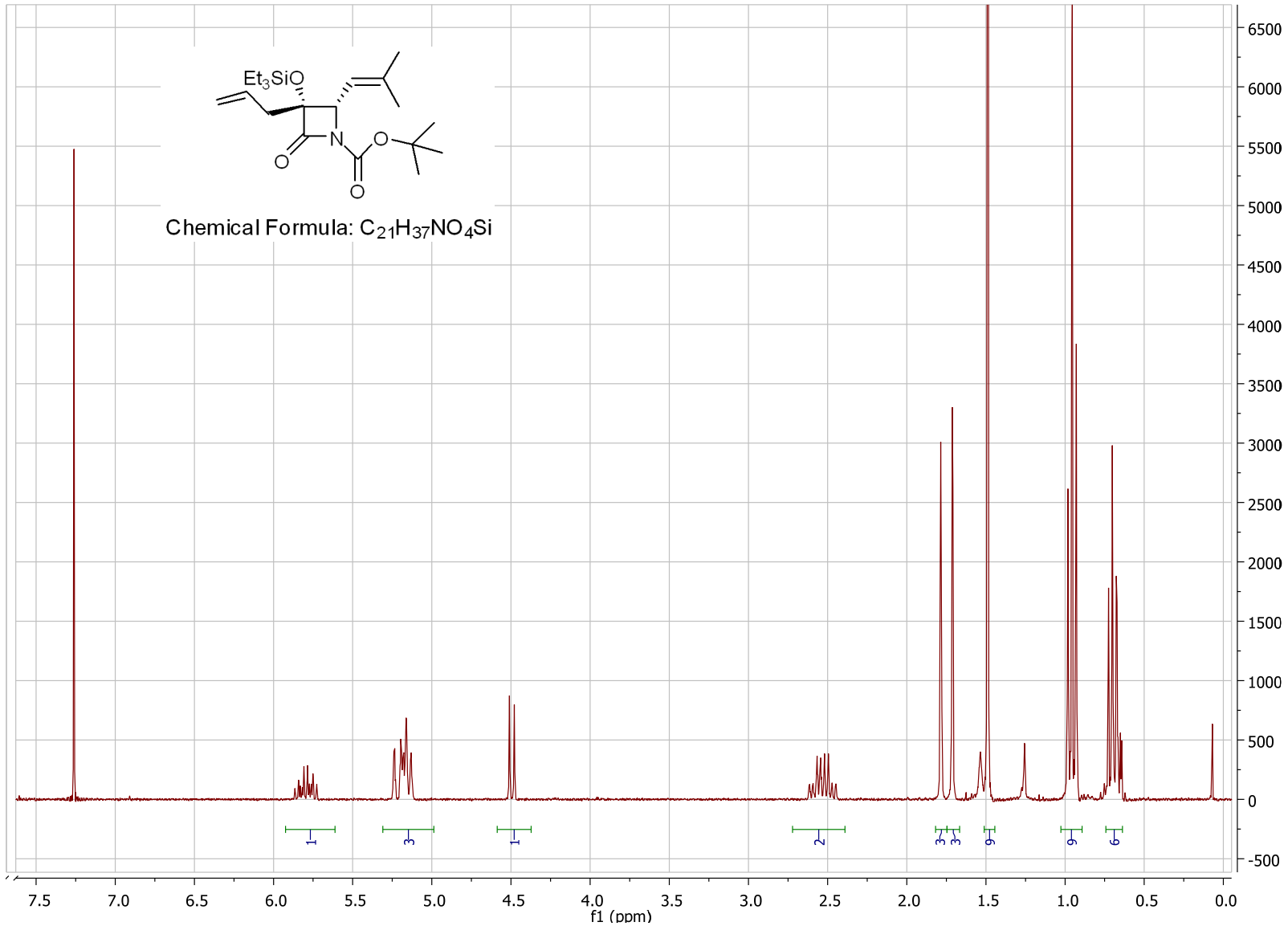

^{1}H NMR Spectrum of **3-14**

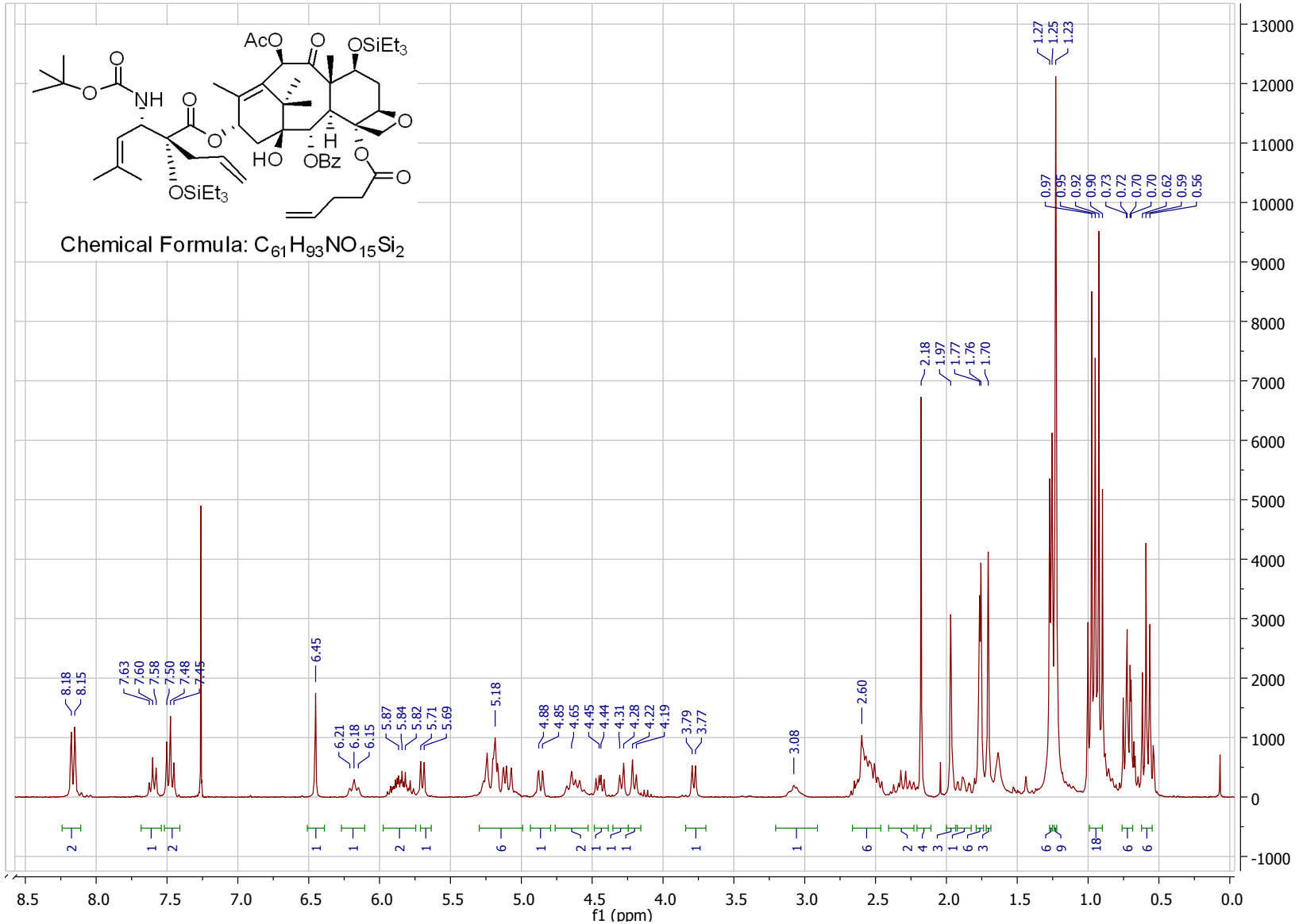

^{1}H NMR Spectrum of **3-15**

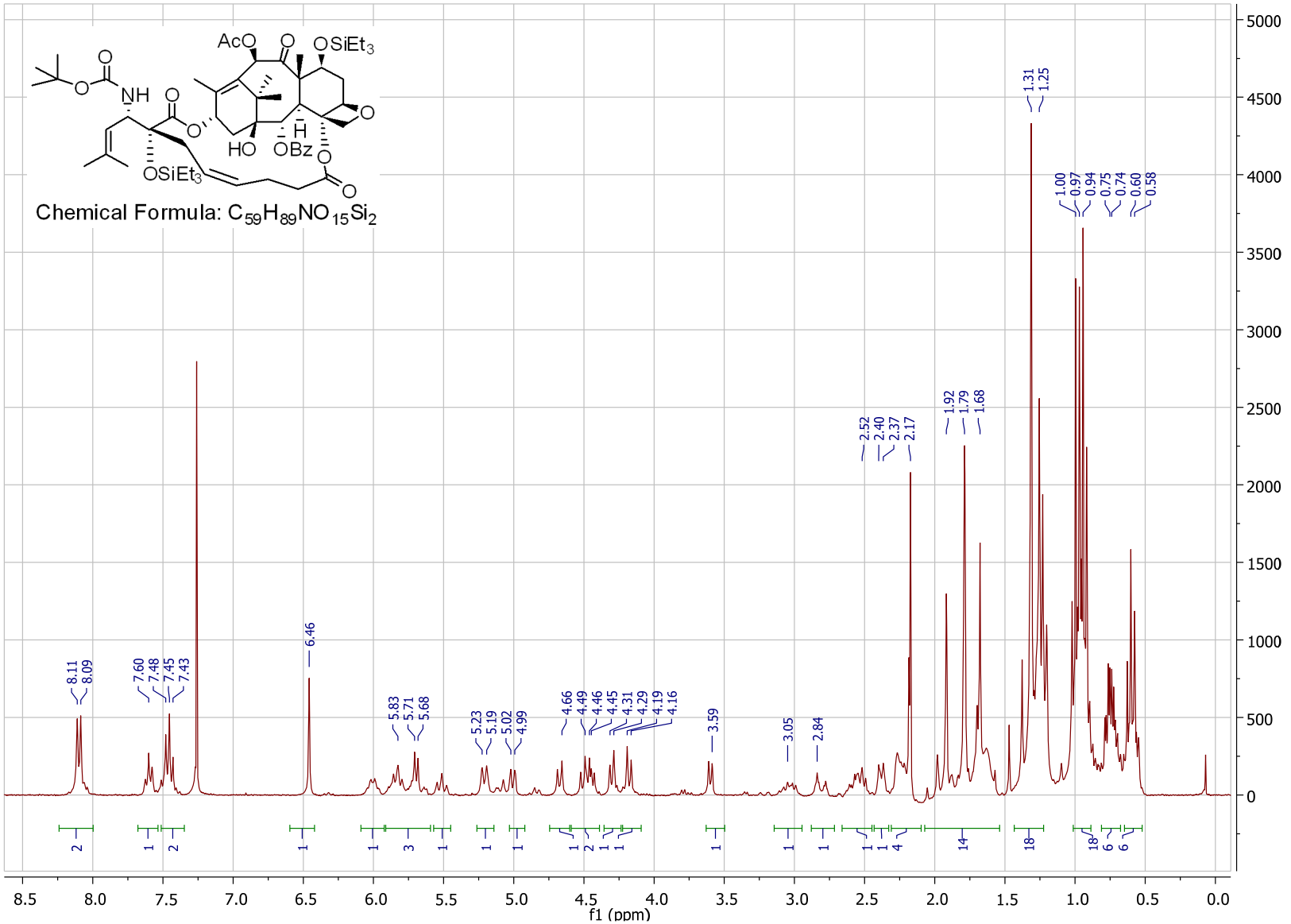

^{1}H NMR Spectrum of **3-16**

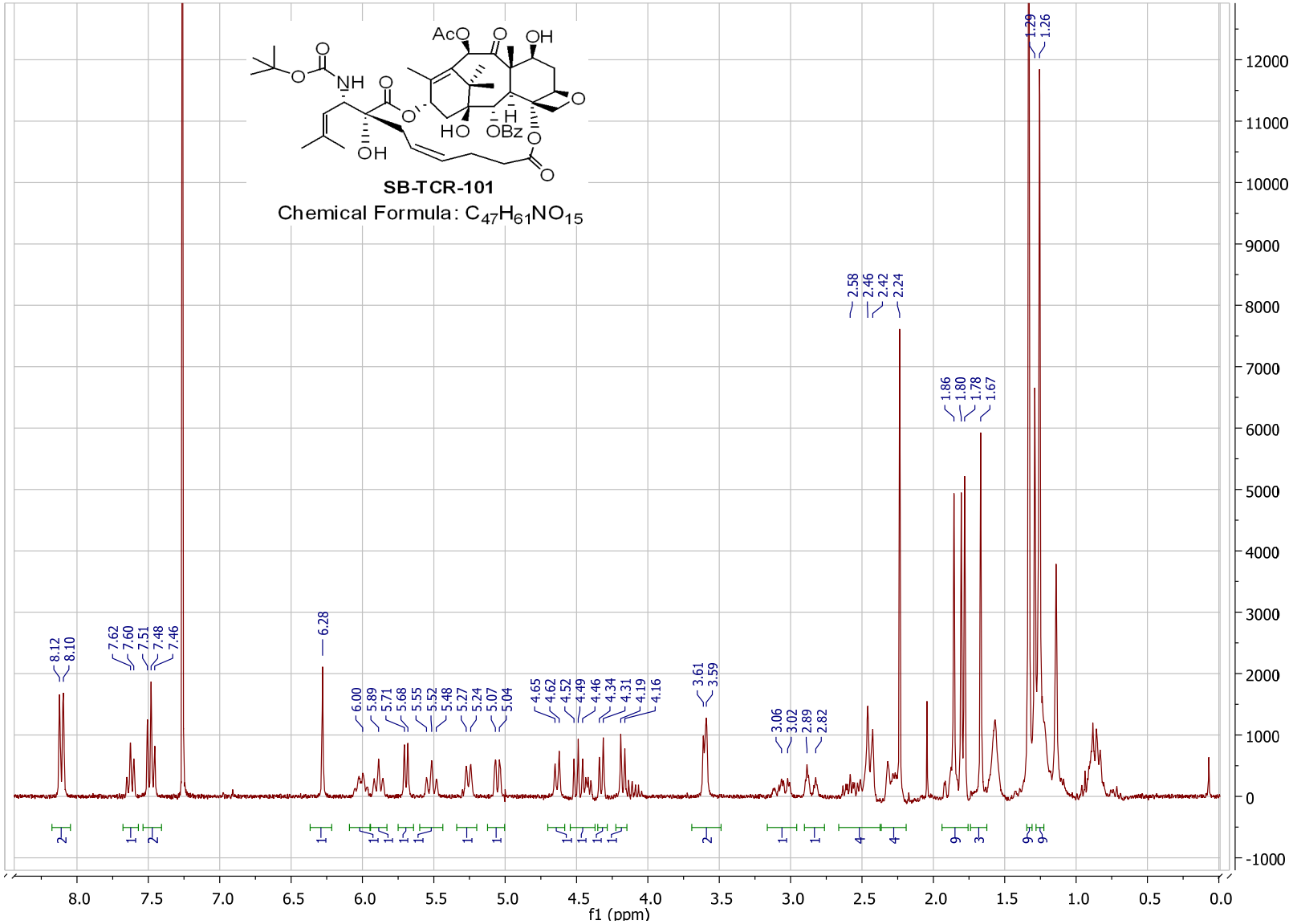

^{1}H NMR Spectrum of **3-17**

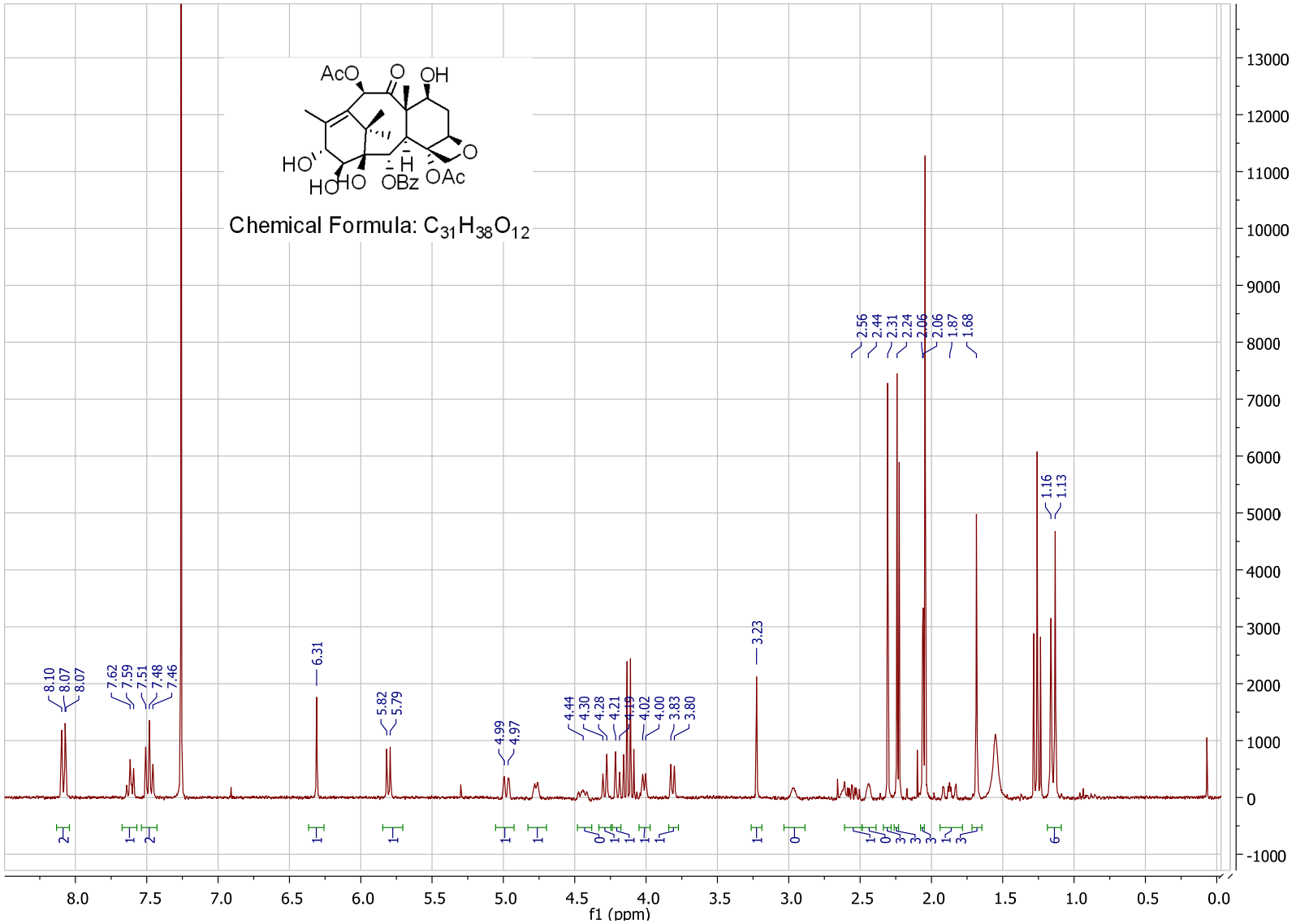

^{1}H NMR Spectrum of **3-18**

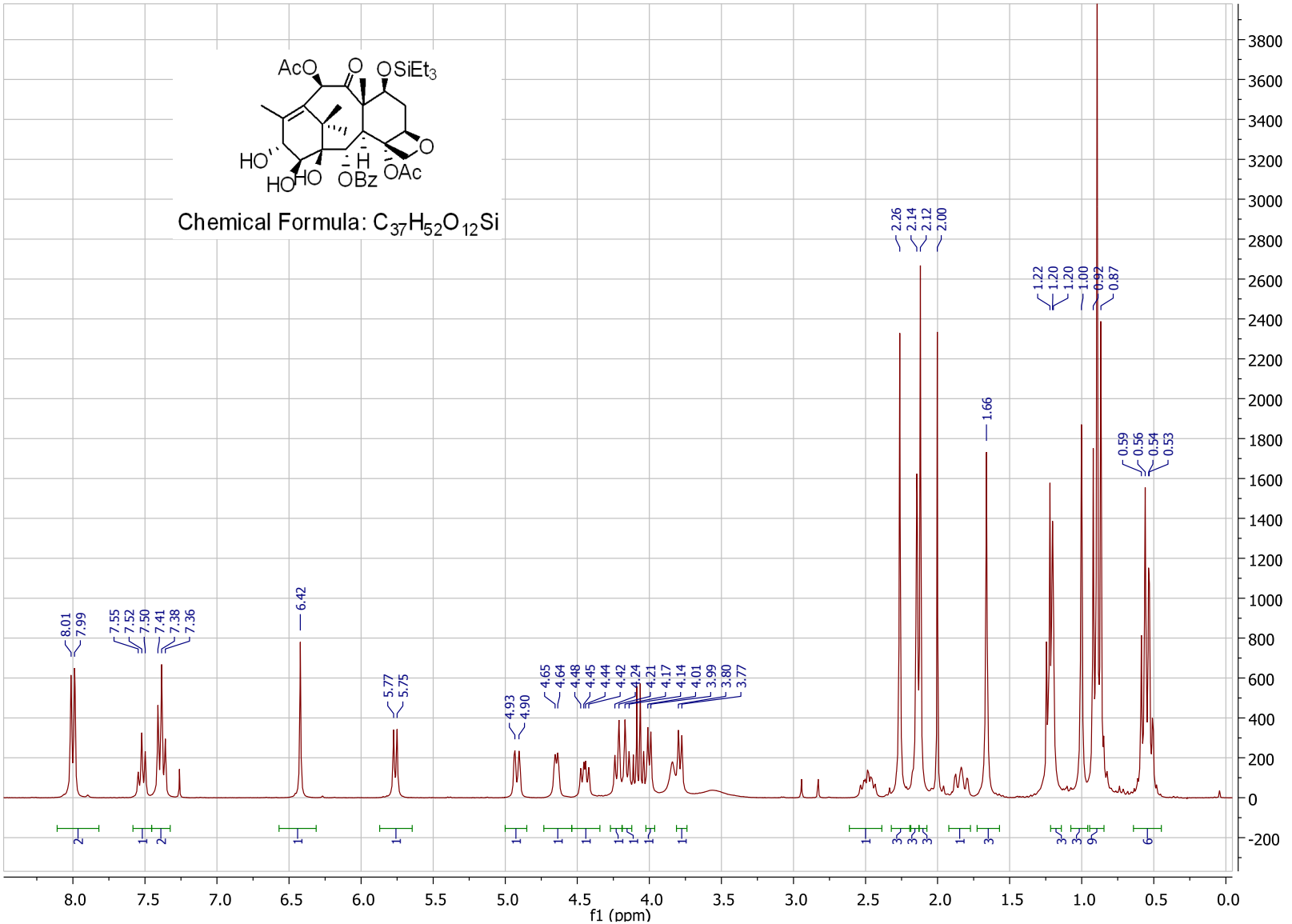

^{1}H NMR Spectrum of **3-19**

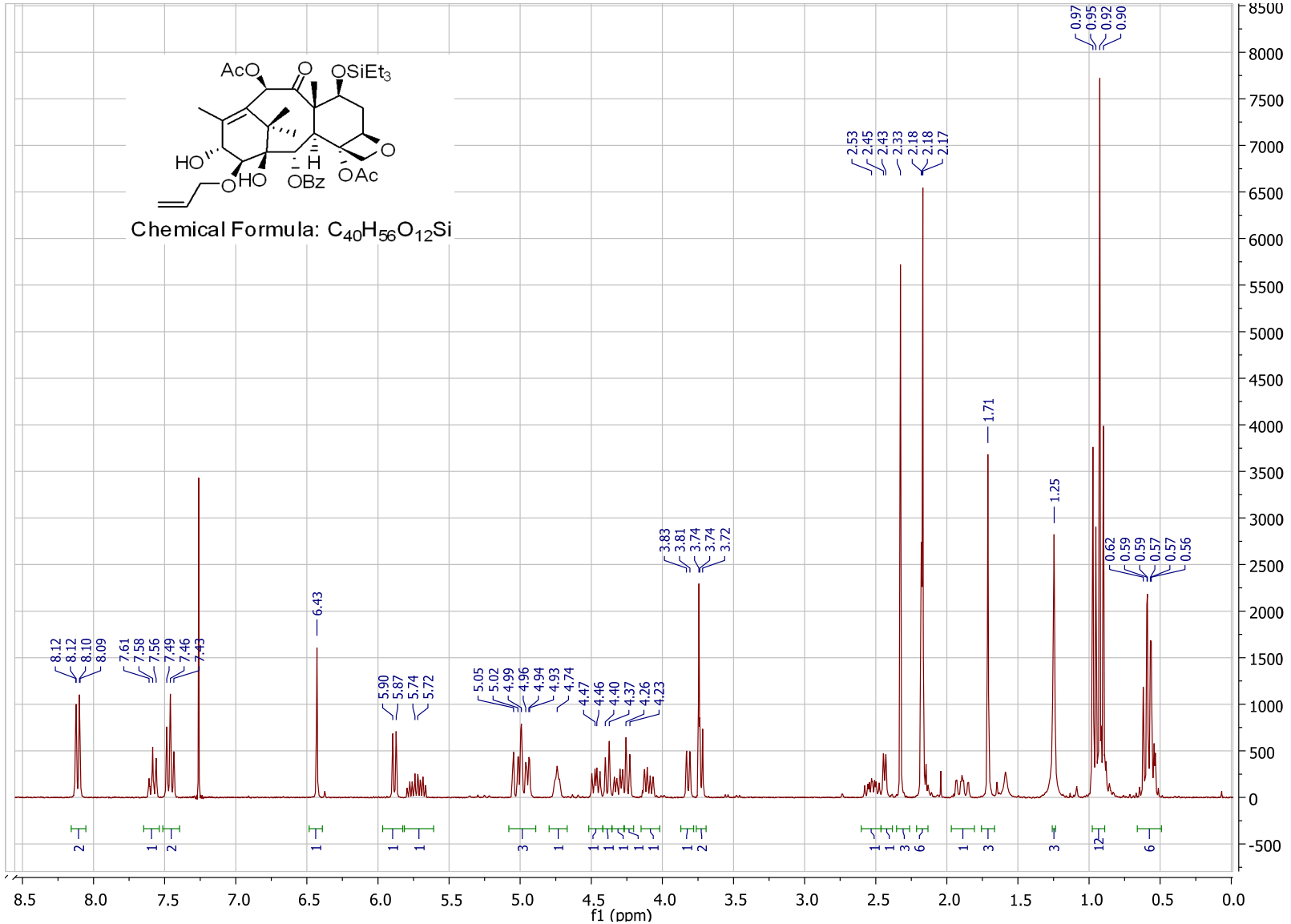

^{1}H NMR Spectrum of **3-20**

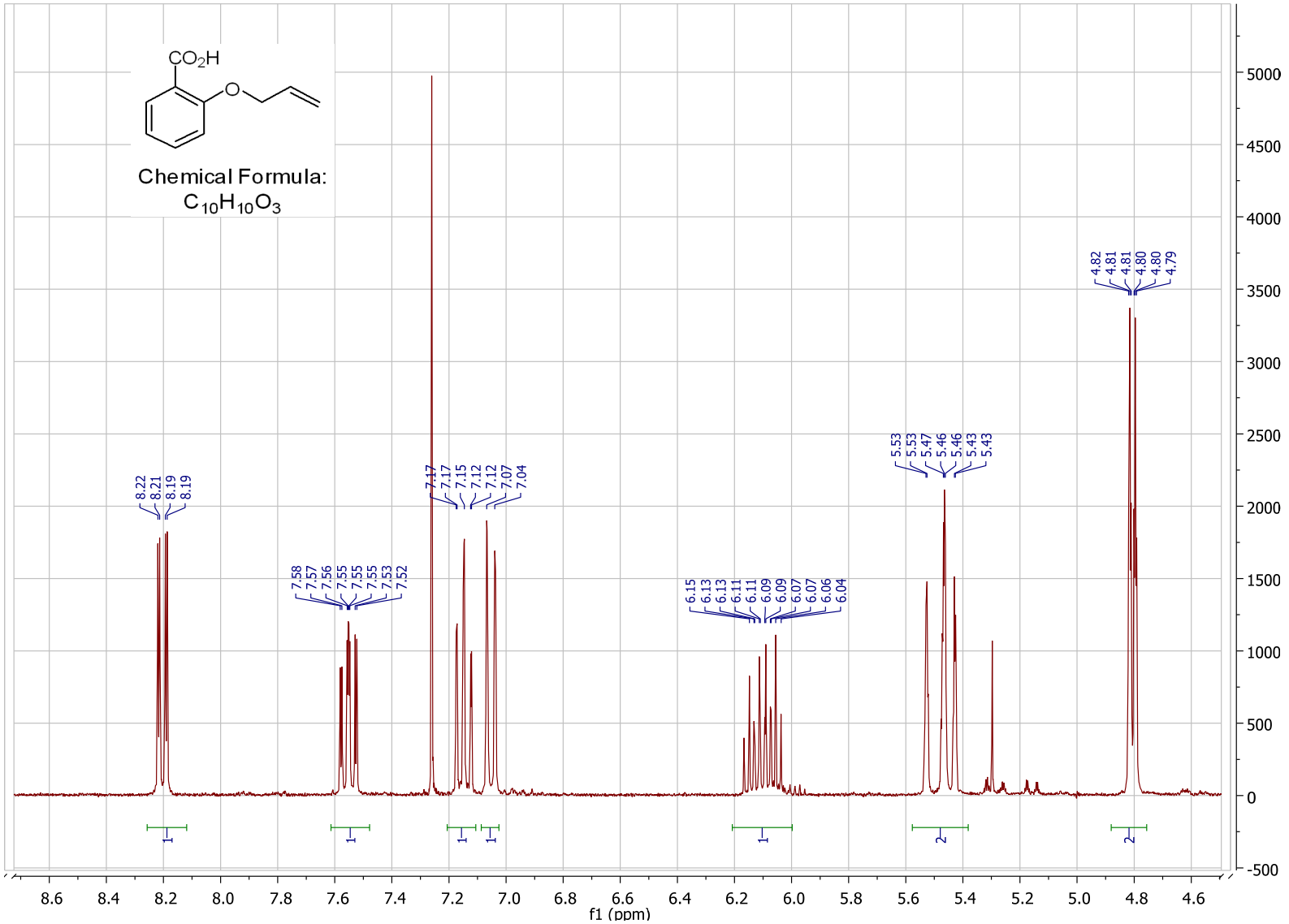

^{1}H NMR Spectrum of **3-21**

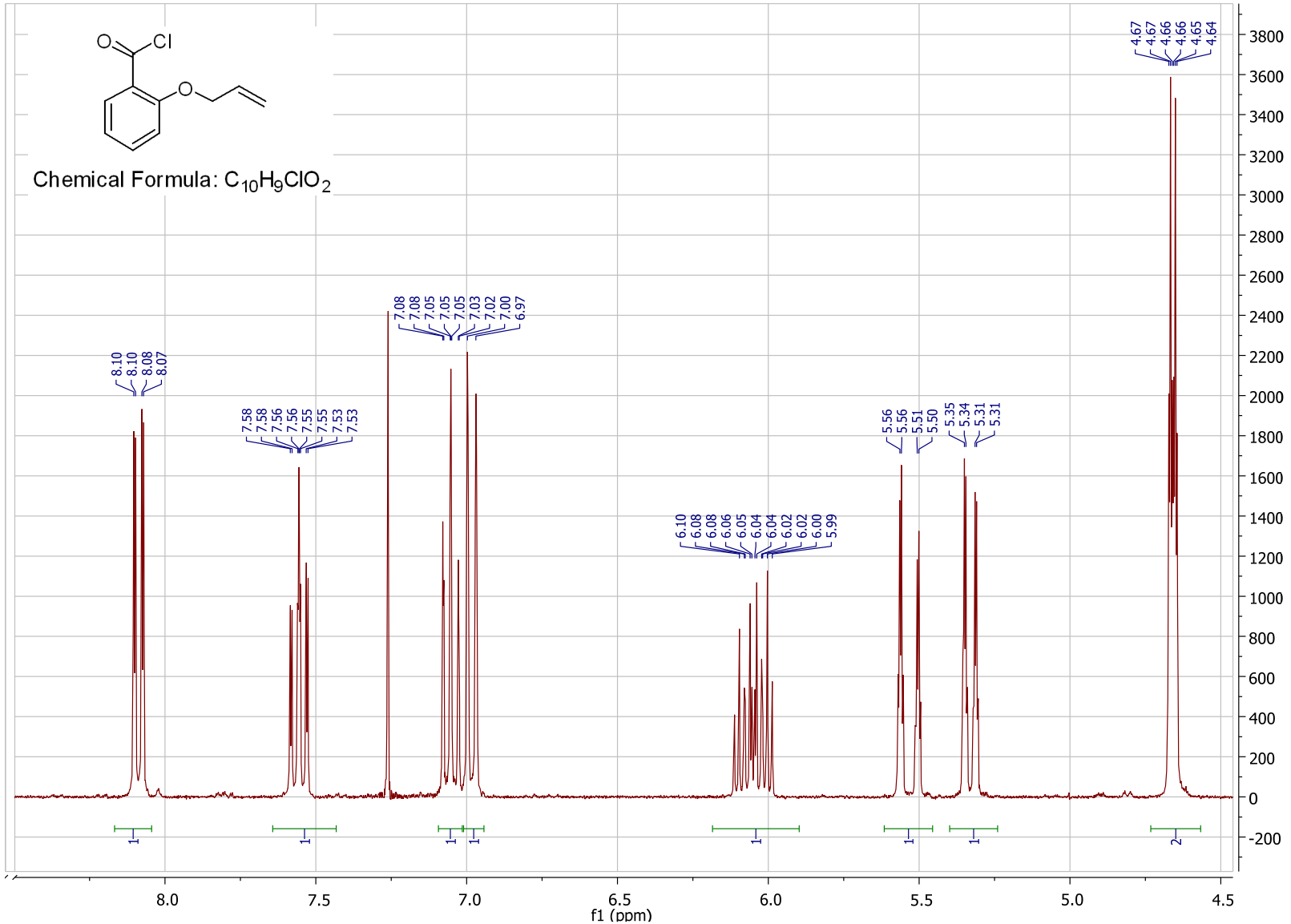

^{1}H NMR Spectrum of **3-22**

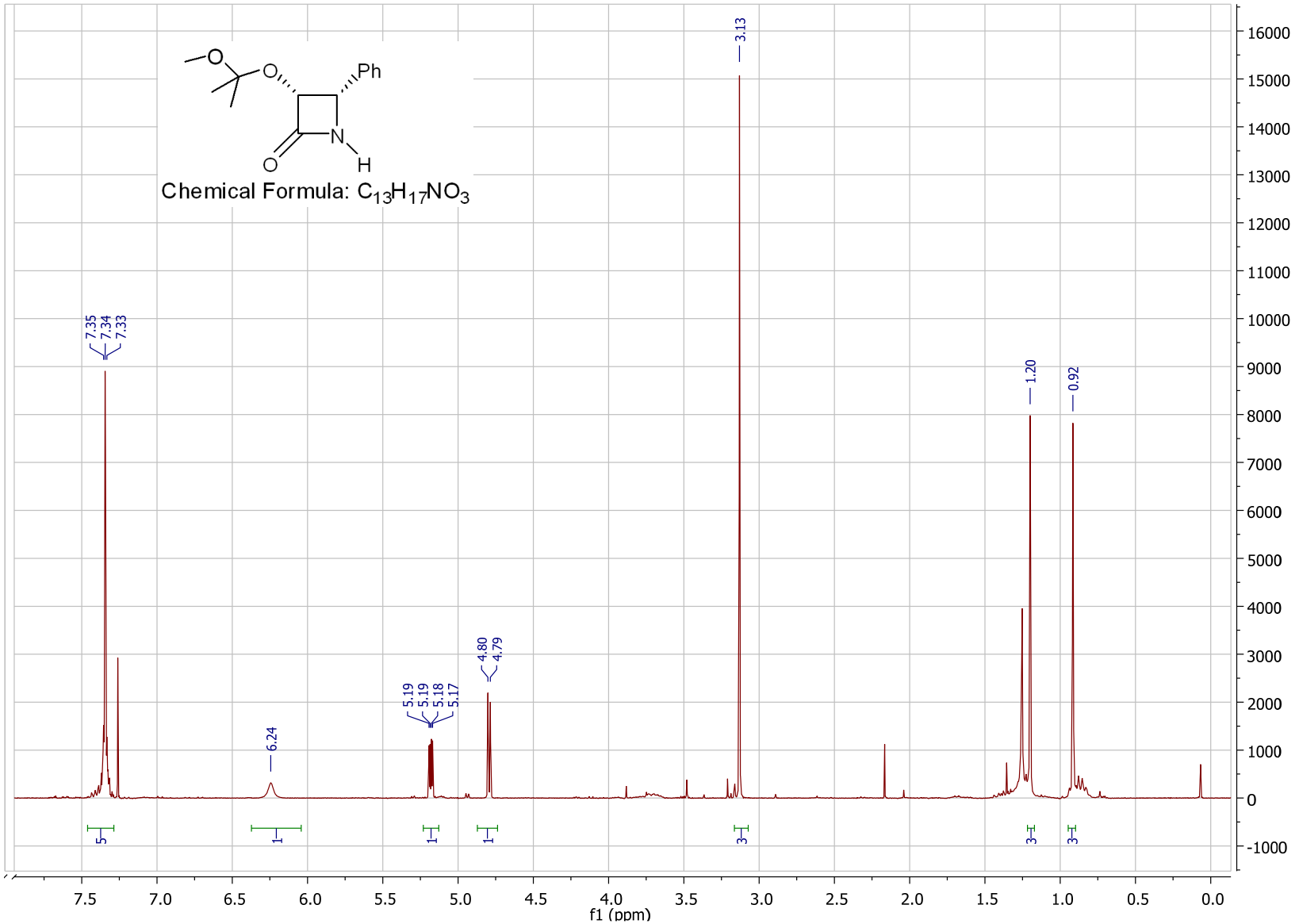

^{1}H NMR Spectrum of **3-23**

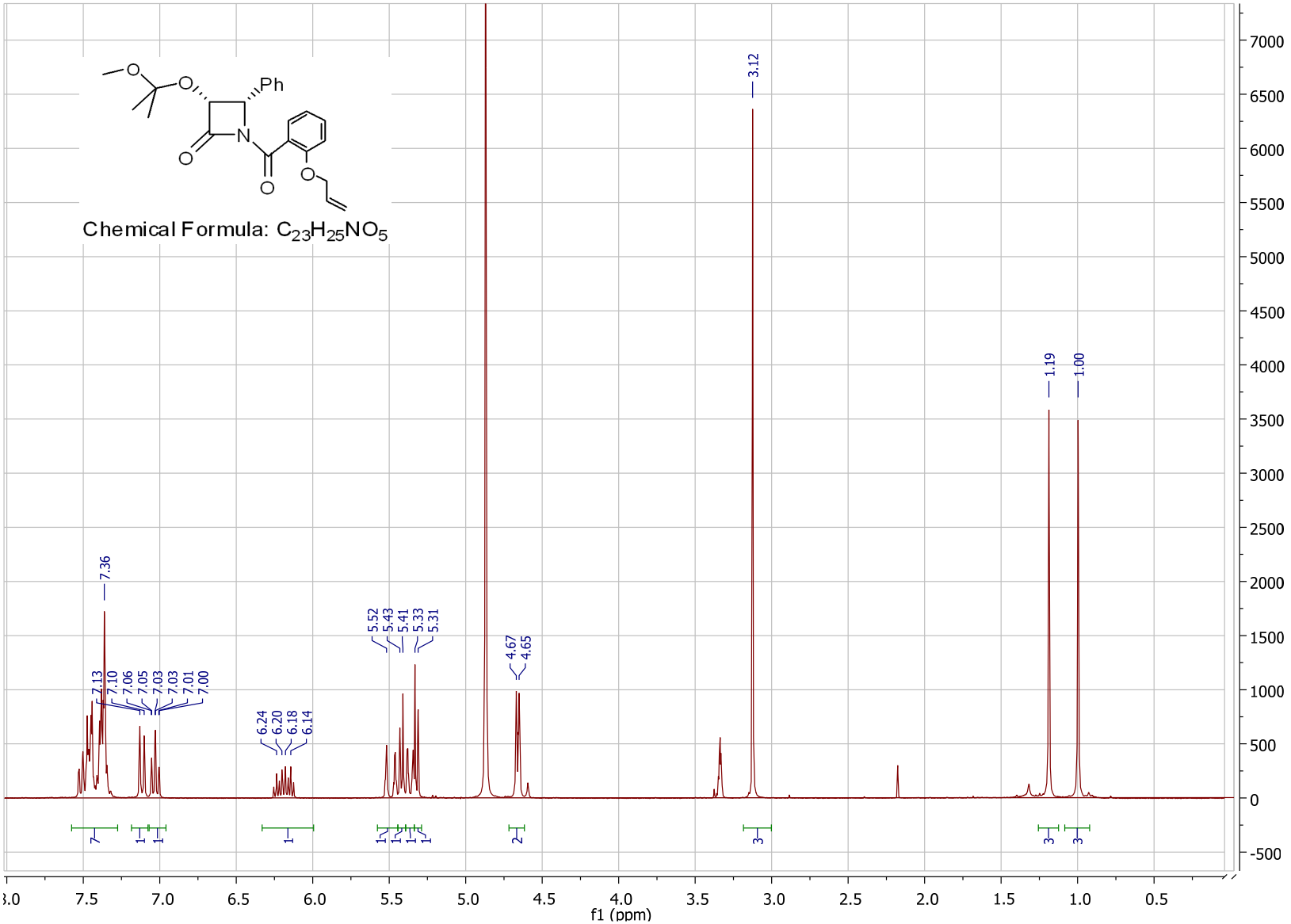

^{1}H NMR Spectrum of **3-24**

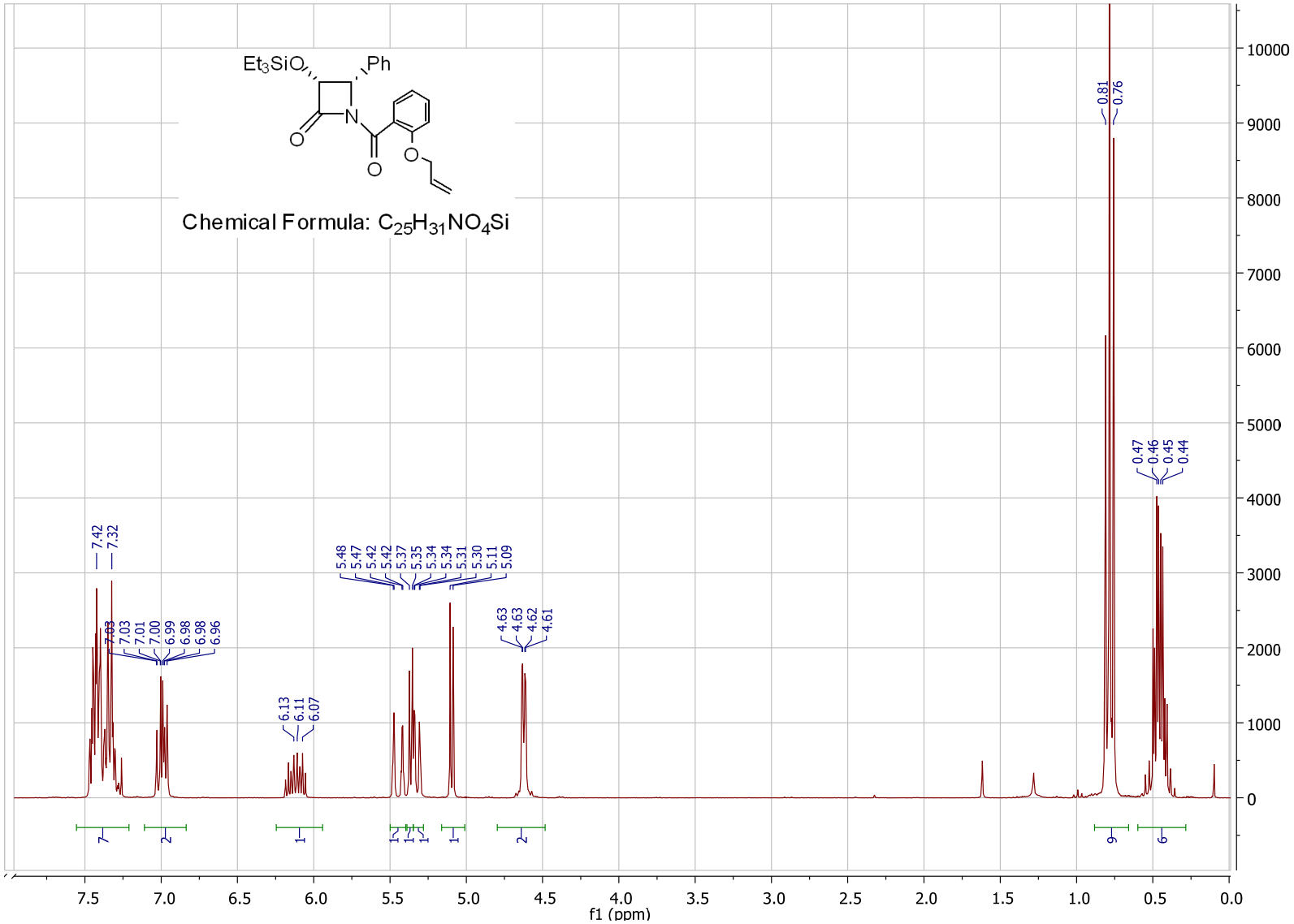

^{13}C NMR Spectrum of **3-24**

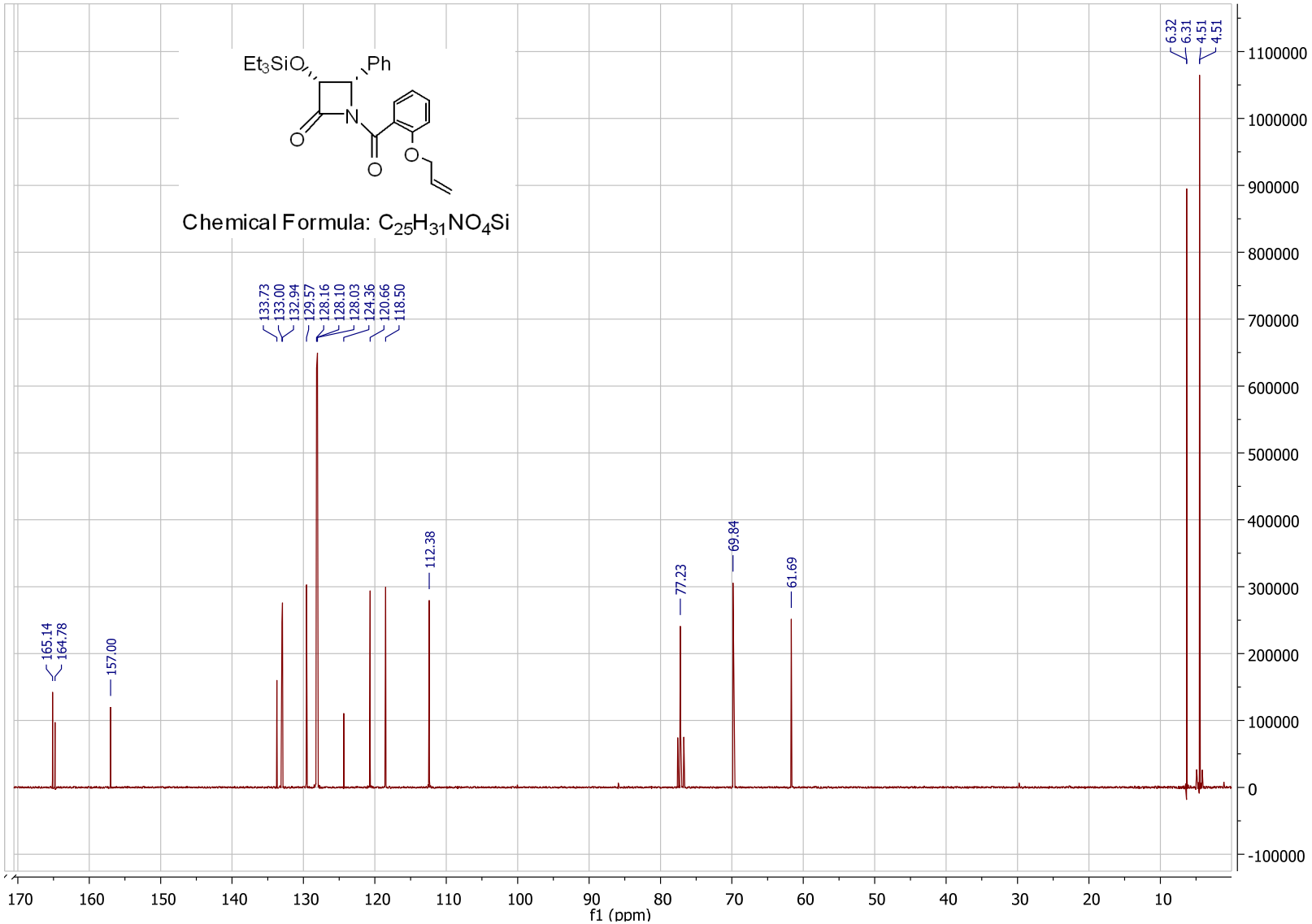

^{1}H NMR Spectrum of **3-25**

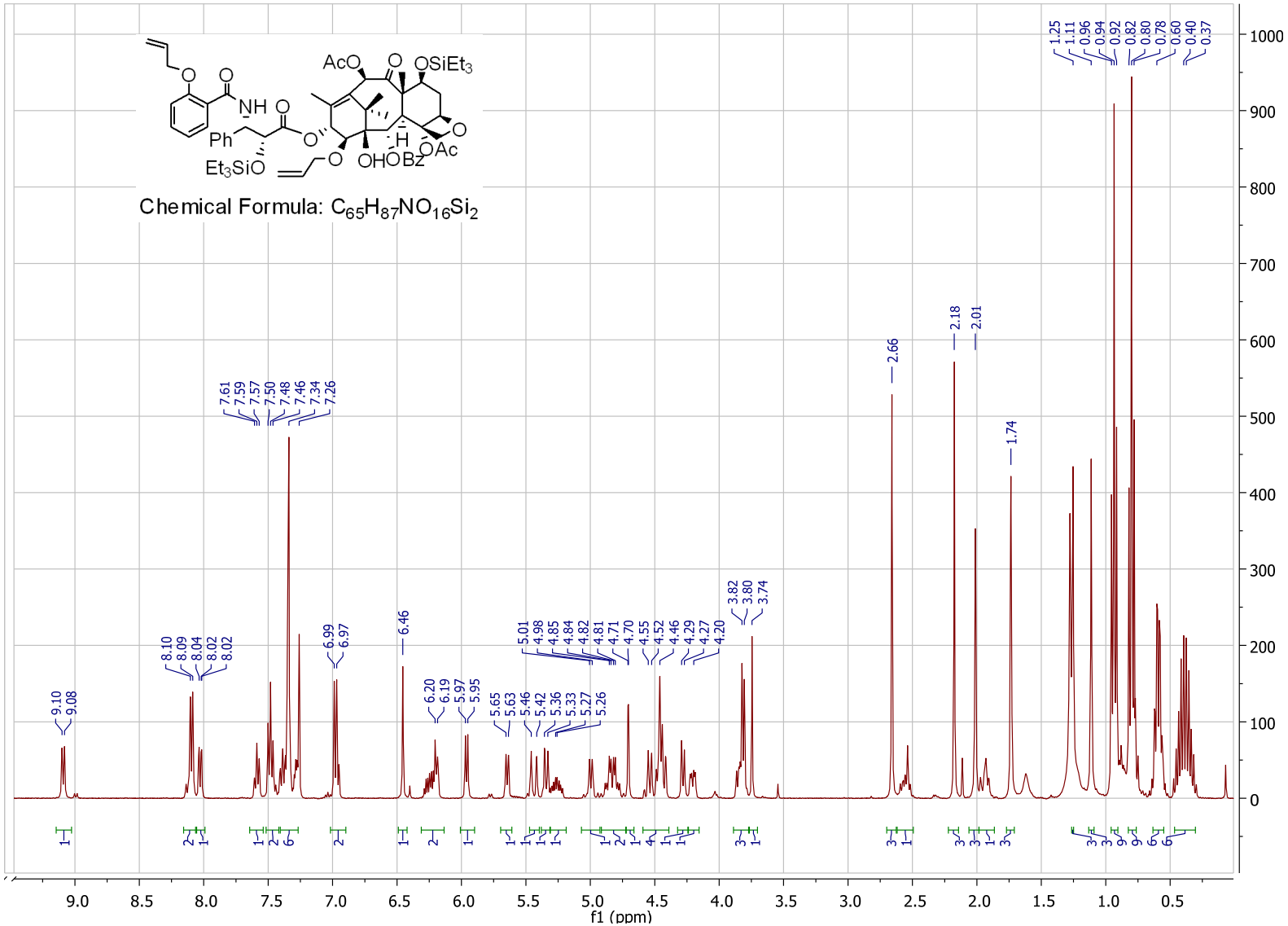

^{13}C NMR Spectrum of **3-25**

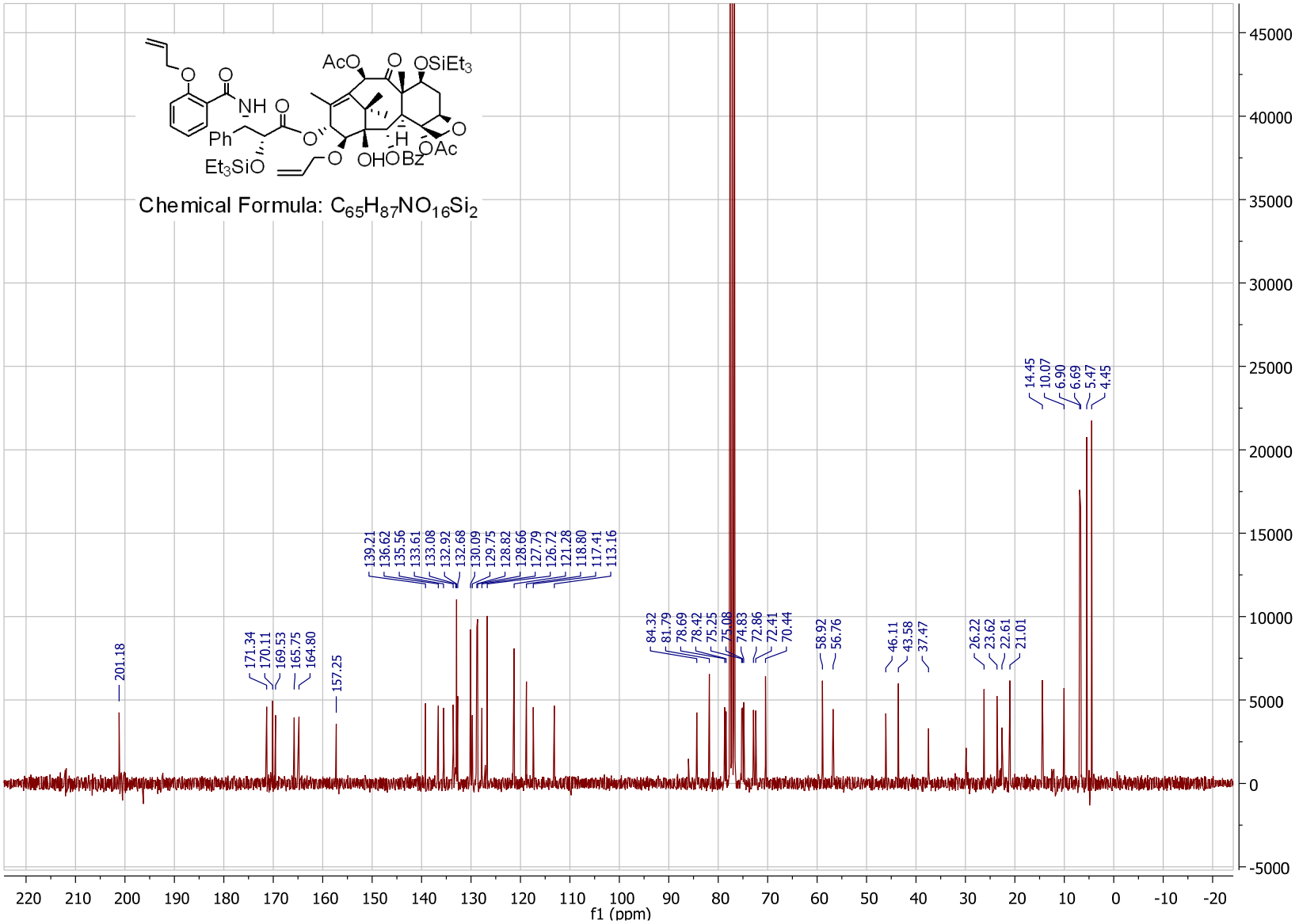

^{1}H NMR Spectrum of **3-26a**

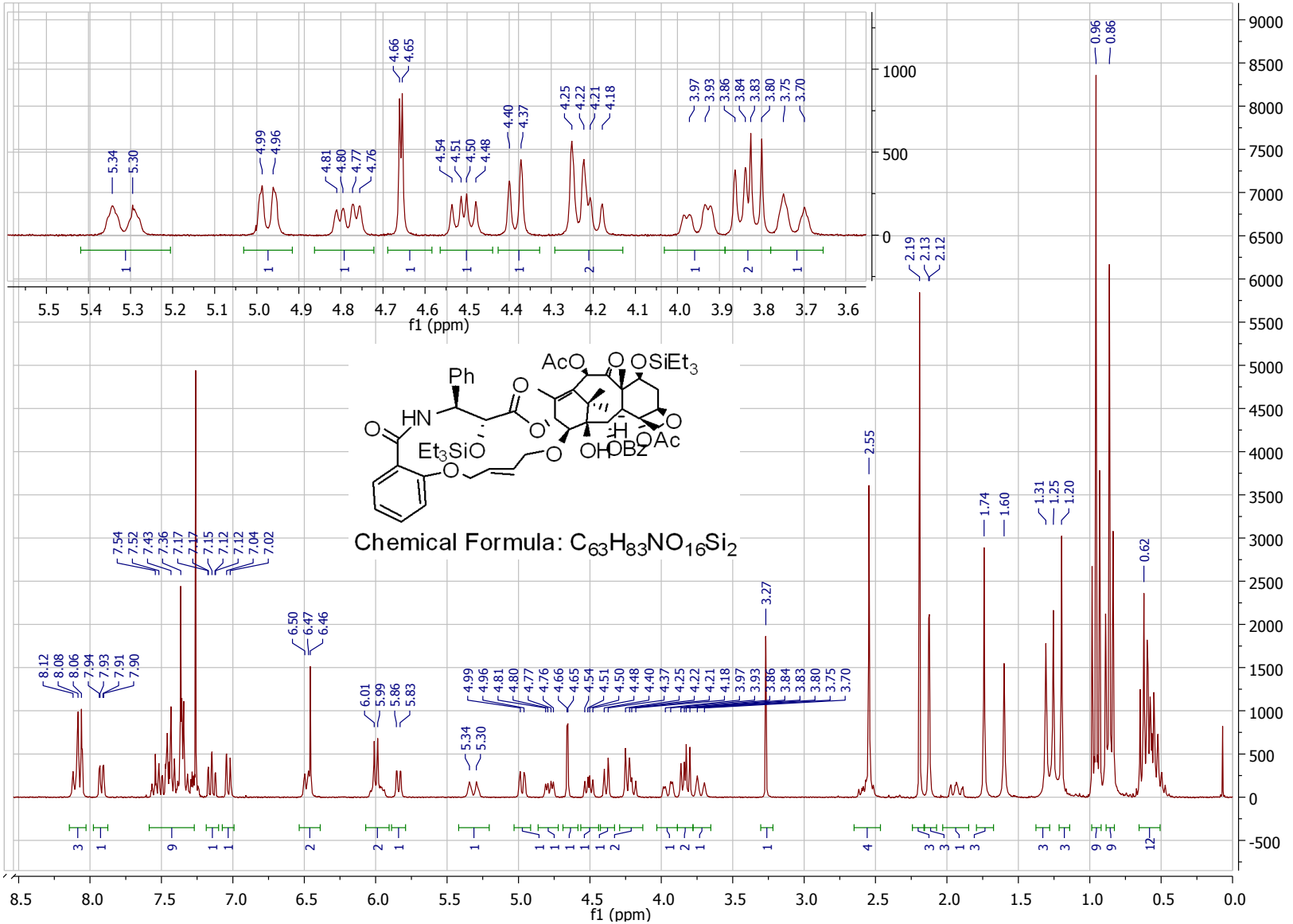

^{1}H NMR Spectrum of **3-26b**

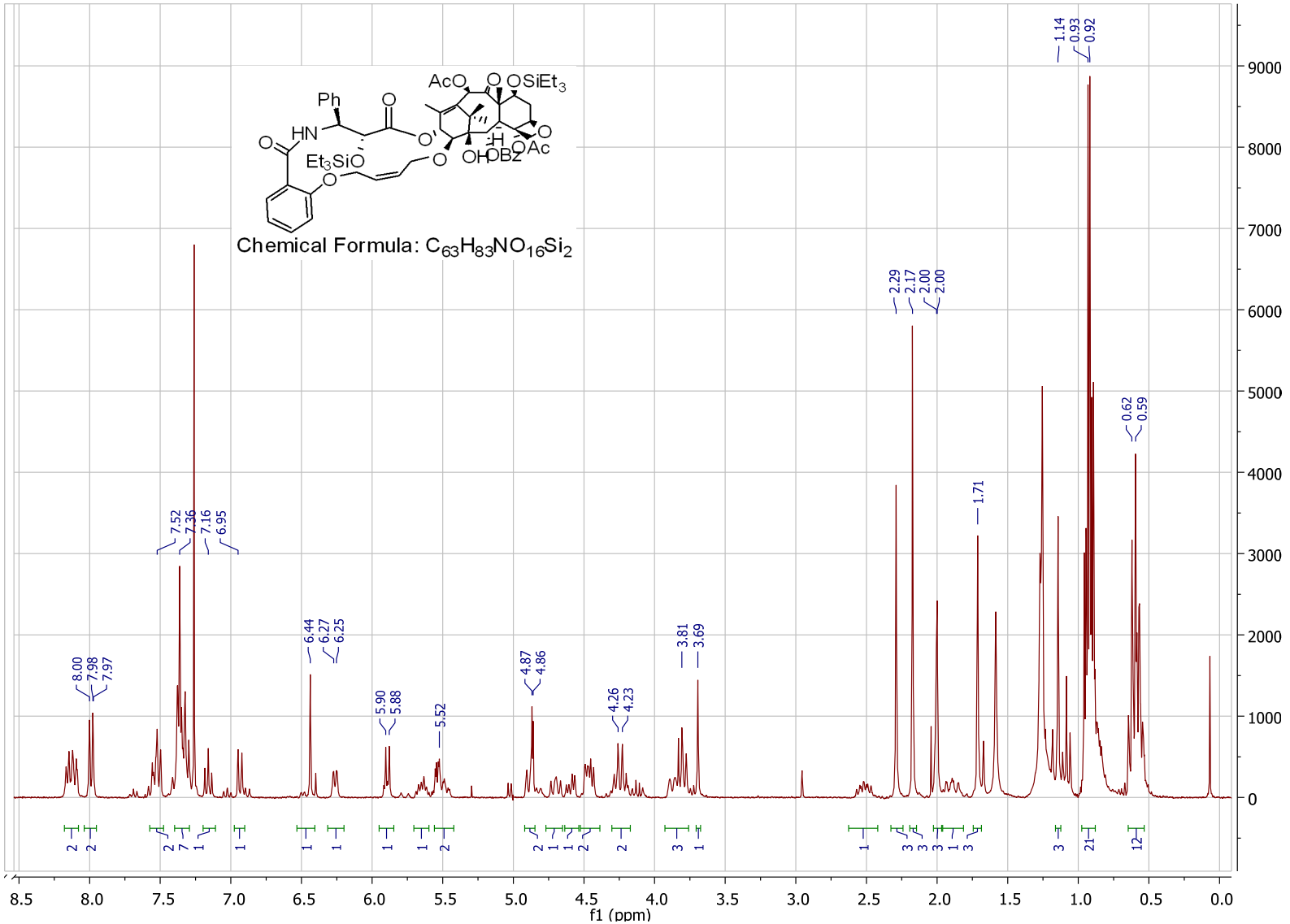

^{1}H NMR Spectrum of **3-27a** (*E*)-**SB-T-2055**

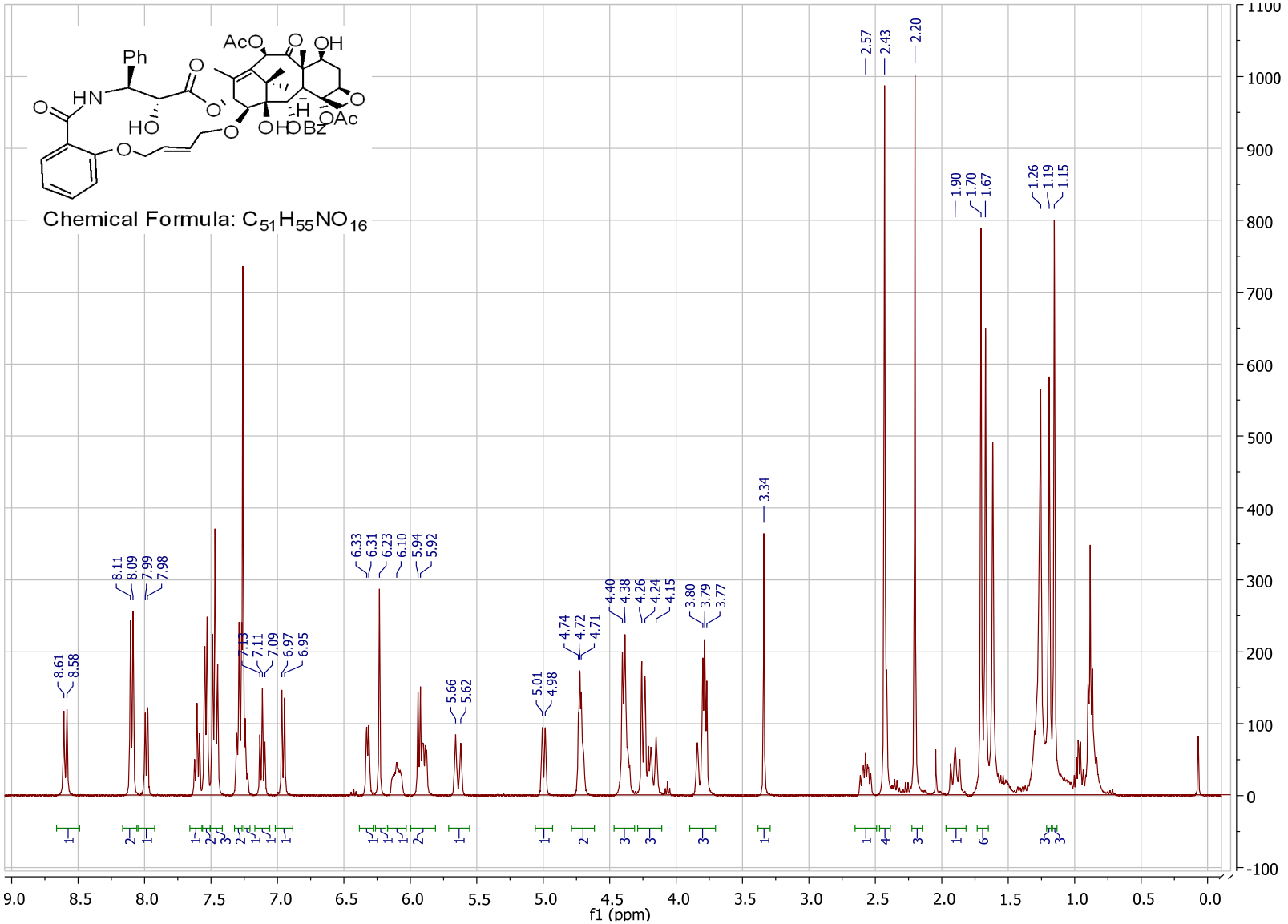

^{13}C NMR Spectrum of **3-27a** (*E*)-**SB-T-2055**

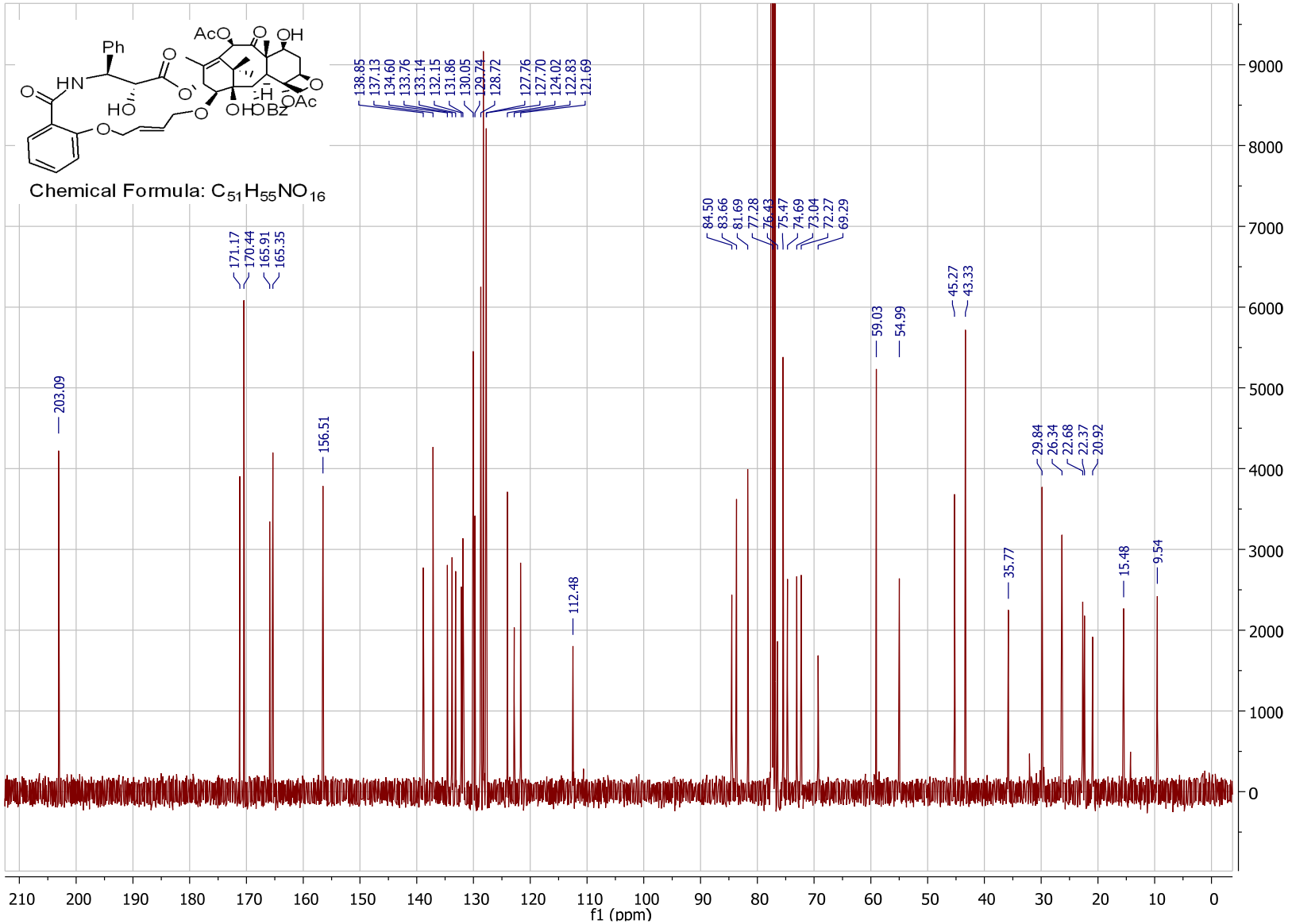

^{1}H NMR Spectrum of **3-27b** (*Z*)-**SB-T-2055**

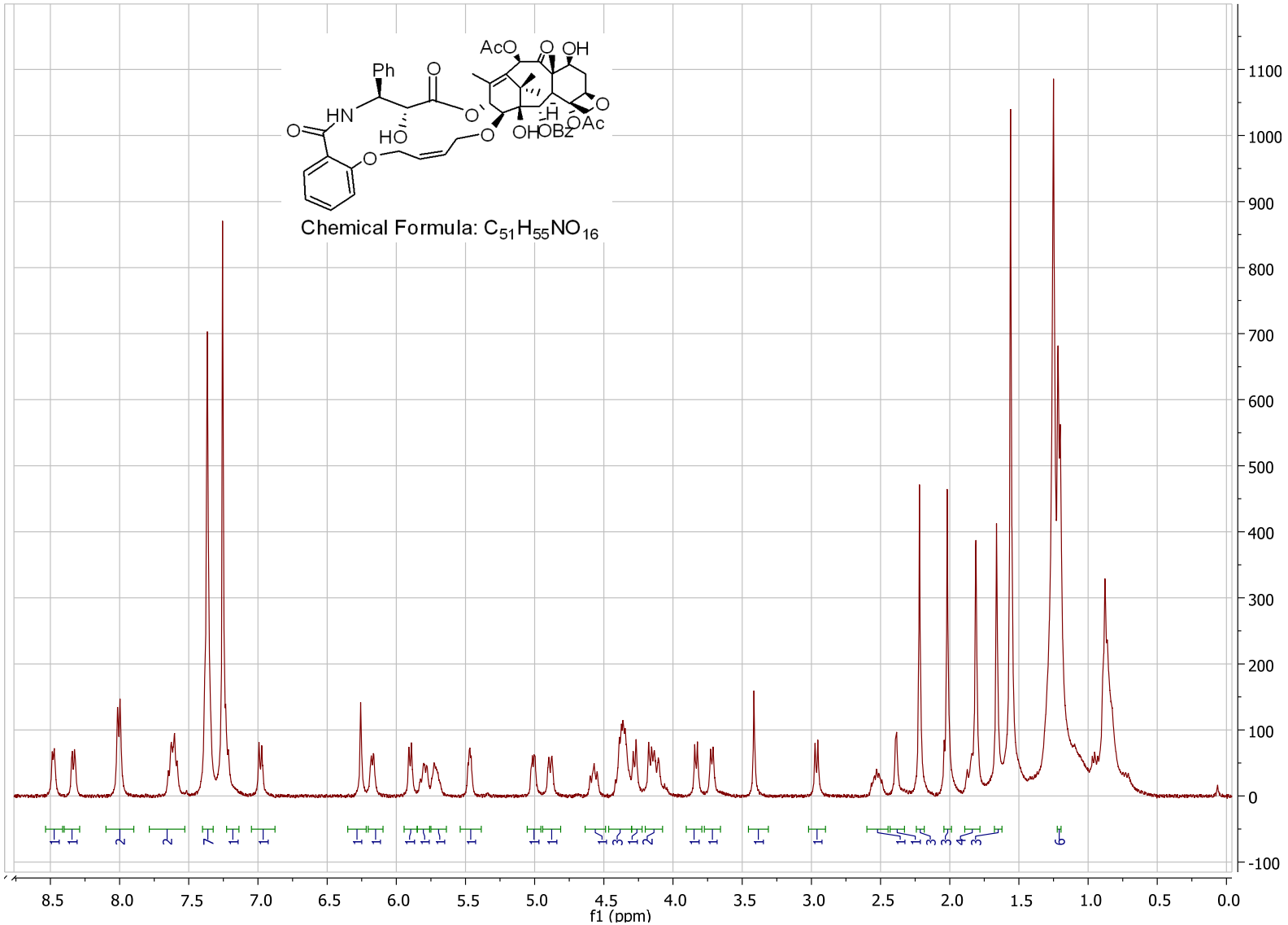

^{13}C NMR Spectrum of **3-27b** (*Z*)-**SB-T-2055**

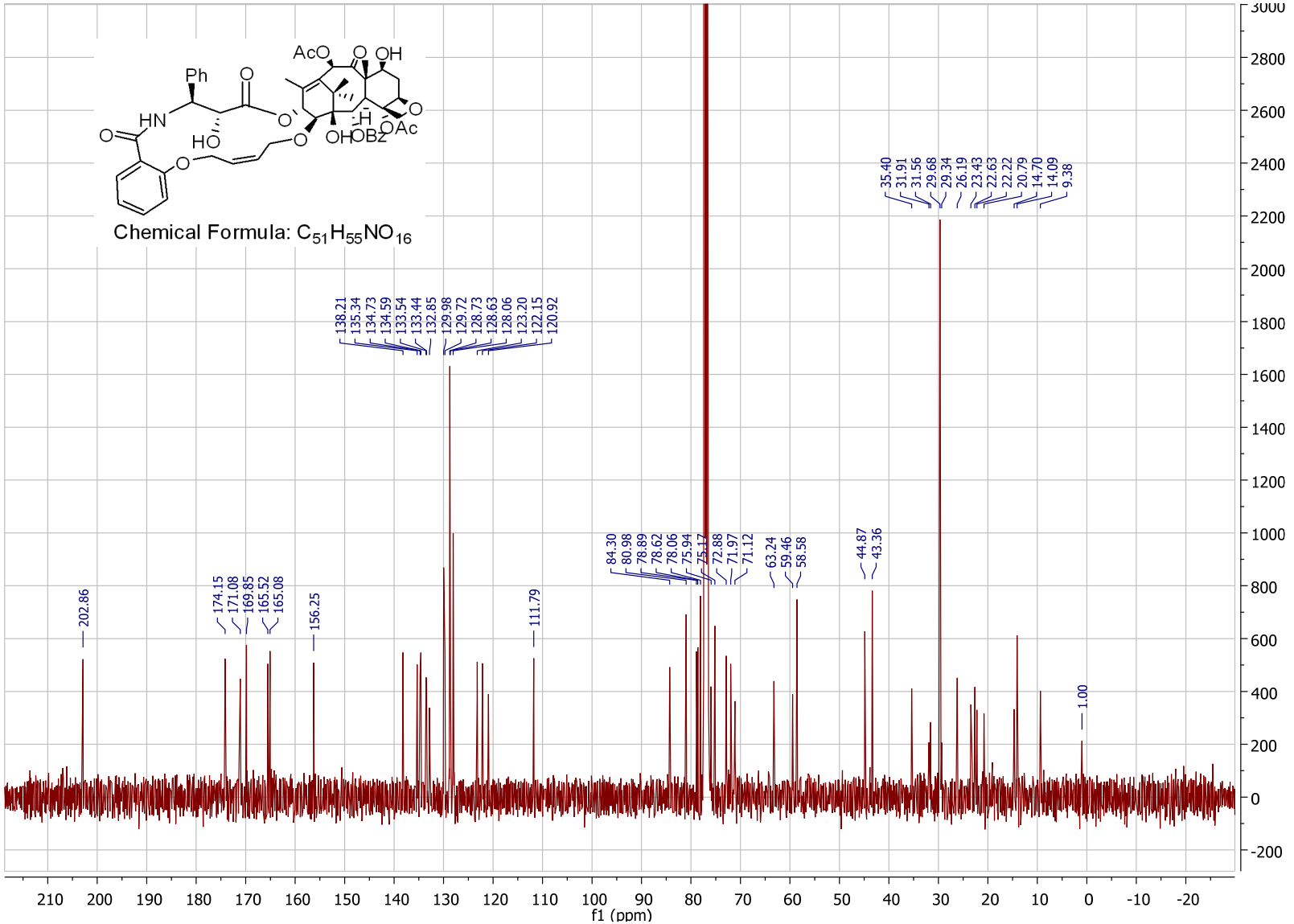

^{1}H NMR Spectrum of **4-6**

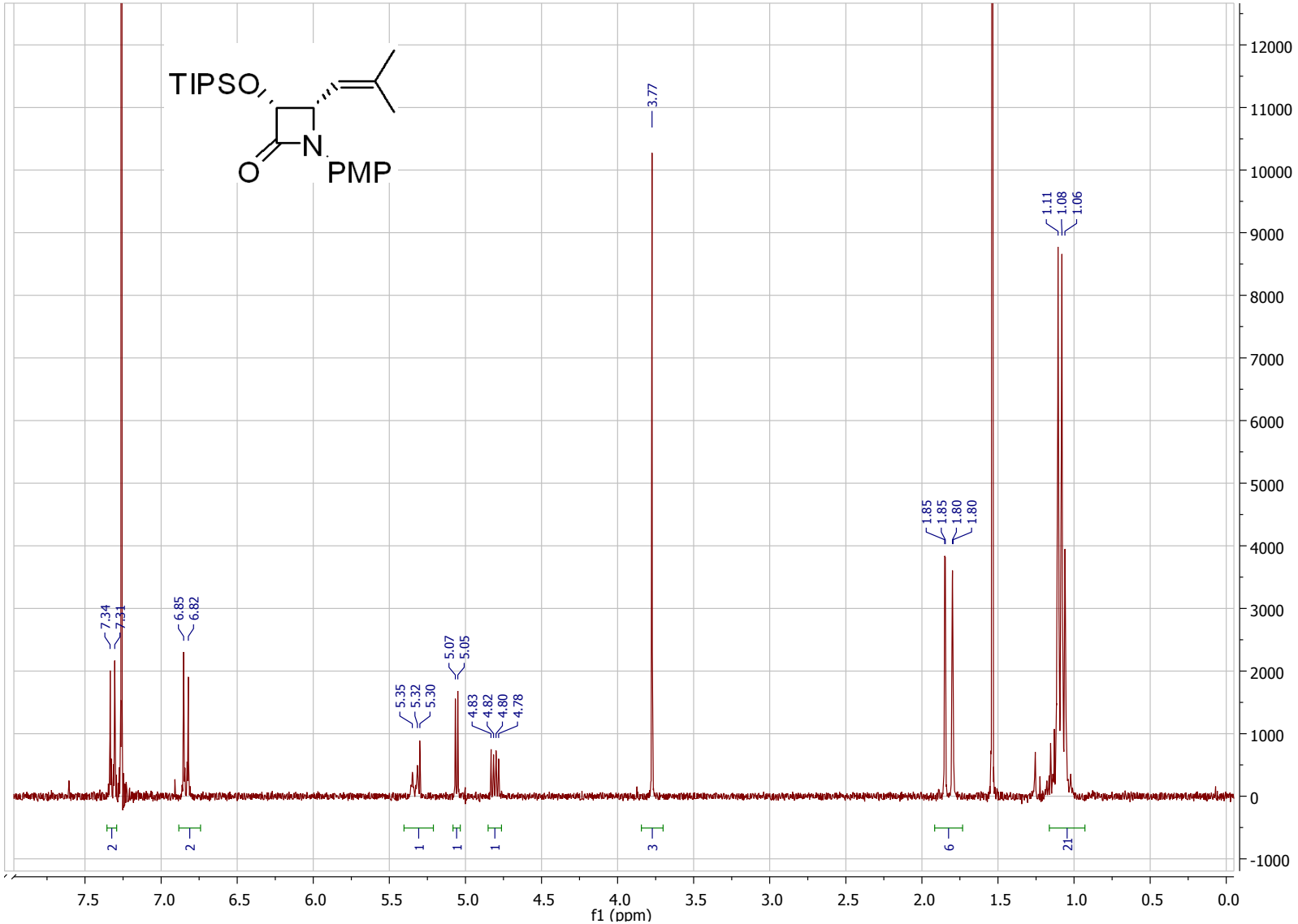

^{1}H NMR Spectrum of **4-7**

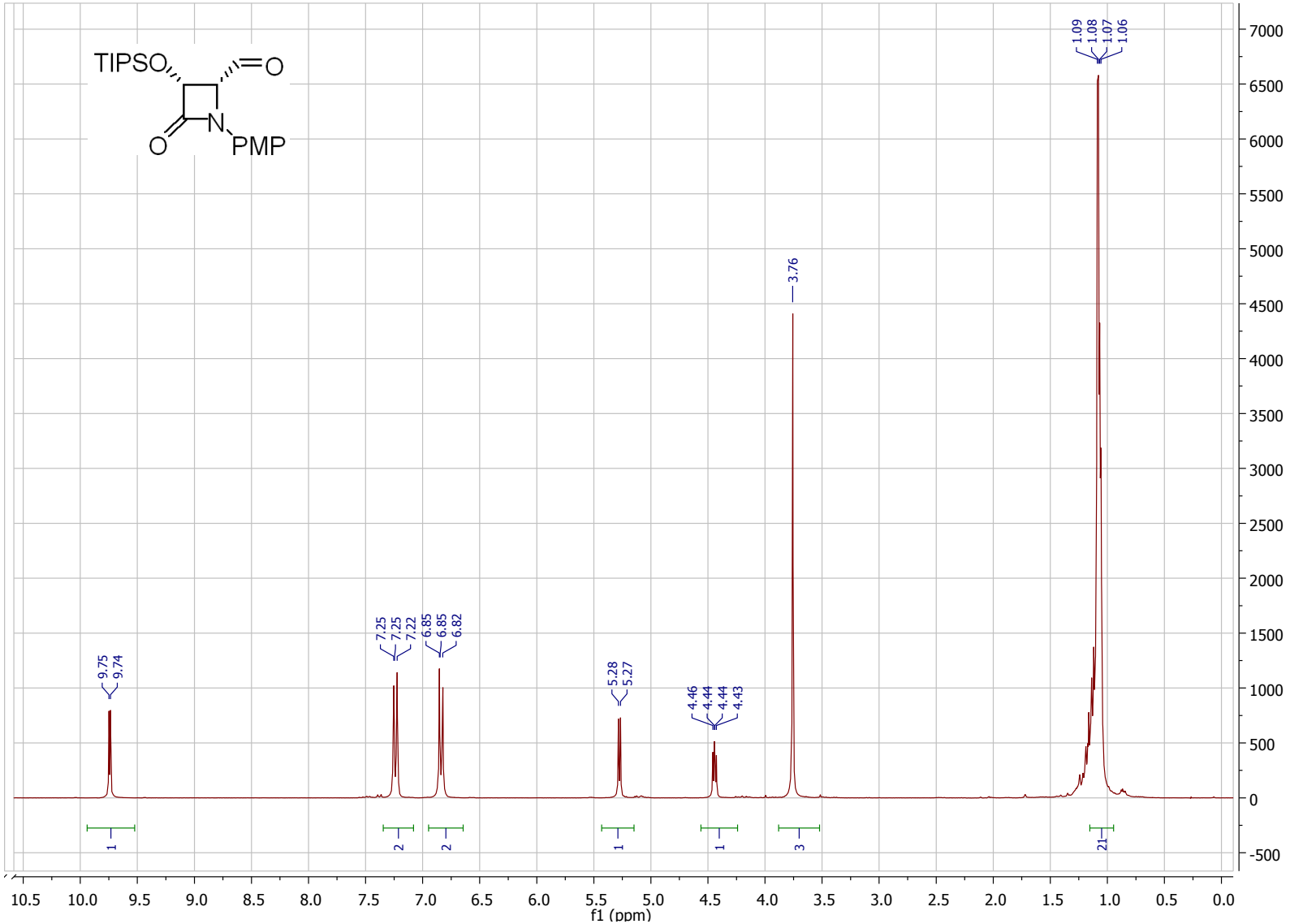

^{1}H NMR Spectrum of **4-8**

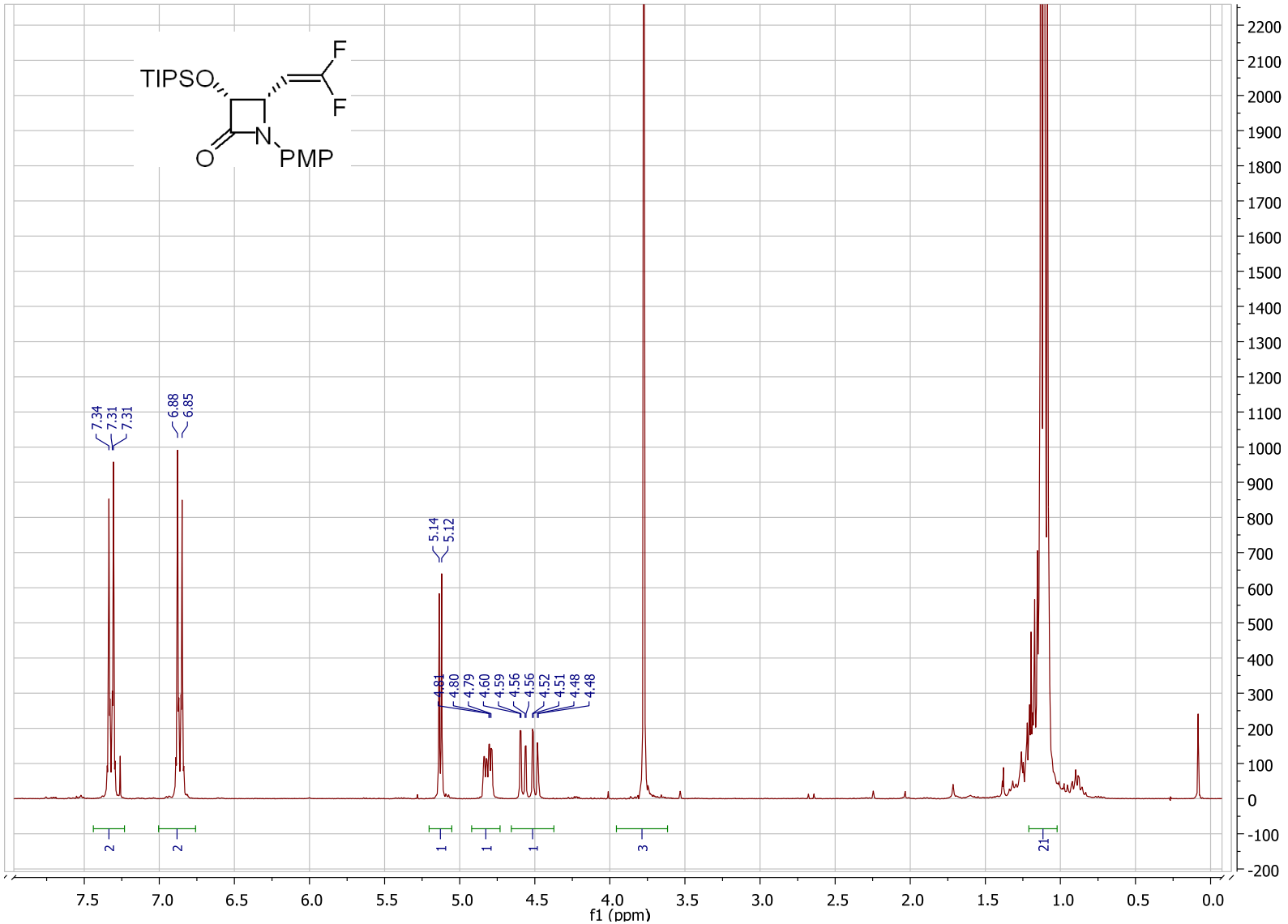

^{1}H NMR Spectrum of **4-9**

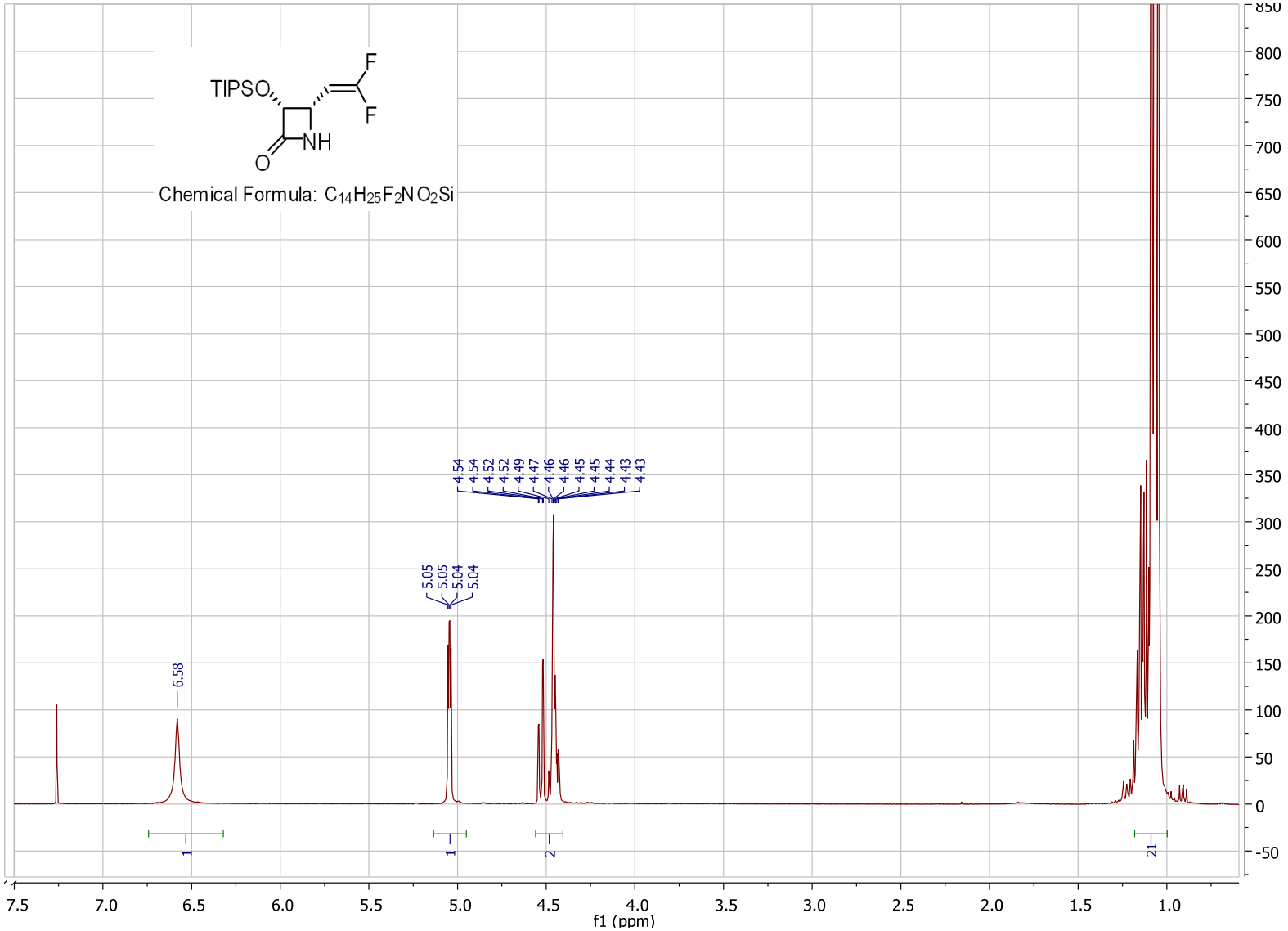

^{1}H NMR Spectrum of **4-10**

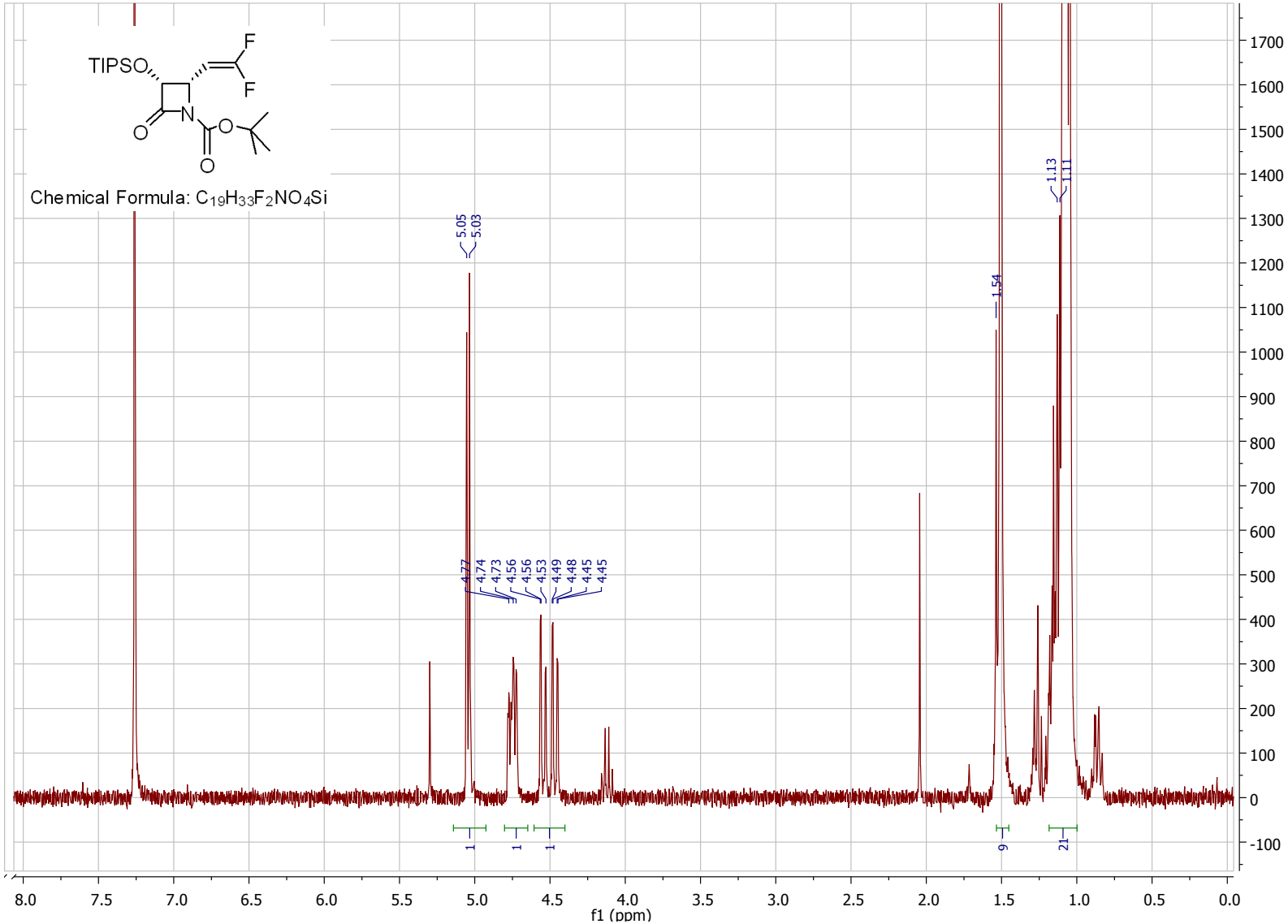

^{1}H NMR Spectrum of **4-11**

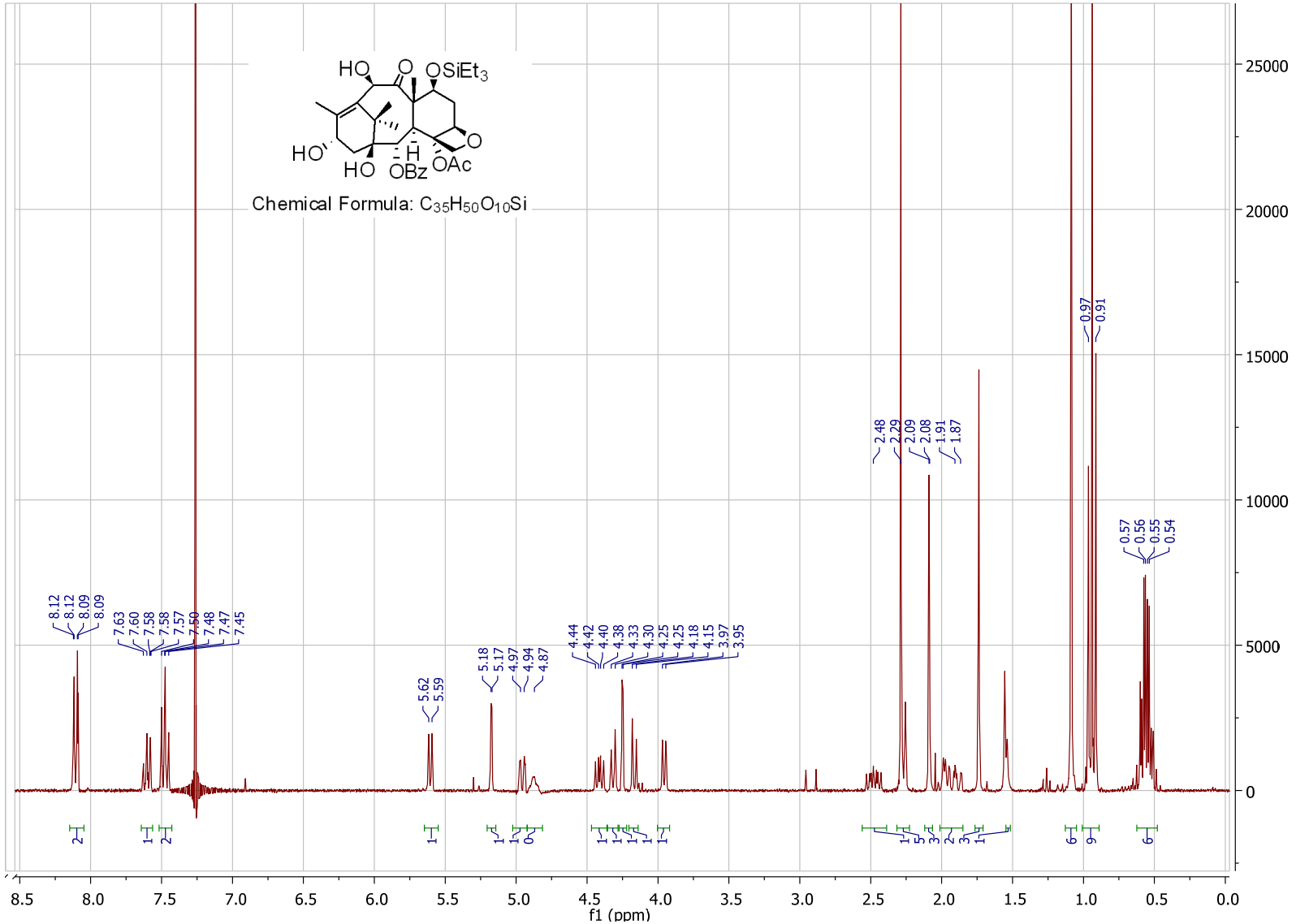

^{1}H NMR Spectrum of **4-12**

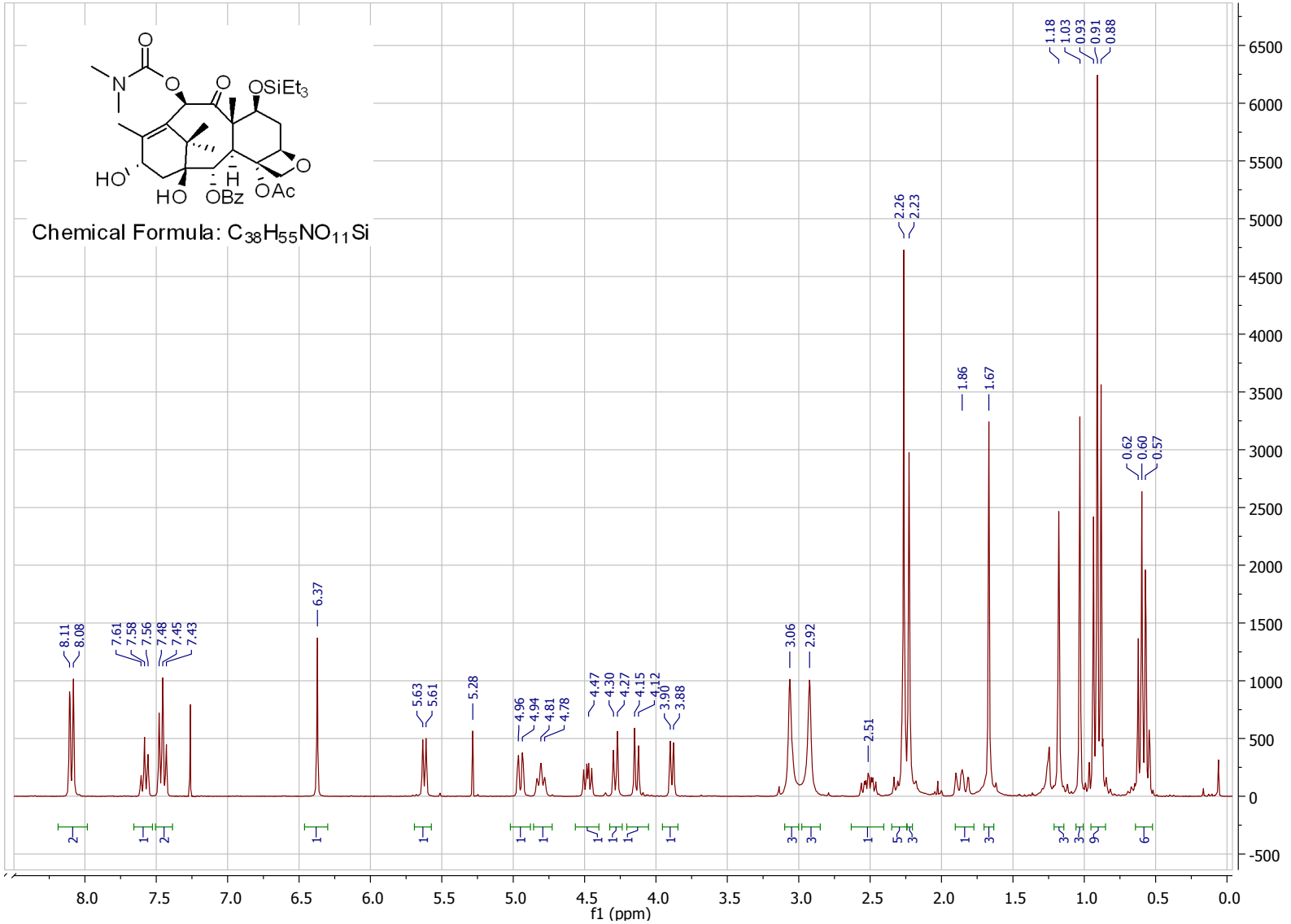

^{1}H NMR Spectrum of **4-13**

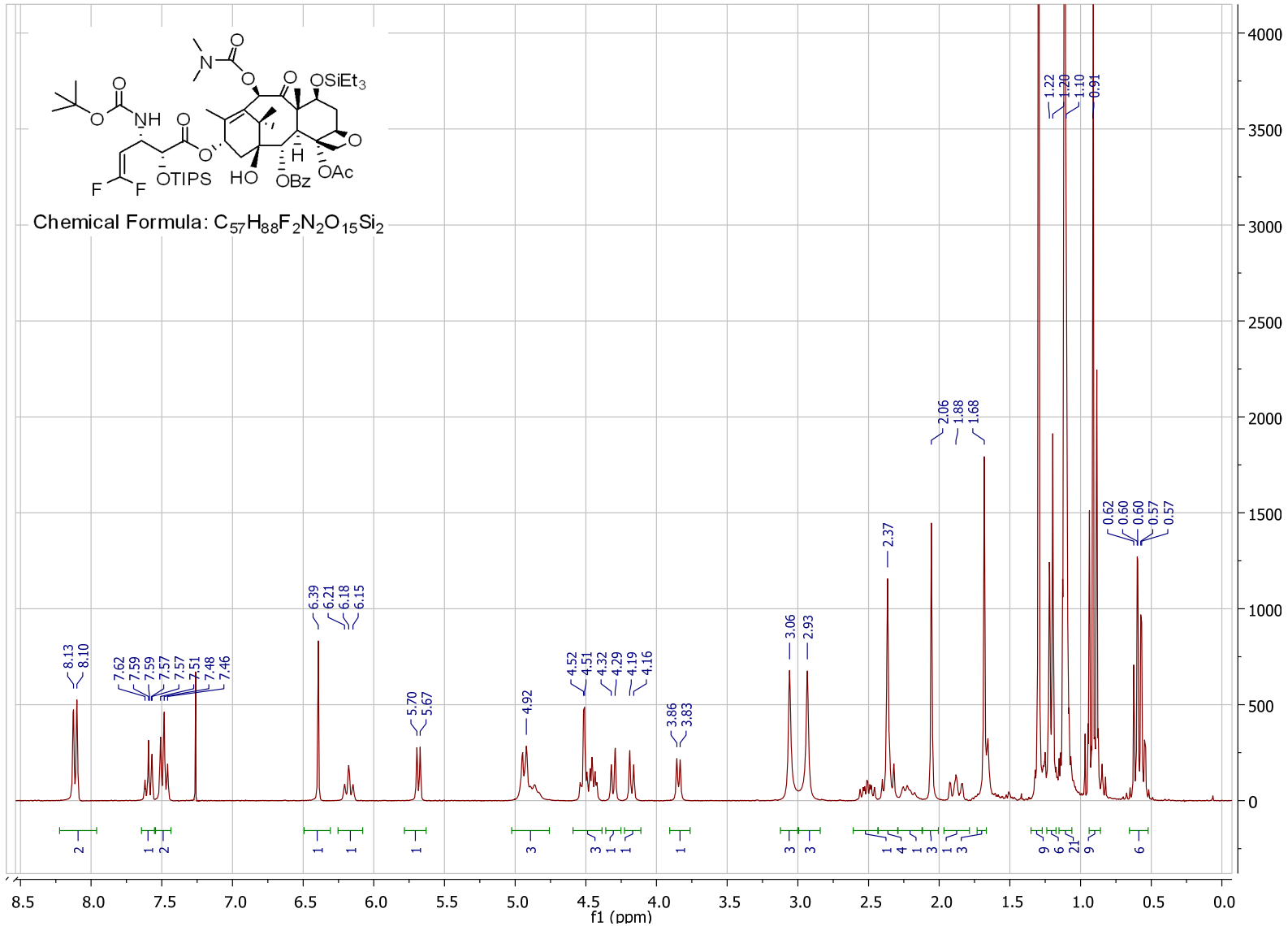

^{1}H NMR Spectrum of **4-14**

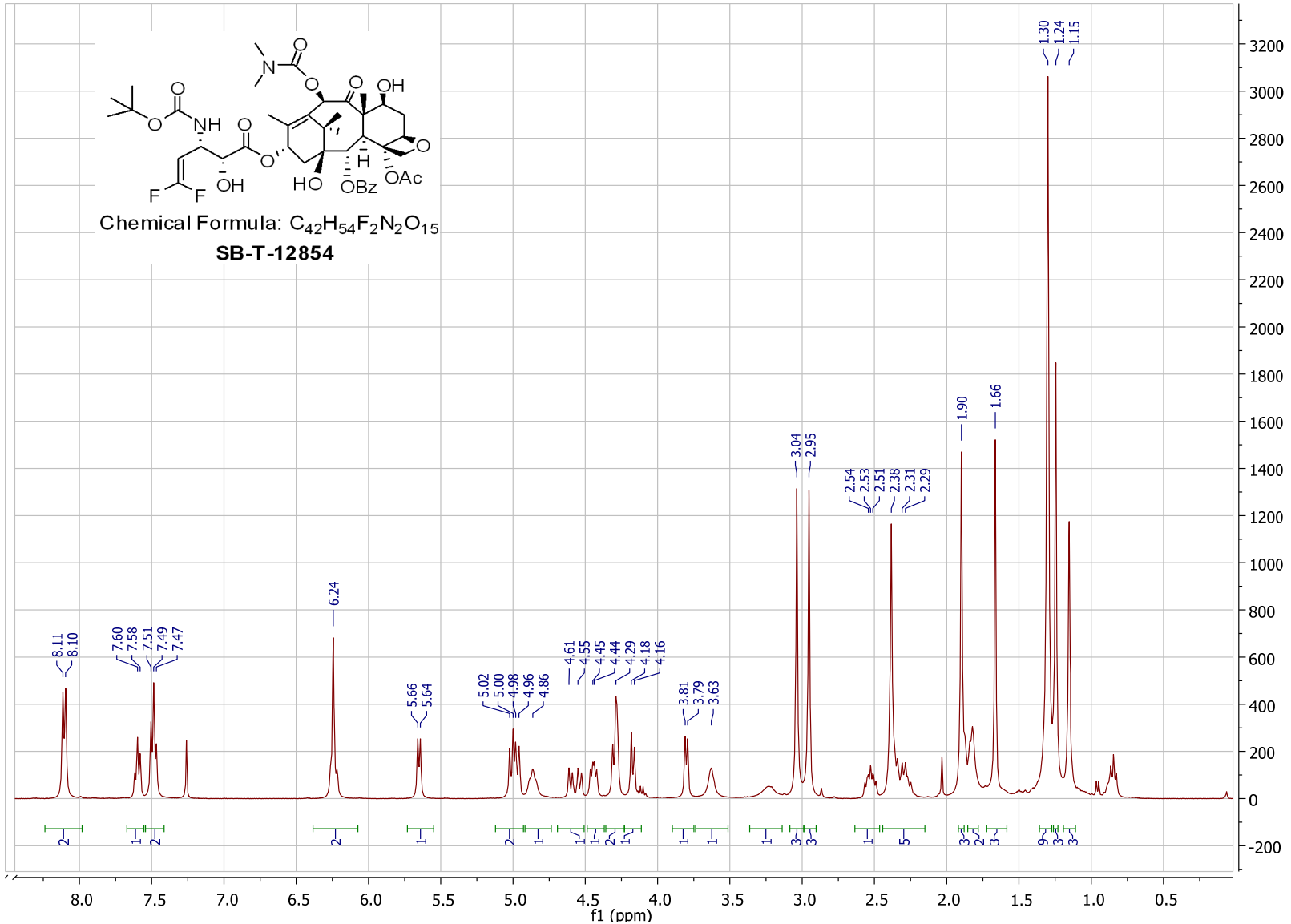

^{1}H NMR Spectrum of **4-15**

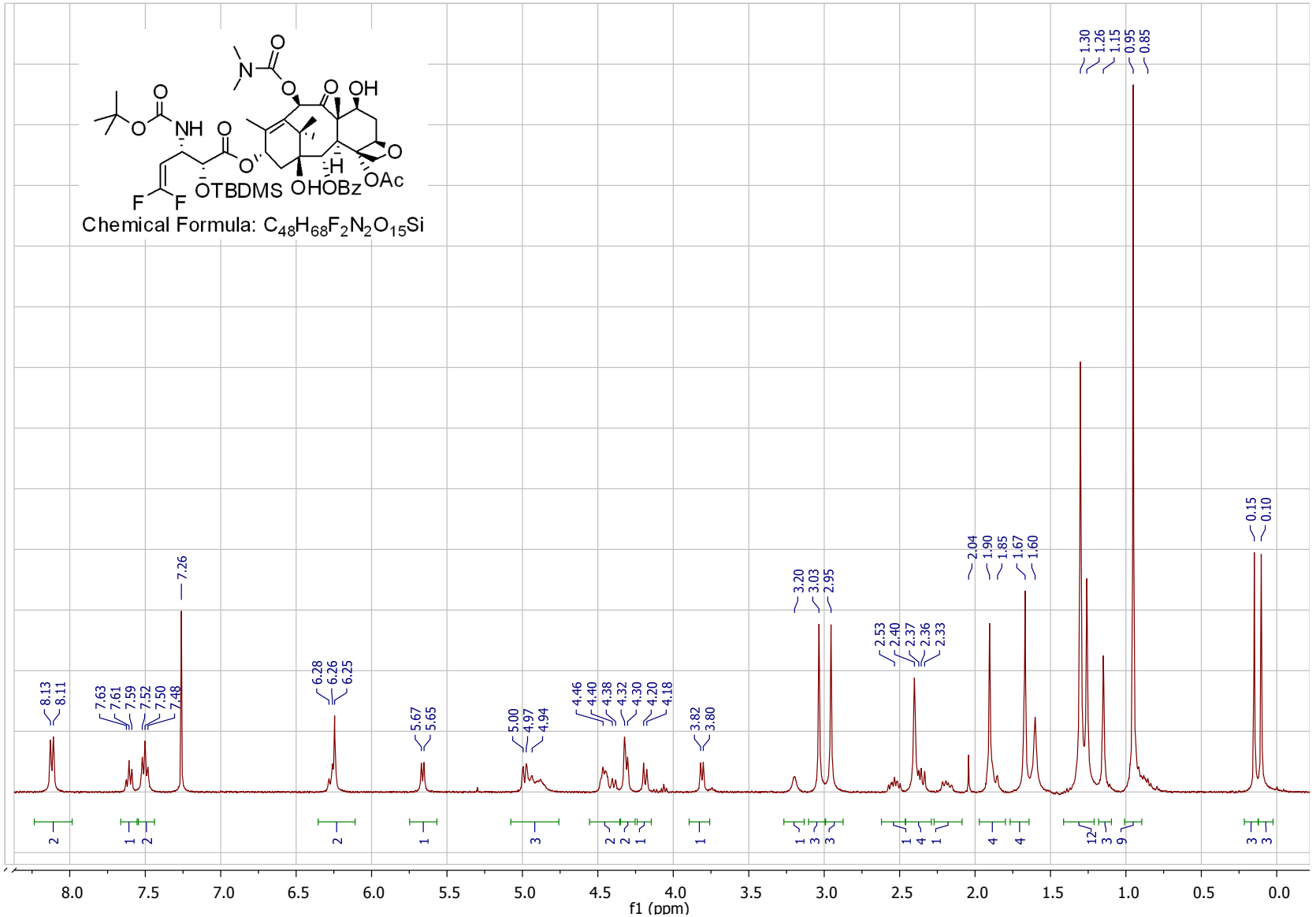

^{1}3C NMR Spectrum of **4-15**

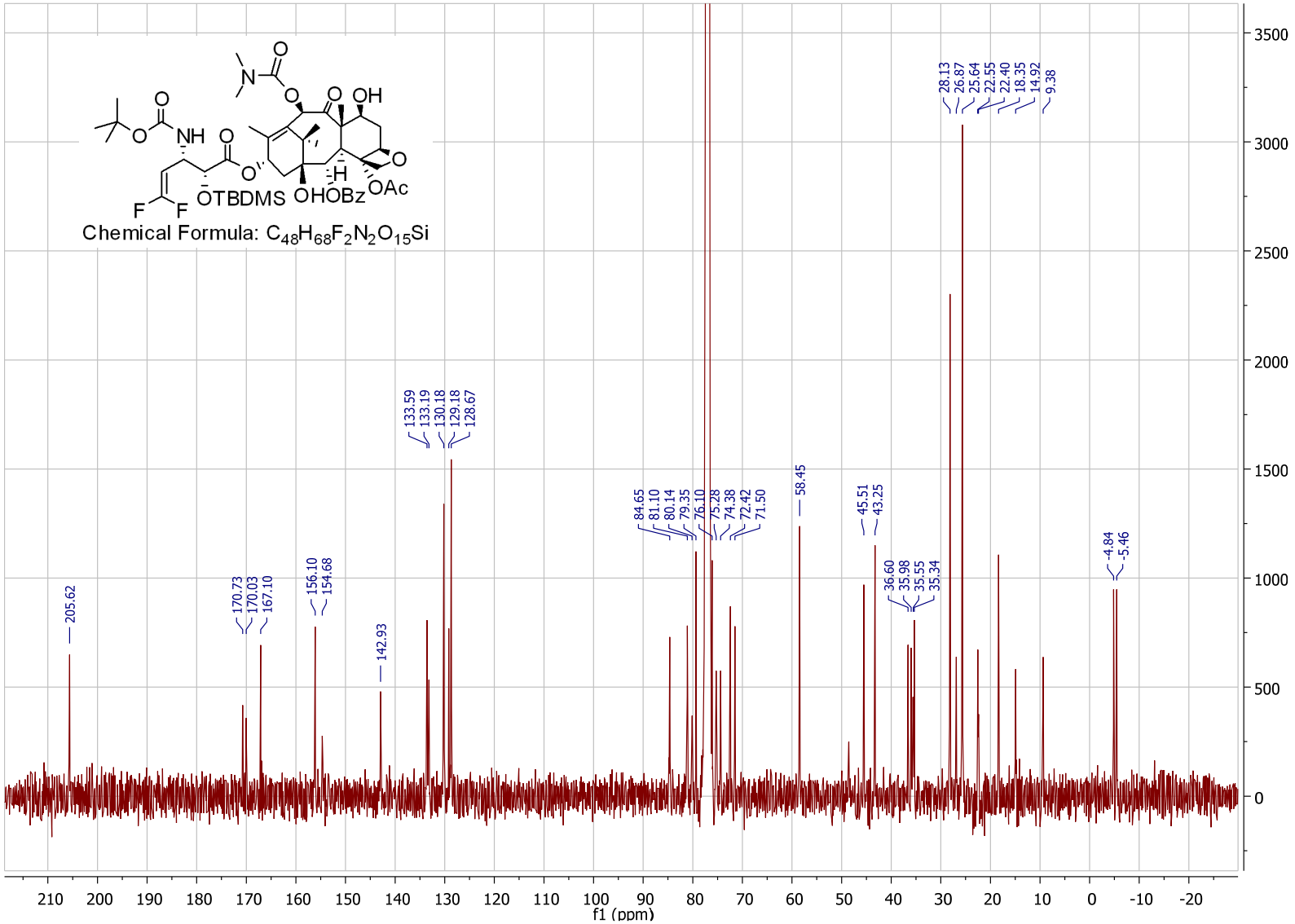

^{19}F NMR Spectrum of **4-15**

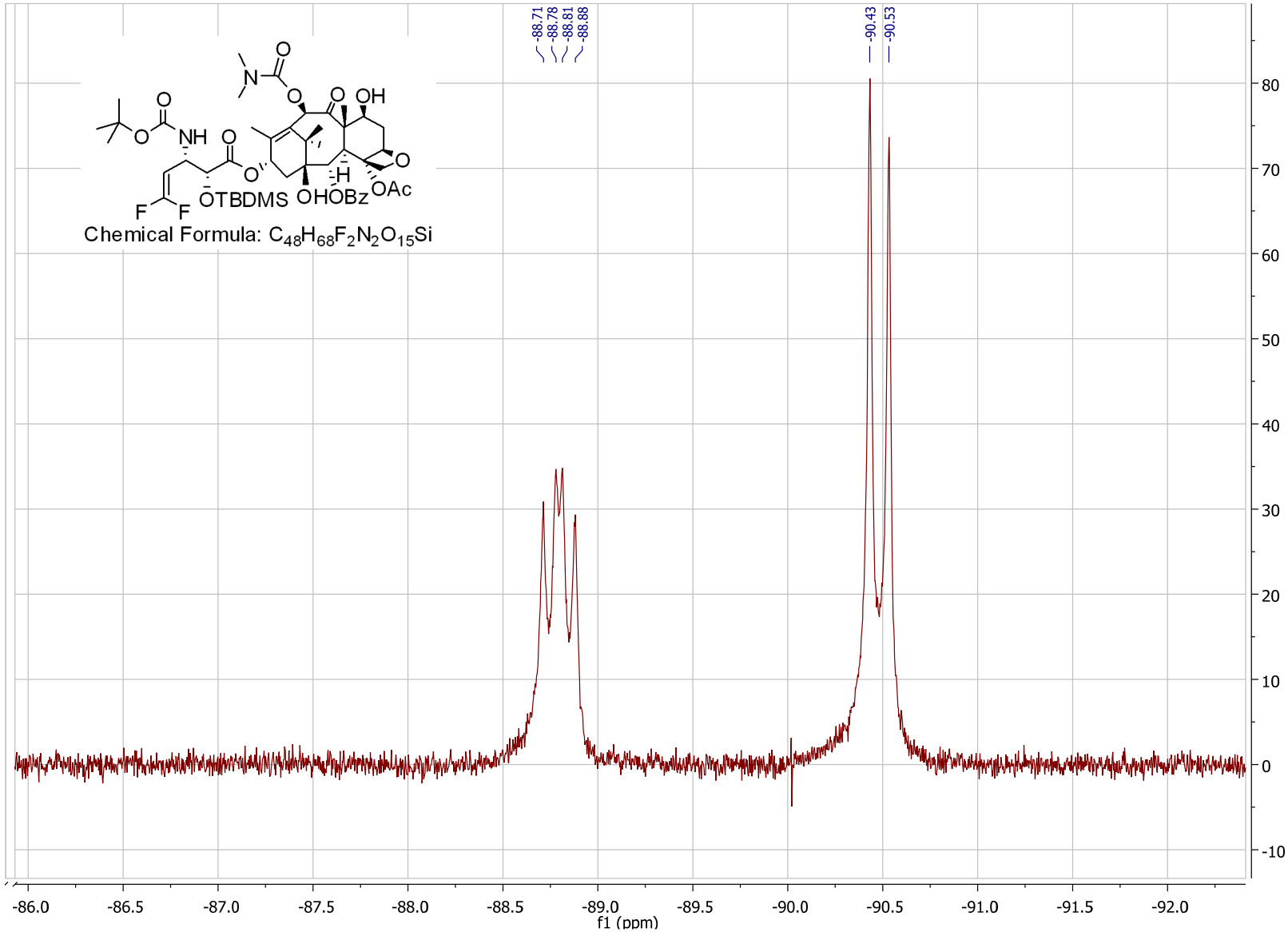

^{1}H NMR Spectrum of **4-16**

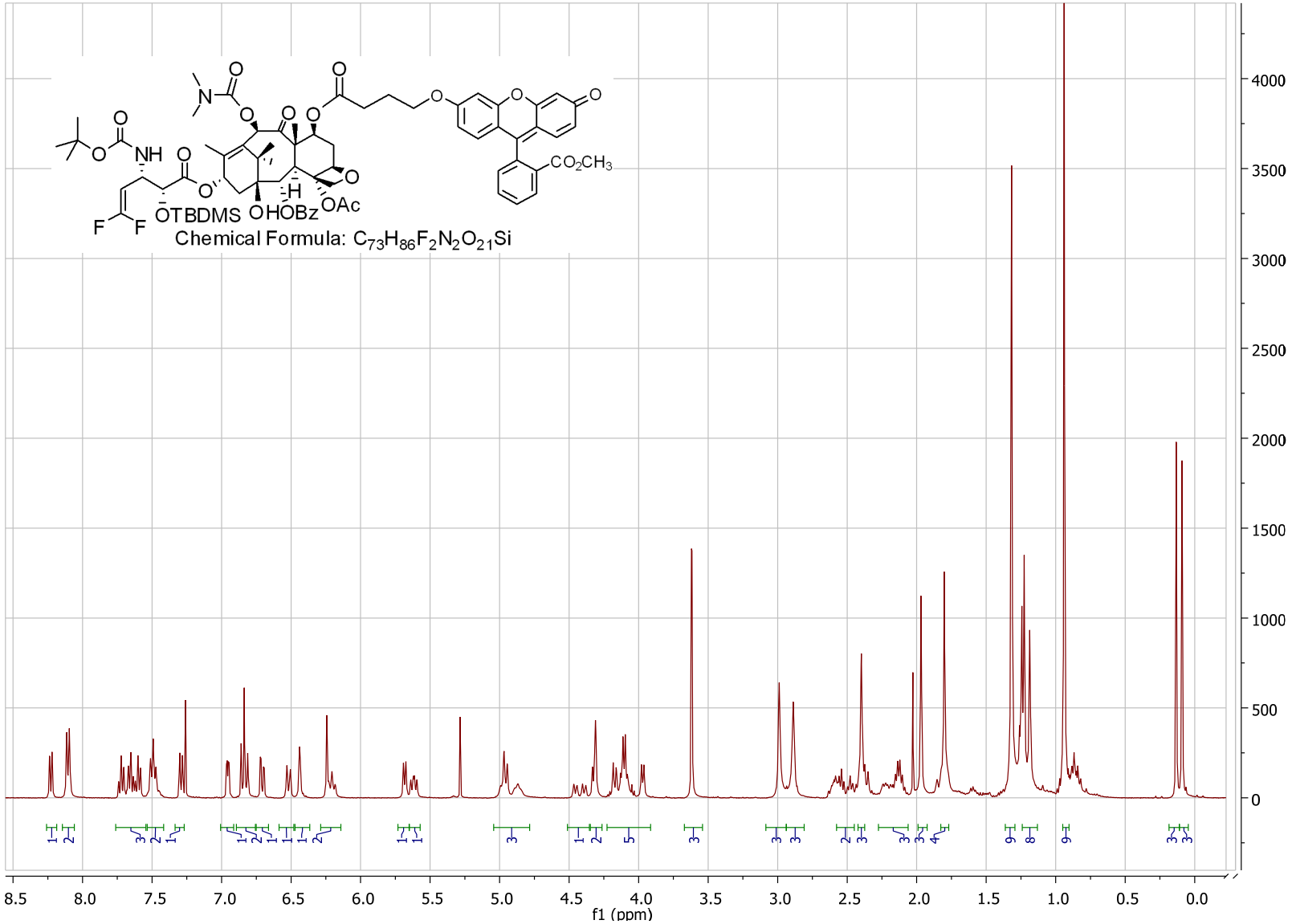

^{13}C NMR Spectrum of **4-16**

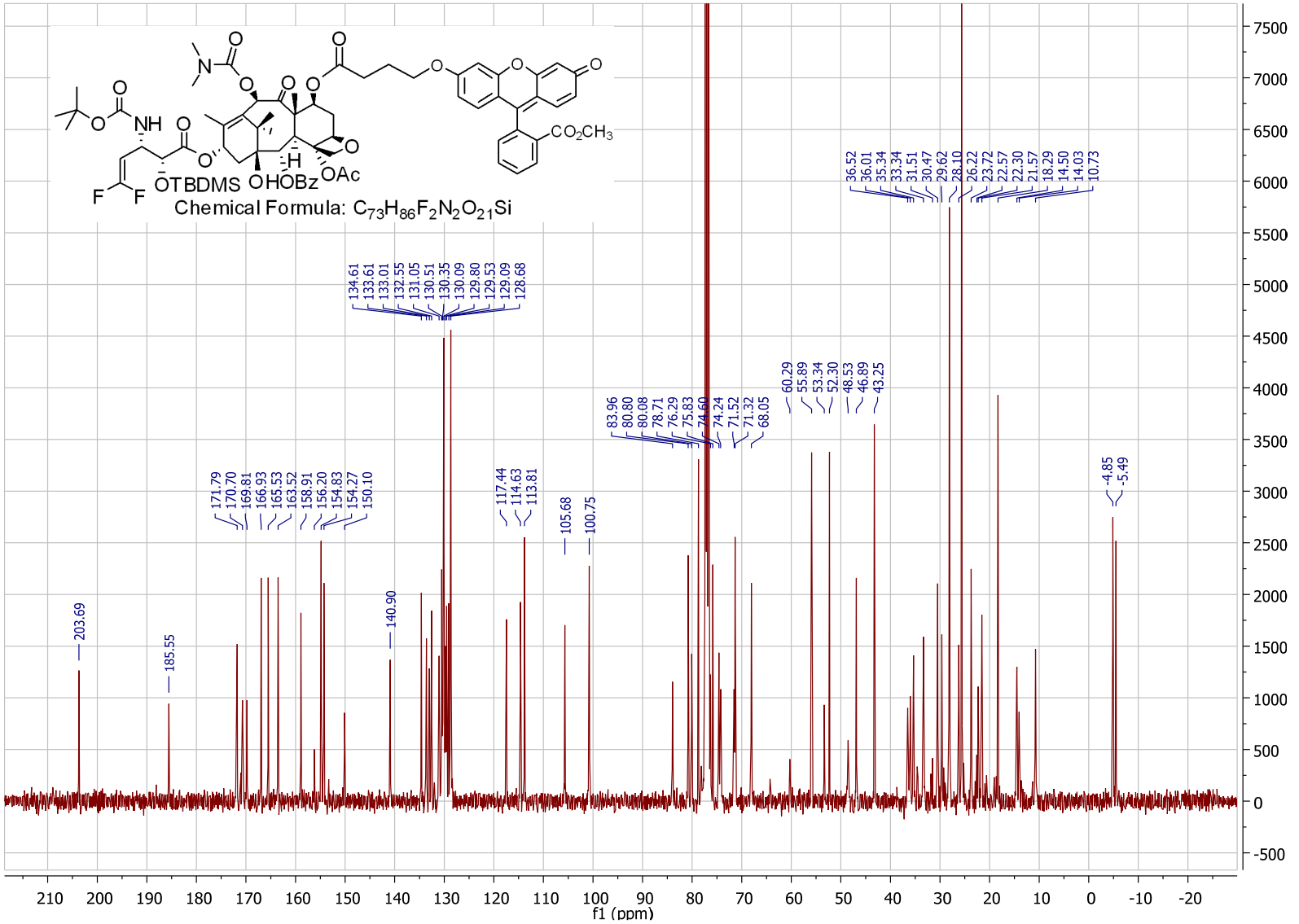

^{19}F NMR Spectrum of **4-16**

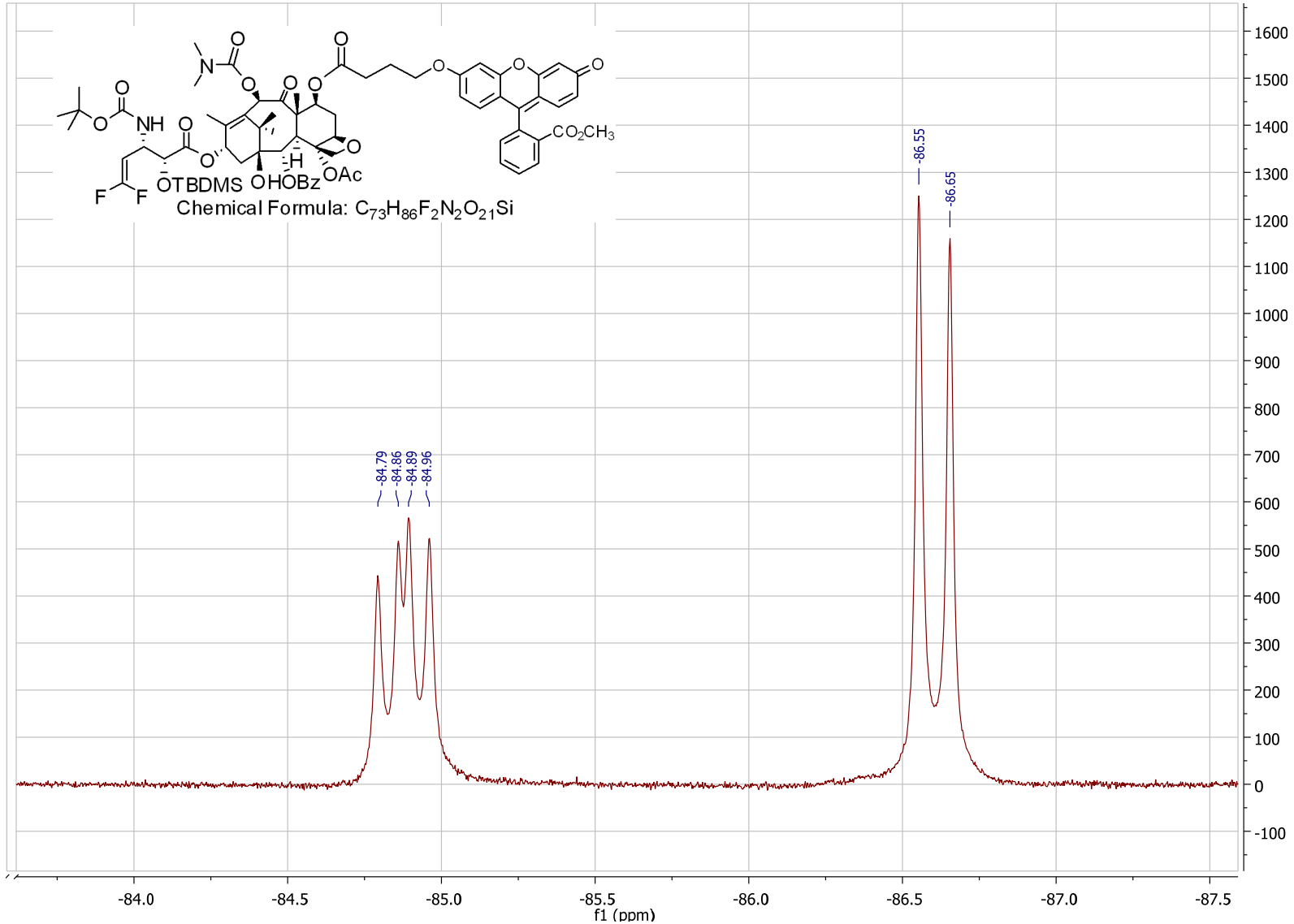

^{1}H NMR Spectrum of **4-17**

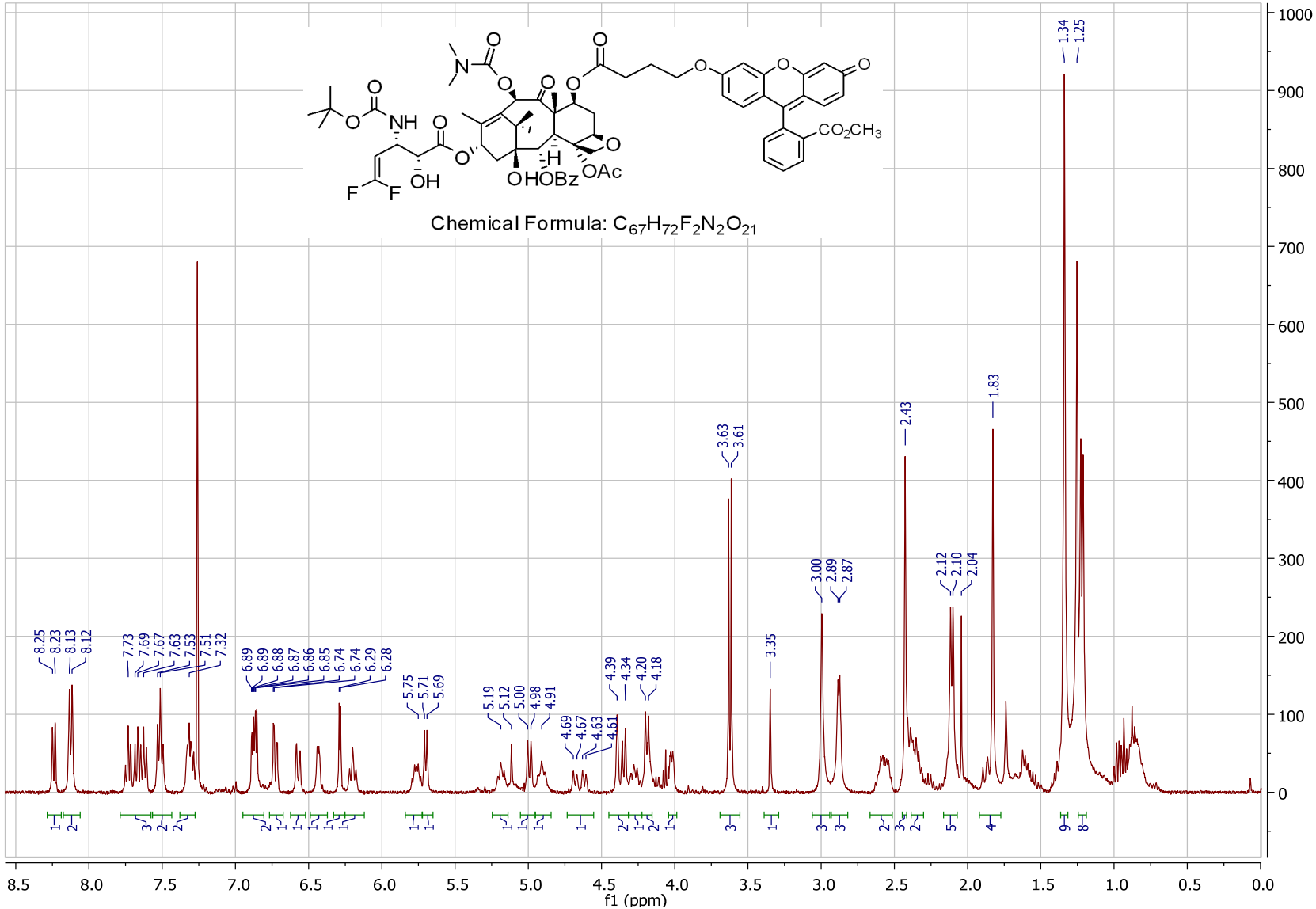

^{13}C NMR Spectrum of **4-17**

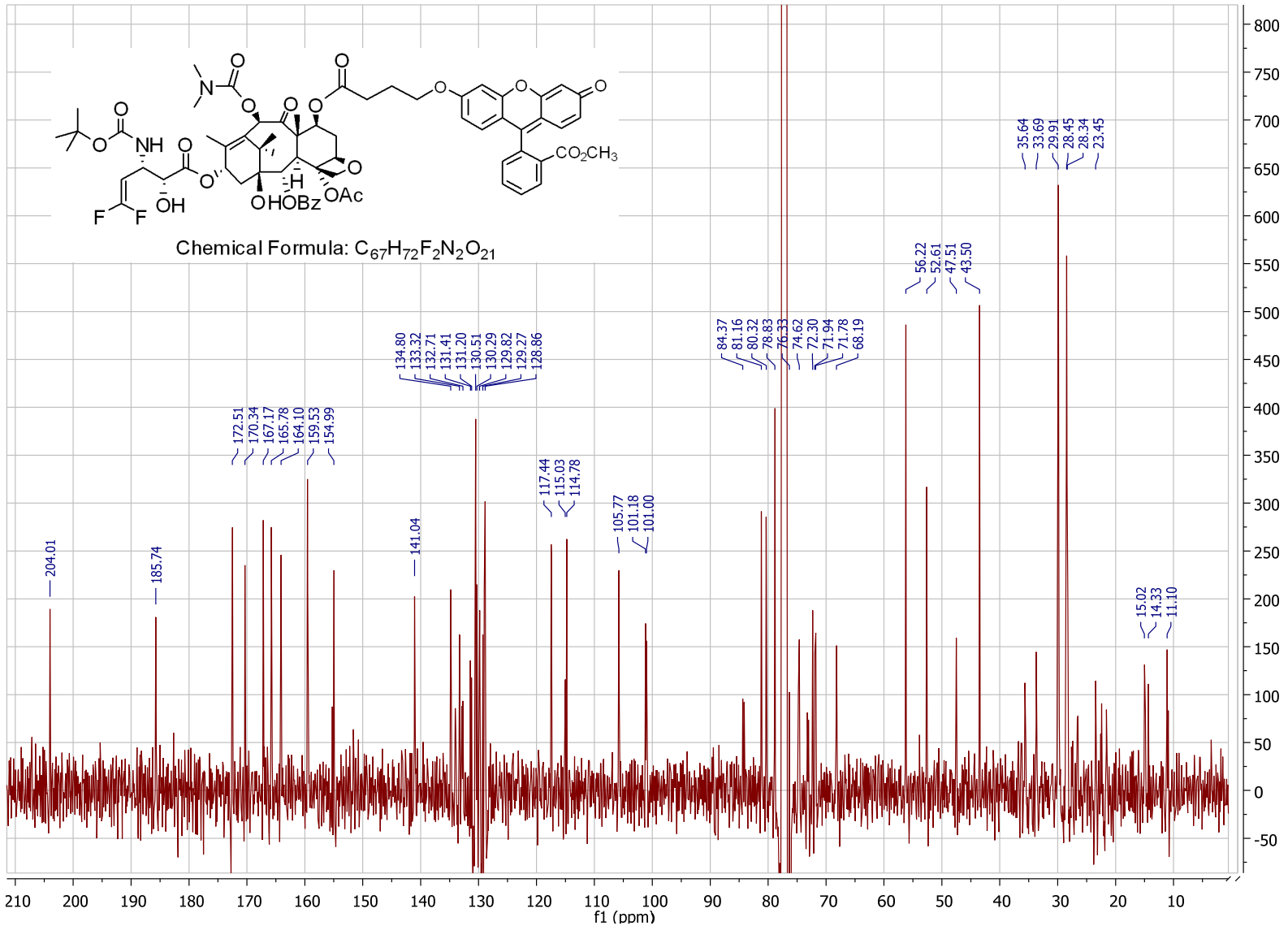

^{19}F NMR Spectrum of **4-17**

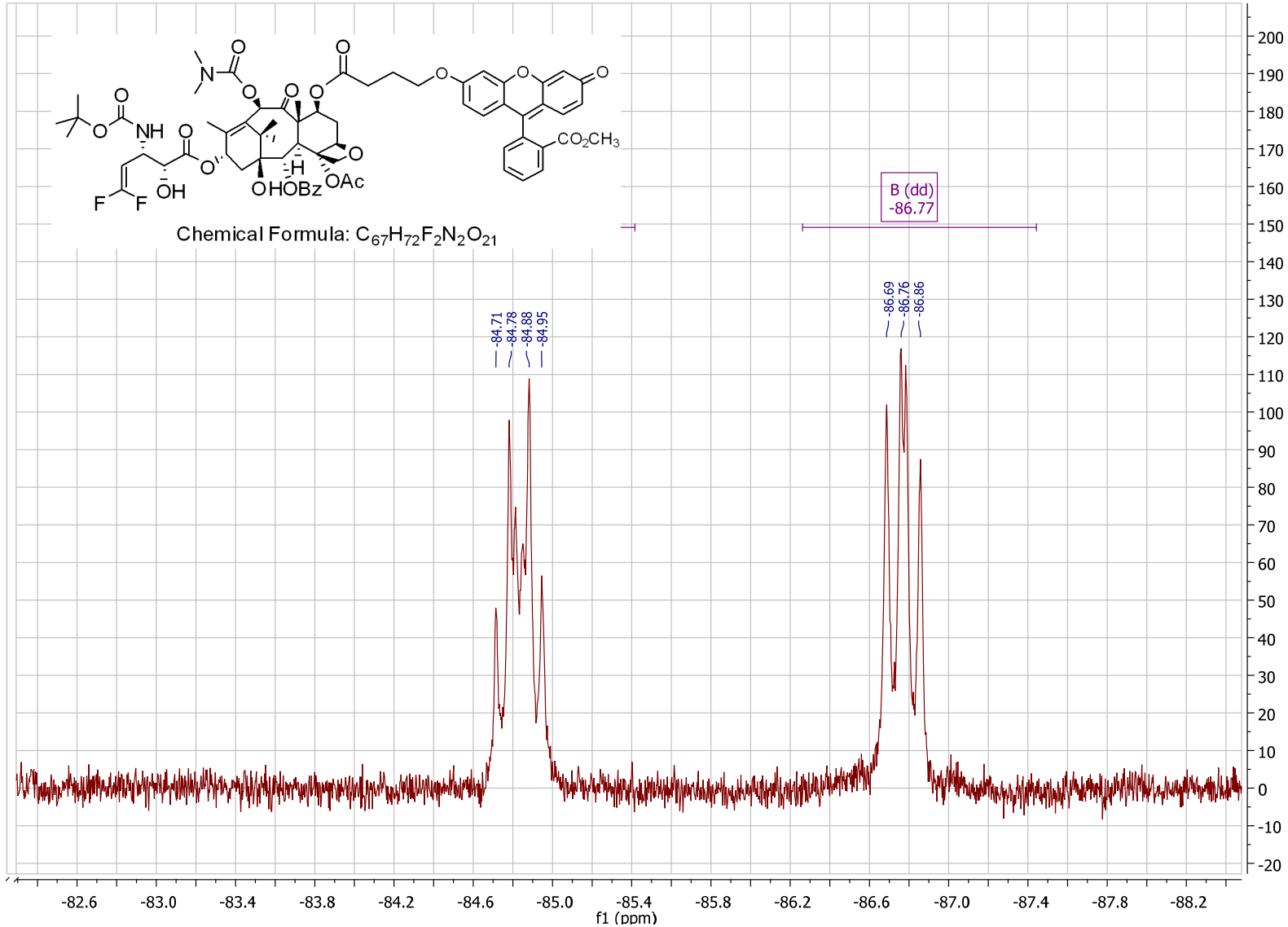

^{1}H NMR Spectrum of **5-1**

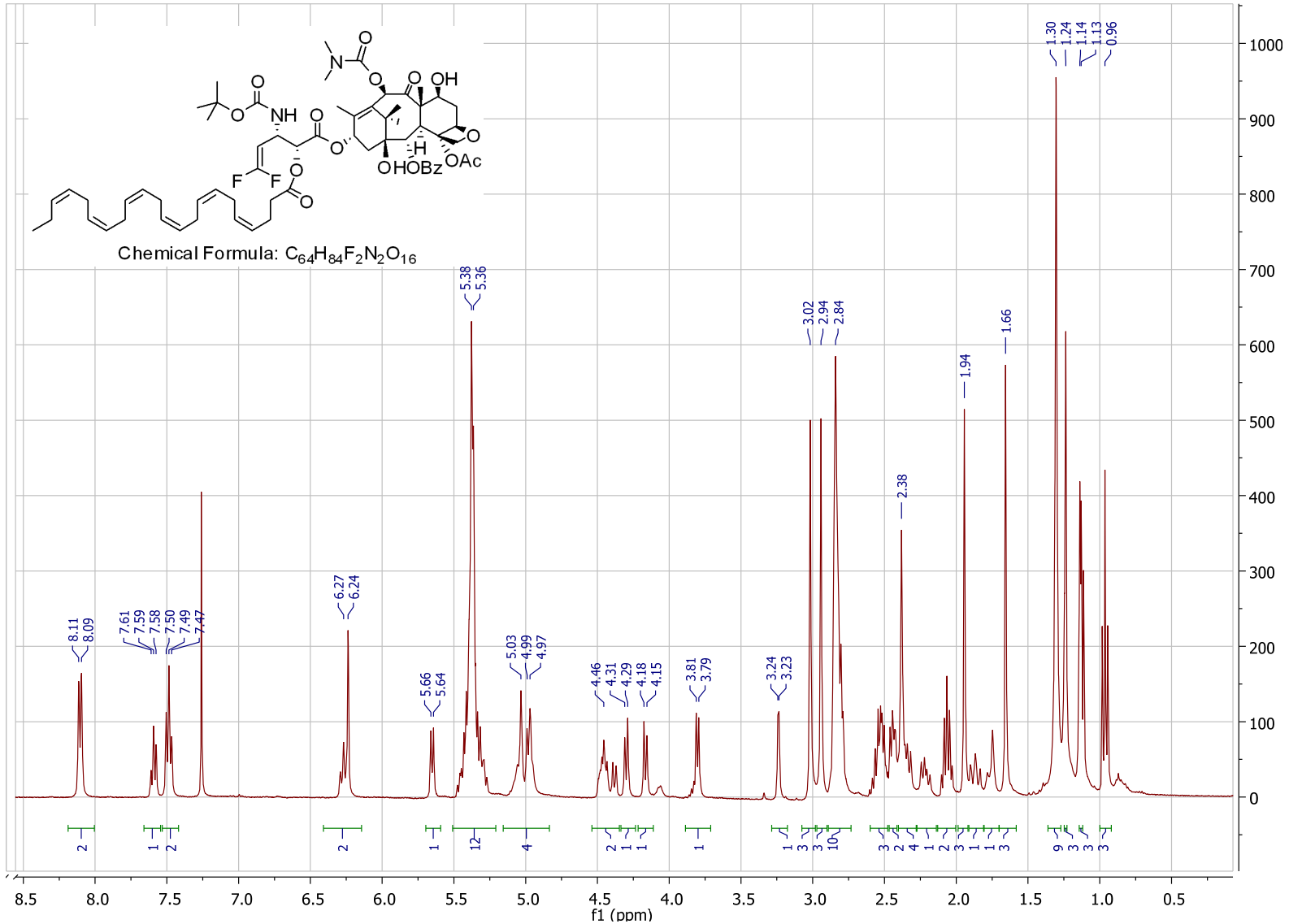

^{13}C NMR Spectrum of **5-1**

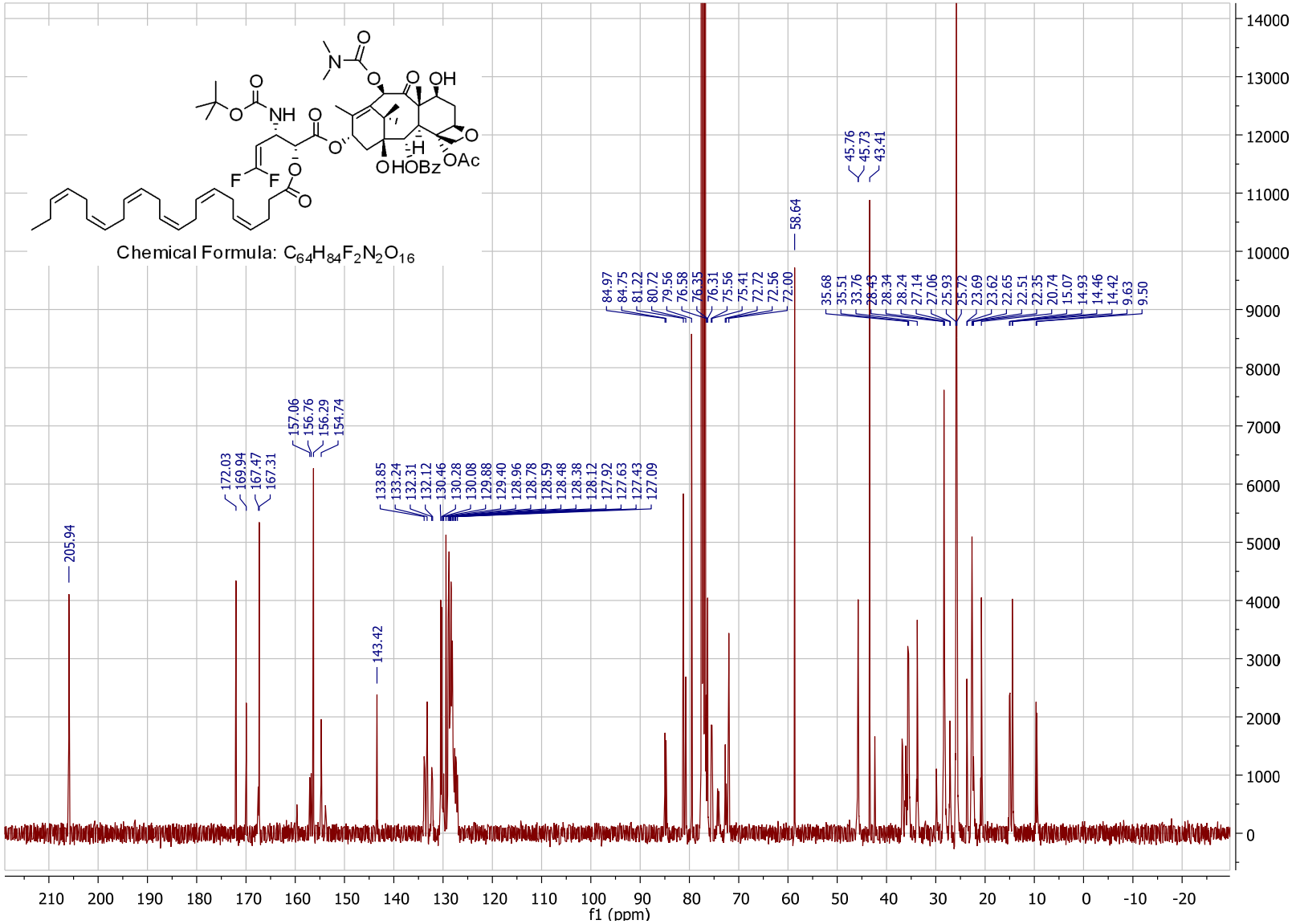

^{19}F NMR Spectrum of **5-1**